

**Developments in Economic Geology**

**30**

**Precambrian  
Ore Deposits of the  
East European and  
Siberian Cratons**

**D.V. Rundqvist and C. Gillen  
(Editors)**

**ELSEVIER**

Developments in Economic Geology, 30

**Precambrian Ore Deposits of the  
East European and Siberian Cratons**

## Developments in Economic Geology

### Further titles in this series

1. I. L. ELLIOTT and W. K. FLETCHER (Editors)  
GEOCHEMICAL EXPLORATION 1974
2. P. M. D. BRADSHAW (Editor)  
CONCEPTUAL MODELS IN EXPLORATION  
GEOCHEMISTRY  
*The Canadian Cordillera and Canadian Shield*
3. G. J. S. GOVETT and M. H. GOVETT (Editors)  
WORLD MINERAL SUPPLIES  
*Assessment and Perspective*
4. R. T. SHUEY  
SEMICONDUCTING ORE MINERALS
5. J. S. SUMNER  
PRINCIPLES OF INDUCED POLARIZATION FOR  
GEOPHYSICAL EXPLORATION
6. R. A. RICH, H. D. HOLLAND and U. PETERSEN  
HYDROTHERMAL URANIUM DEPOSITS
7. J. G. MORSE (Editor)  
NUCLEAR METHODS IN MINERAL EXPLORATION  
AND PRODUCTION
8. M. KUŽVART and M. BÖHMER  
PROSPECTING AND EXPLORATION FOR MINERAL  
DEPOSITS
9. C. R. M. BUTT and I. G. P. WILDING (Editors)  
GEOCHEMICAL EXPLORATION 1976
10. G. B. FETTWEIS  
WORLD COAL RESOURCES  
*Methods of Assessment and Results*
11. R. G. TAYLOR  
GEOLOGY OF TIN DEPOSITS
12. H. K. GUPTA  
GEOTHERMAL RESOURCES; AN ENERGY  
ALTERNATIVE
13. C. R. M. BUTT and R. E. SMITH (Editors)  
CONCEPTUAL MODELS IN EXPLORATION  
GEOCHEMISTRY, 4:  
Australia
14. G. BÁRDOSSY  
KARST BAUXITES  
*Bauxite Deposits on Carbonate Rocks*
15. A. W. ROSE and H. GUNDLACH (Editors)  
GEOCHEMICAL EXPLORATION 1980
16. R. W. BOYLE  
GEOCHEMICAL PROSPECTING FOR THORIUM  
AND URANIUM DEPOSITS
17. G. R. PARSLow (Editor)  
GEOCHEMICAL EXPLORATION 1982
18. M. KUŽVART  
INDUSTRIAL MINERALS AND ROCKS
19. P. LAZNICKA  
EMPIRICAL METALLOGENY  
*Depositional Environments, Lithologic Associations  
and Metallic Ores*
20. O. RUDAWSKY  
MINERAL ECONOMICS  
*Development and Management of Natural Resources*
21. M. KUŽVART and M. BÖHMER  
PROSPECTING AND EXPLORATION OF MINERAL  
DEPOSITS  
*second, completely revised edition*
22. N. DE KUN  
MINERAL ECONOMICS OF AFRICA
23. B. L. GULSON  
LEAD ISOTOPES IN MINERAL EXPLORATION
24. T. A. P. KWAK  
W-Sn SKARN DEPOSITS  
*Related Metamorphic Skarns and Granitoids*
25. P. LAZNICKA  
BRECCIAS AND COARSE FRAGMENTITE  
*Petrology, Environments, Associations, Ores*
26. D. L. BUCHANAN  
PLATINUM-GROUP ELEMENT EXPLORATION
27. G. BÁRDOSSY and G. J. J. ALEVA  
LATERITIC BAUXITES
28. M. VANECEK  
MINERAL DEPOSITS OF THE WORLD  
*Ores, Industrial mineral and Rocks*
29. P. LAZNICKA  
PRECAMBRIAN EMPIRICAL METALLOGENY  
*Precambrian Lithologic Associations and Metallic Ores  
(Volume 2)*

Developments in Economic Geology, 30

# **Precambrian Ore Deposits of the East European and Siberian Cratons**

*Edited by*

**D.V. Rundqvist**

*Russian Academy of Sciences,  
Institute of Precambrian Geology, St. Petersburg, Russia*

*and*

**C. Gillen**

*The University of Edinburgh, Centre for Continuing Education,  
Edinburgh, United Kingdom*



1997

ELSEVIER

Amsterdam – Lausanne – New York – Oxford – Shannon – Singapore – Tokyo

ELSEVIER SCIENCE B.V.  
Sara Burgerhartstraat 25  
P.O. Box 211, 1000 AE Amsterdam, The Netherlands

ISBN: 0-444-82657-2

© 1997 Elsevier Science B.V. All rights reserved.

No part of this publication may be reproduced, stored in a retrieval system or transmitted in any form or by any means, electronic, mechanical, photocopying, recording or otherwise, without the prior written permission of the publisher, Elsevier Science B.V., Copyright & Permissions Department, P.O. Box 521, 1000 AM Amsterdam, The Netherlands.

Special regulations for readers in the USA - This publication has been registered with the Copyright Clearance Center Inc. (CCC), 222 Rosewood Drive, Danvers, MA 01923. Information can be obtained from the CCC about conditions under which photocopies of parts of this publication may be made in the USA. All other copyright questions, including photocopying outside of the USA, should be referred to the copyright owner, Elsevier Science B.V., unless otherwise specified.

No responsibility is assumed by the publisher for any injury and/or damage to persons or property as a matter of products liability, negligence or otherwise, or from any use or operation of any methods, products, instructions or ideas contained in the material herein.

This book is printed on acid-free paper.

Printed in The Netherlands

## Foreword

“Precambrian Ore Deposits of the Russian and Siberian Cratons” is a sequel to “Precambrian Geology of the USSR” published in 1993 (English edition), in which the main emphasis was on the stratigraphy, magmatism and metamorphism of Precambrian assemblages in both ancient cratons (East European and Siberian) as well as in Phanerozoic fold belts and mobile regions. Mineral deposits associated with Precambrian structures were mentioned only in passing, since space restrictions in the earlier work did not allow even a brief outline of major deposits. The present book fills that gap.

Like its predecessor, this work was written by a group of colleagues at the Russian Academy of Sciences Institute of Precambrian Geology and Geochronology in St Petersburg. The overall plan follows the layout in “Precambrian Geology of the USSR” – Parts 1 and 2 provide a regional description of the East European and Siberian Cratons, while Part 3 deals with the time–space distribution patterns of mineral deposits.

During the preparation of this book, several revisions and refinements of previously accepted tectonic and metallogenic regional zonation were introduced; in particular, recently obtained new geochronological data have refined our notions about the geological and metallogenic evolution of the regions of Siberia during the Early Proterozoic and the Late Riphean.

As the compilation of the book progressed, it became abundantly clear that the level of knowledge of Precambrian metallogeny in the regions studied was far from perfect. In a number of cases, for example the Anabar Shield, a complete description of mineral deposits is not offered, and instead we present only the general features of mineral genesis for certain blocks and zones.

In their descriptions of individual deposits, the authors have used their own material, collected over many years of research in the Precambrian of Russia, as well as the published data listed in the references section at the end of the book. This work represents the first step in systematically studying the data on deposits of useful minerals and ore-bearing type structures in the Precambrian.

The material was prepared for publication by V.A. Gorelov and V.Ya. Khiltova; figures were drawn by G.P. Pleskach, A.A. Mikhailova and T.A. Zhuravlyova, to whom the authors express their gratitude. V.G. Kushev and V.A. Semyonov are also thanked for their critical remarks and constructive suggestions.

Authors: V.B. Dagalaysky, V.A. Gorelov, V.Ya. Khiltova, A.M. Larin, D.A. Mikhailov, G.P. Pleskach, D.V. Rundqvist, E.Yu. Rytsk, Yu.M. Sokolov, S.I. Turchenko, A.K. Zapolnov.

This Page Intentionally Left Blank

## Contents

<i>Foreword</i> (D.V. Rundqvist) .....	V
<i>Introduction</i> (D.V. Rundqvist) .....	1
<b>Part I. Mineral deposits of the East European Craton</b>	
<b>Section 1. Eastern Baltic Shield</b>	
<i>General geological features</i> .....	11
<i>Chapter 1. The Kola Terrain</i>	
<i>V.A. Gorelov &amp; S.I. Turchenko</i> .....	15
1 Ore deposits and occurrences .....	16
1.1 Iron .....	16
1.2 Titanium, iron, phosphorus .....	20
1.3 Aluminium (kyanite schists) .....	27
1.4 Nickel, copper, cobalt .....	29
1.5 Lead, zinc .....	41
1.6 Molybdenum .....	43
1.7 Rare metals .....	46
1.8 Graphite .....	50
<i>Chapter 2. Karelia Terrain</i>	
<i>V.A. Gorelov, A.M. Larin &amp; S.I. Turchenko</i> .....	51
1 Ore deposits and occurrences .....	53
1.1 Iron .....	53
1.2 Titanium .....	57
1.3 Nickel, copper, PGE .....	58
1.4 Molybdenum .....	67
1.5 Gold .....	70
1.6 Massive sulphide .....	71
1.7 Shungite .....	74
<i>Chapter 3. Belomorian Belt</i>	
<i>V.A. Gorelov</i> .....	77
1 Ore deposits and occurrences .....	77
1.1 Muscovite .....	77
1.2 Ceramic pegmatites .....	83

## VIII

### *Chapter 4. Ladoga Belt*

<i>V.A. Gorelov &amp; A.M. Larin</i> .....	87
1 Ore deposits and occurrences .....	88
1.1 Tungsten .....	88
1.2 Tin .....	89
1.3 Ceramic pegmatites .....	100
1.4 Graphite .....	102
2 Conclusions .....	103

### **Section 2. Ukrainian Shield and Voronezh crystalline massif**

#### *Chapter 5. The Ukrainian Shield*

<i>V.B. Dagelaysky</i> .....	107
1 Geological structure and metallogeny .....	107
2 Ore deposits and occurrences .....	115
2.1 Iron .....	115
2.2 Chromium .....	123
2.3 Titanium and phosphorus .....	123
2.4 Nickel, copper, cobalt .....	127
2.5 Molybdenum .....	130
2.6 Rare metals and rare earths .....	132
2.7 Graphite .....	141
2.8 Topaz and morion in pegmatites .....	145
2.9 Abrasive garnet .....	149
2.10 Talc and magnesite .....	150
2.11 Pyrophyllite .....	151
3 Conclusions .....	152

#### *Chapter 6. The Voronezh crystalline massif*

<i>V.B. Dagelaysky</i> .....	155
1 Geological structure and metallogeny .....	155
2 Ore-bearing tectonic structures .....	160
3 Ore deposits and occurrences .....	160
3.1 Iron .....	160
3.2 Nickel, copper, cobalt .....	165
4 Conclusions .....	170

#### *Chapter 7. Platform cover of the East European Craton*

<i>A.K. Zapolnov</i> .....	173
1 General features of tectonic evolution and ore content .....	173

## Part II. Mineral deposits of the Siberian Craton

### Section 1. Anabar Shield

<i>Chapter 8. Major features of geological structure and metallogeny</i> <i>S.I. Turchenko</i> .....	185
---	-----

### Section 2. Aldan Shield

<i>Chapter 9. Aldan Terrain</i> <i>D.A. Mikhailov</i> .....	195
--	-----

1.1 Iron .....	198
1.2 Phlogopite .....	202
1.3 Apatite .....	206
1.4 Rock crystal in quartz veins .....	209

<i>Chapter 10. Olyokma Terrain</i> <i>A.M. Larin &amp; D.A. Mikhailov</i> .....	211
--	-----

1 Ore deposits and occurrences .....	212
1.1 Iron .....	212
1.2 Copper .....	215
1.3 Rare metals .....	222
1.4 Apatite .....	224

<i>Chapter 11. Batomga Terrain</i> <i>A.M. Larin</i> .....	227
---	-----

<i>Chapter 12. Dzhugdzhur–Stanovoy Terrain</i> <i>V.A. Gorelov</i> .....	231
---	-----

1 Ore deposits and occurrences .....	232
1.1 Iron .....	232
1.2 Nickel, copper, cobalt .....	232
1.3 Molybdenum .....	235
1.4 Gold .....	236
1.5 Phosphorus, iron, titanium .....	238
2 Conclusions (D.A. Mikhailov) .....	242

### Section 3. Basement inliers around craton margins and fold belts

<i>Chapter 13. Pre-Sayan inlier</i> <i>V.Ya. Khiltova &amp; G.P. Pleskach</i> .....	249
--	-----

1 General geological features(V.Ya. Khiltova) .....	249
2 Ore deposits and occurrences (V.Ya. Khiltova & G.P. Pleskach) .....	250
2.1 Iron .....	250
2.2 Titanium .....	255

2.3	Aluminium (sillimanite schists) .....	257
2.4	Rare metals .....	258
2.5	Talc and magnesite .....	260
2.6	Muscovite .....	265
2.7	Apatite .....	265
2.8	Fluorite .....	269
<i>Chapter 14. Angara–Kan inlier</i>		
	<i>V.Ya. Khiltova &amp; G.P. Pleskach</i> .....	271
1	Ore deposits and occurrences .....	271
1.1	Titanium .....	271
1.2	Gold .....	273
1.3	Muscovite .....	274
<i>Chapter 15. Khamar–Daban and Pre-Olkhon inliers, SW Pre-Baikal</i>		
	<i>D.A. Mikhailov &amp; V.Ya. Khiltova</i> .....	279
1	Pre-Olkhon inlier .....	279
1.1	Manganese .....	280
2	Western Khamar–Daban .....	281
2.1	Phlogopite .....	282
2.2	Lazurite .....	284
<i>Chapter 16. Yenisey fold belt</i>		
	<i>V.Ya. Khiltova &amp; G.P. Pleskach</i> .....	289
1	Ore deposits and occurrences .....	289
1.1	Iron .....	291
1.2	Manganese .....	294
1.3	Lead, zinc .....	298
1.4	Gold .....	302
1.5	Talc and magnesite .....	310
1.6	Rare metals .....	313
2	Conclusions .....	314
<i>Chapter 17. Baikal–Patom fold belt</i>		
	<i>A.M. Larin, Ye.Yu. Rytsk &amp; Yu.M. Sokolov</i> .....	317
1	Geological structure and metallogeny .....	317
2	Ore deposits and occurrences .....	323
2.1	Iron .....	323
2.2	Nickel, copper, cobalt .....	326
2.3	Lead, zinc .....	329
2.4	Tin .....	336
2.5	Rare metals .....	337
2.6	Gold .....	341
2.7	Muscovite .....	349
2.8	Ceramic pegmatites .....	356

2.9	Chrysotile–asbestos .....	356
2.10	Ornamental stones .....	358
3	Conclusions .....	360

**Section 4. Platform cover of the Siberian craton**

<i>Chapter 18. Tectonic evolution and metallogeny</i>		
	<i>A.K. Zapolnov</i> .....	365

1	Mineral deposits and occurrences .....	370
1.1	Manganese .....	370
1.2	Lead, zinc .....	371

**Part III. Patterns of mineral deposit evolution in Precambrian structures**

<i>Chapter 19. Evolutionary patterns of mineral deposits in Precambrian terrains</i>		
	<i>A.M. Larin, S.I. Turchenko &amp; D.V. Rundqvist</i> .....	383

1.1	Archaean metallogenic epochs .....	384
1.2	Proterozoic metallogenic epochs .....	391
1.3	Phanerozoic metallogenic epochs .....	402
2	Conclusions .....	402

<i>Chapter 20. A classification of Precambrian mineral deposit types</i>		
	<i>D.V. Rundqvist, V.A. Gorelov, S.I. Turchenko &amp; A.M. Larin</i> .....	409

References .....	425
Index of mineral deposits and occurrences .....	445
Subject Index .....	451

This Page Intentionally Left Blank

## Introduction

### *1. Types of Precambrian tectonic units*

Precambrian mineral deposits are now becoming more significant in the mineral–raw materials balance for many countries in the world, since the vast majority of ores of iron, titanium, vanadium, gold and uranium, non-metals such as muscovite and phlogopite, and considerable amounts of asbestos and barite are currently being worked from Precambrian deposits. Recently, new types of gold, rare-metal, tungsten, tin, beryllium, rare-earth, radioactive elements, platinoids and manganese ore bodies have been discovered, as well as deposits of unusual geochemical associations such as Ni–U, U–Cu–Au and Pt–Au. The most interesting recent discoveries have been made in Australia, India, South Africa, Canada and Brazil. Statistically, these countries now lead the growth league tables of mineral–raw materials resources, as a direct result of these new deposits being opened in Precambrian complexes.

This phase occurred earlier in the former Soviet Union – the decade 1930–1940 was a period of intense discovery of Precambrian mineral deposits, and coincided with regional geological investigations of the ancient regions of the country, i.e. the Soviet part of the Baltic Shield, the Ukrainian and Aldan shields, the Baikal–Patom province, etc. (Fig. 1). Due to the work of A. Fersman, A. Polkanov, G. Kholmov, V. Kotulsky and other scientists who worked in the Kola Peninsula and Karelia at that time, almost all the currently-known deposits were discovered – Monchegorsk (Cu–Ni), Olenegorsk and Kostomuksha (Fe), Parandovo and Hautavaara (massive sulphide) and others. In the post-war years, exploration led to the discovery of a number of deposits of rare-metal metasomatites, copper–molybdenum–porphyry ores, shungite, ore-bearing black shales and others, but these discoveries enlarged only the areas of U, Pt and Mo without significantly altering the broad metallogenic profile of the region, as established in the pre-war years.

Precambrian deposits continued to be discovered in the Ukraine into the 1950s and 60s, when new types of radioactive, rare-metal and rare-earth deposits were discovered (Perzhan, Zhyoltorechka, etc.) among a variety of metasomatic rocks, altered metamorphic complexes.

In Eastern Siberia, many gold placers in the Lena and Aldan regions and muscovite deposits in the Baikal Highlands were already known at the start of this century, but the general metallogenic pattern of these regions was finally established only in the post-war years after the discovery of native Precambrian gold deposits (Sukhoy Log), exploration of the ferruginous quartzites of the Chara–Tokko region, magnetite and phlogopite skarn deposits (Tayozhnoye and others), apatite deposits (Seligdar), rare metals (Katugin), piezoquartz and asbestos (Molodyozhnoye), as well as the discovery of a major province of polymetallic (Kholodninskoye) and copper ores (the Udokan cupraceous sandstones).

If we also consider other countries in terms of genetic and structural types, then it is worth emphasizing that recently there has been particularly considerable growth in the

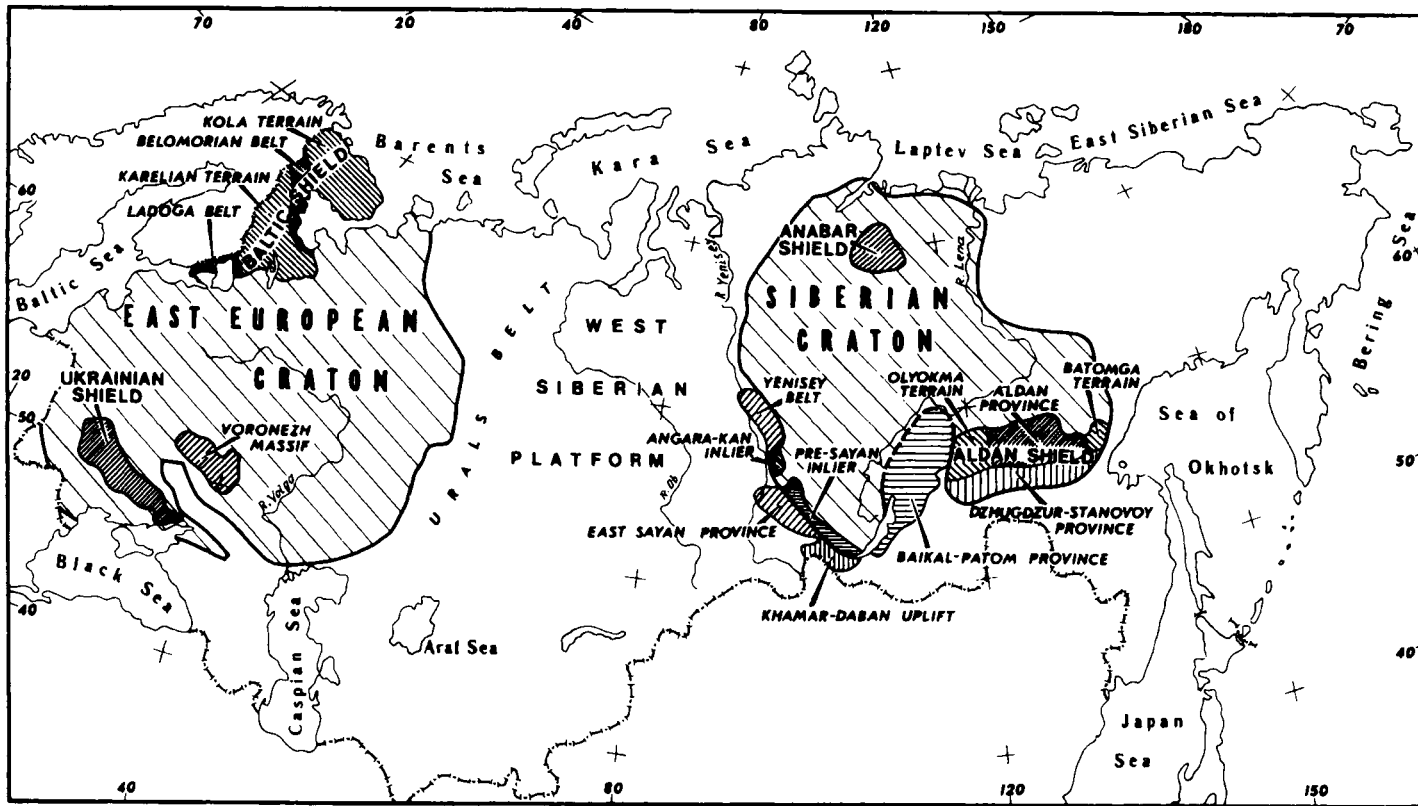


Fig. 1. Main tectonic units in East European and Siberian cratons.

significance of deposits all over the world associated with Archaean greenstone belts, which have become important sources of ferruginous quartzites and manganese, gold, copper–nickel, asbestos, pyrite, copper and base metal ores. Additionally, newly-discovered types of mineralization, in particular platinoids, rare earths, etc., among basic–ultrabasic layered intrusions and basic and alkali dyke complexes have increased the interest in mafic magmatism in rift zones. Greater attention is now being paid to the metallogeny of volcano-sedimentary complexes in Proterozoic epicratonic basins, which contain a unique “variegated” association of useful mineral deposits, including uranium, nickel, cobalt, platinum, gold, copper, base metals, barite and shungite, related to high-carbon, carbonate and terrigenous–carbonate assemblages, ancient residual soils (palaeosoils), and basic volcanics.

The increasing importance of mineral deposits of Precambrian age in countries’ mineral–raw materials balance defines new tasks in metallogenic research. The systematic treatment of data relating to the geodynamics of Precambrian deposits has begun to play an important role, resulting in the identification of the most prospective epochs of ore formation, and the formulation of criteria for forecasting and exploration signatures of new ore types.

One of the major issues in the systematic approach to metallogenic data for Precambrian terrains is to establish principles for metallogenic regional subdivision, the identification of ore-bearing structures of different ranks – metallogenic provinces, zones and ore fields – and the study of their development, reconstruction of formational evolution and changes in geodynamic environments with time.

Using metallogenic regional subdivisions and type classification by area, it is now possible to make broad comparisons between territories on different continents, to identify the most typical deposits in different geological settings and to use patterns of ore mineral distribution using evidence from well-studied regions in newly opened-up territories. These factors were responsible for the recognition a considerable time ago that the study of Precambrian ore-bearing structures was one of the most important aspects of metallogenic analysis. T.V. Bilibina, V.I. Kazansky, V.M. Terentyev, V.M. Popov, S.I. Turchenko, V.G. Kushev, A.V. Sinitsin, D.V. Rundqvist and others proposed different versions of type classifications for metallogenic structures. In the present work, the approach to the systematic treatment of data for Precambrian ore-bearing structures follows that worked out by a team in the Institute of Precambrian Geology and Geochronology (Russian Academy of Sciences, St Petersburg) and accepted for the International Atlas of metallogenic maps for the Precambrian of the continents.

The regional descriptions that follow examine the major types of Precambrian tectonic units, reflecting the broad evolutionary development of the continental crust in the Archaean and Proterozoic respectively. Precambrian specialists are familiar with the geological characteristics of these units, but in order to avoid any ambiguity later, we now explain the meanings of the terms as used here:

*Granulite–gneiss terrains* – extensive areas of ancient crust (> 3 Ga), characterized by intensely deformed metasediments and metavolcanics, transformed at granulite and high-T amphibolite facies and associated with plutonic complexes of various composition. The present authors distinguish principally these areas from linear granulite–gneiss structures of collision zones.

*Granite–greenstone terrains* – extensive areas of Archaean crust, characterized by an association of volcanosedimentary supracrustal assemblages that make up greenstone belts, underlain and surrounded by granitoids (granite and tonalite gneiss, migmatite).

*Tectonothermally reworked belts* – linear structures, developed in the continental crust, starting from the Late Archaean and extending to the Late Proterozoic. They are characterized by polycyclic processes of granulite and amphibolite facies metamorphism of various thermodynamic regimes, and repeated igneous activity, variously expressed as granitoids, migmatitic granites and gabbro–anorthosites. Typical features are polyphase deformation, deep-level thrusts and shear zones. These structures correspond generally to collision-type fold belts.

*Rift belts* – linear Proterozoic tectonic structures, restricted to deep fault zones with layered and differentiated mafic and ultramafic intrusions, dykes and bimodal basalt–rhyolite volcanics, associated with sedimentary rocks. Such belts can be divided into subtypes, depending on a number of factors, including ore content. Metamorphism is predominantly at greenschist facies.

*Fold belts* – Proterozoic tectonic structures, characterized by distinctive zonation, folded sediments, ophiolite, island arc and continental shelf assemblages, with the possible occurrence of ancient reworked crustal fragments, abundant syn- and post-tectonic granitoids, and frequent zonal metamorphism, up to high-T amphibolite facies. These correspond to accretionary belts.

*Volcano-plutonic belts* – Proterozoic linear structures in which the dominant constituents are igneous complexes of mostly acidic composition. Depending on the tectonic setting and the dominant constituent rock association, three types of such belt can be distinguished: a) predominantly volcanic belts, overlying ancient continental crust and structurally related to adjacent fold belts (magmatism of active continental margins); b) predominantly plutonic belts, restricted to deep faults separating major tectonic structures (intraplate magmatism of continental rifting stage); c) predominantly plutonic belts with typomorphic anorthosite–rapakivi granite association and as a rule having an intracratonic setting. They appear as isolated round or chain-shaped bodies. These structures may be considered as equivalent to modern magmatism of intraplate hot spots.

*Pericratonic basins* – belts and basins with a long history of formation (usually 600–1000 Ma) around craton margins, which in the shape of oblique troughs (grabens) may cut into the interior of a craton.

*Intracratonic basins* – isolated sediment-filled basins and depressions within cratons, representing the early stages in the development of the platform cover. Within or on the flanks of shields are basins or remnants of basins with substantial volcanism, later and more localized non-magmatic grabens and troughs (sometimes minor basins, up to 200 × 400 km). The formation of ancient platform basins often concludes with intense displays of basic and ultrabasic magmatism as layered intrusions and, or dyke complexes. Within platforms are basins which completed the growth of previously existing downwarps (e.g. aulacogens) and, as a rule, overstepped and extended beyond their borders.

*Aulacogens* – major intracratonic basins bounded by syntectonic faults, superimposed along regenerated deep faults in the crystalline basement of a craton. Aulacogens

usually form basin systems. Their development immediately precedes the formation of the sedimentary assemblage of the platform cover.

*Platform cover* – a sedimentary blanket covering most of the craton and consisting of marine terrigenous and carbonate rocks. Igneous activity in the form of plateau lavas is possible.

In compiling this monograph, the authors were confronted with a number of difficulties related to assigning ore deposits to one or other tectonic unit, particularly with reference to Proterozoic deposits located within Archaean granulite–gneisses or younger Late Riphean deposits found in Early Proterozoic tectonic units. In this case, should we consider deposits naturally belonging to their host tectonic units and blocks, or should we consider them related to the processes of subsequent crustal rejuvenation that affected the entire region? We should not lose sight of the well-known fact that many deposits are controlled by suture zones bounding tectonic structures. The difficulties encountered in referring deposits to particular types of tectonic structure are also related to the lack of convincing evidence for the age and genesis of the deposits, especially those which evolved over a prolonged period and for which we can trace a complex history in the transformation of primary ore concentrations during recrystallization, metamorphism and subsequent intrusive igneous activity or the effect of weathering processes.

When all these factors were taken into account, we adopted the simplest plan of presentation: firstly, there is a brief geological outline of a region and the distribution of deposits based on the type of ore-bearing tectonic units, followed by a description of individual deposits by content: iron, manganese, gold, apatite, etc. (in the sequence ferrous metals – base metals – rare metals – non-metals).

The book concludes with a summary of data about particular features of the ore content of each typical Precambrian terrain and the major ore-forming epochs, and typical groups and kinds of ore deposits.

A few words are also necessary about the genetic classification adopted here. Precambrian terrains are well known for their wide variety of useful mineral deposits. For those in which the ores are essentially unaffected by metamorphism, the conventional Phanerozoic genetic classification system has been used, in the variant set out most fully by V.I. Smirnov. This identifies true magmatic liquation and segregation types, skarn, greisen, numerous and varied high-, medium- and low-temperature hydrothermal deposits, clastic sedimentary, organic and chemical. In addition, Precambrian terrains contain various exceptionally widely distributed metamorphic deposits belonging to different P–T conditions.

In the generally accepted classification of useful mineral deposits, starting with Bogdanovich (1913) and continuing up to the most recent summaries by Tatarinov, Smirnov and Belevtsev, there has been a strong tendency to identify two classes of deposit of metamorphic origin – metamorphosed (e.g. metamorphosed cupraceous sandstones, massive pyrite ores, copper–nickel sulphides, etc.) and truly metamorphic (e.g. graphite, rutile and kyanite deposits in schists).

However, such a simple and intelligible division of deposits based on their metamorphism has been shown by more recent research to be insufficient at present. A different approach to the genetic classification of useful mineral deposits of meta-

morphic type has been proposed in recent years – one based on the source of the ore concentrations. Sokolov, Glebovitsky and Turchenko (1975) proposed three classes of metamorphic deposit: *prometamorphic*, *orthometamorphic*, and *rheometamorphic*.

It is also particularly worth emphasizing the importance of determining the age of Precambrian deposits. In most of the cases described, the age has been determined both from geological relationships and in individual cases, which are particularly contentious, by isotope geochemical investigations. The geological age is usually based on information about the age of the rocks which are the direct host for the ore mineralization – ore-bearing, genetically related, or those associated with the mineralization; or of younger rocks overlying the mineral deposit, or in pebbles of which the ores are found; or of rocks cross-cutting the deposit (dykes, veins, stockworks, etc.). In a number of cases, significant help is obtained from evidence about the time of folding, whether or not the ores were involved in the folding, and data about metamorphism.

The complexity of using field relationships for age dating Precambrian ores and mineral deposits is due to the wide distribution in the Precambrian of mineralization in “featureless” metamorphic assemblages. In this regard, data on the age or mineralization is based in most cases on the results of isotopic dating of rocks – ore-bearing, ore-producing formations and post-ore dyke complexes. There are significantly fewer data on the isotopic ages of hydrothermal–metasomatic ore-bearing rocks, vein minerals, etc. and also the lead model age of ore minerals.

The problem of isotopic dating of mineral deposits has been addressed by A.A. Polkanov, E.K. Gerling, I.M. Gorokhov, L.A. Neymark, and others. In so far as the age dates obtained from the various isotopic systems K/Ar, Rb/Sr, U/Pb, Pb/Pb, Sm/Nd respectively also reflect different geological processes, the book quotes alongside specific age dates the method, and in a number of cases also the author and the laboratory where the determination was made.

Generalizing the available data on the age dating of mineral deposits obtained in the Academy of Sciences Precambrian Institute laboratories as well as in other Russian organisations and abroad, allows us to caution against the uncritical use of the numbers obtained. This is due in the first place to the difficulty of separating the age of the source of the ore material and the age of formation of the ore in a given deposit, the age of the primary deposition of the ore and the age of episodes of subsequent redistribution and redeposition, recrystallization and metamorphism. In addition, using different isotopic dating methods for a single deposit practically always allows us to trace a prolonged history of formation.

The clearest and best studied examples of the rare-metal deposits around Lake Ladoga, the pyrite–base metal and gold ores of the north Lake Baikal region, and the apatite and phlogopite deposits of the Aldan Shield are evidence that modern mineral parageneses, their textures and structures, the morphology of ore bodies, are all the result of a very long, multi-stage history. Individual episodes of this history – the initial accumulation of disseminated concentrations in rock assemblages, concentrations of ore elements during regional or contact metamorphism, metasomatism, the formation of veins, stockworks, etc. may be relatively brief and “contained” within the margins of error of a particular “isotopic age” determination. But the overall total history of formation may stretch out over many hundreds of millions of years. Generally, all the

presently available data on the geochronology of ore forming processes, including many Phanerozoic deposits also, point to the prolonged formation of deposits, ore fields and zones. With this in mind, in the majority of cases the long period of formation is such that quiescent pauses between individual relatively brief active ore-forming impulses were quite long.

Overall, the evidence obtained from geochronological dating of ore processes substantially modifies and complements our traditional ideas about the interrelation of geological and ore formations: the formation of ore zones, fields, deposits and in a number of cases, individual ore bodies, must be compared not with the formation of one geological sequence, but with an evolutionary series of geological sequences, which developed over tens or even hundreds of millions of years.

Since the present work is a sequel to material on the geology and mineral deposits of the Precambrian set out in the book "Precambrian Geology of the USSR", we briefly refer to the tectonic and age subdivisions adopted previously, and note their metallogenic equivalents (Table A).

In a more detailed characterization of the ore content of any one terrain, we usually employ the following hierarchical series of subdivisions, from the general to the more particular: metallogenic region (zone) → ore-bearing field (zone) → ore deposit → ore body. In this sequence, the terms are proposed for relatively isometric spatial distributions (in plan view), and in parentheses for strongly-oriented linear distributions.

The following geochronological subdivisions, accepted in the former USSR, are used in accounts of geological periods (Table B).

In the previous work these age intervals were called crust-forming periods or stages. Their metallogenic equivalents were taken as metallogenic epochs (Katarchaeon, Early Archaean, etc.). In order to signify more detailed intervals, characterizing their specific metallogeny, Kratz and Sokolov (1984) proposed the concept of a metallogenic pulse (e.g. at  $2600 \pm 100$  Ma,  $1800 \pm 100$  Ma) and noted the nine most typical. It is worth noting that in 1990, based on the generalization of new data, a refinement of several boundaries was proposed. Thus, it was proposed to put the Archaean-Proterozoic boundary at  $2500 \pm 50$  Ma. The  $2000 \pm 50$  Ma boundary in the Lower Proterozoic was taken to mark two subdivisions of the Early Proterozoic, the Karelian and the

Table A

Hierarchy of tectonic and corresponding metallogenic subdivisions

Tectonic subdivisions	Metallogenic subdivisions
Global tectonic province – craton (East European, Siberian, etc.)	Global metallogenic province (belt)
Global tectonic belt (e.g. Urals-Mongolia)	
Tectonic superprovince (Central Province of East European craton, uniting several granite-greenstone terrains)	Metallogenic superprovince
Tectonic province (e.g. granite-greenstone terrain)	Metallogenic province
Tectonic zone (for instance: greenstone belt, intracratonic basin, etc.)	Metallogenic zone

Table B

Geochronological subdivisions used in this work (age in Ma)

		Subdivision		Age intervals, Ma	
Late Precambrian	Vendian	Riphean			650–570
	Upper Proterozoic (PR <sub>2</sub> )	Upper Middle Lower	R <sub>3</sub> R <sub>2</sub> R <sub>1</sub>		1050–650 (± 50) 1350–1050 (± 50) 1650–1350 (± 50)
Early Precambrian	Proterozoic	Lower	PR <sub>1</sub>		2500–1650 (± 100)
	Archaean	Upper	AR <sub>2</sub>		3000 (± 200)–2600 (± 100)
		Lower	AR <sub>1</sub>		3500 (± 100)–3000 (± 200)
	Katarchaeon				3500 (± 100)

Svecofennian. The boundary between the Lower and Upper Archaean was also refined, and is now taken to be at  $3100 \pm 100$  Ma. However, these changes as a whole are not particularly significant, as we shall see.

An independent category of geochronological and at the same time tectonic subdivisions is represented by tectono-magmatic cycles and megacycles. The following periods are used in this work: Aulian ( $> 3.4$  Ga), Saamian (Aldanian) (3.4–3.0 Ga), Rebolian (3.0–2.6 Ga), Seletskian (2.5–2.3 Ga), Svecofennian (Udokanian in the Aldan Shield) (2.2–1.7 Ga), Gothian (1.7–1.2 Ga), Dalslandian (1.2–0.9 Ga) and Baikalian (1.0–0.6 Ga).

In concluding this introduction to the book, we emphasize once again that the authors consider the material presented here as the first essential step on the road to a general systematic description of ancient mineral deposits. Further work needs to be done in collecting and analyzing data both in order to solve common scientific problems: the classification of ore formations, the evolution of ore formation in time; and to solve tasks in applied geology: elaborating a theory for forecasting and exploring for useful mineral deposits within the confines of Precambrian terrains.

## **Part I**

### **Mineral deposits of the East European Craton**

This Page Intentionally Left Blank

## Section 1:

### Eastern Baltic Shield

#### *1. General geological features*

The Precambrian deposits of the eastern Baltic Shield constitute an important potential in the mineral-raw materials base of the country in terms of iron, titanium, nickel, alumina (kyanite schists), muscovite, ceramic feldspar and shungite. There are also small deposits of molybdenum, tin, tantalum, niobium, cesium, pyrite, graphite, and occurrences of copper, tungsten, cobalt and noble metals which merit further investigation and evaluation.

A significant addition to the mineral resources of the region is to be found in Phanerozoic deposits (not dealt with here), the main ones being multicomponent ores (P, Fe, Ti, Al, Ta, Nb, Sr, Zr, REE, F, phlogopite, vermiculite) in the Khibiny, Lovozero, Kovdor and other alkali-ultrabasic and carbonatite intrusions.

The region is divided into four first-order tectonic structures: the Kola, Karelian, Belomorian and Ladoga terrains (Fig. 1). The Kola and Karelian terrains were Archaean cratons (3.1–2.6 Ga) with their own individual evolutionary features, which determine whether they are classified as granulite-gneiss or granite-greenstone terrains respectively, and stabilized by the Early Proterozoic (Rundqvist and Mitrofanov, 1992). The Ladoga belt forms part of the Early Proterozoic Svecokarelian fold domain. The Belomorian belt, which formed as a collision zone between the Kola and Karelian terrains, is a mobile polycyclic belt with tectonothermal reworking of older crust. Typical are large-scale horizontal and vertical movements of geological structures in the belt, with exposure at the present erosion surface of the deepest levels of Archaean crust showing uneven reworking in the Early Proterozoic.

The dominant trend of rock complexes and fold axes is NW, which coincides with the strike of most of the Archaean and Early Proterozoic deep faults, which are both terrain boundaries and boundaries of major fold structures. Synchronous with these faults, and also in later epochs, there appeared variously oriented, mostly perpendicular faults extending to various crustal depths, with the result that the region has a complex fault pattern.

According to the classification of Precambrian tectonic units adopted here, the structural types identified in the region are: granulite-gneiss and granite-greenstone terrains, intracratonic basins, tectonothermally reworked belts, fold belts, rift belts, and volcanoplutonic belts (Fig. 2). The volcanoplutonic belts can be considered as zones of tectonomagmatic activity. A recent review of the metallogeny of these units has been published (Turchenko, 1992).

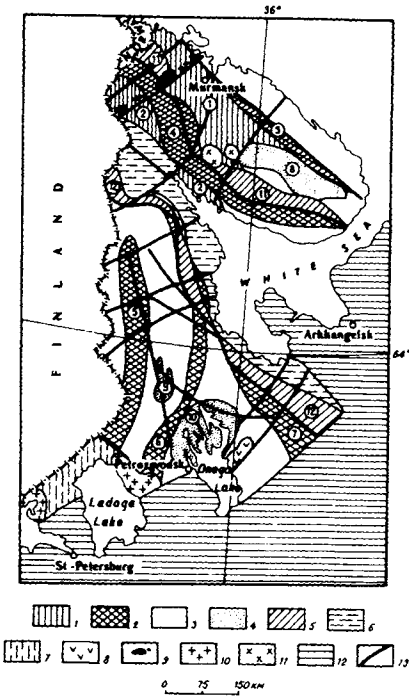


Fig. 2. Tectonic sketch map showing early Precambrian tectonic units and intrusions in the eastern Baltic Shield. 1) granulate-gneiss blocks, zones; 2) greenstone belts & zones of belts; 3) granite-gneiss areas; 4) intracratonic basins; 5) rift belts; 6) Belomorian belt of tectonothermal reworking; 7) Ladoga zone of Svecokarelian fold belt; 8) Burakov basic-ultrabasic intrusion; 9) Uruguba granites & granodiorites; 10) rapakivi granites; 11) Palaeozoic alkaline intrusions; 12) platform cover; 13) faults. *Named structures (circled numbers):* 1 - Central Kola block, 2 - Korva-Kolvitsa zone, 3 - Kolmozero-Voronya belt, 4 - Tersk-Allarechka belt, 5 - West Karelian zone, 6 - Central Karelian zone, 7 - East Karelian zone, 8 - Keivy basin, 9 - Segozero-Yangozero basin, 10 - Onega basin, 11 - Pechenga-Varzuga belt, 12 - Kuola-Vygozero belt.

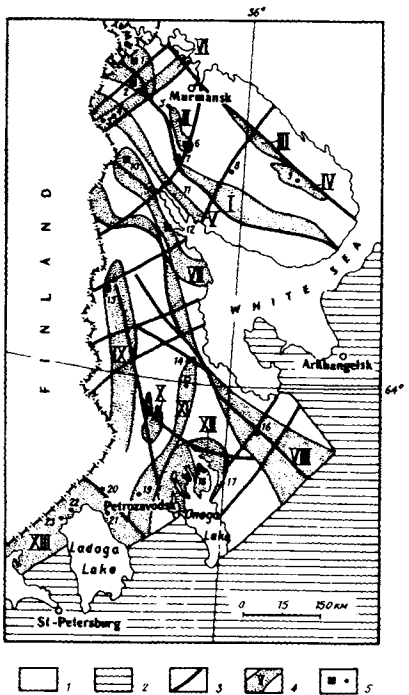


Fig. 3. Sketch map of Precambrian metallogenic zones and deposits in the Eastern Baltic Shield. Compiled using material from Bilibina et al. (Anon., 1985). 1) early Precambrian; 2) platform cover; 3) faults; 4) metallogenic zones: I - Pechenga-Varzuga (Ni, Cu, Ti, P), II - North Imandra (Fe), III - Kolmozero-Voronya (REE), IV - Keivy (Al), V - Korva-Kolvitsa (Ni, Ti), VI - Uruguba (Mo), VII - Belomorian (Mu, Sp), VIII - Kuola-Vygozero (Ni, Cu, Ti, P), IX - Himola-Kostomuksha (Fe), X - Yangozero (Cu), XI - Hautavaara (Py), XII - Onega (shungite, Cu), XIII - North Ladoga (Sn, W, Gr); 5) ore regions and ore fields (a), ore deposits (b): 1 - Pechenga (Ni), 2 - Allarechka (Ni), 3 - Jaurijoki (Mo), 4 - Lovnozero (Ni), 5 - Gremyakhya-Vyrmes (P, Ti), 6 - Olenegorsk (Fe), 7 - Monchegorsk (Ni), 8 - Tsagin (Ti), 9 - Shuururta (Kyanite), 10 - Yona (Mu), 11 - Central (Ti), 12 - Chupa (Mu), 13 - Kostomuksha (Fe), 14 - Lobash (Mo), 15 - Parandovo (Py), 16 - Lebyazhi (Ni), 17 - Zazhogino (shungite), 18 - Pudozhgora (Ti), 19 - Hautavaara (Py), 20 - Jalonvaara (Py, Cu), 21 - Pitkäranta (Sn), 22 - Latvasyrjä (W), 23 - Ihala (Gr).

Table 1

Examples of ore deposits and occurrences, localized in tectonic structures of the eastern Baltic Shield

Tectonic structure	Deposits & occurrences	Main ore signature
1. Granulite–gneiss blocks, zones	Pinkelyavr	iron
	Tsentralnoye (Central)	titanium
	Lovnozero	nickel
2. Greenstone belts	Olenegorsk, Kostomuksha	iron
	Allarechka, Lebyazhi	nickel
	Pellapahk, Lobash	molybdenum
	Kolmozero–Voronya zone	rare metals, pyrite, graphite
	Hautavaara, Skalistoye Occurrences	copper, zinc, gold, muscovite
3. Intracratonic basins	Shuururta (Keivy)	aluminium, shungite
	Zazhagin, Occurrences	copper, cobalt, zinc, gold
4. Rift belts	Gremyakh–Vyrmes	titanium, phosphorus
	Kaula, Monchegorsk Occurrences	nickel
		copper, gold, asbestos
5. Belomorian belt of tectono-thermal reworking	Yona and Chupa pegmatite elds	muscovite, feldspar raw materials
6. Ladoga fold belt	Latvasyrjä, Ihala	tungsten, graphite, feldspar
	Lyupiko, Linnavara Occurrences	titanium, nickel, copper, rare metals
7. Volcano-plutonic belt	Pitkäranta, Kittilä	tin, zinc
8. Zones of tectono-magmatic activity	Jauri	molybdenum
	Tsagin, Pudozhgora	titanium
	Bazarnaya Bay	lead, zinc

Coinciding with first-order tectonic structures are metallogenic provinces of the same name. At the boundaries of the above type structures, structural–metallogenic zones are localized, with one or more economically important mineral deposits and ore occurrences (Fig. 3, Table 1).

This Page Intentionally Left Blank

## Kola Terrain

V.A. GORELOV and S.I. TURCHENKO

The Kola terrain is subdivided into several ore-bearing tectonic structures. These are: Archaean granulite–gneiss terrains, the Central Kola block and the Korva–Kolvitsa zone; Late Archaean greenstone belts, the Kolmozero–Voronya and Tersk–Allarechka; the Late Archaean–Early Proterozoic Keivy intracratonic basin; the Proterozoic Pechenga–Varzuga rift belt; and zones of early tectonomagmatic activity, including the Uraguba belt (Fig. 2).

The structural position of the Korva–Kolvitsa zone, which unites the Lapland and Kandalaksha–Kolvitsa granulite–gneiss terrains and runs along the boundary between the Kola and Belomorian geoblocks, remains far from unambiguous in the regional tectonic scheme. As well as being considered to belong to the Upper Archaean–Lower Proterozoic (Sumian) complex of the Kola terrain (Rundqvist and Mitrofanov, 1992), some workers assign it to the Belomorian geoblock. In this work, the zone is also referred to the Late Archaean granulite–gneiss structures of the Kola terrain.

The granulite–gneiss terrains consist of two-pyroxene and felsic granulites, pyroxene–amphibole schists and amphibolites, high-alumina gneisses and partial-melt rocks belonging to the charnockite–enderbite series with a NW-trending fabric in the rocks. Intrusions in this complex include granitoids of the tonalite–trondjemite series. Typical for the Korva–Kolvitsa zone are Late Archaean gabbro–labradorite and clinopyroxenite–wehrlite intrusions. Numerous intrusive websterite–gabbro–norite and granodiorite–granite associations belonging to the Lower Proterozoic are found locally in different parts of the granulite–gneiss terrains. Mineral deposits located within the granulite–gneiss terrains include small ore deposits (e.g. Pinkeljavr) and numerous occurrences of ferruginous quartzites belonging to the eulysite type, titanomagnetite, copper–nickel sulphides and muscovite.

Tholeiitic basalts predominate in the greenstone structures, associated with peridotitic to basaltic komatiites. There are minor amounts of felsic volcanics and sediments: tuffite, greywacke, arkose, graphitic and pyritic shales, quartzite, ferruginous quartzite and carbonates. Intrusive igneous rocks are represented by ultramafic, gabbro–labradorite, gabbro–trondjemite, migmatitic granite and granite associations. Greenstone belts contain small deposits of ferruginous quartzite (BIF), copper–nickel sulphide ores, copper–molybdenum (porphyry?) ores, rare metals and graphite, and copper and zinc occurrences.

The Keivy intracratonic basin consists of supracrustal assemblages, represented by various paragneisses and schists, meta-andesitic basalts, meta-andesites and meta-rhyolites, with a predominance in the upper parts of the succession of acid volcanics

and the weathering products of underlying rocks, represented by high-alumina staurolite–kyanite schists, with which the kyanite deposits are associated. Early Proterozoic alkaline granites are developed over a broad area in the SW part of the Keivy basin.

The Pechenga–Varzuga rift belt consists of an Early Proterozoic assemblage, represented by conglomerate, sandstone, clastic terrigenous–carbonate rocks, picritic basalts and tholeiitic basalts. The volcanosedimentary assemblage attains a thickness of 13 km, of which more than 10 km belong to volcanic formations. Along faults and in fault intersection zones, numerous basic–ultrabasic intrusions formed, and the gabbro–alkali association of the Gremyakha–Vyrmes pluton. Associated with this belt are apatite–iron–titanium and copper–nickel sulphide deposits, as well as copper and asbestos occurrences.

## 1. Ore deposits and occurrences

### 1.1. Iron

Iron-ore deposits in the Kola terrain are represented by the ferruginous quartzite formation which constitutes the Trans-Imandra metallogenic zone with the Olenegorsk economic ore region (Fig. 3), and the Shonguy–Volshpakh zone to the north, with the unproductive deposits of Simbozero, Polovinnaya and Pinkeljavr, together with numerous ore occurrences.

The Olenegorsk iron-ore region occupies an area of 600 km<sup>2</sup> (30 km × 20 km) in the centre of the Kola Peninsula near the NW end of Lake Imandra in the Trans-Imandra structure, which is called a greenstone belt (in Rundqvist and Mitrofanov, 1992), but this interpretation is rare. The iron-ore region is found at the boundary between the greenstone belt and the Central Kola granulite–gneiss block. Some workers (including Goryaninov and Balabonin, 1988) consider the ore region to belong to the granulite–gneiss block.

The region consists of rocks of the productive Upper Archaean Zaimandra (Trans-Imandra) Fm, which had earlier been dated at 2.7–2.4 Ga (Nalivkin and Yakobson, 1985), but now at 2.83 Ga (Glebovitsky and Shemyakin, 1995). The productive assemblage overlies an oval and slightly flattened basement block consisting of granodiorite gneiss (Fig. 4).

The constituents of the formation from bottom to top are: biotite, sillimanite–garnet–biotite, and hornblende–biotite gneisses, corresponding to a basal terrigenous assemblage; hornblende amphibolites with thin gneiss bands, representing basic volcanics with minor thin bands of tuffaceous rocks from basic to felsic composition; ferruginous quartzite (magnetite and hematite–magnetite); amphibole and biotite gneisses, and “leptites” – acid and intermediate metavolcanics (Gorbunov, 1981). This formation varies in thickness from 200 to 600 m. The productive formation is overlain by the Volchezero Fm aluminous gneisses. The ferruginous quartzites which are up to 300 m thick can be traced, with minor breaks, throughout the entire outcrop area of the Zaimandra Fm in the ore region.

Due to the tectonic movements responsible for folding and faulting the iron ore assemblage, the basement rocks took on the same foliation as the rocks in the Zaimandra Fm. The folds in this region have a pronounced NW trend, with deviations from this direction only in zones where granodiorite domes are abundant. The structure has an overall SW dip.

Faults are abundant in the region, and have various orientations. The earliest syn-folding faults, along which imbricate-monoclinical structures of the ore region formed, cannot be interpreted with total certainty due to the fact that repeated movements took place along them. A regional NE fault is situated on the NW flank of the Olenegorsk region, separating it from the rest of the Trans-Imandra structure. The downthrow to the NW is thought to have been significant, and the productive formation is mostly overlain by the next formation in the succession (Gorbunov, 1981). The ferruginous quartzites of the Olenegorsk region display many of the features of jaspilites, although they differ in a number of respects due to amphibolite and granulite facies metamorphism.

Ten deposits have been discovered and prospected in the region: Olenegorsk, Kirovogorsk, Komsomolsk, Professor Bauman, "15 Years of October", Pecheguba, South Kakhozero, Zheleznaya Varaka, Kurkenpakhk, Aivar, and several ore shows (Fig. 4). Total reserves and resources of the region have been estimated at 3 billion tonnes of ore, to a depth of 1–1.2 km, containing 23–33% iron ore in the form of

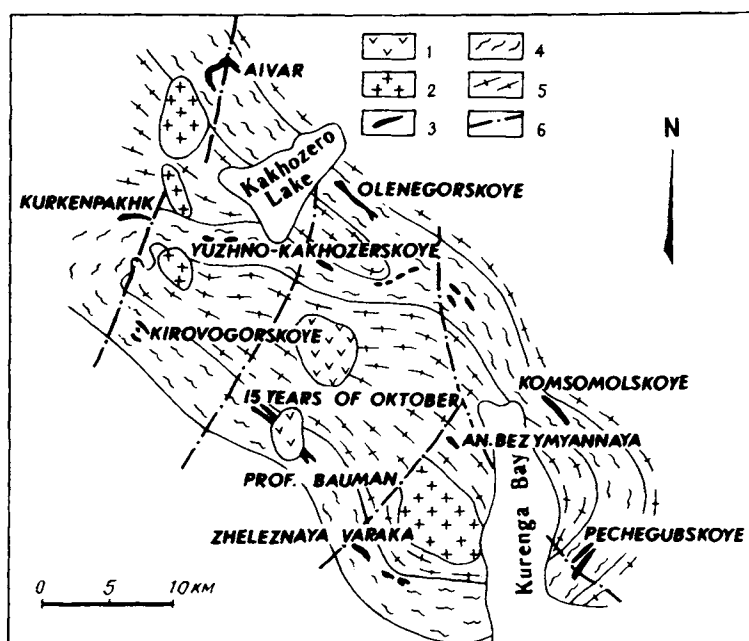


Fig. 4. Geological sketch map of the Olenegorsk iron ore region (based on Sevzapgeologiya materials). 1) basic & ultrabasic intrusions; 2) granite; 3) ferruginous quartzite; 4) hb gneiss; 5) granodioritic gneiss; 6) faults.

magnetite and hematite. The ore deposits in the region are generally of one type in terms of the composition and structure of the ore bodies, and they differ in the scale and degree of post-ore tectonic effects which complicate the general structure of the deposits, as well as in the ore granularity which determines its technical properties. Most workers adhere to the view that these deposits have a volcanosedimentary origin and underwent amphibolite to granulite facies metamorphism. The Olenegorsk deposit is the best studied of those named above and descriptions are to be found in the "Sevzapgeologiya" geological exploration company archives, and in Goryainov (1976).

The *Olenegorsk deposit* is situated 5 km NW of the Olenya station on the Murmansk to St Petersburg railway line. It consists of a sheet-like deposit, extending in a NW direction for some 4 km, with a steep ( $55\text{--}70^\circ$ ) monoclin dip to the SW (Fig. 5). The deposit can be followed to depths greater than 1200 m and its central part has not been fully contoured. The thickness varies from 20–30 m on the limbs to 300 m at the centre. Throughout their entire extent, the ferruginous quartzites are conformable with the host gneisses. On the SE limb, the deposit branches into a number of thin seams. The ore deposit consists of magnetite and hematite–magnetite quartzites. The magnetite : hematite ratio is around 3 : 1 on average for the deposit. There is an increase in hematite on the hanging wall of the deposit (Fig. 6).

Zones of tectonic disruption are developed in the ferruginous quartzites and especially along their margins. In the quartzites, these zones are expressed as intraformational fine flow folding, while in the contact parts of the deposit, zones of

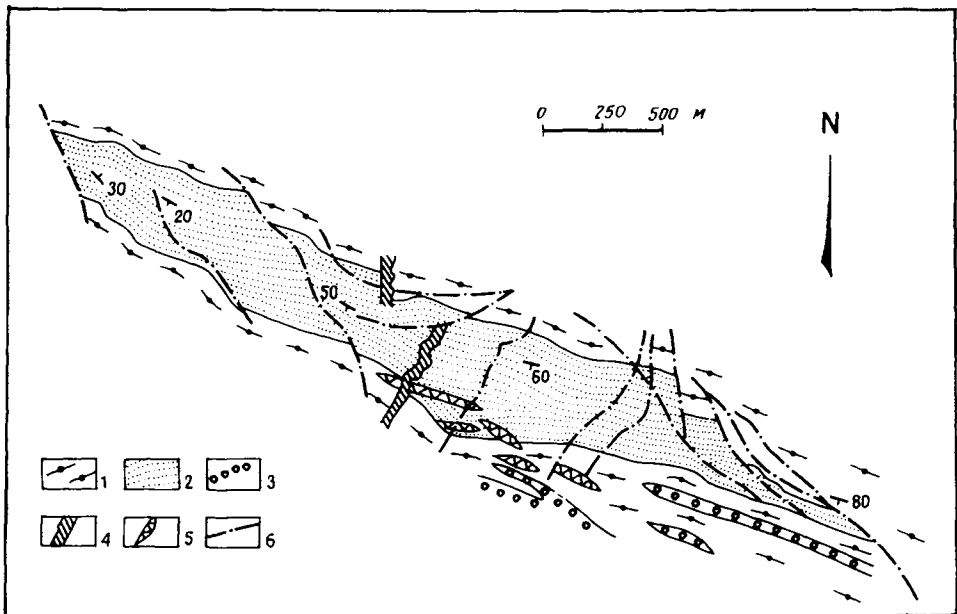


Fig. 5. Geological sketch map of the Olenegorsk deposit (simplified, after Goryainov, 1976). 1) hb-bi gneiss; 2) Fe quartzite; 3) "leptite"; 4) foliated dolerite dykes; 5) pegmatite; 6) faults.

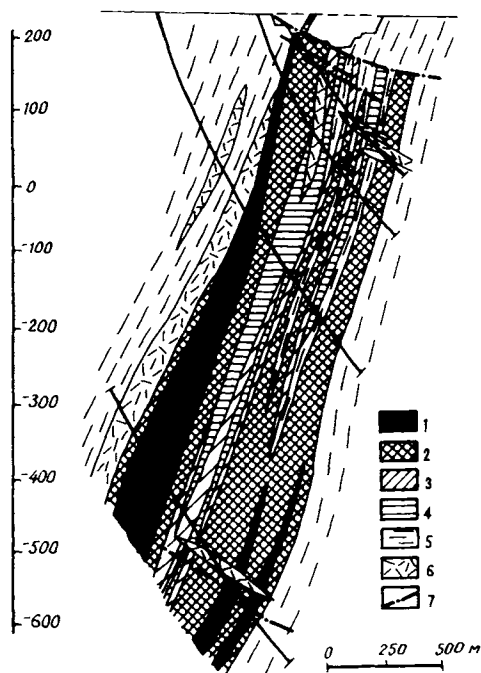


Fig. 6. Geological section through the Olenegorsk deposit (Goryainov, 1976). 1-4—mineral types of ferruginous quartzites in ore body: 1) pegmatite-magnetite, 2) magnetite, 3) magnetite-silicate, 4) sulphide-silicate; 5) hb-bi gneiss, amphibolite, "leptite"; 6) pegmatite; 7) faults.

interlayer delamination and slip with retrogressed rocks form, utilized by numerous bodies of granitic pegmatites. Young faults include flat-lying thrusts, extended along the ore body and expressed as shear zones with displacements of up to 150 m.

Goryainov (1976) has divided the ferruginous quartzites into seven types, according to their degree of ore mineralization and mineral composition: ore quartzites ( $\text{Fe} > 27\%$ ): 1 – hematite, 2 – hematite-magnetite, 3 – magnetite; ore-poor quartzites ( $\text{Fe} = 20-27\%$ ): 4 – magnetite-silicate, 5 – silicate; barren quartzites ( $\text{Fe} < 15\%$ ): 6 – sulphide-silicate, 7 – monoquartz, sulphide. There is a close association between hematite and hematite-magnetite ores with the upper part of the deposit, and sulphide and sulphide-silicate ores with the lower part. In idealized form, the same change in ore type occurs from hanging wall to footwall, although all seven ore types have never been observed in sections through the deposit.

The ores in this deposit are fairly simple in their mineralogy and chemical composition. The major ore minerals are magnetite and hematite, while pyrite, pyrrhotite and chalcopyrite are minor. Non-ore minerals include, together with quartz which forms the main constituent in the ferruginous quartzites, tremolite, actinolite, cummingtonite, pyroxenes, alkaline amphiboles, garnet, calcite and siderite. High-grade ores contain 95% magnetite and quartz. As the soluble iron content decreases, there is an increase in the content of magnesium, calcium and to a lesser extent

sulphur oxides. Since impurities in the ores – sulphur, arsenic, phosphorus and zinc – do not in general exceed 0.01%, the ores in this deposit are referred to as high-grade. Due to good crystallinity, ore mineral extraction in the concentrate is very high, over 90%. Reserves down to a depth of 1200 m amount to 800 million tonnes, for an average iron content in the ore of 31%.

### 1.2. Titanium, iron, phosphorus

The well-known magmatic deposits of titanomagnetite, ilmenite–titanomagnetite and apatite–ilmenite–titanomagnetite ores in the region associated with the Early Proterozoic gabbro–labradorite, clinopyroxenite–wehrlite, gabbro–wehrlite and alkali gabbro intrusions and are represented by early to late magmatic genetic types. Early magmatic mineralization is seen only in gabbro–wehrlite intrusions, while late magmatic mineralization occurs in clinopyroxenite–wehrlite intrusions. Both types of mineralization are seen in the other types of intrusion. Table 2 shows the Precambrian titanium ore deposits discovered in the region (Gorbunov, 1981)

Three titanomagnetite and ilmenite ore deposits are associated with the gabbro–labradorite intrusions which occur along deep faults on the western and northern margins of the Keivy structure – Tsagin, Magazin–Musyur and Acha. Of these, the Tsagin deposit has been studied in greatest detail (Gorbunov, 1981; Yudin, 1980, 1987).

*The Tsagin deposit* is spatially and genetically related to the Late Archaean Tsagin gabbro–labradorite intrusion which formed in a N–S zone of deep faults. The intrusion consists of a layered lopolith within an Archaean granite–gneiss and tonalite–gneiss complex, stretched out along a fault for 23 km, with a width of up to 9 km. Around the edges of the lopolith, the layers and trachytic banding dip at 30–40° towards the centre, and there is a gradual decrease in dip to horizontal in the axial zone (Fig. 7).

The intrusion consists of separate units. The outer contact parts consist of medium-grained gabbro and gabbro–norite with subordinate olivinite, troctolite,

Table 2  
Precambrian titanium deposits in the eastern Baltic Shield

Deposit	Magmatic formation	Type of substance	Mineral type	Tectonic structure
Tsagin Acha Magazin–Musyur	gabbro– labradorite	iron–titanium	ilmenite–titano- magnetite	marginal zone of the Keivy structure
Tsentralnoye Magnetitovy Log Zhdanov	clinopyroxenite– wehrlite gabbro–wehrlite	iron–titanium	ilmenite–titano- magnetite	Korva–Kolvitsa zone
Greymykh– Vyrmes	alkaline gabbro	phosphorus–iron– titanium	apatite–ilmenite– titanomagnetite	Pechenga–Varzuga rift belt

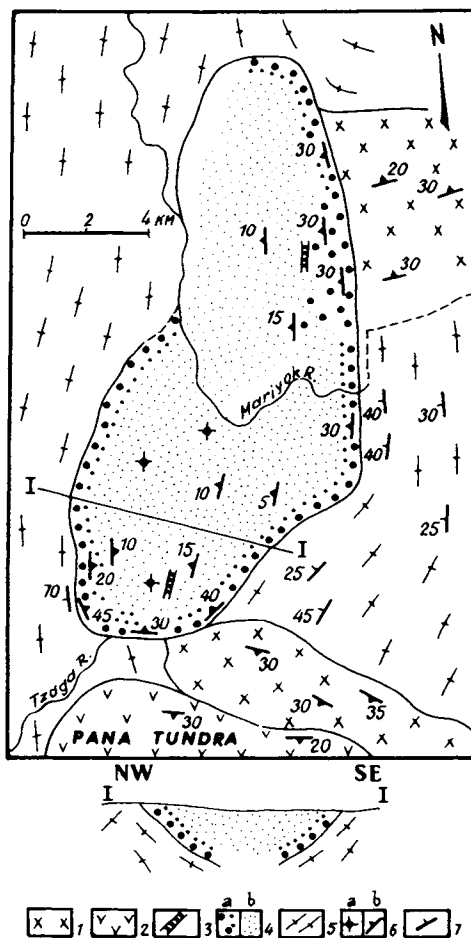


Fig. 7. Geological sketch map of the Tsagin intrusion (Yudin, 1980). 1) alkaline granite; 2) gabbro & gabbro-norite; 3) hornblende dolerite & gabbro dykes; 4) Tsagin gabbro-labradorite intrusion: (a) medium-grained gabbro & gabbro-norite, (b) coarse gabbro & labradorite; 5) granite-gneiss & granite; 6) primary gneissosity & trachytic texture: (a) horizontal, (b) dipping; 7) secondary gneissosity with dip angle.

plagioclase and clinopyroxene. Early magmatic schlieren-segregation titanomagnetite ore shows are restricted to this zone which, on the whole, typically show low titanium and vanadium concentrations. The highest titanomagnetite concentration is found in the NE part of the massif – the Marijoki section. The centre of the intrusion consists of coarse-grained and megacrystic gabbro and labradorite, alternating with late-magmatic essentially titanomagnetite ores which may have potential economic significance. These ores form three ore body types of different ages.

(1) Primary stratiform layered and podiform titanomagnetite bodies, conformable with the primary layering of the rocks. The bodies range in thickness from a few tens of cm to 20 m, the average being 10 m. The ores have a banded texture, as a rule.

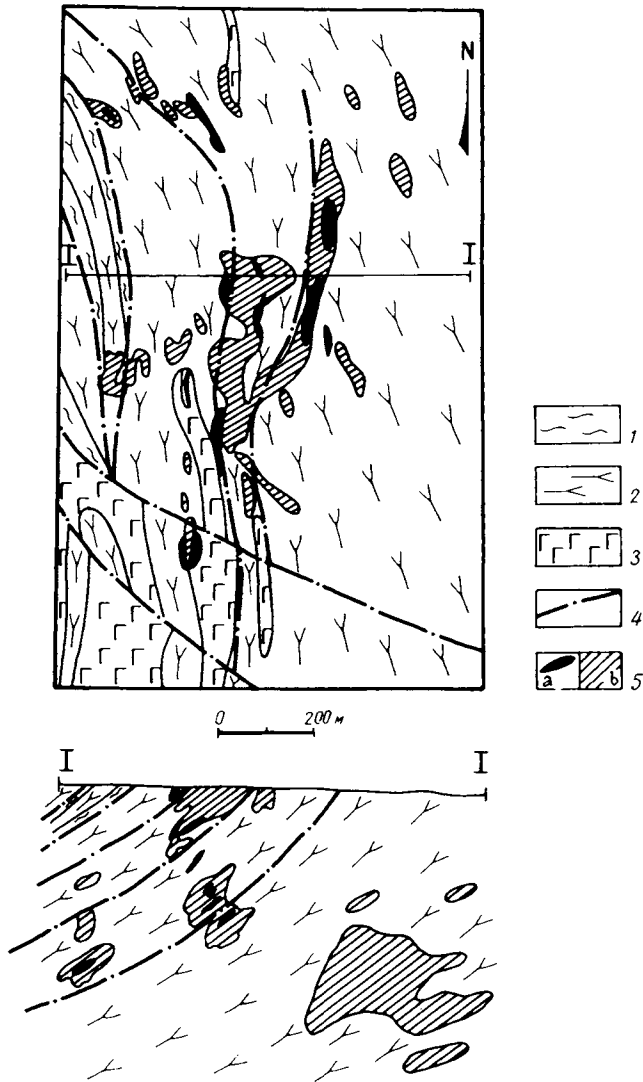


Fig. 8. Geological sketch map of the Tsagin deposit (based on Sevzapgeologiya materials) and section I—I. 1) mylonitized gabbro-amphibolite; 2) coarse and megacrystic labradorite & gabbro-labradorite; 3) gabbro, olivine gabbro, gabbro-norite; 4) faults; 5) titanomagnetite ores.  $\text{TiO}_2$  content: (a)  $> 10\%$ , (b) 2–10%.

(2) Lenticular titanomagnetite bodies, lying unconformable to the general structure in the central part of the intrusion, but conformable with the structure of the nearest margin of the gabbro-labradorite rocks, with which they have sharp contacts. The largest titanomagnetite ore body – the Tsagin deposit itself – is 200 m long and 30–40 m thick (Fig. 8) and has a characteristic banded texture, similar to stratified bodies.

(3) Cross-cutting titanomagnetite veins up to 1 m thick in gabbro–labradorites and primary stratified titanomagnetite deposits.

These late-magmatic ores consist of two types: dissemination-rich, and dense with massive and banded textures. The dense varieties locally contain a pyrrhotite–titanomagnetite type.

The main ore minerals are titanomagnetite and ilmenite, which account for over 95% of the ore mass volume. The amount of ilmenite in free grains does not exceed 10%. Secondary ore minerals are pyrrhotite and chalcopyrite, while there are minor amounts of pentlandite, pyrite, marcasite, valleriite, cubanite, violarite and millerite. The average content of useful components in the ores of the deposit is as follows: 35% total iron, 4.2% titanium, 0.2% vanadium, 0.04% nickel, 0.06% copper, 0.01% cobalt, 0.2% sulphur, 0.01% phosphorus. Ore mineral extraction in the concentrate is high. The titanomagnetite concentrate has the following composition: total iron 58–59%, titanium dioxide 11–12%, vanadium pentoxide 0.5%.

*The Central deposit.* The Korva–Kolvitsa granulite–gneiss zone contains clinopyroxenite–wehrlite intrusions which have undergone amphibolite facies metamorphism and in which are situated the Central and South-Western deposits in the Kandalaksha–Kolvitsa block, and Magnetitovy Log in the Lapland block. The Central deposit is regarded as a type example, using material from Yudin (1987).

The deposit is situated 12 km north of Kandalaksha Bay on the White Sea and is associated with the Central clinopyroxenite–wehrlite intrusion which measures 4 × 1 km in plan, lying in metamorphosed basic rocks (Fig. 9). The main minerals forming the intrusion are clinopyroxene and olivine. The ore minerals are titanomagnetite, ilmenite, pyrrhotite and chalcopyrite. Apatite and spinel are also encountered. Metamorphism of the intrusion is shown by the fact that pyroxene is replaced by hornblende and olivine is intensely serpentinized. Garnet, biotite, phlogopite, chlorite, talc and carbonate also formed as metamorphic minerals.

The intrusion contains 22 conformable, closely-spaced, parallel vein-like titanomagnetite bodies, forming a zone that stretches for over 3 km. The ore bodies strike at 320–330° and dip to the SW at 60–80°. They are from 0.5 to 50 m thick and from 40 to 1500 m long, and have numerous bifurcations. The ore zone has not been delineated down dip. Along strike, the zone displays differentiation in the morphology of ore types. In the SE the main ores are disseminated, while in the NW part of the zone they are dense. The zone is broken into blocks by numerous cross-faults, with throws of up to 40 m in plan. The scale of vertical displacements has not been established. The ores in this deposit are late-magmatic and belong to the titanomagnetite type. The amount of titanomagnetite and ilmenite in them is around 70% on average, with ilmenite not exceeding 10% of the ore mass, the remainder of the ore being mostly clinopyroxene. The titanium content in the ores varies from 5.4% to 7.8%, and vanadium from 0.15% to 0.35%.

*The Gremyakh–Vyrmes deposit* is situated in the NW of the Pechenga–Varzuga rift belt, 40 km SW of Murmansk on the right bank of the river Tuloma, in an economically developed region. Genetically and spatially, it is associated with a highly complex fracture-type Proterozoic intrusion of the same name, which formed in an Archaean gneiss unit. The massif has an area of around 100 km<sup>2</sup> (19 × 6–4 km)

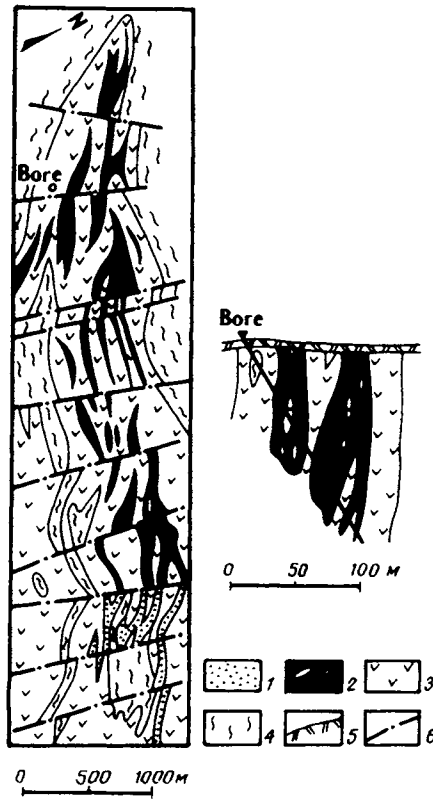


Fig. 9. Geological plan-view and section of the Tsentralnoye (Central) deposit (Yudin, 1987). 1) disseminated ores; 2) massive ores with country rock xenoliths; 3) clinopyroxenite & wehrlite; 4) metadiorite; 5) moraine; 6) faults.

and conformably follows the NW strike in the host gneisses, and has a WSW dip. According to Polkanov and Yeliseyev (1967), the intrusion formed in three stages. During the first stage in the sequence, a pyroxenite–gabbro–anorthosite and akerite–pulaskite complex formed, making up the southern part of the intrusion, equal to almost half of its area. In stage two, an alkaline rock complex formed – nepheline syenite, yuvite and ijolite, resulting in a steeply-dipping N–S sheet-like body, 1–1.5 km thick and some 4 km long. This rock complex stretches along the axial part of the first complex. In the final stage, alkaline granites and granosyenites formed, making up the northern part of the massif (Fig. 10). Various researchers consider that the late complex is only spatially associated with the two earlier ones. The massif has an age of 1.9–1.8 Ga (Anon., 1985).

The ores of the Gremyakha–Vyrmes deposit are represented by an apatite–ilmenite–titanomagnetite association which occurs in rocks of the first intrusive type, where two ore-bearing rock series can be identified: a) olivinite–peridotite–pyroxenite–gabbro–anorthosite, forming the eastern and central parts of the massif, and b)

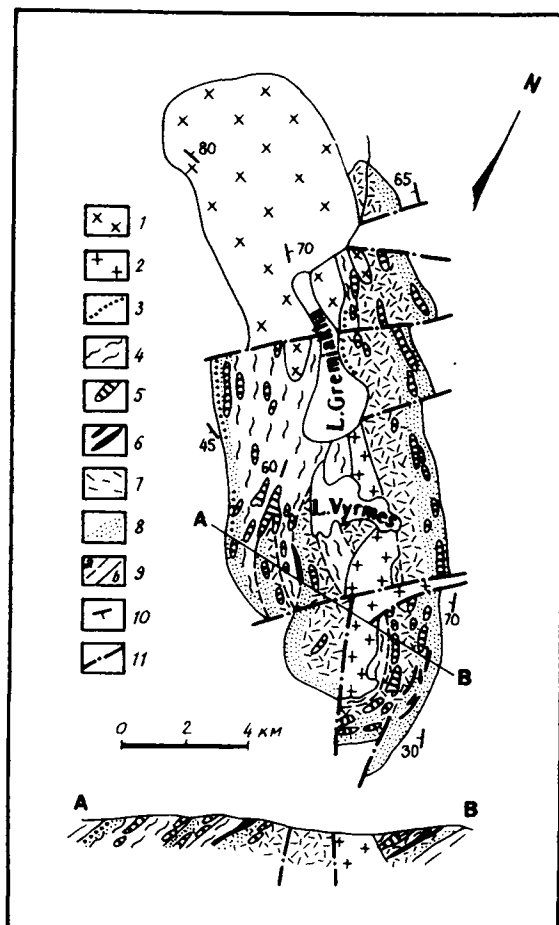


Fig. 10. Geological sketch map of the Greymyakh-Vyrmes intrusion (after Polkanov et al., 1967, with additions). 1) alkaline granite & granosyenite; 2) nepheline syenite, ijolite, urtite, melteigite, jacupirangite, yuvite, malinite, foyaite, aegerinite; 3) ilmenite-apatite gabbro; 4) alkali gabbro, pulaskite, akерite; 5) peridotite, pyroxenite, olivinite with ilmenite-titanomagnetite ore mineralization; 6) deposits of massive ilmenite-titanomagnetite ore; 7) gabbro, gabbro-anorthosite, anorthosite; 8) zone of complex ilmenite-titanomagnetite-apatite ores; 9) boundaries between (a) individual complexes and (b) country rocks; 10) primary banding and secondary gneissosity with dip angle; 11) strike-slip faults.

an overlying and younger peridotite-oligoclase gabbro-akerite-pulaskite series which forms the western part. Both rock series are differentiated and have a banded structure with bands dipping to the west at 40–45° and up to 70° in the eastern part of the intrusion.

A half-ring ore zone has been mapped in this part of the massif, some 20 km long and associated with the inner contact of the massif. The thickness of the zone with a  $P_2O_5$  cut-off grade of 2% varies from 40 to 500 m. The zone attains a maximum thickness on the NE and SW flanks. Titanomagnetite and ilmenite contents are

characteristically higher in the southern part of the zone. Like the intrusion, the ore zone is cut into blocks by cross-faults. On the eastern and western flanks, the zone is conformable with the intrusion and has a westerly dip; in the south of the massif, the zone dips north at 45–60°.

Two types of mineralization occur in the ore zone – early magmatic segregation, and late magmatic fusive. Segregation ores are restricted to the eastern basal part of the intrusion, forming stratified horizons of disseminated ore, containing numerous segregation varieties from thick disseminations to solid ores, up to 20 m long and 6 m thick. Based on the mineralogy in the silicate portion, the segregation ores can be divided into ore-bearing gabbro, gabbro–norite, troctolite and plagioclase pyroxenite. Solid ores always contain plagioclase, olivine and pyroxene grains. The ore structure is evenly disseminated to patchy, and the texture is predominantly poikilitic. The main ore minerals are titanomagnetite and ilmenite. Free grains of the latter constitute up to 20% by volume of the ore minerals. Secondary minerals are pyrrhotite, chalcopyrite and pentlandite which form small xenomorphic clusters (Osokin, 1987).

Late magmatic ores formed in the upper horizons, and are represented by two morphogenetic types: a) accumulation, forming stratified deposits of disseminated ores, as in segregation types, and b) injection, forming conformable layers and cross-cutting veins of rich disseminated and solid ores. Accumulation ores can be traced along the entire ore zone. These ore deposits vary in thickness from a few tens of metres to 300 m.

Injection-type ore mineralization is typical for the southern part of the ore-bearing zone. In the SE part of the lower units of the pluton, there are six layered bodies 500–600 m long and 10–15 m thick, forming a  $3 \times 0.5$  km zone overlying the segregation ores. The ore bodies have a coarsely banded structure, caused by the interleaving of thin bands of solid and densely disseminated ores, together with gabbro and anorthosite bands. The bands as a rule are asymmetric, the lower parts consisting of densely disseminated and solid ores, and the upper parts being poor disseminated ores. In the southern part of the upper peridotite–pulsaskite series is the largest layered body of solid ores, 30–40 m thick and 1.5 km long, with a steep westerly dip. Vein-type ores are not widely represented. When present, the veins are 1–2 m thick and are usually grouped in ore zones up to 200 m long.

The main ore minerals in the late magmatic ores are titanomagnetite–ilmenite, accounting for up to 30% of the ore mass, and apatite, whose content in the ores varies from 5% to 15–20%. Secondary minerals are pyrrhotite and less commonly chalcopyrite, pentlandite and pyrite, which occur as small xenomorphic grains. Late magmatic ores predominate in the deposit and due to the higher free ilmenite and apatite content, they represent the main economic resource.

The issue of how ores are assigned to one genetic type is particularly relevant to early magmatic segregation and late magmatic accumulation ores, which can be defined with confidence on the basis of the chromium content in titanomagnetite (Gorbunov, 1981). The highest chromium content (0.73%) in this mineral is characteristic for segregation ores; in accumulation ores it is 0.003%, and in injection ores 0.06%.

Ores in this deposit are generally low-grade. The  $P_2O_5$  content in the ore zone ranges from 2% to 8–10%, the average being 3.5%. The titanium content varies from 3% to 14%, and vanadium from 0.01% to 0.03%. Based on these contents, reserves to a depth of 300 m are 160 million tonnes  $P_2O_5$ . The ore quality and the thickness of the zone do not change with depth. Apatite recovery in the concentrate is 90–95%, with around 40%  $P_2O_5$  in the concentrate. Ilmenite and titanomagnetite recovery is also high. The  $TiO_2$  content in the ilmenite concentrate is 42–45%. The titanomagnetite concentrate contains 55% total iron, 7–8%  $TiO_2$  and 0.4%  $V_2O_5$ . The deposit occurs in conditions that favour open-cast mining.

### 1.3. High-alumina raw material (Kyanite schists)

High-alumina raw material deposits are restricted to the Keivy intracratonic basin in the eastern Kola Peninsula. The structure occupies an area greater than 10,000 km<sup>2</sup>, some 200 km long from west to east, and up to 70 km wide. Its internal structure consists of an elongate E–W-striking synclinorium with an E–W fold system. The synclinorium contains four Upper Archaean to Lower Proterozoic supracrustal rock assemblages (Rundqvist and Mitrofanov, 1993), represented by various gneisses, schists and amphibolites. The topmost unit, the Keivy schists, is a high-alumina assemblage, with which the kyanite deposits are associated.

The Keivy ore-bearing zone, which has been studied in detail by Belkov (1963), is the world's largest in terms of kyanite ore reserves. It is part of the Keivy schists, which are up to 1500 m thick. The schists overlie the Lebyazhi biotite, garnet–biotite and hornblende gneisses, and form a syncline some 150 km long and a few km wide on the limbs to 14 km in the core (Fig. 11). The formation consists of a productive member of kyanite and staurolite–kyanite schists, 25 to 400 m thick, overlain by muscovite quartzite and plagioclase–staurolite schist.

The lower part of the productive member is 10–120 m thick and contains kyanite schists proper (the productive horizon), which become poorer in kyanite upwards, and correspondingly richer in staurolite, muscovite and plagioclase. The thickness of

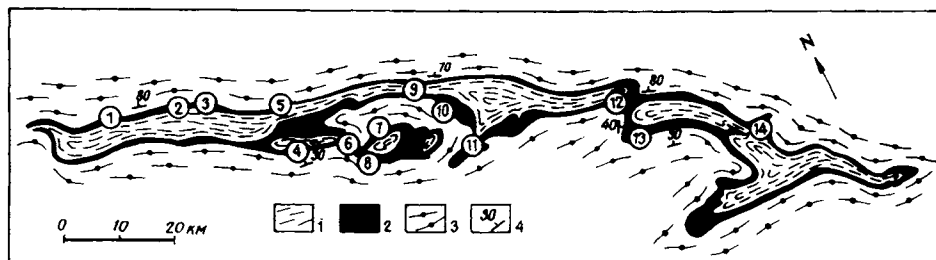


Fig. 11. Geological sketch map of the Keivy synclinorium and location of kyanite deposits (Gorbunov, 1981). 1) Keivy high-Al schists; 2) productive member, Keivy Fm; 3) Lebyazhi gneisses; 4) – orientation. Kyanite deposits (circled numbers): 1 – Vorgelurta, 2 – Tavorta, 3 – Tyapsh–Manyuk, 4 – Chervurta, 5 – Bezmyannaya, 6 – Bolshoy Rov, 7 – Kyrpurta, 8 – Yagelurta, 9 – Shuururta, 10 – East Shuururta, 11 – Malurdayv, 12 – Nussa-1, 13 – Nussa-3, 14 – Manyuk.

the productive horizon is determined by the content of kyanite and other minerals. At the present time, kyanite ores proper are considered to be those schists with >20% kyanite, <10% staurolite, <15% muscovite, and other minerals except quartz, <15% total. Percentage figures for the mineral content of the average ore is kyanite 35, quartz 40, muscovite 10, staurolite 5, plagioclase 5, rutile + ilmenite 1, iron sulphides 2, graphite and accessory minerals 2.

The total extent of the productive horizon at the present erosion level is approximately 420 km around the periphery of the syncline. Poor and non-productive ores (those with <30% kyanite) occupy 35% for the segment with average quality ores, and 10% for the length with >40% kyanite. At present there are 30 deposits in this last segment which are considered to be true kyanite deposits. The largest of these, which are suitable for open-cast mining, are Shuururta, Typash-Manyuk, Vorgelurta and Chervurta which are among the best studied deposits. The possibility that in future similar or more prospective parts of the productive horizon might be discovered as independent deposits cannot be discounted.

The kyanite ore quality is determined by the content of useful and waste components, as well as the kyanite morphology, on which depends the enrichment method used and the quality of the kyanite concentrate obtained. There are three main ore types, depending on the kyanite morphology: finely prismatic, paramorphic, and concretionary. The best ores are the coarsely concretionary types, which yield high quality concentrates on enrichment, with a 57%  $\text{Al}_2\text{O}_3$  content and a minimal impurity content. Ores with finely prismatic kyanite predominate, and the productive horizon on the southern limb of the Keivy synclinorium, which extends for 275 km, is composed of this type. Paramorphic ores predominate on the northern limb. Individual segments of the productive horizon consist of concretionary and concretionary-paramorphic ores, with a total length of 15 km. As an example, the Shuururta deposit is described below in some detail (Belkov, 1963; Gorbunov, 1981; Nosikov, 1960).

*The Shuururta deposit* (Fig. 12) is located in the centre of Keivy, north of Lake Semuzhye, on an upland plateau. It belongs to part of the southern limb of the northern linear synclinal structure in the Keivy belt. Rocks within the deposit dip in a monocline at 30–40° to the NE (020°–030°). At the base of the geological section are the Lebyazhi gneisses which underlie the Keivy schists. The lower member of the Keivy Fm is 10–12 m thick, containing garnet-staurolite and mica-garnet schists, rich in graphite and iron sulphides. Higher in the section they give way to a kyanite schist member, some 300 m thick. The productive horizon in this member attains a thickness of 120–130 m, its surface outcrop width being 200 m, with a length along strike of 6 km. The productive horizon is overlain by muscovite quartzites and kyanite-staurolite schists.

The overturned limb of the ore body (the productive horizon) contains paramorphic ores, 30 m thick. They are replaced upwards in the section by coarsely-concretionary ores with thin intercalations of concretionary-paramorphic, finely-concretionary and fibrous-sheaf varieties. The concretionary ores are 100–120 m thick. The productive horizon continues downdip for over 300 m without any major change in thickness or ore composition. Coarsely-concretionary ores make up

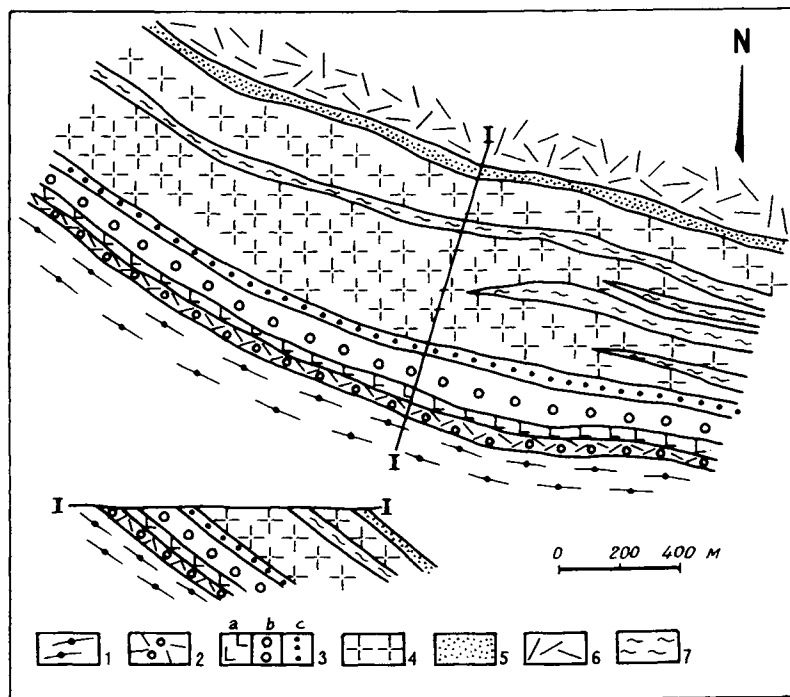


Fig. 12. Geological sketch map and section of the Shuururta deposit (based on Sevzapgeologiya materials). 1) garnet-biotite gneiss; 2) muscovite-garnet schist; 3) kyanite schist (ore layer): (a) paramorphic, (b) large concretions, (c) small concretions; 4) staurolite-kyanite fine concretions, radiating sheaves & porphyroblastic schists; 5) muscovite quartzite; 6) kyanite-staurolite porphyroblastic schist; 7) feldspar & garnet-feldspar amphibolites.

some 65% of the ore composition, and contain 43% kyanite on average; paramorphic ores amount to 30%, with 35% kyanite in them; and finely-concretionary ores form 5% of the ore total, with 38% kyanite content. The deposit occurs in conditions that favour open-cast working. Ore deposits in the Keivy belt belong to the metamorphic type. The formation of the kyanite ores is related to the metamorphism of primary highly aluminous sediments, rich in organic matter.

#### 1.4. Nickel, copper, cobalt

Copper-nickel sulphide ore deposits in the Kola terrain occur in three tectonic structures: the Pechenga-Varzuga rift belt, the Tersk-Allarechka greenstone belt, and the Korva-Kolvitsa granulite-gneiss zone. The first of these contains the Pechenga and Monchegorsk ore regions, the second has the Allarechka ore region, and the third contains the Lovnozero nickeliferous regions with economic deposits and numerous copper-nickel sulphide ore shows (Fig. 3). Ore deposits and occurrences are genetically related to four intrusive formations: gabbro-wehrlite (Pechenga type), peridotite-pyroxenite-norite (Monchegorsk type), olivinite-harzburgite (Allarechka

type), and websterite–gabbro–norite (Lovnozero type) (Rundqvist, 1986; Gorbunov and Papunen, 1989; Gorbunov, 1981).

The formation of nickeliferous intrusions and copper–nickel deposits is associated with the Karelian tectonomagmatic cycle and embraces the period 2.0–1.7 Ga (Nalivkin and Yakobson, 1985; Gorbunov and Papunen, 1985). Rundqvist and Mitrofanov (1992) refer the nickel-bearing intrusions in the Allarechka and Lovnozero regions to the Late Archaean.

The Pechenga–Varzuga rift belt, which formed in an Archaean basement, can be traced from NW to SE through the entire Kola terrain. It has a steep (50°–80°) SSW dip and extends for over 500 km, with a width of up to 70 km. The structure consists of picritic basalts and tholeiitic basalts, with minor amounts of tuffaceous and sedimentary units. Pechenga-type nickeliferous intrusions within this structural belt form rootless phacolithic bodies interlayered predominantly with the tuffaceous–sedimentary rocks. Monchegorsk-type intrusions are represented by major bodies – lopoliths which formed along the northern contact between the rift and the underlying Archaean gneisses in areas where deep faults intersect – the Monchegorsk, Pansky–Fyodorov tundra, Mt Generalskaya and Karikjavr intrusions. In addition to the deposits that form the two ore fields – Pechenga and Monchegorsk – this structural belt is also known to contain the small Karikjavr and Lastjavr deposits in Monchegorsk-type intrusions (Gorbunov and Papunen, 1985).

*The Pechenga ore field* (Gorbunov, 1968; Gorbunov and Papunen, 1985; Gorbunov, 1981; Polkanov, 1961) occurs in the asymmetrical Pechenga graben–syncline, which strikes NW in a broad arc (70 × 35 km). The syncline is filled with four formations of the Pechenga Complex, totalling 10 km thick. Each formation commences with a sedimentary unit and concludes with a volcanic unit. Some 80% of the succession is volcanogenic material – mostly diabase and diabase tuff with much smaller volumes of albitophyre, porphyrite and picrite. The fourth unit is the thickest (up to 2 km) – the ore-bearing tuffaceous–sedimentary unit, called the productive unit. It contains subcordant sheet-like and lenticular gabbro–diabase bodies and nickeliferous basic–ultrabasic rocks.

Over 200 basic–ultrabasic bodies have been found in the productive unit. These bodies vary widely in size, from a few m to several hundred m thick, and a strike length from 0.1 to 6 km, with up to 1 km down dip. A few small, steeply-dipping, fractured, sheet-like ultrabasic bodies occur in diabases underlying the productive horizon. Based on internal structure, the intrusions can be divided into differentiated, with serpentized peridotite and wehrlite at the base, to pyroxenite and gabbro; and undifferentiated, usually thin, and consisting of serpentinite or rare pyroxenite and gabbro. There are no age differences between the types.

Basic–ultrabasic intrusions are widely developed within the productive unit, including the Pechenga ore field (Fig. 13), located in the central part, and with which economic ore concentrations are associated. The copper–nickel deposits in the ore field are grouped into two ore complexes, a western and an eastern. The western complex contains the Kaula, Promezhutochnoye, Kotselvaara, Kammikivi and Semiletka deposits, controlled by a bifurcating intraformational tectonic zone at the top of the productive unit. The Sputnik, Verkhnyeye (Upper), Zhdanov,

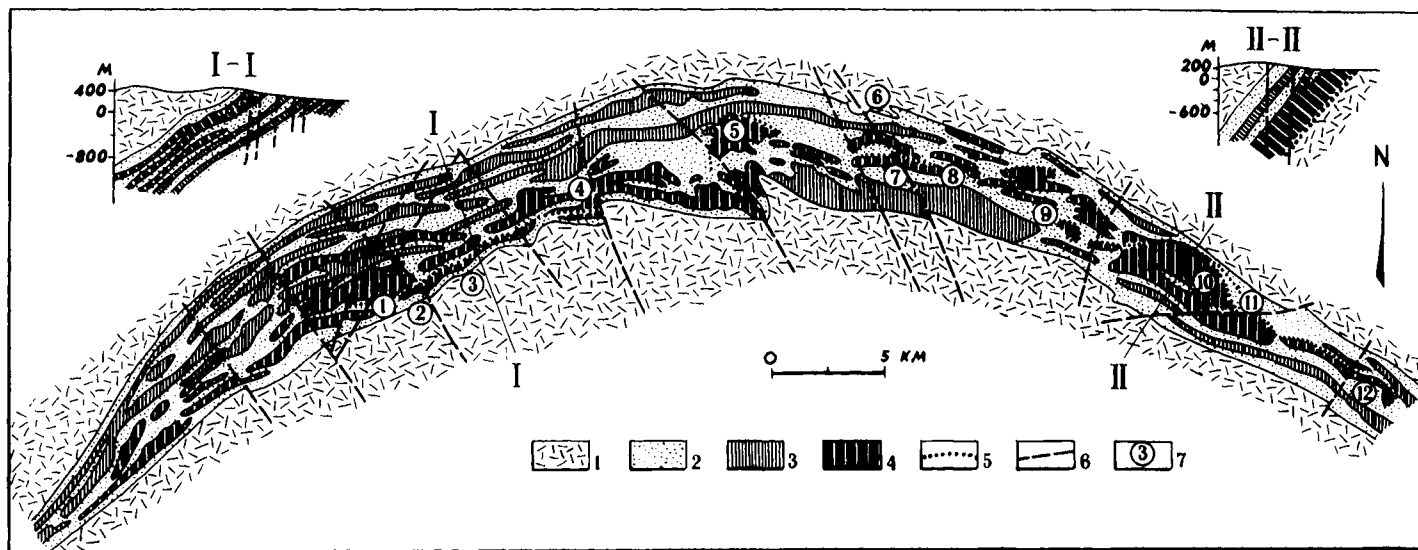


Fig. 13. Geological sketch map of the Pechenga ore field. 1) volcanogenic rocks (metadolerite), suites III & IV; 2) productive tuffaceous-sedimentary unit; 3) gabbro-dolerite intrusions; 4) gabbro-wehrlite intrusions; 5) Cu-Ni sulphide ores; 6) faults; 7) Cu-Ni deposits (circled numbers): 1 - Kaula, 2 - Promezhutochnoye, 3 - Kotselvaara-Kammikivi, 4 - Semiletka, 5 - Souker, 6 - North Souker, 7 - Raisoaiivi, 8 - Mirona, 9 - Sputnik, 10 - Zhdanov, 11 - Zapolyarnoye, 12 - Onki.

Zapolyarnoye and Onki deposits form the eastern complex, controlled by several intraformational tectonic zones, which cut different parts of the productive unit from basal to upper horizons. At various levels within the central part of the productive unit there are uneconomic deposits of intermediate to poor Cu–Ni ores, and small occurrences of rich ores, such as Mirona, North Soukerjoki, Souker and Rajsoaivi. Associated with the intrusives localized in the dolerites of the third flow are the Pahtajärvi and Kolosjoki occurrences. Minor copper–nickel ore shows have been found on the flanks of the productive unit, beyond the margins of the ore field.

All the known deposits are restricted to the lower peridotitic parts of the nickeliferous intrusions. Sulphide ore mineralization in almost all the deposits is not restricted to the parent rocks and is also distributed a little way into the host tuffs and sediments as thin veins and brecciated ores, small veinlets and disseminations. Most of the ores are either sheet-like or podiform. They are commonly more extensive downdip than along strike. Some researchers (Gorbunov, 1968) consider that the deposits in the western ore complex are more deeply eroded than those of the eastern complex, and consist of the lower ore-enriched parts.

The majority of the ore bodies within the deposits of the ore field have an asymmetric banded structure. At the base, within the peridotitic part, are disseminated ores, in which the sulphide content gradually increases towards the footwall. Sulphide dissemination intensifies at the base of intrusions in synclinal fold closures and there is a simultaneous increase in the thickness of the disseminated ore deposits. Massive and brecciated sulphide ores lie at the base of downfaulted intrusions, mostly along the serpentinite–host rock contact, but occasionally spreading beyond the margins of the intrusive bodies for up to 400 m along strike and to 200 m down dip. Rich ores form at complex intersections between intralayer ore-controlling tectonic zones and cross-faults. Post-ore faults are rare. Where present, they displace the ore deposits by a few metres and the ores adjacent to the faults are comminuted, flattened and recrystallized.

Copper–nickel ores can be divided into four types, based on textural and compositional features: 1) disseminated in serpentinites, 2) brecciated, 3) massive, 4) vein disseminations in schists. Disseminated ores in serpentinites predominate in all deposits, and they include the main metal reserves. They are subdivided into nickel-poor and nickel-rich (those with  $> 1\%$  Ni).

The main ore minerals in all the deposits are pyrrhotite, pentlandite and chalcopyrite. Magnetite is the main mineral in impregnated serpentinites, while pyrite plays this role in some parts of the brecciated and massive ores. Secondary ore minerals are violarite, bornite, sphalerite, cubanite, mackinawite and valleriite. There are rare occurrences of chloanthite, nickeline, cobaltine, millerite, galena and various platinumoids. In weakly-altered periodotites, the sulphides display typical "sideronitic" texture – in rich ores, intergrowths between sulphides and secondary silicates are widely developed, forming ore–silicate pseudomorphs after olivine, or rarely pyroxene.

In brecciated ores, fragments of serpentinite, altered to talc, and sometimes tuffaceous–sedimentary rocks, are cemented by sulphides. The rock fragments are lenticular in shape and up to 20 cm in size. In massive ores consisting predominantly of pyrrhotite, pentlandite frequently occurs as porphyritic grains up to 1 cm across.

Intense pyritization of massive and brecciated ores is found along post-ore fault zones. Vein-type disseminated ores in schists consist of finely disseminated, lenticular and veinlet sulphide mineralization, usually oriented along the schistosity. The sulphide content in these ores is up to 70%. The main ore-forming components in the deposits of the Pechenga ore field are iron, nickel, copper, cobalt and sulphur. In addition there are minor amounts of selenium, tellurium, platinoids and gold, forming an assemblage that has economic value. The nickel and copper content in the ores ranges from fractions of 1% to 10–15%. Massive ores contain most nickel, while copper is mostly present in ore-impregnated schists. High cobalt contents, up to 0.25%, are seen in massive ores. The nickel : copper : cobalt ratio is not constant in the ores, and has the following average values: massive ores – 48 : 19 : 1; brecciated ores – 56 : 22 : 1; disseminated ores in serpentinites – 55 : 24 : 1; vein-type disseminations in schists – 47 : 47 : 1; the average ratio for the entire ore field is 40 : 20 : 1. The precious metal content in the ores on the whole increases with increasing content of the main metals.

Most of the previously-mentioned researchers hold the view that the Pechenga deposits formed in three successive phases: magmatic, pneumatolytic–hydrothermal, and hydrothermal, within each of which a number of separate mineralization episodes can be distinguished, but partly-rich ores have a metamorphic genesis (Turchenko, 1987). The magmatic phase involved the formation of intrusions, with early magmatic liquation of sulphides, differentiation and crystallization of magma and subsequent crystallization of liquated sulphides in the ultrabasic wall rocks as sideronitic clusters, schlieren and injection veins. A characteristic feature of the pneumatolytic–hydrothermal phase is autometamorphism – wholesale serpentinization of ore-bearing ultrabasic rocks, accompanied by ore–fluid metasomatism. Further alteration occurred in the ore-enriched rocks during the hydrothermal phase – amphibolization, chloritization, talc and carbonate formation, and local redistribution of sulphides resulting from dynamometamorphism, faulting and hydrothermal metamorphic alteration. This phase concluded with the formation of post-ore calcite and talc–calcite veins which cross-cut the ore bodies.

*The Kaula deposit*, which is now essentially worked out, is the best-studied deposit in the ore field. It occurs in a small serpentinite intrusion, with a lenticular–sheet form and dimensions 400 m along strike × 600 m downdip × 160 m maximum thickness. The intrusion has an E–W strike and dips at 40–50° to the south, conformably with the phyllitic country rocks. It plunges to the SW and wedges out at depth. The anastomosing Main tectonic zone can be traced on its footwall. This is an ore-controlling structure for the Kaula deposit and for the entire western branch of the Pechenga ore field (Fig. 14). Dipping southwards at 35–40°, the zone cuts the tuffaceous sedimentary unit and the basal part of the serpentinite mass at a sharp angle. Throughout the mass and for some distance beyond, the zone is filled with brecciated and massive ores and is surrounded by an “aureole” of rich disseminated ores which grade into normal and poor varieties on the hanging wall. A N–S-striking cross-cutting fault on the western flank also plays an important role in the structure of the deposit, being infilled with predominantly massive ores along that portion which cuts the serpentinites.

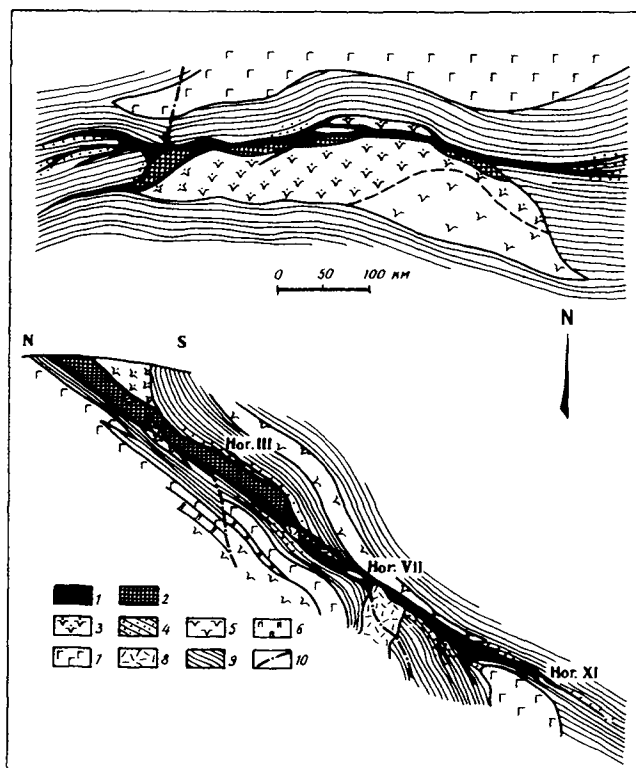


Fig. 14. Geological sketch plan of horizon 312 (a) and geological section (b) of the Kaula deposit (Gorbunov, 1968). 1) massive and brecciated sulphide ores; 2) rich disseminated ores in serpentinite; 3) normal disseminated ores in serpentinite; 4) ore-bearing phyllite; 5) serpentinite; 6) pyroxenite; 7) gabbro; 8) dolerite; 9) phyllite; 10) faults.

The Kaula deposit consists of two ore bodies, the Main ore body and the Satellite Body. The Main ore body is an irregular sheet which broadly mirrors the shape of the serpentinite intrusion and extends below the base of the intrusion into the sedimentary rocks. The ore body is more extensive by a factor of 1.6 downdip compared to its strike length and, like the intrusion, it dips to the SW. Upper horizons vary in thickness from 30 to 70 m and there is a gradual thinning towards the flanks. Disseminated ores predominate, accounting for 84% of the total volume of the ore body, 58% including impregnated serpentinites, and 26% in ore-bearing phyllites. The proportion of brecciated and massive ores in the deposit increases with depth as the serpentinites with disseminated ore mineralization wedge out. As the tectonic zone extends beyond the confines of the ore-bearing mass, these ores decrease in thickness, as do the associated impregnated sedimentary wall rocks. Nickel and copper contents also decrease, while there is a change in the ores to pure pyrrhotite types, which can be traced for large distances beyond the margins of the ore body. Accompanying the ore body, mainly on the footwall side, are ore apophyses up to

100 m long. These apophyses formed as a result of the Main ore-bearing tectonic zone breaking into numerous branches. The Satellite ore body is the largest of the steeply-dipping apophyses that branch off from the Main ore body on its footwall side. It extends along strike for more than 200 m.

*Ore deposits in the Monchegorsk pluton* (Polkanov, 1956; Gorbunov and Papunen, 1985; Gorbunov, 1981). The Monchegorsk nickeliferous pluton is a Lower Proterozoic intrusion belonging to the periodotite–pyroxenite–norite formation. It occurs on the NW shores of Lake Imandra, within the Proterozoic Imandra Group of volcanosedimentary rocks and the underlying Archaean Kola Gneisses. The intrusion has a total area of 50 km<sup>2</sup>, and is up to 600 m thick. In plan view, it is horse-shoe shaped, with the NE branch forming the intrusion in the Nittis–Kumuzhye–Travyanaya hills (NKT), and the WNW branch forming the intrusion in the Sopcha, Nyud and Poaz hills. The bottom of the intrusion is shaped like a symmetrical trough (Fig. 15). The western and central parts of the intrusion (NKT and Sopcha) have peridotite at the base and pyroxenite at the top, with a thick zone of inter-layered peridotite, olivine pyroxenite and pyroxenite between them. The eastern part consists predominantly of norites which become less melanocratic eastwards. At the contact zone between the intrusion and the underlying rocks, there is a thin (up to 10 m) layer of norite and gabbro–norite.

Genetically related to the pluton are several copper–nickel sulphide ore deposits and occurrences, which fall into three genetic types:

- (1) Layered deposits of syngenetic, sparse disseminated ores; the basal deposit of the intrusion and several other deposits associated with the overlying periodotite (“layer 330”) and norite (Nyud–II, Terrasa) layers of the intrusion belong to this type;
- (2) The Nittis–Kumuzhye–Travyanaya (NKT) and Sopcha vein deposits;
- (3) The Moroshkovoye vein-type disseminations at the southern contact of the intrusion.

The basal deposit of disseminated and cluster–disseminated ores has been studied in detail in the NKT intrusion, where it is restricted to a transition zone between peridotite and marginal gabbro–norite. In cross-section, the deposit is sickle-shaped, conformable with the shape of the intrusion. It increases in thickness towards the axis of the intrusion, reaching 20–30 m at the 0.2% nickel cut-off grade. The ore mineralization is separated from the intrusion contact by a 5–10 m thick barren quartz gabbro–norite horizon. Sulphides in the rocks are distributed as a uniform fine dissemination, but there are also instances of ore clusters in various dimensions. The main sulphides are pyrrhotite, pentlandite and chalcopyrite, their average ratio being 3 : 1 : 1, and secondary pyrite, magnetite, chromite and ilmenite. The nickel : copper ratio in the ore is 2–1.5 : 1. Copper-rich ore varieties also display higher PGE contents.

The ore horizon in the *Sopcha intrusion*, or “layer 330”, belongs to a peridotite and olivine pyroxenite layer within pyroxenites and is exposed at the surface in the upper part of the intrusion at the 330 m benchmark. The ore horizon is 1–5 m thick and contains approximately 1.5 times as much sulphides and metals as the basal deposit.

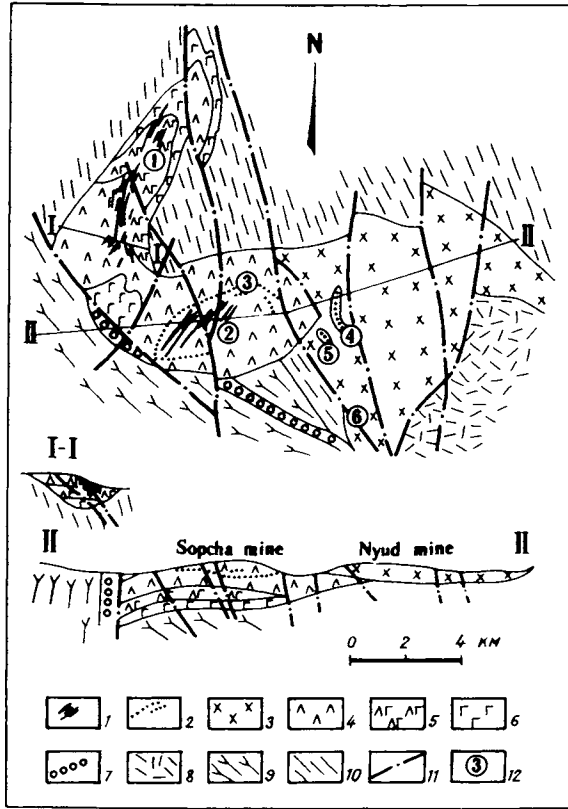


Fig. 15. Geological sketch map of the Monchegorsk pluton (based on Sevzapgeologiya materials). 1) Cu-Ni sulphide veins; 2) disseminated Cu-Ni ores; 3) norite; 4) pyroxenite; 5) pyroxenite-peridotite transition zone; 6) peridotite; 7) basic-ultrabasic transition zone; 8) Imandra-Varzuga metadolerites; 9) metagabbro & gabbro-norite on Main Moncha Ridge; 10) Kola gneisses, diorites, granodiorites; 11) faults; 12) Cu-Ni deposits and occurrences (circled numbers): 1 - NKT, 2 - Sopcha, 3 - "layer 330", 4 - Terrasa, 5 - Nyud-II, 6 - Lake Moroshkovo.

The Nyud-II cluster-disseminated ore deposit is minor in dimensions and ore reserves, which are now exhausted. It occurs in the upper part of the Nyud-Poaz intrusion, in the so-called "critical horizon", in the transition zone between olivine norite and normal norite. Ore types identified in the intrusion are disseminated, vein-disseminated and clusters, with disseminated types predominating. The association between certain areas of sulphide clusters and small veins and a system of tectonic fractures indicates the significant role of tectonics in the formation of the deposit.

Ore-bearing veins in the Nittis-Kumuzhye-Travyanaya (NKT) deposit are represented by over 50 veins containing massive sulphide ores. The veins are restricted to elongate fractures in the axial part of the intrusion, and form a NNE-trending vein field extending along strike for over 3.5 km with a width of up to 200 m (Fig. 15).

Two pre-ore faults cut the deposit into three segments. In the middle segment the veins have a N-S strike, while in the northern and southern segments they strike NNE (5–20°). The veins dip steeply, at 85–90°, in most cases towards the axis of the trough-shaped downwarp that forms the floor of the intrusion. Strike-length is 100–1400 m, down-dip extension is up to 450 m, and vein width is up to 30 cm or 2–3 m in boudin swellings. The middle segment typically has the thickest and most constant veins. A regular decrease in vein thickness down dip has been established, and they wedge out completely in the 500–600 m interval above the base of the intrusion. None of the veins extends as far as the basal deposit of disseminated ores. Individual veins and the entire vein field have a SW dip and the veins in the southern segment do not crop out at the surface – these are referred to as “blind” veins.

The ore veins are slab-shaped, but where cut by dense fracture swarms or diabase dykes they have a complex shape with step-like changes in thickness, swellings and branchings as they cross from one fracture to another. Contacts between veins and wallrocks are sharp. Hydrothermal alteration of wallrocks is insignificant and is represented by the formation of thin (up to 1–2 cm) anthophyllite and talc-breunerite zones. The ore veins are genetically related to gabbro-pegmatite veins into which they gradually merge at the margins over a 1–3 m interval. Individual veins with an essentially chalcopyrite composition are encountered 100–150 m below the vein field, restricted to a feldspar peridotite horizon and filling NE-striking steeply dipping fractures. The veins typically have a high PGE content. The main ore minerals in the veins are pyrrhotite, pentlandite, chalcopyrite and magnetite; secondary minerals are ilmenite, cubanite, mackinawite and millerite.

The *Allarechka nickeliferous region* (Bogachev et al., 1968 Gorbunov and Papanen, 1985; Gorbunov, 1981) occurs at the margins of the Kaskama–Allarechka structure (Rundqvist and Mitrofanov, 1992), which extends for 150 km to the SE from the Russian border to the Litsa granite intrusion, cutting a greenstone belt. It has a boundary in the north with the Pechenga structure, and in the south with the Lotta granulite–gneiss block; these boundaries are marked by deep faults (Fig. 16). Tectonically, the region is divided into two blocks: the eastern Allarechka block and the western Hihnajärvi block with several granite–gneiss dome structures in the Archaean basement. The domes are surrounded by an Upper Archaean supracrustal assemblage, forming synclinal and monoclinical structures. The lower horizons of this assemblage are represented by various gneisses, primarily biotitic, which give way upwards to biotite–amphibole gneiss and amphibolite, compositionally equivalent to picrite, tholeiite, andesite–basalt and andesite (Rundqvist and Mitrofanov, 1992). This supracrustal assemblage contains thin ferruginous quartzite–pyrrhotite mineralization, the Skalistoye graphite deposit being associated with one such zone.

The dome structures have marginal faults striking NE and NW which control the emplacement of numerous (over 200) meta-ultrabasic sheets and lenses with a harzburgite–olivinite composition. These bodies are mainly associated with feldspar amphibolites, being rare in the basement granite–gneisses. They are up to 1.5–2 km long and up to 200 m thick; as a rule, the ultrabasic bodies have been deformed simultaneously with the country rocks and are boudinaged. Most investigators refer

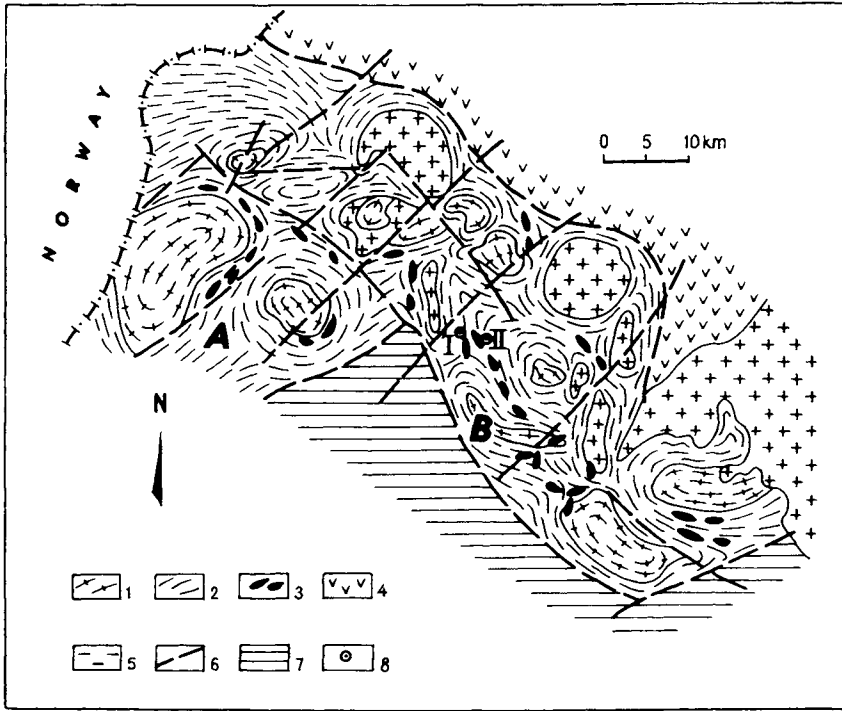


Fig. 16. Geological sketch map of the Allarechka nickel region. 1) granite-gneiss; 2) migmatized gneiss, schist, amphibolite; 3) ultrabasic bodies; 4) Pechenga structure; 5) granite & granodiorite; 6) faults; 7) Lotta granulite-gneiss block; 8) Cu-Ni deposits: I - Allarechka, II - Vostok; tectonic blocks: A - Allarechka, B - Hihnajärvi.

these bodies to Lower Proterozoic intrusive formations, but some (e.g. Rundqvist and Mitrofanov, 1992) associate them with an Upper Archaean komatiitic volcano-plutonic complex, typical of Archaean greenstone belts. Economic copper-nickel sulphide ore deposits are associated with individual intrusions – the Allarechka and Vostok (“East”), situated on the SW flank of a dome structure of the same name (Fig. 16), also the Runnijoki, Akkim and Annama occurrences.

The Allarechka deposit is related to an intralayer body of altered ultrabasic rocks, represented mainly by serpentized and amphibolitized harzburgites. The intrusion occurs in a unit of migmatized amphibolites, biotite and biotite-hornblende gneisses and is elongated in a N-S direction, conformable to the overall strike. The dimensions of the ultrabasic body are  $1.5 \times 0.3$  km, and it is up to 50 m thick. Rocks dip moderately ( $25\text{--}30^\circ$ ) to the west. Gently-plunging parallel and cross-folds are frequent and were responsible for the gross curvature of the intrusion. The western limb of the ultrabasic body is overturned along a steep near N-S fault, giving the intrusion a trough shape (Fig. 17). Throughout its length it is boudinaged and broken into blocks varying in size from 5–10 m to 100–200 m and showing very little relative displacement.

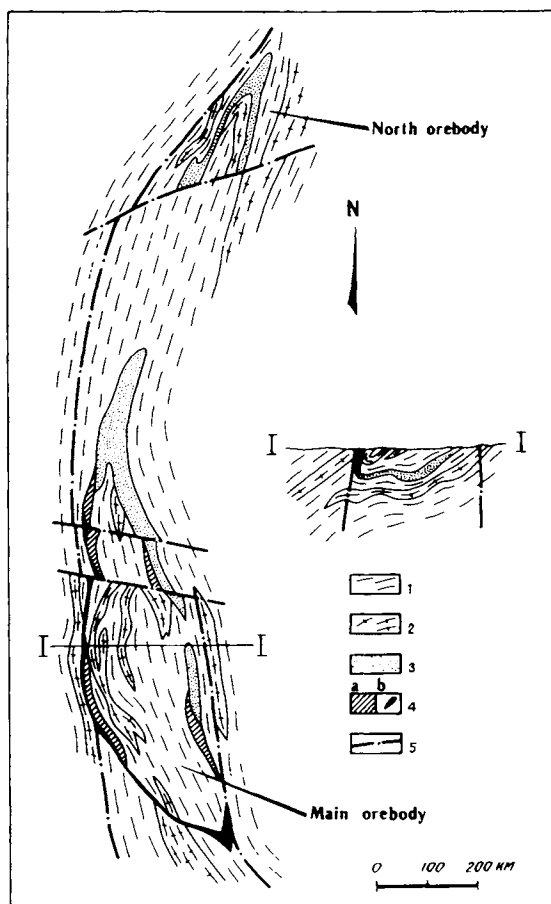


Fig. 17. Geological sketch map of the Allarechka deposit and section I—I.1) amphibolites, migmatites, gneisses; 2) granite-gneiss; 3) meta-harzburgite & meta-olivinite; 4) Cu-Ni sulphide ores: (a) disseminated, (b) massive; 5) faults.

The main structural element in the deposit is a N-S fault, along which massive and rich disseminated sulphide ores formed in the peridotites. Vein apophyses of massive sulphide ores extend beyond the margins of the ultrabasic rocks into the gneiss complex for up to 150 m, exploiting fractures with a variety of orientations. Towards the E and NE flanks of the deposit, the ore mineralization rapidly diminishes and the ores give way to sparsely disseminated sulphides in the ultrabasic rocks. The ore-bearing intrusion is cut by a NE-trending post-ore regional fault at the point where it is deformed by a cross-flexure, which divides the deposit into two ore bodies, the Main and Northern bodies. Most of the ore and metal reserves are concentrated in the Main ore body, which was completely exhausted in the early 1970s.

The Main ore body has an overall trough shape, in conformity with the shape of the intrusion. In the central part its maximum depth is 80 m. The body gradually

rises in the north and south, eventually appearing at the present surface level. Its strike length is a little over 1 km, its downdip extension is up to 200 m, and its thickness is up to 20 m. The ore composition is chalcopyrite–pentlandite–pyrrhotite, secondary ore minerals being magnetite, pyrite, bornite, violarite and mackinawite. Pyritization and violaritization are widespread in the ores. Nickel averages around 4%, but can be up to 15–17% in some parts of the massive ores. For the deposit as a whole, the nickel : copper : cobalt ratio is 40 : 20 : 1 on average and overall is similar to that in deposits belonging to the Pechenga ore field.

In terms of its morphology and ore mineralization characteristics, the Northern ore body resembles the northern flank of the Main body. It consists predominantly of low-grade disseminated ores. Most workers consider this to be a magmatic ore deposit – liquation type with subsequent superimposed autometamorphic and allo-metamorphic processes. The deposit is now exhausted, and mining ceased in 1992.

The *Lovnozero nickeliferous region* (Gorbunov, 1981; Yakovlev et al., 1979). The Korva–Kolvitsa granulite–gneiss zone contains fairly widespread nickeliferous websterite–gabbro–norite intrusions, occasionally ultrabasic bodies. In the Lapland block, this zone contains the Lovnozero nickeliferous region, while small solitary ore occurrences are found in the Kandalaksha–Kolvitsa block, including Poryeguba and others.

Around 300 norite and gabbro–norite intrusive bodies, plus rarer ultrabasic rocks, have been mapped in the Lovnozero nickeliferous region. Associated with some of these are the Lankku, Yunges, Sueynlagash, Luonjoki, Elgorash and other occurrences, and the small Lovnozero deposit. The region is in a granulite complex which consists mainly of hypersthene and pyroxene-bearing plagiogneisses (gneissose diorites), felsic granulite and minor garnet–biotite gneiss, hornblende–diopside gneiss and amphibolite, forming a synformal structure with a pronounced E–W strike and northerly dips that vary from 30° to 80°.

The Lovnozero deposit occurs in the Lotta valley, on the shores of Lake Lovnozero. It is represented by several ribbon-shaped nickeliferous intrusions, mostly noritic in composition. Gabbro–norite and rare plagioclase pyroxenite are present in some individual bodies in addition to norite. Country rocks are mostly hypersthene diorite and subordinate felsic granulite. Boundaries between the intrusions and the country rocks are both gradual and sharp, with essentially no wall-rock alteration.

The Main ore body, or No. 1 body, forms the base of the deposit, and includes the bulk of the ores. The ore body is restricted to a weakly gneissified massif of fine- to medium-grained norite and in part gabbro–norite. The intrusion has an elongate lenticular shape, conformable with the host gneissose diorite and felsic granulite, NE strike and NW dip at angles of 40–70°; it plunges towards the NE at 20–25°, parallel to the orientation of a mineral lineation. Dimensions of the intrusion are around 200 m along strike, up to 400 m down dip, outcrop width is more than 1 km, and thickness is up to 80 m (Fig. 18). Both the intrusion and the country rocks are broken into blocks that are displaced from one another along a system of NW-striking faults. The faults are identified on the basis of cataclastic and mylonite zones up to a few tens of metres thick. Displacements along these faults reach a few hundred metres.

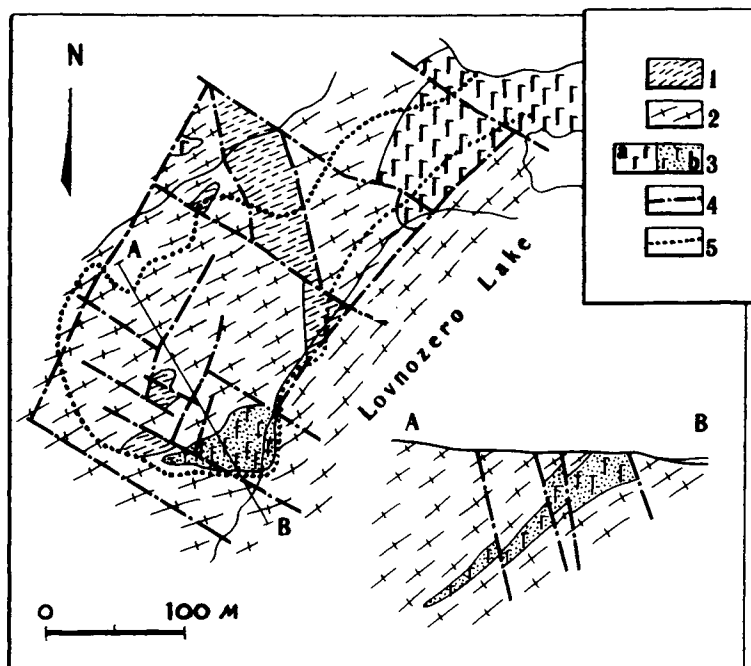


Fig. 18. Geological sketch map and section of the Lovnozero deposit (based on Sevzapgeologiya materials). 1) felsic granulite; 2) gneissose diorite (basic granulite); 3) norites: (a) barren, (b) ore-bearing; 4) faults; 5) contours of ore deposit; 6) exploration boreholes.

The Main ore body completely mimics the outlines of the intrusion, in places adhering to its upper horizons. Disseminated and cluster-disseminated ores predominate in the body, with a gradual increase in useful constituents downdip. Rich disseminated ores usually adhere to melanocratic norite varieties. There are small veins and veinlets of massive and brecciated sulphide ores, restricted to areas where plagioclase pegmatite veins are developed in norites. The veins are up to 1.5 m thick, with some individual veins being traceable into the country rocks for up to 50 m beyond the margins of the norites. The main ore minerals are pyrrhotite, pyrite, pentlandite and chalcopyrite; secondary: titanomagnetite, ilmenite, rutile, magnetite and violarite. The ores in this deposit are poorer than those in the Pechenga and Allarechka deposits, with an average cobalt : copper : nickel ratio for the whole ore body of 1 : 13 : 26 (0.034% : 0.43% : 0.88%). In addition to the Main ore body, the deposit also has several smaller ore bodies with negligible reserves of nickel and copper.

### 1.5. Lead and zinc

Polymetallic ore vein fields are located along the coast of the Kola Peninsula. On a regional scale they are associated with extension fractures of major faults that separate the Kola province from the Riphean (Late Proterozoic) geosynclinal zones

(Varanger–Rybachiy zone). Argentiferous polymetallic veins were first discovered in 1732 on Medvezhye (Bear) Island in Kandalaksha Bay in the White Sea. These are now completely exhausted. Veins with a similar composition but with a low silver content were subsequently discovered on the Pechenga coast of the Barents Sea and at the mouth of the river Ponoy. The Pechenga veins have also been worked out. Studies on the isotopic composition of lead in veins from the Pechenga coast have shown its age to be 630–1020 Ma (Bilibina, 1980; Gorbunov, 1981), corresponding to the Late Proterozoic tectonomagmatic activity that affected the Baltic Shield. No relationship has been established between intrusive complexes and the veins. The polymetallic veins include sphalerite–galena, chalcopyrite–sphalerite–galena and galena mineralogical types. A description of the polymetallic veins on the Pechenga coast will serve as a case study.

The *polymetallic veins on the Pechenga coast* form the largest such concentration on the Kola Peninsula (Gorbunov, 1981; Fedotova, 1978; Fedotova et al., 1971). The vein field occurs to the west of the Pechenga inlet, between Bazarnaya Bay and Dolgaya Bay in Kola Gneisses, the dominant varieties being biotite, garnet–biotite and hornblende–biotite, which are often interleaved (Fig. 19). The gneisses contain small amphibolite lenses and associated magnetite quartzites. The gneisses are strongly folded and intensely migmatized by granites and cross-cutting granite pegmatite veins. The rocks have a NW strike and dip steeply (at 60–90°) NE. Numerous altered diabase, gabbro–diabase and porphyritic diabase dykes cut the gneisses; they are up to 1.5 km long and up to 100 m wide. Most have a NE strike and a steep-to-vertical dip to the SE.

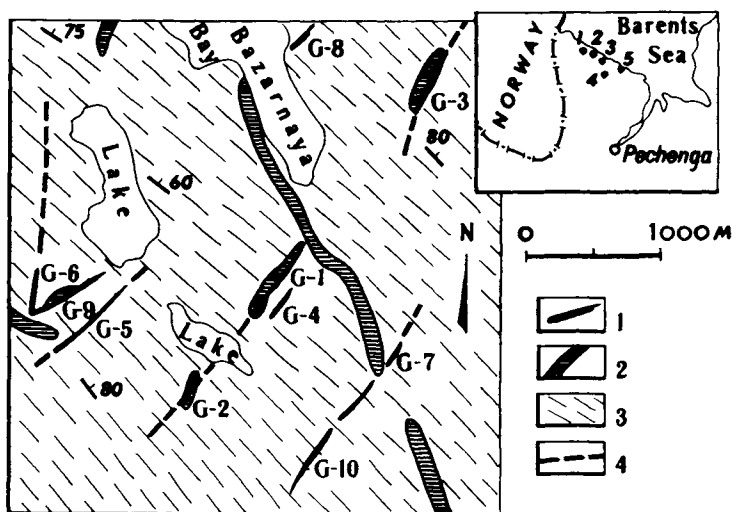


Fig. 19. Geological sketch map of the Bazarnaya Bay occurrence (based on Sevzapgeologiya materials). 1) quartz & quartz–barite veins with Pb–Zn mineralization and number; 2) dolerite dykes; 3) biotite & garnet–biotite gneisses; 4) faults. *Inset*: location of polymetallic occurrences in the Bazarnaya Bay zone: 1 – Bazarnaya Bay, 2 – Raisa, 3 – Dolgaya Bay, 4 – Sofia, 5 – Samuil.

The polymetallic veins are associated with two directions of shear zones and mylonite zones – NE to SW and E to W. Most of the veins are steeply-dipping slab-like, with a NE strike and lie wholly within the gneisses or along dolerite dyke margins, frequently cutting the dykes. The E–W veins are localized in mylonite zones, concordant with the strike of the gneisses. They have a more complex shape and structure, and are characterized by frequent anastomosing, brecciated zones and polyphase mineralization. The veins are up to 0.7 m thick, or 2.5 m in boudins, up to 1 km strike length, or in rare instances 1.5 km. The longest vein in the ore field is the “Victoria-1” vein, at 2450 m. As a general rule the veins are disrupted, with the intervening gaps being up to tens or hundreds of metres wide. Wall rocks adjacent to the vein contacts have been hydrothermally altered, mainly by silicification and chloritization. Altered rocks also contain sparsely disseminated sulphides and higher lead, zinc and silver contents.

Lead–zinc mineralization in the veins is highly irregular and occurs mainly as veinlets and clusters. Ore structures are massive, banded, brecciated, veined, clustered and disseminated, and the texture is granular or cataclastic. Principal ore minerals are galena and sphalerite; pyrite, chalcopyrite and marcasite are secondary, while gersdorffite, ulmanite, millerite, bornite and native silver are rare. Hypergene minerals are known to include chalcocite, covellite, malachite, azurite, smithsonite, calamine, cerussite, brochantite, erythrene, anabergite, psilomelane and iron hydroxides. Gangue minerals are quartz, barite and calcite, with dolomite and microcline also recorded, with quartz predominating, frequently making up to 60–90% of the vein mass.

The complete mineralization process includes six phases: sphalerite, quartz–galena, quartz–chalcopyrite, carbonate, barite and pyrite–quartz (Fedotova et al., 1971). Vertical mineralogical and geochemical zonation have been identified, expressed as zinc replacing lead with depth, and decreasing concentrations of silver, gallium and germanium in the major ore minerals, and a change in the gangue mineral ratio; barite is dominant in the upper parts of the veins, which is replaced first by calcite then quartz with depth. An oxidation zone is only weakly developed in the veins. These polymetallic veins in all probability had a hydrothermal origin.

### 1.6. Molybdenum

There are two uneconomic molybdenum deposits known in the Kola terrain – the Jaurijoki, associated with granites in the Uraguba zone of tectono-magmatic activity, and the Pellapahk deposit in the Kolmozero–Voronya greenstone belt.

The *Jaurijoki deposit* is situated in the SW part of the Uraguba fault zone, which extends from the Barents Sea SW into Finland. Within Russia it is about 200 km long and up to 40 km wide. The clearly delineated zone can be easily traced on the basis of mesabyssal, hypabyssal and sub-volcanic polyphase granitoid intrusions along the margins. These granites show different erosion levels and belong to the late Karelian granite–granodiorite suite of a granite–latite series, dated at  $1840 \pm 50$  Ma (Vinogradov et al., 1987). The Uraguba zone has 12 major granitic intrusions totalling 1100 km<sup>2</sup> in area. All the intrusions within the Kola terrain are characterized

by molybdenite mineralization. The deposit is genetically and spatially associated with two closely adjacent subvolcanic granitic intrusions, the Yuvoaivi and the Uchabyuoaiivi, which cut Upper Archaean garnet-quartz-feldspar granulites (Fig. 20).

The Yuvoaivi intrusion is oval-shaped in plan, with dimensions  $6 \times 8$  km and an area of some  $42 \text{ km}^2$ . Six different age phases of granite formation were responsible for the pluton (Vinogradov et al., 1987; Dubrovsky, 1963). Most of the pluton consists of third-phase uneven-grained, leucocratic microcline-plagioclase granite. A NNW-striking ( $345^\circ$ ) greisen zone passes through the western part of the intrusion; it is up to 1.5 km wide, with *en échelon* bunches of quartz veins with the same strike. Adjacent veins in these bunches vary from two to 23 in number. Vein length is from 5 to 400 m, and thickness from 0.3 to 1.2 m. Quartz-rich vein cores contain fluorite nests and muscovite patches. Greisens from vein selvages have variable compositions of quartz, muscovite and fluorite. Molybdenite occurs in isolated segments.

The apex of the Uchabyu intrusion crops out 3 km east of the Yuvoaivi intrusion. It is almost oval in plan view, with dimensions  $0.8 \times 0.5$  km ( $0.5 \text{ km}^2$ ). Much of its exposed surface consists of medium-grained fluorite-muscovite-quartz greisens, within which are preserved blocks of weakly reworked two-mica and muscovite-quartz porphyries, in which the fine-grained groundmass contains up to 20% quartz phenocrysts and solitary oligoclase phenocrysts (Vinogradov et al. 1987). From geophysical data, a granitic crest can be traced at a depth of around 600 m beneath this sub-volcanic structure, joining the two granite intrusions. In the outer contact zone of the intrusion there is a breccia of intensely biotitized and sericitized country rocks with garnet granulite relicts, termed "metagranulites". The breccia belt is asymmetric to the stock: in the N and E it is up to 0.5 km wide, 0.2 km in the S, and only a few metres in the W. Cementing the breccia are rock types varying from aphanitic felsite porphyry to fine-grained porphyritic microgranite and fine-grained

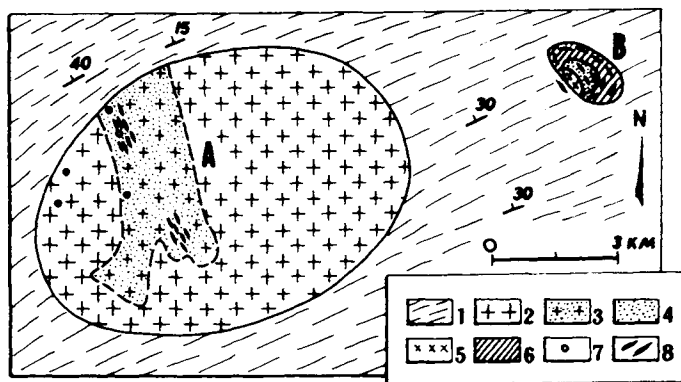


Fig. 20. Geological sketch map of the Jaurijoki deposit (based on Sevzapgeologiya materials, with additions). 1) granulite; 2) granite; 3) greisenized granite; 4) greisens; 5) quartz porphyry; 6) eruptive breccia (from granulites); 7) Mo occurrences; 8) quartz veins with molybdenite. A -- Yuvoaivi intrusion. B -- Uchabyuoaiivi intrusion.

granite. A fluorite–quartz stockwork occurs in the centre of the greisens, approximately 25 m in diameter, and with a network of anastomosing feldspar–quartz and muscovite–quartz veins (Fig. 21).

The bulk of the molybdenum ores in the deposit are related to the Uchabyuoaiivi intrusion. Molybdenite forms sporadic disseminations in greisens and brecciated granulites. Most of the molybdenite is concentrated in an arcuate zone of quartz veins, 1200 m long, which extends into the metagranulite breccia. Quartz veins in this zone are represented by several morphological types: steeply-dipping *en échelon* types, stock-like and cavity infillings containing molybdenite, and steeply-dipping planar sheets which are usually barren. Ore veins are 10–700 m long and up to 1 m thick, or 3 m in boudins. Places where quartz veins are pinched or wedge out are enriched in molybdenite. Ore mineralization increases with depth. In addition to molybdenite, the quartz veins also contain fluorite, muscovite, calcite, biotite, pyrite, magnetite and hematite. Scheelite and wolframite are found occasionally. The ores contain gallium, zirconium and rhenium in small quantities.

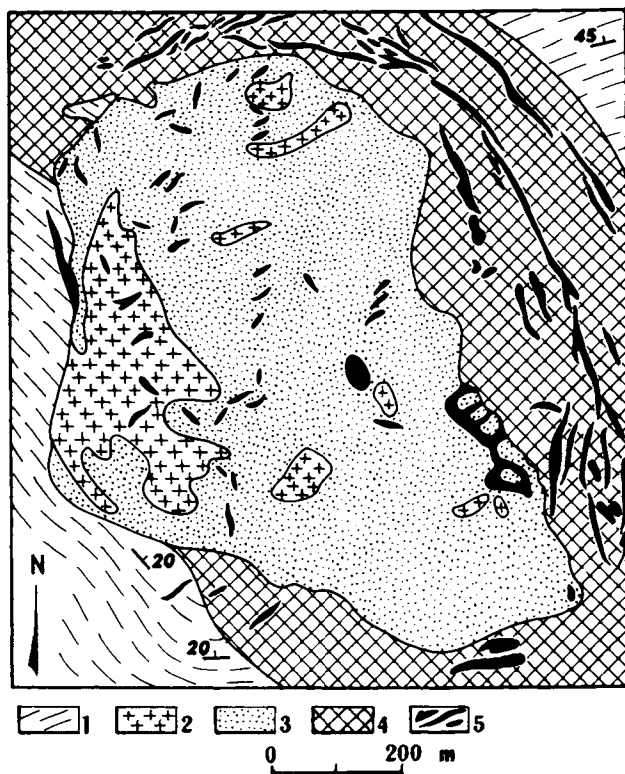


Fig. 21. Geological sketch map of the Uchabyuoaiivi pluton (based on Sevzapegeologiya materials, with amendments). 1) metagranulite; 2) quartz porphyry; 3) greisen; 4) eruptive breccia (from granulites); 5) fluorite–quartz veins with molybdenite.

Based on the major component the ore complex can be classified as a vein-stockwork type of porphyry–molybdenum formation, with signs of a transition to a tungsten–molybdenum greisen formation. The intensity of ore-concentrating processes in the granite intrusion was less pronounced than in the subvolcanic facies.

The *Pellapahk deposit* (description based on materials from the “Sevzapgeologiya” [“North-west Geology”] production company) is situated in the NW of the Kolmozero–Voronya greenstone belt in the highlands of the same name. It is associated with a metasomatic zone which formed along the contact between a quartz porphyry sheet and the Chervurta high-alumina plagioclase schists (AR<sub>1</sub> age). The metasomatic zone is conformable with the schists, striking NW (280–300°) and dipping steeply (70–80°) to the NE. The metasomatic zone is over 4 km long and up to 800 m wide.

The aluminous schists in the zone are converted to muscovite–quartz metasomatites (with kyanite and andalusite), forming an outer sub-zone 480 m thick; quartz porphyries in the zone are intensely sheared, with muscovite and microcline growth continuing right up to the formation of the quartz–microcline metasomatites, forming an inner subzone 320 m thick.

Metasomatites in the outer subzone have the composition 50–60% quartz, 5–20% muscovite, 10–30% andalusite + kyanite, plus small amounts of corundum, plagioclase and biotite. Those in the inner subzone consist of 60% microcline, 25–30% quartz, 6–8% muscovite, with epidote and biotite also present. There is a highly distinctive “layer” of muscovite–quartz metasomatites around 80 m thick at the boundary between the two subzones, which is totally lacking in high-alumina minerals. Silicification and tourmalinization were superimposed on the metasomatic zone. Quartz nests and finely acicular varieties of tourmaline (1–2%) are scattered throughout the whole zone. Cutting the metasomatic zone are vertical post-ore muscovite–tourmaline granitic pegmatites 50–60 m thick and gabbro–dolerite dykes containing no ore mineralization.

Finely disseminated sulphide mineralization is observed throughout the metasomatic zone. The sulphide content is 5–6% on average for the zone, 90% of which is pyrite and the remainder molybdenite, chalcopyrite and a negligible amount of sphalerite. There is a direct correlation between the molybdenite and chalcopyrite contents. Molybdenite is mostly concentrated in the centre of the outer subzone, where it amounts to 0.1–0.3% over a thickness of 40 m, based on a visual estimate in the southern ore-bearing horizon. A second, northern, ore-bearing horizon up to 190 m thick can be traced 250 m north of the first ore horizon in the outer contact zone of quartz porphyries. The ore-bearing horizons typically have higher gold and silver contents. The Pellapahk deposit is a copper–molybdenum–porphyry type.

### 1.7. Rare metals

Precambrian rare metal deposits in the Kola province are associated with granite pegmatites in the Kolmozero–Voronya greenstone belt (Rundqvist and Mitrofanov, 1992). The belt comprises Upper Archaean volcanosedimentary deposits, metamorphosed in the kyanite–staurolite subfacies of the amphibolite facies and altered

to various gneisses, schists and amphibolites. The amphibolites occur as a wide-spread and extensive set of sheet-like bodies tens and hundreds of m thick and stretching for many km. A characteristic feature of the Kolmozero–Voronya zone are numerous pegmatite bodies, from extensive sheet-like veins to lenticular and barrel-shaped bodies, mostly localized in the amphibolites. Rare metal deposits of cesium, lithium and accompanying tantalum, beryllium and other rare elements are associated with some of the pegmatite bodies (Smirnov, 1974).

Pollucite-bearing pegmatite veins have been discovered in a pegmatite field in the centre of the Kolmozero–Voronya zone. Small ore-rich veins are associated with a system of cross-cutting fractures in amphibolites; they are arranged in an *en échelon* pattern and have a complex shape (Fig. 22), but few are exposed at the present-day surface. The veins dip gently at 10–30° and are often more extensive downdip than along strike. In some places the pegmatite veins are cut by post-ore faults with negligible displacements. Thin centimetre-scale amphibole–tourmaline selvages, biotitization zones and holmquist-bearing aureoles up to 2 m wide are found at the outer contacts of the amphibolites that are host to the pegmatites.

The pollucite pegmatites typically have a variable internal structure and a complex mineral composition with various paragenetic associations. Zoning, structural inhomogeneity and cesium mineralization are found locally in pegmatites where they have been swollen by boudinage. In pinch structures granitic and sometimes pegmatoid textures are present in the pegmatites. Zahlbands in the bodies show quartz–albite pegmatite development, sometimes as impersistent selvages up to 1 m wide, consisting of saccharoidal albite, quartz grains and rare tantallite, spodumene and

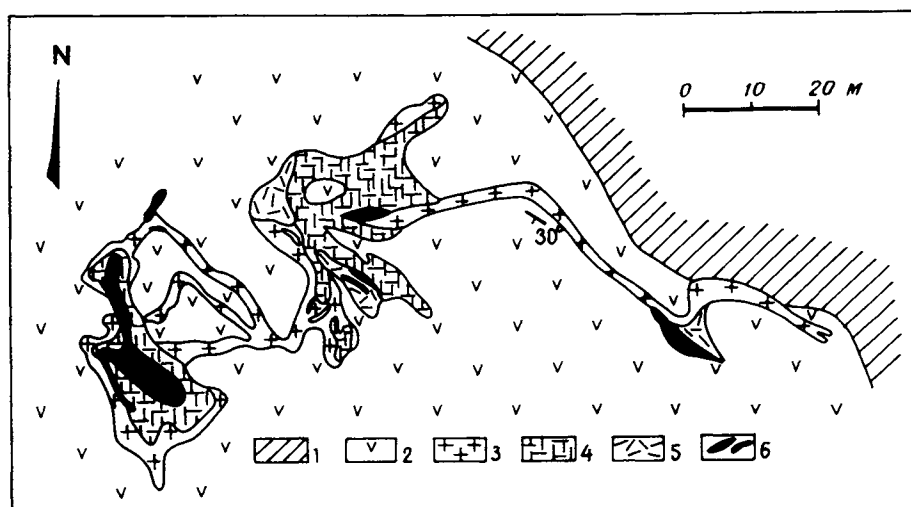


Fig. 22. Sketch showing structure of pollucite-bearing pegmatite veins (Smirnov, 1974). 1) hornblende-biotite schist; 2) sheared amphibolite; 3) aplitic quartz-albite pegmatite; 4) massive microcline pegmatite; 5) apographic pegmatite; 6) pollucite pegmatite.

beryl crystals. This pegmatite variety is widespread down the dip of pegmatite veins and in individual cases makes up most of the bodies.

Quartz–albite selvages in the central parts of the bodies are sometimes replaced by albite zones in which small microcline blocks (up to 10%) and spodumene crystals appear, sometimes also quartz–spodumene cavity infillings (10–15%). Areas showing zonation have albite varieties succeeded by essentially microcline or quartz–microcline pegmatite with a coarse blocky or apographic texture, in which the microcline is always more or less, sometimes completely, replaced by albite such that the albite aggregate not infrequently preserves the quartz intergrowths that typify graphic pegmatite. In addition to microcline, quartz and platy albite, this zone also contains spodumene, tantallite and beryl.

Mineralogically, the most complex pollucite zone is associated with the axial parts of boudin swellings or is localized as discontinuous nests in the hanging wall of the body. The zones have a banded structure with various replacement textures. Pollucitic pegmatite makes up around 20% of the volume of the pegmatite bodies. Always associated with the pollucite are albite–clevelandite, lepidolite, pink spodumene, quartz, coloured tourmaline, montebasite, rare cesium beryl, lithiophyllite, apatite, tantallite, microlite, and other minerals. Large patches and clusters of pollucite, albite and quartz are characteristic. Pollucite patches are up to 1.5 m across, with an irregular shape and consisting of fine-grained aggregates. It commonly forms thin veinlets in the quartz–albite groundmass. Cesium is also present in increased quantities in accessory beryl, lepidolite and muscovite, where the proportion of dispersed cesium can amount to 15% of its total mass in this rare-metal pegmatite field. Tantallum is an accessory in the pollucite pegmatites.

A second spodumene pegmatite field is found in the SW part of the Kolmozero–Voronya zone. Country rock gneisses in the pegmatite field strike NW, generally concordant with the zone; the gneisses are deformed by steep linear folds and are cut by various Upper Archaean intrusions. The earliest of these are represented by gabbro–anorthosites up to 5 km long, filling fractures and intruded along a fault that goes along the boundary between Archaean oligoclase gneissic granites and the Upper Archaean metamorphic complex. The pegmatite field is associated with the hanging wall of a gabbro–anorthosite intrusion and does not extend beyond its margins.

Spodumene pegmatites are genetically related to small (3 × 1.5 km) tourmaline–muscovite granites with numerous apophyses which pass into pegmatites and which are found 10 km from the spodumene pegmatites. The granites have an isotopic age of 2.4 Ga (K–Ar method), while the Rb–Sr age data of the rare metal pegmatites yield 2.3–2.2 Ga. Gabbro–anorthosites which host the ore-bearing pegmatites are amphibolized to varying degrees and in places are converted to amphibolites. These rocks strike parallel with the host gneisses.

The ore field is linear in shape and its trend is conformable with the strike of a basic intrusion; it is several kilometres long and 200–600 m wide (Fig. 23). The pegmatites fill a shear-vein system, subparallel to the dominant structural trend but cutting across the dip of the banding in the gabbro–anorthosites. Pegmatite bodies are grouped into two parallel zones which are spaced 100–200 m apart. Each zone

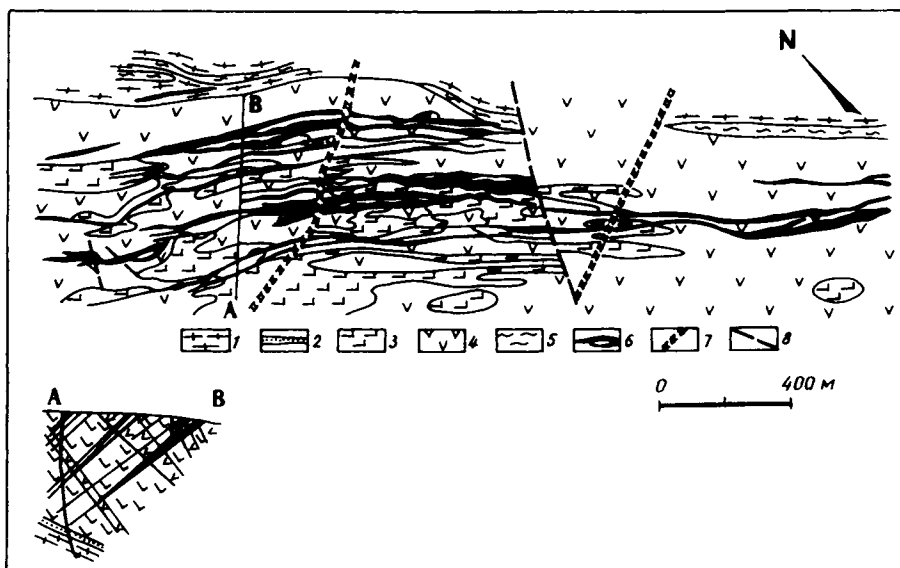


Fig. 23. Geological sketch map of rare-metal pegmatites in gabbro-anorthosite (Smirnov, 1974). 1) granite-gneiss; 2) conglomerate; 3) gabbro-anorthosite; 4) amphibolite; 5) talc-chlorite schist; 6) pegmatite; 7) dolerite dykes; 8) faults.

consists of a series of close, branching pegmatitic bodies. All the bodies dip at  $50^\circ$  to the SW. Post-ore tectonics resulted in the formation of steep ( $70\text{--}85^\circ$ ) tensional cross-fractures, filled with dolerite dykes, and a series of faults.

In the centre of the deposit the pegmatite bodies display a minor flexural bend, at which they attain their maximum thickness. They have a constant dip and gradually decrease in thickness with depth. The bodies are sheet-like, varying in thickness from 1–2 to 20 m. Contacts with the gabbro-anorthosites are sharp, and the gabbro-anorthosites are sheared and altered adjacent to the pegmatites. Alteration zones, up to 5 m wide, have plagioclase replaced by anorthite and contain widely distributed holmquistite, zoisite and epidote. Close to the outer contact, biotitization and tourmalinization are intensely displayed, with 2–5 cm wide biotite-tourmaline selvages formed.

The central portions of pegmatite veins consist of large blocky microcline-spodumene pegmatite varieties, which are fringed by essentially quartz-albite zones containing small spodumene crystals. On the flanks and at depth, where the ore bodies wedge out, pegmatites consist of a quartz-albite aggregate with rare spodumene crystals.

The main ore mineral in the pegmatites is spodumene, which has a uniformly high content in pegmatite. Around 5–7% of the lithium in the pegmatites is associated with lithium phosphates – trifiene, lithiophyllite and amblygonite, and small amounts with holmquistite and muscovite. The pegmatites contain small amounts of beryl, manganapatite, spessartine and tantalite-columbite group minerals.

### 1.8. Graphite

Numerous graphite occurrences were discovered in the Allarechka nickeliferous region in the early 1960s during exploration for copper–nickel ore deposits, forming together with pyrrhotite an intralayer graphite–pyrrhotite zone many kilometres wide mainly in biotite and garnet–biotite gneisses, less commonly in hornblende–biotite gneisses, feldspar amphibolites and migmatized granites. Graphitic gneisses surround granite–gneiss dome structures of the region.

The *Skalistoye graphite deposit* (description based on material from the “Sevzappegeologiya” production company) is situated on the SW limb of the Allarechka dome structure 20 km south of the Allarechka copper–nickel deposit. It is restricted to the NE limb of a broad syncline whose interlimb distance is around 8 km. The region around the deposit consists of interleaved gneisses and amphibolites, and migmatized granites. The rocks in the deposit are arranged in a monocline with steep (75–90°) dips to the SW (210–230°).

No. 1 sector in the deposit has the two largest sheet-like ore bodies, conformable with biotite and garnet–biotite gneisses. Both wall rocks and ore horizons are cross-cut by vertical faults with up to 300–400 m displacement. The ore bodies are 1.1 km long, 4–40 m thick, with a graphite content of 2–8%, or 4% on average for the whole deposit. The graphite is flaky or in large flakes. Ores are rich (graphite recovery = 94–96%, ash content = 2–4%) and are amenable to the extraction of the main economic graphite grades. In terms of its geological structure and the ore quality, the Skalistoye deposit bears a very close resemblance to the Zavalevskoye deposit in the Ukraine. The Allarechka graphite-bearing region has good prospects for finding more commercial graphite ores.

## Karelia Terrain

V.A. GORELOV, A.M. LARIN and S.I. TURCHENKO

### *1. Introduction*

The Karelian granite–greenstone terrain is typified by the extensive development of Late Archaean (Lopian) greenstone belts, which represent the relicts of elongate zones preserved after Late Archaean granite formation, metamorphism and folding events. The spatial boundaries of the greenstone belts and the extent to which individual structures are assigned to them are constrained by the geology and geochronology. The many greenstone structures in Karelia are combined into six greenstone belts (Sokolov, 1987; Rybakov et al. 1985, 1987; Turchenko, 1992; see Fig. 24): Himola–Kostomuksha and Yalonvaara, forming the West Karelian zone; Vedlozero–Segozera and Parandovo–Tikshozero (Central Karelian zone); Sumozero–Kenozero and South Vygozero (East Karelian zone). In terms of their constituents, these belts are similar to the greenstone belts of the Kola terrain. Extensive areas of granite–gneiss within the granite–greenstone terrain are inliers of the Saamian basement, regenerated during Lopian time (2.9–2.66 Ga).

Typical deposits in the Karelian greenstone belts are ferruginous quartzites (BIF), copper–nickel sulphide ores, molybdenum and massive sulphide, together with chromium, titanium, copper, zinc and asbestos occurrences (Sokolov, 1987; Kratz, 1983; Turchenko, 1992).

Several intracratonic basins formed in the Karelian geoblock, cratonized during the Late Archaean, the largest of which are the Onega and Segozero–Yangozero in the southern and central parts of the geoblock respectively (Fig. 2). The basins are filled with supracrustal assemblages, geological successions of which show predominantly a basalt volcanic formation, with clearly subordinate felsic volcanics and sedimentary rocks. Mostly the rocks in these basins display greenschist facies metamorphism. Typical mineral deposits in the intracratonic basins of the Karelian terrain are shungite and numerous copper and cobalt–copper occurrences, as well as gold occurrences.

During the Early Proterozoic, an elongate rift, the Kuola–Vygozero belt, formed conformable with the strike of Archaean rock complexes in the stable Karelian terrain, along the boundary between this terrain and the Belomorian belt of tectonothermal reworking (Turchenko, 1992). The rift belt can be traced SE from the Russian–Finnish border for 750 km, until it is overstepped by the platform cover (Fig. 2). A Lower Proterozoic volcanosedimentary rock assemblage (picritic basalt and tholeiitic basalt) formed in the elongate synclinal downwarps and graben–synclines which make up the greater part of the belt. Synclines in the Kuola–Vygozero belt are, from N to S:

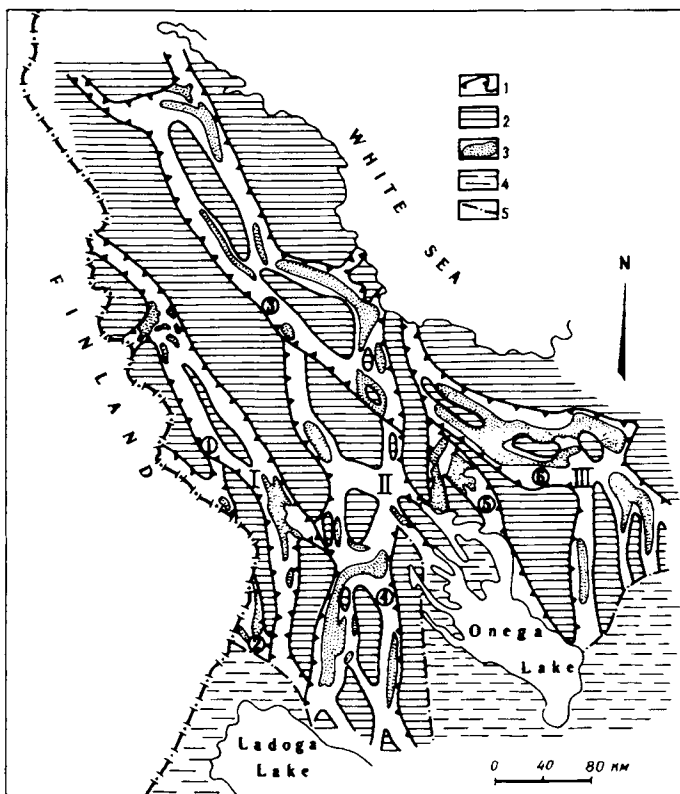


Fig. 24. Sketch reconstruction of Archaean greenstone belts in the Karelian granite-greenstone province (Rybakov et al., 1987). 1) Lopian greenstone belts *Numbers in circles*: 1 – Himola-Kostomuksha, 2 – Yalonvaara, 3 – Parandovo-Tikshozero, 4 – Vodlozero-Segozero, 5 – South Vygozero, 6 – Sumozero-Kenozero; 2) basement blocks; 3) local greenstone structures; 4) post-Lopian sediments; 5) faults.

Kuolajärvi, Kukasozero, Shombozero–Lehta, and the Vetrenny belt. As is the case in the Pechenga–Varzuga belt, the structure of the rift belt is complicated by flexural folding, and both parallel and cross-faults that extend to various depths.

Nickeliferous basic-ultrabasic rocks of the Olanga group were intruded along these faults and in fault intersection zones. The Burakovka zone of deep faults in the SE part of the Karelian province belongs to the largest cross-fault which is probably associated with the rift structure and which controls the Burakovka peridotite-gabbro-norite layered intrusion, the largest such body in the Baltic Shield (700 km<sup>2</sup>). Ore-bearing alkali gabbro and ultrabasic-alkali gabbro intrusions were emplaced in the NW part of the rift. Associated with the rift are deposits and ore shows belonging to phosphorus-iron-titanium and copper-nickel sulphide formations, and chromium, copper, gold and asbestos occurrences, as well as PGE mineralization (Turchenko, 1992). The descriptions of ore deposits in the Karelian granite-greenstone terrain that follow are presented in the same order as for the Kola terrain.

## 2. Ore deposits and occurrences

### 2.1. Iron

Ferruginous quartzites were first discovered in Karelia in 1946–47. Major magnetic anomalies were found by aeromagnetic methods and confirmed by field observations overlying the ferruginous quartzites of the West Karelian iron-ore zone. This zone contains several iron ore regions (Gorkovets et al., 1986): Kostomuksha, Hedozero–Bolshezero, Voloma, Tumbarechka, Himola, Sovdozero, Notozero–Hizavaara, Lake Motko, with two economic deposits – Kostomuksha and Korpanga, belonging to the Kostomuksha ore region, and numerous uneconomic deposits and manifestations (Fig. 25).

The *Kostomuksha ore region* (Sokolov, 1987; Gorkovets et al., 1981, 1986; Lazarev, 1971; Chernov et al., 1970) is located in the NW part of the West Karelian Zone of greenstone belts, and occupies an area of some 1000 km<sup>2</sup> (35 × 35 km). In addition to Kostomuksha and the Korpanga deposit 7 km to the north, this region also contains several groups of magnetic anomalies corresponding to small-scale ferruginous quartzite deposits. This region is made up of rocks belonging to the Upper Archaean Lopian complex, with the iron–silica formation occupying the middle part of the Himola Group, in the Kostomuksha Fm, up to 1.2 km thick (Gorkovets et al., 1981, 1986). Table 3 illustrates a section through the Himola Group. The ore-bearing unit is

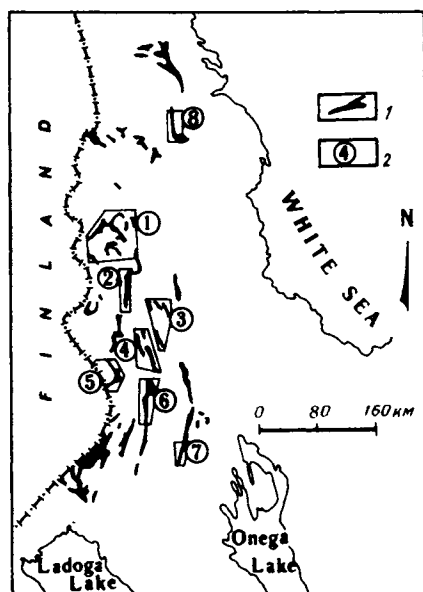


Fig. 25. Sketch map showing iron ore regions of Karelia (Gorkovets et al., 1986). 1) U. Archaean (Lopian) complex with ferruginous quartzite fm; 2) iron ore regions and clusters: 1 – Kostomuksha, 2 – Hedozero–Bolshezero, 3 – Voloma, 4 – Tumborechka, 5 – Lake Motko, 6 – Himola, 7 – Sevdozero, 8 – Notozero–Hizovara.

Table 3  
Stratigraphic section of the Himola Group (AR<sub>2</sub>) in the West Karelian greenstone belt zone

Age, Ma	Group	Formation	Member	Lithology	Thickness, m
2700 ± 100	Himola	Suurilampi		Mica schists with garnet, staurolite, andalusite	100–1300
		Kostomuksha	Upper Kostomuksha	Mica schists and graphitic schists, magnetite quartzite	50–720
			Lower Kostomuksha	Magnetite quartzites, graphitic and mica schists	30–420
		Mezhozero	Upper Mezhozero	Schists (from rhyodacitic volcanics)	hundreds of metres
			Lower Mezhozero	Gneisses (from andesite–dacite volcanics)	hundreds of metres
2850 ± 30		Sukkozero		Polymict conglomerates, grits, and greywackes	10–450

underlain by schists after rhyodacitic volcanic rocks and overlain by mica schists. The iron ore unit contains grünerite–magnetite, biotite–magnetite, riebeckite–magnetite and other varieties of ferruginous quartzites, interleaved on a large scale with rhythmically-banded mica schists, the metamorphosed equivalents of flysch-type terrigenous sediments, and with graphite-bearing phyllitic schists. The number and thickness of iron–silica bands decrease up the succession, and the volume of mica schist increases.

Isotopic dating of the base of the Himola Group in the Kostomuksha region, using authigenic zircon in a conglomerate cement, yielded an age of 2.85 Ga. The upper age of the Lopian complex is 2.7 Ga (Gorkovets et al., 1981, 1986). The structural plan of the Kostomuksha region is defined by a cluster of Archaean dome–block structures, made of granite–gneiss and various migmatites. These structures are surrounded by iron-ore units to form a 4.5–7 km wide complex network of variously oriented synclines which partly touch each other and stretch for over 25 km in a N–S direction. Total resources for this region have been estimated at 3.5 billion tonnes of ore (to a depth of 1000 m), containing around 30% of iron. All the deposits found in the region are of a uniform type, and differ from those in the Olenegorsk region by having suffered a lower grade of metamorphism, as well as displaying a number of other geological features. The Kostomuksha deposit proper has attracted greatest attention. Exploitation is by opencast mining and the pits are projected to yield 24 m.t. of ore annually.

*The Kostomuksha deposit* (Gorkovets et al., 1981, 1986) lies in western Karelia. Structurally, it belongs to the central part of the Kostomuksha synclinorium and is restricted to the western limb of a rather narrow and markedly asymmetric syncline, as measured by limb thickness (Fig. 26), whose axial surface strikes 010–015° in the northern part, and swings round to a more ENE strike in the central part. The ferruginous quartzite bands and the various schists, which decrease in thickness with depth, have steep E or SE dips of 80–85°, while in the southern part of the deposit the rocks dip to the N and NE at angles of 60–70°, which become shallower at depths greater than 3 km.

The deposit comprises two conformably interfolded sheet-like bodies: the Main ore body and the Interbedded Deposit. The Main ore body occurs on the footwall of the productive unit, and can be traced for 14.5 km along strike, but the down-dip extension has not been constrained. In its central part, the deposit attains 300 m thickness at the fold closure and it becomes gradually wedged out towards the limbs. From the central part to the northern limb, the deposit splits into two branches – western and eastern members, consisting of graphitic phyllites and quartz–biotite–amphibole schists up to 40 m thick. In places these schists are enriched in pyrite and pyrrhotite. On the footwall side the host rocks for the ore body are quartz–biotite, phyllitic, biotite–quartz–amphibole and talc–chlorite schists, together with ore-free quartzites. In the central and southern parts, the Main ore body on the hanging wall side is overlain by felsic volcanics – helleflintas (fine-grained, quartz-rich, hornfelsic rock) – from a few metres to 400–600 m thick, a thickness which increases with depth.

The Interbedded Deposit lies 50–600 m east of the Main ore body. It consists of alternating bands of ferruginous quartzite and mica schist, with the proportion of ferruginous quartzite generally not exceeding 20–25% of the total volume. The

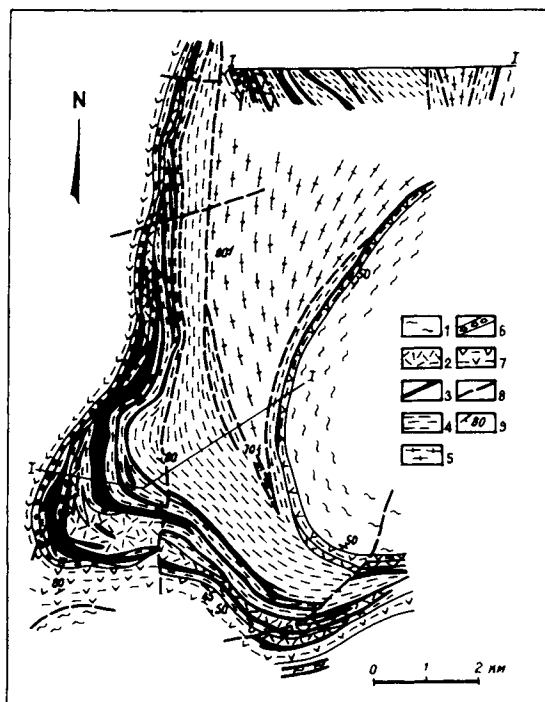


Fig. 26. Geological sketch map of the Kostomuksha iron ore deposit (Gorkovets et al., 1986). 1) gneiss, granite-gneiss, migmatite; 2) plagioclase porphyry, heffintas; 3) ferruginous quartzite; 4) mica schist; 5) migmatized & granitized mica schist; 6) conglomerate; 7) metabasalt; 8) faults; 9) orientation.

Interbedded Deposit differs from the Main ore body in having a more complex structure and a greater variation in thickness, from 100–400 m in the north, to 800–900 m in the central part of the deposit. Various individual ferruginous quartzite bands within the deposit are from a few metres to 80 m thick, and from a few hundreds of metres to 6.7 km long. The barren units interbedded with the ore bands are 5–160 m thick. Over 40 ore bodies have been counted in the deposit.

Predominant among the ferruginous quartzites that make up the ore deposits are magnetic varieties, which are divided into four mineralogical types: alkali-amphibole, biotite, amphibole, and grünerite-magnetite quartzites. All these varieties are most fully represented in the Main ore body. Alkali-amphibole and biotite varieties have high magnetite contents, and the largest magnetite grain size, and also have less sulphur. The main rock-forming minerals in the deposit are magnetite and quartz, both of which can attain 50% in the ores. Ores which contain 30%  $\text{Fe}_3\text{O}_4$  consist as a rule of 95% magnetite + quartz. Hematite is the second main ore mineral, with up to 10–15% being present in the ore. Secondary ore minerals are pyrite, pyrrhotite and chalcopyrite. Amphibole (up to 20%) and biotite (up to 40%) are also always present. Harmful impurities in the ore are sulphur (0.25 av.%) and phosphorus (0.07 av.%). In terms of their engineering properties, the ores in this deposit are fine- and medium-grained,

easily enriched, with 93–95% magnetite being extracted in the concentrate, which contains up to 66–69% iron. Most researchers class this deposit as belonging to the metamorphosed volcanosedimentary type.

## 2.2. Titanium

The Pudozhgora and Koikari titanomagnetite deposits are found on the SE and NW edges of the Onega trough. They are of the same type and are genetically associated with gabbro–dolerite dykes. The following description of the Pudozhgora deposit is based on Yudin (1987) and material provided by the Sevzapgeologiya (“North-west Geology”) production company.

*The Pudozhgora deposit* is situated on the eastern shore of Lake Onega and was discovered in 1939. It occurs in a gently-dipping gabbro–dolerite dyke, cutting a granite–gneiss complex, and formed during the Early Proterozoic (2.1–1.8 Ga). Country rock xenoliths are found in the dyke. It can be followed for over 7 km along strike and has an overall trend of 310–320°; dips are 3° to 48° to the SW. The sheet is 120–180 m thick, decreasing to 40–50 m on the flanks; its shape is tabular with wavy outlines, corresponding to fracture surfaces in the country rocks. Compositionally, the sheet changes gradually upwards from basic to more felsic gabbro dolerite. There is a very pronounced 1.5–5 m chilled margin in which the rocks are represented by aphanitic and fine-grained amphibolized varieties.

A sub-ore gabbro dolerite horizon, 10–40 m thick containing low-grade titanomagnetite dissemination, occurs on the footwall of the sheet above the chilled margin. The overlying ore horizon has a high titanomagnetite content, in contrast to the barren gabbro–dolerites. This horizon is divided into three isolated deposits at the present-day erosion surface, which merge into a single ore body at 60–80 m depth, with the same thickness as at the surface. The ore horizon mimics the irregular outlines of the sheet, forming flexures downdip and along strike. The ore deposit can be traced for 7.1 km along strike and 400 m down dip; no wedging-out of the ores downdip has been established. Both the ore deposit and the country rocks dip to the SW at 50° in the NW of the deposit to 8–12° on the SE flank; the average dip angle for the deposit 30°. The ore body is 7–23 m thick, 15 m on average (Fig. 27). The main part of the body consists of rich disseminated ores – the first ore variety – containing 45–75% titanomagnetite. Characteristically, the deposit maintains a constant 0.5–4 m thickness in the dip and strike direction. Rich ores give way to poorer ores – the second variety – on the hanging wall and footwall of the ore body.

Mineralogically, the ores in this deposit have a uniform composition. Titanomagnetite is the main ore mineral; chalcopyrite, pyrite and pyrrhotite are present in negligible quantities. Gangue minerals are represented by a typical amphibolized gabbro–dolerite mineral assemblage, together with apatite, quartz, sphene and leucoxene. The disseminated ore shows a hypidiomorphic grain texture. Titanomagnetite predominates as isomorphic grains, 0.3–0.8 mm in size. The ores are impoverished and require enrichment. Average metal contents in the ore are Ti 8%, Fe 28.7% and V<sub>2</sub>O<sub>5</sub> 0.43%. All researchers classify this deposit as a true magmatic type, except that some regard it as melt-type, while others consider that it is a segregation-type.

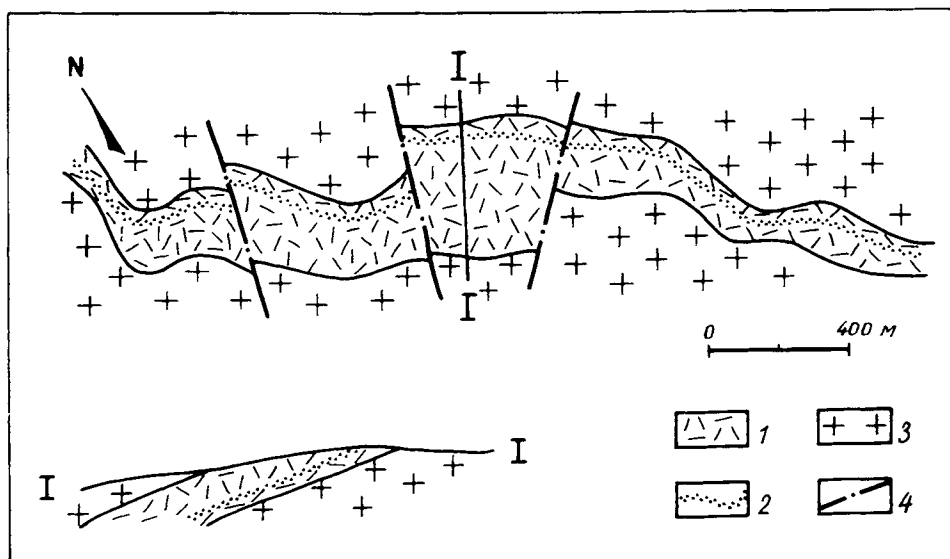


Fig. 27. Geological sketch map of the Pudozhgora deposit (Dubrovsky, 1969). 1) gabbro-diabase; 2) titanomagnetite ore horizon; 3) microcline granite; 4) faults.

### 2.3. Nickel, copper and PGE

The Karelia terrain has known uneconomic copper–nickel sulphide ore deposits and occurrences, localized in several tectonic structures. A suite of nickeliferous dunite–peridotite intrusions in the middle of the Sumozero–Kenozero greenstone belt forms the Lake Kamennoye nickeliferous region. The Olanga group of nickeliferous and platinumiferous peridotite–gabbro–norite intrusions occurs on the NW flank of the Kulo–Vygozero rift belt – Lukkulaisvaara, Kivakka and Tsipringa (Sokolov, 1987; Turchenko, 1992). Nickel prospects for the Burakov intrusion are unknown. The Vedlozero–Segozero and South Vygozero greenstone belts contain ultrabasic intrusions with poor copper–nickel sulphide mineralization (Kratz, 1983).

*Mineral deposits in the Lake Kamennoye region* (Sokolov, 1987; Kratz, 1983; Gorbunov and Papunen 1985). The Lake Kamennoye nickeliferous region is located on the margins of the Lake Kamennoye depression, which is around 35 km long by 10 km wide. The depression formed along a NW- and NE-trending system of deep faults, and is divided into two branches which are infilled with Upper Archaean volcanosedimentary successions in which basic volcanics, including sheared varieties, predominate, together with felsic volcanics and pyrite–graphite schist horizons containing massive pyrite–base metal ore occurrences (e.g. Zolotyye Porogi, “Golden Rapids”).

The Lake Kamennoye structure is bounded to the north and south by blocks of undifferentiated Archaean granitic rocks. Two of the large Lower Proterozoic intrusions – the Vozhminskoye and Kumbuksinskoye of similar type – and several smaller

intrusions are emplaced in the NE branch of the depression. They all belong to a dunite–peridotite suite. Genetically associated with the intrusions are the small Vozhminskoye and Lebyazhi copper–nickel sulphide deposits and the Svetlozero occurrence among others (Fig. 28). The ore deposits and occurrences are broadly the same type, differing only in the scale of ore mineralization. The best studied deposit is the Lebyazhi, which will serve as an example, since exploratory–evaluation work has been undertaken on it.

The *Lebyazhi deposit* (Kratz, 1983; Gorbunov and Papunen 1985) was discovered in 1973 by exploratory drilling to investigate a complex magnetic and electrical anomaly. It is situated 150 km SE of the Nadvoitsy railway station, and is genetically and spatially related to Kumbuksinskoye intrusion. The intrusion is a lenticular sheet

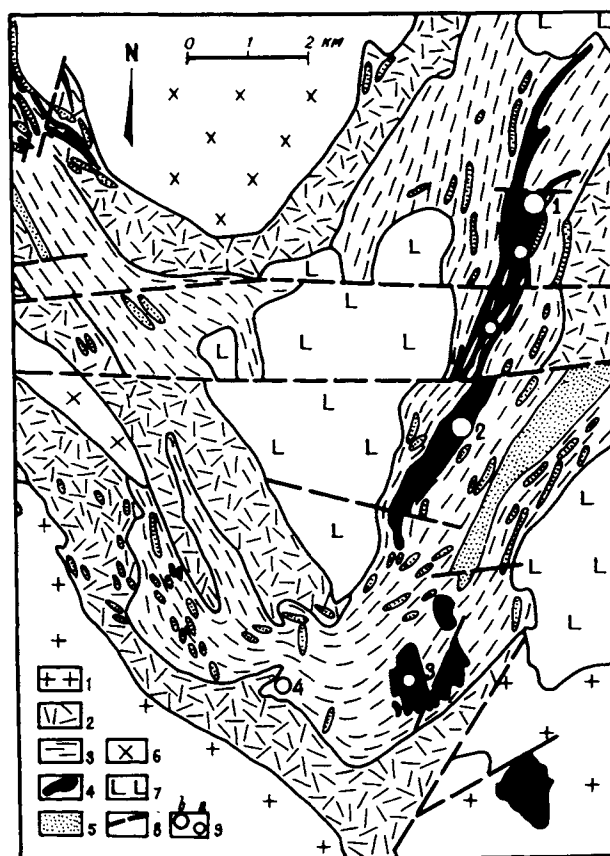


Fig. 28. Sketch showing the geological structure of the Lake Kamennoye belt (Gorbunov and Papunen, 1985). 1) migmatitic granite; 2) metabasalt and komatiite; 3) andesite–basalt, tuffaceous sandstone, black schist; 4) basic–ultrabasic intrusions: olivinite, harzburgite, wehrlite, pyroxenite; 5) gabbro; 6) trondhjemite; 7) basalt & tuff; 8) faults; 9) Cu–Ni sulphide deposits (a): 1 – East Vozhminskoye, 2 – Lebyazhi, (b) occurrences: 3 – Lake Svetloye, 4 – Zolotyeye Porogi.

extending 7 km in a NE direction and is up to 800 m wide at the centre; it dips to the NW at  $20^\circ$  in the N and  $70-90^\circ$  in the southern part and cuts obliquely across the country rocks. Changes in the dip angle are related to E-W faults which cut the intrusion. Associated with these faults are cross folds, accompanied by flexures and sags at the base of the intrusion (Fig. 29).

The intrusion is in two phases, with first phase rocks accounting for most of the body; these are highly altered olivinite, wehrlite, pyroxenite and gabbro. Second phase rocks are represented by wehrlite, pyroxenite and gabbro-pyroxenite, forming discontinuous dyke-like bodies developed in tectonic zones that run along the footwall of the intrusion and the upper boundary of first phase olivinites.

Rocks hosting the ores are highly altered, although relict textures are preserved that enable the primary rock compositions to be reconstructed. Rock alteration was poly-

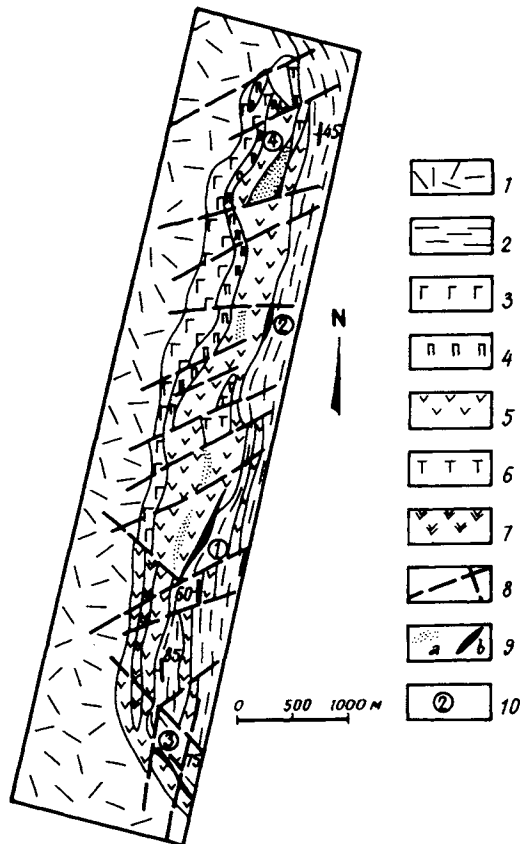


Fig. 29. Geological sketch map of the Lebyazhi deposit (based on Sevzapgeologiya materials). 1) basic volcanics - metadolerites; 2) felsic volcanics & tuffo-sediments; 3-5): first phase intrusive complex, 3) metagabbro, 4) metapyroxenite, 5) serpentinized olivinite & peridotite; 6) second phase metawehlrite & metapyroxenite; 7) metagabbro-dolerite dykes; 8) faults; 9) Cu-Ni sulphide ores: a - disseminated, b - massive, brecciated; 10) ore deposits: 1 - Main orebody; 2, 3, 4, - No. 1, 2, 3 deposits.

phase, leading to the formation of several generations of secondary minerals, divided into a sequence of four mineral transformation stages (Kratz, 1983): autometamorphic chrysotile–lizardite serpentinization → allometamorphic antigorite serpentinization → allometamorphic chlorite–amphibole stage → talc–carbonate stage concluding the alteration processes and having a marked retrogressive character. Alteration is bounded by narrow but extensive zones of close-spaced fractures, forming a complex network in the serpentinites.

The following sequence of first phase rocks is observed from the footwall to the hanging wall: apoperidotitic serpentinites (10–50 m), intensely carbonatized and altered to talc–carbonate rocks; serpentinites after pyroxene olivinites (10–30 m), serpentinites after olivinites (50–200 m), serpentinites after pyroxene olivinites and harzburgites (50–200 m), metapyroxenite (0–60 m) and gabbro (0–300 m). Rare gabbro–dolerite and dacite porphyry dykes are found in the intrusion.

The Lebyazhi deposit incorporates a series of ore bodies within the Kumbuksinskoye intrusion. The bodies are located in the Eastern and Central ore-controlling zones. The Eastern zone, containing the richest ores, lies at the eastern contact, the footwall of the intrusion. It has mostly epigenetic ores, with some syngenetic types also developed. In a practical context, the most interesting epigenetic ore bodies occur in shallow synformal depressions at the intrusion base and characteristically have greatest extent down-dip – 300–400 m – and along pitch (to the north) – over 1.5 km. The zone has three ore bodies, Main, No. 1 and No. 2.

The Central ore-controlling zone is traced by metawehrlite, pyroxenite and gabbro–dolerite dykes, rodingite and talc–carbonate veins, developed along the intrusion axis and clearly marked by magnetic anomalies of tens of thousands of gammas. The zone is 10–100 m wide and is traceable for 7 km along the entire intrusion. Disseminated ore mineralization is dominant in the zone. Epigenetic mineralization follows dykes of different compositions where metasomatic alteration has affected both rocks and ores. A No. 4 ore body has been delineated in the zone, and contains over 0.5% nickel.

The Main ore body, which occurs in the lower part of the intrusion, completely mimicks the outlines of the intrusion base (Fig. 30). It dips at 30–60° to the NW and is 14 m at its maximum thickness in places where the footwall of the intrusion shows the greatest sagging, beyond which the thickness decreases to 1–2 m. The ore body is 5 m thick on average and can be traced for 1.8 km along pitch to the north and 450 m down-dip. Ore types are disseminated, brecciated and massive. Brecciated and massive ores occur at the contact between the intrusion and the volcanosedimentary wall rocks. Over 70% of the nickel is concentrated in the predominant disseminated ores. Ore minerals (in decreasing order of content) are pyrrhotite, pyrite, pentlandite, magnetite, chalcopyrite, millerite, chromite, rutile, galena and sphalerite. The ores are rather impoverished, and are represented by millerite–magnetite, heazlewoodite–magnetite and widespread pentlandite–pyrrhotite types. The nickel content of the ores varies within wide limits, reaching 9% and with an average of 0.45% and a 0.3% metal content cut-off grade; copper – up to 1.6% (av. 0.22%); cobalt – up to 0.25% (av. 0.024%). Ore enrichment is difficult.

**Stratiform copper ore** occurrences are common in Early Proterozoic depressions in the Karelia terrain (Bilibina, 1980), represented by two mineral types: chalcopyrite–

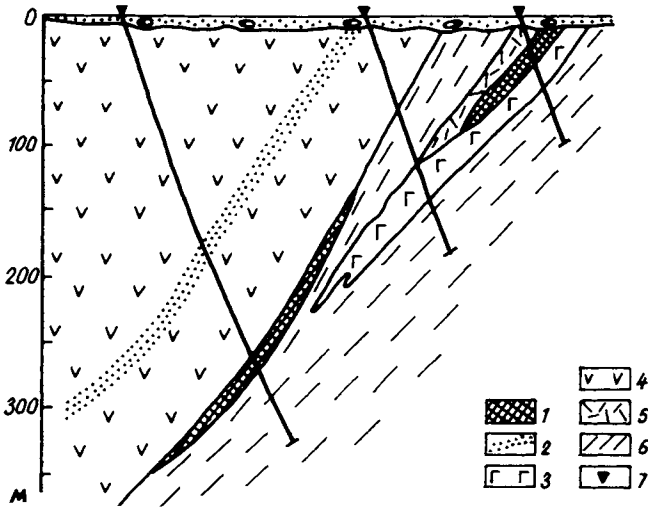


Fig. 30. Geological section of the Main orebody in the Lebyazhi deposit (based on Sevzapgeologiya materials). 1) Cu-Ni sulphide ore; 2) heazelewoodite mineralization; 3) gabbro-dolerite; 4) apo-olivinite serpentinite; 5) meta-andesite; 6) albite-quartz-sericite tuffite; 7) boreholes.

pyrite-cobalt in shales and calcareous rocks, and chalcopyrite-chalcosite, sometimes gold-bearing, in sandstones and quartzites.

*The Kuzoranda occurrence* in the Onega depression belongs to the first mineral type; its ore-bearing sequence contains three members. The lowest member is 40–50 m thick and consists of shungitic siltstones with polymict sandstone lenses; the middle member is around 100 m thick – dolomites and siliceous-limey siltstones; the top 10–15 m thick member is made of siltstones with calcite porphyroblasts. Sulphide mineralization is evident in all three members and can be followed along strike for 10 km in discrete rock exposures, where the sulphide content reaches 90% over a thickness that ranges from 5 cm to 3.5 m. The average sulphide content in the lowest member is 3.5%, and around 1% in the other two members. The sulphides – pyrite and chalcopyrite – form disseminations, merging into thin interlayers and lenses.

*The Maimjärvi occurrence* in the SE of the Yangozero depression is an example of a chalcopyrite-chalcosite ore type. Jatulian sediments in the area include a 200 m thick quartzitic sandstone unit, underlain by a quartzite-conglomerate horizon and overlain by metadolerites. Several ore-bearing horizons have been found in the quartzitic sandstones, the thickest of which attains 37 m with an average copper content of 0.82% (Bilibina, 1980). Compositionally similar occurrences are the Hirvi-Navolok in the Kukasozero belt in the north of the Karelia terrain, the Ushkovo in the Lehta graben-syncline, and others.

*Ores in the Burakov intrusion.* The Burakov peridotite-gabbro-norite layered intrusion is situated between the eastern shore of Lake Onega and Lake Vodlozero, within a NE-trending deep fault zone associated with the Kuola-Vygozero rift structure. The massif is the largest layered igneous body in the Baltic Shield and Russia. In

plan view it is an oval body, cut by late fractures, stretching for 50 km along the fault, and is 13–17 km wide (Fig. 31), with a total area of some 700 km<sup>2</sup>. The pluton is a lopolith which was formed under stable conditions such that the magma chamber adopted a layered structure. Its contacts dip inwards at 40–50° and up to 70°. The SE contact is steeper than the NW. The base of the intrusion has been estimated to lie at 7–9 km. K–Ar radiometric data suggest an age of  $2360 \pm 60$  Ma or  $2449 \pm 1.5$  Ma (U–Pb zircon method, Yu. Amelin) for the pluton, which together with evidence that it cross-cuts the Lower Proterozoic Pudozhgora gabbro–dolerite dyke swarm means that the massif probably belongs to the Early Proterozoic magmatic event.

The intrusion was emplaced into Archaean migmatites and migmatitic granites. NW-trending faults divide the pluton into three major blocks, which from SW to NE are the Burakov, Shalozero and Aganozero. The Aganozero block is at a higher level than the first two and erosion has revealed deep-level ultrabasic differentiates. From bottom to top the pluton contains ultrabasic, transitional, gabbro–norite and gabbro–diorite zones. Its outer contact has a marginal zone up to 250 m wide, consisting of gabbro–norite and pyroxenite. Typically, it is “contaminated” with country rocks and contains syenite–diorite and granophyric diorite veins. Negligible amounts of ore

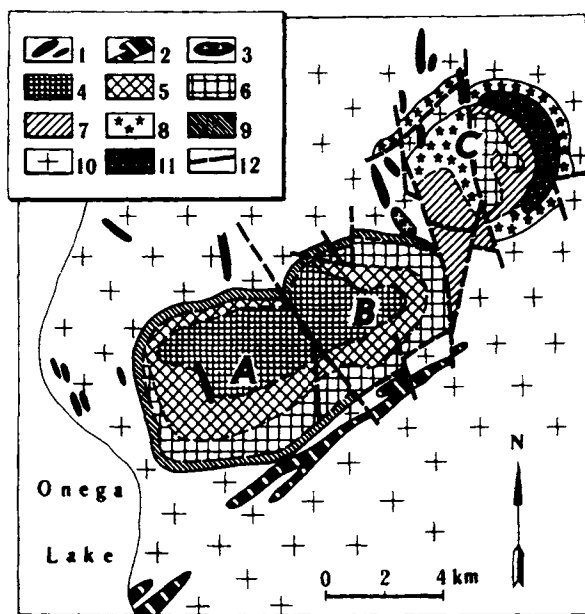


Fig. 31. Sketch showing geological structure of the Burakov intrusion (Kratz, 1983). 1) gabbro–dolerite, Pudozhgora complex; 2) microcline granite; 3) South Burakov gabbro–norites; 4–9) Burakov intrusion: 4) gabbro–diorite, 5) gabbro–norite zone, upper subzone, 6) gabbro–norite zone, lower subzone, 7) transition zone – peridotites, pyroxenites and part of the gabbro–norites, 8) ultrabasic zone – apodunite & apoperidotite serpentinites, 9) marginal zone – gabbro–norite, pyroxenite; 10) granitic & dioritic gneisses, migmatites; 11) faults; 12) Ni ore deposit; 13) tectonic blocks in Burakov intrusion: A – Burakov, B – Shalozero, C – Aganozero.

minerals are found in the zone: magnetite, ilmenite, chalcopyrite, pyrite and rarer pyrrhotite and pentlandite. The ultrabasic unit is exposed by erosion only in the Aganozero block and consists of apodunite at the base with apoperidotitic serpentinite above. Ore minerals in this zone are disseminated chromite phenocrysts from single grains to 3–5%, disseminated pyrite and pyrite veins, chalcopyrite, pyrrhotite and sporadic grains of millerite.

The transition zone also appears only in the Aganozero block. Its constituents are alternating layers of peridotite, augite and bronzitite containing thin plagioclase and gabbro–norite interlayers. Layers vary in thickness from a few cm to a few m. Ore mineral types and their percentages are the same as in the ultrabasic zone on the whole.

Gabbro–norite and gabbro–diorite zones are typical for the Burakov and Shalozero blocks. The lower part of the gabbro–norite zone, which replaces the transition zone, appears in the central part of the Aganozero block. In the gabbro–norite zone, there is frequent alternation of leucocratic to melanocratic gabbro–norites of varying grain size, containing sporadic disseminations and rare thin veins of magnetite, titanomagnetite, pyrite, chalcopyrite and pyrrhotite. At the top of the pluton is the gabbro–diorite zone, up to 415 m thick. Titanomagnetite predominates among the ore minerals in this zone, with magnetite and sulphides present in significantly smaller amounts.

Mineralogically and chemically the Burakov intrusion is similar to the Monchegorsk pluton and the intrusions in the Olanga group. Two types of mineralization occur in the intrusion – nickel and chromite.

*Nickel mineralization.* During recent exploration of the intrusion for copper–nickel sulphide ores in apo-dunitic and apo-olivinitic serpentinites in the ultrabasic zone of the Aganozero block, hydrotalc–lizardite rocks were discovered over a large area (around 75 km<sup>2</sup>), and they spontaneously disintegrated into separate grains on being extracted from depth.

These rocks, given the name “sapolite” or “kemistite” were treated with weak acids (hydrochloric or sulphuric) and rather easily yielded up to 70–90% nickel and 20–25% magnesium, when the average content of these elements in the serpentinites was 0.3% and 30% respectively. Thanks to this property of the rocks to disintegrate, the high nickel extraction and the straightforward removal of magnesium, the kemistites may be regarded as a new ore type, and the entire area in the Aganozero block over which the kemistites are developed is considered to be a new ore deposit type in economic geology and unique in its nickel–magnesium reserves. The following description of this ore target is based on material held with the Sevzapgeologiya Production Company.

The ore deposit occupies almost the entire NE, E and S parts of the apo-dunites and apo-olivinites in the Aganozero block. It is sickle-shaped in plan view and rimmed by gabbro–norite. The most prospective part is a segment in the NE, 1.5 to 3 km wide and 35 km<sup>2</sup> in area. The deposit is at least 200–350 m thick and geophysical data indicate that its bottom edge lies some 900–1400 m deep. It occurs in massive lizarditic serpentinites as a sub-horizontal body with complex outlines both in plan and in section. Serpentinites which overlie the deposit vary in thickness from 30 to 80 m. Kemistite is a friable variety of hydrotalcite–serpentinite which differs from its host serpentinite in containing 10–17% fine flaky hydrotalcite. Chemical determination of nickel, magnesium and iron extraction is used to isolate the useful mineral component.

Internally, the deposit has a relatively simple structure. Different grain-size varieties of kemistite form large horizontal or gently inclined lenses 15–250 m thick. Sand-sized fractions, 0.5–0.074 mm, predominate and account for 65–75% of the composition. Crumbly sand-sized kemistite predominates at the edges of the deposit, where the nickel recovery rate drops sharply to 50–65%. Nickel and magnesium contents are uniform throughout the deposit.

The deposit consists of lizardite (71–73%) and hydrocalcite (22–24%); secondary minerals are chlorite, magnetite, calcite + siderite, hydrohematite; accessories – pyrite, pyrrhotite, pentlandite and ilmenite. Nearly all the nickel (76%) and magnesium (89%) occur in the serpentine, with 10% and 6% respectively in the talcite.

The origin of kemistites is not entirely clear. They are not a typical weathering product, since there are no indications here of a normal weathering crust. A characteristic feature of the kemistites, as distinct from the host serpentinites, is secondary low-temperature alteration involving H<sub>2</sub>O and CO<sub>2</sub> influx and hydrocalcite formation, loss of monomineralic composition and transfer of components in mobile form.

Thus, the value of kemistites as ores is due to special mineral–geochemical forms which are mobile in acid solutions under normal conditions. Despite the low nickel content in the ore, significant cost savings can be made thanks to the possible use of simpler hydrometallurgical processing techniques without any preliminary crushing and roasting stages. An additional and important positive factor in nickel extraction technology is the recycling of most of the acids and a presumed environmentally clean process which is achieved in a closed system.

*Chromite mineralization* is encountered in the lower part of the transition zone in the Aganozero block, where an extensive 3 m thick stratiform horizon that stretches for over 10 km has formed in rhythmically interlayered rocks in a peridotite–pyroxenite member, constituting a finely-banded olivine–chromite cumulate (Sokolov, 1987; Kratz, 1983). Interstitial material in the rock is made up of large poikilitic augite and bronzite crystals, including olivine and numerous small chromite grains. Chromite forms fine, relatively evenly dispersed disseminations, thin layers and clustered aggregates of massive ore. Chromite averages 45% in the ore horizon (Sokolov, 1987). From the cation ratio, the ore chrome spinel is close to that in the Bushveld, Stillwater and Great Dyke intrusions. The chromite is characterized by a higher iron content and by high chromium and titanium. The presence of a chromite horizon and the widely dispersed chrome spinel content in the transition and ultrabasic zones make it reasonable to expect new ore horizons to be discovered.

*Ore occurrences in the Lukkulaivaara intrusion.* Recent exploration in a nickeliferous layered intrusion suite of peridotites and gabbro–norites in the Karelia–Kola region has enabled a platiniferous horizon in the Lukkulaivaara intrusion to be identified and traced. It belongs to the Olanga group of layered intrusions, the others being Tsipringa and Kivakka. They are located in the northern part of the Kuola–Vygozero rift belt in the Panajärvi region and were emplaced during the Karelian tectonomagmatic cycle. Cutting Late Archaean migmatite–granites, the intrusions in turn experienced crushing at the margins and are broken into separate blocks, related to superimposed folding, which is considered to be a Lower Proterozoic event. Amphibolization in the marginal portions is related to this event. The isotopic age of the

rocks forming the intrusion has been estimated to be 2430–2450 Ma (Sokolov, 1987; Turchenko, 1992).

The Lukkulaivaara intrusion (Fig. 32) lies to the east of Lake Tsipringa. It is oval-shaped in plan view, slightly elongate in an E–W direction, and is around 10 km<sup>2</sup> in area (4 × 2.5 km). It shows all the typical features of the other layered intrusions belonging to the peridotite–gabbro–norite suite in this region. Its basal part consists of a thin marginal gabbro–norite zone, which gives way upwards to olivinite, peridotite, pyroxenite, interleaved with fine- and medium-grained leucocratic and mesocratic norite and gabbro–norite. At the top are amphibolized gabbro and gabbro–norite. The layers strike almost E–W and dip at 50–65° to the north. Thrust zones can be traced along the northern and southern contacts of the intrusion.

In the norites and gabbro–norites in the middle of the intrusion, where copper–nickel sulphide mineralization with platinoids was discovered earlier, a platiniferous horizon has been found which is traceable along strike and down dip. Minerals belonging to the platinum group metals (PGE) are also found on rare occasions in rocks other than this horizon. Platinum mineralization in this ore horizon is distributed in a narrow (up to 3 m) vertical range in the intrusion, including norites, plagioclases and also in a glomero-porphyrific (orthopyroxene + plagioclase) microgabbro–norite body containing coarse-grained and pegmatitic plagio-pyroxenite schlieren. Platinum

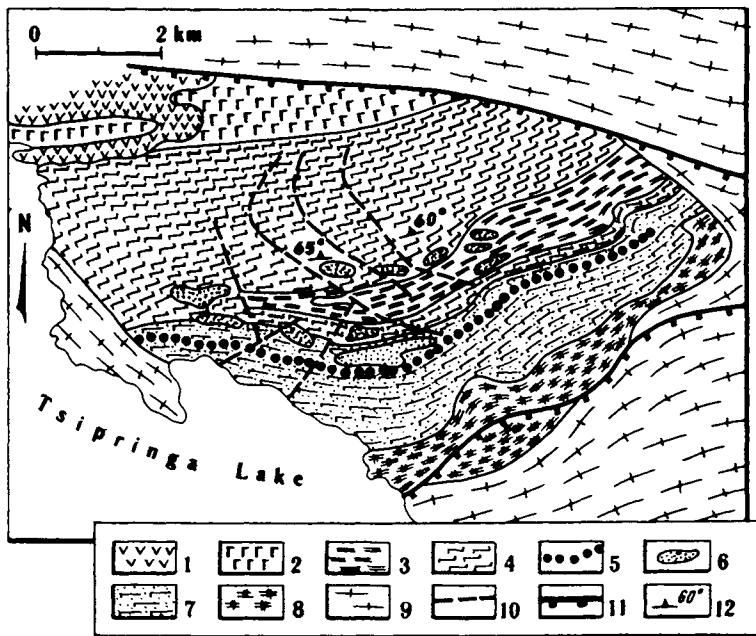


Fig. 32. Sketch showing geological structure of the Lukkulaivaara intrusion. 1) basalt; 2) amphibolized gabbro & gabbro–norite; 3) finely interbanded leuconorite & anorthosite; 4) gabbro–norite; 5) ore horizon; 6) microgabbro–norite; 7) norite; 8) interbanded dunite, olivinite, pyroxenite; 9) migmatite–granite; 10) faults; 11) thrust zones; 12) dip & strike of ig. layering.

group elements are always associated with sulphide-bearing zones, although the degree to which platinoid minerals are concentrated there shows no correlation whatsoever with the overall sulphide enrichment (Grokhovskaya et al., 1989). PGE minerals occur both as sulphide aggregates and among the rock-forming minerals.

In the sulphide-rich zones, the sulphides form several mineral associations, of which the most widespread are rich chalcopyrite parageneses: pyrrhotite + pentlandite + chalcopyrite; pentlandite + chalcopyrite; millerite + bornite + chalcopyrite. Schlieren-type segregations in the coarse-grained and pegmatitic pyroxenites and in the microgabbro–norites have the assemblages chalcosite + bornite + magnetite with heazelewoodite and godlevskite (Grokhovskaya et al., 1989). Altogether 16 PGE minerals have been identified in the platiniferous horizon, including sperrylite, merteite, isomerteite, majakite, stillwaterite, kotulskite, moncheite, etc. (Grokhovskaya et al., 1989). The majority of these minerals are found in the sulphide assemblages where chalcopyrite predominates. The PGE mineralization in the coarse-grained and pegmatitic plagiopyroxenites that make up the schlieren segregations in microgabbro–norites is significantly different from that described above. It is genetically related to the millerite–bornite–chalcopyrite assemblage and is typical for sulphide-rich intrusions, with which copper–nickel ore deposits are associated. Moncheite, kotulskite, telargpalite, sperrylite, braggite and tulaminite have been discovered in these rocks (Grokhovskaya et al., 1989). Platinoids are unevenly distributed in the platiniferous horizon, in that the horizon contains separate layered ore deposits 1–3 m thick and extends along strike for up to 500 m with an average PGE content in the deposits of 5 to 7 g/t.

#### 2.4. *Molybdenum*

Precambrian molybdenum porphyry and copper–molybdenum porphyry type deposits have been discovered in recent years in the Superior province of the Canadian Shield, the Pilbara block in the western Australian Shield, in Sweden and in other places. Closely related types of deposit have been found more recently in the Kola–Karelia region of Russia. Molybdenum deposits occur in the Yalonvaara and Lobash deposit within the granite–greenstone terrain. The Pellapahk copper–molybdenum deposit in the Kolmozero–Voronya greenstone belt (Kola Peninsula) has been described above (Chapter 1).

*Karelian molybdenum deposits* are restricted to the edges of the Karelian craton at its boundaries with the Svecokarelian fold belt (Yalonvaara) and the Belomorian tectono-thermal reworking belt (Lobash). The deposits occur mainly in supracrustal assemblages in Upper Archaean greenstone belts and are associated with late-folding hypabyssal intrusions belonging to a granite–trondhjemite suite which cuts the volcano-sedimentary rocks in the greenstone belts. The intrusions have a three-phase structure: 1) metagabbro, 2) granodiorite and trondhjemite, 3) microcline–plagioclase and plagioclase granite porphyries.

Economic molybdenum enrichment in the *Lobash deposit* is a stockwork mineralization type (Fig. 33) restricted to a zone lying above the intrusion of unexposed leucocratic trondhjemite–porphyry stock-like bodies. A network of variously oriented

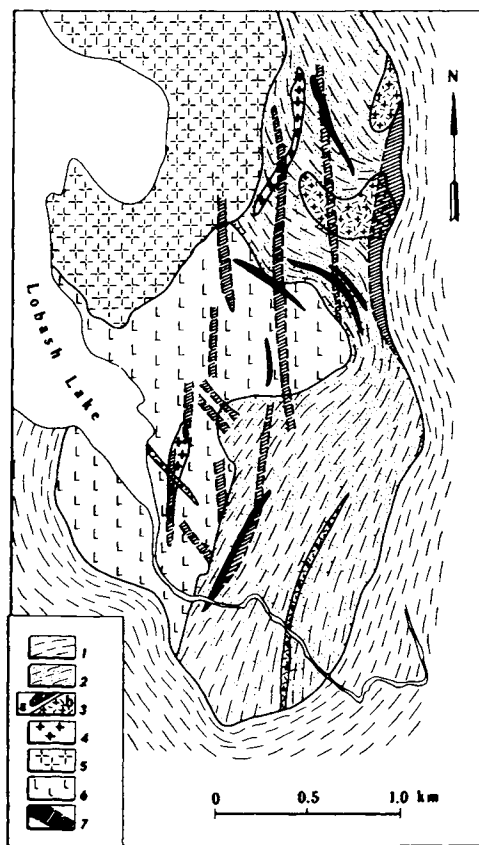


Fig. 33. Sketch showing geological structure of the Lobash molybdenum deposit. 1) Karel'ian metavolcanics & metasediments (2.35–2.45 Ga); 2) Lopian schists & metavolcanics (2.9 Ga); 3–6) Late Archaean gabbro–trondhjemite complex (~2.6 Ga): 3a) fine-grained porphyritic granite, 3b) fine-grained feldspathized and beresitized granite, 4) medium-grained trondhjemite, 5) coarse-grained trondhjemite & granodiorite, 6) metagabbro; 7) Mo ore zone.

quartz and epidote–quartz veinlets with pyrite–molybdenite mineralization is associated with a near N–S linear tectonic zone mainly within first-phase gabbros and basic metavolcanics. Furthermore, dispersed molybdenite mineralization is present in the apical parts of feldspathized trondhjemite–porphyries, intruded into Upper Archaean metavolcanics and schists.

Metasomatic alteration appears as pre-ore biotitization and amphibolization of metagabbros and schists, and syn-ore propylitization. Intense feldspathization, beresitization and weak fluoritization are evident in the apical parts of molybdenite-bearing trondhjemite–porphyries. Spatially, the mineralization displays weak zoning. In the centre of the deposit, above ore-bearing granite roofs, almost exclusively pyrite–molybdenite mineralization is developed, which is replaced towards the flanks by pyrite–pyrrhotite and still farther by polymetallic mineralization.

Indirect geological evidence suggests that the mineralization has an upper age limit of pre-Early Proterozoic. This is supported by the fact that the supposedly ore-bearing granites are overlain by Lower Proterozoic volcano-sedimentary formations, and by the complete absence of any kind of ore mineralization in the Lower Proterozoic rocks.

In order to solve the problems related to the time of formation of the molybdenum mineralization, an isotope geochronological study of the ores was conducted at the Academy of Sciences Institute of Precambrian Geology and Geochronology (St Petersburg) using Pb–Pb methods on sulphides, and the supposed ore-bearing granites with which molybdenum mineralization is associated (U–Pb and Rb–Sr methods; Larin et al., 1990; Ovchinnikova et al., 1995). The age of granites was determined by the U–Pb method on zircons. Three analyzed zircon fractions do not form isochrons, and the least discordant point on the  $^{207}\text{Pb}/^{206}\text{Pb}$  ratio gives an age estimate in the order of 2.6 Ga.

The Pb isotope data for ore sulphides (molybdenite, pyrite, galena) and feldspars from host granites show a significant range of isotopic compositions ( $^{206}\text{Pb}/^{204}\text{Pb}$  from 15.157 to 30.583,  $^{207}\text{Pb}/^{204}\text{Pb}$  from 15.247 to 18.291). On the Pb–Pb plot (Fig. 34) the data points form a single straight line that might be interpreted either as a primary isochron corresponding to Pb-isotope evolution in a source with variable  $\mu$  ( $^{238}\text{U}/^{204}\text{Pb}$ ) since 2.6 till 1.7 Ga, or as a mixing line reflecting mixing of Pb derived from high- $\mu$  and low- $\mu$  end members. In both cases a Proterozoic age for the mineralization is implied. A Rb–Sr study of metasomatically altered trondhjemites showed that the Sr isotopic composition was homogenized  $1818 \pm 73$  Ma ago. The large time interval (over 1 b.y.) separating the onset of metasomatic processes from granite crystallization is underlined by the very high initial  $^{87}\text{Sr}/^{86}\text{Sr}$  ratio, which is 0.791. A

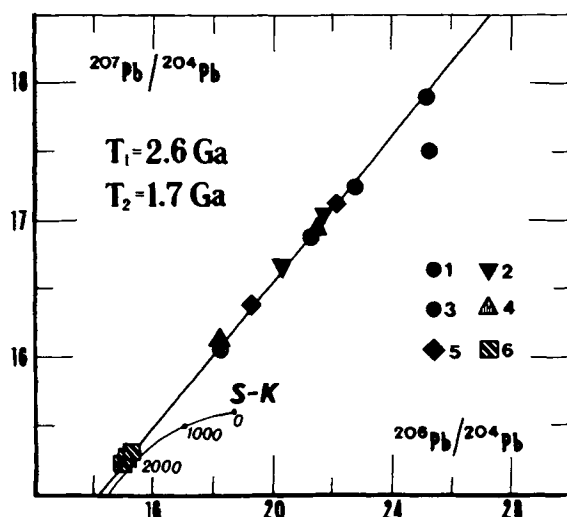


Fig. 34. Lead–lead plot for ore lead in galena, molybdenite and pyrite in the Lobash molybdenum deposit and common lead in feldspars from associated granites. 1) molybdenite; 2) acid-leached molybdenite; 3) pyrite; 4) acid-leached pyrite; 5) acid-leached feldspar, data corrected for *in-situ* U decay, 6) galena.

figure close to this value was obtained from the U–Pb system in sphene from these granites. Recently obtained Re–Os data on a molybdenite sample from the Lobash deposit (K. Suzuki, 1995, written communication) indicated that the Re–Os system in this ore mineral had been disturbed during post-crystallization alteration. The indication of an open-system behaviour in ore sulphides requires a reconsideration of Pb-isotope data. Two pyrites and two molybdenites were leached with dilute acid (1 N HBr) and Pb-isotope compositions were measured for both leaches and residues. Measurable differences in the isotopic compositions allowed us to construct four 2-point leach-residue Pb–Pb isochrons that gave a range of apparent ages from 1.7 to 2.9 Ga. The data show that the primary mineralization in the Lobash ore deposit was formed in the Late Archaean (probably in connection with the emplacement of spatially related granitoids). The ores experienced a superimposed Proterozoic event which caused disturbance of Re–Os and Pb–isotopic systems.

In addition to the molybdenum deposits in the Karelian granite–greenstone province described above, there are also those associated with meso-abyssal and abyssal potassic granites, for which a preliminary isotopic age of 2.75 Ga has been determined by the Pb–Pb zircon evaporation technique (unpubl. data of Neymark and Larin, Institute of Precambrian Geology and Geochronology). Ore deposits of this type – Päävaara, Kichany, Hukkala in Karelia, Matasvaara and Autajauri in Finland – are most often stockwork types, associated with microcline granites and located within granitic massifs at the roof of the body where it meets the supracrustal rocks, and also in the immediate exocontact zones. Host rocks are silicified and feldspathized to the point where ore-bearing feldspar metasomatites have formed.

The ore mineralization (molybdenite, chalcopyrite, pyrite, pyrrhotite, sphalerite, galena, scheelite, bismuthite) is associated with quartz, quartz–feldspar and feldspar veins and stringers. This type of molybdenum ore in Finland has yielded an age of 2.7 Ga using the Re–Os method and practically coincides with the U–Pb age for ore-bearing potassic granites – 2.66 Ga (Haapala, 1983).

## 2.5. Gold

Gold occurrences are found in the Kuola–Vygozero rift belt, within Lower Proterozoic volcanogenic (Mayskoye, cf. Turchenko, 1992) and sedimentary (Voitskoye) assemblages and belong to a gold–sulphide–quartz formation (Zhdanova et al., 1975; Kairyak et al., 1975).

*The Voitskoye occurrence* (description based on Sevzapgeologiya company material) has been known since the 18th century. It is in northern Karelia, 4 km SE of Nadvoitsy station on the St Petersburg–Murmansk railway line, on the right bank of the river Vyg where it flows into Lake Vygozero, and occurs in the Vygozero syncline. That segment containing the ore occurrence consists of a 500 m thick Lower Proterozoic terrigenous assemblage – interbedded quartzose sandstones and sericite–quartz schists. Within the schists is a gold-bearing quartz vein that strikes NE and dips steeply to the SE (Fig. 35). The vein extends for some 50 m along strike and over 200 m down dip and is 1.5 to 8 m thick. It splits up at depth. A sericite–ankerite–quartz metasomatic zone can be traced along the hanging wall and a pyrite–sericite–quartz zone along the footwall,

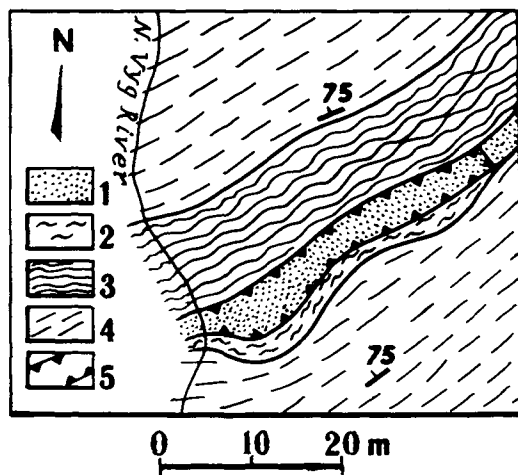


Fig. 35. Geological sketch map of the Voitskoye occurrence (based on Sevzapgeologiya materials). 1) ore-bearing quartz vein; 2) pyrite-sericite-quartz metasomatite; 3) sericite-ankerite-quartz metasomatite; 4) quartzose sandstone, quartzite, sericite-quartz schist; 5) outline of open-cast pit in worked-out part of vein.

5–20 m wide. Ore minerals in the vein are present as disseminations, large clusters and fine veinlets, and are represented by gold, chalcopyrite, bornite, native copper and chalcocite. Native silver, pyrite, scheelite, grey copper ore, covellite and malachite are present, but are rare. Gold occurs as isomorphic grains up to 2 mm across with a characteristic honeycomb surface; and chalcopyrite as clusters and large phenocrysts. The gold content in the worked-out part of the vein (to 130 m depth) was 10 g/t and copper 1.3%. Higher gold grades are associated with sulphide mineralization portions.

### 2.6. Massive sulphide

Greenstone belts in Karelia contain widespread massive sulphide mineralization, which can be divided into iron pyrites (Hautavaara, Parandovo, etc.), copper pyrites (Yalonvaara, etc.), massive sulphide-polymetallic (Zolotyie Porogi, "Golden Rapids"), copper-lead-zinc-massive sulphide (Vozhminskoye) compositional types (Sokolov, 1987). All these mineralization types with the exception of iron pyrites, are represented by small occurrences and occasional minor ore deposits such as Yalonvaara.

Pyrite deposits form a typical feature in Central Karelian greenstone belts in which the fairly major Hautavaara and Parandovo deposits are located, as well as the smaller Shuya, Nyalmozero, Chalka, Vedlozero and Bergaul deposits and numerous minor occurrences. The deposits display a very strong association with the dacite-rhyolite volcanosedimentary formation and are stratiform in type (Robonen et al., 1983). Despite regional metamorphism from greenschist to amphibolite facies and complete recrystallization, primary textural features have been quite well preserved in the rocks. Two volcanosedimentary rock groups can be distinguished in the regions where these

deposits occur: sequentially differentiated basalt–andesite–dacite–liparite and undifferentiated spilite–basalt (Robonen et al., 1983; Sokolov, 1978).

Host rocks for the mineral deposits are quartzite, sericite–quartz schist, siliceous tuff and tuffite. The deposits have tabular, podiform and rarely vein shapes, up to 25 m thick and 750 m long, and they are generally conformable with the country rocks. Massive pyrite occupies the central part of the deposits, with banded and disseminated pyrite–pyrrhotite ores on the flanks. Aside from the main ore minerals, pyrite and pyrrhotite, there are also small amounts of chalcopyrite, sphalerite, and rare examples of magnetite, galena, pentlandite, molybdenite, sparse chromite, ilmenite, barite and arsenopyrite. Ores can be divided into rich with over 25% sulphur and low-grade, containing 15–25% sulphur.

The mineral deposits and their host rocks have undergone two regional metamorphic events: a prograde stage from epidote–amphibolite to amphibolite facies, and a retrograde stage. Retrograde metamorphism is expressed in the replacement of prograde assemblages by lower temperature mineral associations – biotite + epidote + clinozoisite + quartz + carbonate. Genetically related to this stage is pyrrhotite mineralization, which formed as a result of pyritic ores having been redistributed by metamorphic fluids and the influx into the ore zone from the wall rocks and serpentinites of copper, zinc, arsenic, nickel, etc., creating discrete ore deposits consisting of economic concentrations of these components.

Evidence from the isotopic composition of lead from sulphides in the massive sulphide ores demonstrates that the processes which formed the mineral deposits occupied a significant time interval. Formation began 2.3–2.4 Ga ago with pyrite ores. Pyrrhotite ores are dated at  $1875 \pm 50$  Ma, reflecting the retrograde metamorphic event (Sokolov, 1978). Robonen and others (Robonen et al., 1983; Turchenko, 1978) have demonstrated that the ores formed in two stages: a volcanosedimentary stage, with which pyrite ore deposition is associated, and a metamorphic stage, causing pyrite ores to be recrystallized and regenerated, and metamorphic–hydrothermal pyrrhotite mineralization. An inherent feature of Karelian ore deposits are general indications of volcanosedimentary massive sulphide mineralization, the ore component source of which was basic volcanism.

*The Hautavaara deposit* is a suitable example to describe (Robonen et al., 1983; Sokolov, 1978). It occurs in the southern part of the Vodlozero–Segozero greenstone belt, 3 km from Hautavaara station on the Petrozavodsk–Sortavala–St Petersburg railway line and belongs to the NNE-striking ore zone which extends for over 30 km. Several other deposits have been explored in this same zone – Shuya, which forms a single ore field with Hautavaara, Nyalmozero, Vedlozero, Chalka and Ulyaleg, with Hautavaara being the largest.

The deposit is associated with an 800–900 m thick ore-bearing volcanosedimentary shale sequence, which has spherulitic dolerites from the undifferentiated formation above and below. At the base is a rhythmically-bedded tuffaceous quartz sandstone member with thin conglomerate interbeds, hornblende schists and dacite plagioclase–quartz porphyry bodies. Higher up in the section tuffaceous quartz sandstones, siliceous tuffites, chemogenic quartzites with acid tuff–conglomerate lenses and thin graphitic schist layers predominate. The rock succession containing the ore is overlain

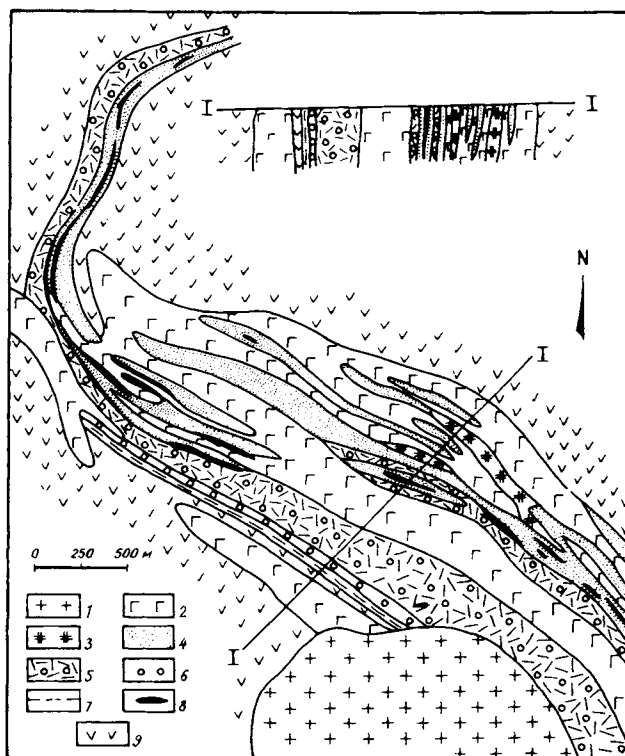


Fig. 36. Geological sketch map of the Hautavaara deposit (Robonen and Rybakov, 1983). 1) granite & granodiorite; 2) gabbro-dolerite; 3) serpentinite; 4) sericite-quartz schist, graphitic, quartzose & siliceous tuffites; 5) dacitic porphyry tuffs & tuffites; 6) tuffoconglomerate; 7) quartz-magnetite-amphibole schist; 8) pyrite deposits; 9) pillow dolerite.

by a thin, basic tuffo-conglomerate horizon, in which dolerites have been emplaced above the ores (Fig. 36). The ore zone can be followed for 7 km as an S-shaped fold in plan view. Its SE limb strikes NW ( $330\text{--}340^\circ$ ), which swings round through N to S to NE ( $040^\circ$ ) in the NE limb.

The bulk of the ore deposits are restricted to the contact between quartzose tuffaceous sandstones and quartzites with graphitic schists. In part some ore bodies lie in the lower half of the graphitic schist member. The entire volcanosedimentary assemblage hosting the ores is cut by metamorphosed gabbro-dolerite sheets and dykes, ultrabasic rocks and porphyritic dacites. The mutual relationships with the ore show that the intrusions are younger than the pyrite mineralization but older than the pyrrhotite. Several parallel and *en échelon* ore bodies have been delineated in the deposit, the largest being the Main ore body and the Parallel ore body.

The Main ore body is an asymmetric lenticular sheet, 750 m long and 22 m thick at its maximum at the NW termination, and traceable at depth to 480 m. Its dip varies from SW to NE at angles of  $80\text{--}87^\circ$ , concordant with the general dip of the wall rocks.

The ore consists of massive banded pyrite and pyrrhotite–pyrite to 80–120 m depth. Massive pyrite ores are dominant from 80 to 120 m, and at 250–300 m depths, beds of country rock appear in the ores.

Other ore bodies have smaller dimensions but the same shape and structure. A characteristic feature of the ore bodies in the deposit is their banded or layered structure; as a rule, the bodies consist of several pyrite ore beds, separated by thin sericite–quartz schist and quartzite intercalations, containing irregularly disseminated pyrite phenocrysts. A gradual transition from densely disseminated to massive pyrite ores is frequently observed. Pyrite ore–wallrock contacts are everywhere conformable. Pyrrhotite stringers cut the pyrite bodies and are mostly developed in zahlbands and on the flanks of the ore bodies. Graphite schists contain particularly large amounts of pyrrhotite.

### 2.7. Shungite

Shungite rocks occur in the middle member of the North Onega Fm, which is in the lower part of the sequence in the Onega depression. It is 400 m thick and consists in the main of ash tuffs with subordinate dolomite, siltstone and argillaceous shales. Most rocks in the member contain a few percent shungite and it is considered to be a productive unit. Present-day outcrops of the productive unit in a strip along the western and northern contours of the depression (the Lake Onega shoreline) form the West and North Onega regions with all the known high-carbon shungite deposits – Zazhogin, Faimoguba, Chebolak and Shunga (Sokolov, 1975, 1981, 1982, 1987). Rocks in the North Onega Fm have experienced weak regional metamorphism – the initial stages of the greenschist facies, which is a necessary condition for evaluating the engineering properties and economic significance of shungite as a mineral raw material. Low-carbon shungitic schists with around 1% free C (the Nigozero deposit) yield shungizite, a lightweight concrete filler; high-carbon schists with over 20% free C can be used in metallurgical processes as reducing agents, fluxes or as a substitute for graphite.

*The Zazhogin deposit* is used as a case study, the description being based on materials owned by the Sevzapegeologiya Production Company. The deposit lies in the NE part of the North Onega peninsula, 80 km SE of the town of Medvezhegorsk. A large percentage of the area of the North Onega shungite region (1000 km<sup>2</sup>) containing this deposit, consists of shungitic rocks. Linear folds striking NW (330°) are developed in the region, extending for 30–50 km in 8–10 km wide synclines and 2–5 km wide anticlines with synclinal limbs dipping at 10–30° and anticlinal limbs steeper, up to vertical. Suitably thick (over 30 m) conditioned shungitic rocks in the Zazhogin deposit have been discovered only in the northern half of the Tolvuy syncline (Fig. 37).

The deposit extends for 15 km to the NW, is 4–7 km wide, and occupies an area of some 80 km<sup>2</sup>. Nine shungite horizons have been counted in the productive rock assemblage, horizon IV being the thickest. Later generation folds parallel to the main axis of the structure complicate the syncline within the confines of the mineral deposit. Dome structures appear in second-order anticlinal axes, measuring 300–700 m across. Shungite horizons form bulges in dome cores.

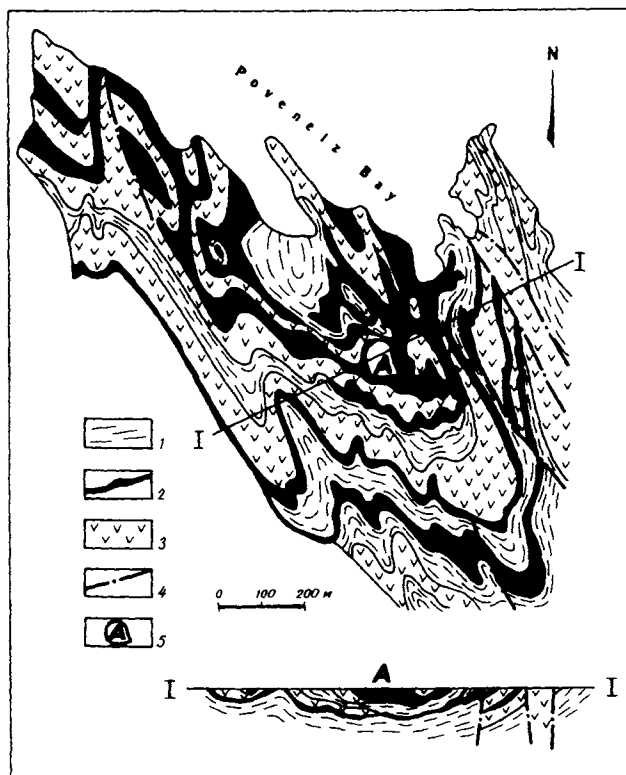


Fig. 37. Geological sketch map of the Zazhogino deposit (based on Sevzapgeologiya materials). 1) siltstone, dolomite, tuff; 2) shungitic rocks; 3) metadolerite sills & lava flows; 4) faults. A - Part of Maksovo deposit surveyed in detail.

The massive-brecciated shungite rocks forming the bulges contain almost no gangue as dispersed pyroclastic material and barren beds. Bulges which have been investigated are oval in plan and up to 200–700 m across. The thickness at the centre of the deposits is 40–120 m and there is a gradual wedging-out towards the periphery. The highest quality raw material and the most suitable for extraction is concentrated in the Maksov deposit, which contains most of the deposit reserves. The deposit is lenticular, slightly extended along an anticline, 700 m long by 500 m wide and up to 120 m thick at the centre and thinner at the edges until wedging out completely.

In the middle of the area where the deposit crops out, its top and bottom coincide with the top and bottom of horizon VI. At the periphery the deposit occupies the middle part of the horizon, where it consists of brecciated and massive shungite rocks. Brecciation increases towards the top of the deposit and in plan view towards its centre. The centre of the deposit is exposed, while on the flanks it is overlain by younger unproductive beds of shungitic rocks.

The main components in the rocks that form this deposit are free carbon as shungite, and quartz. In brecciated and massive varieties, the free carbon and quartz total is

85%;  $\text{Al}_2\text{O}_3$ , mostly in sericite, is 3.5–5%; 1.5–2.5%  $\text{Fe}_2\text{O}_3$ ; and 1–2% each for S,  $\text{CO}_2$ ,  $\text{K}_2\text{O}$ , CaO, MgO and other elements. The maximum free carbon content, 35–45%, was found in an area belonging to the long axis of the deposit. Quartz increases from the base to the middle, to 60–65%, then decreases towards the top. The main quality index for the raw material is the free carbon (shungite) content, the minimum content of which has been defined to be 20% for the deposit.

## Belmorian Belt

V.A. GORELOV

The Belmorian belt is a structure which has experienced tectonothermal reworking. Separated from the Karelian and Kola terrains by deep faults, the belt extends in a NW direction for 1500 km and is up to 200 km across. Its central and southern portions are covered by the White Sea and by the Phanerozoic sedimentary cover (Fig. 2). Based on current evidence, the belt is considered to be a complex structure which underwent multiple stages of reworking from Early Archaean to mid-Proterozoic time.

Along the Belmorian belt from its NW flank to the latitude of Lake Engozero in the SE lies a clearly delineated zone of muscovite and ceramic pegmatites with two economic regions – Yona and Chupa–Loukhi (Fig. 3). The zone is around 500 km long by 50–200 km wide. No other economically significant targets for other types of useful minerals have been found in the Belmorian belt.

### *1. Ore deposits and occurrences*

#### *1.1. Muscovite*

Muscovite deposits in the region are genetically and spatially related to a series of muscovite pegmatites which are now considered to have a metamorphic origin (Sokolov 1988; Salye, 1975, 1976; Sokolov, 1970). The pegmatites occur in Belomorian (Archaean) gneisses, metamorphosed under kyanite–sillimanite type amphibolite facies conditions, migmatized and granitized to varying degrees.

Geologically, the base of the Belomorian zone is a polyphase deformed, poly-metamorphic complex of Belomorian gneisses: 1) mainly biotite, sometimes hornblende–biotite gneiss; 2) high-alumina garnet–biotite and productive biotite gneiss; 3) amphibolites, hornblende and hornblende–biotite gneiss and associated garnet–biotite and kyanite–garnet–biotite gneiss. Associated with the metamorphic complex are metamorphosed intrusive diorites with corona textures (“drusites”), granites and pegmatites of various ages (Sokolov, 1987; Gorlov, 1975). The Belomorian fold belt displays two main trends over much of its area (Gorlov, 1975), i.e. two mutually perpendicular fold directions – NE and NW (Fig. 38). The NE-trending folds are almost at right angles to the general strike direction of the rocks and form a huge fan across their length (35 km), open to the NE. The folds are up to 8 km wide and plunge towards the NE. In vertical section they are disharmonic and display the most developed forms in the aluminous gneisses. The NW folds are oriented parallel to the

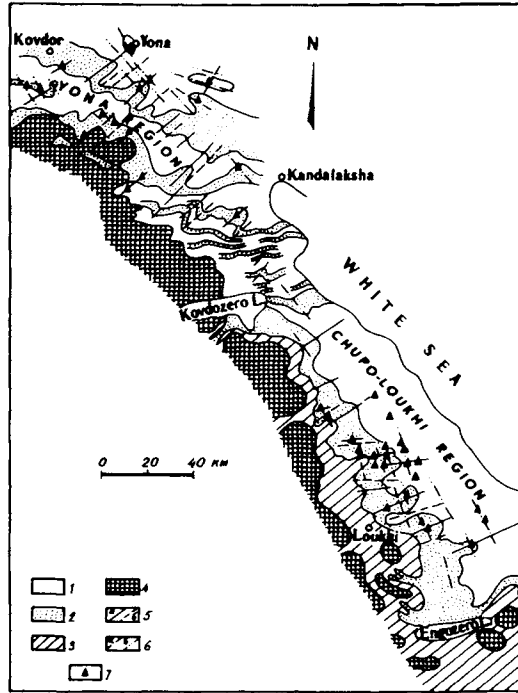


Fig. 38. Geological sketch map of the Belomorian muscovite and ceramic pegmatite zone (Gorlov, 1975).  
 1) biotite & hornblende gneisses with thin amphibolite bands and lenses; 2) high-alumina gneiss;  
 3) Kotozero amphibolites & gneisses; 4) undifferentiated Belomorian basement granite-gneisses; 5) NE  
 fold axes: a) anticlines, b) synclines; 7) pegmatite vein clusters.

western edge of the belt and are developed mostly in the gneisses that lie structurally above the aluminous gneisses. In areas where the two phases are seen together, the NW folds are superimposed on those trending NE, forming a cross-shaped interference fold pattern which is very prominently displayed in both mica-bearing regions in the Belomorian zone. These two regions are separated by an area where the cross-folding effect is weakly developed. Pegmatite veins known here have no economic importance. Isotopic studies put the mica pegmatites at 2100–1750 Ma, i.e. Proterozoic (Nalivkin and Yakobson, 1985; Rundqvist, 1986a).

A very strong control is evident for the muscovite pegmatites: they are all associated with garnet–biotite, kyanite–biotite, biotite and two-mica plagioclase gneisses, with a mica content not less than 15% (Rundqvist, 1986a). Favourable structures for the formation of pegmatites with high-quality muscovite are those within which tectonic and metamorphic processes concluded with the stage at which muscovite pegmatites were generated. Subsequent events – superimposed metamorphism – led to the deformation of the mica, with a sharp reduction in quality, to the point where it is completely unusable.

Depending on the style of pre-pegmatite fault tectonics and the physico-mechanical properties of the country rocks, the pegmatites form zones of cross-cutting or strike-

parallel veins. Vein morphology is variable, with lenticular and tabular bodies predominating. They are a few metres wide, although some are up to 20–30 m and their length along strike is from tens to a few hundred metres. Veins are traceable down dip and hade for up to 600 m. They extend for more than 1 km at depth, as proven by drilling evidence.

In terms of mineral composition, microcline–plagioclase varieties are dominant among the muscovite pegmatites, with occasional essentially plagioclase veins with well-expressed differentiation. Muscovite in the quartz–muscovite core of these veins displays a megacrystic form, with a characteristic ruby or brown colour. Muscovite pegmatites formed during a single complete cycle of pegmatite formation. In polyphase pegmatites the muscovite is generally low-quality.

Several economic pegmatite fields are known in the mica-bearing regions of the Belomorian belt, named after particular deposits: Yona, Rikolatva and Neblogorsk in the Yona region of the Murmansk province; Tedino, Chupa, Malinovaya Varaka and others in the Chupa–Loukhi region in Northern Karelia. Most are being exploited using underground methods.

*The Rikolatva deposit* is presented as a case study, based on information from the Sevzapgeologiya Production Company, and Proskurina (1974). This deposit is located 50 km SE of Kovdor in the fold closure of the Vysokogora anticline. The fold core contains garnet–biotite and biotite gneisses belonging to the Rikolatva productive formation which is at least 850 m thick, while the periphery consists of amphibole gneisses and amphibolites (Fig. 39). At least two fold phases have affected the rocks, with NE and WNW axial trends, producing a rather complicated pattern, with limbs dipping generally north: the N limb dips at  $50^\circ$ , and the S limb at  $70^\circ$ . Local domes formed within the Rikolatva structure due to folding: the Central, Western and Southern arches, whose shape is emphasised by basic intrusions intruded along litho-

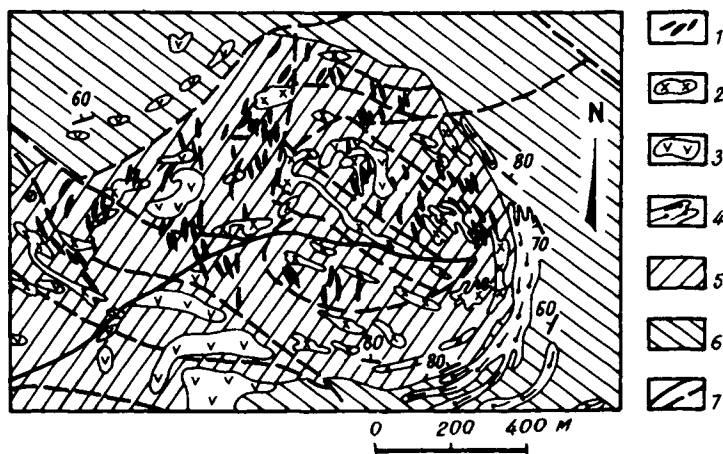


Fig. 39. Geological sketch map of the Rikolatva deposit (Gorlov, 1975). 1) pegmatite veins; 2) granite-gneiss, granite, aplite; 3) gabbro-norite; 4) layered amphibolite; 5) Rikolatva kyanite-garnet-biotite & biotite gneisses; 6) biotite and hornblende-biotite microcline-bearing gneisses; 7) faults; 8) dip and strike of foliation.

logical banding in the structures. These domes appear to have been peculiar structural traps for pegmatite bodies, the largest being the Central dome, surrounded on its north side by a gabbro–norite intrusion.

The deposit is bounded to the S, SW and NW by faults which intersect on the west flank where a series of thrusts developed to produce the closure pattern. The Rikolatva structure is divided into several blocks by faulting. Pegmatite veins formed in this fault system and along accompanying fractures, creating the Central, Western and Southern vein fields. Essentially microcline veins formed close to the faults, with only low economic mica contents. Mica increases away from the faults, eventually reaching significant concentrations.

Igneous rocks make up about 25% of the deposit's area, the oldest being Early Proterozoic basic and ultrabasic rocks, now altered to amphibolite, lying between lithological bands. These were followed by gabbro and peridotite with corona textures (the so-called "drusite" suite), which cut the fold structures in the deposit. The latest-formed igneous rocks are plagioclase–microcline granite veins and pegmatites.

The deposit is characterized by a high concentration of pegmatite veins which number more than 1100, including over 200 with economic mica content. The greatest pegmatite density is in the central and northern part of the Rikolatva structure. Around two-thirds are not exposed at the surface. Muscovite pegmatites fall into three fracture systems: NE (015–030°), N to S and NW (300–330°). Most of the veins in the west strike NNE, and in the east to NW. Some veins have several different strike directions simultaneously, resulting in a complex shape. Most are cross-cutting veins and are simple tabular bodies with steep easterly dips. The overall pitch of the veins, vein zones and the ore field is 60° to the north. In plan view, veins measure from a few tens of metres up to 200 m, averaging 80 m. Thicknesses range from a few cm up to 22 m, 1–2 m being the norm. There is an overall decrease in vein thickness from west to east across the deposit.

According to L.L. Grodnitsky, the deposit has five pegmatite vein types, one of which, Va, has the main economic significance. Morphologically, these are large bodies with an irregular lenticular shape, discontinuous, pinched out and with apophyses. Internally, they display a partial zoned structure of plagioclase and microcline with quartz blocks in the middle of the veins which can be followed for tens of metres and usually surround blocky microcline. Microcline pegmatite occupies up to 50% of the volume of a vein and is usually concentrated in intermediate and central sectors of a vein. Large tabular biotite crystals are common, sometimes intergrown with muscovite. Blocky-graphite texture is widely developed. Vein zahlbands contain an almost continually traceable fine-grained plagioclase pegmatite fringe. In addition to the quartz–muscovite complex, a muscovite pegmatite type is also widespread, usually at the boundary between blocky quartz and blocky microcline, less often with plagioclase. Muscovite in this vein type ranges from 8 to 55 kg/m<sup>3</sup>, the average being 20–25 kg/m<sup>3</sup>. Reserves are up to 2,500 tonnes of muscovite. The muscovite in cross-cutting veins provides a good source of mica for use in radio spares and capacitors. The average economic yield from mica-rich veins in the deposit is 46%. A by-product from the pegmatite veins is lump microcline, pure microcline pegmatite with a high potash value (4.4–7.6), and quartz.

*The Loukhi-Chupa mica region* occurs in the SE part of the Belomorian mica-bearing belt. Its geological evolution was punctuated by three tectonic cycles of deformation and synchronous magmatic activity. The main elements in the Late Archaean block-fold structure are the NW-trending Primorye ("Coastal") and Western anticlinoria (second-order structures), separated by the Chupa fault-bounded basin. These folds are complicated by Early Proterozoic NE-trending fault zones with large displacements in plan, which led to the formation of NE block-fold structures, late block-dome structures with unevenly expressed granite diapirism in domal uplifts, and with shear zones around their edges. During the latest event in the geological evolution of the region – the Svecofennian cycle – a discontinuous system of discrete superimposed shear zones and faults was established that controlled the localization of the economic muscovite pegmatites. The association of economic pegmatite veins with discrete late shear zones, which were accompanied by local high-pressure, medium-temperature metamorphism (kyanite-muscovite subfacies of the amphibolite facies and the high temperature subfacies of the epidote-amphibolite facies) is considered to be the main structural and metamorphic factor controlling the economic mica pegmatites in Chupa high-alumina gneisses, for which a lithostratigraphic control on the pegmatite veins had previously been established.

Economic mica pegmatite mineral deposits (Tedino, Malinovaya Varaka, Chupa, etc.) are situated in the Chupa basin, filled mainly with polymetamorphosed Chupa high-alumina plagioclase gneisses, and are controlled by third and fourth order block-fold, block-dome and flexural structures. The Tedino deposit is described as a typical example, using material held by the Sevzapgeologiya Production Company.

*The Tedino muscovite pegmatite deposit* includes part of the mica pegmatites associated with fourth-order anticlinal highs which affect the Tedino syncline, itself a third-order structure. Within the deposit, three blocks of pegmatite veins can be identified: Eastern, Western and North-western. The blocks consist of fine-grained, indistinctly banded, weakly foliated garnet-biotite gneiss with a steep (60–70°) ESE dip, separated by an assemblage of medium-grained, banded, highly sheared garnet-biotite gneiss (Fig. 40). Regarding a structural classification, this deposit would be treated as a mixed type of pegmatite field, in which three different groups are combined, depending on their mode of occurrence: cross-cutting, banding-parallel, and inter-boudin.

Economic mica veins are associated with discrete zones of late, repeated shearing and local metamorphism. The veins strike NW and NE and fill a system of tension gashes which cross-cut at right angles, and exfoliation fractures. Groups of cross-cutting and banding-parallel pegmatites, controlled by gentle NE late anticlines and open flexures, have conjugate geometry both in plan and in section: as the brittle behaviour of country rocks increases, the vein bodies change shape and mode of occurrence. Cross-cutting veins in relatively brittle rocks become banding-parallel in relatively ductile rocks. A necessary accompaniment to this is the appearance of repeated shearing and metasomatism during retrograde metamorphism of the kyanite-muscovite gneisses.

Cross-cutting veins are represented by slab-like, lenticular or distinct bodies, 30–50 m to 200 m strike length, 100–200 m down dip and 0.5–10 m thick. Filling

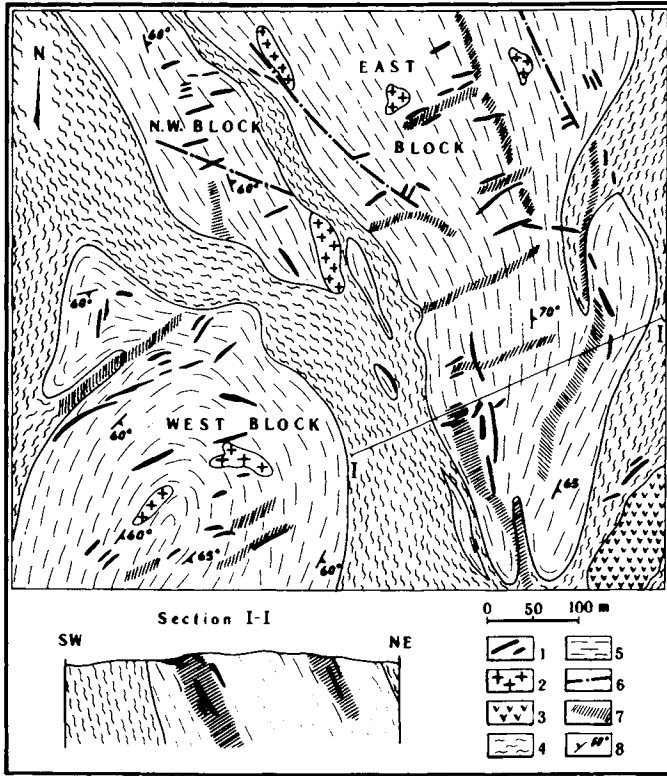


Fig. 40. Geological sketch map showing structure of the Tedino deposit (based on Scvzapgeologiya materials). 1) pegmatite veins; 2) granite; 3) peridotite; 4) medium-grained banded, intensely sheared garnet-biotite gneiss; 5) fine-grained indistinctly-banded, weakly sheared garnet-biotite gneiss; 6) shear zones; 7) zones of secondary schistosity favouring pegmatite vein emplacement; 8) dip and strike of gneissose banding.

variously-oriented fractures, the veins form knee-shaped bends. They form groups up to 70–170 m wide, separated by muscovite-free gaps 80–200 m wide. Around 40% of the reserves in the deposit are accounted for by the cross-cutting veins.

Veins emplaced parallel to gneissose banding are relatively rare, but since they have large dimensions and a high mica content, they account for some 60% of all known reserves. These veins have a lenticular shape, mostly complex, with sharp outlines, pinch-and-swell form and offshoots. Strike length varies from 40 to 300 m, 80–90 m being the average. Down dip extension exceeds 50–70 m, reaching 110 m; they are 2–3 m thick, and up to 16 m thick in boudin swellings.

Five pegmatite vein types have been identified on the basis of mineral composition, structural and textural features, distribution pattern, and variations in economic mica content. Type III, with 90% of all extracted mica, forms the main economic type: these are zoned microcline pegmatite veins with a blocky texture.

Economic veins typically have a relatively high average muscovite content: 56 kg/m<sup>3</sup>, the range in individual veins being from 9 to 134 kg/m<sup>3</sup>. The mica in the

deposit is high quality, with an average hand-picked yield of 36% from the raw material, including around half that destined for use in televisions, capacitors and radio spares. Quartz and lump microcline in small quantities can be extracted from the veins.

### 1.2. Ceramic pegmatites

The European part of North Russia has more than four-fifths of all known reserves of high-quality ceramic raw materials, associated with microcline granite pegmatites. Most ceramic pegmatite deposits occur in the same zones as the muscovite pegmatites, and occupy a lower position in the section relative to the mica pegmatites and usually found in microcline-bearing biotite–amphibole gneisses and amphibolites (Gorbunov, 1981). As is the case with the mica pegmatites, ceramic pegmatites are represented by cross-cutting vein bodies, often with an irregular shape and variable thickness, forming fields containing tens and hundreds of veins. The most important targets within the Belomorian belt are Hetolambi and Pirtima in North Karelia and Kuru-Vaara and Otradnoye in the southern Kola Peninsula (Fig. 41). All the targets are situated in areas which have been opened up economically and have a suitable transport infrastructure. Ceramic pegmatite resources in the Belomorian belt assure the development of high-quality microcline, microcline pegmatite and quartz–feldspar mineral raw material extraction for a long period in the future.

*The Kuru-Vaara deposit is chosen as a case-study. It is located 6 km from the Yona railway station on the Kandalaksha–Kovdor branch line in the Upolaksha ceramic*

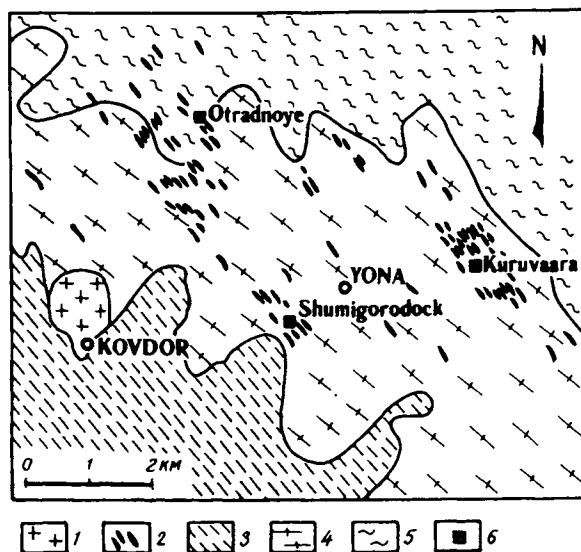


Fig. 41. Location of ceramic pegmatites in the Yona region (Gorbunov, 1981). 1) Kovdor alkali-ultrabasic intrusion; 2) ceramic pegmatite veins; 3) kyanite–garnet–biotite & garnet–biotite gneisses; 4) hornblende & biotite gneisses, amphibolite; 5) biotite gneiss & granite–gneiss; 6) ceramic pegmatite deposits.

pegmatite zone (Gorbunov, 1981). Several fields of ceramic pegmatites are known in this zone, including Shumigorodok and Otradnoye (Fig. 42), Otradnoye being the largest. The Kuru-Vaara deposit contains over 200 pegmatite veins with ceramic raw material reserves exceeding 50 m.t. in open-cast pits, and has been successfully exploited. The pegmatites occur in Keret gneisses on the northern limb of an E to W anticlinal flexure, and occupy a NW system of steep fractures oriented oblique to the strike of the gneisses. The gneisses are biotitic to amphibolitic, with biotite and garnet-biotite varieties predominating. Small stock-like gabbro-amphibolite bodies intrude the gneisses. In the best studied part of the pegmatite field, prepared for exploitation by open-pit methods, over 100 economic pegmatite bodies 3-10 m wide have been exposed. Generally the bodies are well differentiated with increasing grain size towards vein centres and with a change from apographic and graphic textures to blocky. The axial parts of some veins

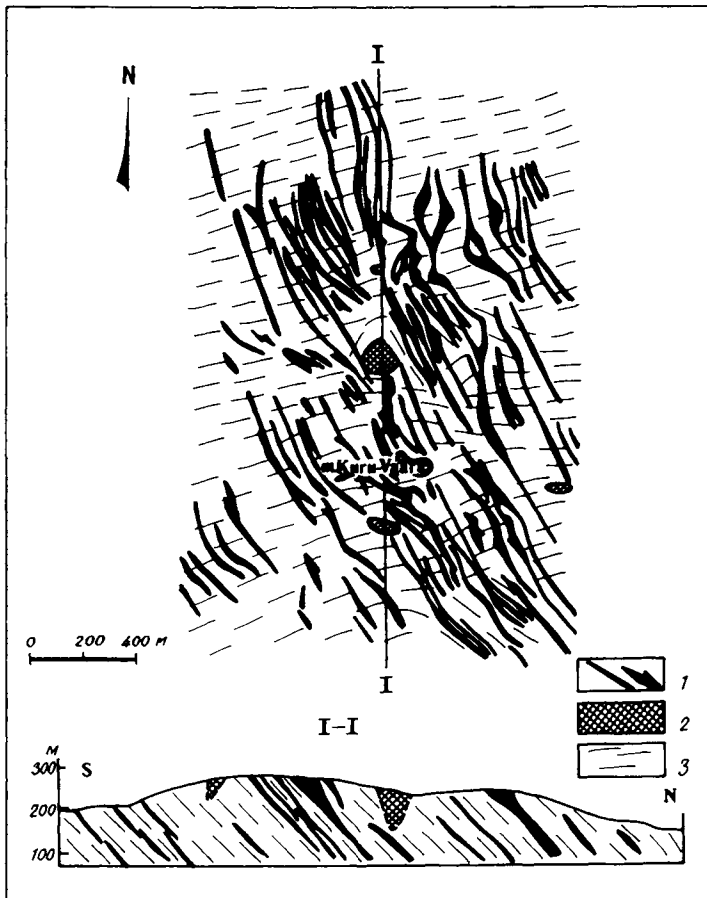


Fig. 42. Geological sketch map of the Kuruvaara deposit (simplified from Gorbunov, 1981). 1) ceramic pegmatite veins; 2) gabbro & gabbro-amphibolite; 3) garnet-hornblende, garnet-biotite, biotite & hornblende-biotite gneisses.

have blocky quartz. The main minerals in the pegmatites are microcline, quartz and plagioclase, with minor amounts of biotite, muscovite, magnetite, rare tourmaline, orthite, zircon, sphene, apatite and garnet. Microcline varieties predominate in the deposit; the microcline is high-quality, with 11–12%  $K_2O + Na_2O$  and  $K_2O/Na_2O$  ratio  $> 3$ . Harmful impurities are  $Fe_2O_3 - 0.1-0.15\%$  and  $CaO - 0.4-0.5\%$ .

This Page Intentionally Left Blank

## Ladoga Belt

V.A. GORELOV and A.M. LARIN

The Ladoga Belt comprises the area around the NW shores of Lake Ladoga and belongs to the Early Proterozoic Svecokarelian domain, which lies mostly in Finland and Sweden. To the NE, the Ladoga Belt is in faulted contact with the Karelian terrain, and to the SE it is covered by platform sediments (Fig. 2).

The northern part of the belt is made up of the Lower Proterozoic Ladoga complex, while the central and southern parts contain Archaean granite–gneiss domes, basement inliers which were reworked during the Early Proterozoic. Domes are enveloped by Ladoga complex rocks, a supracrustal sequence consisting of the Sortavala Group and the overlying Ladoga Group. At the base of the succession in the Sortavala Group are quartzite–carbonate units alternating with volcanogenic–carbonate–schist units and at higher levels with Ladoga Group flysch-type schists. The Ladoga complex is intruded by syn-folding and post-folding granitoids, as well as by basic and ultrabasic bodies. Metamorphism in the Ladoga belt varies from greenschist to granulite facies, in a single Barrovian-type zonal sequence (Rundqvist and Mitrofanov, 1992).

Hoglandian volcanogenic rocks – comagmatic anorthosite–rapakivi granite suites – are developed only to a very limited extent. They have been identified on Hogland island near the southern edge of the Vyborg massif and in roof pendants of this massif. Volcanic rocks form a bimodal complex and occur interleaved with coarse clastic terrigenous rocks.

The Ladoga belt is part of the Ladoga–Bothnian ore belt, characterized by varied ore mineralization types (Sokolov, 1987; Khazov, 1982). Occurrences belonging to several ore formations are found in the belt: copper pyrites–polymetallic (Mursula, Varalahti), copper–nickel (Armin-Lampi, etc.), titanomagnetite (Velimäki, etc.). Economic deposits belonging to this formation are found in Finland. Associated with the anorthosite–rapakivi granite suite are titanomagnetite, polymetallic, tin, rare metal and fluorite deposits and occurrences. In the Ladoga belt, tin and ceramic pegmatites have economic significance, while tungsten and graphite may be considered to have economic potential.

## 1. Mineral deposits and occurrences

### 1.1. Tungsten

Tungsten mineralization in the Ladoga belt, represented by small skarn deposits and occurrences, was discovered in the 1960s during 1:50,000 scale geological surveying (Makarova, 1971). Ore targets in this formation – Latvasyrjä, Mensunvaara, Kommunar, Heinäjoki, Jokiranta, Jakkima) occur in the Savo–Ladoga zone of the Svecokarelian fold belt within Early Proterozoic Sortavala carbonate horizons which surround granite–gneiss domes, and are associated with late orogenic granitoids (Fig. 44). Small granite intrusions and dykes are located along predominantly NE-striking fault zones. This formation is a product of a crustal palingenic–anatectic magma, formed during the concluding stages of partial melting (“ultrametamorphic” processes).



Fig. 44. Structural sketch map of the Sortavala ore region (after Ivashchenko, with the author's amendments). 1) late-orogenic granite; 2) granite–gneiss domes & migmatites; 3) early-orogenic granitoids; 4) metagabbro, quartz diorite; 5) metadolerite, metagabbro–dolerite, gabbro–amphibolite; 6–8) Sortavala Gp: 6) dolomitic marble, calciphyre, magnesian & apomagnesian lime skarns (u. carb. horizon), 7) amphibolite, amphibole–biotite & graphite schists with thin skarn layers, 8) magnesian & apomagnesian lime skarns; 9) quartz–biotite schist, migmatite, quartzite, quartzose sandstone (Ladoga Gp); 10) faults; 11) tungsten skarn ore occurrences.

The K–Ar muscovite age of rocks belonging to this formation is 1875–1897 Ma. Geochemically, it belongs to an ultra-acid K–Na series of potentially W-bearing granitoids (Ivashchenko, 1987). Compositionally the granitoids range from fine-grained biotite granite to pegmatitic muscovite and tourmaline–muscovite granites. They possess a characteristic geochemical signature across the entire spectrum of rare elements: Mo, W, Sn, Nb, Be, Li, Pb. Accessory minerals are apatite, columbite, scheelite, monazite and thorite. Rare-metal pegmatites are associated with the pegmatitic granites of this suite. Albitization, muscovitization and greisenization are widespread both in the granites themselves and particularly so in the pegmatites. Higher W contents (8–11 ppm) in biotites and feldspars indicate their potential tungsten-bearing nature.

Tungsten is the main ore element in the deposit, accompanied by Be, Mo, Pb, Zn, Cu and Bi. Magnesian-lime skarns are the dominant metasomatic rock type. Skarn bodies are up to 5–7 m wide and 400 m long. Their composition is pyroxene, pyroxene–garnet and vesuvian; closely associated with them are pyroxene–plagioclase and pyroxene–scapolite skarn-like rocks. Iron-rich pyroxenes are the main variety – hedenbergite and salite, while the garnet is mainly grossular. Skarn emplacement was controlled by exfoliation fractures parallel to lithological banding. The most favourable members for skarn formation are finely interbanded aluminosilicate and carbonate rocks. Infiltration and infiltration–bimetasomatic skarns are the main types, belonging to the wollastonite-free pyroxene–garnet depth facies. The magnitude of the plagioclase–scapolite equilibrium is evidence for the deep conditions under which the skarns formed.

Less widespread are earlier magnesian skarns belonging to the abyssal depth facies whose formation was related to regional metamorphism and partial melting. The major minerals in these skarns are fassaite, forsterite, spinel, humite, phlogopite and serpentine. Tungsten mineralization is superimposed on the skarns and is related to acid-phase aposkarn metasomatites. Dominant types are epidote, quartz epidote, quartz–epidote–clinozoisite, actinolite and other aposkarn propylites forming tabular bodies, metasomatic deposits, and rarer veins up to 3–4 m wide and 35–40 m long. Occasionally quartz–plagioclase and manganapatite–plagioclase vein metasomatites with poor Mo–W and W mineralization accompanied by propylite aureoles in the host skarns are encountered. The ores are represented by single phenocrysts and cluster disseminations or rarer veinlets of scheelite, sometimes accompanied by pyrite, pyrrhotite, chalcopyrite, molybdenite, sphalerite, and galena. Wolframite, cassiterite, helvite, bismuthite and native bismuth are occasionally found in ore bodies. The  $WO_3$  content in the ores varies enormously, reaching a few percent.

### *1.2. Tin*

Economic tin deposits in the eastern Baltic Shield are known only within the Pitkäranta ore region (Fig. 45) in southern Karelia (North Ladoga region) at the edge of the Svecokarelian fold belt close to its boundary with the Karelian craton. A typical feature of the geological structure of the region is the widespread development of granite–gneiss domes containing basement rocks remobilized in the Early Proterozoic.

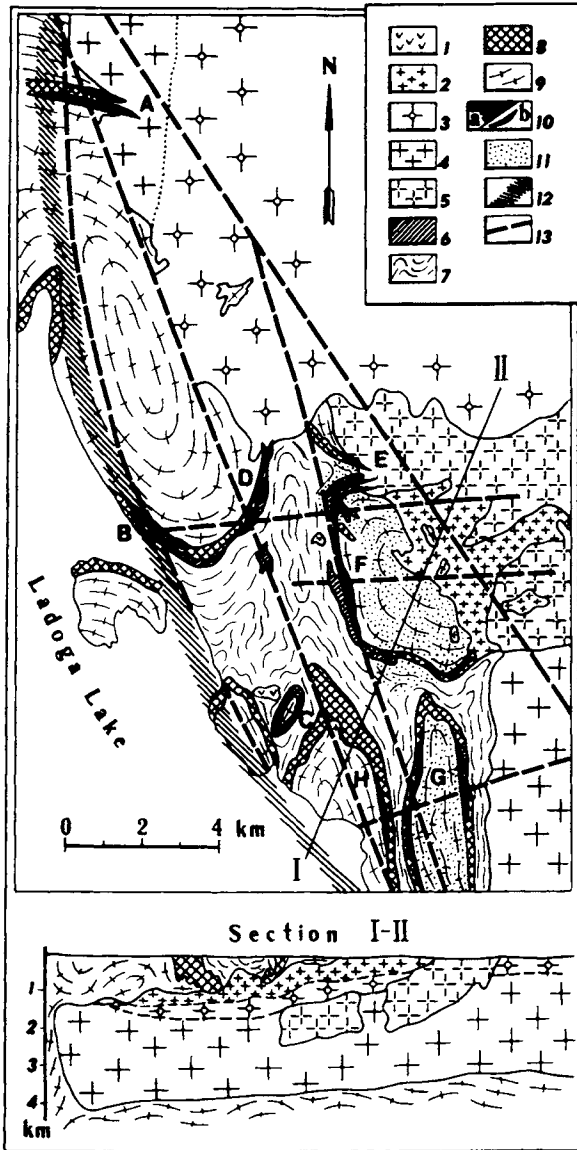


Fig. 45. Structural sketch map of the Pitkäranta ore region. 1) Jotnian volcanosedimentary & intrusive rocks; 2-5) Salmi rapakivi granites: 2) albite-protolithionite granite, 3) porphyritic biotite granite with fine-grained groundmass, 4) even-grained biotite granite, 5) coarse-grained porphyritic biotite-amphibole granite; 6-9) Svecokarelian complex: 6) ceramic pegmatites, 7) high-alumina schists, Ladoga Gp, 8) amphibolite & amphibole schist with carbonate horizons, Pitkäranta Fm, 9) granite-gneiss domes; 10) ore deposits: A-C tin-polymetallic, A - Kittelä, B - Old Ore Field, C - Heposelkä; D-H) beryllium-tin-polymetallic, D - New Ore Field, E - Hopunvaara, F - Lyupikko, G - Uksa, H - Ristiniemi; 11) projection on dome-like offshoots of the Salmi batholith of albite-protolithionite granite onto present erosion surface (depths from 70 to 400 m); 12) projection of boundary of sharp bend (gentle dips become vertical) in roof of Salmi batholith onto present erosion surface; 13) faults.

The domes are surrounded by Pitkäranta hornblende–biotite schists and amphibolites with carbonate horizons, which are overlain by the Ladoga flysch complex. Pitkäranta Fm (Sortavala Group) and Ladoga Group rocks are Early Proterozoic in age and are intensely deformed and metamorphosed at amphibolite facies conditions. All these rock groups are cut by the large (4,500 km<sup>2</sup>) Salmi anorthosite–rapakivi granite intrusion. The intrusion lies at the E end of the Early Riphean Ladoga–Dalekarlian anorogenic volcano-plutonic belt, which runs in an ENE direction along the southern border of the Baltic Shield (Fig. 43). The massif was emplaced in a large thrust zone between the Svecokarelian fold belt and the Karelian craton. Rocks in the SW part of the intrusion have a weathering crust and are overlain by subhorizontal unmetamorphosed Jotnian clastic terrigenous–volcanogenic rocks (the Salmi Fm) and are cut by small layered basic intrusions and dykes, comagmatic with Salmi volcanics.

The isotopic age of rapakivi granites in the Salmi intrusion is  $1543 \pm 8$  Ma, determined by the U–Pb isochron method on zircon; and a Sm–Nd isochron constructed using whole rocks and minerals with high REE concentrations (amphibole, apatite, bastnesite) yields an age of  $1560 \pm 45$  Ma,  $\epsilon_{Nd}(T) = -6.9$  (Amelin et al., 1990, 1991; Neymark et al., 1994).

The Salmi pluton is a typical polyphase anorogenic intrusion which cuts fold structures and metamorphic zones in Lower Proterozoic and Upper Archaean supra-crustal rocks. The time difference between the conclusion of orogenic processes in the host rocks belonging to the Svecokarelian fold belt and the Salmi intrusion is not less

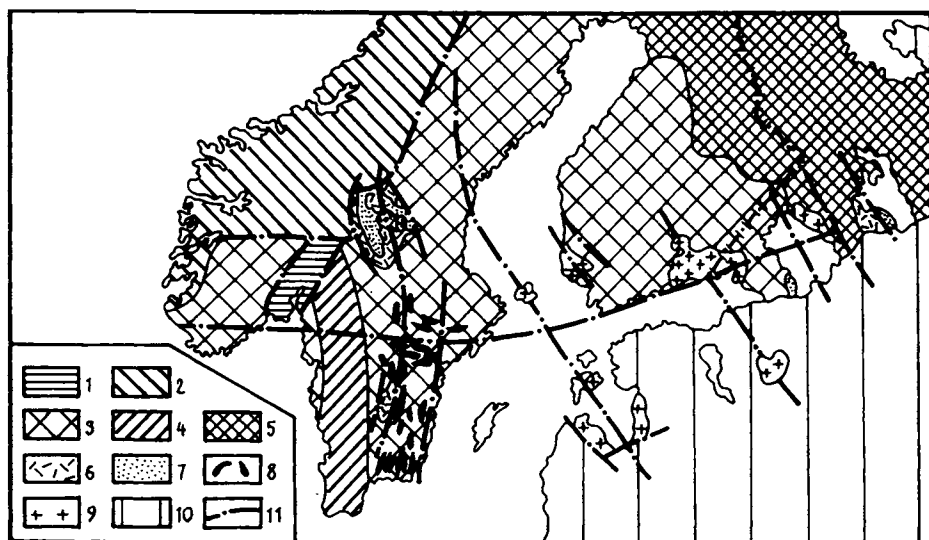


Fig. 43. Sketch map showing the position of the Ladoga–Dalekarlian volcanoplutonic belt within structures of the Baltic Shield. 1) Oslo graben; 2) Caledonian fold belt; 3) Svecokarelian fold belt; 4) Trans-Scandinavian granite belt; 5) Karelian granite–greenstone terrain; 6–8 – Ladoga–Dalekarlian volcanoplutonic belt; 6) acid and mafic volcanics in basins; 7) Hoglandian–Jotnian terrigenous rocks in basins; 8) basic dykes and sills; 9) rapakivi granite; 10) Russian Platform sedimentary cover; 11) faults.

than 300 million years. The massif contains two compositionally distinct rock complexes: gabbro–anorthosite–monzonite, and a later rapakivi granite which has a three-phase structure (Khazov, 1973).

Phase one was coarse-grained porphyritic biotite–amphibole granite (vyborgite and piterlite), phase two – coarse-grained biotite granite, and phase three – fine-grained porphyritic and uneven-grained leucocratic biotite granite. Phase three granites typically display uneven albitization, reaching up to the stage where albite–protolithionite topaz-bearing granites appeared in apical parts of the intrusion. These are extremely like Phanerozoic lithium–fluorine granites. A number of authors (Belyayev and Lvov, 1981) consider the albite–protolithionite granites to be the concluding magmatic phase of the pluton.

Rapakivi granites in the Salmi massif are generally characterized by enrichment in  $\text{SiO}_2$ ,  $\text{K}_2\text{O}$ , F, Rb, Y, Nb, Zr, Sn, REE (except Eu) and are poor in  $\text{Al}_2\text{O}_3$ , CaO, MgO, Sr. Elements such as Nb, Sn, Be, U, Th, Y, Rb, F and Zr are most intensely accumulated in late phases (Khazov, 1973; Belyayev and Lvov, 1981). Zircon, ilmenite, fluorite and orthite are the main accessory minerals. In addition, rare-element accessory minerals also appear in late phases – tantaloniobates, cassiterite, beryl, danalite, monazite, scheelite, etc. Rock-forming minerals are notable for their higher tin content. Sn concentrations in late phase biotites are up to 200–500 ppm (Rub et al., 1982) which corresponds to the tin content in Phanerozoic tin-bearing granites. Geochemically, the Salmi granites are totally comparable with A-type granites and lie on the Pearce tectonomagmatic plots (Pearce et al., 1984) in the within-plate granite field (Fig. 46).

All the ore targets in the region lie in the NW outer contact zone of the Salmi intrusion where its late phases are most developed. They are restricted to a strip with a maximum width of up to 4–5 km that extends along the contact for almost 50 km, and coincides with the contact metamorphic zone of the intrusion. The external boundary of the zone practically coincides with a line identified geophysically, along which a steep bend in the roof of the rapakivi granites has been located beneath the country rocks. The SW dip of the roof becomes vertical at this bend. The largest number of ore targets is concentrated in the middle of this strip where the roof of the rapakivi granites dips down relatively gently and is united into the Pitkäranta ore region.

Skarn deposits with complex tin, rare metal, polymetallic, iron and fluorite mineralization constitute the main type of deposit in the region with economic significance. They are associated with carbonate horizons in the Pitkäranta Fm which mantle granite–gneiss domes. Tantalite mineralization has been discovered in unexposed roof projections of the Salmi intrusion, consisting of albite–protolithionite granites. Linear greisen zones with Be, Mo, Sn and Cu mineralization are frequently located among different varieties of rapakivi granites and granite–gneiss domes. Moreover, clastic terrigenous rocks at the base of the Salmi Fm are known to contain cassiterite placer concentrations which evidently formed from the erosion of skarn deposits (Khazov, 1973)

Two groups have been identified among the skarn ore deposits of the region (Larin, 1980), with gradual transitions between the two: beryllium–tin–polymetallic (Uksa, Lupikko, Hopunvaara, New Ore Field, Ristiniemi) and tin–polymetallic (Kittelä, Old

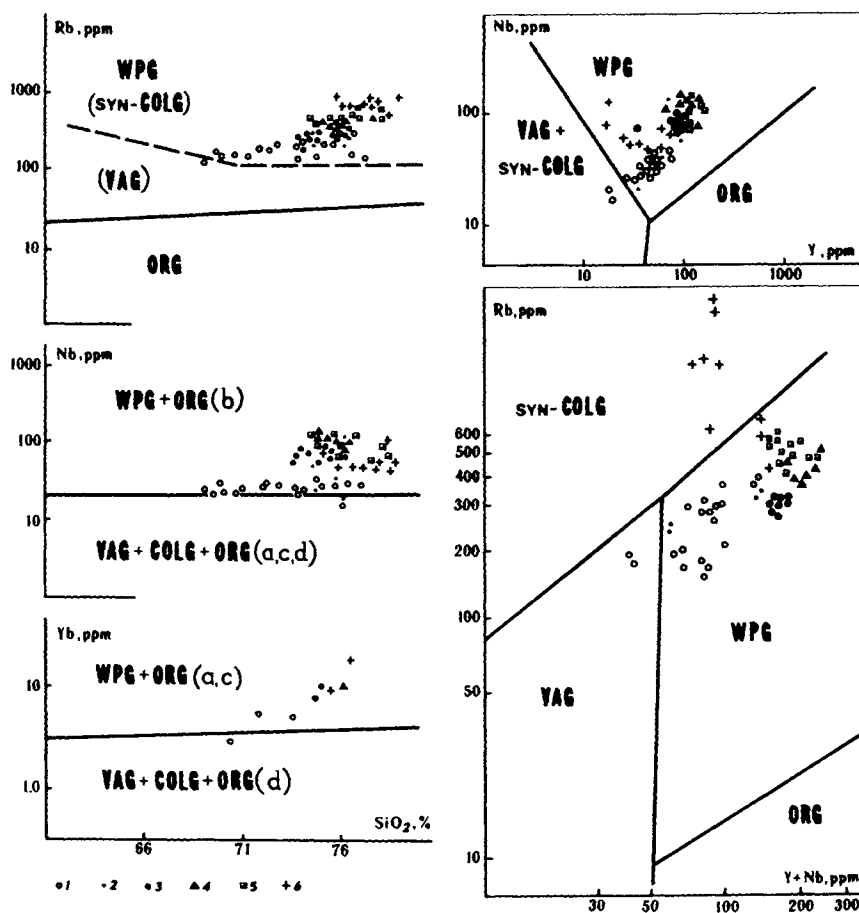


Fig. 46. Salmi rapakivi granite compositional points on a Pearce tectonomagmatic discrimination plot (Amelin et al., 1991). 1–2 biotite–amphibole granites: 1) coarse-grained. 2) fine-grained veins; 3–5 biotite granites: 3) even-grained, 4) porphyritic with fine-grained groundmass. 5) fine-grained veins; 6) albite–protolithionite granites. ORG – ocean ridge granites. VAG – volcanic arc granites. COLG – collision zone granites. WPG – within-plate granites.

Ore Field, Heposelkä) (Fig. 45). The first type occurs in the over-intrusion zone of the Salmi massif, which is characterized by a relatively gentle tip of the roof beneath the country rocks. As a rule they are restricted to roof offshoots of albite–protolithionite granites, exposed in drill cores that penetrate to 70 to 400 m depths. Dykes of these granites and stockscheiders are also widespread here. A broad spectrum of ore elements is characteristic of the first type of deposit: Be, Li, Sn, W, Cu, Zn, Pb, Fe, As, Bi, Au, Ag, Cd and In. However, only Be, Sn, Cu, Zn and fluorite have any economic importance.

Deposits belonging to the second group are localized either in the contact zone of the intrusion, where the granites have a steep dip (Kittelä), or in the zone where there is

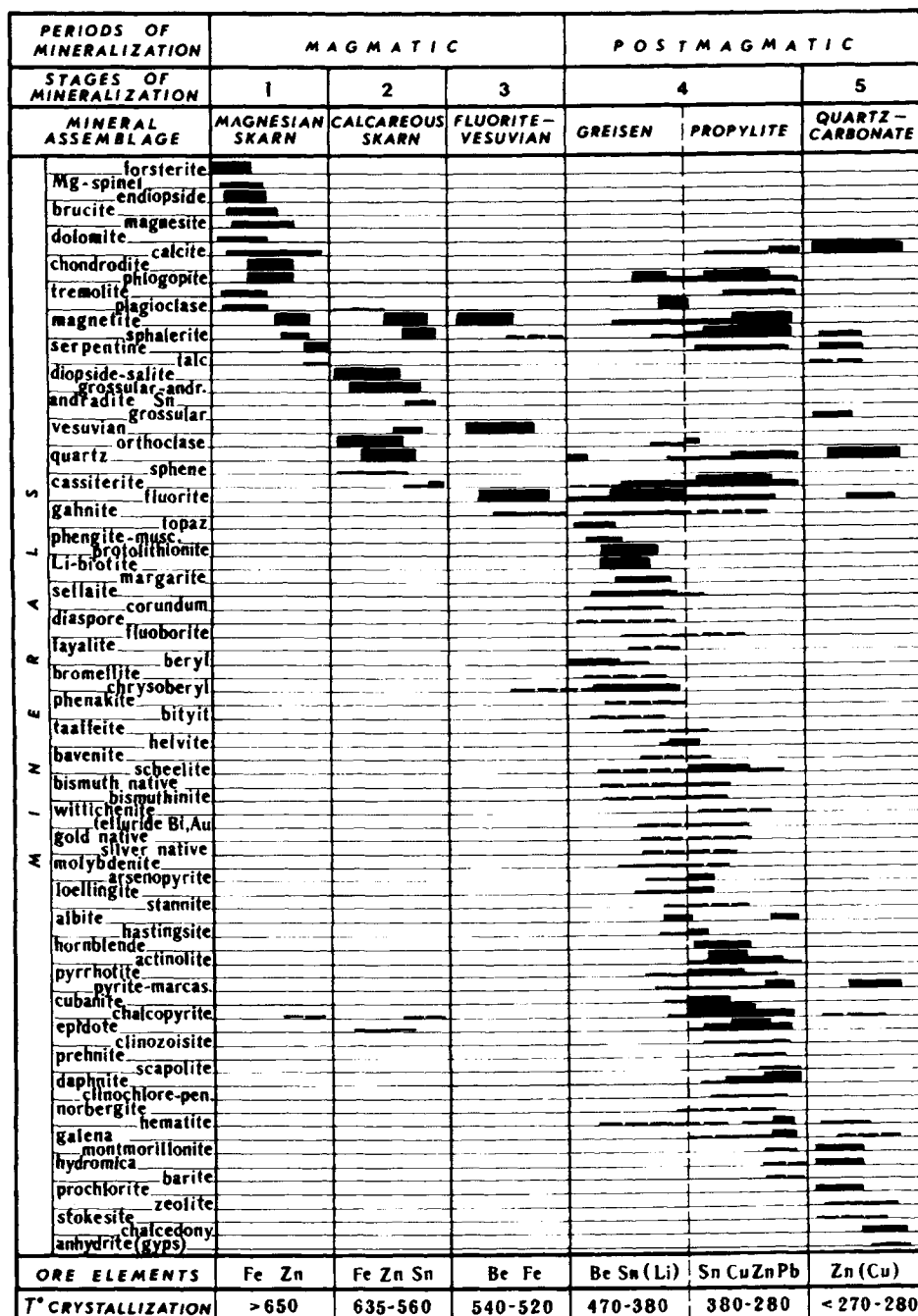
a steep flexural bend of the rapakivi granite roof beneath the country rocks at which the gentle dip becomes vertical. In the latter case, the ore deposits are at their maximum distance away from the intrusion (Old Ore Field, Heposelkä). The roof of the intrusion is usually over 1 km deeper than them. Albite–protolithionite granite dykes are either absent or very sparse. This type of deposit characteristically has a poorer ore element association: Sn, Cu, Zn, Pb, Fe, W, Bi, Ag, Au, Cd, In. Only Sn, Cu and Zn are important economically. In terms of scale, deposits in the second group are much larger than the first.

The ore deposits have a predominantly tabular shape and have a conformable relationship with the country rocks and only in the immediate contact zone with granites of the Salmi intrusion do cross-cutting veins, pipes and irregularly-shaped contact bodies begin to appear. Deposits extend for up to 1.8 km along strike and 700 m down dip and are from 2–3 m to 10–15 m thick. As a general rule they have a complex structure due to the occurrence of bodies of ore-bearing metasomatic rocks belonging to different mineral-forming stages, and the presence of facies zoning within “simple” bodies of metasomatites. For the ore deposits in this region as a whole, it is possible to identify the following main types of ore-bearing metasomatites: magnesian and lime skarns, fluorite–vesuvian–magnetite metasomatites, aposkarn greisens and propylites, late carbonate–quartz metasomatites. Figure 47 shows the mineral composition of these rocks. Magnesian skarns with their accompanying Fe–Zn mineralization, despite having the widest distribution area, are generally found as relicts among lime skarns and later metasomatites.

Lime skarns with syngenetic Fe–Zn and Sn mineralization are the most widespread type of metasomatic rocks in the region. Bimetasomatic skarns predominate, having formed at the contact between primary carbonate and aluminosilicate rocks, mainly hornblende schists. Typically they have clearly-expressed metasomatic zoning, illustrated in Table 4. Most of the Sn occurs isomorphically in garnets (Larin et al., 1986). The Sn concentration in late andradite reaches 2.20%. Cassiterite is present as an additional phase.

Fluorite–vesuvian–magnetite metasomatites are found exclusively in the first type of deposit. Associated with them is beryllium mineralization, where all the Be occurs as an isomorphic impurity in vesuvian. In these rocks, as distinct from the skarns, vesuvian is highly enriched in beryllium (to 0.85%) and fluorine (0.77–1.23%). Aposkarn greisens also occur exclusively in the first type of deposit. Beryllium, tin, lithium and fluorite mineralization are associated with them. Aposkarn greisens are zoned and frequently form a single zoned body with aposkarn propylites (Table 5). Aposkarn propylites occur in all the deposits of the region and the bulk of the tin–polymetallic ore mineralization is associated with them. Late carbonate–quartz metasomatites occur in all deposits, but they are small in scale. Copper–zinc and rarer tin mineralization in them is generally redeposited.

An analysis of the ore zoning (Larin, 1980) has shown that lateral zoning along the strike of the ore bodies has low-contrast differences relative to the ore-controlling NW and WNW faults, and also relative to the Salmi intrusion contact zone. Zoning across the width of ore bodies practically always has a contrastive, asymmetric, unidirectional character. In the lower carbonate horizon, where the majority of the ore bodies are



■ major minerals; ■ additional minerals; — minor minerals; — accessory minerals.

Fig. 47. Paragenetic diagram for deposits in the Pitkäranta ore region.

Table 4  
Metasomatic column for bimetasomatic skarn bodies in the Kittilä deposit

Zones	Endoskarn rocks and wallrocks					Exoskarns and calciphyres			
	feldspathized schists	quartz-feldspar	pyroxene-garnet-feldspar	feldspar-pyroxene-garnet	garnet	pyroxene-magnetite	pyroxene-garnet	pyroxene	calciphyre
Rock-Forming minerals	<b>amphibole</b> <b>biotite</b> <b>quartz</b> <b>orthoclase</b> <b>plagioclase</b> chlorite pyroxene sphene	<b>quartz</b> <b>orthoclase</b> <b>plagioclase</b> pyroxene garnet sphene	<b>orthoclase</b> <b>pyroxene</b> <b>garnet</b> quartz plagioclase sphene	<b>pyroxene</b> <b>garnet</b> orthoclase sphene	<b>garnet</b> pyroxene calcite sphene	<b>pyroxene</b> garnet	<b>pyroxene</b> <b>garnet</b>	<b>pyroxene</b> garnet calcite	<b>dolomite</b> <b>calcite</b> pyroxene garnet phlogopite serpentine
Ore minerals			cassiterite	cassiterite	cassiterite	<b>magnetite</b> <b>marmatite</b> cassiterite	magnetite cassiterite marmatite	magnetite	
Ore elements			Sn	<b>Sn</b>	<b>Sn</b>	<b>Fe, Zn, Sn</b>	<b>Sn, Fe, Zn</b>	Fe, Zn	

Note: Major minerals and ore elements are shown in **bold**.

Table 5

Reference metasomatic column for aposkarn greisens, greisen–propylitic and propylitic bodies

Zones	Topaz–quartz	Fluorite–topaz–mica	Fluorite–mica	Fluorite–feldspar	Amphibole	Phlogopite–epidote	Quartz–chlorite
Rock-forming minerals	<b>topaz</b> <b>quartz</b> muscovite protolithionite fluorite	<b>fluorite</b> <b>topaz</b> <b>Li-biotite</b> <b>protolithionite</b> margarite gahnite	<b>phlogopite</b> <b>fluorite</b> sellaite gahnite corundum Li-biotite margarite fayalite diaspore fluoborite	<b>plagioclase</b> (An <sub>21–51</sub> ) <b>albite</b> <b>orthoclase</b> <b>fluorite</b> <b>hornblende</b> hastingsite phlogopite quartz gahnite	<b>actinolite</b> <b>hornblende</b> phlogopite epidote hastingsite quartz fluorite calcite gahnite	<b>epidote</b> <b>phlogopite</b> <b>actinolite</b> <b>quartz</b> <b>calcite</b> fluorite turingite clinozoisite	<b>turingite</b> <b>quartz</b> <b>calcite</b> <b>epidote</b> phlogopite scapolite albite actinolite prehnite
Ore minerals	<b>beryl</b> chrysoberyl cassiterite	<b>chrysoberyl</b> beryl cassiterite	<b>chrysoberyl</b> helvite group cassiterite scheelite loellingite arsenopyrite magnetite	<b>cassiterite</b> <b>helvite group</b> <b>phenacite</b> arsenopyrite loellingite chalcopryite sphalerite scheelite bismuthite tellurides	<b>cassiterite</b> <b>chalcopryite</b> <b>sphalerite</b> <b>pyrrhotite</b> <b>magnetite</b> pyrite cubanite bismuthite tellurides scheelite	<b>cassiterite</b> <b>sphalerite</b> <b>chalcopryite</b> <b>pyrrhotite</b> <b>magnetite</b> galena scheelite	<b>galena</b> <b>sphalerite</b> <b>cassiterite</b> <b>hematite</b> <b>mushketovite</b> <b>magnetite</b> pyrite chalcopryite
Ore elements	<b>Be,</b> Sn, Li	<b>Be,</b> Sn, Li	<b>Be,</b> Sn, W	<b>Sn, Be,</b> Zn, Cu, W, As	<b>Sn, Cu,</b> Zn, W, As	<b>Sn, Zn, Cu,</b> W, Pb	<b>Pb, Zn, Sn,</b> Cu

Note: Major minerals and ore elements are shown in **bold**.

localized, zoning appears relative to the contact between this horizon and granite-gneiss domes.

Vertical zoning in the general case is symmetric. It is more contrastive in the first type of deposit than in the second. For the first type the general zoning order is **Be, Li, F, (Sn) → (Be), F, Sn, W, Cu, Zn, (Fe) → (F), Sn, (W), Cu, Zn, Fe, (Pb) → (Cu), Zn, Pb, Fe**; and for the second: **Sn → Sn, Cu, Fe, (Zn) → Cu, Zn, (Fe) → Zn, (Pb)**. Ore zonation is regularly associated with zoning in the metasomatic rocks.

It is important to note that the centres of ore deposits relative to which symmetrical vertical zoning occurs, are located at practically the same depth for all the deposits in the region. The richest mineralization in all types of deposit is controlled by this surface. Sn and Be-Sn pay shoots are associated with it, having a tendency to lie subhorizontally along carbonate bedding planes. Mineralization almost appears to “flow” from steeply-dipping ore-conducting channels along bedding-plane parallel zones where the surface of these horizons intersects the controlling depth level (Fig. 48). Pay shoots gradually change orientation to become subparallel to the roof as they approach the Salmi intrusion.

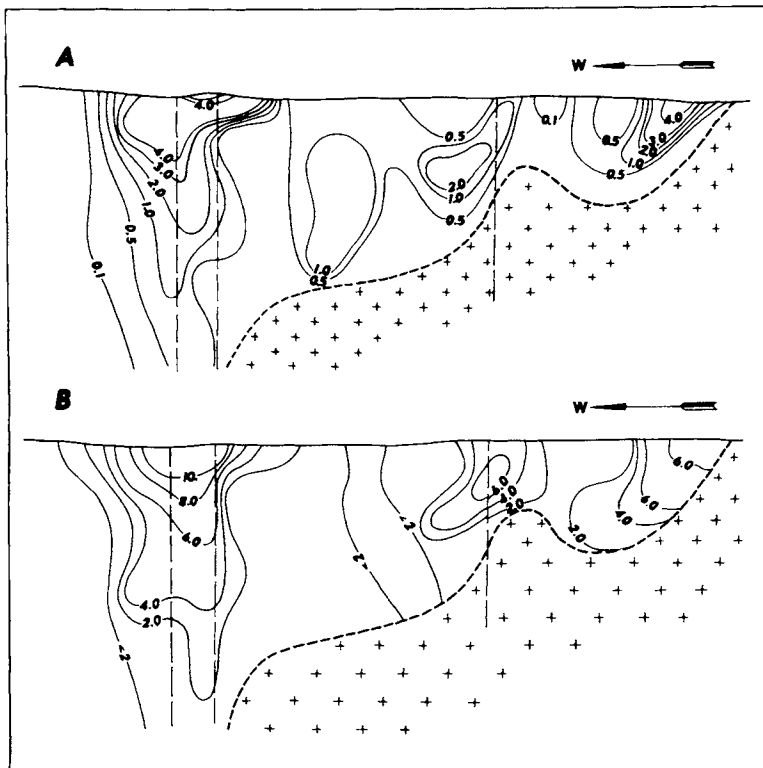


Fig. 48. Distribution of (A) tin in metre-percent and (B) aposkarn propylites (total cross-sectional thicknesses) on vertical projection surface for the Kittelä deposit.

For the ore region as a whole, zoning is such that in a SE to NW direction there is a gradual change from beryllium–tin–polymetallic to tin–polymetallic mineralization as the depth of apical offshoots of albite–protolithionite granites increases. Against this background, the zonal series in the first type of deposit undergoes a gradual change, with initial (Be, Li, F) and final (Pb, Zn) members of the ore element series being reduced in importance, while the middle (Sn, Cu) members play a greater role. The range of basic ore-bearing metasomatites and their ore mineral content alter. Aposkarn greisens and fluorite–vesuvian–magnetite metasomatites become gradually less important, while propylites play a greater role and carry more ores, and the tin content of lime skarns increases. Contrasts in ore zoning decrease and the vertical range of mineralization increases with depth (over 700 m). Similar zoning is also observed away from the Salmi intrusive contact in the direction towards which the intrusion roof is more deeply buried beneath the country rocks.

Two ore-forming stages have been distinguished in the deposits of this region: syn-magmatic and post-magmatic. Each stage can be broken down into several mineralization episodes which replace one another in sequence (Fig. 47), characterized by a particular set of metasomatic rocks and ores, associated with facies zoning and formed within a specific range of physicochemical conditions (Larin, 1980). Metasomatites belonging to the first stage formed under conditions prevailing when the granite magma had not yet crystallized. Evidence for this is the fact that rapakivi granites cut the skarns, and the absence of endo-skarns in the rapakivi granites. Second stage ore-bearing metasomatites formed after the rapakivi granites had completely crystallized, and they are closely associated with post-magmatic granite alteration which was expressed most intensely in apical parts of intrusions consisting of albite–protolithionite granites.

Dating of the ore-bearing metasomatites using the Sm–Nd method on internal isochrons (Amelin et al., 1990, 1991; Larin et al., 1991) confirms the validity of identifying two ore-forming stages, separated in time. An isochron constructed using tin-bearing pyroxene–garnet skarn samples from the Kittelä deposit (two garnet generations, clinoenstatite, diopside and whole rock) corresponds to an age of  $1546 \pm 28$  Ma,  $\epsilon_{Nd}(T) = -10.6$ . An isochron for aposkarn greisen samples from the Lyupikko deposit (two fluorite generations, topaz, oligoclase, muscovite, protolithionite and whole rock) corresponds to an age of  $1492 \pm 25$  Ma,  $\epsilon_{Nd}(T) = -7.4$ .

The age of the skarn coincides with that for the rapakivi granites, while the  $\epsilon_{Nd}(T)$  value differs significantly from  $\epsilon_{Nd}(T)$  for Salmi intrusion rocks and is intermediate between the latter and  $\epsilon_{Nd}(1550 \text{ Ma}) = -12.9$  for the country rock granite–gneiss domes. Evidently the formation of first-stage ore-bearing metasomatites was related to the separation of fluid at an early stage in the evolution of the source magma. Volatile separation may have been due to decompression as a result of a sharp drop in pressure during rapid upward movement of the magma from where it was generated to the level at which it was finally emplaced. The  $\epsilon_{Nd}(T)$  values for skarns confirm the geological field evidence regarding the extensive development of first-phase metasomatic processes with the involvement of a large volume of country rock material, mainly the granite–gneiss domes.

The formation of second-phase ore-bearing metasomatites is significantly separated in time (c. 50 Ma) from the crystallization of the rapakivi granites. The age of these

metasomatites is intermediate between the age of rapakivi granite crystallization and the age at which post-magmatic processes in the rocks of the intrusion were complete, determined from the Rb–Sr isochron method to be  $1455 \pm 17$  Ma (Amelin et al., 1990; Larin et al., 1991). Values of  $\epsilon_{\text{Nd}}(T)$  for aposkarn greisens and the rapakivi granites are very close, indicating that the second-phase ore-bearing metasomatites may have formed during post-magmatic processes mainly due to the influx of material from the rapakivi granites.

A study of the isotopic composition of lead ores from galena in the Pitkäranta ore region deposits (Larin et al., 1990) compared with the isotopic composition of lead ores from galena in Early and Middle Proterozoic deposits in the Svecokarelian fold belt and the Karelian craton (Vaasjoki, 1981), showed that they differed sharply from all the others on the basis of lead isotopic composition (Fig. 49), which contradicts the point of view (Popov, 1975) that the Pitkäranta ores could have formed due to the redeposition of older Svecofennian ore concentrations. An analysis of data on the isotopic composition of common lead residues after acid leaching of feldspars from igneous and partial melt rocks in the region and lead ore from the Pitkäranta deposits (Larin et al., 1990) provides evidence for the greater similarity between the latter and the igneous rocks of the Salmi intrusion (Fig. 49). This confirms the view that the ore material and the rapakivi granites have a single source.

A characteristic feature of ore lead from galena in the Pitkäranta ore region and common lead in feldspars from rocks in the Salmi intrusion is the low  $^{238}\text{U}/^{204}\text{Pb}$  ratio and higher Th/U ratios in the source (Larin et al; 1990). According to the “plumbotectonics” model (Zartman and Doe, 1981), these data may indicate a mantle–lower crustal source for the ore material and the Salmi intrusion igneous rocks. Similar isotopic characteristics for ore lead and common lead in igneous rocks, as well as older values for model ages compared with isotopic dating of granites and ores bring these deposits closer to those in “rejuvenated cratons”, identified by Doe and Zartman (1979). It should be noted that data published by Zartman (1984) for similar deposits differ, as a rule, by a large margin. The absence of major deposits in the Pitkäranta region may be due to the relative antiquity of the mineralization and the destruction of large volumes of ore by intense erosive processes.

### 1.3. Ceramic pegmatites

Ceramic pegmatite bodies in the Ladoga fold belt – Lyupikko, Seraya Gorka (“Grey Hill”), Krasnaya Gorka (“Red Hill”), Bulka, Heponiemi, Linnavaara – are located in the region of Pitkäranta, forming the Pitkäranta pegmatite field. The largest of these are Lyupikko, undifferentiated pegmatites, and Linnavaara, differentiated pegmatites (Sokolov, 1987; Pekki et al., 1977).

*The Lyupikko deposit* is one of the largest in the country (Pekki et al., 1977) and contains over 30 pegmatite veins in the contact zone of the Lyupikko granite dome and surrounding supracrustal assemblages belonging to the Pitkäranta Fm in the Sortavala Group. The largest veins occur in a 0.5–0.8 km wide zone that stretches for 3 km. Relationships with the country rocks are sub-concordant. Pegmatite bodies have a complex morphology; they contain country rock xenoliths, which have been assimi-

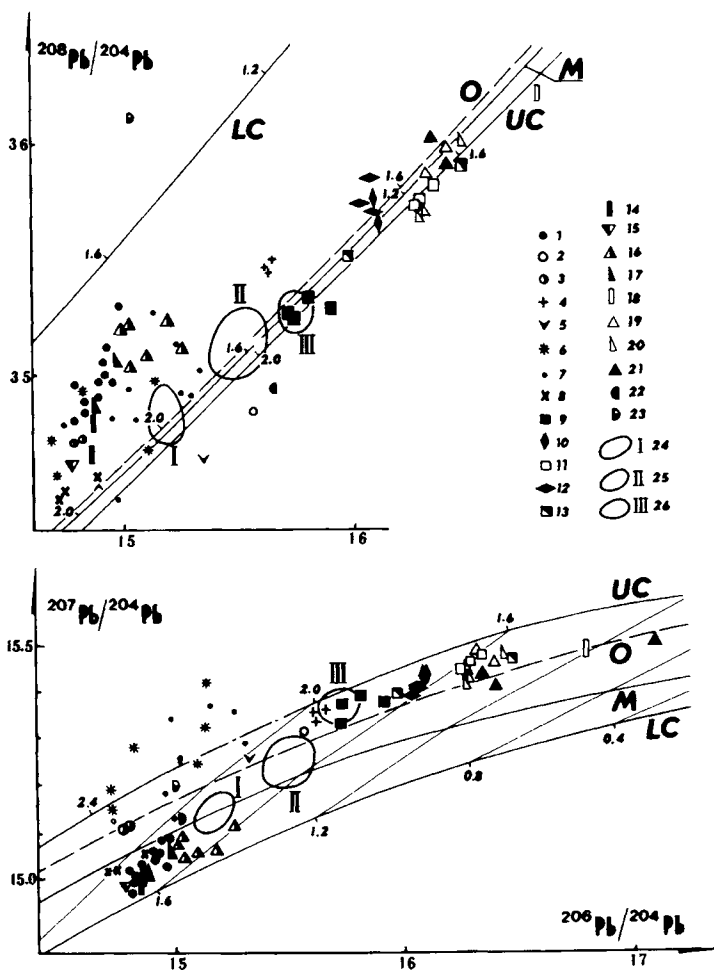


Fig. 49. Lead isotope ratios for galena in North Ladoga ore deposits, a number of sulphide deposits in Finland (Vaasjoki, 1981), and common lead in feldspars from igneous rocks in the Pitkäranta ore region. 1) galena from Pitkäranta ore region; 2-5)  $PR_1$  galena from N. Ladoga ore occurrences: 2) Pb. 3) W-polymetallic, 4) Pb-Zn, 5) Mo; 6-13) galena in Finnish deposits: 6) sulphide occurrences in Archaean basement, 7) epigenetic Cu, Pb, Zn occurrences in Karelide zone, 8) Outokumpu Ni-Zn-Cu deposit, 9) sulphide occurrences in exocontact zones of rapakivi granites, 10) Be-Sn greisen occurrences in Vyborg rapakivi granite intrusion, 11) quartz-sulphide veins in Vyborg intrusion, 12) Be-Sn greisen occurrences in Laitila rapakivi granite intrusion, 13) quartz-sulphide veins in Laitila intrusion; 14-21) feldspars from anorthosite-rapakivi granite intrusions (14-20 residues after acid treatment), 14-17) Salmi massif: 14) plagioclase from anorthosite, 15) orthoclase from monzonite, 16) orthoclase from vyborgite, 17) orthoclase from vyborgite ovoids; 18-20) Vyborg intrusion: 18) plagioclase from porphyrite, 19) orthoclase from vyborgite, 20) orthoclase ovoid from vyborgite; 21) orthoclase from Laitila rapakivi granite intrusion; 22-23) feldspars from granite-gneiss domes in Pitkäranta ore region (acid residues): 22) plagioclase, 23) K-feldspar; 24-26) galena compositional fields for Finnish deposits: 24) polymetallic deposits in Main Sulphide Ore Belt, 25) sulphide occurrences in Central Finnish batholith, 26) epigenetic polymetallic deposits in Svecofennian zone. LC - lower crust, M - mantle, OR - orogen, UC - upper crust. After Zartman and Doe (1981).

lated with the pegmatites, forming dark contact hybrid rocks, enriched in iron-bearing silicates. Two of the largest stock-like bodies occur amongst the pegmatites, 1500 m long and 80–120 m wide or 160–200 m in boudin swellings. The pegmatites are undifferentiated with a plagioclase and microcline–plagioclase composition with rare offshoots of graphic microcline pegmatite. The pegmatites will guarantee a source of crushable quartz–feldspar raw material for the glass industry. Relatively small veins of differentiated pegmatites are found in the deposits, which lie totally within the granite–gneisses. The content of microcline varieties in this type of vein varies from 5% to 35%, the average being 15–18%. Reserves of the microcline varieties account for around 2% of the reserves of all the pegmatite raw material in the deposit.

The Linnavaara deposit occurs in hornblende–biotite schists and amphibolites belonging to the Pitkäranta Fm, and has a near N–S strike and easterly dip. The deposit consists of several veins, the largest being the North vein which is over 400 m long and up to 75 m wide and contains most of the reserves. The pegmatites are differentiated. The internal structure and composition of the veins are complicated by tectonic stresses and subsequent albitization and greisenization. Fine flaky muscovite and biotite formed together with feldspar and quartz in the pegmatite, and in places garnet and tourmaline have developed, with appearances of accessory beryllium and tantalocolumbite mineralization. Microcline pegmatite accounts for 14% on average of the content of the North vein.

#### 1.4. Graphite

Small deposits of crystalline graphite in the Lake Ladoga region were discovered and exhausted in the last century. During 1968–1971, the largest prospective graphite-bearing assemblage in the NW Ladoga region was discovered around the village of Ihala (Biske et al., 1977; Sokolov, 1987). This is an economically developed region, with the St Petersburg–Petrozavodsk railway line running along its NW border. Graphite prospects lie 3–20 km from the nearest railway stations and connecting main roads.

The graphitic complex in the Ihala region is associated with highly metamorphosed volcanosedimentary rocks of the Proterozoic Sortavala Group. A graphitic horizon 170–500 m thick and up to 20 km long mantles granite–gneiss domes. The assemblage consists of biotite, amphibole–pyroxene–biotite and garnet–biotite gneisses. The rocks were metamorphosed at amphibolite facies, in places up to granulite facies. The gneisses everywhere display *lit-par-lit* migmatization, with vein material accounting for 10–15% of the entire volume of a rock. Graphite–biotite gneisses are of practical interest, forming patches and lenses up to 100 m thick, separated by graphite-free biotite, garnet–biotite and other gneiss and schist bands. Individual graphitic gneiss bands are up to 30 m thick and can be traced for up to 700 m along strike. The productive horizons are steeply dipping and deformed by minor folds.

Forecast reserves of graphite ores in the most prospective sectors (Tervijärvi, Huhtervu, Raivamäki, etc.) have been estimated at 15–20 million tonnes, with each prospect having an average of 3–5% graphite in the ores, i.e. close in quality to ores in the Skalisty deposit. Graphitic rocks occupy an area of around 15 km<sup>2</sup> and are overlain

by a thin cover of loose sediment, hence the resources represent a major graphite deposit. The area is suitable for developing open-pit extraction facilities. The mineral composition of the graphite ore is represented by quartz (30–40%), plagioclase (15–35%), microcline (10–20%), biotite (10–20%), iron sulphides (2–10%) and graphite (3–5%). The graphite is flaky, with flakes being 0.01–0.02 mm to 1.5–2 mm in size, 0.2–0.6 mm on average and 0.01–0.03 mm thick. Flotation enrichment yields a high (96%) recovery rate for carbon in the concentrate, which has an ash content of 10–12%.

In many respects the geological setting of the Ihala graphite region is similar to that of the Zavalevo deposit in the Ukraine. Ihala graphite has properties that are no less than Zavalevo, and the yield of refractory graphite from Ihala ores is comparable with the yield of similar graphite from Zavalevo (Biske et al., 1977). Graphite deposits in this region belong to the metamorphic genetic type and formed as a result of amphibolite facies metamorphism of sedimentary assemblages containing organic matter.

## 2. Conclusions

The ore deposits of the eastern Baltic Shield considered here represent the most important part of the ore formations in this region and fall into several metallogenic zones (Fig. 3). Each province or geoblock in the region, which differ from one another in their deep structure and geological evolution, as well as petrophysical parameters and geochemical signatures (Bilibina, 1980), has characteristic features of mineral genesis. The Kola and Karelian terrains had common metallogenic signatures in the Precambrian for iron, titanium, nickel, copper, cobalt, aluminium, phosphorus, molybdenum, tantalum, niobium, noble metals, occurring on varying scales in these structures. Characteristic differences in these provinces show up as rare metal deposits in pegmatites of the Kola terrain and massive sulphide deposits in Karelia.

Precambrian mineral deposits in this region formed in the time interval spanning the Early Archaean to the Late Proterozoic. During the Early–Middle Archaean, small uneconomic ferruginous quartzite deposits formed. The Late Archaean epoch is characterized by iron ore (ferruginous quartzites), iron–titanium, alumina (kyanite schists), rare metal (tantalum, niobium, cesium, etc.), massive sulphide and graphite deposits. During the Proterozoic, deposits containing more numerous ore formations appeared: phosphorus–iron–titanium, copper–nickel sulphides, molybdenum, tin ores, tungsten, muscovite and ceramic pegmatites, graphite and shungite; copper and gold occurrences.

This Page Intentionally Left Blank

**Section 4:**

Platform cover of the Siberian Craton

This Page Intentionally Left Blank

## Ukrainian Shield

V.B. DAGELAYSKY

### *1. Geological structure and metallogeny*

The Ukrainian Shield is a Precambrian basement structure with a long and complex history spanning an interval greater than three billion years during which tectonic structures evolved, ranging from granulite–gneiss and granite–greenstone terrains in the Early and Late Archaean, to intracratonic basins and troughs and zones which became active for the first time in the Late Proterozoic. Another significant feature in the formation of the shield structure were block movements along tectonic zones belonging to different depth levels.

The geological structure of the Ukrainian Shield has been considered in detail in a number of works (Shcherbak et al., 1989; Belevtsev and Galetsky, 1984; Rundqvist and Mitrofanov, 1992; Dagelaysky, 1988), which demonstrated the contribution made by local researchers to the study of various geological, geochronological, petrological and metallogenic problems in the Precambrian of the Ukrainian Shield, as well as outlining the composition, age and spatial relations of metamorphic (primary sedimentary and volcanic) and igneous complexes. This section is restricted to a brief survey of the major geological features and composition of Precambrian complexes in the Ukrainian Shield essential for understanding of subsequent sections relating to the ore deposits of the region. Figure 50 is a sketch map showing the distribution of Precambrian rocks in the Ukrainian Shield.

In this work we adhere to the Precambrian stratigraphic scheme and sequence of igneous complexes as set out in (Belevtsev and Galetsky, 1984). The following structural–lithological units have been identified among the metamorphosed volcanosedimentary successions and igneous formations. The Lower Archaean complex consists of the Dnestr–Bug, Aul and West Pre-Azov Groups, the Nemirov and Dnepropetrovsk granitic complexes, with basic and ultrabasic rocks. The Upper Archaean complex contains the Rosinsk–Tikich and Konka–Verkhovtsevo groups, and the Sursk–Tokov and Zvenigorod granitic complexes. The Lower Proterozoic complex includes the Krivoy Rog, Ingul–Ingulets, Central Pre-Azov, Bug, Teterev, Klesov and Pugachev Groups; the Berdichev, Osnitsk, Pre-Azov, Kirovograd–Zhitomir, East Pre-Azov and Korosten granitic complexes; basic and ultrabasic rocks; and the Korosten basic igneous complex. The Ovruch Group and the Perzhan igneous and metasomatic formations are referred to the Upper Proterozoic complex. It is important to note that certain changes were made to the Precambrian stratigraphic correlation scheme for the

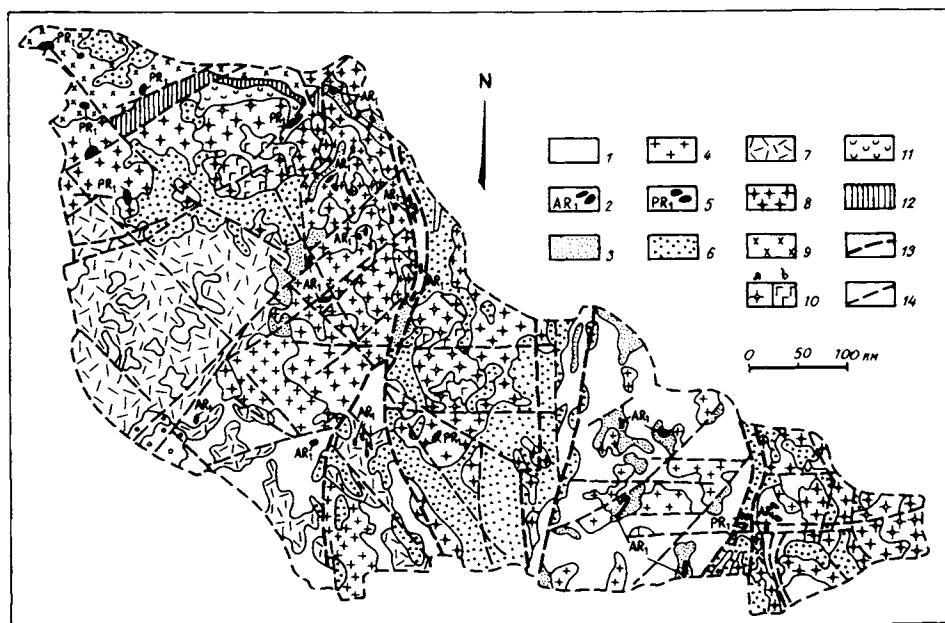


Fig. 50. Distribution of Precambrian rocks in the Ukrainian Shield (after Galetsky et al., 1984, simplified). *Early Archaean*: 1 – groups: Dnestr–Bug, Aul, West Pre-Azov; granitic complexes: Dnepropetrovsk, Nemirov; 2 – basic-ultrabasic complex. *Late Archaean*: 3 – Rosin–Tikich, Konka–Verkhovtsevo Groups; 4 – Zvenigorod, Sursk–Tokov granitic complexes; *Early Proterozoic*: 5 – basic-ultrabasic complex, 6 – groups: Teterev, Bug, Ingul–Ingulets, Krivoy Rog, Central Pre-Azov, Klesov, Pugachev; 7 – Berdichev granitic complex; 8 – Kirovograd–Zhitomir granitic complex; 9 – Osnitsk gabbro–diorite–granodiorite complex; 10 – Korosten complex: a – granitoids, b – basic-ultrabasics. *Late Proterozoic*: 11 – Ovruch Group; 12 – Perzhan metasomatites; 13 – deep tectonic zones; 14 – tectonic zones, faults.

Ukrainian Shield after 1984 (Etingof et al., 1986), the most important being: the subdivision of the Aul, Dnestr–Bug and West Pre-Azov groups into a number of formations whose mutual relations have yet to be established; and the identification of a Lower Archaean basic–ultrabasic igneous complex and the Gaivoron granite complex (AR<sub>2</sub>, replacing the Nemirov complex), the Gaisin, Uman and Shevchenko granitic complexes (all three are PR<sub>2</sub>).

A combined analysis of geological and geophysical data together with drillcore information has demonstrated that it is possible to identify three major provinces or geoblocks within the shield (and further subdivision of these into blocks), distinguished by different stratigraphic successions, internal crustal processes and specific metallogenic features (Belevtsev and Galetsky, 1984). These are the Azov province (including the East Azov and West Azov blocks), the Central Ukraine province (Dnieper and Kirovograd blocks), and the West Ukraine province (Volyn, Podolsk and Belotserkov blocks). The sketch map of the block structure of the Ukrainian Shield (Fig. 51) also shows the suture zones which separate the delineated provinces – the Golovanevsk suture in the west and the Orekhovo–Pavlograd suture in the east. The suture zone between the Dnieper and Kirovograd blocks is particularly significant, being an Early

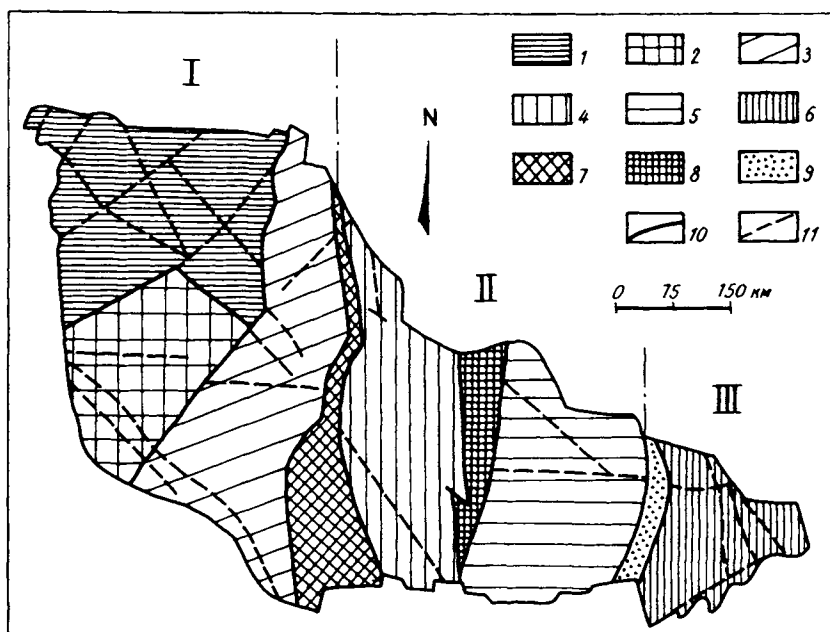


Fig. 51. Block structure and metallogenic regions of the Ukrainian Shield (Galetsky et al., 1984). Blocks and corresponding metallogenic provinces: 1 – Volyn, 2 – Podolsk, 3 – Belotserkov, 4 – Kirovograd, 5 – Dnepropetrovsk, 6 – Azov. Sutures between blocks and respective metallogenic zones: 7 – Golovanevsk, 8 – Krivoy Rog–Ingulets, 9 – Orekhovo–Pavlovgrad, 10 – deep tectonic zones, 11 – faults. Geoblocks: I – West Ukrainian (Volyn–Podolsk), II – Central Ukrainian, III – East Ukrainian (Azov).

Proterozoic rift belt, coinciding with the Krivoy Rog–Ingulets (Krivoy Rog–Kremenchug) zone.

The northern part of the West Ukraine province (the Volyn block) is made up of an Archaean granulite basement and metamorphosed Proterozoic sequences in which sub-platform and platform successions are widespread (the Pugachev and Ovruch Groups and Korosten granitoids). Overall, the West Ukraine province is characterised by widespread granitic rocks and migmatites which stitch together the Lower Archaean supracrustal rocks belonging to the Dnestr–Bug Group.

In the Kirovograd block of the Central Ukraine province intense granitization occurs in anticlinal culminations and synclinal cores containing the volcano-sedimentary assemblages of the Bug and Ingul–Ingulets Groups. The Dnieper block has major synclinoria consisting of metamorphosed Archaean volcanics and sediments (mainly the Konka–Verkhovtsevo Group), separated by granite–gneiss anticlinoria in which dome structures are widely developed.

The Azov province contains Lower Archaean and Lower Proterozoic formations in which two sedimentary and volcanic cycles have been identified; these produced the West Pre-Azov and Central Pre-Azov Groups respectively. In addition there are the Early Proterozoic Pre-Azov and East Pre-Azov granitic complexes.

The Archaean is characterised by the presence of basic volcanic rocks and less commonly by intermediate and acid volcanics at the top of the succession. Thin concordant sedimentary–volcanogenic ferruginous quartzites have been observed. Lower Proterozoic assemblages frequently contain conglomerates at the base and typically show interbedded volcanics, argillaceous rocks and carbonates as well as graphitic layers. An interesting feature is the development of thick iron ore formations which have a primary sedimentary (clastic terrigenous–chemogenic) origin.

Intense migmatitisation and metasomatism occurred in the Archaean, with the development of broad migmatite fields and partial-melt granites – the Dnepropetrovsk granite gneisses and gneissose granites, as well as the Sursk–Tokov granites in the Dnieper granite–greenstone terrain, the Nemirov and Zvenigorod granites in the West Ukraine province. Typically during the Early Proterozoic the partial-melt Berdichev granites formed, also not infrequent allochthonous intrusions of the Kirovograd–Zhitomir plagioclase–microcline granites and the analogous Pre-Azov complex. During the protoplatform evolutionary stage of the shield at the end of the Early Proterozoic, the Korosten granite and alkali-granite complex was emplaced, with associated basic and ultrabasic multiple plutons – Korosten and Korsun–Novomirgorod – and smaller intrusions in the East Azov block.

Several metamorphic episodes have been identified in the Ukrainian Shield, which differ in scale of development and P–T conditions. The Early Archaean regional metamorphic episode typically had granulite and amphibolite facies conditions, and partial-melting processes proceeded under the same pressure and temperature conditions (in the Podolsk and West Azov blocks).

Greenschist and epidote–amphibolite facies metamorphism appeared during the Late Archaean (in the Belotserkov and Dnieper blocks). Early Proterozoic regional metamorphism and partial melting took place under greenschist to granulite facies conditions; local retrogression of Archaean granulite complexes occurred (in the Volyn, Podolsk and Azov blocks). The granulite facies had a restricted development in the Podolsk block and the Golovanevsk suture zone. In the Kirovograd block and the Krivoy Rog–Ingulets zone, granulite facies rocks form a discontinuous strip, while in the Azov block they occur as inclusions within migmatites and granites. The metamorphic rocks of the Ukrainian Shield correspond to medium- and low-pressure facies series.

Metallogenic research in the Ukrainian Shield, the study of specific ore-forming processes and their relationships to particular geological complexes and formations has developed at a particularly intense rate in the last 30 years. General works have been published dealing with metallogeny, distribution and evolution with time of ore-forming processes in the Ukrainian Shield (Belevtsev et al., 1984; Bilibina et al., 1978; Galetsky et al., 1986; Gladky et al., 1971; Galetsky, 1974; Belevtsev and Yepatko, 1986). Criteria for forecasting mineral deposit occurrences in Precambrian complexes in the Ukrainian Shield and ore deposit distribution patterns in structural belts were considered (Belevtsev and Galetsky, 1984; Bepalko, 1975; Ryabenko, 1976). Generalizations relating to questions concerning metamorphic ore formation (Belevtsev et al.) and geological, formational and age type classifications of iron ore complexes were arrived at on the basis of data collected across the shield.

Regional metallogenic subdivisions of the Ukrainian Shield from Belevtsev and Galetsky (1984) showing provinces and zones corresponding to the Precambrian block structure, are illustrated in Figure 51. These metallogenic provinces and zones have the following characteristic features (Galtesky, 1974):

*The Volyn province* – titanium, tin, kyanite, chamber pegmatites and graphite ore deposits and occurrences; molybdenum, nickel, lead and zinc, and tungsten occurrences.

*The Podolsk province* – pegmatite deposits and occurrences; iron, titanium, copper, molybdenum, nickel, zirconium, apatite, graphite and fluorite occurrences.

*The Belotserkov province* – nickel and cobalt, iron, graphite, sillimanite, pegmatite ore deposits and occurrences; titanium, bismuth, molybdenum, lead and zinc, tungsten, apatite and corundum occurrences.

*The Kirovograd province* – pegmatite deposits; titanium, bismuth, copper, molybdenum, nickel, lead, tungsten, zirconium and silver occurrences.

*The Krivoy Rog–Ingulets zone* – iron, graphite and talc deposits and occurrences; titanium, copper, molybdenum, nickel, gold, silver, apatite and asbestos occurrences.

*The Dnieper province* – iron, aluminium, nickel and cobalt, talc and pegmatite deposits and occurrences; titanium, copper, molybdenum, lead, tungsten and gold occurrences.

*The Azov province* – iron, titanium, molybdenum, graphite, fluorite and rare-metal pegmatite deposits and occurrences; copper, nickel, tin, lead and zinc, apatite and asbestos occurrences.

Table 6 shows each metallogenic province and zone (see also the map, Fig. 51), with the geological groups, complexes, major ore-bearing and ore formations, as well as examples of ore deposits and occurrences.

### 1.1. Ore-bearing tectonic structures

Recently the dominant trend in metallogenic research has been the identification of ore-bearing tectonic structures with characteristic specific time and space evolutionary features and particular ore-forming processes. This is especially important in the evolution of provinces during the Precambrian, due to the intense and repeated appearance in them of different regimes of magmatic, metamorphic and metasomatic processes closely tied to tectonics, with the formation during primary concentration, or with subsequent redeposition, of a large number of important ore-formational types of useful mineral deposits (Fe, Mn, Cr, Ti, Cu–Ni, W, Au, etc.). The oldest structures in the Ukrainian Shield (Fig. 52) are *granulite-gneiss terrains* (Podolsk and West Azov), consisting of relicts of Lower Archaean supracrustal sequences and ancient granite-gneisses and younger remobilized granitoids, as well as *the Dnieper granite–greenstone terrain* in which Upper Archaean greenstone belts developed in the basement, surrounded by tonalite gneiss and granitoids. During Early Proterozoic time, tectono-thermal reworking processes developed in the older structures, with the formation of extensive fields of partial-melt granitic rocks – the northern and central parts of the Podolsk block and the Azov province (in granite–gneiss terrains), the northern part of the Belotserkov zone and the north-eastern part of the Podolsk block (in the Rosinsk–

Table 6  
Some metallogenic features of the Ukrainian Shield

Metallogenic province; major metallogenic epochs	Geological Groups and Formations	Main ore-bearing geological formations or groups of formations	Ore formations (ore deposits and minor occurrences)
Volyn; Early Proterozoic and Late Proterozoic epochs	Ovruch Group Teterev Group	trachyandesite-sandstone carbonate schist; graphitic schist; ferruginous schist	quartz-pyrophyllite (Nagoryansk, Zbrankov); metamorphic carbonate; graphitic gneiss; metamorphic iron ore
	Korosten Complex	leucocratic granite; rapakivi granite; gabbro-anorthosite	ceramic and micaceous pegmatites; chamber pegmatites (Volyn pegmatite field); titanium (Volodar-Volyn and Chepovich intrusions);
Podolsk; Archaean and Early Proterozoic epochs	Perzhan metasomatites Dnestr-Bug Group	alkali granite kinzigite	tin-tungsten-molybdenum; fluorite graphitic kinzigite (Makharinetsk); high-alumina garnet (Slobodov)
	Berdichev Complex Complex of alkali-ultrabasic rocks and carbonatites	leucocratic granites alkali-ultrabasics and carbonatites	tungsten-copper-molybdenum (Lyubar, Ostropol) apatite-carbonatite
Belotserkov; Archaean and Early Proterozoic epochs	Bug Group; basic and ultrabasic complex	khondalite, dunite-peridotite; dunite-clinopyroxenite- gabbro; komatiite-tholeiite	graphitic khondalite (Zavalyevskoye); chromite (Kapitanov); copper-nickel sulphide
Kirovograd; Early Proterozoic epoch	Bug Group; Kirovograd-Zhitomir complex;	flyschoidal; sub-alkaline granitoid;	graphitic gneiss; copper-molybdenum; tin-tungsten skarn
	Korosten Complex	rapakivi granite;  gabbro-anorthosite	quartz; tungsten-molybdenum;  apatite-titanium; high-alumina feldspathic

West Ingulets–Krivoy Rog zone; Early Proterozoic epoch	Ingul–Ingulets Group;	silica–schist–carbonate; iron–chert; iron–chert meta-andesite– meta-basalt;	graphitic gneiss; volcano-sedimentary & sedimentary iron ore; copper–nickel sulphide (Karachunovo–Lozovat);
	Krivoy Rog Group	jaspilite–chert	metamorphic and metasomatic iron ore; sedimentary iron ore (Krivoy Rog–Kremenchug iron ore basin)
Dnepropetrovsk; Archaean and Early Proterozoic epochs	Aul Group; Konka–Verkhovtsevo Group;	jaspilite–meta-tholeiite; dunite–peridotite; dunite–pyroxenite– gabbro; iron–chert;	volcanogenic iron ore; talc–magnesite (Pravdin); copper–nickel sulphide; volcanogenic iron ore (Verkhovtsevo, Chertomlyk);
	Krivoy Rog Group;	minor intrusions in aplite– pegmatite granites;	tungsten–molybdenum;
Azov; Archaean, Early and Late Proterozoic epochs	East Pre-Azov Complex	alkali nepheline syenite	phosphorus
	West Pre-Azov Group;	iron–chert	volcanogenic–sedimentary iron ore;
	Central Pre-Azov Group;	khondalite;	graphitic khondalite;
	Gulyaipole and Osipenkovo Formations;	iron–chert;	volcanogenic–sedimentary iron ore (Mariupol and others);
Pre-Azov Complex;	metasomatitic; granodioritic;	chemogenic–sedimentary iron ore;	
East Pre-Azov Complex;	syenitic–granosyenitic;	pegmatitic;	
Kamennomogilsk Complex;	alkali–nepheline syenitic;	nepheline–feldspar–apatite;	
Chernigov Complex	alkali–granitic;	fluorite;	
	alkali–ultrabasic	apatite–carbonatitic	

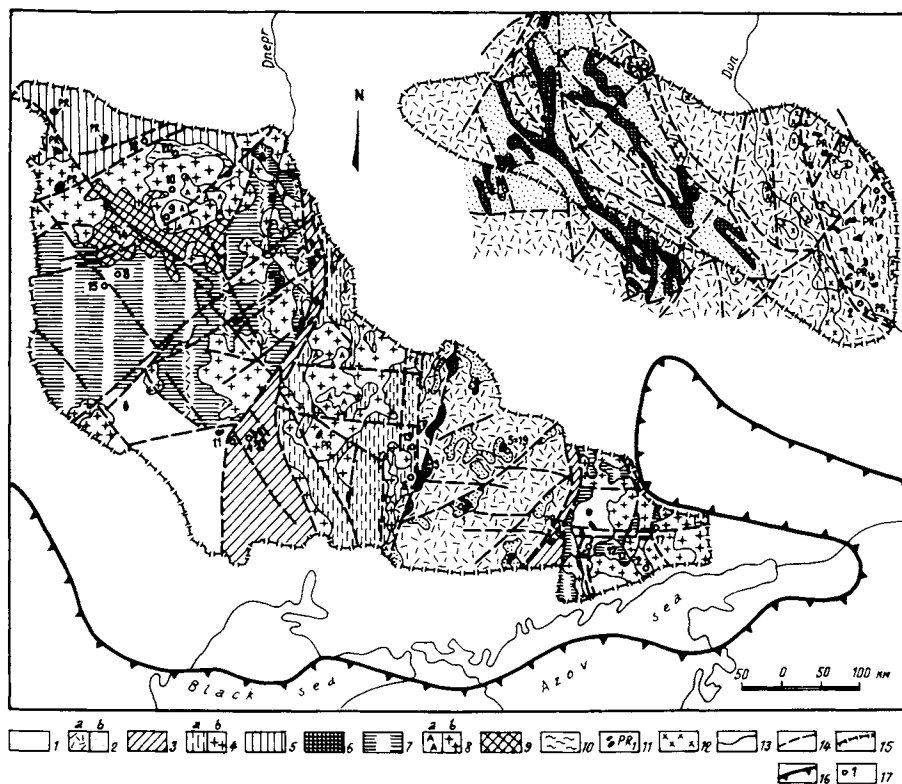


Fig. 52. Sketch map of ore-bearing tectonic structures in the Ukrainian Shield and the Voronezh Massif. Compiled by V.B. Dagelaisky using material from Dagelaisky (1988) and Galetsky et al. (1984). 1 - granulate-gneiss terrain; 2 - granite-greenstone terrain: a - tonalite-gneiss & granite-gneiss areas, b - greenstone belts; 3 - collisional suture zone; 4 - fold belt (a), synorogenic granitoids in fold belt (b); 5 - volcanoplutonic belt; 6 - rift structure; 7 - area (belt) of tectonothermal reworking (symbol in narrow strip = pre-existing structure); 8 - igneous complexes: a - gabbro-anorthosite, b - rapakivi granite; 9 - intracratonic fold belt; 10 - intracratonic basin; 11 - Archaean (or Proterozoic PR<sub>1</sub>) basic-ultrabasic rocks; 12 - post-deformational granites in Voronezh Massif; 13 - geological boundaries; 14 - faults; 15 - conventional edge of Ukrainian Shield and Voronezh Massif (based on 300 m sub-surface datum); 16 - boundary of East European craton; 17 - ore deposits (numbers as in Table 5).

Tikich granite-greenstone terrain). Rapakivi granite intrusions were emplaced at the end of the Early Proterozoic during a tectono-magmatic proto-activation process as subplatform bodies (the Korosten, Korsun-Novomirgorod, East Pre-Azov and Moldavian intrusions).

*Early Proterozoic fold belts*, consisting of volcano-sedimentary assemblages, metamorphosed to varying degrees, together with syn-tectonic granites, mainly developed in the Kirovograd block. Early Proterozoic syntectonic granites (Kirovograd-Zhitomir and Pre-Azov complexes) are also present in older Archaean structures.

The narrow Krivoy Rog-Kremenchug suture zone is a *rift structure*, consisting mainly of the Krivoy Rog Group, a predominantly sedimentary sequence with sub-

ordinate volcanics and containing significant thicknesses of ferruginous quartzites. Development of this zone concluded with the formation of intense alkali (mainly soda) metasomatism.

An *intracratonic fold belt* is situated in the south of the Volyn block, surrounding the younger Korosten sub-platform pluton. It consists of Teterev Group formations, predominantly clastic terrigenous and carbonate–terrigenous. Amphibolite and epidote–amphibolite metamorphism is characteristic. Andesite–basalt series volcanics are present, altered to amphibole and pyroxene-bearing gneisses and schists, as well as amphibolites.

A *volcanoplutonic belt* has been delineated in the extreme north west of the shield, forming part of the Volyn–Polessye belt (Galetsky, 1987), which embraces the edges of the Belorussian and Voronezh massifs. It consists of the Osnitsk diorite–granodiorite–granite complex and metamorphosed essentially acid volcanics (basalt–andesite–liparite series) of the Klesov assemblage which occur as small areas within the granitoids. An interesting feature in the SE marginal part of the belt is the existence of intense metasomatic reworking with the formation of specific rocks – apo-granites with varied mineralization – the Sustchan-Perzhan zone.

*Intracratonic basins* – platform structures – appeared in the Late Proterozoic. These are the Ovruch structure around the northern edge of the Korosten pluton – volcanics belonging to a trachybasalt–trachyandesite–trachyliparite formation with thin horizons of coarse clastic rocks and quartzitic sandstones, and possibly also the Novograd–Volyn structure in the south of the Volyn block, consisting mainly of intermediate volcanics with a patch of meta-siltstones and meta-sandstones at the top of the succession.

*Suture zones* constitute a special type of structure. They are characterised by a connection to deep faults and the existence of blocks of different rock types within their confines which developed at different times, the presence of basic–ultrabasic bodies, uneven metamorphism as a result of individual blocks having different geological histories, and frequent episodes of granite formation. The Ukrainian Shield has two such suture zones: the Golovanev zone, containing tonalite gneiss and granite gneiss, segments of greenstone belts, zones containing supracrustal assemblages in fold belts, basic–ultrabasic bodies; and the Orekhovo–Pavlovgrad zone. Table 7 shows the relationship between a number of ore deposits and occurrences and ore-bearing tectonic structures in the Ukrainian Shield. The map in Figure 52 shows these deposits and occurrences (numbered) within the structures of the shield.

## 2. Ore deposits and occurrences

### 2.1. Iron

The Ukrainian iron ore province occupies the entire area of the Ukrainian Shield. During the last decade there has been intensive research conducted due to the great importance of Precambrian iron ore mineralization for the Ukraine. This is reflected in the large number of general reviews devoted to various aspects of mineralization

(Belevtsev, 1986a, 1986b, 1987; Dagelaisky, 1984; Semenenko et al., 1978, 1988; Belevtsev et al., 1981; Grechishnikov, 1983). Characteristic features of iron ore deposits in the Ukrainian Shield are detailed in a collection of papers edited by Belevtsev (Belevtsev et al., 1981). Figure 53 illustrates the distribution of iron ore deposits in the Ukrainian Shield; and Table 7 sets out their tectonic settings.

A study of iron-bearing sedimentary and volcanogenic assemblages and of iron ores themselves has demonstrated the fruitfulness of employing the formational approach to problems relating to their distribution, genesis and economic importance. Several different classification schemes for iron ore formations have been developed during the last 25 years (in publications by Shatsky, Semenenko, Goryainov, Formozova, Shchegolev, Belevtsev, Kalyayev and others). According to Belevtsev (1986), Belevtsev and Galetsky, (1984) and Belevtsev et al. (1981), the Ukrainian iron ore province includes a number of lower order metallogenic units containing iron ores belonging to particular formations. These are the Odessa–Belotserkov metallogenic zone (ores in volcanic and

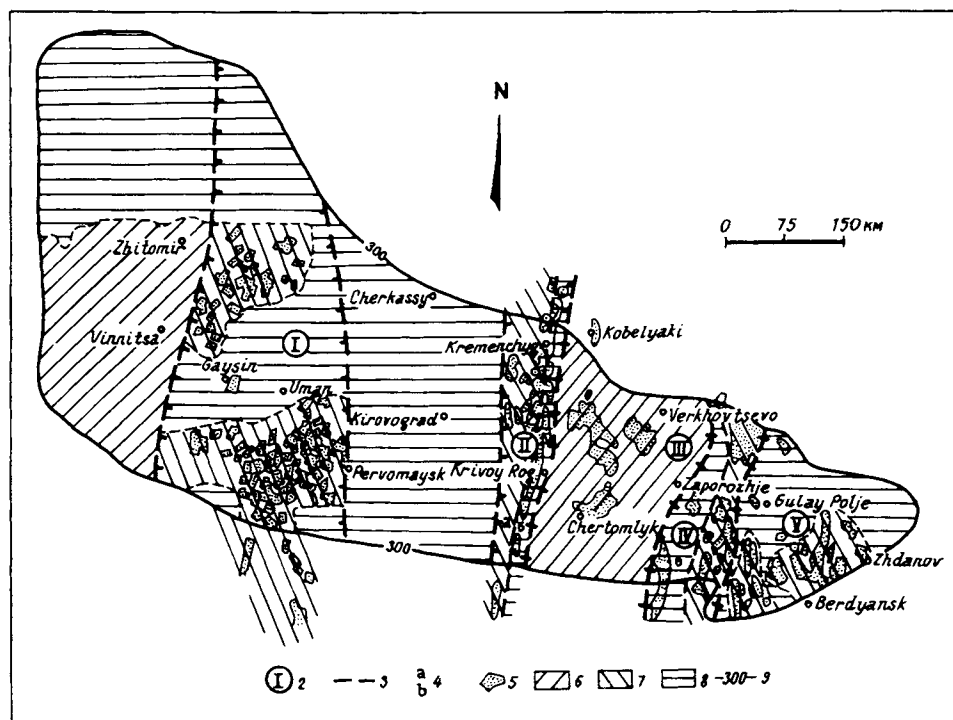


Fig. 53. Sketch map showing distribution of ferruginous rocks in the Ukrainian Shield (Belevtsev et al., 1981; Anon., 1982). 1 - boundary of metallogenic zones and provinces for iron; 2 - provinces and zones: I - Odessa-Belotserkov zone, II - Krivoy Rog-Kremenchug zone, III - Dnieper province, IV - Orekhovo-Belozero province, IV - Azov province; 3 - subzone boundaries; 4 - iron-rich rocks; 5-6 - iron-chert formations: 5 - volcanogenic (3.5-2.7 Ga), 6 - volcanosedimentary (3.5-2.7 and 2.6-1.8 Ga), 7 - sedimentary and clastic-chemogenic (2.6-1.8 Ga); 8 - edge of Ukrainian Shield (from 300 m sub-surface datum).

Table 7

Relationship between mineral deposits (6) and occurrences (+) and tectonic structures in the Ukrainian Shield

Useful\Structures minerals	I	II	III	IV	V	VI	VII	VIII	IX	X	XI	XII
Fe	+		<u>1</u>	+	<u>2</u>	<u>3</u>						+
Cr				<u>4</u>								
Cu, Ni Cu (Ni, Co)			<u>5</u>		+	<u>6</u>						+
Cu-Mo, Mo				7+		<u>+</u>	8+			+		
Ti									<u>+9</u>			
Topaz, morion									<u>10</u>			
Graphite				<u>11</u>	<u>12</u>	<u>13</u>					<u>14</u>	
Garnet							<u>15</u>					
Apatite						+			+			
Rare carths, rare metals						<u>21,</u>			17+	<u>18</u>		
Magnesite, talc			<u>19</u>			<u>16</u>						
Pyrophyllite, Al-raw materials												<u>20</u>

*Notes:* Ore-bearing tectonic structures: I – granulite-gneiss terrain; II-III – granite-greenstone terrain. II – tonalite- and granite-gneiss areas, III – greenstone belt; IV – collision zone (suture zone) between different structures; V – fold belt; VI – rift belt; VII-IX – structures due to tectono-thermal reworking, VII – of granulite-gneiss terrain, VIII – of granulite-greenstone province, IX – region of tectono-magmatic proto-activation, X – volcano-plutonic belt; XI – intra-cratonic fold belt; XII – intra-cratonic basin (trough).

*Ore deposits:* 1 – Chertomlyk, 2 – Mariupol, 3 – Krivoy Rog-Kremenchug basin, 4 – Kapitanov, 5 – Pravdin-1, 6 – Karachunov-Lozovat zone, 9 – Stremigorod, 10 – Volyn pegmatite field, 11 – Zavalyevskoye, 12 – Troitskoye, 13 – Petrov, 14 – Burtyn, 15 – Slobodov, Kamenskoye, 16 – Chernigov, 18 – Sustchan-Perzhan zone, 19 – Pravdin-2, 20 – Zbrankov, 21 – Zheltorechka.

*Ore occurrences:* 7 – Lipovenkovo, 8 – Lyubar, Ostropol, 17 – October, Petrovo-Gnutovo.

volcano-sedimentary formations), the Krivoy Rog–Ingulets metallogenic zone (iron–silica clastic terrigenous–chemogenic sedimentary formation), the Dneprovsk metallogenic province (ores in a volcanosedimentary formation), the Azov metallogenic province (sedimentary and volcanosedimentary ores).

Iron ore deposits in the Ukrainian Shield generally belong to the prograde metamorphic (Kratz, 1984; Sokolov et al., 1975) or metamorphosed class (Belevtsev, 1981), including ferruginous quartzites and rich iron ores. The iron ores found in the Ukrainian Shield can be divided into five groups according to their genetic features and mining properties relating to extraction and procession (Belevtsev et al., 1981): rich iron ores – the Saksagan, Pervomaysk, Ingulets and Pobug types; poor iron ores – the Skelevat, Verkhovtsevo and Mariupol types. The stratigraphic position of the iron ores can be characterised as follows. Iron ore horizons, beds and lenses are known to be intimately interbedded with the host rocks of Archaean Dnestr–Bug, West Pre-Azov, Rosinsk–Tikich and Konka–Verkhovtsevo groups and the Lower Proterozoic Bug, Ingul–Ingulets, Krivoy Rog and Central Pre-Azov groups. Iron ore formations in the Ukrainian Shield basically belong to two epochs – Archaean and Early Proterozoic. Characteristics of the Ukrainian Shield iron ore formations and specific geological settings for several typical ore deposits or groups of deposits, as summarised below, are based on work by Belevtsev (1986) and Belevtsev et al. (1981).

#### 2.1.1. *Krivoy Rog type (clastic terrigenous–chemogenic formation)*

This type makes up the Krivoy Rog–Kremenchug rift belt and occurs in Early Proterozoic synclines, sometimes monoclines, 2.6–1.8 Ga old. There are two formations: Gdantsevo and Saksagan. The Gdantsevo iron–silica–carbonate formation typically displays iron–silica horizons alternating with carbonate members and graphitic–carbonaceous shales. The Saksagan iron–silica–silicate formation is represented by iron–silica horizons interleaved with chlorite, biotite and amphibole schists. Greenschist to amphibolite facies metamorphism is typical for these iron ore formations, which constitute the most important type in the Ukrainian Shield. Four types of ore have been identified: Skelevat (low-grade ores, ferruginous quartzites), Saksagan, Pervomaysk, Ingulets (rich ores).

*Skelevat* ferruginous quartzites have a predominantly magnetite and martite composition and occur within the Saksagan Fm of the Krivoy Rog Group (Kremenchug and Pravobereg regions, Krivoy Rog basin). Sheet deposits are up to 200–300 m thick and extend for several kilometres along strike. Depth of occurrence depends on the plunge depth of fold structures. Ferruginous quartzite deposits may occur in 1) fold hinges (Skelevat–Magnetitovoye, Gorishneplavinskoye, Ingulets); 2) fold limbs (Bolshaya Gleyevatka); 3) cross-fold zones (Pervomaysk). Ferruginous quartzites have magnetite, hematite–magnetite, silicate–magnetite and carbonate–silicate–magnetite compositions and are found in greenschist and epidote–amphibolite facies metamorphic rocks. Skelevat type ores contain 34–35% iron in carbonates.

The *Saksagan* ore type (85% rich iron ores in the Krivoy Rog basin) is also associated with the Saksagan Fm, Krivoy Rog Group (5th and 6th iron horizons). The rocks typically display greenschist facies metamorphism. Ores occur in folded and

fractured parts of synclines and basically have a martite composition. Deposits of rich ores are restricted exclusively to deep oxidation zones.

The *Pervomaysk* ore type (9% of the reserves) is also observed in ferruginous quartzites and shales in the Saksagan Fm and consists of silicate–magnetite and carbonate–magnetite varieties. Deposits of such ores are encountered in intensely faulted zones. They occur amongst rocks belonging to the epidote–amphibolite facies in which alkali and carbonate metasomatic aureoles appear around the ore bodies.

The Ingulets ore type (7% of rich ore reserves) has a silicate–magnetite and carbonate–hematite–magnetite composition. The ores are associated with the junction between Saksagan Fm and Gdantsevo Fm rocks (Krivoy Rog Group), or in the lower part of the Gdantsevo Fm; they are sheet-like or podiform in shape.

Most of the iron ore deposits belonging to this formational type are concentrated in the Krivoy Rog basin, where ferruginous rocks crop out in a near N–S strip 100 km long by 2–7 km wide. The Krivoy Rog basin consists of Archaean trondhjemites and migmatites with relicts of basic and ultrabasic igneous rocks and gneisses and Lower Proterozoic formations. The Krivoy Rog Group (PR<sub>1</sub>) containing all the ore deposits in the basin, lies above a weathered mantle of granitic rocks belonging to the Dnepropetrovsk complex (AR<sub>1</sub>, basement). The group is subdivided into five formations, the lowest being the *Novokrivoy Rog Fm* of amphibolite with subordinate hornblende–biotite schist, metasandstone and quartzite, up to 1.2 km thick. The *Skelevat Fm* overlies the Novokrivoy Rog Fm above a stratigraphic unconformity and consists of metamorphosed clastic sediments – conglomerates and sandstones – and aluminous schists; the thickness is 100–250 m. The *Saksagan Fm* (iron ore) is conformable on the Skelevat Fm and has a characteristic alternation of iron–silica rocks with shale beds of varying composition. The complete succession has seven ferruginous and seven shale horizons which vary in thickness along strike and down dip. The formation has a maximum thickness of 1.6 km. The 700–800 m thick *Gdantsevo Fm* consists of conglomerates, metasandstones, chlorite schists, and associated chlorite–magnetite ores. The *Gleyevat Fm*, consisting of conglomerate, metasandstone, biotite, carbonate and graphite schists, contains ferruginous quartzites; the formation is 3–4 km thick. Figure 54 illustrates the distribution of ferruginous rocks in the Krivoy Rog basin.

Rocks belonging to the Krivoy Rog Group occur in a near N–S strip, complicated by folding and faulting – the Main syncline with the Saksagan fold–thrust zone on the eastern limb, and the Tarapak–Likhmanovo anticline on the western limb (Fig. 55). In the north of the basin the western limb of the Main syncline is missing. Barrovian-type regional metamorphism from greenschist facies to epidote–amphibolite facies has affected rocks of the Krivoy Rog Group. The Saksagan iron ore formation consists of quartz–sericite schists with graphite, chlorite, biotite and amphibole, and ferruginous rocks (iron–silicate quartzites and jaspilites). Authigenic mineral zoning has been observed.

Due to the fact that ferruginous quartzites vary in amount in different parts of the Krivoy Rog basin and are interleaved with schist horizons, the total thickness of the iron ore assemblage varies from 150 m in the south to 800 m around Krivoy Rog town and 1600 m to the north; farther north the thickness decreases again. The iron content of ores in the Krivoy Rog basin is 46–70% rich ores and 15–20% to 30–35% poor ores.

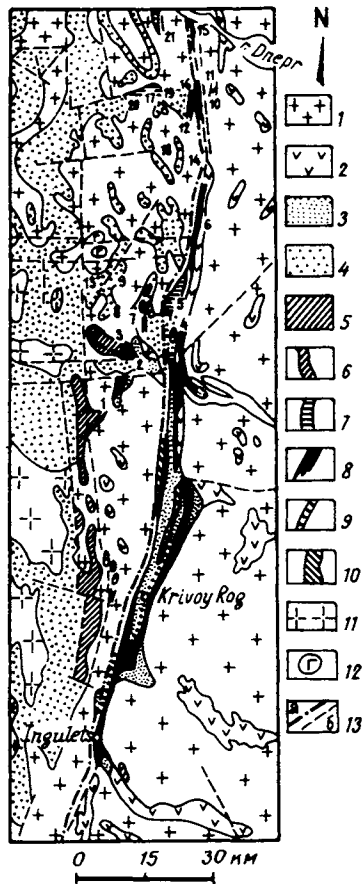


Fig. 54. Distribution of iron-chert rocks in the Krivoy Rog iron ore basin (Reshetnyak and Yefimenko, 1984). 1 - Dnepropetrovsk granitic complex (AR<sub>1</sub>); 2 - Konka-Verkhovtsevo Group (AR<sub>2</sub>); 3 - Krivoy Rog Group (PR<sub>1</sub>); 4 - Ingul-Ingulets Group (PR<sub>1</sub>); 5 - Rodionov Fm (in 4). Iron ore formations: 6 - iron-chert-metabasite (AR<sub>1</sub>-AR<sub>2</sub>); 7 - iron-chert-gneiss (AR<sub>1</sub>-AR<sub>2</sub>); 8 - iron-chert-schist (PR<sub>1</sub>); 9 - iron-chert-clastic (PR<sub>2</sub>); 10 - iron-chert-meta-ultrabasic (PR<sub>2</sub>); 11 - Kirovograd-Zhitomir granitic complex (PR<sub>1</sub>); 12 - basic-ultrabasic complex (PR<sub>1</sub>); 13 - faults: a - regional, b - splay. Numbers in circles - ore deposits and sectors: 1 - Petrov, 2 - Artemov, 3 - Bereznevat, 4 - Kamchatsky, 5 - Zheltyansk, 6 - Popelnastov, 7 - Zelenov, 8 - Ivanov, 9 - Lenin, 10 - Nikolayev, 11 - Mlynkov, 12 - Uspenov, 13 - Ovnyakov, 14 - Proletarsky, 15 - Orekhov, 16 - Lozovat, 17 - Maryevsky, 18 - Chervono-Bratsk, 19 - Krasnofedorov, 20 - Zybkovsky, 21 - Kamennopotok.

Rich ores are observed amongst jaspilites and form sheets, thick deposits, ore pipes and pockets. Iron ores formed in the Krivoy Rog basin by the accumulation of iron during the sedimentary process, and subsequent metamorphism (ferruginous quartzites - poor ores). The development of later rich ores was due to the simultaneous action of tectonics and hydrothermal-metamorphic processes: silica being removed from zones of compression, and Mg-Fe metasomatism.

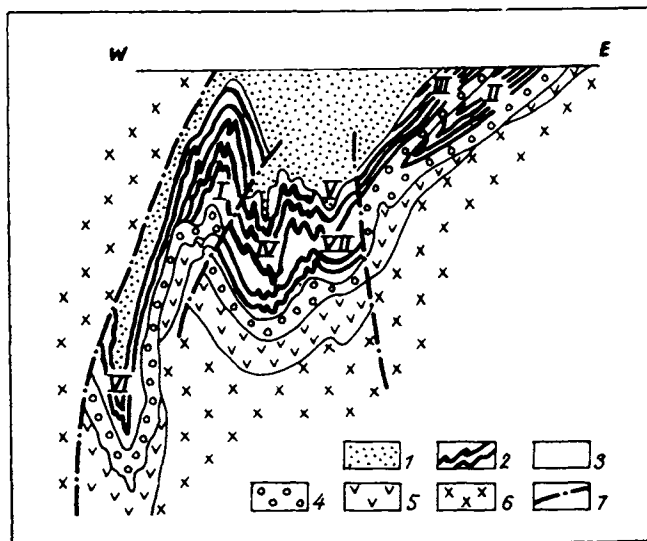


Fig. 55. Geological-structural sketch map of the Krivoy Rog basin (Belevtsev, 1986). Krivoy Rog Group: 1 – Gdantsev Fm (upper); 2–3 – Saksagan Fm: 2 – iron ore horizons, 3 – schists; 4 – Skelevat Fm; 5 – Novo-Krivoy Rog Fm; 6 – Archaean basement (granites & migmatites); 7 – tectonic breaks. Structures: I – Tarapak-Likhmanov anticline; II, III – Saksagan synformal anticline; IV–VII – synclines: IV – West Ingulets, V – East Ingulets, VI – Ingulets, VII – Novo-Krivoy Rog.

### 2.1.2. *Volcanosedimentary type (Verkhovtsevo)*

This type is developed mostly in the Verkhovtsevo, Chertomlyk and Sursk regions in the Dnieper metallogenic province and is associated with the Upper Archaean Konka-Verkhovtsevo Group which forms greenstone belt structures. (It is present amongst 2.8–3.0 Ga old metamorphic and granitized basic rocks). Ferruginous quartzites are interbedded with basic metavolcanics and metamorphosed volcano-sedimentary rocks. Volcanogenic rocks of ultrabasic, intermediate and acid composition are encountered less frequently. Most often the ferruginous rocks are thin, with carbonate-magnetite and silicate-carbonate-magnetite compositions. Ferruginous quartzite beds extend along strike from a few hundred m to 5–8 km and vary in thickness from a few m to 250 m, but most commonly from 5–8 m to 30–50 m. Beds thicker than 100 m are rare and cannot be traced for more than 700–900 m along strike. The beds dip steeply, conformable with the host rocks, and the non-productive rocks account for much the greater proportion of the thickness of a formation. Both the ferruginous quartzites and their host rocks typically display greenschist facies metamorphism, occasionally amphibolite facies. Verkhovtsevo type ores contain 10–19% iron as magnetite, and 4.5–18.7% iron in carbonates.

The *Chertomlyk* ferruginous quartzite deposit is located on the eastern limb of the Chertomlyk synclinerium, the western limb of which is cut by a north-easterly thrust. The strike on the eastern limb is to the NE, and nearly N–S in the north, with steep westerly dips. Two ferruginous quartzite beds occur within micaceous quartzites,

ultrabasic rocks and schists. The first bed is 120–250–300 m thick, giving way to two beds each 15–30 m thick, and the second bed is 20–30 m to 65–85 m thick. Both beds can be mapped for around 8 km long.

In this deposit the ferruginous quartzites are represented by silicate–carbonate–magnetite varieties and consist of quartz, magnetite (14–25%), carbonate (sideroplesite, 23–52%), biotite, amphibole and chlorite. The total Fe content varies from 20% to 43%, and is around 30% on average; Fe in magnetite is 10.0–19.2%, around 15% on average; and Fe in carbonate is 4.5–18.7%, around 7% on average. At present there is no industrial extraction of ores in this deposit due to the relatively low magnetite content, the complex mineral composition, and the fine-grained nature of the ore components (0.007–0.1 mm).

### 2.1.3. *Volcanosedimentary formation – leptite<sup>1</sup> type*

This type is developed most widely in the Azov metallogenic province (Mariupol, Kuksungur and other ore deposits in fold belt structures), in the Odessa–Belotserkov zone and other regions. They are represented by banded iron–silicate rocks associated with paragneisses and orthogneisses, metavolcanics (amphibolites, apo-keratophyres and meta-ultrabasic igneous rocks), and migmatites. They usually form single beds or drawn-out lenses with a limited strike length. Less commonly, two or three ore bands are observed. Metamorphism is typically amphibolite and granulite facies, occasionally greenschist facies. Two ore types have been distinguished (Belevtsev et al., 1981): Mariupol (poor ferruginous quartzites) and Pobug (rich ores).

*Mariupol type* ferruginous quartzites are mainly silicate–magnetite (pyroxene– and amphibole–magnetite and others) and rarer magnetite varieties. Associated with the ferruginous quartzites in the formation are barren quartzites, calciphyres, graphitic and high-alumina schists and gneisses (primary sedimentary rocks), as well as meta-volcanics belonging to the Early Proterozoic Central Pre-Azov Group. The ferruginous quartzites are up to 200–300 m thick. Individual deposits and ore bands form disconnected monoclinical and brachysynclinal folds amongst granitoids and migmatites. Mariupol type ores contain 32–42% total iron and 22–40% iron as magnetite; iron in carbonates is almost completely absent.

Rich *Pobug type* ores have a carbonate–magnetite composition and are associated with basic ortho- and para-rocks. Dolomite–magnetite ores occur adjacent to calciphyre, pyroxene–plagioclase schist and garnet–biotite gneiss; pyroxene–garnet gneiss and amphibolite may be found here and there. A characteristic association is dolomite–magnetite ore and ferruginous quartzite, the first such occurrence in the Ukrainian Shield. Ores of this type form conformable sheet-like and podiform bodies.

*The Mariupol ore deposit* is located in the axial zone of the Central Azov syncline. Ore bands stretch in a strip that extends in a nearly N–S direction for 20–25 km. Segments of the deposit are the cores of shallow synclines. The host rocks of the Central Pre-Azov Group (PR<sub>1</sub>) consist of various gneisses, schists, marbles, metabasics (amphibolites), barren quartzites, and migmatites.

<sup>1</sup>Leptite in Russian is used to signify high-grade regional metamorphic quartzofeldspathic rock with a granular or granoblastic texture and fine grain size; usually considered a primary sedimentary rock.

There are one or two (depending on the area) sheet deposits of pyroxene–magnetite quartzite, 30–150 m thick and 300–8000 m long. Ore beds in synclines near the surface dip steeply and flatten out to 30° at depth. The dip is steep (80–85°) where the ore beds occupy monoclinical structures. Deposits contain significant numbers of barren and weakly mineralized rocks, up to 15 m thick. Ore-bearing quartzites consist of magnetite (10–59%), quartz (30–64%), pyroxene (1.3–35.9%), plagioclase (up to 17%), garnet (up to 25%), and other minerals. The total iron content in the ores is 32–42%, with 8–40% Fe in magnetite.

## 2.2. Chromium

Chromite mineralization in the Precambrian of the Ukrainian Shield occurs in the west, predominantly in the Volyn and Podolsk (eastern part) blocks and the Golovanevsk zone. Individual chromite deposits and particularly ore occurrences are spatially and genetically associated with Archaean ultrabasic intrusions belonging to the dunite–peridotite formation (Galetsky et al., 1984). In the Northern Pobug region, dunite–peridotite massifs are located within a collision zone setting – the Golovanevsk suture zone which along the Pobug fault zone consists of rocks belonging to the Bug Group and Late Archaean–Early Proterozoic granitoids. The intrusions extend for 260–1800 m and are 12–162 m wide (Kanevsky, 1981). Harzburgites predominate over lherzolites, and wehrlites are almost completely absent, but serpentinites are present.

In the established chromium deposit – the *Kapitanov* and a number of small occurrences – the Lipovenkovo and other ore bodies have a lenticular and tubular shape and occur within serpentinites usually at the contact with pyroxenites, less commonly within the pyroxenites. Ore bodies are 50–150 m long by 0.5–8.0 m wide. The ores are massive (40–41% Cr<sub>2</sub>O<sub>3</sub>) and densely impregnated (28–29% Cr<sub>2</sub>O<sub>3</sub>). The main ore mineral is chrome spinel (chromite); magnetite, pyrite, pyrrhotite, chalcopyrite and pentlandite are also present (Zlobenko et al., 1977). Sulphides constitute a sparsely distributed dissemination. A study of variations in chrome content in rocks from nine dunite–peridotite intrusions in the Middle Pobug region has shown (Kanevsky, 1981) that the chrome-bearing intrusions have a particular range of chromium concentration coefficient: 2.8–9.6. Platinum and palladium has been discovered in ultrabasic rocks in the region of the *Kapitanov* intrusion. These metals occur as accessories in the basal parts of dunite intrusions and in chromite-enriched rock varieties (Belevtsev et al., 1974). Potash metasomatism along a fault zone in the *Kapitanov* intrusion produced mica rocks containing up to 25% corundum in addition to biotite (70–75%).

## 2.3. Titanium and phosphorus

Titanium–phosphorus ore mineralization (ilmenite, titanomagnetite, apatite) within the Ukrainian Shield is generally associated with rocks in the gabbro–anorthosite–rapakivi granite association (Dagelayskaya, 1987). This rock association is localized in the Korosten and Korsun–Novomirgorod plutons, which have a total area of some 25,000 km<sup>2</sup>, and represent a product of tectonomagmatic activity that first occurred at the end of the Early Proterozoic. The plutons occupy a sharply discordant position in

relation to the country rocks – metamorphosed assemblages of the Terev and Ingul–Ingulets groups and non-metamorphic volcano-sedimentary rocks of the Pugachev Group. Rocks which overlie the Korosten pluton are platform sediments of the Ovruch Group. Rapakivi granites form by far the greatest component of the plutons (around 75% of the area). The remainder consists of rocks in the gabbro–anorthosite association, forming discrete intrusions within the granites and commonly with a zonal structure, polyphase history and elements of layering (Fig. 56). Gabbro–anorthosites and anorthosites account for around 75% of the area of the intrusions. There are limited amounts of gabbroic rocks (up to 23%) and very restricted ultramafic rocks (c. 2%), including ore-bearing types – apatite- and ilmenite-bearing gabbroic and ultramafic rocks. The geological and petrographic sketch map of the Korosten pluton (Fig. 57) shows the age divisions of the gabbroic complex. The earliest (pre-anorthosite) phase contains a group of “marginal” gabbroic rocks – gabbro-norite, norite, gabbro, often containing olivine. The second phase is gabbroic rocks, forming schlieren among anorthosites, with which they are contemporaneous. The third (post-anorthosite) phase

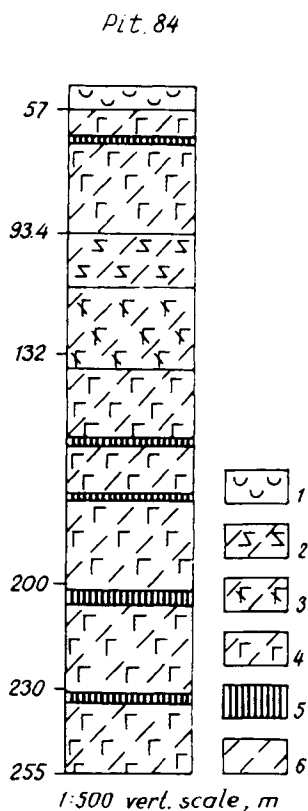


Fig. 56. Rhythmic structure of titaniferous basic body. 1 – gabbro weathered crust; 2 – leucocratic ore-rich gabbro; 3 – melanocratic ore-rich gabbro; 4 – melanocratic olivine gabbro & ore-bearing troctolite; 5 – ore-bearing plagioclase peridotite; 6 – orientation of parallel texture.

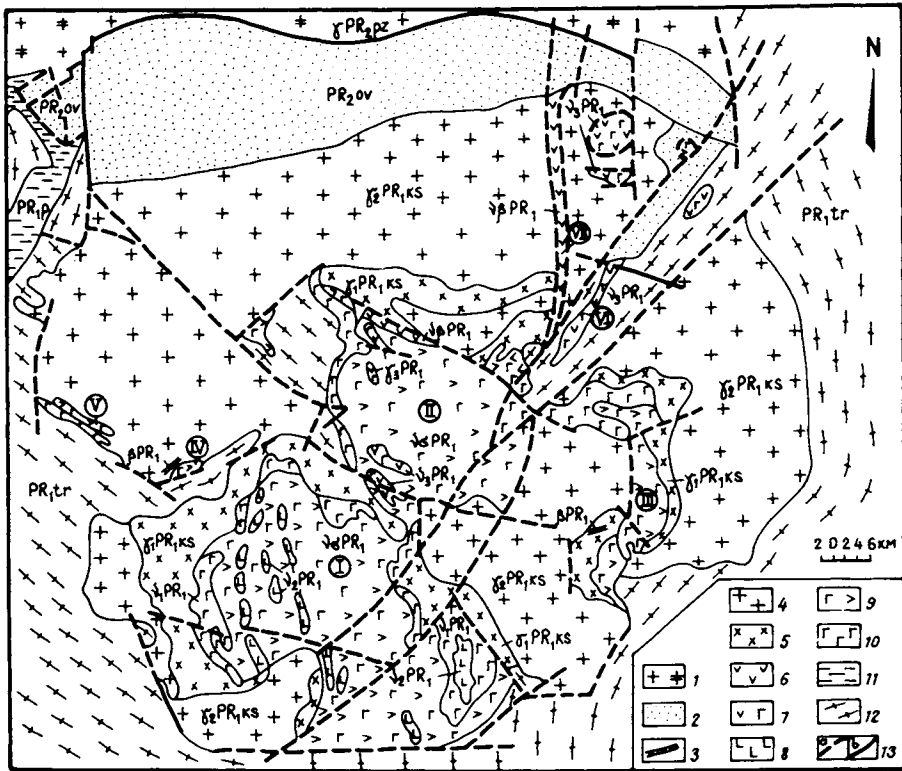


Fig. 57. Geological-petrographic map of Korosten pluton. Compiled by I.N. Dagelayskaya, based on a map by Bukovich et al. (1979). 1 – Perzhan granitoid complex ( $\gamma PR_2 pzh$ ); 2 – Ovruch lavas & sediments ( $PR_2 ov$ ); 3–5 – Korosten granitic complex: 3 – diabase ( $\beta PR_1$ ), 4 – rapakivi granite ( $\gamma_2 PR_1 ks$ ), 5 – hybrid granite, syenite, monzonite ( $\gamma_1 PR_1 ks$ ); 6–10 – Korosten gabbro-anorthosite complex: 6 – gabbro-diabase, diabase porphyry ( $v\beta PR_1$ ), 7 – olivine gabbro, troctolite, including ore-rich ( $v_3 PR_1$ ), 8 – gabbroic & ore-bearing ultramafic rocks in striped zones ( $v_2 PR_1$ ), 9 – gabbro-anorthosite & anorthosite ( $v\alpha PR_1$ ), 10 – “marginal” gabbro ( $v PR_1$ ); 11 – Pugachev lavas & sediments ( $PR_1 p$ ); 12 – Teterev gneiss & migmatite ( $PR_1 tr$ ); 13 – faults (a), geological boundaries (b). *Intrusions*: I – Volodar-Volyn, II – Chepovich, III – Fedorov, IV – Ushomir, V – Krivotin, VI – Rudnya-Bazarskoye body, VII – Zvizdal-Zalesskaya dyke.

consists of gabbro belonging to the so-called stripe zones, occupying a cross-cutting position in the intrusions. These gabbroic rocks are enriched in ore minerals (ilmenite and titanomagnetite) and are associated with ore-bearing ultramafic rocks with known titanium occurrences (Ryzhany, Paromovka and other regions). The fourth phase consists of stock-like and cross-cutting vein bodies, some of which are ore-bearing apatite-ilmenite gabbroic rocks, troctolites and ultramafics (a body in the southern part of the Chepovich intrusion). Dolerite and gabbro-dolerite dykes make up the fifth phase.

In the contact zones between gabbro-anorthosites and rapakivi granites there are hybrid rocks, granitized to a greater or lesser extent, represented by monzonite, syenite and pyroxene-bearing granite. Also associated with the same contact zones are topaz-morion (rock crystal) chamber pegmatites, which are considered further below.

Titanium and accompanying phosphorus ore mineralization are associated with gabbro-anorthosite intrusions, their overall area being up to 6,000 km<sup>2</sup> – the Korosten intrusion in the Volyn block and the Korsun-Novomirgorod intrusion in the Kirovograd block. The titanium content of the Korosten pluton has been studied to a greater extent, and is known to consist of placer, residual deposits and *in-situ* titanium ore bodies, some of which are being exploited. During the 1960s–70s, Gerasimchuk, Proskurin, Timofeyev, Shvayberov, Tarasenko, Boyko, Dagelayskaya and Kudinova investigated the titanium mineralization in the gabbro-anorthosite complex. These authors' information was used in compiling this summary.

All rock varieties in the gabbro-anorthosite complex contain titanium (ilmenite-titanomagnetite) and the frequently accompanying phosphorus (apatite) mineralization, but high economic titanium contents and higher phosphorus contents are associated with melanocratic gabbroic and ultramafic rocks of varying origins, and residual weathering deposits from these rocks. Titanium mineralization occurs as magmatic, late metasomatic, and surficial. Orthomagmatic ores are associated with various phases in the formation of rocks in the gabbro-anorthosite association: early gabbroic rocks and gabbro-anorthosites contain poor syngenetic (disseminated)–segregation apatite-ilmenite mineralization and richer magmatic (fusion) mineralization. The first of these is widespread in early differentiates from basic magma – gabbroic rocks of the “marginal” complex, which are the source of weathered mantles with economic ilmenite contents. Later gabbroic rocks typically display fusive mineralization, associated with feldspar ultramafics. Such mineralization occurs in the Paromovka, Ryzhany and Styrtva areas in the Korosten pluton; and evidently also most of the apatite-ilmenite ores within the Korsun-Novomirgorod pluton – the Mezherich, Ternovka and Novomirgorod areas. Fusive late-magmatic mineralization is found in troctolites, gabbroic and ultramafic rocks, late stocks and dyke-like bodies – the *Stremigorod* type.

Superimposed hydrothermal-metasomatic ore mineralization is related to the influence of rapakivi granites in the Korosten complex on basic rocks and is restricted to contact zones between basic rocks and granites. Representative forms are veinlets, lenses, clusters or densely disseminated and massive ores. This type is often associated with tectonic zones in gabbro-anorthosites (Mezherich-Obikhodovo zone) and granite contacts (the zone in the area around Pinyazevichi). From their TiO<sub>2</sub> (ilmenite) and P<sub>2</sub>O<sub>5</sub> (apatite) contents, the ores are subdivided into poor (TiO<sub>2</sub> up to 5%, P<sub>2</sub>O<sub>5</sub> to 2.5%), average (TiO<sub>2</sub> 5–10%, P<sub>2</sub>O<sub>5</sub> 2.5–5%) and rich (TiO<sub>2</sub> > 10%, P<sub>2</sub>O<sub>5</sub> > 5%). Most ore-bearing gabbroic and ultramafic rocks belong to poor ores. In ore-bearing gabbros and troctolites from cross-cutting stock-like and vein bodies, ore element contents have the following ranges: TiO<sub>2</sub> 7.5%–12%, P<sub>2</sub>O<sub>5</sub> 3.5%–5.6%, V<sub>2</sub>O<sub>5</sub> up to 0.5%. The highest content of these elements (especially TiO<sub>2</sub>, 17–20%) on average is characteristic for the late superimposed hydrothermal-metasomatic type that occurs at contacts between gabbroic rocks and rapakivi granites. Rich phosphorus-titanium mineralization is also known at present from several sectors in the Korsun-Novomirgorod pluton (data from Vorobey et al., 1984). It is represented by apatite-ilmenite ores with 15–27% TiO<sub>2</sub> content. The genesis of the ore is debatable, as is the genesis of a number of the other above-mentioned P-Ti ore mineralization types associated with the Korosten complex. Some workers (for example Tarasenko et al.,

1982) link their formation to hydrothermal–metasomatic processes transforming gabbroic rocks under the effect of rapakivi granites, where there is significant redistribution of ore material with the formation of densely disseminated apatite–ilmenite ores (basification process). However, other researchers consider that the magmatic factor plays the leading role in P–Ti mineralization in rocks of the gabbro–anorthosite complex (Proskurin, 1984; Dagelayskaya et al., 1983), although superimposed mineralization did play a significant role. The highest  $\text{TiO}_2$  and  $\text{P}_2\text{O}_5$  contents have been found in late differentiates and intrusive phases of gabbroic magma, enriched in phosphorus and titanium. These contain both disseminated and fusive mineralization types, the latter being predominant. Examples of such types are the ore gabbroic and ultramafic rocks in the stock-like body in the SW part of the Chepovich intrusion which cuts rocks belonging to the gabbro–anorthosite complex.

A characteristic feature for all the ore-bearing rocks in the gabbro–anorthosite complex is an increase in the iron content and total iron, which increases towards the ore-rich troctolites and ultramafics, i.e. it depends on how melanocratic the rock is, since iron mainly occurs in olivines and pyroxenes, not in the ore minerals. All the ore rocks typically have higher (relative to clark values) vanadium, zinc, cobalt, copper, zirconium and barium contents and anomalously low Ni and Cr, and in the case of Stremigorod ores – Y, Rb and Sc.

Favourable criteria for P–Ti ore mineralization in intrusions belonging to the gabbro–anorthosite association are high degree of differentiation in the complexes (anorthosites–ultramafics). End members of the differentiation series are enriched in iron and titanium. High-iron and high-titanium mafic and ultramafic late phases in the formation of the intrusions are widespread, and hydrothermal–metasomatic alteration zones have been observed at contacts with rapakivi granites and elsewhere.

#### 2.4. *Nickel, copper, cobalt*

Copper–nickel sulphide with cobalt ore mineralization has been discovered in the Volyn, Podolsk and Dnieper blocks – these are metallogenic provinces of the same names. They are associated with a dunite–pyroxenite–gabbro suite of Archaean ultramafic intrusions. Rocks belonging to this suite form lenticular and sheet-like bodies, localized mainly within greenstone belt structures (as well as regions where they have been reworked) and the collision suture zone. In terms of their structural setting, they are conformable in synclines of various orders as intrusive interlayer deposits. Host rocks are the Rosinsk–Tikich ( $\text{AR}_2$ ) and Teterev ( $\text{PR}_1$ ) groups in the NW of the Ukrainian Shield, the Bug Group ( $\text{PR}_1$ ) in the centre of the shield, and the Konka–Verkhovtsevo Group ( $\text{AR}_2$ ) in the Dnieper block (Ilvitsky et al., 1969). The intrusions are 210–3350 m long by 70–640 m wide and consist of serpentinized dunite and peridotite, pyroxenite, gabbro–norite and amphibolized gabbro (Galetsky et al., 1984; Zlobenko et al., 1977). Rocks in this series typically display a differentiated composition, high magnesium content, and low alkalis. For the Bug region, ore mineralization is characterized by the presence of chalcopyrite, pyrrothite and pentlandite. Useful components attain the following maximum contents: nickel 0.65%, copper 0.34–0.52%. Sulphide-bearing zones are up to 10 m thick with a sulphide content of 5–35%.

Sulphides form dispersed disseminations, grain clusters and occasionally sulphide veinlets up to 2 cm across. Present amongst the ore minerals are also magnetite, ilmenite, pyrite, millerite, gersdorffite, nickeline and cobaltite. The nickel concentration coefficient was determined for 130 intrusions in the dunite–pyroxenite–gabbro suite in the North Bug region (Kanevsky, 1981), and was found to be greater than 1.4 (simultaneously, that for cobalt exceeds 0.7), which indicates the prospects for nickel sulphide ores in that type of intrusion.

Copper–nickel sulphide occurrences have been found in the suture zone in the Bug region, associated with metamorphic rocks belonging to a komatiite–tholeiite association. Basic–ultrabasic igneous intrusions associated with synclines and faults in the Rosinsk–Tikich and Teterev Groups are characterized by the same assemblage of ore minerals, forming dispersed disseminations or clusters of sulphide grains. The nickel content is up to 0.42%, copper to 0.3%.

In the Sursk–Verkhovtsevo–Chertomlyk zone of the Dnieper metallogenic province, copper–nickel sulphide mineralization has been discovered in the Pravdin ultrabasic intrusion (the *Pravdin* deposit), which together with other intrusions forms interlayer deposits in folds affecting the Konka–Verkhovtsevo Group (AR<sub>2</sub>). A belt of ultrabasic intrusions stretches for around 30 km, with a width of 300–2500 m. Host rocks are basic volcanics and schists of the Konka Fm that make up the greenstone belt. The Pravdin intrusion has dimensions 300–2500 m × 5000 m and consists of serpentized dunite and peridotite, serpentinite, talc–carbonate, amphibolitic and chloritic rocks. Syngenetic copper–nickel mineralization has been identified (Ilvitsky et al., 1969). Figure 58 illustrates the two representative associations: 1) chalcopyrite–pyrrhotite; 2) pentlandite-bearing (with polydymite, maucherite and chalcopyrite) and millerite type. The first type is restricted to zones in which amphibole and chlorite–amphibole rocks are developed, 10–20 m to 100–200 m thick. Mineralization has various characteristic morphological types: vein-disseminated (the main type), clustered, disseminated, etc. Chalcopyrite and pyrrhotite are the most widespread minerals; also present are pyrite, bornite, covellite, plus rare sphalerite. The copper content varies from 0.5% to 7.6% in drill core intervals where intense pyrite–pyrrhotite–chalcopyrite mineralization is observed, such intervals being 0.5–3.2 m thick. Gold (up to 2 g/t), silver (up to 10 g/t), cobalt, nickel and other metals have been found.

The second type of nickel sulphide mineralization is controlled by NW-striking tectonic zones coincident with the strike of the intrusion. Various morphological types of mineralization are observed here too: vein-disseminated (the main type), cluster-disseminated and dispersed-disseminated. Sulphides are irregularly distributed in the zones – from single grains, to 20–30%. Zones with higher sulphide contents are 0.15–1.6 m thick and are localized in brecciated areas amongst serpentinites and talc–carbonate rocks. The primary sulphide mineral (apart from chalcopyrite) is pentlandite, subsequently replaced during a hydrothermal event by polydymite and maucherite. The nickel content varies from 0.16 to 12.48%. Figure 58 illustrates the nature of the localization of the nickel sulphide ore mineralization in rocks of the Pravdin ultrabasic intrusion.

The *Karachunovo–Lozovat* sulphide mineralization zone (mainly copper) has been identified in a rift structure to the west of Krivoy Rog town in the Krivoy Rog–Ingulets metallogenic zone (Belevtsev et al., 1974; Dovgan et al., 1964) and has been traced in a

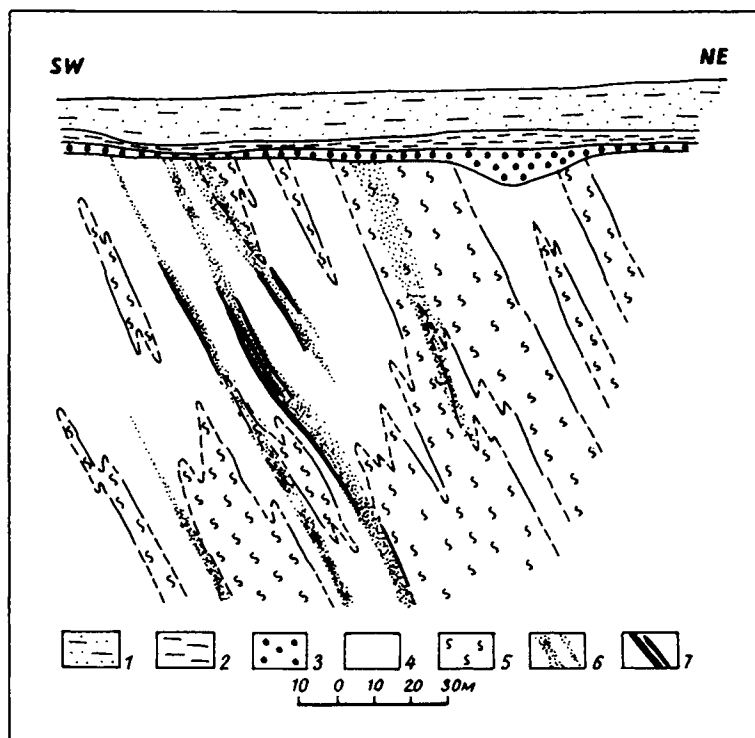


Fig. 58. Nickel sulphide ore mineralization in Pravdin ultrabasic intrusion. Section from drillcore data (Ilvitsky and Shrubovich, 1969). 1 – marls, 2 – sandy-clayey sediments, 3 – weathered mantle on ultrabasics, 4 – talc-carbonate rocks, 5 – serpentinite, 6 – zones of dispersed nickel sulphide dissemination, 7 – vein-disseminations of nickel sulphide ores.

near-N-S direction for over 20 km, with a width of around 4 km. Bismuth-copper, nickel-copper, lead and cobalt mineralization have also been observed. The most important sulphide contents have been noted in ferruginous quartzites belonging to Lower Proterozoic supracrustal assemblages – the Ingul-Ingulets and Krivoy Rog Groups – as well as in schists and migmatites of the Ingul-Ingulets Group. Bands of sulphide ore mineralization are associated with steeply-dipping near-N-S zones of schistosity, crushing, shearing and mylonitization. These sulphide-bearing strips are a few tens of metres across, although overall they have low ore element contents (copper – hundredths of one per cent, occasionally a few tenths of one per cent). Additionally, sulphide veins a few centimetres wide and mineralized breccia zones have been noted, in which the copper content reaches a few tenths of one per cent. Sulphide veins have sharp contacts and are controlled by shear joints. The main sulphide minerals in the veins are pyrite and chalcopyrite. Essential chalcopyrite ores contain chalcopyrite 5–50%, pyrite 0–15%, magnetite 0.5–15%, ilmenite 0.1–3%, pyrrhotite 0–10%, chalcocite 0–3%, cubanite 0–2%, marcasite 0–10%; bismuth and cobalt minerals have also been found (Dovgan et al., 1964).

In addition to sulphide veins, veinlet, dissemination and breccia types of copper mineralization have also been identified. Ore minerals form cross-cutting and concordant narrow (up to 1–2 cm) veinlets, essentially chalcopyrite. Disseminated mineralization is usually present at the contact between migmatites and basement relicts, forming bands up to 2 m wide and with copper contents up to hundredths of one per cent. Greatest interest attaches to brecciated ores, in which the ore minerals (mainly chalcopyrite) cement and replace rock fragments in crush zones. Other ore minerals observed include chalcosite, galena, native bismuth, pentlandite, cobaltite, etc. The copper content in this ore type ranges from a few tenths of one per cent to a few per cent. Useful mineralization in this zone belongs to the hydrothermal–metasomatic vein type.

2.5. Molybdenum

Molybdenite is quite widely distributed in the shield (Fig. 59; Galetsky et al., 1974; Belevtsev and Galetsky, 1984; Metalidi et al., 1986; Belevtsev, 1974; Pochtarenko et al., 1974) and is associated with several different Precambrian complexes (Nechayev et al., 1987). Rhenium is typically found with the molybdenite, the amount depending on how deep was the environment of formation. A broadly chalcophile geochemical signature with molybdenum has been identified in the Volyn and Podolsk metallogenic provinces, the Golovanevsk zone, the Krivoy Rog–Kremenchug belt, and the Azov met-

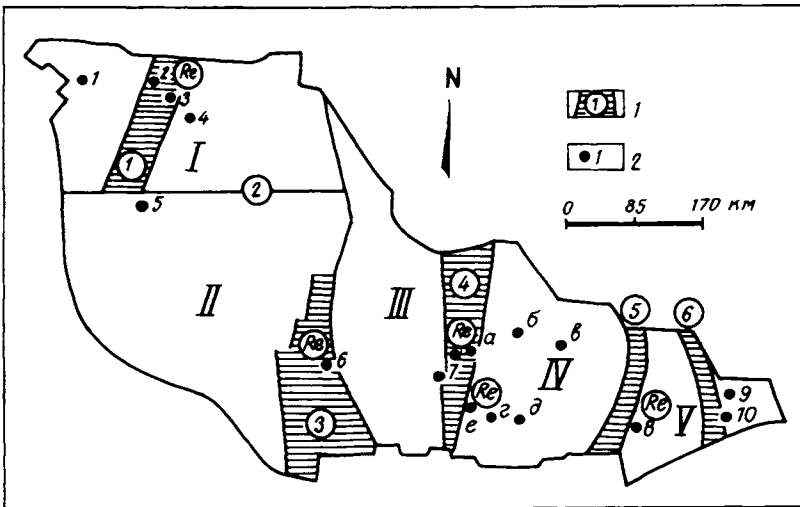


Fig. 59. Molybdenum mineralization in the Ukrainian Shield and rhenium-bearing molybdenites (Nechayev et al., 1987). *Shield blocks*: I - Volyn. II - Podolsk. III - Kirovograd. IV - Dnieper. V - Azov geoblocks. *Zones between blocks* (numbers in circles): 1 - Usovo-Dubrovsk, 2 - Andrushevo, 3 - Golovanevsk, 4 - West Ingulets, 5 - Orekhovo-Pavlovgrad, 6 - Central Azov. *Molybdenum mineralization* (filled circles): 1 - Virov, 2 - Perzhan, 3 - Verbin, 4 - Korosten, 5 - Malobratulov, 6 - Lipovenkovo, 7 - Maleyevo, 8 - Chernigov, 9 - October, 10 - Kalchik, a - Pervomaysk and Moiseyevo, b - Pervozvanov, c - Sursk, d - Aleksandrov, e - YUGOK.

allogenic province, i.e. in different structural settings – collisional suture zones, rift belts, areas of tectonothermal reworking affecting granulite–gneiss terrains, and a volcanoplutonic belt. In the western part of the shield molybdenite forms disseminations in quartz veins, as well as in metasomatic rocks in the Perzhan zone. In the middle of the shield, molybdenite has been found in conglomerate pebbles, pegmatites and skarns in the Krivoy Rog region. It has been found in the Chernigov carbonatite intrusion in the east of the shield (the Chernigov rift zone). Rhenium-bearing molybdenite is typically restricted to rocks from deep crustal sections, exposed in suture zones – Golovanevsk, Krivoy Rog–Kremenchug (rift-type) and Central Azov (inter-block-type). Rhenium-bearing molybdenite is also characteristic for an ultrabasic rock complex (the Lipovenkovo occurrence in the Golovanevsk zone).

The *Lyubar* and *Ostropol* occurrences have some interest. In addition to higher molybdenum, compared to other occurrences these two contain other metals, rare elements and rare earths. These occurrences are situated in the NW of the Podolsk metallogenic province in a belt of tectonothermal reworking in a granulite–gneiss terrain (Galetsky et al., 1974; Belevtsev and Galetsky, 1984). Dome structures are common in the area where these occurrences are located, and are developed within a larger-scale NW-striking syncline. Early Proterozoic ultrametamorphic Berdichev granites, garnet- and cordierite-bearing, migmatites of the granitoid formation, charnockite and enderbite are the most widespread rocks. There are also outcrops of leucocratic aplite–pegmatite granite and pegmatite. Proterozoic granites are present – the younger Kirovograd–Zhitomir complex – forming small intrusions. Granitic rocks contain remnants and xenoliths of biotite, amphibole–pyroxene and graphitic gneisses and schists and amphibolites, forming narrow synclines, also pyroxenite and gabbro–norite, and rarer marble and calciphyre. The main ore-bearing rocks in the region belong to the charnockite–migmatite suite, and to a lesser extent the granite–migmatite suite that represents remobilised granulite basement (Belevtsev and Galetsky, 1984).

As may be seen from the geological and structural sketch map of the region (Fig. 60), the *Lyubar* and *Ostropol* copper–molybdenum occurrence is associated with the intersection between the NE-striking Khmel'nitsky and the E–W-striking *Ostropol* tectonic zones. Nearly all the rocks from this region display a molybdenum geochemical signature, in association with copper, lead and zinc. Average molybdenum contents (0.0014%) have been found in pegmatitic pyroxene granite in the *Lyubar* occurrence and in cataclasite and mylonite in *Ostropol*. Small amounts of molybdenum (0.0004%) are present in garnet–biotite and biotite gneisses, pyroxene–biotite granite (charnockite), and aplite–pegmatite granite. True molybdenum mineralization in the form of molybdenite is associated with E–W fault zones along the contacts of Berdichev granites and charnockites. The rocks in these zones have suffered cataclasis and mylonitization as well as having been subjected to metasomatic alteration – albitization, potash-feldspathization and occasionally silicification, chloritization and carbonatization.

Molybdenite is not infrequently associated with coarse-grained and pegmatitic pyroxene granites, which typically have high silica and sulphur contents and low alkalis. Finely dispersed molybdenite dissemination is usual, as well as laminated-sheet aggregates with individual flakes measuring up to 0.2–0.3 cm. In the *Ostropol* occurrence,

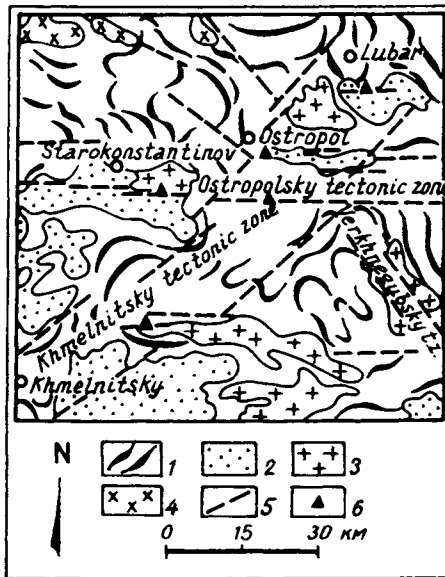


Fig. 60. Lyubar molybdenum occurrence (Pochtarenko and Bachay, 1974). 1 – Berdichev granite and migmatite complex (PR<sub>1</sub> – Chudново–Berdichev granites); 2 – gneiss, schist, amphibolite, charnockite; 3 – aplitic-pegmatitic granites, intrusive and metasomatic (AR–PR<sub>1</sub>); 4 – intrusive granites (PR<sub>1</sub>–PR<sub>2</sub>); 5 – faults; 6 – molybdenum occurrences.

molybdenite is present along the contact between pegmatitic granite and amphibolitized charnockite. The average molybdenum content in pyroxene granites is 0.07% and up to 0.2% at particular depth intervals over a thickness of 1.2 m. In cataclastic silicified varieties of pegmatitic granite, the molybdenum content reaches 0.01%. Present with the molybdenite are disseminated pyrrhotite, pyrite, chalcopyrite, magnetite and ilmenite; zircon, cyrtolite and apatite have also been found. Enhanced levels of tungsten (up to 0.02%) and Pb, Zn, Sb, Ag, B, Ni, Co have been noted in rocks from the molybdenum occurrences. Tungsten appears in skarns at the contact between marble and leucocratic microcline granite; Sn and Nb have been found mainly in leucocratic pegmatitic granites. The molybdenum occurrences referred to above belong to a molybdenum (molybdenum–copper) ore formation associated with a granitic group of formations. Hydrothermal genetic types are represented, forming stockworks, pipes and columns with disseminated ore mineralization.

## 2.6. Rare earths and rare metals

This type of mineralization occurs in the Azov region, the SE part of the Ukrainian Shield. Rocks in the region are Archaean gneisses and migmatites belonging to the West Pre-Azov Group, forming a granulite–gneiss terrain; Lower Proterozoic assemblages belonging to the Central Pre-Azov Group; and Early Proterozoic syn-orogenic granites of the Pre-Azov complex, forming isolated structures within an area of tec-

tonothermal reworking during Early and probably Late Proterozoic time. A gabbro–granite–syenite complex formed towards the end of the Early Proterozoic, in areas of primary tectonomagmatic activity, and an alkali–ultrabasic–carbonatite complex, localized within rift-type structural belts (the Chernigov zone). These rock complexes are the source of titanium and rare metal–rare earth mineralization (zirconium, niobium, tantalum, hafnium, cerium, lanthanum, etc.).

Intrusions of the gabbro–granite–syenite complex include the October, South Kalchik, Kalmius, and Yelanchik bodies (Ainberg, 1933; Yeliseyev et al., 1964; Rudenko, 1962; Tsarovsky, 1958, 1962, 1964), which are fault intrusions of Proterozoic age, discordant to the dip and strike of the country rocks and located in near-N–S and NW-striking faults. Compositionally, these intrusions are all fairly similar, but the greatest variety of rock types and associated petrogenetic and ore-forming processes are characteristic for the October intrusion, and the ore occurrence of the same name.

*The October intrusion* occupies an area of approximately 100 km<sup>2</sup>. Zones within the body are alkali–earth–quartz and quartz syenites which cut granites and gneisses. The central part of the massif consists of alkaline rocks proper (alkaline syenite, nepheline syenite and mariupolite<sup>2</sup>). Their contacts with alkali–earth syenites are gradual and non-intrusive, although they are considered to be an independent intrusive phase (Yeliseyev et al., 1964), since their primary structures display a different pattern (Fig. 61). The NE part of the intrusion contains a block 1.5 × 3.0 km in area, consisting of gabbro, pyroxenite and peridotite segregations. Contacts between these rocks and the syenites are tectonic. Nepheline syenites form a horseshoe-shaped body and have gradual contacts with alkali syenites. Mariupolites form two fields – in the NE part amongst gabbroic and ultramafic rocks, and in the SW amongst alkaline syenites. In the SW they gradually merge into nepheline syenites, at the expense of which they form. Associated with the mariupolites are albite–nepheline and microcline–nepheline pegmatites and albitites which formed like the mariupolites during metasomatic and auto-metamorphic transformation processes. Dykes are widespread in the intrusive massifs; these belong to two types: 1) compositionally similar to the country rocks and geologically related to them – syenite–aplite, granite–porphyry, etc., and 2) basic dykes that can be followed for 50–100 m up to several km and which are concentrated in NW-trending swarms. These are dolerite, lamprophyre, quartz porphyry, monchiquite, tinguaitite dykes, and other compositions.

Other metasomatic rocks are represented in the massif in addition to mariupolites. Fenite, glimmerite, albite–phlogopite metasomatite, carbonatite and carbonate–fluorite metasomatites form at the contact between basic rocks and nepheline syenites. Soda-rich metasomatites occur as alkalization zones in linear cataclastic zones. These are known in the Kalmius and Yelanchik intrusions, as well as amongst granites and gneisses, and are 5–20 m wide by 4–20 m long. Newly-formed minerals are albite, aegirine, alkali amphibole, micas and carbonates. The carbonate in these rocks is represented by parisite. Zircon, pyrochlore, sphene, rare-earth apatite, beckelite and

<sup>2</sup>mariupolite = variety of albite–nepheline syenite with 74% albite, 13% eleolite (greenish nepheline), 7% acmite, 4% lepidomelane, biotite, 2% zircon (large crystals), apatite, beckelite, etc., usually no orthoclase; obsolete term.

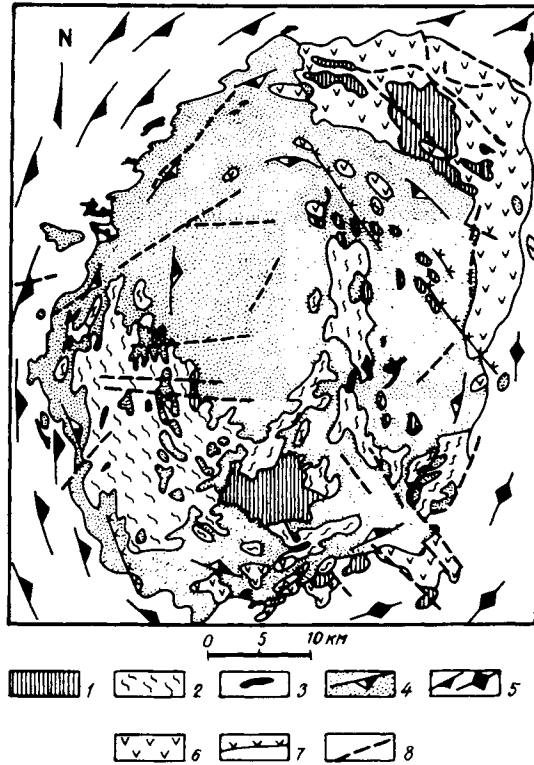


Fig. 61. Geological sketch map showing structure of October intrusion (Yeliseyev and Kushev, 1964). 1 – metasomatites, 2 – nepheline syenite. 3 – alkaline syenite-pegmatite. 4 – alkaline syenites & orientation, 5 – quartz syenites & orientation of trachytic texture. 6 – basic & ultrabasic rocks. 7 – lamprophyre dykes. 8 – faults.

fluorite appear in metasomatites. Geochemical features of the process are the appearance of rare earths, mainly in the cerium group, in parisite and fluorite. Similar metasomatites have been described by Kuzmenko (1946) in the Petrovo-Gnutovo zone between granite-gneisses and albitites; the zone is 0.3–3 m wide. Zirconium, tantalum-niobium and rare-earth mineralization are associated with the mariupolites and syenite pegmatites of the October intrusion.

The *Petrovo-Gnutovo* rare-earth occurrence is situated within the East Azov block in the southern part of the Kalmius alkali granite, quartz syenite and syenite intrusion belonging to the Early Proterozoic East Pre-Azov complex. The intrusion is dominated by quartz syenite with clinopyroxene (diopside-hedenbergite series), amphibole (hornblende), aegirine and alkali amphibole (crossite etc.). A vein phase is represented by aplite, aplite-syenite and pegmatite. The youngest veins associated with the alkaline intrusion include N-S veinlets (up to 10 cm wide) of aegirine, aegirine-crocidolite, amphibole, apatite-amphibole, aegirine-amphibole-fluorite-carbonate composition, and thicker fluorite and fluorite-carbonate veins. They occur in a 4–5 km wide belt, elongated in a N-S direction.

An irregular, steeply-dipping ore body 0.3–2.85 m thick is present in pyroxene–hornblende granosyenites. Vein constituents include carbonates, fluorite, quartz, chalcedony and ore minerals – sphalerite, galena, chalcopyrite, pyrite and argentite. Carbonates (calcite and parisite) and fluorite are the main useful minerals, their content varying from 1% to 54%. *Parisite* forms isolated pockets and bands or scattered disseminations. Chemical analyses (Kuzmenko, 1946) reveal that the parisite contains 18.8–24.2%  $Ce_2O_3$  and 18.5–24.46%  $(La, Dy)_2O_3$ . Elements in the yttrium group amount to 0.07–0.32%.

*Fluorite* forms pockets, lenses and bands up to 0.7 m wide, as well as scattered clusters and disseminations. The genesis of this ore occurrence is variously considered to be hydrothermal or post-magmatic, associated with the granite–granosyenite suite.

*The Chernigov apatite-carbonatite and rare metal-rare earth deposit.* The Chernigov carbonatite intrusion (Glevassky et al., 1977, 1978, 1981; Rusakov et al., 1980, 1986) is situated in the West Azov block of the Ukrainian Shield and includes the Novopoltava, Begim–Chokrak, Prostorov and Chernigov–Tokmachan occurrences, thus forming an ultrabasic–alkali–carbonatite rock complex with an associated mineral deposit of the same name. It is represented by carbonatites (amongst which Glevassky et al. (1978) have identified sövite, alvikite, beforsite and kimberlitic carbonatites), pyroxenite, alkali syenite, nordmarkite and fenite. The rocks form a strip that extends for up to 13 km along strike in which dykes and veins are subcordant to assemblages in the Archaean West Pre-Azov Group and the Early Proterozoic Pre-Azov granosyenite and granite complex. The West Pre-Azov Group includes pyroxene–amphibole–biotite gneiss, pyroxene schist and amphibolite, which were metamorphosed in the high-temperature amphibolite–granulite facies. Migmatization and granitization have been observed in rocks of the West Pre-Azov Group. Figures 62 and 63 present schematic illustrations of the geological structure of the Chernigov massif.

Carbonatites proper occur as dyke-like bodies in fenite, nepheline syenite and pyroxenite, such that these bodies coincide with the general trend of the Chernigov fault zone. The carbonatite bodies vary in thickness from a few cm (veinlets) to 50–60 m, occasionally up to 100 m (dykes). Parallel dyke swarms are frequently observed. Contacts between carbonatites and the country rocks are sharp as a rule, and a narrow biotite reaction rim (up to 1.5 cm) is present; the carbonatite grain size decreases towards the contact. The country rocks are fenitized at the contact with carbonatites, alteration aureoles being 10–20 m wide. Carbonatites include rocks containing not less than 50% carbonates (calcite and, or dolomite), while only kimberlitic carbonatites contain 25–50% carbonates. Silicate minerals are represented by olivine, clinopyroxene, amphibole, mica, and occasional feldspar and nepheline. Apatite and magnetite are essential components; in the southern occurrence, for example, the  $P_2O_5$  content in carbonatites is 2.36–4.66% (Rusakov et al., 1980). Accessory ore minerals are pyrochlore, hatchettolite, columbite, cerium-fergusonite, monazite, ancylite, carbocernaite, ilmenite, sulphides, etc.

Based on drill core data and geophysical interpretation, Rusakov et al. (1986) concluded that the arcuate plan of the rock strips making up the carbonatite complex probably closes towards the south, conformable with a dome structure consisting of country rocks. The Chernigov ultrabasic–alkali–carbonatite complex is a central-type

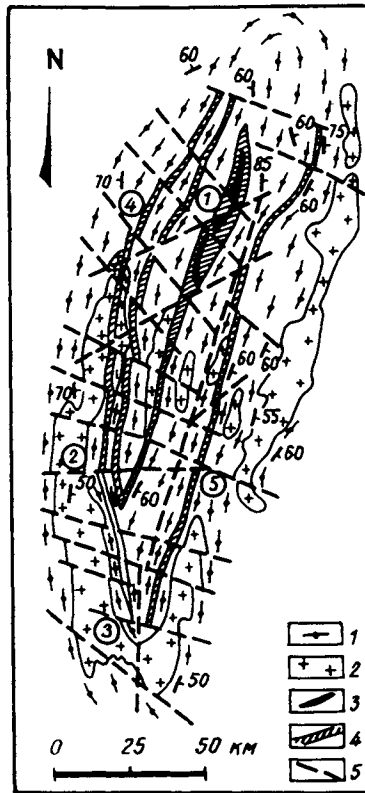


Fig. 62. Geological sketch map of Chernigov carbonatite intrusion (Rusakov, 1986). 1 – West Pre-Azov gneisses (AR<sub>1</sub>); 2 – Pre-Azov granitoid complex (PR<sub>1</sub>); 3 – carbonatite; 4 – carbonatitic complex rocks; 5 – faults. Carbonatite occurrences (*numbers in circles*): 1 – Novopoltava, 2 – Begim-Chokrak, 3 – Prostorov; fenite occurrences: 4 – Novokazankovat, 5 – Chernigov-Tokmachan.

igneous intrusion (Glevassky et al., 1981; Rusakov et al., 1986) whose base is now exposed after prolonged erosion. Carbon and oxygen isotopic compositions in calcites from the carbonatites indicate a deep (mantle) origin. Isotopic dating has proven an Early Proterozoic age for the rocks in the Chernigov intrusion: 2020 Ma (from the  $^{207}\text{Pb} : ^{206}\text{Pb}$  ratio in sphene from a pyroxenite) and 1900–1920 Ma (K–Ar method on phlogopite from pyroxenite and carbonatite).

Apatite mineralization localized in 10–30 m wide zones and with 10–15% apatite is a characteristic feature in the Chernigov alkali ultrabasic and carbonatite intrusion (Belevtsev and Galetsky, 1984). The ore formation is an apatite–carbonatite type associated with an alkali-ultrabasic group of geological complexes. It has also been established that the carbonatite varieties identified here differ in their metallogenetic signatures. For example, sövites typically display zircon–pyrochlore–hatchettolite mineralization; for beforites, fergusonite, columbite, monazite and baddeleyite are typomorphic; alvikites and kimberlitic carbonatites do not contain niobium minerals, but apatite has been found to be uniformly distributed (around 5%  $\text{P}_2\text{O}_5$  on average).

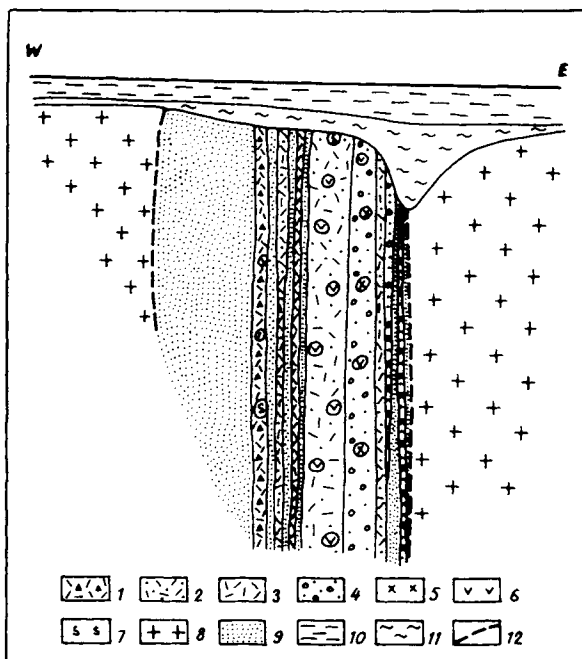


Fig. 63. Schematic section through S. part of Chernigov fault zone. From drillcore data (Glevassky and Krivdik, 1977). 1 – kimberlitic carbonatite; 2 – dolomite–calcite beforosite; 3 – dolomitic beforosite; 4 – alvikite; 5 – ijolite–melteigite; 6 – olivinite–glimmerite; 8 – host rocks (gneiss, amphibolite, granite); 9 – fenite, alkali syenite; 10 – unconsolidated sediment; 11 – weathering crust; 12 – faults.

The overall geochemical signature of the Chernigov massif is typical for carbonatite rock complexes, i.e. phosphorus, rare elements (Nb, Ta, Zr), cerium group rare earths, and Fe to a lesser extent (Glevassky et al., 1978, 1981).

It is essential to note that there is an alternative viewpoint on the metasomatic origin of the carbonatites in the Chernigov intrusion in the Azov region (Osadchy et al., 1977). The carbonatites which formed and the metasomatising solutions which produced the rare elements are considered to be products of post-magmatic pneumatolytic–hydrothermal activity of ultrabasic alkaline magmas. Carbonatite metasomatism has particular significance in the development of rare-metal and rare-earth mineralization.

Useful mineralization (rare metal–rare earth and tin–tungsten–molybdenum) is especially interesting in the *Sustchan–Perzhan zone* (Bespalko, 1975; Galetsky, 1970, 1974; Belevtsev and Galetsky, 1984; Metalidi et al., 1983), which is situated in the NW of the Ukrainian Shield in the Volyn block. It forms a linear structure as part of a volcano–plutonic belt with extensive alkali granitic magmatism, cataclasis and shearing, and intense metasomatic alteration which can be traced for 200–500 km along strike, with a width of 0.5–3 km on the flanks and 10–30 km in the centre. The zone strikes NE and its structural elements dip at 50–80° to the NW. It shows up clearly in geophysical fields. In the gravity field it is expressed as a sharp gravity step striking NE.

with a 5–15 km width and 10–18 km amplitude. In the magnetic field it appears as a mainly negative anomaly along its entire length.

The Sustchan–Perzhan zone includes rocks belonging to the Kirovograd–Zhitomir, Osnitsk and Korosten granite complexes (Early Proterozoic) and also the Perzhan alkali granite complex. Granitic and metasomatic rocks crop out most extensively in the middle of the zone and with their accompanying mineralization they are associated with a complex tectonic intersection formed by several cross-cutting structural elements of different ages in the north of the Volyn block (Metalidi et al., 1983). This structural complexity arose from the intersection of orthogonal and diagonal faults and is situated between the Khochin and Ustin faults in the north, which strike almost E–W, and between the Yurovo and Plotnitsky diagonal fault system in the west. The most productive part of the Perzhan complexity is located between the Plotnitsky and Ubortsky faults where there are metasomatic syenitic rocks with associated zirconium–rare earth, tantalum–niobium and fluorite occurrences; and with the Perzhan granites – productive metasomatic rocks containing tin, tungsten, molybdenum, etc.

In the central part of the zone, the dominant Perzhan complex rocks are characterized by being differentiated, with the development of essentially potassic syenite and granite, enriched in volatiles, and the widespread appearance of metasomatic processes. The Perzhan granites in this complex have been studied in detail by Galetsky (1970), who identified a new apo-granite<sup>3</sup> type with a complex palingenic-metasomatic origin and specific mineralization (siderophyllite-K-feldspar-perthite apo-granites). Figure 64 is a sketch map showing the geological structure in the central part of the Sustchan–Perzhan zone (after Galetsky, 1974).

Various kinds of metasomatic rock types are locally distributed within the confines of the zone. According to Bospalko (1975), these may be grouped into apo-granitic, alkali fenite–syenite, greisen and propylite branches. Compositionally the metasomatites can be divided into quartz–feldspar, essentially feldspathic (K-feldspar and albite), mica–enriched, mica–quartz (greisens), and quartz veins (Galetsky, 1974). A geochemical investigation by Metalidi and Nechayev (1983) has shown that such elements as fluorine, beryllium, tin, tantalum, niobium, rare earths, zirconium, lead, zinc, lithium, rubidium, cesium, gallium, thallium and cadmium are typical for syenite–apo-granitic metasomatites. Relatively enhanced amounts of most of these elements are observed in the most intensely metasomatized rocks. The following relationship has been noticed between these higher contents and the different metasomatite compositions:

- with feldspathic types – zinc, lead, molybdenum, thallium, gallium and fluorine;
- with quartz–feldspar–siderophyllite types – zinc, zirconium, rubidium, cesium, lithium, germanium, cadmium, tantalum and niobium;
- with quartz–feldspar types – tin.

Particular importance attaches to the characteristic features of uranium mineralization in the sedimentary iron ore unit in the Krivoy Rog–Kremenchug zone (Belvtsev et al., 1987; Yeliseyev et al., 1981; Kazansky et al., 1974; Petrov et al., 1969). The *Zheltorechka* uranium deposit is located in the north of the zone. It was opened in 1946

<sup>3</sup>Apo-granite = albitized and greisenized granite around intrusion margins commonly mineralized in rare elements (Nb, Ta, Li, Rb, Be, Sn, W, Mo, etc.).

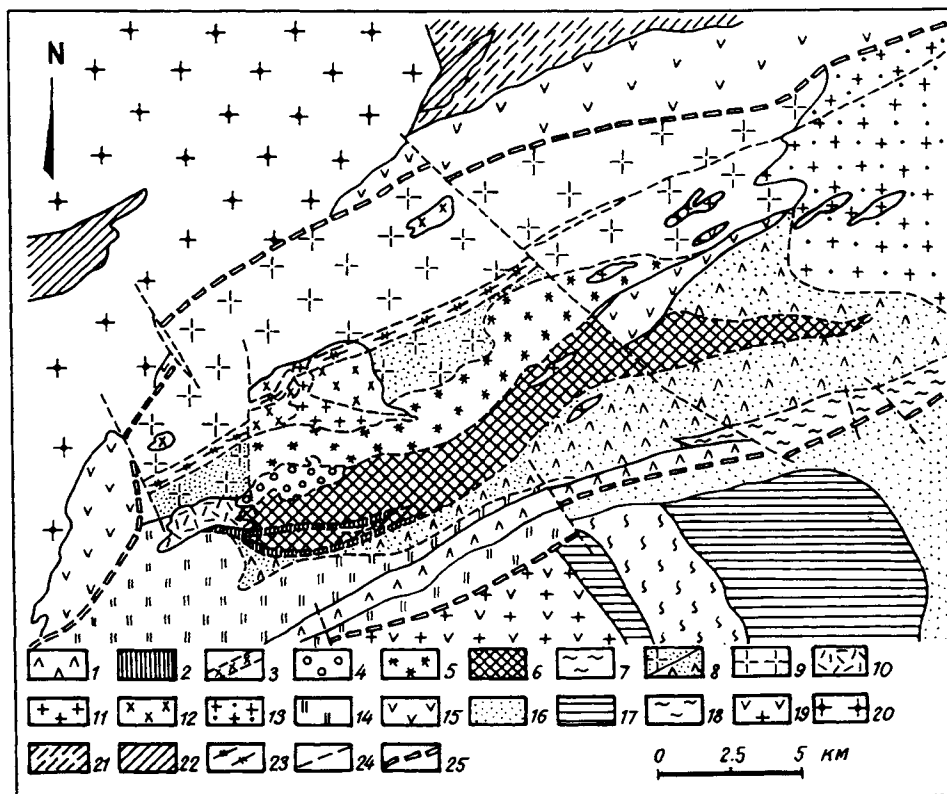


Fig. 64. Geological sketch map showing structure of central part of Sustchan-Perzhan zone (Galetsky, 1974). 1 – secondary quartzites; 2 – qz–musc greisens; 3 – alkali metasomatites; 4–8 – Perzhan granites: 4 – Perzhan with milky quartz (late), 5 – medium- to coarse-grained (after Khochin granites), 6 – fine- to medium-grained, 7 – intensely albitized & greisenized granophyres, 8 – metasomatically altered; 9 – Khochin granites; 10 – granite-porphyrries; 11 – fine-grained granites; 12 – syenites; 13 – granophytic granites; 14 – Lvovkov granites; 15 – gabbro; 16 – quartzite & pink sandstone; 17 – grey sandstone; 18 – qz–chl–seri schist; 19 – granitized amphibolite; 20 – Osnitsk granites; 21 – Kirovograd-Zhitomir migmatites; 22 – biotite gneiss; 23 – cataclastic, mylonite & breccia zones; 24 – tectonic lines; 25 – boundaries of Sustchan-Perzhan tectonic zone.

and is still being exploited at present (Belevtsev et al., 1987). Iron ores have been worked in this complex iron–uranium deposit since 1898. It is located in the northern continuation of the Krivoy Rog–Kremenchug rift structure and is restricted to Lower Proterozoic Krivoy Rog Group metamorphic rocks, which appear among Archaean granitoids. The belt of metamorphic rocks is 0.5–2 km wide and extends for 9 km.

There are three stratigraphic units in the Precambrian rocks of the region: from the base upwards these are Demurino (Late Archaean migmatites), Krivoy Rog (four formations which correlate with corresponding formations in the centre of the Krivoy Rog structure), and Checheliyevka (gneisses and schists with thin quartzite and marble bands, totalling over 4.5 km thick).

The productive Krivoy Rog Group in the area around the ore deposit includes the underlying formation (which correlates with the Novo-Krivoy Rog), 200–400 m thick and represented by amphibolite, amphibole schist and quartzite; a lower formation (analogous to the Skelevatka Fm), 10–250 m thick, consisting of biotite gneiss, schist and quartzite; a middle formation (analogous to the Saksagan Fm), 250–450 m thick alternating amphibole–magnetite and hematite–magnetite quartzites and hornblende–garnet schist; and an upper formation (analogous to the Gleyevatskaya Fm), around 300 m thick, consisting of dolomite, quartzite and biotite schist. Structurally, the deposit is a narrow apressed syncline with steep sub-vertical dips on the fold limbs. Figure 65 illustrates the structure of the deposit.

Uranium and iron ores proper in this deposit owe their origin to the effects of a number of stages in the metasomatic process – magnesium–iron, soda–carbonate, carbonate, late-alkaline, and sulphide–pitchblende. Widespread magnesium–iron metasomatism produced amphibole-bearing iron ores with hematite and magnetite due to the redistribution of magnesium and iron in primary ferruginous rocks. Uranium mineralization proper is related to the limited development of soda–carbonate and

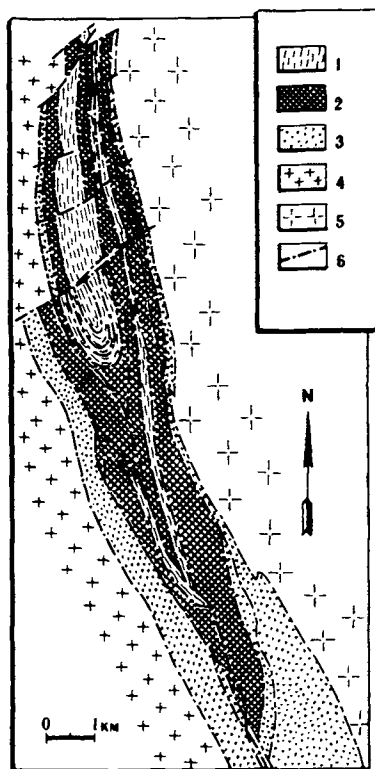


Fig. 65. Geological sketch map showing structure of Zheltorechka deposit (Belevtsev et al., 1984). 1–3 – Krivoy Rog Group: 1 – upper fm, 2 – middle fm, 3 – lower and underlying formations; 4 – Dneprov-Tokov granitic complex; 5 – Saksagan trondhjemite; 6 – tectonic breaks.

carbonate metasomatic processes and also to the formation of the latest cross-cutting uraniferous veins. Albitic ores with uraninite, brannerite and nenadkevite-type (coffinite) uranium silicates are associated with albitization (mainly in rocks in the middle and partly the upper formations of the Krivoy Rog Group – quartz–biotite and amphibole–biotite schists). Uranium mineralization is absent in aegirine metasomatites as a rule. Economic uranium–iron–carbonate ores in the Zheltorechka (“Yellow stream”) deposit accumulated during carbonate metasomatism. The products of this process form large podiform bodies after iron ores and ferruginous quartzites as well as magnetite–amphibole schists. The main ore mineral is uraninite. Vein-type sulphide–pitchblende mineralization is represented by nasturan (pitchblende), uraninite, coffinite, magnetite, iron and copper sulphides, graphite, organic matter, and a few non-ore minerals. The deposit thus contains complex metasomatic zoning which formed due to the superimposition of different metasomatic episodes. Belevtsev et al. (1987) consider the Zheltorechka deposit to represent a uranium ore formation that is related to Early Proterozoic carbonate–soda metasomatism.

### 2.7. Graphite

Graphite deposits and occurrences in the Ukrainian Shield are spatially and genetically related to carbonaceous metasedimentary assemblages (Galetsky et al., 1986; Dubyna, 1939; Ivantsiv, 1972; Kalyayev, 1967; Lazko et al., 1975; Nikolaev et al., 1985; Ryabenko and Moskina, 1978) which formed over an extensive time interval from 3.3 to 1.2 Ga ago. The most productive formations (Galetsky et al., 1986) are kinzigite, high-alumina quartzite and khondalite, carbonate–terrigenous, flyschoidal carbonaceous metasiltstone–metacarbonate. Earlier workers (Ryabenko and Moskina, 1978) identified a single productive formation. According to Galetsky et al. (1986), the kinzigite formation crops out in Early Archaean basement highs (granulite–basic rocks in the Podolsk metallogenic province) and is represented by cordierite-bearing aluminous gneiss with graphite, interleaved with basic gneiss, schist and calciphyre. The high-alumina quartzite and khondalite formations are present in sutures and inter-block zones (the Golovanevsk and Central Azov zones) and are represented by aluminous gneiss (with cordierite and corundum) and schist with graphite–silica rocks, quartzite and calciphyre. The main graphite deposits (Zavalyevskoye, Troitskoye, and others) are associated with these formations. The carbonate–terrigenous formation crops out in the Krivoy Rog–Kremenchug zone, the main rock type being graphite–biotite gneiss (the Petrov and Balakhovskoye deposits). A flyschoidal metasiltstone–metasandstone formation is present in the Volyn and Kirovograd metallogenic provinces and is mainly represented by biotite gneiss with garnet and sillimanite. The Berdichev graphite region has been discovered for the first time, and a major new graphite deposit – the Burtyn. Metamorphism of the graphitic rocks varies from greenschist to granulite facies.

As is shown in the sketch of ore-bearing structures in the Ukrainian Shield (Fig. 43), graphite deposits and occurrences are found in various structures, including collision zones (granulite–gneiss terrains within them), a fold belt, a rift belt, and an intracratonic fold belt.

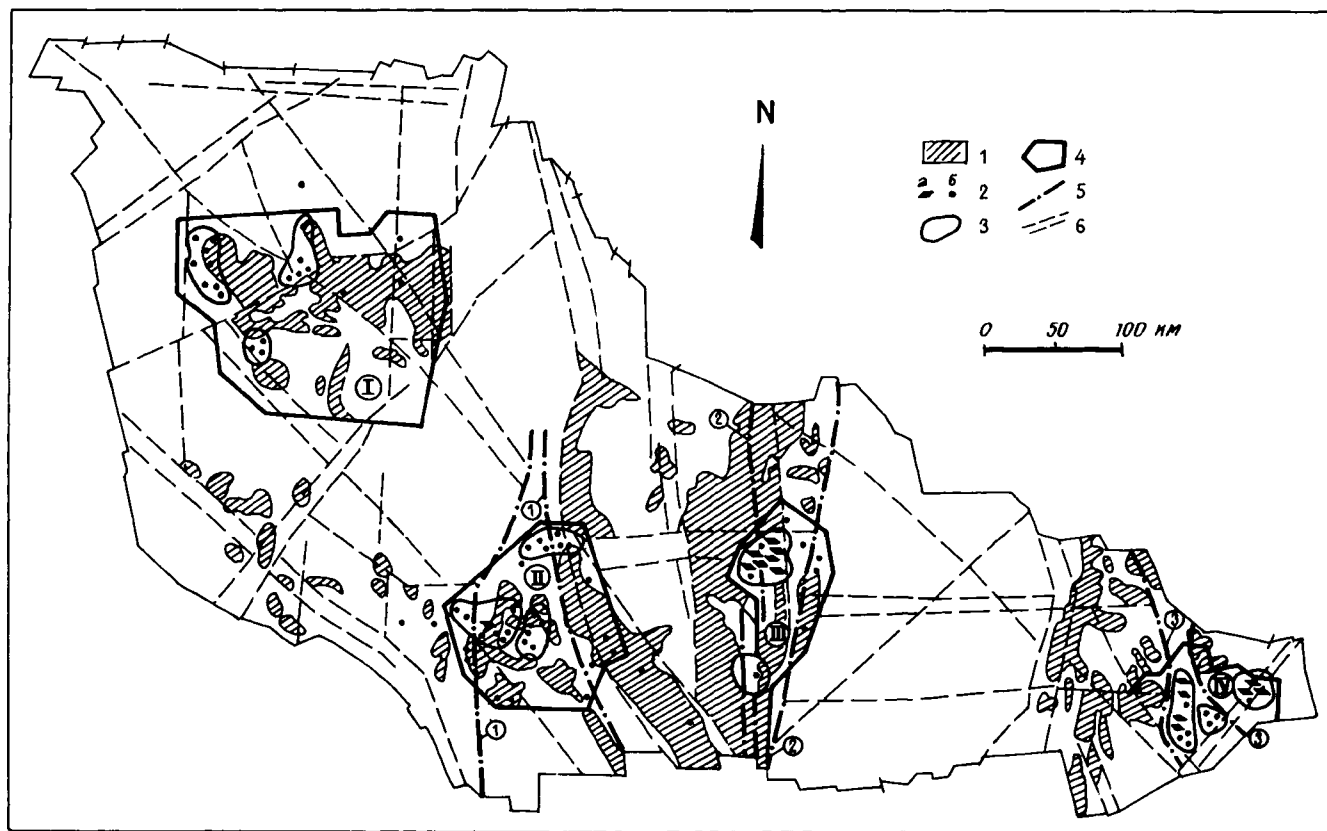


Fig. 66. Sketch map showing location of carbonaceous formations and graphite deposits (occurrences) in the Ukrainian Shield (Galetsky et al., 1986).  
 1 - carbonaceous formations; 2 - graphite deposits (a) and occurrences (b); 3 - ore fields; 4 - graphite regions: I - Berdichev, II - Bug, III - Krivoy Rog, IV - Azov; 5 - zones between blocks (arabic numbers in circles): 1 - Golovanevsk, 2 - West Ingulets, 3 - Central Azov; 6 - tectonic zones.

The Ukrainian graphitic province coincides in area with the whole Shield (Fig. 66) and includes the following regions: Bug, Krivoy Rog, Azov, and Volyn. Graphite deposits and occurrences are found in rocks belonging to the Bug, Ingul–Ingulets, Teterev, Krivoy Rog and Central Pre-Azov Lower Proterozoic groups, and to a lesser extent in the Lower Archaean Dneestr–Bug Group.

The Bug region in the Volyn–Podolsk geoblock is situated in the middle reaches of the river South Bug and is one of the main graphite-bearing regions in the Ukrainian Shield. Graphitic rocks occur mainly in the middle Bug region and in the Teterev river basin and are associated with the Bug Group, particularly the Kosharo–Alexandrovka Fm. Compositionally it includes feldspathic quartzite, aluminous gneisses (cordierite- and garnet–biotite with sillimanite), mafic schists (biotite–pyroxene, amphibole–pyroxene, occasionally with garnet), and garnet–biotite schist. The formation is over 2500 m thick and shows granulite and high-temperature amphibolite facies metamorphism. Graphite is also always present in the middle of the Khastchevat–Zavalyevsk Fm of the Bug Group, among aluminous gneisses interleaved with marbles and calciphyres. Graphitic gneisses in the Bug Group form the limbs of deeply eroded major synclinal structures in the shape of small bodies 1–3 km wide by 10–20 km long, narrow (100–500 m) strips, lenticular bands among granitoids and charnockites, and bands in the migmatite substrate. Most graphite deposits and occurrences are related to second- and higher-order folds and faults.

The *Zavalyevskoye graphite deposit* (Ivantsiv, 1972; Nikolayev et al., 1985; Ryabenko and Moskina, 1978) is situated in the southern part of the Golovanevsk zone within a brachyantyclinorial structure, on the limbs of the E–W Zavalyevsk syncline (Fig. 67). The northern limb of the syncline is vertical and the southern limb dips

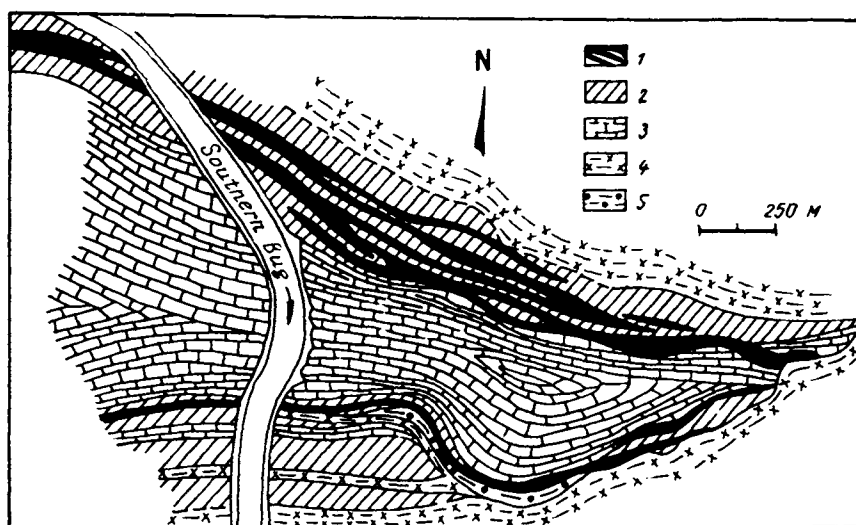


Fig. 67. Sketch map showing geological structure of Zavalevskoye graphite deposit (Ivantsiv, 1972). 1 – graphitic gneiss; 2 – barren gneisses; 3 – crystalline limestone; 4 – granite charnockite; 5 – migmatite.

steeply (70–75°) to the south. Fold cores contain banded marble, while biotite, garnet- and sillimanite-biotite, pyroxene, amphibole and graphite gneisses form the limbs, interbanded with calciphyre and magnetite-garnet-pyroxene quartzite and schist. This assemblage is around 450 m thick on the northern limb of the syncline and between 20–80 to 800 m on the southern limb.

Graphitic gneisses in the deposit form a series of strips extending in a SE direction, 5–10 to 100 m wide and from a few hundred metres to 1–2 km long, as well as a number of thin bands in limestones. Conformable pegmatite and quartz veins are present in the gneiss unit, genetically related to the Kirovograd-Zhitomir granitic complex. Lamellar graphite is almost uniformly distributed throughout the rock, but sometimes forms clusters and pockets (up to 5–6 mm), oriented along the schistosity, and occasionally thin veinlets 1–2 mm across. The graphite content is 6–10% on average, sometimes up to 15–20%. In partial-melt and intrusive rocks, graphite is present only in contact zones close to graphite-bearing rocks. Graphite mineralization in the Middle Bug region is frequently associated with charnockitic rocks, where it is found in lenses, thin bands and xenoliths of graphitic gneiss. The graphite content in charnockites themselves does not exceed 2–3%.

*The Krivoy Rog graphite region* encompasses the Kirovograd block and the Krivoy Rog-Kremenchug zone in the centre of the shield. Graphite deposits and occurrences are mainly associated with rocks in the Ingul-Ingulets Group (Rodionovka and Spasovka Fms), less commonly the Krivoy Rog Group (Saksagan and Gdantsev Fms). In the Ingul-Ingulets Group, graphite is present in biotite and sillimanite-biotite gneisses, less usually in quartzite, skarn, marble and schist. Gneisses are intensely granitized and form broad (up to 20 km) N-S striking belts with steep dip angles. Graphitic rocks form strips 0.5–1.2–1.5 km, occasionally 2.5 km long among biotite schist and biotite-plagioclase gneiss; the strips vary in width from 50 to 100–150 m.

The largest graphite occurrences are found in the *Petrov group* of deposits in synclinal folds. Graphitic members (graphite-biotite, graphite-plagioclase and graphite-biotite-chlorite gneisses and schists) are up to 50 m thick and 1300 m long and regularly include thin limestone and quartzite beds up to 1 m thick. The graphite content in graphite-biotite gneiss is 2–23% (7–9% on average). Lamellar graphite is usually evenly distributed in the rock, or occurs as conformable elongate segregations. The total thickness of the graphite-bearing rock assemblage in the region of the Petrov deposits is 600 m. Metamorphic rocks are cut by pegmatites and quartz veins.

*The Azov graphite region* is located in the middle of the Azov geoblock. Graphite deposits and occurrences are associated with graphitic gneiss, sometimes with graphitic schist, quartzite and crystalline limestone of the Central Pre-Azov Group. The rocks of this group (Temryuk, Sachka and Karatysh Fms) are aluminous and mafic gneisses and schists, quartzite, limestone and calciphyre, which occur as conformable lenses and beds several hundreds of metres thick amongst migmatites. The most important graphite deposits are the Troitskoye, Sachkinsko-Vishnyakovskoye and Starokrymskoye.

*The Troitskoye deposit*, which has been worked since 1917, is in a synclinal fold closure in graphite-biotite and garnet-biotite-graphite gneisses which form thin (from 10–20 to 50–60 m) bands amongst biotite-garnet and hornblende gneisses. Lamellar graphite is present on average up to 7–9%.

*The Sachkynsko-Vishnyakovskoye deposit* occurs in a gneiss belt that is over 300 m wide and which can be traced along strike for more than 6 km. Gneiss varieties include biotite, biotite-garnet and graphitic types. Graphitic gneisses proper occupy bands that are 100–200 and 700 m wide, 2.5–3 km along strike; individual ore-bearing strips are 1–10 m thick. The graphite is lamellar, medium- to fine-grained, and its average content is 6–10%.

*The Starokrymskoye deposit* is situated in a 150–500 m wide belt of graphitic gneisses with biotite, biotite-garnet and biotite-pyroxene compositions. Graphite-biotite gneiss and graphite-biotite-chlorite gneiss and schist form lenticular belts 500 m long and 40–50 m wide. Graphite occurs in finely lamellar form averaging 3–5% with a range of 6 to 20%. Graphite mineralization is not uncommonly associated with cross-cutting aplite, pegmatite and granite veins both as disseminations within the veins and as clusters of coarsely-lamellar graphite at contacts between granite and pegmatite veins and the gneisses.

*The Volyn graphite region* in the Volyn block consists mainly of partial-melt and intrusive granitoids. Lower Proterozoic metamorphosed volcanosedimentary assemblages are present to a lesser extent (Teterev, Klesov and Pugachev Groups), and the Upper Proterozoic Ovruch Group. Graphite is associated with the Vilen and Gorod gneisses (Teterev Group) and occurs in graphitic and biotite-graphite gneisses as thin bands amongst pyroxene-biotite and biotite gneisses. The average graphite content in the ore is 2–8%. Isolated graphite mineralization has been observed in anorthosite and gabbro-anorthosite as well as in Korosten-type rapakivi-like granites. Most of the graphite occurrences in this region are insignificant in size. However, a new graphite region has been discovered, the Berdichev, which contains the major Burtyn graphite deposit. Forecast reserves of graphite ores for the Ukrainian Shield have been estimated at 100 M tonnes of graphite, to a depth of 2100 m.

### 2.8. Topaz and morion in pegmatites

Chamber pegmatites which are spatially and genetically associated with Early Proterozoic Korosten granites form the source for piezo-optical and gem-quality raw materials in the form of morion, rock crystal, topaz and beryl deposits. These pegmatites are developed in two regions: 1) the Volyn pegmatite field in the Volyn metallogenic province, associated with the Korosten pluton of basic and granitic rocks; and 2) the Konstantinovo pegmatite field in the Kirovograd metallogenic province, associated with the Korsun-Novomirgorod gabbro-anorthosite and rapakivi granite pluton. Both plutons consist of rocks from the Korosten complex which contains three rock groups (Galetsky et al., 1984): the oldest is gabbro, gabbro-norite and norite, anorthosite and gabbro-anorthosite; a hybrid group developed at the contact between basic rocks and granites – gabbro-syenite; the youngest group is rapakivi and similar granite type, sub-alkaline granite, granite-porphiry, pegmatite and aplite.

Long-term research by large groups of Russian and Ukrainian geologists has demonstrated the major forecasting significance of the contact between rapakivi granites and basic rocks for this type of mineralization, in particular the close association between pegmatite bodies and so-called "hybrid" rocks which originated during

reworking of older basic rocks, as well as cover rocks (sandstones and lavas). Chamber pegmatites containing rock crystal are found only along the SW contact of the Volodar–Volyn gabbro–anorthosite intrusion and are not found in the contact zones of other granites. The geological setting of areas with pegmatite bodies in the SW part of the Korosten pluton is illustrated in Figure 69.

The *Volyn pegmatite field* is situated in the SW part of the Korosten pluton in a strip of hybrid granitic rocks (Fig. 68) along the western contact of the Volodar–Volyn intrusion. The strip of hybrid granites runs NW for 30 km and is 10–12 km wide; it has a border with Lower Proterozoic gneissose migmatites in the west. The pegmatite-bearing zone in the granitic rocks is 0.5–4 km wide. The strip of hybrid granites and the pegmatite field are associated with a NW-striking regional-scale deep fault in which the

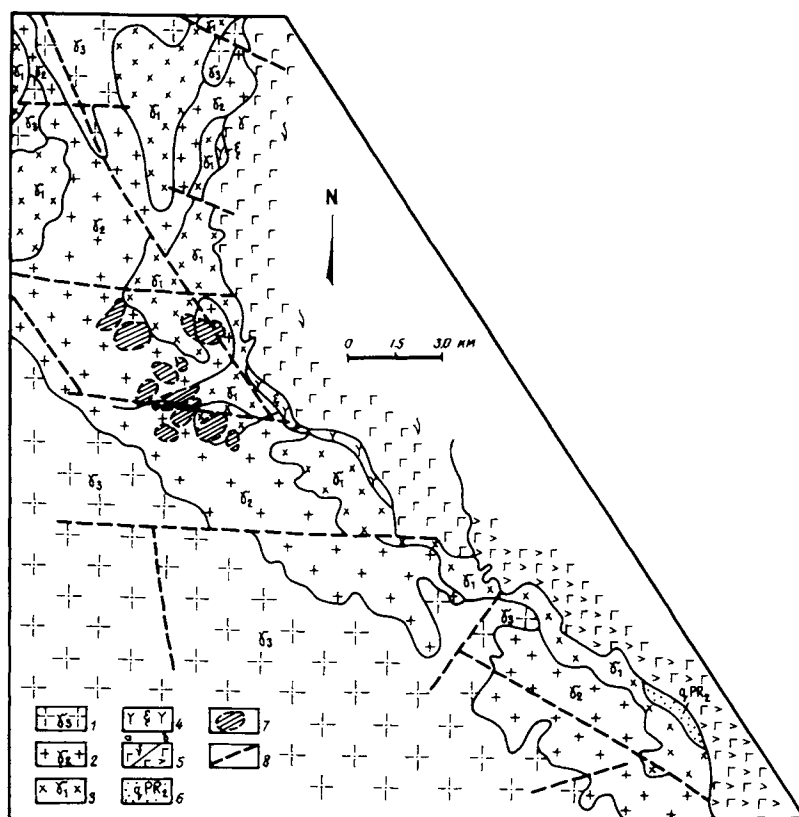


Fig. 68. Sketch map showing geological structure of Volyn pegmatite field (SW contact of Volodar–Volyn gabbro–anorthosite intrusion). Compiled by I.N. Dagelaiskaya, 1987. 1 – aplitic–pegmatitic and pegmatitic ovoidal bi-amph and bi granites ( $\gamma_3$ ); 2 – aplitic–poikilitic ovoidal px–amph granites ( $\gamma_2$ ) with olivine; 3 – hypidiomorphic px–amph non-ovoidal granites ( $\gamma_2$ ) with ol; 4 – syenite and granosyenite (x); 5 – gabbro in marginal complex (a), gabbro–anorthosite (b); 6 – Ovruch quartzites and quartzitic sandstones (qPR<sub>2</sub>); 7 – outlines of areas with pegmatite bodies; 8 – tectonic zones.

greatest thickness of granites has been identified from geophysical data. Later faults have an E–W orientation and were responsible for producing block movements of rocks in the contact zone and for dividing the zone into blocks – low-yielding (Northern and Dashen), and those that are saturated with pegmatite bodies (Vis-hnyakov and Dvoristchan blocks).

Available geophysical data and drilling results have shown that the contact between basic and acid rocks is a complex zone, characterized by alternating gabbroic rocks, anorthosites, granites and various hybrid rocks. The contact between basic rocks, here represented by various gabbroids of the “marginal” complex, and rapakivi granites is a major structural element which determines many features in the geological structure of the pegmatite-bearing region (Fig. 69).

The observed inhomogeneous composition and structure of the hybrid rock zone is directly related to the contact between basic rocks and granites. All the hybrid rock varieties and xenolith orientations are parallel to the contact. Definite zoning is observed in a cross-section at right angles to the contact, expressed as a regular east–west change in hybrid rock types. Monzonite and gabbro–monzonite occur at the immediate contact, also syenite and granosyenite, which give way westwards to hybrid rapakivi-type granites ( $\gamma_{\Gamma 1}$ ,  $\gamma_{\Gamma 2}$ ,  $\gamma_{\Gamma 3}$ , etc.) which in their turn replace each other in sequence. Only

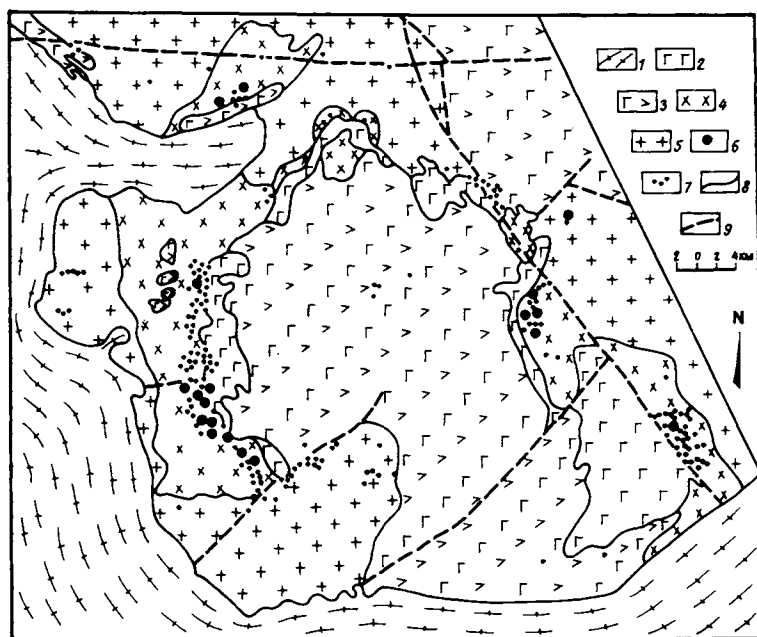


Fig. 69. Pegmatite areas in SW of Korosten pluton. Compiled by I.N. Dagelaiskaya, based on material by O.F. Bernasovskaya (1975). 1 – Terev gneisses and migmatites ( $PR_1$ ), 2 – marginal gabbros, 3 – basic rocks, 4 – hybrid granitoids, 5 – Korosten rapakivi granites, 6 – areas with productive pegmatite bodies, 7 – areas with individual pegmatites, 8 – geological boundaries, 9 – faults.

$\gamma_{T2}$  granites are pegmatite-bearing, plus a few  $\gamma_{T1}$ , while the other varieties contain no pegmatite bodies. The Volyn pegmatite field is thus characterised by a unique zonation, expressed as a regular pattern of alternations and sequential changes in hybrid granitic rock varieties in an east–west direction, i.e. away from the gabbro–anorthosite contact.

The emplacement of the Volyn chamber pegmatites, like the hybrid granitoids, was also controlled by the contact between granites and gabbros. The strip in which pegmatite bodies are distributed is 2–4 km wide and is drawn out parallel to the contact between acid and basic rocks. Pegmatite bodies are irregularly arranged within this strip. A genetic model for the pegmatites described here, based on the work of many Russian and Ukrainian researchers, illustrates their main distribution patterns. It has been demonstrated that the Volyn pegmatites are localized in inner contact zones between rapakivi-like granites and basic rocks, since according to the model adopted here the apical part of the intrusion contained a large quantity of volatiles (fluorine, carbon dioxide, alkalis), which acted as mineralizing fluids.

A second feature in the emplacement of productive pegmatites is their relationship to particular hybrid granite varieties, notably granites  $\gamma_{T2}$  and to a lesser extent  $\gamma_{T1}$ , which seem to have formed close to each other in time. If such is the case, then only  $\gamma_{T2}$  granites are pegmatite-forming, while  $\gamma_{T1}$  granites may also have been a “screen”, near which pegmatite formation was most intense. Depending on the position of the pegmatites relative to the contact between granites and basic rocks, differences in their composition and structure are observed. Thus, low-grade pegmatites with many cavities occur immediately adjacent to the contact, while cavernous varieties are restricted to the axial zone of the belt. Moreover, large groups of up to 10 bodies measuring 60–80 m across form in the central and southern part of the Volyn pegmatite field, with regularly developed inner and outer zones, where morion crystals weighing up to 10 tonnes are found in cavernous areas, together with large topaz, beryl, microcline and mica crystals. Pegmatite bodies in the north are no wider than 10–20 m and are scattered over a wide area. Marginal zones in the bodies are well developed here, but block and cavernous structures only poorly.

There are also several prospective areas within the Korsun–Novomirgorod pluton at the contacts between gabbro–anorthosite intrusions and rapakivi granites. Pegmatite fields are found which are associated with the inner contact zones of granitic intrusions. Productive pegmatites in the Korosten pluton have a rock crystal–topaz–morion composition, with in addition beryl, phenacite, fluorite, cassiterite and lithia mica.

The Volyn pegmatites are divided in two morphological and genetic types, based on the currently available classification systems (Lazarenko et al., 1978): 1) schlieren or residual types formed *in situ*, and 2) injection or squeezed-out types, formed from transported melts. The first group includes non-chamber and chamber pegmatite bodies. Non-chamber pegmatites are compositionally similar to their host granites and are characterized by small dimensions, indistinct margins and incomplete zoning. They are represented by minor aplite–pegmatite bodies and pegmatitic schlieren – small bodies of no economic importance. Those with most practical significance are chamber pegmatites. Such pegmatites are usually located in contact zones of  $\gamma_{T1}$  and  $\gamma_{T2}$  hybrid granites. In shape they are irregular to isometric, flat horizontal sheets or elongate stock-like bodies. Sizes range from a few metres to several hundred metres. Hydro-

thermal activity is widely represented in this type of pegmatite – solution and recrystallization processes, etc. There are multi-chambered pegmatites with several structural centres around which concentric zoning is developed, and single-chambered pegmatites with a large cavity or chamber having concentrically-arranged zones. These bodies have an isometric shape, 10–30 m across, with complete differentiation. Chamber pegmatites proper are completely differentiated bodies, with the following zones: aplite, graphic, pegmatitic feldspathic, quartz, cavities, and an alkali-leaching zone. The second group contains only one type of pegmatite body – veins within granites or basic rocks. These are around 1.5 m wide and up to 50 m long and their composition depends on that of the host rock.

Mineralogically, the Volyn pegmatites are highly varied and have been the subject of many research papers, particularly the highly detailed work by Lazarenko et al. (1978). The main rock-forming minerals in the Volyn pegmatites are feldspar, quartz and mica; secondary minerals are topaz, fluorite, siderite, hydromica, chlorite, phenacite, opal, chalcedony; rare minerals are pyrite, ilmenite, zircon, apatite and garnet. Economically important minerals are quartz (morion), topaz and beryl.

It should be emphasised in conclusion that the main specific feature of the Volyn chamber pegmatites is their close genetic relationship to early intrusive granite phases,  $\gamma_{T2}$  and to a lesser extent  $\gamma_{T1}$ . This relationship is underlined by the spatial association between the pegmatites and these granite types, the existence of gradual contacts between granites and pegmatites, the widespread development of graphic and pegmatitic textures in the granites, the isometric shape of pegmatite bodies, close chemical composition based on a number of elements in rock-forming and accessory minerals, and similar petrochemical features in the pegmatites and granites.

### 2.9. Abrasive garnet

Garnet deposits (mainly almandine) as a source of abrasive raw material, are known from several localities in the Ukrainian Shield. The *Slobodov garnet deposit* (Grivakov, 1971) is situated in the north of the Podolsk block in the Khmelnytsky metallogenic zone and is associated with leucocratic granites belonging to the Early Proterozoic Berdichev complex. The granites consist of quartz (34% on average), plagioclase (oligoclase,  $An_{28-30}$ , 20%), microcline–perthite (17%), biotite (7%), garnet (16%), and cordierite (8%, with 30–35% Fe). Ore minerals present are ilmenite, magnetite and pyrite; accessories are zircon, rutile, monazite and apatite. Garnet grains are 4–6 mm or up to 10 mm in size and are disseminated as phenocrysts or form small clusters with 15–20% garnet on average. Garnet isomorphic molecular composition is ~62% almandine, ~30% pyrope, ~7% grossular,  $\leq 1\%$  andradite, and  $< 1\%$  spessartine. Quartz and biotite inclusions are common in garnet crystals, also rarer zircon, rutile and apatite. Total garnet reserves have been estimated at 1–10 million tonnes. The deposits belong to a high-alumina garnet ore formation associated with leucocratic granites. Early Proterozoic Berdichev partial-melt granites crop out in a belt of tectonothermal reworking in Archaean high-alumina gneisses – relict rocks of a granulite–gneiss terrain. Disseminated garnet which originally formed during an Archaean metamorphic event has been recrystallized and a new generation formed during Early

Proterozoic partial melting (ultrametamorphism), when the mineral deposit itself formed.

Garnet in the *Kamenskoye deposit* (Anon., 1977) is also essentially almandine and occurs in tourmaline and muscovite-bearing pegmatites in an Early Proterozoic gneiss complex. Pegmatite veins are 8–10 m long and 0.2–5 m wide (mostly 1.0 m) and are zoned. Garnet is present in all zones – aplite, graphic and pegmatitic. The highest garnet contents are found near zahlband parts of pegmatites. Garnet grains vary in size from 3 mm to 50 mm in the pegmatoid zone.

### 2.10. Talc and magnesite

Talc and magnesite deposits occur in the Dnieper granite–greenstone terrain in the north of the Dnieper block. Ultrabasic sills were intruded into Upper Archaean Konka–Verkhovtsevo Group volcano-sedimentary rocks in the Sursk region of the Ukrainian Shield. A continuous belt of ultrabasic intrusions from 300 to 2500 m wide can be followed for 30 km – the Pravdin, Pavlov and Petrov intrusions (Ilvitsky and Shrubovich, 1969).

*The Pravdin deposit* (Romanovich, 1973) is situated in the SE part of the Pravdin ultrabasic intrusion, which has dimensions 300–2500 m by 5000 m. Host rocks are apo-diabase and apo-spilitic amphibolites and schists belonging to the Konka–Verkhovtsevo Group. The intrusion consists of serpentized dunite and peridotite, chrysotile with relict olivine, chrysotile–antigorite and antigorite–talc–carbonate serpentinites, talc–carbonate, chlorite and amphibole rocks. Carbonate ores and carbonate serpentinites have economic importance, forming a deposit with a thickness of 300–600 m and length of 2.5 km, striking NW and dipping steeply (60–85°) to the NE. A crush zone, 10–45 m wide, divides the deposit into a SW and a NE part. Carbonate serpentinites form irregular and lenticular bodies within the productive deposit. Raw materials in the deposit have the following composition (Romanovich, 1973): talc–carbonate ores (40–45% talc and 50–55% breunerite; dolomite is present close to the fault zone) – MgO 35.4%, SiO<sub>2</sub> 28.4%, Al<sub>2</sub>O<sub>3</sub> 0.57%, CaO 0.51%; carbonate–serpentine ores – MgO 38.5%, SiO<sub>2</sub> 32.3%, Al<sub>2</sub>O<sub>3</sub> 0.52%, CaO 0.41%. The carbonate concentrate contains 8–10% FeO and 0.15–0.35% Fe<sub>2</sub>O<sub>3</sub>.

*The Veselyansk deposit* (Romanovich, 1973) is also represented by an ore body of talc–carbonate rocks in an ultrabasic intrusion. Host rocks are quartz–biotite, quartz–chlorite–biotite and quartz–sericite schists, magnetite quartzite and biotite–amphibole schist in the Upper Archaean Konka–Verkhovtsevo Group. A 5.5 km long, 30–300 m wide productive horizon consists of talc and magnesite (breunerite) in approximately equal quantities with small serpentinite, chlorite and actinolite schist inclusions. Minor amounts of chlorite, magnetite and single quartz, chromite and pyrite grains are present in the mineral deposit.

These Late Archaean deposits are located in the Sursk–Verkhovtsevo–Chertomlyk metallogenic zone. The useful mineral belongs to a talc–magnesite ore formation associated with a dunite–peridotite suite. According to the genetic classification of magnesite mineralization types (Smolin et al., 1984), the minerals in the deposits outlined above belong to a hypogene type – apo-ultrabasic talc–magnesite (breunerite) rocks.

### 2.11. *Pyrophyllite*

*The Zbrankovsk and Nagoryansk pyrophyllite deposits* are both being worked at present. They are associated with Upper Proterozoic Ovruch Group rocks which crop out locally in the extreme NW of the Volyn block (Lychak, 1959, 1972). This rock group occupies an intra-cratonic basin-type structure which formed in the Late Proterozoic along the edge of an Early Proterozoic granitic complex (the Kirovograd–Zhitomir and Osnitsk granitoids) and Early to Late Proterozoic granites in the Korosten massif. Alkali metasomatites (Perzhan type) are developed along the N and NW tectonic contacts of the Ovruch structure as E–W-striking zones in a recognised volcanoplutonic belt. The Ovruch Group contains two formations (Drannik and Bogatskaya, 1967): a lower Zbrankov Fm, mainly volcanic, and an upper Tolkachev Fm, mainly sedimentary, which correspond to two stages in the formation of the group under platform conditions. Volcanic processes, which played an important role in the formation of the Ovruch Group, were initially fissure eruptions, followed later by central-type effusive–explosive eruptions, alternating with sediment deposition (Tankilevich and Kulikovsky, 1977).

The Zbrankov Fm (from base to top – plateau basalt, quartz porphyry and trachyandesitic porphyry, separated by thin sedimentary and pyroclastic members) lies on a weathered mantle of Korosten granite or on polymict sandstones belonging to the early-Late Proterozoic Pugachevka Group (in the Belokorovich structure). Conformably above is the Tolkachev Fm, consisting of basal grit, sandstone, tuffite and siltstone containing volcanoclastic material, sericitized and pyrophyllitized; a quartzitic sandstone unit occurs above, in places frequently interleaved with pyrophyllite– and sericite–hematite schists. The stratigraphic position of pyrophyllite-bearing rocks in the Ovruch Group is shown in Figure 70. It has been established that the localization of conformable deposits of pyrophyllite rocks in the Zbrankovsk and Nagoryansk deposits is controlled essentially by N–S and E–W trending tectonic zones. Pyrophyllite schists form sheet-like and lenticular deposits from 20–30 cm to 1.8 m thick.

The acicular–prismatic habit of pyrophyllite in weakly altered primary rocks and the presence of inclusions in small angular quartz grains would appear to provide evidence for a volcanoclastic origin for pyrophyllite schists which developed at the expense of quartz porphyry lavas and pyroclastics, ash tuff, tuffaceous siltstone and tuffite as a result of superimposed solfatara–fumarole alteration (sericitization, pyrophyllitization, secondary silicification, and hematitization). Morphologically variable pyrophyllite is typical for various stages in the alteration of primary rocks, from finely lamellar acicular–prismatic intergrowths with hematite to coarsely foliated lamellae, free of hematite, in lenticular aggregates. According to Tankilevich (1976), the formation of pyrophyllite schists in the Zbrankovsk deposit is related to the metamorphism of washed-in tuffaceous–kaolinitic material (altered quartz–porphyry and orthophyre tuffs and intermediate tuffites). The Nagoryansk deposit is related to the recrystallization and metamorphism of slightly reworked intermediate to basic tuffites with a significant quartz admixture. These pyrophyllite deposits belong to a quartz–pyrophyllite type of useful mineral formation in the metamorphic–hydrothermal genetic class.

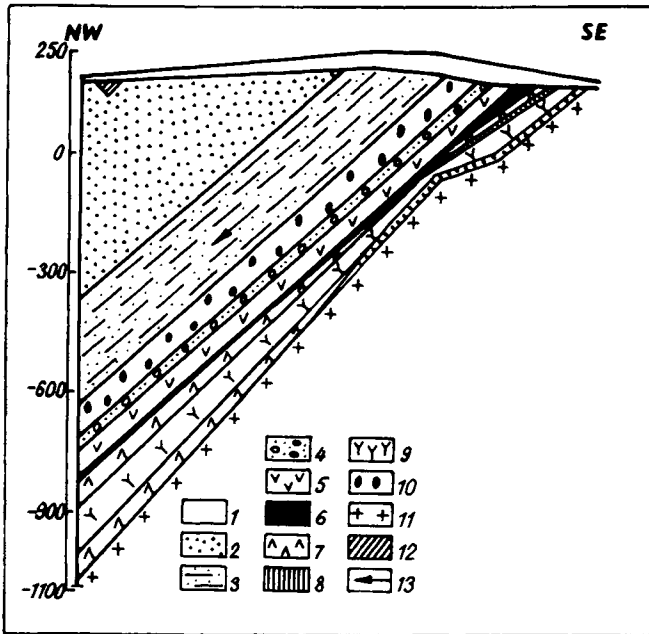


Fig. 70. Pyrophyllite-bearing rocks in the Ovruch Group (Tankilevich, 1976). 1 – post-Proterozoic formations; 2–4 – Tolkachev Fm: 2 – quartzose sandstone with pyrophyllite cement. 3 – sandstones interbedded with tuffites, ash tuffs, tuffaceous siltstones, sericitized and weakly pyrophyllitized, 4 – volcanomict grits: sandstone, tuffite, siltstone, pyrophyllitized & sericitized; 5–10 – Zbrankov Fm: 5 – porphyrite, orthopyre, 6 – tuffo-conglomerate, -sandstone, -siltstone, pyrophyllitized & sericitized, 7 – diabase, 8 – tuffolavas & lava conglomerates of qz porphyries, pyrophyllitized & sericitized, 9 – qz porphyry, pyrophyllitized & sericitized, 10 – polymict sandstone; 11 – rapakivi granite; 12 – pyrophyllite schists (tuffites), Nagoryansk deposit; 13 – combined metasomatic & pyrophyllite alteration zones.

### 3. Conclusions

It is possible to identify the following metallogenic epochs in the geological history of the Ukrainian Shield – Archaean, Early Proterozoic and Late Proterozoic, each with its own characteristic assemblage of useful minerals regularly associated with identified formational types and located in particular ore-bearing tectonic structures. During the *Archaean* epoch, iron accumulated in volcanosedimentary units, carbonaceous and high-alumina units, and a number of elements (chromium, nickel and copper) in basic to ultrabasic rocks; talc–magnesite deposits also formed at this time. Useful components were then concentrated in subsequent epochs. Evidence for the Archaean epoch is seen in the Podolsk, Belotserkov, Dnieper and Azov metallogenic provinces. Iron accumulated in sedimentary units during the *Early Proterozoic* epoch, forming rich ores; copper and molybdenum occurrences formed, and deposits of rare metals and rare earths, also apatite and abrasive garnet. Specific geological formations originated during the concluding stage of the Early Proterozoic epoch, with associated titanium and phosphorus,

topaz–morion pegmatites, etc. This epoch is widely represented in the Volyn, Kirovo-grad and Azov metallogenic provinces. The *Late Proterozoic* epoch is characterized by the formation of rare metal–rare earth and tin–tungsten–molybdenum deposits and occurrences related to metasomatic rocks in regions of crustal activation; also the formation of kyanite and pyrophyllite occurrences. This epoch affected the Volyn and Azov metallogenic provinces and the Krivoy Rog–Ingulets metallogenic zone.

This Page Intentionally Left Blank

## The Voronezh crystalline massif

V.B. DAGELAYSKY

### *1. Geological structure and metallogenic features*

The Voronezh crystalline massif – the Kursk–Voronezh block in the Precambrian basement of the Russian Platform – lies to the north of the Ukrainian Shield, from which it is separated by the Palaeozoic Dnieper–Donetsk aulacogen-type basin. Precambrian rocks in the Massif (Fig. 71) typically display complex geological structure and ore mineral prospects due to the effects of various tectonic and ore-forming regimes, as is the case for the Ukrainian Shield (Galetsky et al., 1987; Gorbunov et al., 1969; Golivkin, 1982; Zaitsev et al., 1970; Leonenko et al., 1976a, b; Shchegolev, 1985).

Precambrian assemblages in the Massif are represented by four complexes: Early Archaean (Oboyan Group), Late Archaean (Mikhailov Group, Sergeyev basic–ultrabasic and Saltykov trondhjemite–migmatite complexes), early–Early Proterozoic (Kursk Group, Oskolets trondhjemite–migmatite complex), late–Early Proterozoic (Oskol Group, Stoylo–Nikolayev ultrabasic–granodiorite, Ataman–Pavlov and Liskin subalkaline granitic complexes), Late Proterozoic (Smorodin basic complex, Baigora Group).

The Lower Archaean Oboyan Group consists of migmatized and granitized rocks over 2 km thick, the main constituents being gneisses (biotite, biotite–amphibole, pyroxene–amphibole, garnet–sillimanite, cordierite- and graphite-bearing), with bands of iron ore (two-pyroxene–magnetite with occasional garnet, and amphibole–magnetite), amphibolite, granite gneiss and migmatite (Shchegolev, 1985). The rocks are commonly migmatized by plagioclase-rich granites belonging to the Saltykov and Oskolets complexes and microcline granites from the Ataman complex.

The Upper Archaean Mikhailov Group varies in thickness from a few tens or sometimes hundreds of metres to 3 km and is the most widespread group in the region, forming the structure of Upper Archaean greenstone belts (Krestin, 1988). Metamorphic grade ranges from greenschist to amphibolite facies. Typically present are basic and ultrabasic volcanic products at the base, sedimentary rocks in the middle of the succession, and acid to intermediate volcanic products at the top.

The Lower Proterozoic Kursk Group is over 4.5 km thick and lies with an angular stratigraphic unconformity on units belonging to the Mikhailov or Oboyan Groups. It forms the limbs of major and minor synclines. According to Plaksenko (1966), the Kursk Group is divided into three metasedimentary formations, the middle being iron-ore proper. Volcanogenic members are encountered only at the bottom of the basal

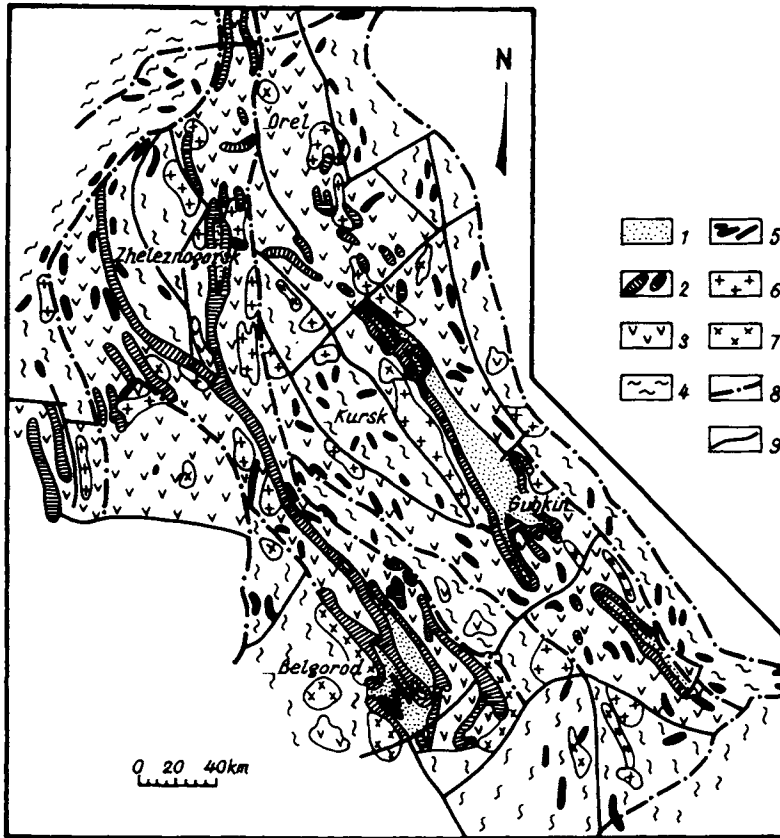


Fig. 71. Sketch map showing geological structure of the Precambrian in the Kursk Magnetic Anomaly (KMA), after Shchegolev, 1985, simplified. 1 – Oskol Group (Yakovlev, Tim, Shchigrov-Oskolets, Kurbakin Fms); 2 – Kursk Group PR<sub>1</sub>; 3 – Mikhailov Group AR<sub>2</sub>; 4 – Oboyan Group AR<sub>1</sub>; 5 – iron-chert rocks (silicate-magnetite ores) in Mikhailov & Oboyan groups; 6 – post-Kursk granitoids; 7 – pre-Kursk granitoids; 8 – first-order tectonic breaks; 9 – second-order tectonic breaks.

horizon in the lowermost formation, as tuffaceous sandstones and talc-amphibole schists. The lowermost formation is widely distributed and varies from a few metres to 2 km thick. Conglomerate beds and lenses up to 9 m thick are found at the base, interleaved with metasandstones and schists. Higher in the sequence come schists, carbonate rocks, phyllitic and carbonaceous slates, thin quartzites without ores. The middle formation gradually oversteps the lowermost, and consists of ferruginous quartzites or iron ores interleaved with schists, the total thickness varying from hundreds of metres to 2500 m in the ferruginous quartzites of the Mikhailov deposit. The topmost formation is conformable, with a gradual transition, and is up to 300 m thick of phyllitic, carbonaceous-clay, biotite-, garnet- and cummingtonite-bearing schists, with carbonate-bearing schists and metasandstones increasing at the top of the succession. Golivkin (1982) divides the Kursk Group into two: a lower Stoylen Fm (sandstones and schists) and an upper Korobkov Fm (iron ores).

The Early to Late Proterozoic Oskol Group in the Kursk Magnetic Anomaly (KMA) region lies with stratigraphic and angular unconformity on rocks belonging to the Kursk Group, and is up to 2.5 km thick. Typically present are coarse clastic rocks (conglomerate, breccia and grit with ferruginous quartzite clasts) at the base, where banded iron formations are also found. Overlying these rocks are quartz-mica schist with thin limestone and dolomite beds, together with graphitic schist.

Upper Proterozoic formations are represented by volcanosedimentary assemblages, the Baigora and Glazunov Groups (Fms). The Baigora Group, around 400 m thick, consists of tuffaceous shale and sandstone, chloritic slate and quartzose sandstone; thin (10–20 m thick) conglomerates occur at the base. The Glazunov Fm in the KMA region consists mainly of subhorizontal basaltic rocks, a few hundred metres thick.

Igneous rocks in the Voronezh Crystalline Massif have been investigated mainly by geophysical methods and by drilling (Gorbunov et al., 1969; Golivkin, 1982). The Late Archaean *Sergeyev complex* is represented in most places by pyroxenite, serpentinite, tremolite and carbonate-talc rocks, forming thin layer-parallel lenticular bodies. Trondhjemites of the *Saltykov complex* intrude and migmatize rocks of the Mikhailov and Oboyan Groups. The trondhjemites have a pre-Kursk weathered mantle. The early-Early Proterozoic *Oskoletsk complex* is represented by trondhjemites and migmatites, developed at the expense of Kursk Group rocks and other formations, together with basic and ultrabasic dykes. Late-Early Proterozoic igneous complexes within the KMA area include the *Stoylo-Nikolayev*, Smorodin and Ataman complexes, and the Mamon and Bobrov complexes in the east of the Voronezh Crystalline Massif (Gorbunov et al., 1969). During the initial phase of the *Stoylo-Nikolayev complex*, stock-like and lenticular gabbro, gabbro-dolerite and pyroxenite bodies formed, intruding Oskol Group rocks. Biotite-hornblende gabbro-diorite, diorite and granodiorite formed several intrusions during the second phase, including the *Stoylo-Nikolayev*, Trosnyan and other massifs. Final phases are represented by granodiorite, lamprophyre and diorite porphyry.

Simultaneously, the polyphase *Mamon intrusive complex* was emplaced. Its constituent rocks are peridotite, dunite and other ultrabasics, gabbro and gabbro-diorite, granodiorite and their vein equivalents (Gorbunov et al., 1969; Chernyshov, 1971). The *Smorodin complex* consists of differentiated gabbro-dolerite intrusions. The polyphase *Ataman complex* consists of biotite-hornblende granodiorite, granite, granosyenite and syenite (first phase); subalkaline microcline granite; aplitic granite, pegmatite and albitite veins. Alkaline ultrabasic rocks have been found in the Novo-oskol region. The *Bobrov granitic complex* in the east of the Massif consists of biotite granite, granodiorite, and pegmatite, biotite granite and adamellite veins.

Metallogenic features of the Voronezh Massif owe their origin to a prolonged, complex, polycyclic evolutionary history during the Precambrian in this part of the Earth's crust, and multiple volcanosedimentary and magmatic events that played a role in constructing the Massif. From detailed studies of the geological formations and associated ore formations and genetic types (Plaksenko et al., 1976, 1977; Poltorykhin, 1986; Chernyshov, 1976), it has been possible to establish specific features for the metallogeny of this buried Precambrian basement segment. Table 8 shows the volcanic and sedimentary groups and igneous complexes forming the Voronezh Crystalline

Table 8  
Some metallogenic features in the Precambrian of the Voronezh Crystalline Massif (after Plaksenko et al., 1976)

Epoch	Group. complex	Ore formation	Typical mineral assemblage	Examples of <u>ore deposits</u> and occurrences
Late Proterozoic	Smorodin	titanium-magnetite with vanadium	ilmenite, titano-magnetite, sulphides	Smorodin
	Baigora	metalliferous conglomerates	quartz, chlorite, sericite, pyrite, gold	Bobrov
Early Proterozoic	Oskol	iron-chert-clastic	hematite, magnetite, quartz, pyrite	Mikhailov, Zhideyev, Yakovlev
	Oskol	pyrrhotite-pyrite	pyrrhotite, pyrite, chalcopyrite, sphalerite, gold	Tim-Yastreb, SW Voronezh Massif
	Vorontsov	graphite	graphite, pyrite, pyrrhotite, high-Al minerals	Podkolodnovo, Annin
	Vorontsov	high-alumina	garnet, sillimanite, graphite	Podkolodnovo, Annin
	Mamon	copper-nickel sulphides; Co-bearing nickel sulphides	pyrrhotite, pentlandite, chalcopyrite, platinoids	<u>Nizhne-Mamon, Podkolodnovo, Yubileynoye, Yelan</u>
	Mamon	chromite	chrome spinels, chrome magnetite	Mikhailov, Sadov
	Mamon	ilmenite-magnetite	ilmenite, magnetite, sulphides	North Mamon
	Pavlov, Bobrov	rare-metal pegmatites	tantalum, niobium, other such metals	<u>Volotov</u>
	Liskin	molybdenite-quartz	molybdenite, quartz	Vislov, Liskin
	Stoylo-Nikolayev	gold-sulphide-quartz	pyrite, arsenopyrite, pyrrhotite, chalcopyrite, gold, quartz	Lebedino, Tmsk
Kursk	iron-silica-schist metalliferous conglomerates	hematite, magnetite, quartz	<u>Lebedin, Mikhailov, Stoylen, Korobkov, Ignatyev, Mikhailov, Lebedin</u>	

Late Archaean	Mikhailov	iron-silica-metabasite	magnetite, quartz, silicates	Usozhsk and Manturov anomalies
		metalliferous conglomerates iron pyrites	quartz, chlorite, sericite, gold pyrite, chalcopyrite, sphalerite, pyrrhotite	Ignatyev, Lebedin
Early Archaean	Oboyan	iron-silica-gneiss	magnetite, quartz, silicates	Kursk-Besedin, Komarich anomalies
	Oboyan	graphite	graphite, high-alumina minerals	Kursk-Besedin
	Oboyan	high-alumina	garnet, sillimanite, graphite	Kursk-Besedin
	Oboyan	iron pyrites	pyrite, chalcopyrite, sphalerite, pyrrhotite	Kursk-Besedin

---

Massif, together with ore formations and examples, most of which are minor occurrences.

## *2. Ore-bearing tectonic structures*

Recent studies (Galetsky et al., 1987) have demonstrated the possibility of directly correlating tectonic structures and constituent rock complexes between the Ukrainian Shield and the Voronezh Massif. A similar comparison may be made between the ore-bearing tectonic structures, shown in Figure 52. Currently, most workers identify the Kursk granite–greenstone terrain over a significant part of the massif (Lobach-Zhuchenko, 1988; Krestin et al., 1988). It consists of narrow greenstone belts (the Upper Archaean Mikhailov Group) in a granite–gneiss basement with relict Lower Archaean Oboyan Group rocks. We do not exclude the interpretation that individual segments of the basement to the granite–greenstone terrain and the high-grade Oboyan gneisses are structures of granulite–gneiss terrains. A typical feature in the Kursk granite–greenstone terrain are iron ore deposits and occurrences in essentially ferruginous quartzite–metabasic (Mikhailov Group) assemblages. Nickel and chrome occurrences in this structural region are associated with an ultrabasic dunite–harzburgite suite. Narrow apressed linear rift-type structures filled with early-Lower Proterozoic Kursk Group rocks are present where the Kursk granite–greenstone terrain is developed. The major iron ore deposits of the Kursk Magnetic Anomaly, in a ferruginous silica–schist formation, are associated with precisely this group. In the east of the Voronezh Massif is an intracratonic basin filled with Lower Proterozoic Vorontsov Group and equivalent Oskol Group sandy–shaly and volcanogenic sequences. Large copper–nickel sulphide deposits and small occurrences (also with cobalt, platinum and palladium) are associated with late-Early Proterozoic basic and ultrabasic igneous complexes. Ore-bearing basic–ultrabasic bodies are mainly located in the Vorontsov intracratonic basin. The distribution of ore deposits (and small occurrences, which are in the majority) in the Voronezh Massif according to ore-bearing structural types is shown in Table 9.

## *3. Ore deposits and occurrences*

### *3.1. Iron*

The Kursk iron ore province (known historically as the Kursk Magnetic Anomaly, KMA) is situated in the Kursk granite–greenstone terrain of the Voronezh Massif and is the country's main iron ore base. Five metallogenic zones and one metallogenic province including six ore regions have been defined (Fig. 72) on the basis of geological evolution, composition and structure of iron ore formations. The most important are the Mikhailov–Belgorod zone (rich iron ores) and the Orel–Oskol zone (slightly enriched ferruginous quartzites). All the zones have a NW strike and continue for 180–425 km with a width of 35–125 km.

Table 9

Relationship between mineral deposits and occurrences (+) and tectonic structures in the Voronezh Crystalline Massif

Mineral \ structures	I	II	III	VI	XII
Fe	+	+	+	1	
Fe (pyrites)		+	+		+
Cr	+	+			
Cu-Ni			+		2
Cu (Ni, Co, Pt, Pd)					3
Graphite	+				+
Alumina (staurolite, sillimanite)					+

*Ore-bearing tectonic structures (same numbering as in Table 5 for the Ukrainian Shield):* I – granulite-gneiss terrain; II-III – granite-greenstone terrain: II – tonalite- and granite-gneiss areas, III – greenstone belt; VI – rift belt; XII – intracratonic basin.

*Mineral deposits:* 1 – Mikhailov (Kursk Magnetic Anomaly, KMA); 2 – Nizhne-Mamon, Podkolodnovo; 3 – Yelan.

The following iron-silica ore-bearing formations have been identified in the Kursk iron ore province, as in the Ukrainian province (Shchegolev 1981): gneiss (AR<sub>1</sub>), metabasite (AR<sub>2</sub>), schist and clastic sediments (PR<sub>1</sub>). Most researchers consider that the formations are distributed according to stratigraphic subdivisions: Oboyan, Mikhailov, Kursk and Oskol Groups. Each formation includes definite ore types: ferruginous quartzites (Golivkin, 1982).

*Ores in the iron-silica-gneiss formation.* This includes Komarich-type high-grade metamorphic ores, developed in the granite-gneiss basement and in the Oboyan Group. Most gneisses contain no more than 10% ores. Ferruginous quartzites form beds and lenses 0.1–40.0 m thick and 500–600 m long, occasionally up to 25 km, with a magnetite and silicate-magnetite composition. Total iron content ranges between 20% and 42%, with 17–35% iron in magnetite.

*Ores in the iron-silica-metasite formation.* Two types of iron-silica rocks have been identified – Beregov and Besedin.

*Beregov type ores* are associated with greenstone belts and form part of the Upper Archaean Mikhailov Group as a minor component in the Alexandrov Fm. Ore deposits are typically small and scattered. Interbedded ore layers and lenses 0.2–16.0 m thick extend for tens of m up to a few km. Rock types include amphibole and garnet schists, meta-ultrabasics, and chlorite-biotite schists. Silicate-magnetite and carbonate-magnetite varieties of ferruginous quartzite predominate. Total iron in the ores is 16.7–23.3% and iron in magnetite is 6.7–16.8%; iron carbonates are always present. This ore type is comparable to the Verkhovtsevo ore type in the Ukrainian Shield.

*Besedin type ores* are found in the granite-gneiss basement of the Kursk granite-greenstone terrain and typically show ferruginous quartzites interbedded with high-alumina and mica schists, amphibolite, gneiss and granite gneiss, and leptite (fine-grained granoblastic quartzofeldspathic gneiss). Ore horizons are 1–40 m and more thick, 0.5–6.0 km long, sometimes up to 15 km. Ferruginous quartzites, which were

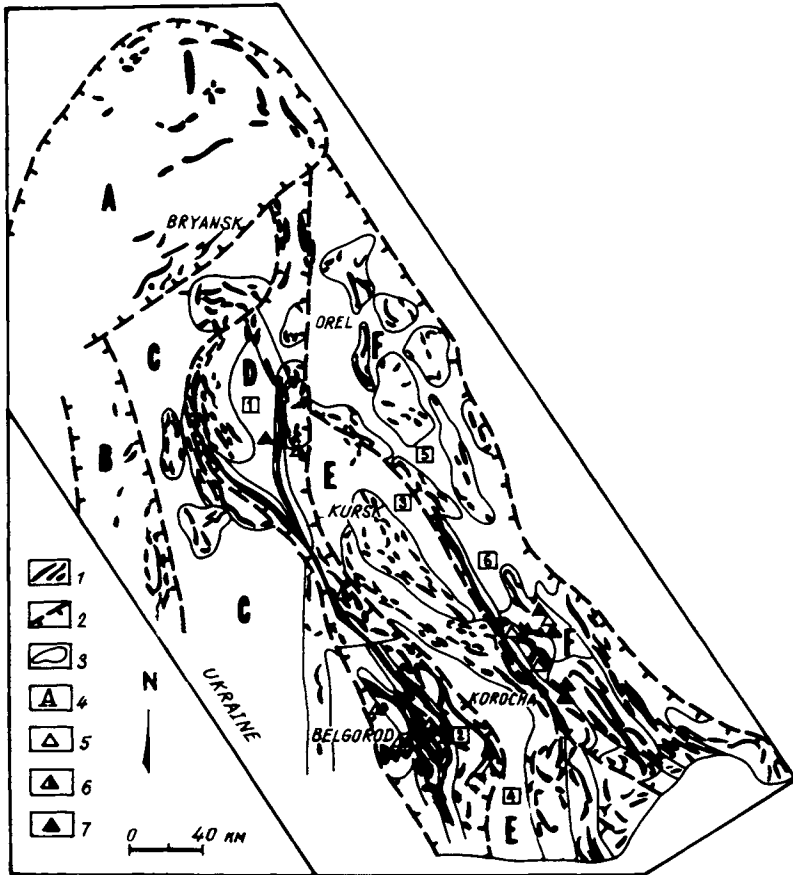


Fig. 72. Regional map of Kursk metallogenic provinces (Anon., 1974). 1 - ore-bearing iron-chert rocks; 2 - boundaries of metallogenic zones & provinces; ore regions (*roman numerals*): I - Mikhailov, II - Belgorod, III - Kursk, IV - Valuy, V - Orlov, VI - Oskol; 3 - boundaries of ore zones & complexes; 4 - metallogenic zones & provinces: A - Baryatinsk, B - Krupetsk, C - Rylsk-Rakityansk, D - Mikhailov-Belgorod, E - Kursk-Korochan, F - Orlov-Oskol; 5-7 - ore deposits: 5 - ferruginous quartzite, 6 - rich residual iron ores, 7 - ferruginous quartzite & rich residual iron ores.

metamorphosed at amphibolite and granulite facies conditions, have the composition silicate + magnetite, sometimes magnetite and hematite + magnetite. Total iron in the ores is 20-45%; iron in magnetite is 10-35%; iron carbonates are practically absent.

*Ores in the iron-silica-schist (chemogenic) formation.* This group includes Krivoy Rog type ferruginous quartzites in the Lower Proterozoic Kursk Group, which has the most extensive occurrence and is confined to synclines of various orders. Ore content in the productive Kursk Group is 30-55%, up to 75%. Ore horizons are from a few metres to 500 m or more thick and extend for 3 to 100 km. The ores are represented by silicate-magnetite, carbonate-silicate-magnetite, magnetite and hematite-magnetite ferruginous quartzites. Total iron varies within the 15-45% range; iron in magnetite is

10–36% and in carbonates, up to 5%. Metamorphic grade corresponds to greenschist facies (in the Mikhailov–Belgorod zone), epidote–amphibolite facies (in the Orlov–Oskol zone), and occasionally amphibolite facies. Rocks of the iron–silica–schist formation in the KMA region include huge iron ore deposits (Shchegolev, 1985): Mikhailov, Lebedin, Korobkov, Stoylen, etc., as well as the Yakovlevo, Gostishchevo and Chernyansk deposits. One typical deposit is described below.

The Mikhailov iron ore deposit (Figs 73 and 74) is situated in the Mikhailov–Belgorod metallogenic zone (Golivkin, 1982; Shchegolev, 1985) and belongs structurally

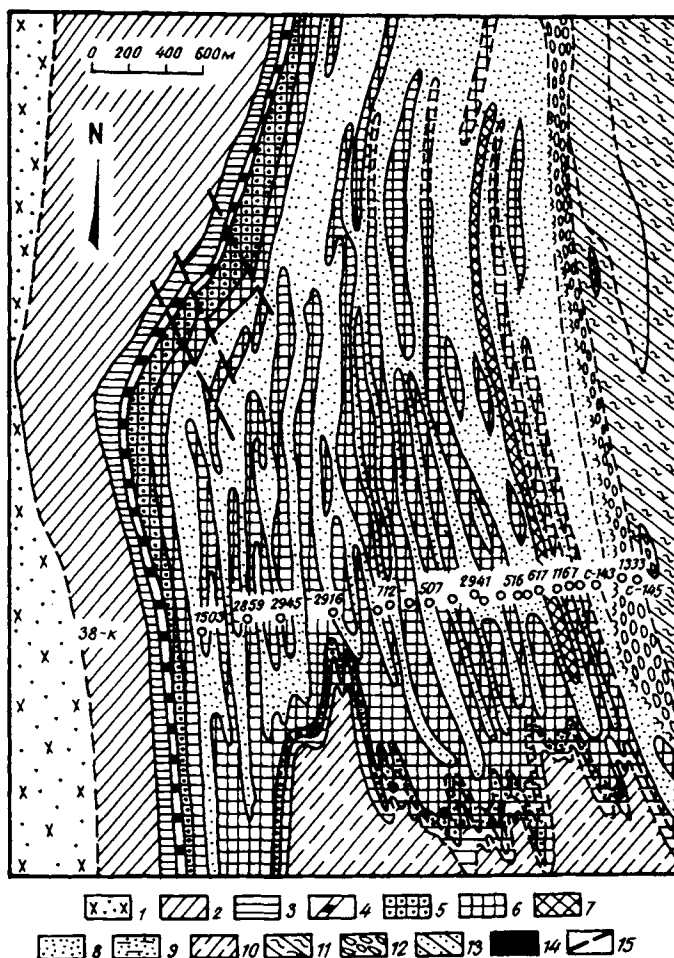


Fig. 73. Geological structure of Mikhailov iron ore deposit (Shchegolev, 1985). *Kursk Group* 1–2 – lower fm: 1 – metasandstone, grit, slate; 3–10 middle fm: 3 – alternating barren and ore-poor mag quartzites, 4 – carb-mag quartzite, 5 – mag quartzite, 6 – mag & hem-mag quartzite with green bi, 7 – py-mag quartzite, 8 – hem & mag quartzites, 9 – hem quartzite, 10 – intra-ore schists. *Oskol Group* 11 – breccioconglomerate, metasandstone, slate, 12 – breccioconglomerate of ferruginous quartzite interleaved with metasandstones, 13 – undifferentiated clastic ferruginous quartzites, 14 – hypergene iron ores; 15 – faults.

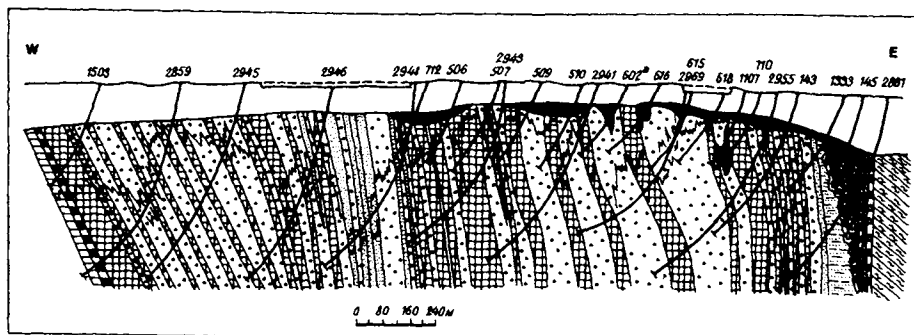


Fig. 74. Geological section through Mikhailov deposit (Shchegolev, 1985). Legend as Fig. 73.

to the western limb of a syncline of the same name. Two ferruginous quartzite members 200 m (lower) and 700 m thick are underlain by metasandstones, grits and schists of the lower or Stoylen Fm which gradually give way upwards in the succession to barren quartzites or rocks with a very low ore content (small amounts of magnetite). Ore-bearing ferruginous quartzites belong to the middle or Korobkov Fm and occur as two members separated by graphite, quartz-sericite and quartz-chlorite-sericite schists, 180–200 m thick. The lower ore member is divided into six horizons on compositional grounds. Each member displays a regular structure, expressed as a sequential alternation of the following rock types (upwards in the succession from schists): barren quartzite with schist interbeds, ore-poor with magnetite, silicate-magnetite, magnetite, and hematite-magnetite quartzites. Carbonate-magnetite quartzite with 15–20% sideroplesite + pistomesite is seen in the upper member. Two economic ferruginous quartzite varieties make up the ore deposit: magnetite (20% of the ore thickness) and hematite-magnetite (75%). Magnetite quartzites contain on average 37.5% total iron, and 25.7% Fe in magnetite; the figures for hematite-magnetite quartzites are 39.2% and 20.8% respectively. The average Fe content in rich siderite-martite and martite ores is about 54%.

*Ores in the iron-silica clastic formation* make up part of the Lower Proterozoic Oskol Group and occur mainly in the Belgorod syncline. Ore types are referred to as *Yakovlev* (clastic terrigenous) and *Belgorod* (clastic terrigenous-chemogenic).

*Yakovlev type ores* characteristically display conglomerates and ferruginous quartzite (chert) breccio-conglomerates interbedded with ferruginous metasandstone, siltstone and schist. Thin chlorite-magnetite and chlorite-hematite iron ores and ferruginous quartzites are present. The country rocks in the Rogov, Kurbakin and Yakovlev Groups contain no more than 1–5% ore material. Ore lenses and beds vary in length from tens of m to a few km, and in thickness from 0.2 to 25.0 m, sometimes up to 100–130 m. Metamorphism was at greenschist facies. The total Fe content in ferruginous quartzites is 16.6–27.8%, and Fe in magnetite = 0.3–18.9%. Maximum comparable figures for breccio-conglomerates are 32.7% and 1% respectively. This ore type has no economic significance.

*Belgorod type ores* are interbedded with graphite, carbonate and mica schists and metasiltstone; limestone, dolomite and metasandstone beds are also present. Meta-

morphism was at greenschist facies. Ore members are 1–150 m thick and extend for 2–20 km. Compositionally the ferruginous quartzites, alternating with schists, are magnetite, hematite–magnetite, carbonate–magnetite and silicate–carbonate–magnetite types. Host rocks in the Belgorod Group contain up to 17% ore minerals. The total iron content in the ores is 22–32%; and 9–29% Fe in magnetite.

In certain parts of the KMA there are rich iron ore occurrences associated with alkaline metasomatism zones in Kursk Group ferruginous quartzites. They are represented by magnetite (martite)–hematite and dolomite–magnetite ores, forming sub-concordant bodies up to a few metres thick and with 45–65% total Fe. They occur within alkali amphibole–hematite–magnetite and cummingtonite–magnetite quartzites.

### 3.2. *Nickel, copper, cobalt*

Copper–nickel sulphide ore mineralization in the Precambrian of the Voronezh Crystalline Massif is associated with a number of basic–ultrabasic rock complexes located in particular structures and represented by various formational types (Chernyshov, 1986). The Early Archaean (3.5–3.0 Ga) has numerous small (up to 1.5 km<sup>2</sup>) intrusions belonging to a *peridotite–pyroxenite–gabbro–norite* suite (the Besedino complex of Chernyshov et al., 1981), associated with ancient granite–gneiss blocks (Kursk–Besedino, Bryansk, etc.). Ultramafics of this type are associated with two-pyroxene schists and amphibolites, forming together with granite gneiss and gneissose granite the basement to greenstone belts and possibly also relicts of granulite–gneiss terrains. A typical accessory mineral assemblage is sulphide (pyrite, chalcopyrite, pyrrhotite)–chrome–spinel–magnetite. Nickel accumulated mainly in silicate form; less commonly it is concentrated in sulphides, forming scattered disseminations. This type has no economic importance.

A Late Archaean komatiite–basalt and dunite–harzburgite suite is associated with the Belgorod–Mikhailov and Orlov–Tim greenstone belts within the Kursk granite–greenstone terrain. Associated with the komatiites are sheets and podiform bodies 3–5 km long and 20–90 m thick of the dunite–harzburgite ultramafic suite containing a sulphide (millerite, pyrite, pyrrhotite, pentlandite and chalcopyrite)–chrome–magnetite accessory mineral assemblage. Nickel is also present, mainly in silicate form.

Copper–nickel sulphide ores proper and nickel ores within the Voronezh Massif are associated with basic and ultrabasic igneous intrusions of the Mamon complex – a dunite–peridotite–gabbro–norite suite (Gorbunov et al., 1969; Chernyshov, 1972, 1976) and are widely developed in the East Voronezh zone, which contains a late-Early Proterozoic intracratonic basin. More than 300 intrusions have been proven by drilling and geophysical methods, but copper–nickel mineralization has been found in only a few. Chernyshov (1986) distinguishes several groups of intrusive bodies differing in composition, degree of differentiation and ore content, amongst which the most important are true ultramafic differentiated plutons, low in magnesium (MgO = 12–30%) with predominantly syngenetic mineralization (Nizhne-Mamon, Podkolodnovo deposits) and polyphase complexly differentiated ultrabasic–basic low-magnesium Yelan type plutons with Cu–Ni sulphide mineralization in early ultrabasics and

essentially Ni and Ni-Co (with Pt, Pd, etc.) ores in norite and norite-diorite bodies (*Yelan deposit*).

Intrusions are restricted to narrow (15–40 km) and extensive (upto 300 km long) NW-trending belts: the Losevo–Mamon essentially ultramafic belt in the west; and the Yelan–Ertil belt in the east, consisting of complexly differentiated Yelan type ultrabasic–basic plutons. Nickeliferous intrusions, round or elongate in shape, are emplaced into a sandstone–shale assemblage in the Vorontsov Group, enriched in carbonaceous matter and containing pyrite–pyrrhotite mineralization.

*The Nizhne-Mamon deposit* (Glazkovsky et al., 1974) occurs in a differentiated gabbro–peridotite intrusion with an area of around 6 km<sup>2</sup>, running for 4 km in a NW direction parallel to the strike in the Vorontsov Group country rocks (Fig. 75). Rocks in the intrusion dip steeply (70–80°) to the NE. The main rock types are ultrabasic: peridotite (over 70%) and dunite (about 2%), which are intensely serpentinized, plus olivine pyroxenite, which are cut by gabbro–norite and gabbro belonging to the second intrusive phase. Dunites form a relatively constant horizon, 7–15 m thick, on the hanging wall of a peridotite band and constitute the main bulk of disseminated copper–nickel sulphide ores. Exploration has been carried out in two ore bodies, the “Main ore body” and the “Lower ore body”.

The “Main ore body” occurs at the contact zone between serpentinized dunite and peridotite and olivine pyroxenite. The deposit, which has indistinct boundaries, extends for over 2000 m and can be traced to a depth of 250–350 m. Poor-quality disseminated ores with 0.2–0.6% nickel and 0.15–0.40% copper are present in peridotite and olivine pyroxenite at the base of the deposit. Higher up, in serpentinized dunite, the richest deposits occur as evenly and densely disseminated ores with 0.5–0.95% Ni and upto 0.8% Cu, as massive and brecciated sulphides. The top of the deposit is mineralized serpentinite in which the amount of useful mineralization decreases towards the hanging wall. Zones of disseminated sulphide mineralization are present.

The “Lower ore body” also occurs in a serpentinized dunite layer and is composed of patchy, densely disseminated ores with a banded texture. Vein-type bodies containing massive sulphide ores 300–400 cm thick occur at the contact between ultrabasics and cross-cutting granitic dykes. The nickel content in massive sulphide ores does not exceed 2–3%.

*The Podkolodnovo deposit* (Glazkovsky et al., 1974) has a similar setting to the Nizhne-Mamon deposit described above. It occurs in a stock-like steeply-dipping ultrabasic intrusion with an area of some 3 km<sup>2</sup> and a concentric zoned internal structure. Serpentinite is the main rock type in the intrusion (at 55–60%); peridotites (wehrlite, harzburgite, lherzolite) amount to 20–25%, and olivine pyroxenite 1–2%. Disseminated sulphide mineralization, forming two deposits, is also restricted to serpentinized dunite or places where dunite alternates with peridotite and olivine pyroxenite.

The Western deposit is over 1000 m long and can be traced to depths of 250–300 m. Sulphide mineralization forms lenses and bands in the deposit, 0.5–5 m thick and upto 600 m long. At the base are cluster-type disseminated ores in amphibolitized peridotite, while at higher levels are uniformly disseminated ores in serpentine. The nickel content ranges from 0.4 to 1.2%. The Central deposit is 300–350 m long and contains densely

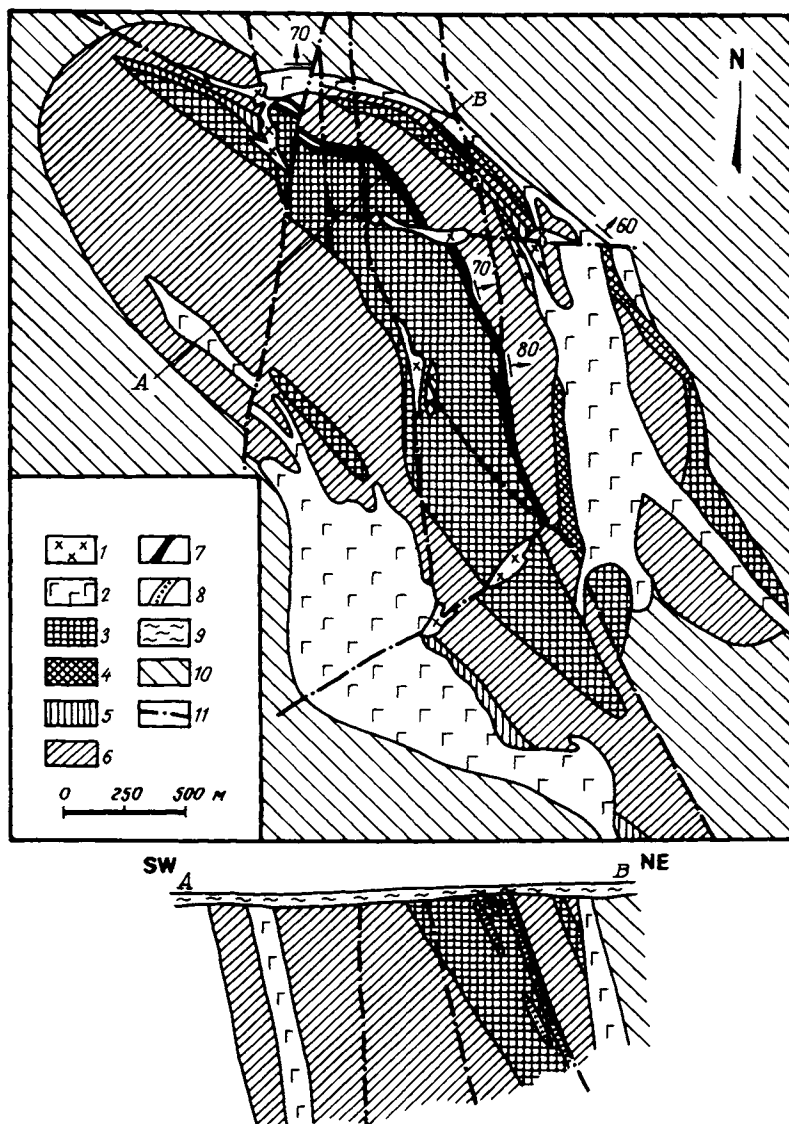


Fig. 75. Geological sketch map of Nizhne-Mamon ore deposit (Glazkovsky et al., 1974). 1 – diorite, 2 – gabbro–norite, 3 – peridotites (lherzolite, harzburgite, wehrlite), 4 – plag peridotite, 5 – ol pyroxenite, 6 – serpentinite, 7 – ore-rich serpentinite, 8 – ore mineralization, 9 – sedimentary cover rocks, 10 – Vorontsov sandy–shaly succession, 11 – faults.

disseminated ores in lenticular bodies conformable with the layering in the intrusion. This deposit is restricted to serpentinized dunite bands or to places where dunite is interbanded with peridotite and olivine pyroxenite. Overall, copper–nickel sulphide ore deposits fall into two types: 1) disseminated, the main type; and 2) massive and

brecciated. Pyrrhotite is the major component in both types (at 85–95%), with 3–8% pentlandite and chalcopyrite. Secondary sulphides are cubanite, mackinawite, vallerite, pyrite, marcasite, bornite, chalcocite, etc. Chrome spinel and magnetite are typical for the disseminated ores. Metasomatic processes in the ores led to sulphides being replaced by magnetite pseudomorphs. So-called “shadow” ores (after N.M. Chernyshov) formed in cases where complete pseudomorphing occurred.

Besides the copper–nickel deposits described above, a new type of deposit has been found in the Voronezh Massif (Chernyshov 1986; Chernyshov et al., 1978), where Ni–Co sulphide mineralization with minor copper is associated with orthopyroxenite and quartz norite in polyphase differentiated magma chamber plutons. Particularly interesting is the Yelan basic–ultrabasic pluton (*the Yelan deposit*) in the Yelan–Ertil syncline, which contains Lower Proterozoic Vorontsov Group rocks. Figure 76 shows the geological structure of the Yelan pluton.

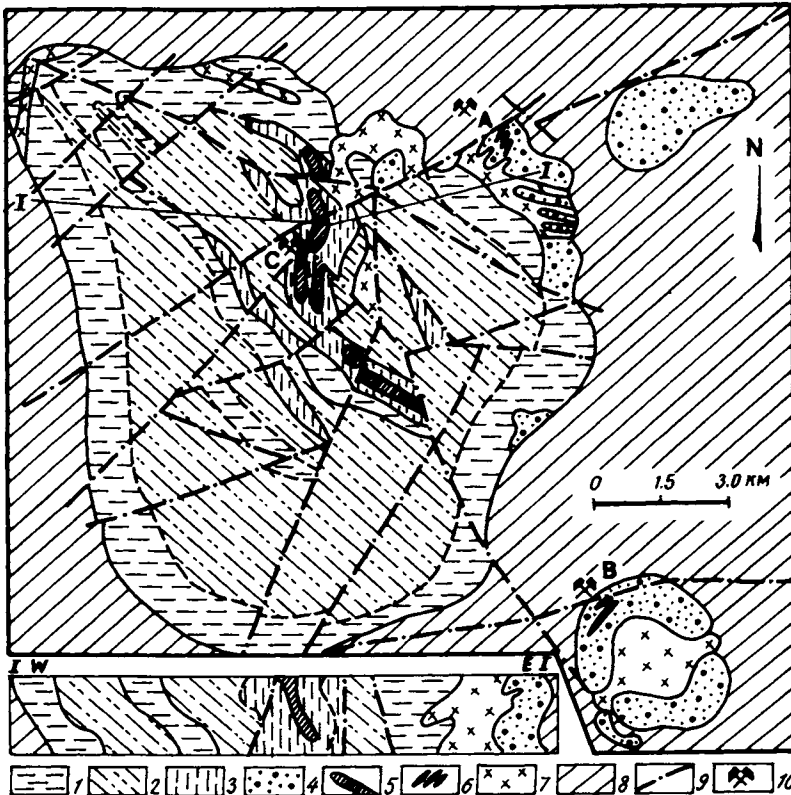


Fig. 76. Schematic structure of Yelan polyphase ore-bearing pluton in the Voronezh Crystalline Massif (Chernyshov, 1986). 1 – ol gabbro–norites with thin plag peridotite, dunite & troctolite layers; 2 – ol-orth & ol-free gabbro–norites; 3 – bi-hb gabbro–norite & bi-hb websterite, hb gabbro, hb pyroxenite & hornblendite; 4 – sulphide-bearing norite; 5 – metasomatic orthopyroxenite with copper–nickel sulphide ore mineralization; 6 – ore bodies; 7 – diorite; 8 – Vorontsov Group sandy–shaly rocks; 9 – faults; 10 – ore deposits & occurrences: A – Yelan, B – Yelkin, C – Central.

The Yelan lopolith formed in three phases: 1) basic-ultrabasic, 2) sulphide-bearing norite, 3) diorite. The first phase is the most extensive, and is represented by two rock associations: an early layered series (dunite, peridotite, websterite, troctolite, orthoclase gabbro, norite) and a late olivine-free hornblende series (hornblende pyroxenite, pyroxene hornblendite, hornblende gabbro-norite, etc.). Among first phase rocks, ultrabasic differentiates in the layered series amount to 3–5%. The second phase includes quartz-bearing norites of varying grain-size and colour index, and pyroxene diorites. The third phase consists of quartz diorites with biotite and hornblende. Dyke complexes were associated with the relevant intrusive phases. An isotopic age has been obtained for the basic-ultrabasic rock association ( $2060 \pm 25$  Ma) and sulphide-bearing norites (2020 Ma) by the Pb–Pb method on zircon, the average of several determinations. Spatially associated with early-phase olivine-free differentiates in the pluton are orthopyroxenite bodies with copper–nickel sulphide mineralization.

Ore-bearing norites form steeply-dipping pipe-, slab- and stock-shaped bodies with an area of 0.5–10 km<sup>2</sup>, mostly in the NE and E inner contact zones of the intrusion, or in Vorontsov Group rocks. Ore bodies are sometimes arranged *en échelon* and can be traced for more than 1300 m deep. Identified ore types are disseminated, vein-disseminations, brecciated and massive (solid), differing in nickel : copper and nickel : cobalt ratios. In the quantitatively predominating disseminated ores, these ratios (according to Chernyshov, 1986) are: 1) in chalcopyrite–pentlandite–pyrrhotite ores (chalcopyrite + pentlandite upto 10–15%) Ni : Cu = 4 : 1–6 : 1, Ni : Co = 10 : 1–15 : 1; 2) in pentlandite–pyrrhotite ores (pentlandite upto 35–45%) Ni : Cu = 17 : 1, Ni : Co = 13 : 1 → 40 : 1. In vein-disseminated and brecciated ores, Ni : Cu = 25 : 1–30 : 1, Ni : Co = 14 : 1–30 : 1; the ore composition is pentlandite (20–35%, sometimes upto 80%)–pyrrhotite, less commonly chalcopyrite–pentlandite (upto 30% in total)–pyrrhotite with nickel and cobalt arsenides and sulpharsenides. In massive ores (pentlandite–pyrrhotite, also with nickel and cobalt arsenides and sulpharsenides) Ni : Cu = 60 : 1, Ni : Co = 17 : 1 → 20 : 1. The total ore composition in norites is typically: a quantitative predominance of pyrrhotite, limited distribution of chalcopyrite (1.5–5 to 10–15% of the ore volume), high pentlandite content (to 30–50%), constant presence of nickel and cobalt arsenides and sulpharsenides (cobaltite–gersdorffite, löllingite, cobaltite and nickelite, rammelsbergite, smaltite–skutterudite, etc.), molybdenite, native copper, arsenopyrite, pyrite, chrome spinel, ilmenite, graphite, etc. A specific feature of the ores is the low heavy sulphur isotope content compared to copper–nickel sulphide deposits.

Ore formation is associated with magmatic processes (copper–nickel sulphides in orthopyroxenite and nickel in norites), and high-temperature post-magmatic processes (nickel–cobalt mineralization). The nickel–cobalt ore mineralization described above in norites of the Voronezh Massif is comparable to the Sudbury deposits in Canada, on the basis of the type of sulphide-rich norite magmas, magmatic redeposition of sulphides from ultrabasics in earlier phases, mineral composition, and geochemical signature.

In addition to the useful mineralization referred to above, which has economic importance, the Precambrian of the Voronezh Massif contains some other ore formations (Plaksenko and Shchegolev, 1977), associated with which are particular ore

occurrences (Table 7). *Metalliferous conglomerates* include coarse clastic rocks at the base of the Mikhailov and Kursk Groups (Novoyalta, Mikhailov, Yakovlev and Staro-oskol regions of the KMA), as well as the Baigorov assemblage in the SE of the Voronezh Massif. Basal conglomerates in the lower Kursk Group contain *gold* and *rare elements*, the highest content being characteristic of metaconglomerates with quartz pebbles and an essentially pyrite cement. Lower Proterozoic conglomerates attain a maximum thickness of 600 m in the Staro-oskol region (Poltorykhin, 1986). A *graphite* formation embraces graphite-bearing rocks in the Kursk-Besedino anomaly region (the granite-gneiss basement of a granite-greenstone terrain or a local granulite-gneiss terrain) and graphite gneisses of the Vorontsov Group in an intracratonic basin. In the Podkolodnovo and Annin sections, graphite gneisses are interbanded as 1–25 m thick bands with high-alumina biotite and amphibole gneisses. The graphite content is 3–50% and over, and forms individual 0.2–0.3 mm flakes and aggregates. Graphite is associated with ore minerals – pyrite, pyrrhotite and occasionally chalcopyrite, marcasite, molybdenite, magnetite and hematite. Fine graphite-sulphide intergrowths are found. A *high-alumina* rock formation includes gneisses with high-alumina minerals (staurolite, cordierite, sillimanite), varying from 5 to 7%, which are found in the SE of the Massif and within a number of anomalies in the KMA. Corundum-muscovite schists in the Mikhailov Group, upto 20 m thick, are found above amphibolites in the Staro-oskol region. Pyrite-pyrrhotite mineralization in a pyrite formation is present in various structures: the granite-gneiss basement and greenstone belts in the Kursk granite-greenstone terrain (the Oboyan and Mikhailov Groups), in sandy-shaly and volcanogenic assemblages in an intracratonic basin (the Vorontsov and Oskol Groups in the Vorontsov structure), and in Late Proterozoic Glazunov plateau basalts. The main ore minerals are pyrite and pyrrhotite; chalcopyrite, sphalerite, magnetite and hematite are also present, and native gold has been observed. The sulphide content varies from 5% to 60%. Conformable zones of sulphide mineralization are tens of metres thick.

#### 4. Conclusions

The material presented above enables us to draw brief conclusions about the number and specific features of metallogenic epochs in the Precambrian of the Voronezh Massif. The *Early Archaean* epoch is characterized by metamorphic ore formations: iron-silica-gneiss, pyrite, graphite, and high-alumina types. During the *Late Archaean* epoch, the following ore formations originated: iron-silica-metabasite, massive sulphide, chromite. The most varied ore formations that make up the known ore deposits and occurrences in the Voronezh Massif belong to the *Early Proterozoic* epoch. Metamorphic formations belong to the early stage – iron-silica-schist, and metalliferous conglomerates. Metamorphic formations in the later stage include iron-silica-clastic, metalliferous conglomerates, massive sulphide (pyrrhotite-pyrite), graphite and high-alumina types; also magmatic formations: rare-metal pegmatites, copper-nickel sulphides (with cobalt and platinoids), chromite and ilmenite-magnetite; hydrothermal-metasomatic ore formations: gold-sulphide-quartz, molybdenite-quartz. The

*Late Proterozoic* epoch includes the following ore formations: metalliferous conglomerates, titanium-magnetite (with vanadium), and low-Ni sulphide types. Precambrian ore deposits in the Voronezh Massif with the greatest practical interest are mainly iron ore and copper-nickel sulphide ore deposits.

This Page Intentionally Left Blank

## Platform cover of the East European Craton

A.K. ZAPOLNOV

### *1. General features of tectonic evolution and ore content*

Upper Proterozoic Riphean and Vendian sediments are included in this work as part of the Precambrian of the East European Craton platform cover. Riphean sediments for the most part are localized in relatively narrow elongate furrows in the crystalline basement, such sedimentary basin structures usually being referred to as aulacogens. Riphean and Vendian are also constituents of intracratonic and pericratonic basins which are mostly developed around the craton margins. Upper Vendian sediments (Valdai Group and its analogues) are more widespread. These sediments, together with the Lower Palaeozoic, constitute the lower structural stage of the upper platform assemblage, forming a sedimentary blanket on the craton.

Structures in the platform cover have been poorly investigated in terms of their metallogeny. This is particularly the case for structures belonging to the Riphean–Lower Vendian (palaeocratonic) structural stage, buried beneath a thick sedimentary mantle of the craton cover assemblage. Economic concentrations of metals associated with Riphean sediments are known only in the Bashkirian region of the Urals, which historically belongs to the East European Craton, and in the modern structural plan forms part of the Urals fold belt. For these reasons we can present only an outline of the main features relating to the evolution of ore formation in the late Proterozoic across the Russian Platform. The most important feature is the sharp increase in the number of ore occurrences at the transition from the palaeocratonic to the neocratonic stage. Within the framework of the palaeocratonic stage, there is a slight increase in the productiveness of sedimentary assemblages towards later stages in their development. Peripheral regions of the platform have the greatest prospects for mineral exploration in this regard.

In historical tectonic terms, there is a definite pattern in the sequence of events that make up the exceedingly long palaeocratonic period. The overall tectonic activity of this period can be described by a complete cycle of archogenesis, including the formation of a gentle arch (stage 1), further upwelling of central regions (stage 2) and finally rapid subsidence (stage 3). During stage 1, a broad arch formed with a gently dipping central segment and steeper marginal zones, complicated by a system of major radial fractures – grabens. Peri-cratonic troughs or basins formed around the edges of this mega-arch on a fractured crystalline basement at the beginning of the stage. These structures continued to develop in subsequent stages to the extent that they contain the most complete late Precambrian reference sections.

The main useful mineral concentrations are associated with pericratonic basins. A relatively well-studied example in the Russian Platform is the Bashkirian peri-craton, where a varied complex of ore deposits and occurrences is known. For this reason it is worthwhile dwelling on the metallogenic features of this region, however briefly, despite the fact that the greater part (and the only part so far investigated) of the pericratonic basin lies outside the platform in the modern structural plan.

Stratified iron deposits have been known here since the 18th century. The *Bakal group* of deposits (Novobakal, Shikhan, Rudnichnoye, etc.) occur on the limbs of the Bakal syncline. Ore bodies, which have slab-like, pocket and podiform shapes, occur in Bakal Fm ( $R_1$ ) carbonate rocks. Ore deposits range in thickness from 4 m to 120 m, and they can attain lengths of 3.5 km. The main ore mineral is magnesium-bearing siderite (sideroplesite,  $(Fe, Mg)CO_3$ ), with brown ironstones present in the oxidation zone – hydrogoethite, hydrohematite and goethite. Ankerite is a secondary ore mineral. Ore bodies in the Zigazin–Komarov group of iron ore deposits ( $R_2$  age) have a similar structure. Here the ore field extends for some 40 km, with an area of 250 km<sup>2</sup> in which about 30 deposits are concentrated (Tukan, Tussagan, Tarskoye, and others). Ore deposits average 10–15 m in thickness, with beds and lenses extending for about 1 km, sometimes up to 3–4 km. The ores are sideritic, with brown ironstones in the oxidation zone.

The *Satka group* of crystalline magnesite deposits (Stepnoye, Volchegorskoye, Gologorskoye, Karagai and others) has been known since the end of the 19th century. More than 100 ore bodies are located in a 300–500 m thick carbonate unit in the Satka Fm ( $R_1$ ), with dips of up to 45°. Sheet deposits are 5–40 m thick and up to 2.5 km long, and the bodies can be traced for several hundred metres downdip. The ore deposits are conformable with the host dolomites and have sharp contacts. The ores are considered to be metasomatic formations, having originated under the influence of magnesium-rich hot solutions. The hottest fluids are associated with dolerites which cut both the ore bodies and the wall rocks. Ore bodies are composed almost exclusively of magnesite, with minor amounts of calcite, aragonite, quartz and pyrite.

Other mineral occurrences associated with sedimentary assemblages in the pericratonic basin worthy of mention include the ancient coastal marine zirconium–titanium placer deposits in the volcanogenic–clastic terrigenous Ay Fm ( $R_1$ ) and the clastic Zilmerdak Fm ( $R_3$ ), also stratiform type occurrences of barite, fluorite, polymetallic deposits, and cupraceous sandstones. In addition, titanium–iron–vanadium mineralization is associated with igneous complexes (Kusin layered gabbro complex,  $R_2$ ), and small hydrothermal copper occurrences (the Mashak rhyolite–basalt complex,  $R_2$ ).

During the course of the subsequent stage, from the Middle Riphean, the entire Russian platform area experienced further up-arching. This process was particularly intensive in central, eastern and north-eastern regions, where a network of relatively narrow, elongate grabens (aulacogens) formed. It is important to emphasise that the newly established aulacogen system was at the same time subordinate to the regional structural plan of the pre-Riphean crystalline basement. Aulacogens are spatially and apparently genetically related to the most active zones between crustal blocks, in complete agreement with the block structure of the basement (Rundqvist and Mitrofanov, 1993, p. 195).

Practically no mineralization has been found to date in aulacogens in the Russian Platform. However, considering that they are only imperfectly known, we cannot completely rule out the possibility of finding, in particular, stratiform deposits of non-ferrous metal ores and occurrences of certain other types. This is indirectly confirmed by noting that the network of aulacogens continued to play a tectonic role in the emplacement of useful minerals in sediments belonging to the overlying Phanerozoic cover (Valeyev, 1978).

The third and final phase in the Riphean to Early Vendian evolution of the platform was characterized by overall subsidence of the cratonic mega-arch. This process developed gradually and commenced with sedimentation extending beyond basin (aulacogen) margins. In regions where aulacogens had not developed, small imperfectly isometric sedimentary basins emerged during this period. The location of these primary basins, as well as that of the aulacogens, is conformable with the sites of zones between pre-Riphean crystalline basement blocks. Sedimentation subsequently extended sharply beyond the confines of the aulacogens (or primary sedimentary basins) with the formation of broad intracratonic basins possessing particular features of similarity with synclises of the upper platform structural stage. The overall extensional dynamic regime, during which arch-shaped geostructures subsided, is underlined by the intense display of continental basaltic volcanism in western regions. Throughout the entire Late Riphean, the transition to the third phase did not occur simultaneously across the platform.

The intracratonic basins (mostly epi-aulacogens) which formed during this stage are of practical interest with respect to exploration for economic metal ore concentrations. However, the metallogenic content of the intracratonic basins has been poorly researched to date, and there is essentially no targetted study being conducted with regard to any ore occurrences in the basins.

In the far NE of the platform, in the area near the Timan basin, grey clastic terrigenous Safonov Group (Upper Riphean or Kudash) sediments contain low-grade lead mineralization, expressed as finely disseminated galena. A manganese-bearing clastic terrigenous-carbonate formation is also associated with continental basins. According to Yakobson (in Anon., 1985), manganiferous dolomites in the Orsha basin (Lapich Fm, R<sub>3</sub>) may be considered to be a product of effusive and explosive carbonatite volcanism. Supporting this viewpoint are textural features of dolomites, together with geochemistry (up to 1% Fe, Mn, P and Ba present) and the presence of an ultrabasic accessory mineral assemblage which is not typical for the sedimentary cover. Similar manganese-bearing dolomites are also known from the Ladoga basin (the top of the Priozersk Fm, a probable analogue of the Lapich Fm) and from the Pachelma epi-aulacogen basin (the Peresytkin Group).

Copper occurrences and titanium-zirconium placer deposits are associated with late sediments of this stage. Up to 20 native copper occurrences are known from within the Volyn intracratonic basin, where they are associated with plateau basalts (the Volyn Group, V<sub>1</sub>). Most occurrences are concentrated in a narrow (15–20 km) strip, in which Volyn basalts lie at shallow depth beneath Upper Cretaceous sediments (near the settlements of Malorita and Zaboloty, the towns of Ratno, Kamen-Kashirsky and Rafalovka, and north of the town of Rovno). Copper most commonly occurs in

basalts, less often in tuffs. The largest occurrences are in zones where the jointing is closely spaced. Native copper is the main ore mineral, with individual slabs weighing up to 1 kg. Secondary minerals are chalcocite, bornite, covellite, cuprite, malachite and azurite. These minerals are seen as disseminations in quartz and calcite veins and in the cement in volcanic breccias, or as encrustations and films along fractures. Copper minerals plus chlorite, zeolites, quartz, etc. may also fill amygdales in basalts. Chalcocite and chalcopyrite are most often encountered in tuffs, forming disseminations or small pockets up to 2–3 cm (Belevtsev et al., 1974). Most mineral occurrences in the Volyn basin seem to have formed due to leaching of cupraceous basalts as a result of the activity of post-volcanic hydrothermal solutions. Native copper may have crystallized in part during magma cooling.

In the Orsha intracratonic basin, Volyn lavas are replaced by the Svisloch tuffaceous–sedimentary formation, with which are associated placer deposits containing higher concentrations of ilmenite, leucogene, zircon and magnetite. On structural and sedimentological grounds, it can be argued that similar placers could possibly be found in other intracratonic basins.

The next major period in platform evolution began in the Late Vendian. Starting in Valday times, most of the Russian Platform was drowned during an extensive marine transgression, marking the transition to the late platform regime with a regular alternating pattern of regional transgressive and regressive epochs. Typical for this period was the formation of a thick sedimentary blanket in predominantly large-scale structures with extremely gently-dipping limbs (fractions of a degree) – synclises and anteclyses\*. Mineral genesis in the platform cover during the late platform period was perceptibly richer and more varied, although at the very base of this assemblage in Upper Vendian sediments, practically no economic mineral deposits have been found.

The Late Vendian transgression encroached onto the Russian Platform from two sides, NE and SW, such that by the beginning of the Cambrian, two non-adjacent basins existed on the platform: the South-Eastern (Volyn–Dnestr) and Central basins, situated in the future Moscow and Mezen synclises. Currently available data on Upper Vendian metallogeny are almost exclusively for the Volyn–Dnestr basin.

In the north of the Dnestr part of the basin (Podolsk region around the river Dnestr), complex fluorite–polymetallic ore mineralization has been discovered at several stratigraphic levels. Most of the occurrences are associated with Mogilev Fm sediments (quartzose and arkosic sandstones of the Olchedayevo and in part the Yampol beds). For the ore region as a whole, a clear zoned mineralization structure has been established, in the form of well-expressed alternating mineral zones, in the direction from the Ukrainian Shield towards the SW: fluorite (partly with copper), baryte, galena, and sphalerite zones.

Important fluorite concentrations (over 10% for bodies at least 0.1 m thick) have been observed at over 20 places (the Murovan–Kurilovets, Krivokhizhintsovo and

---

\* synclise = negative or depressed structure on continental platform; broad, regional extent, tens-thousands km<sup>2</sup>; anteclyse = positive or uplifted structure on continental platform; broad, regional extent, tens-thousands km<sup>2</sup>; both are produced by slow crustal downwarp during the course of several geological periods.

other occurrences). Economic deposits have been discovered in the Bakhtyn deposit. Sheet-like ore bodies are conformable with host sandstones at the top of the Olchedayev member. The thickness of four ore deposits is 0.1–0.7 m, for a width of 50–600 m and a length of up to 2.8 km. The total mineralized area is around 10 km<sup>2</sup>. Fluorite in the deposits averages 17.4%, with the maximum reaching 49% (Nechayev, 1978). Mineralization is dissemination type, and as the fluorite content increases, individual phenocrysts grow into ore lenses and beds.

Zones with fluorite vein-type mineralization are also encountered and in some occurrences this type plays an independent role. For example, in the Voyevodchino occurrence, calcite–fluorite veins with pyrite in Yampol sandstones (at the top of the Mogilev Fm) and in the crystalline basement are associated with subvertical breccia zones, up to 0.5 m wide and usually containing not more than 5% fluorite. Various temperature intervals are quoted in the literature for ore-forming fluids: from 200–145°C (Belevtsev et al., 1974) to 165–130°C (Nechayev, 1978). In any case, sheet-like fluorite occurrences belong to medium- and low-temperature events. The lowest homogenization temperatures for fluid inclusions (110–120°C) were obtained for vein fluorite.

Spatially associated with the fluorite zone are copper occurrences at the base of the Mogilev Fm. Copper minerals are chalcopyrite, malachite, azurite, covellite and bornite. Chalcopyrite forms disseminations in sandstones, or fine vein networks together with quartz and pyrite. Malachite and azurite are present as films and encrustations along joints and fractures in brecciated zones. In the largest occurrence, Ozarino, the copper content in sandstones does not exceed a few tenths of one percent.

A zone with baryte concentrations exists in certain places between fluorite and galena zones. The most significant concentrations are found around the village of Savka, where mineralization affects the entire succession of the Mogilev Fm. The richest interval, 2 m thick, contains up to 15% baryte.

Galena and sphalerite zones have over 20 mineral occurrences. Ore bodies are sheet-like and conformable with host sandstones and grits of the Mogilev Fm. Mineralization is expressed as disseminations, pockets, lenses, occasionally as crystal clusters in calcite veins. According to the zoning referred to above, either galena or sphalerite predominates in individual mineral occurrences. In ore bodies at least 0.1 m thick, the lead concentration can reach 17%, and zinc 13%. No economic ore finds have been made to date. Sphalerite in association with chalcopyrite in the Olkhovskoye occurrence is observed in calcite veins and their inner contacts in zones of increased fracturing in the crystalline basement and the immediately overlying sediments.

Nearly all the ore leads are J-anomalous (containing excess radiogenic lead), although the lead isotopic composition becomes closer to normal with increasing distance away from the edge of the Ukrainian Shield (Nechayev, 1978). The isotopic composition of leads from the Mogilev Fm appears to be controlled to a large extent by the composition of basement rocks in the source region.

Upper Vendian stratified ore mineralization in the Podolsk area around the river Dnestr has all the hallmarks of a sedimentary origin, with subsequent redistribution of the ore material during epigenesis. Insignificant galena mineralization is also known in sandstones and shales from the Upper Vendian Gdovsk horizon on the southern buried edge of the Baltic Shield.

The oldest phosphorite-bearing formation on the Russian Platform occurs in the middle of the Volyn–Dnestr basin. In the north of the Dnestr part of the basin, phosphorites are found as fluorapatite concretions in several (up to 5) ore-bearing horizons amongst marine silt–clay sediments in the Upper Vendian Nagoryan Fm. Large concretions, up to 25 cm, are usually found in lower horizons. Smaller concretions are more typical for upper horizons, and they often grow into each other, forming solid phosphorite lenses up to several m long. Cavities in the concretions, especially the

Table 10  
Ore deposits in the Precambrian cover of the East European Craton

Useful component	Ore formation	Age	Tectonic setting	Ore deposit, Occurrence
Iron	Stratiform siderite in carbonates	R <sub>1</sub> , Bakal Fm	Bashkirian pericratonic basin	Bakal group of deposits
Iron	Stratiform siderite in carbonates	R <sub>2</sub>	Bashkirian pericratonic basin	Zigazin–Komarov group of deposits
Iron–titanium–vanadium	Titanomagnetite in basic rocks	R <sub>2</sub> , Kusin complex	Bashkirian pericratonic basin	Kusin deposit
Magnesite	Magnesite in dolomites	R <sub>1</sub> , Satka Fm	Bashkirian pericratonic basin	Kopan deposit
Zirconium–titanium	Ilmenite–zircon–rare-earth placer formation	R <sub>1</sub> , Ay Fm; R <sub>3</sub> , Zilmerdak Fm	Bashkirian pericratonic basin	Satka group of deposits
Zirconium–titanium	Ilmenite–zircon–rare-earth placer formation	V <sub>1</sub> , Svisloch Fm	Orsha intra-cratonic basin	Numerous minor occurrences
Lead	Galena in grey sandstones	R <sub>3</sub> , Safonov Group	Safonov intra-cratonic basin	Numerous minor occurrences
Lead–zinc	Fluorite–galena–sphalerite–baryte in sandstones	V <sub>2</sub> , Mogilev Fm	Dnestr downward	Numerous minor occurrences
Manganese	Manganiferous dolomite formation	R <sub>3</sub> , Lapich Fm, Priozersk Fm	Orsha intra-cratonic basin Ladoga basin	Numerous minor occurrences
Copper	Native metal in basalts	V <sub>1</sub> , Volyn Group	Volyn intra-cratonic basin	Numerous occurrences in the Zabolotye–Ratno–Rafalovka strip
Fluorite	Fluorite & fluorite–galena–sphalerite–baryte in sandstones	V <sub>2</sub> , Mogilev Fm	Dnestr downward	Bakhtyn and numerous occurrences in the Podolsk–Dnestr region
Barite	Fluorite–galena–sphalerite–baryte in sandstones	V <sub>2</sub> , Mogilev Fm	Dnestr downward	Savka and other small occurrences
Phosphorite	Phosphorite concretions in silty–clayey sediments	V <sub>2</sub> , Nagoryan–sk Fm	Dnestr downward	Numerous small occurrences in Dnestr region

largest ones, are usually filled with calcite and kaolin, with grains and crystals of galena as well as irregular patches of sphalerite, pyrite and chalcopyrite.

Thus, despite the fact that Precambrian structures in the platform cover of the East European craton are characterized by a sufficiently wide spectrum of useful minerals, very few mineral occurrences have so far been discovered, and none has any economic importance. Nevertheless, Late Proterozoic sediments have not been well studied, even those lying at shallow depths, and a comparison with the Precambrian sedimentary cover on other cratons suggests that there are positive prospects for finding major deposits of various kinds, especially stratified ore deposits and buried placers. Table 10 presents the basic known facts concerning mineral occurrences in the sedimentary platform cover of the East European craton.

This Page Intentionally Left Blank

## **Part II**

### **Mineral deposits of the Siberian Craton**

This Page Intentionally Left Blank

## **Section 1:**

### **Anabar Shield**

**S.I. TURCHENKO**

The Anabar Shield is a basement inlier in the North of the Siberian craton, which coincides with the Anabar Plateau of the Central Siberian Highlands. The crystalline rocks which make up the shield are covered around the edges by gently-dipping Riphean sediments of the platform cover. Geological research in the shield began with its discovery in 1905 by I.I. Tolmachev and O. Backlund, though survey mapping was carried out in 1946–60, when the major features of its geological structure were established. At the same time, rocks of the Anabar complex were commonly found to contain ferruginous quartzites; titanomagnetite, base metal ores, phlogopite and apatite occurrences were discovered, but were not prospected in detail due to the difficulty of access. In recent years, graphite and apatite–ilmenite ore prospects have been confirmed.

This Page Intentionally Left Blank

## Major features of geological structure and metallogeny

S.I. TURCHENKO

### 1. Tectonic structure

The Anabar Shield forms the northernmost exposed part of the first-order Aldan–Anabar geoblock and is a separate component of the basement to the Siberian craton. Crystalline rocks of the shield are mostly considered to be Archaean in age, and are divided into three groups: Daldyn, Upper Anabar and Khapchan, consisting of pyroxene gneiss and schist with varying amounts of marble, calciphyre, hypersthene–garnet and other paragneisses, belonging to the granulite facies. Intrusive rocks include enderbite, charnockite and ultramafics, also later granitoids. Tectonically, the shield has two major structural elements: ancient blocks consisting of granulite complexes, and linear NW-striking shear zones with superimposed low-grade metamorphism. Five such zones have been identified within the shield, extending for hundreds of km, each being a few tens of km wide. The zones have an *en échelon* block structure and characteristically display widespread granitization and amphibolite facies retrograde metamorphism; plutonic igneous rocks are also present – anorthosite, gabbro and norite. Most of these zones formed in the period from the Late Archaean to the end of the Early Proterozoic. These shear zones divide the Anabar Shield into three blocks: Central Anabar, Magan and Khapchan (Fig. 77), which differ in their granulite facies P–T conditions, lithological composition and geophysical fields (Vishnevsky, 1978; Grishin et al., 1982; Rabkin, 1959). Ore mineral assemblages inherent to these blocks and in cross-cutting zones are also different.

Major structural forms – antiforms and synclinoria – can be mapped according to the outcrop pattern of the identified rock groups and on this basis an overall domal structure of the shield has been established, with the oldest rocks of the Daldyn and Upper Anabar groups cropping out in the centre of the shield. On the NE and SW margins they give way to carbonate–clastic terrigenous rocks of the Khapchan Group. The overall arched structure is complicated by second-order flexures (synforms and antiforms) which can be traced for 200–300 km in a NW direction, with a width of a few tens of km. The major mappable structural forms are folds which are a few km or a few hundred m across. Various minor structural forms have also been observed: boudins and small-scale shear folds. Dislocations of various ages are represented by crush zones, shearing and mylonitization. Some of these zones, especially those trending almost N–S, appear to be very old, probably Archaean and were reactivated during the Early Proterozoic stage in the evolution of the shield. East–west fractures can be traced by the strike of Late Proterozoic and Mesozoic dolerite dykes (Mashak, 1973).

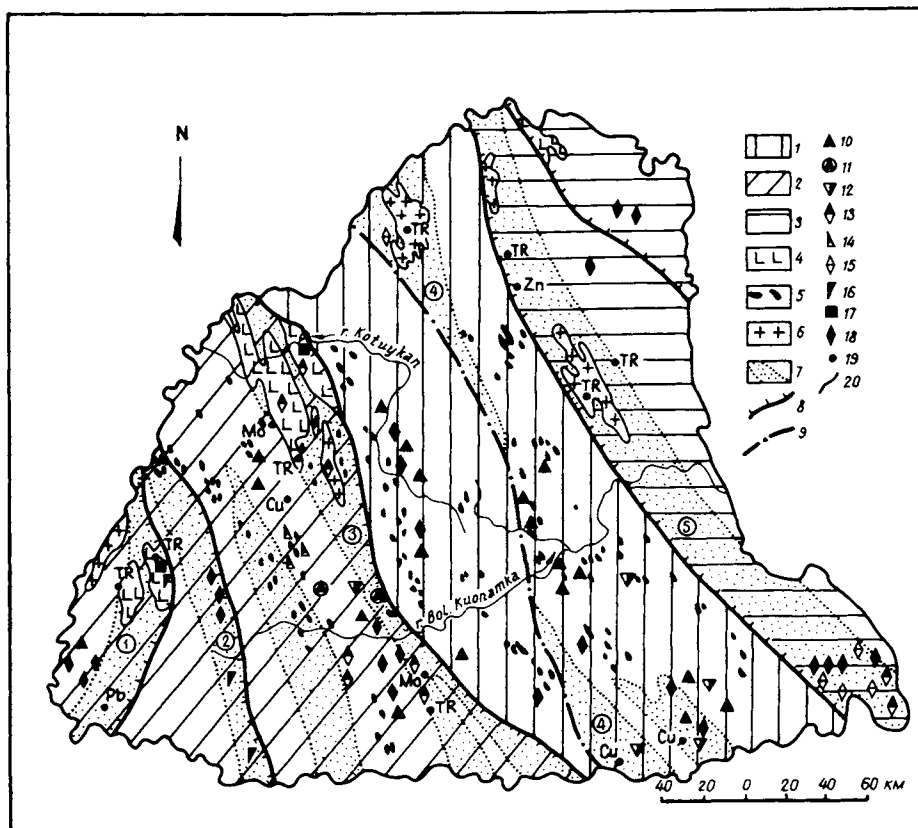


Fig. 77. Structural sketch map of metallogenic regions and location of mineral deposits in the Anabar Shield. *Archaean complex, metallogenic provinces and blocks*: 1 – Central Anabar, 2 – Magan, 3 – Khapchan; 4 – gabbro–anorthosite; 5 – meta-ultrabasics; *Early Proterozoic complex*: 6 – granitoids, 7 – retrograde zones, partial melting, amphibolite facies metamorphism & structural–metallogenic zones (*numbers in circles*: 1 – Magan, 2 – Lamuy, 3 – Monkhoolin, 4 – Khapchan, 5 – Billyakh); 8 – deep-seated thrusts, 9 – Anabar fault; mineral occurrences: 10 – Fe, 11 – Cr, 12 – Ni, 13 – musc, 14 – gt & silli, 15 – phlog, 16 – apatite, 17 – Ti & apatite, 18 – graphite, 19 – base metals & rare metals; 20 – boundary of Anabar metallogenic province.

The Anabar Shield as a tectonic structure evolved over a protracted time interval as the result of many deformations of different nature and was formed by two early Precambrian complexes: Archaean and Early Proterozoic. The Riphean stage was expressed as igneous activity in the form of alkali ultra-basic and carbonatite intrusions in the SE Billyakh zone, which is considered to be Early Riphean (Shpunt et al., 1981).

**Rock complexes.** The Archaean complex consists of supracrustal volcanics and clastic sediments, metamorphosed at granulite facies. Mafic schists in the Daldyn and Upper Anabar groups are analogues of tholeiitic basalts, while pyroxene–plagioclase gneisses (enderbites) are analogues of dacites and andesites (Lutz, 1984; Rozen, 1981). From their petrochemistry, these rocks form a continuous volcanic series with a basalt–

andesite–dacite composition. Meta-ultrabasic rocks, ranging in composition from peridotite to pyroxenite are considered at present to form parts of layered intrusions. Chemically they are comparable with komatiites (Lutz, 1984; Rozen, 1981). Most rocks in the Daldyn Group together with ferruginous quartzites can thus be considered to be a komatiite–tholeiite–basalt formation. Rocks in the Upper Anabar Group together with garnet–biotite gneisses, which are comparable with clastic terrigenous rocks (Rozen, 1981; Rozen et al., 1982) constitute a volcanogenic–clastic formation (basalt–andesite–dacite with terrigenous sediments) with a metamorphic age of  $2890 \pm 80$  Ma, based on U–Pb zircon dating (Bibikova et al., 1985). In the upper part of the sequence, these formations give way gradually to carbonate–flysch formations in the Khapchan Group. The rock association in this group – garnet–biotite gneiss – corresponds to grey-wacke-type sediments (Rozen et al., 1982).

The blocks referred to above differ in terms of the depths at which they underwent granulite facies metamorphism. Typical mineral assemblages in the Central Anabar block are hypersthene + sillimanite + quartz, as well as parageneses with sapphirine and cordierite in peraluminous rocks. Garnetiferous mafic schists are also widespread in the complex – eclogitic garnet–pyroxene, garnet–two pyroxene and garnet–hypersthene rocks. Metamorphic conditions in this complex, based on an analysis of mineral assemblages (Vishnevsky, 1978; Lutz, 1964) correspond to the garnet–hypersthene–sillimanite and sillimanite–biotite–orthoclase subfacies, i.e. high- to medium-P granulite facies (820–950°C, 8–11 kbar). Practically all the metamorphic rock types that characterize the Anabar Shield are to be found in the Magan Block. Common assemblages are those suggesting that the Magan block belongs to the garnet–hypersthene–cordierite–orthoclase and sillimanite–biotite–orthoclase subfacies of the granulite facies. Estimated metamorphic P–T conditions are 780–850°C and 7–8.5 kbar.

Mineral parageneses in peraluminous rocks in the Khapchan block are mainly sillimanite–garnet–cordierite–orthoclase and (only partially) sillimanite–biotite–garnet–orthoclase subfacies of the granulite facies. P–T conditions during metamorphism were 5.5–7.5 kbar and 750–820°C.

The Early Proterozoic complex is represented in the main by retrograde rocks, formed in linear shear zones at the expense of granulite facies assemblages, in various subfacies of the amphibolite and epidote–amphibolite facies. Retrogression was preceded by intense blastocataclasis and blastomylonitization. Compositional types among retrograde rocks are biotite, amphibole, biotite–garnet, garnet–amphibole gneisses and plagioclase gneiss, and amphibole, garnet–amphibole, biotite–amphibole schists.

The Early Proterozoic complex is also represented by igneous rocks, developed mainly in linear shear zones with superimposed metamorphism. This stage was accompanied by partial melting, expressed as injection-type migmatites with a garnetiferous granite and granodiorite composition, as well as intrusive bodies of alaskite and biotite granite. Individual major linear zones also include intrusive bodies of gabbro–anorthosite. Gabbro–anorthosites form sheet-like bodies, deformed into asymmetric folds, and contain elements of compositional layering, to gabbro and gabbro–norite. Titanomagnetite and apatite mineralization are associated with the latter (Sukhanov et al., 1984).

**Metallogenic regions.** The Anabar Shield developed as a unit in the Archaean–Early Proterozoic stages, hence the shield can be taken as the Anabar metallogenic province which formed during two metallogenic epochs corresponding to these stages. The oldest event, belonging to the Archaean was the formation of a granulite–gneiss terrain with its own specific assemblage of useful mineral occurrences.

The second metallogenic epoch is associated with the final phase in the formation of the continental crust within the shield during the Early Proterozoic epoch. The main feature of this epoch was the appearance of major magmatic and metamorphic processes related to the formation of deep-level thrust–shear zones striking almost N–S and expressed in the emplacement of gabbro–anorthosite and granitic intrusions, migmatization, and amphibolite facies retrograde metamorphism. Migmatization and metamorphism display a strongly lithophile–chalcophile mineralization signature. Since the mineral assemblages in granulite–gneiss terrains and in linear zones differ markedly, they are treated separately in the following description.

## *2. Ore mineralization in granulite–gneiss blocks*

Mineral deposits in granulite–gneiss blocks belong to various classes of metamorphic-type deposits (Sokolov et al., 1975). The main group consists of metamorphosed mineral deposits and occurrences (pro-metamorphic) which include iron ore (BIF type), high-alumina industrial minerals, also graphite and abrasive garnet.

BIF-type ore occurrences are represented by magnetite quartzite within magnetite–two pyroxene–garnet schists which form lenticular and ribbon-like bodies up to 50 m thick and from 2.5 to 4.0 km long. The iron oxide content ranges from 33–38% to 60–80%. Forecast reserves of rich ores in an area of some 200 km<sup>2</sup> in the Central Anabar Province have been estimated at over 2 billion tonnes. These ores also contain high titanium and vanadium concentrations.

High-alumina industrial mineral occurrences are represented by sillimanite bodies in aluminous schists, associated with quartz-rich assemblages in the granulite complex. Beds containing sillimanite lenses are up to 100 m thick and can be traced along strike for 1 km to 20–30 km. Sillimanite is unevenly distributed, its content ranging from 5–10% to 20–30%.

A separate genetic category is true metamorphic occurrences of high-Mg garnet, cordierite and sapphirine, metasomatically associated with hypersthene–garnet–sillimanite and cordierite schists. Garnet from these rocks can be used as an abrasive material, while cordierite and sapphirine are partly semi-precious decorative stones. Garnet occurrences are fairly major, but semi-precious stones and decorative materials are less extensive and not yet completely investigated. Metasomatic garnet–cordierite–hypersthene rocks contain up to 60–70% garnet, and forecast reserves of high-quality abrasive garnet are over 50 million tonnes.

Graphite–sillimanite–garnet schists occasionally with up to 20% graphite occur as patches in areas where the Khapchan Group crops out, especially in the Magan block. Individual graphite occurrences can be traced along strike for 20 km, and the average thickness of graphite-rich layers is up to 0.5 m. In carbonates in the same area are

apatite-rich layers which could form sources for stratiform-type phosphate raw material.

In addition, chromite and copper–nickel mineralization are found in association with ultrabasic bodies, spatially related to the Daldyn Group, within granulite–gneiss blocks. These bodies are usually 15–20 m thick and several hundred m long. As a general rule, the bodies are rootless and have been significantly altered by metamorphism and metasomatism. The largest bodies display a weak zoning due to the preservation of olivine-rich rocks in their central parts. Meta-ultrabasics are distinguished by higher Ni, Co, Cu and Cr contents, concentrated in both primary and metamorphic silicates. Less commonly, dispersed disseminations of pyrrhotite, chalcopyrite, chromite, pentlandite and chrome spinels are to be found.

### *3. Ore mineralization in linear zones of tectono-thermal reworking*

Occurrences of useful minerals in these zones are usually represented by the following types: 1) sulphide mineralization with molybdenum, copper, rare metals in mylonites and shear zones; 2) gold-bearing sulphides, rare-earth and rare-metal mineralization in metasomatic aureoles close to granitic intrusions and in areas of intense migmatization; 3) muscovite and rare-metal mineralization in pegmatites; 4) apatite and titanomagnetite mineralization in gabbro–anorthosites.

A typical feature in the Lamuy zone is intense granitization, expressed as migmatites and minor alaskite bodies with rare-metal mineralization (zircon and monazite). Sulphide mineralization with copper, molybdenum, lead and zinc is restricted to aureoles of hydrothermally-altered rocks (the Magan zone). The Khapchan zone contains numerous pegmatites and pegmatitic granites, with associated muscovite–rare-earth element mineralization. Granodiorite and granosyenite bodies, the largest of which are found in the Billyakh zone, have associated rare-earth element mineralization (cerium–yttrium and zirconium).

Locally, especially in the Khapchan zone, where granitization and potash metasomatism are most intense, the main phlogopite occurrences are concentrated and are restricted to areas where two-pyroxene schists and calciphyres crop out. Areas where carbonates crop out have prospects for strontium and boron mineral occurrences, since higher geochemical anomalies have been found for these metals.

### *4. Titanium–apatite occurrences*

A characteristic feature of linear tectono-thermal reworking zones are gabbro–anorthosite intrusions showing apatite and titanomagnetite mineralization (Sukhanov et al., 1984). The largest such intrusion occurs in the north of the Monkhoolin zone, where apatite- and titanomagnetite-bearing gabbro–norites have been discovered, concentrated in the *Vostochny* (“Eastern”) *massif*, which has an area of some 120 km<sup>2</sup>. The body is lenticular in plan and consists of anorthosite in the centre, with gabbro–norite, jotunite and mangerite at the edges. Contacts with basic country rocks are

tectonic and there are persistent gradations between the rocks of the massif, reflecting primary layering.

Apatite and titanium-bearing gabbro-norites are located in the centre of the intrusion and occur as layers alternating with anorthosites (Fig. 78). The  $P_2O_5$  content reaches 3.64%. Apatite occurs as isometric or elongate hypidiomorphic crystals (2–5 mm), forming 5–10% of the rock, sometimes up to 15%. Titanomagnetite forms xenomorphic crystals 0.2–1.0 mm in size (5–11%) and sometimes reaches up to 50% of the rock. The significant thickness and extent of apatite- and titanium-bearing gabbro-norites (Fig. 78) and the high apatite and titanomagnetite contents suggest a possible economic value for these ore occurrences, which have an igneous-cumulus genesis.

**Crustal evolution and general features of metallogenesis.** The formation of the crust in the Anabar Shield took place in several distinct stages. The age of protoliths, measured by U–Pb zircon dating, is in excess of 3.3 Ga. The Archaean complex was metamorphosed under high pressure and temperature granulite facies conditions, which occurred at 2.9 Ga (Bibikova et al., 1985). Metamorphism was accompanied by the earliest partial melt event, with which the oldest pegmatites are associated. This resulted in the formation of the early Precambrian crust of the Anabar Shield, representing part of the extensive Anabar–Aldan granulite-gneiss terrain that constitutes the basement to the Siberian craton. Deep-level thrusts formed in the Late Archaean stage (close to 2.7 Ga ago), probably reflecting early horizontal crustal movements leading to the formation of the block structure of the Anabar Shield. These movements were accompanied by intense folding which obliterated the primary stratification of rock complexes, and granulite facies metamorphism at various depths. Simultaneously, plutonic magmas were emplaced in tectonically compressed zones, to form gabbro-anorthosite (2.7 Ga, Sukhanov et al., 1984), charnockite and enderbite bodies. During

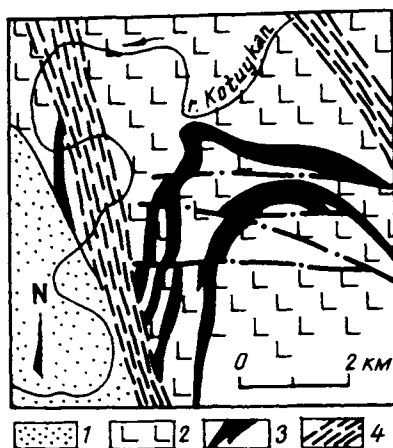


Fig. 78. Sketch map of apatite-titanium mineral occurrence in gabbro-anorthosites of the Vostochny intrusion, Monkhoodin zone (Sukhanov and Rachkov, 1984). 1 – bi-amph gneiss in retrograde zone, 2 – anorthosite & gabbro-anorthosite, 3 – apatite- and Ti-bearing gabbro-norite, 4 – blastomylonite & catclastic zones.

this stage therefore, linear belts of tectono-thermal reworking began to form in the Anabar Shield while individual blocks were subjected to various P-T types of granulite facies metamorphism. The sequence of geological events is summarised in Fig. 78a.

The crustal structure was made more complex during the Early Proterozoic episode (2.0–1.8 Ga ago). Initially, the Archaean craton was fragmented along deep-seated faults that originated along Late Archaean precursor tectonic zones into a number of major blocks that are identifiable within the shield. These movements were accompanied by cataclasis of Archaean complexes and blastomylonitization in thrust-faulted tectonic shear zones under amphibolite facies metamorphic conditions. Subsequently, intense granitization of rock assemblages occurred in tectonic zones, with the emplacement of granites and pegmatites.

The Riphean stage reflects an essentially new character in the evolution of the Anabar crust, when initially rifting along inherited linear tectonic zones (e.g. the south of the Billyakh zone, 5 on Fig. 77) caused the emplacement of alkali-ultrabasic and carbonatite intrusions displaying titanomagnetite-rare-earth element mineralization. Subsequently, at the end of the Early Riphean and in the Middle Riphean the sedi-

AGE Ga		GEOLOGICAL EVENTS		Metallog. signature		
Phanerozoic	0.8	250–170 Ma kimberlites fission track zircon				
		230–220 Ma dolerite & gabbro-dolerite dykes				
	Late	Platform cover			dolerite dykes	
		Billyakh Group	K-Ar on glauconite		carbonatites	
		Mukun Group			alkali-ultrabasic intrusions	
		angular unconformity				
	Early	granitization, intrusion of granites, pegmatites, amphib. facies metam.			shear zones blastomylonites	
		+ supracrustal complex ?			K-Ar U-Pb	
	Late Archaean	2.6	intrusion of gabbro-anorthosites 2700–2770 Ma		Pb-Pb isochron	
		2.7	partial melting, enderbites, charnockites			
2.9		deep-level thrusting, HP & LP granulite facies metamorphism		U-Pb zircon isochron		
3.0		Khapchan Group	clastic-carbonate )	sedimentation		
	Upper Anabar Gp	volcano-clastic ) assemblages	intrusive & effusive			
	Daldyn Group	volcanogenic )	magmatism			

Fig. 78a. Scheme of geological events affecting the Anabar Shield.

mentary platform cover formed, consisting of clastic terrigenous and carbonate sediments belonging to the Mukun and Billyakh groups with basaltic volcanics and gabbro-dolerite dykes dated at 1570–1400 and 1318–1250 Ma (Mashak, 1978). During the Mesozoic, the development of the shield was characterized by igneous activity, expressed as dolerite dyke intrusions (at  $242 \pm 5$  Ma) and kimberlites (250–170 Ma, Komarov et al., 1978).

Precambrian ore-forming processes in the Anabar Shield have particular features that are defined in two metallogenic epochs: 1) Archaean, during which the Anabar granulite complex was formed, and 2) Late Archaean–Early Proterozoic, expressed as the formation of linear structural–metallogenic zones. Mineral deposits associated with Archaean granulite–gneiss terrains belong to the metamorphic genetic type, represented by iron, graphite, garnet and sillimanite deposits. In addition, chromite and copper–nickel magmatic mineralization are associated with meta-ultrabasic bodies.

Magmatic rock assemblages comprising linear zones are characterized by a rare metal–rare earth element signature, typical for granodiorites and alaskites, and also apatite–titanomagnetite mineralization in gabbro–anorthosite intrusions. Here, zones of superimposed metamorphism, blastomylonitization and granitic magmatism are characterized by particular metallogenic signatures, expressed as the formation of metamorphic–metasomatic ore mineralization and hydrothermal mineralization. Minor industrial mineral occurrences of a metamorphic nature are represented by phlogopite, strontium- and boron-bearing apo-carbonate metasomatites, and also muscovite and rare metal-bearing pegmatites. Occurrences with a hydrothermal genesis are hosted in areas of mylonitization and shearing. These metasomatites occur in association with granitic intrusions and are accompanied by copper, molybdenum, lead, and zinc sulphide mineralization.

## Section 2:

### Aldan Shield

D.A. MIKHAILOV

The Aldan Shield is the major basement inlier in the Siberian craton, overlain in the north by Riphean and Palaeozoic to Mesozoic platform assemblages; in the south it borders on the Mongolia–Okhotsk belt, and its western edge is bounded by the Baikal fold belt. The varied nature of events and the protracted Precambrian time interval over which the shield evolved geologically have determined its heterogeneous structure. The shield consists of a central part, the Aldan crystalline massif or granulite–gneiss terrain, and the Olyokma and Batomga granite–greenstone terrains situated to the west and east (Fig. 79). The southern part of the shield consists of the Dzhugdzhur–Stanovoy terrain, where several cycles of tectonic activity occurred, beginning in the Early Archaean, then reaching a climax in the Late Archaean (3.0–2.7 Ga) with the formation of greenstone belts and extensive fields of granitization, and ending in the Early Proterozoic (2.2–2.0 Ga). Early Precambrian granulite–gneiss terrains in the west of the Aldan Shield and granite–greenstone complexes belonging to the Olyokma terrain are unconformably overlain by the Early Proterozoic Udokan Group and its analogues. They form the major Udokan basin and a number of minor graben–synclines representing a stage when intracratonic basins formed. The Early Proterozoic is represented in the eastern part of the shield by the formation of the Ulkan volcanoplutonic complex within the Batomga granite–greenstone terrain.

Iron, phlogopite, apatite, rock crystal and other mineral deposits are widespread in the Aldan Shield, belonging to magnesian skarn, iron–silica, rock crystal, phosphorus–rare earth and other formations. Specific mineral deposit localities within crystalline complexes are determined by lithological and geochemical features of the rocks, the evolution of regional metamorphism, magmatism and folding. A significant number of the deposits are concentrated in the centre of the shield, which led to the creation of the Aldan mining region, the importance of which is also due to the existence of younger gold deposits.

Phlogopite and magnetite deposits belonging to a magnesian skarn formation are the commonest types in the territory described here. Several also include apatite, boron, sulphide and rare-earth mineralization which geologically and structurally are unique targets, without analogues in other regions. Ferruginous quartzite deposits as distinct from magnesian skarn deposits are found in almost every part of the region, varying in size from minor occurrences to relatively large deposits. Mineral deposits in the Aldan Shield are located in the granulite–gneiss terrain of the West Aldan block, and belong to magnesian skarn, rock crystal, phosphorus–rare earth and to a lesser extent iron formations; greenstone belts in the Olyokma block have mainly the iron–silica formation.

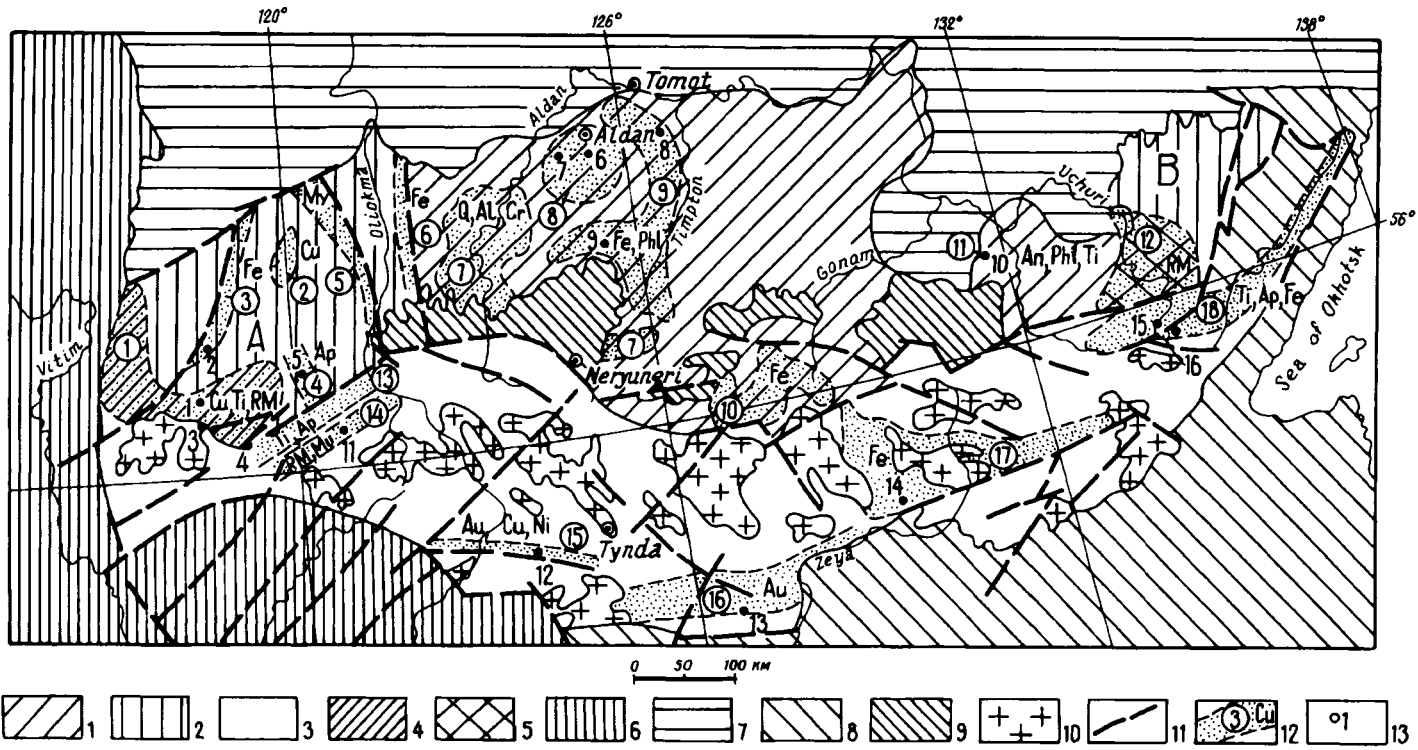


Fig. 79. Metallogenic sketch-map of the Aldan Shield (from Rundqvist and Mitrofanov, 1993 and material from L.I. Krasny, N.S. Malich et al.) 1-5 tectonic structures: 1 - Aldan granulite-gneiss terrain; 2 - granite-greenstone terrains: A - Olyokma, B - Batomga; 3 - Dzhugdzhur-Stanovoy terrain; 4 - Udokan intracratonic basin; 5 - Ulkan volcanoplutonic belt; 6 - Baikal-Patom fold belt; 7 - cover sediments; 8 - Mongolia-Okhotsk Phanerozoic fold belt; 9 - Mesozoic-Cenozoic basins; 10 - Mesozoic granitoids; 11 - faults; 12 - metallogenic zones (numbers in circles): 1 - Udokan (Cu, Ti, RM), 2 - Uguy (Cu), 3 - Chara-Tokk (Fe), 4 - Khanin (Ap), 5 - Temulyakit (Mu), 6 - Nelyuk (Fe), 7 - Upper Aldan-Timpton (Q, Al, Gr), 8 - Seligdar (Ap), 9 - Timpton (Fe, Phl), 10 - Sutam (Fe), 11 - Arbarastakh (Ap, Phl, Ti), 12 - Ulkan (RM), 13 - Kalara (Ti, Ap) 14 - Imangr (RM, Mu), 15 - Dzheltulak (Au, Cu, Ni), 16 - South Stanovoy (Au), 17 - Bomnak (Fe), 18 - Dzhugdzhur (Ti, Ap, Fe); 13 - mineral deposits (black dots) 1 - Udokan, 2 - Chara, 3 - Chiney, 4 - Katuga, 5 - Ukdus, 6 - Seligdar, 7 - Inaglin, 8 - Emeldzhak, 9 - Tayozhnoye, 10 - Arbarastakh, 11 - Okhok, 12 - Lukinda, 13 - Zolotaya Gora ("Golden Hill"), 14 - Sivakan, 15 - Gayum, 16 - Maymakan.

## The Aldan terrain

D.A. MIKHAILOV

The Aldan crystalline massif, which forms the granulite–gneiss terrain under discussion, is divided on geological and geophysical grounds into the West Aldan and East Aldan blocks, with the linear Idzhek–Sutam shear zone lying between them. In the west, the Aldan granulite–gneiss terrain borders on the Olyokma granite–greenstone terrain along a collision zone up to 70 km wide within which several N–S zones have been delineated with higher gravity gradients, basic intrusions and magnetic anomalies. Based on structural and petrological analyses, the complexly folded, polymetamorphic early Precambrian rocks of the Aldan terrain are divided into an unstratified infracrustal complex and a supracrustal complex of stratified formations, metamorphosed under granulite facies conditions and known as the Aldan megacomplex. It consists of the Iyengr and Kurultin Groups in the western block; the Timpton and Dzheltulin Groups in the eastern block. The most typical mineral deposits in the Aldan granulite–gneiss terrain are phlogopite and magnetite in the magnesian skarn formation, several of which include apatite, boron, sulphide and rare-earth mineralization, and from the multi-element composition of the ores these deposits are unique, although from a number of geological features they are comparable with targets of these ore types in other regions.

Magnesian skarn deposits occur in the central Aldan Shield in the region between the upper reaches of the Aldan river and its tributary the Timpton, forming a huge arcuate zone (Fig. 80). Its configuration is defined by the outcrop pattern of the crystalline rocks that surround a dome-shaped structure. These rocks are referred to as the “Fyodorov Group” and contain dolomitic marbles, one of the main factors in the formation of magnesian skarn rocks. The role of marbles as a lithological factor is also clearly expressed in other regions – Lake Baikal, SW Pamirs, the Canadian Shield, Madagascar – where there are mineral deposits associated with magnesian skarns. Moreover, in the Aldan region the magnesian skarns have regional metallogenic features. Skarn bodies with magnetite and apatite occurrences are also developed beyond the edges of marble members, associated with mafic schists and amphibolites. The Aldan region is not only one of the world’s largest phlogopite provinces but is almost the only example of major iron ore deposits in Precambrian magnesian skarn bodies. Magnetite ores have also been discovered in magnesian skarns in the west of the Ukrainian Shield. The absence of lazurite deposits, which are usual components of magnesian skarns in other regions, in our opinion is due to the relatively small thickness of dolomitic marbles and the weak development of dislo-

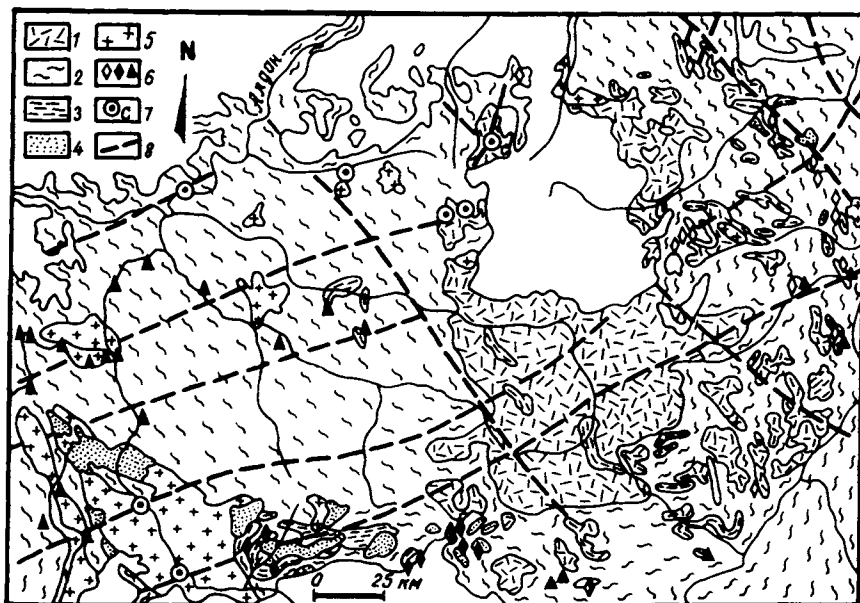


Fig. 80. Structural-metallogenic sketch map of the central part of the Aldan massif. Compiled by D.A. Mikhailov, using material by V.L. Dook and V.I. Kitsul. 1 – high-grade AR-PR<sub>1</sub> basement; 2 – PR<sub>1</sub> folding, metamorphism & partial melting; 3 – mafic schist & dolomite marble bands; 4 – PR<sub>1</sub> gabbro-anorthosite suite, partially metamorphosed; 5 – PR<sub>1</sub> granite; 6 – magnesian skarns (a – phlogopite deposits, b – magnetite deposits, c – minor magnetite occurrences); 7 – apatite deposits; 8 – regional faults.

cations in them, along which minor granite injections could penetrate, which would also have been the substrate for the growth of zones of recrystallization and skarns, with the formation of lazurite-bearing metasomatites. In addition to phlogopite and magnetite, magnesian skarns in some places contain boron, apatite, rare-earth and sulphide mineralization.

A necessary prerequisite for phlogopite deposits is the formation of thick skarn bodies in which metasomatic contraction was extensively developed, leading to the recrystallization of skarns and the formation of thick zones of coarse and megacrystalline monomineralic phlogopite masses. The intensity of skarn formation depends, in addition to the presence of dolomitic marbles, on the deformation style and the development of associated retrogression, partial melting and magmatism. Phlogopite deposits are situated in granulite-gneiss terrains with locally-expressed later isoclinal folding, amphibolite facies retrograde metamorphism, and repeated partial melting. Intense deformation in these areas and the formation of fault zones aided the wide development of skarns around dolomitic marbles, which are almost completely recrystallized into calciphyres in areas with major phlogopite deposits, i.e. they are metasomatic calcite marbles with diopside, amphibole and phlogopite. On a regional scale, phlogopite deposits also occur along major faults in addition to being associated with zones of repeated isoclinal folding. This is much clearer in other regions, particularly around Lake Baikal.

The commercial value of the Aldan phlogopite deposits is also determined by the iron content of the phlogopite which is higher here than in the Baikal region and the SW Pamirs and which depends not on the composition of aluminosilicate rocks, which are directly replaced by skarns, but is determined by the total iron content of the crystalline rocks in which skarn formation took place. The appearance of tholeiitic and alkali-basaltic magmatism in the Aldan Shield led to the widespread development of mafic schists, during the metamorphism of which iron was mobilized and redistributed into the skarns, with the formation of magnetite ores.

Magnetite mineralization in skarns is evident throughout almost the entire central Aldan area. Major magnetite deposits are distinct from phlogopite deposits and are localized in a particular zone, named the Ungra–Dyos–Melemken synclinorium, a tectonically and magmatically active zone (Fig. 80). It contains gabbro intrusions, which also served as a source of the iron that was redeposited in skarn bodies during the metamorphism of these rocks. The regional extent of the amphibolite facies metamorphism in this zone also determined the widespread mobilization of iron from the rocks undergoing metamorphism. The observed increase in the structural and metamorphic reworking of the gabbros from west to east within the Ungra–Timpton synclinorial zone coincides with the increase in size of the iron ore deposits which make up the Dyos, Sivaglin and Leglier group. The linear nature of Proterozoic folding, the association of a gabbro–anorthosite formation with wide fold zones, and the development of extensive blastomylonite zones predetermined the emplacement of deep faults, which were instrumental in the formation of other metamorphic ore types – rock crystal and phosphorus–rare earth.

*Apatite–hematite–rare earth* metasomatites formed in fault zones which intersect dolomitic marbles, mafic schists and magnesian skarn rocks. The Seligdar apatite deposit in the central Aldan Shield is a representative of this type. The metallogenic significance of long-lived deep fault zones also shows up in the localization of ferruginous quartzites belonging to the Charo–Tokk group in the Olyokma block. These zones, which are 1–3 km wide and strike N–S and NE for up to 80–100 km, were previously described as trough complexes consisting of metasedimentary and metavolcanic rocks. Detailed study of these zones has shown that they have a tectonic origin and are blastomylonites after various rock types – schists, gneisses, enderbites, and gabbroids. Ferruginous quartzite bodies occur within the zones, and they metasomatically replace sheared and metamorphosed gabbroic rocks, with the formation around them of skarn-like garnet–amphibole and aluminous rocks. Studies by Devi et al. (1983), Krivenko (1981, 1983) Kulakovskiy et al. (1987) and Mironyuk et al. (1976) have demonstrated the association between ferruginous quartzite deposits of the Imalyk and Charo groups and a large, extensive zone of deep faults. The ferruginous quartzites lying within blastomylonitized rocks do not themselves bear any signs of mylonitization.

In concluding this brief outline of the Precambrian metallogenic features of the Aldan terrain, the following must be emphasised. The origin of ore deposits belonging to magnesian skarn, iron–silica, rock crystal and apatite–rare earth formations is linked to the development of hydrothermal–metasomatic processes. In addition to these types, copper and other metal deposits are known in the west of the shield, associated with other Precambrian complexes – layered gabbro–norite intrusions and

Proterozoic carbonate–clastic sediments. This complexly folded region evolved over a long period with repeated episodes of granulite and amphibolite facies regional metamorphism (the oldest zircon dates being 3.4 Ga, and the youngest 2.0 Ga), magmatism and faulting, resulting in the formation of granulite–gneiss and granite–greenstone terrains. Against this background, the ore-bearing formations described above originated in the interval 1900–1700 Ma ago. This metallogenic pulse corresponds to the time of cratonization, i.e. the transition from mobile fold belt conditions to a platform regime, such that the change in deformation style from folding to blastomylonite and cataclastic fault zone formation predetermined the emplacement of plutonic magmas, enriched in ore elements, and the infiltration nature of metasomatism with the formation of huge masses of metasomatic rocks.

## 1. Ore deposits and formations

### 1.1. Iron

Iron ore deposits in this region are represented by two main formations – magnesian skarns and ferruginous quartzites.

*Magnetite ore mineralization in skarns* has been observed almost throughout the central Aldan area, although major deposits are separate from phlogopite deposits and are localized in a particular zone, the Ungra–Dyos–Melemken synclinorium, a zone of tectonomagmatic activity. Iron ore deposits in Central Aldan form the Dyos, Sivaglin and Leglier groups, with over a dozen deposits containing known reserves of 1.5 million tonnes and forecast reserves of over 10 billion tonnes.

*The Tayozhnoye deposit* is one of the largest and best studied iron ore deposits in the magnesian skarn formation of the Aldan Shield (Pukhorev, 1959). It is situated in the upper reaches of the river Leglier and is associated with the western termination of the Leglier syncline which stretches eastwards and contains a number of small deposits. This sigmoidal fold has steep axes and its constituent metamorphic rocks crop out as lens-shaped beds (Fig. 81). The crystalline assemblage around the Tayozhnoye deposit is subdivided into three, with barren units above and below the productive horizon. The lowest unit consists of pyroxene–amphibole and biotite–amphibole schists and gneisses with hypersthene- and garnet-bearing varieties. The productive Leglier horizon consists of diopside–plagioclase and amphibole–plagioclase schists with marble bands. The unit above the productive horizon is represented by quartzite and cordierite–sillimanite gneiss with thin bands of biotite, tourmaline and graphite varieties. In the Tayozhnoye deposit area, surface outcrops of rocks belonging to this horizon are found in the fold hinge zone and form a series of lenses with complex shapes within granite–gneisses. Individual lenses are up to 400 m thick. All the horizons contain abundant migmatites, granitized rocks and granitoids of various ages and compositions. Granite bodies are relatively small and roughly concordant with host metamorphic rocks. Later granites occur as cross-cutting veins.

The hinge zone of the sigmoidal fold is complicated by minor folding with numerous flexures and fracture zones. Marble lenses often occur in the flexures and their distri-

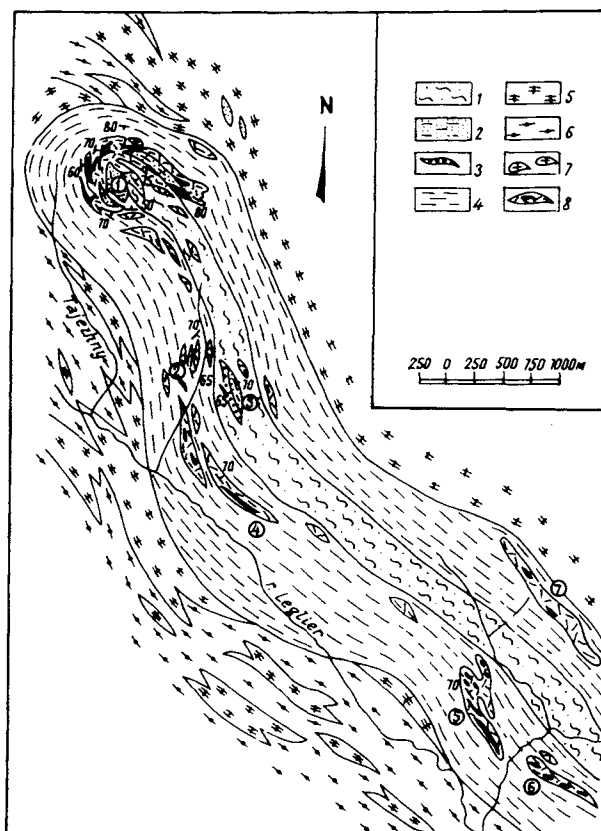


Fig. 81. Geological map of region around the Leglier group of iron ore deposits. Compiled by D.A. Mikhailov (with material from the Yakutsk Geological Survey). 1 - granitized bi gneiss; 2 - silli-cord & tourm gneiss & quartzite; 3 - hema quartzite; 4 - bi-amphibolite gneiss; 5 - hyp gneiss & schist; 6 - granitized hyp gneiss; 7 - granite; 8 - mag skarn. Mineral deposits (numbers in circles): 1 - Tayozhnoye, 2 - Magnetitovoye, 3 - Leglier, 4 - Tinskoye, 5 - Zarechnoye, 6 - Utomitelnoye, 7 - Bolotnoye.

tribution usually determines the location of skarn bodies. The lenticular shape of individual rock members with clearly expressed banding and boudinage is further emphasised by the morphology of the ore bodies and their internal structure. Skarns not only have metasomatic zoning, but also an inherited banding. The main mass of magnetite ores is concentrated along the outlines of skarn bodies and in marble and calciphyre areas associated with these bodies. Over 20 ore bodies have been discovered, varying in size and being up to 1 km long and several tens of m wide.

Although ore-bearing skarn bodies are also concordant with the metamorphic rocks, their undulose contacts and numerous vein apophyses cut the crystalline schistosity. The largest magnetite skarn bodies have a distinct but irregular shape and are massive, branching, partially concordant, and sometimes also sharply cross-cutting veins with numerous relicts of metamorphic and intrusive igneous rocks. The mineral

content of the magnetite ores varies depending on which rocks were replaced by skarns. In the Tayozhnoye deposit the main ore mass is represented by magnetite–forsterite (serpentine) varieties, which are metasomatically altered marbles – ore impregnated calciphyres. Also present with these are clinohumite–magnetite and phlogopite–forsterite–magnetite ores. The remaining types are diopside–magnetite (frequently with scapolite), amphibole–magnetite and phlogopite–magnetite varieties. In all the mineralogical types of ore, magnetite is found to have crystallized later than aluminosilicates and carbonates.

There is usually a gradual transition from poor disseminated ores to almost monomineralic sectors. Structural and texture features of the ores are mainly determined by host-rock characteristics. Banded ores develop in metamorphic rocks, and massive types in granites. In some of the Aldan iron ore deposits, such as Pionerka and Komsomolskoye, the main magnetite ore mass is represented by sheet-like bodies, consisting of banded diopside–scapolite varieties, almost without vein offshoots. The combination of magnetite-bearing sheet-like skarn bodies and branching veins has led some workers to view this as evidence for a “pre-metamorphic” concentration of the main magnetite ore mass in these deposits, and that it was partially redeposited during later skarn-forming processes. The following facts must be taken into account when determining the genesis of magnetite ore mineralization developed in the Tayozhnoye and other Aldan deposits.

(1) Magnetite mineralization is developed only in infiltration magnesian skarn bodies, forming either minor occurrences or large ore deposits. It is regionally distributed throughout the entire Central Aldan area, although the largest deposits are situated in the Ungra–Trompton synclinorium. Magnetite ore mineralization is absent from magnesian skarns formed in the early stages of endogenic cycles (metamorphic diopside rocks and contact-reaction skarns).

(2) The geographical association between the largest magnetite ore deposits and metabasites in the Ungra synclinorium does not suggest that “volcanogenic–sedimentary” concentrations of iron were genetically related to them, and converted into skarn-like ore bodies during metamorphism. Basic rocks themselves often contain no major concentrations of magnetite, but dispersed magnetite disseminations in them could have been the source of the iron that is concentrated in skarn bodies.

(3) Magnetite ore mineralization in skarns, like the skarn-forming process itself, has a strict geological and geochronological association with a particular stage in the geological evolution of this region. In each deposit it has been established that magnetite-bearing skarns replace granitized gneisses, migmatites and granites that formed during amphibolite facies retrogressive metamorphism, and that skarn formation was controlled by folding and faulting in the concluding stage of crustal activity.

(4) In all of the ore mineralogical varieties, magnetite replaces diopside, scapolite, amphibole, phlogopite and calcite skarns and is thus localized in any skarn zone, superimposed on metasomatic zoning and reflecting the banding inherited from substrate rocks which is also taken to be a “primary ore banding”.

(5) From its geochemical features, i.e. the exceptional paucity of impurity elements, the magnetite in magnesian skarns corresponds to magnetite of a hydrothermal origin.

Magnesian skarn bodies thus acted as structural (increased porosity) and geochemical (basic composition) traps for magnetite mineralization which formed in the final acid stage of the skarn-forming process. Besides magnetite ores, the magnesian skarns of the Tayozhnoye deposit contain other types of ore mineralization. It is essential to note that during preliminary exploration the Tayozhnoye deposit was known for its phlogopite. Skarns replacing granites contain large phlogopite crystals. Moreover, the Tayozhnoye skarns contain borates, including ludwigite ( $Mg_2FeBO_5$ ) and serendibite ( $Ca_2(Mg, Al)_6O_2[(Si, Al, B)_6O_{18}]$ ). Further details of the boron mineralization can be found in Pertsev and Kulakovskiy (1988). Tourmaline-bearing quartzites could have been the source of the boron, since these are common in the deposit. Also widespread in the skarns is vein-type disseminated sulphide mineralization, mainly represented by pyrrhotite, and molybdenite occurs frequently. In addition, platinoids have been found in the deposit (Kulakovskiy, 1985), the source of which appears to be a basic-ultrabasic rock complex.

The irregular nature of subsidiary ore mineralization in skarns, and its association with particular portions of skarns, replacing certain rock types, suggests that metamorphic and intrusive igneous rocks were the source of a number of ore elements. Magnesian skarn deposits in the Aldan Shield contain skarns enriched in apatite and in rare earth-bearing minerals – sphene, zircon and orthite (Fig. 82). This type of ore

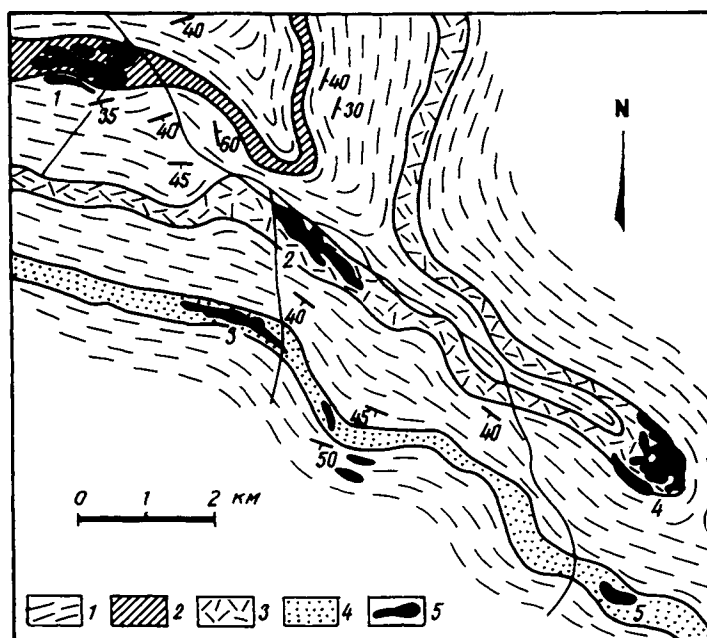


Fig. 82. Phlogopite deposits in the Emeldzhak group, Central Aldan. 1 – schist & gneiss; 2–4 – stratigraphic horizons (2 – Leglier, 3 – Keribikan, 4 – Khatymin); 5 – phlogopite deposits in magnesian skarn bodies (numbers in circles): 1 – Emeldzhak, 2 – No. 2 sector, 3 – No. 7 sector, 4 – Upper Emeldzhak, 5 – Tabornoye.

mineralization is interesting, since thorianite deposits are known in Madagascar, containing 7–25% uranium, hosted in phlogopite-bearing skarn bodies.

*Ferruginous quartzite deposits* are found in many parts of the Aldan province. The Olympic, Yaginda, Goluboye, Yuktin, Khuduchin, Subtugur and other deposits are known in the Sutam, Kholodnikan and Larbin regions in the southern part of the West Aldan block. They are represented by a series of sheet-like bodies of magnetite–hypersthene quartzites varying in length and thickness and lying within complexly deformed high-grade metamorphic Archaean assemblages. Magnetite ore mineralization is also present in schists and gneisses hosting the ferruginous quartzites. Peculiar pyroxene–amphibole–garnet–magnetite schists form envelopes around ferruginous quartzite sheet-like bodies. The quartzites in each region occur in definite stratigraphic formations (Kudryavtsev et al., 1985) – Dzhelindin (Kholodnikan region), Seym (Sutam region) and Khorochin (Larbin region), which underwent metamorphism at granulite and amphibolite facies conditions.

A typical feature of these formations is the common occurrence of mafic schists with thin gneiss and granite–gneiss bands. Ferruginous quartzites are mainly represented by magnetite varieties, with hematite occurring only sporadically – in the Yaginda deposit for example it amounts to around 40%. Textures in the ferruginous quartzites are usually coarsely banded with irregular grain size. Banded rocks usually contain rich ore segregations in the form of clusters and cross-cutting zones. The transition to banded varieties is gradual. The magnetite content in rich ores reaches 80–90%, while in banded types it varies within the 25–35% range. Apatite is a common accessory mineral in ferruginous quartzites, and sulphides are rare. The magnetite content in banded ores is 25.8–36.9%, and in rich ores 59.2–61.0%; sulphur = 0.08–0.13%;  $P_2O_5$  = 0.25%. These ores are easily enriched.

## 1.2. Phlogopite

Phlogopite deposits occur in the middle of the West Aldan block in granulite–gneiss areas locally affected by superimposed isoclinal folding, amphibolite facies retrograde metamorphism and repeated partial melting (Mikhailov, 1973). The intensity of deformation in these areas and the development of fault zones aided extensive skarn formation around dolomite marble members. Deposits occur in the Emeldzhak, Fyodorov, Kuranakh, Elkon, Nyeakuin, Oyumrak and Uchur groups with dozens of deposits in each, varying widely in size. The main distinguishing feature in the morphology of phlogopite bodies in this province is the occurrence of megacrystic monomineralic phlogopite masses as vein segregations within sheet-like diopside–scapolite, –amphibole, –spinel and –phlogopite skarns.

*The Emeldzhak deposit* is one of the best-studied in the Aldan terrain and reflects the main features of the phlogopite deposits in this province. It is situated in the NE of the province, 80 km E of Aldan town. The deposit lies on the SW limb of an anticline containing a number of “productive” horizons in which skarn bodies are hosted (Fig. 82). The productivity of horizons is determined by the presence of dolomitic marble lenses, surrounded by aluminosilicate rocks and magnesian skarn bodies. In the phlogopite deposits there is usually an inverse relationship between the size of dolomite

marble members and skarn bodies. Marbles are not common in the Emeldzhak deposit and occur only as small calciphyre bodies, i.e. metasomatically reworked rocks, which can be accounted for by the recrystallization of marbles with the removal of significant quantities of magnesium and calcium to aluminosilicate rocks during skarn formation. Dolomitic marbles are usually surrounded by calciphyre zones in small deposits.

Metamorphic rocks hosting skarn bodies in the Emeldzhak deposit are represented by granitized two-pyroxene schists and gneisses with thin bands of almost monomineralic diopside and wollastonite rocks and quartzites (Fig. 83). The Emeldzhak anticline is affected by widespread minor folding which produces "packets" of rocks oriented obliquely to the main strike. Minor folds as a rule lie in an *en échelon* fashion relative to one another, in a direction parallel to axial surfaces. Rocks in areas where such displacements have occurred are mostly represented by strongly granitized finely-banded gneisses with boudinage structures and narrow blastomylonite zones. Deformation is most intense on fold limbs. Since they have steeper dip angles, they cut the schistosity of the rocks. Skarn bodies occur in fault and blastomylonite zones and as a result are stretched out along strike but have steeper dip angles. Granitoids are widespread among the metamorphic rocks. Early granite bodies took part in folding and are cut by fault zones. Late-folding and post-folding granites and pegmatites form irregular cross-cutting bodies or dykes.

From their geological setting, morphology and internal structure, skarn bodies reflect the structures and geometry of the rocks which they replace. The main mass of metasomatic bodies, consisting of diopside, diopside–scapolite, –spinel, –amphibole and –phlogopite varieties, is stretched out along the strike of the metamorphic assemblages. Metasomatites replace various schists, gneisses, migmatites and granites and only post-folding granite–pegmatite veins cut the phlogopite skarns. The largest skarn bodies are situated in areas with the most intense folding, and are localized in fault zones or along banding-parallel and oblique fractures. The skarns, which merge into one other, form a single field with numerous relicts of substrate rocks. The skarns have a complex

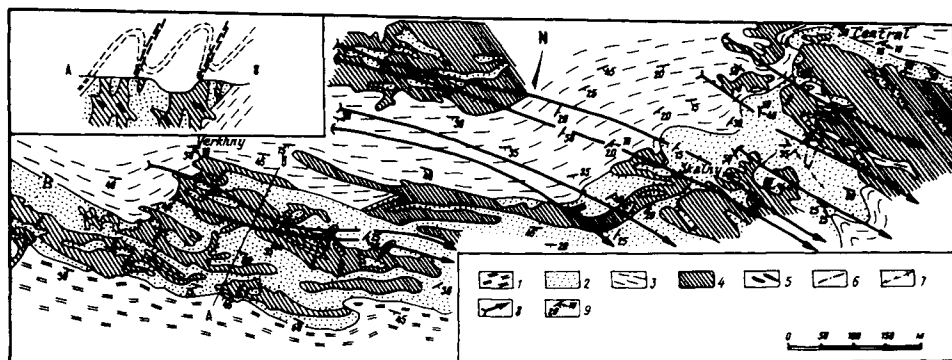


Fig. 83. Geological map of the Emeldzhak phlogopite deposit. Compiled by D.A. Mikhailov. 1 - bi-amph–di schist & gneiss; 2 - di schist with marble, woll & di bands, & qzt; 3 - hyp–amph schist & gneiss; 4 - skarn; 5 - orientation of largest phlog bodies; 6 - orientation of cross-cutting skarn zones; 7 - pegmatite; 8 - orientation of fold axes; 9 - schistosity & lineation.

internal structure. On the one hand they reflect banding, folding and boudinage inherited from the host rocks and on the other hand metasomatic zoning, expressed as a change in bimineralic zones in sections through the bodies, and a tendency for metasomatites in each zone to be monomineralic. This latter effect is expressed in numerous clusters and veinlets consisting of coarsely crystalline scapolite, amphibole and phlogopite aggregates. Monomineralic phlogopite clusters are represented by two morphological types – banded zones (so-called “micaceous”), consisting of aggregates of phlogopite crystals 0.3–0.5–1.0 cm across and which preserve relict banding, and coarsely-crystalline to megacrystic pockets and veins. The number and dimensions of veins and pockets determines the economic value of a deposit. As well as pockets and veinlets, monomineralic phlogopite clusters form sharply cross-cutting zones up to 1 m and more wide, the largest of which extend beyond the margins of sheet-like skarn bodies as symmetrically zoned veins (Fig. 84).

Cross-cutting phlogopite veins in the Emeldzhak deposit strike NE and dip at 50–70° to the NW. Oblique and banding-parallel phlogopite zones inside sheet-like skarn bodies often intersect each other and the largest pockets of gigantic phlogopite crystals are usually found at intersection points. Such pockets vary in size and can be up to 8–10 m across, with phlogopite sheets reaching 1–1.5 m. The number of monomineralic phlogopite zones and their dimensions usually decrease adjacent to where sheet-like skarn bodies wedge out along strike. The thicker the skarns the greater the number of pockets, cross-cutting phlogopite zones and vein apophyses they

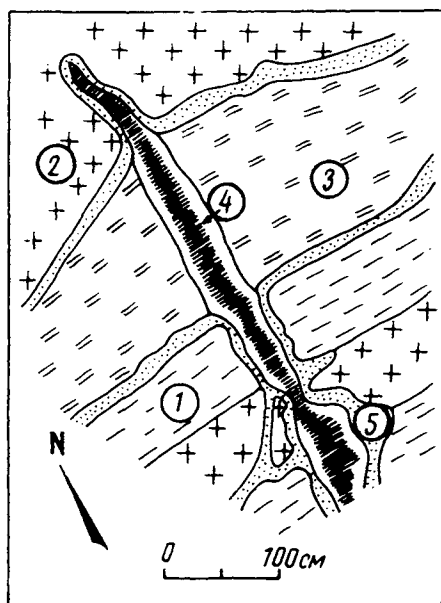


Fig. 84. Vein segregations of megacryst phlogopite masses (black) in sheet-like zoned magnesian skarn bodies replacing gneiss and granite. Emeldzhak deposit. 1 – bi-amph granitized gneiss; 2 – granite; 3 – di-amph, –spinel, –phlog skarns with relict banding; 4 – coarse-grained phlogopite; 5 – di-scaph zone.

contain. It is worth emphasizing that the scale of economic phlogopite content is mainly determined by the thickness of skarn sheets and not their along-strike length.

The economic phlogopite content of skarns depends on the size of mica zones, which in turn depends on the variation in composition of the rocks replaced by skarns. The phlogopite content in skarns depends on the amount of silica, alumina and alkalis in substrate rocks. Therefore skarn bodies with high phlogopite contents as a rule occur in granitic rocks, which also acted as a source for these components. The cross-cutting nature of monomineralic megacrystic phlogopite zones indicates that they formed in the concluding stages of skarn development. Their appearance was determined by the main feature of metasomatic process – the trend from bimineralic to monomineralic zones. As a result of increased porosity in the final stages of formation of each zone, smaller crystals were dissolved and larger crystals grew, so that monomineralic patches of scapolite, amphibole or phlogopite grew in each zone. During the intense development of the metasomatic process, increasing porosity in the growing skarn bodies led to their spontaneous fracturing and recrystallization, with the formation of larger aggregates. Since the diopside–phlogopite zone in magnesian skarns is a closed metasomatic system, and its appearance reflects the culmination of skarn formation, metasomatic contraction occurred to a greater extent in this zone, which also produced major monomineralic phlogopite deposits.

The orientation of monomineralic phlogopite masses in axial zones of sheet-like bodies is defined by their geometry, and in cross-cutting zones by fracture tectonics of metamorphic assemblages. Metasomatic contraction was the main ore-generating factor and the extent to which it is developed depends on the thickness of the skarn bodies. The formation of very large skarn bodies, i.e. the intensity of Mg–Ca metasomatism around dolomite marble members, was determined by zones of repeated deformation, along which infiltration of solutions took place. As a result, the Emeldzhak phlogopite deposit and a number of other smaller mineral deposits in this region are hosted in a linear deep fault zone which formed after the skarns. Intense deformation in the Emeldzhak deposit is expressed as mylonite zones which cut skarn bodies and displace the fragments relative to one another. Mylonite zones, up to 10–15 m wide, formed under low-temperature amphibolite facies conditions. Granite pegmatites were emplaced along mylonite zones, and this event concluded the Proterozoic cycle of internal processes. Thus, phlogopite-bearing magnesian skarn bodies are superimposed on fold structures in metamorphic rocks on the one hand, inheriting the textures of the host rocks, and on the other hand they are restricted to linear fault zones on a regional plan. This suggests that skarn formation took place during a retrogressive regional stage of amphibolite facies metamorphism, while the morphology of skarn bodies and their geological setting reflect a change in the style of deformation from folding to faulting. The formation of monomineralic zones of large phlogopite sheets is related to the concluding stage of skarn formation, therefore on a structural scale the morphology of phlogopite deposits (linear zones) reflects intense shearing. Statistical measurements on phlogopite-bearing zones demonstrate a coincidence between their orientation and the geometry of granite pegmatite dykes localized in blastomylonite zones. Zircon, sphene, orthite and apatite containing rare-earth elements are common in the Emeldzhak deposit (Mikhailov, 1973). In addition,

molybdenite is often found. It should be noted that the skarns in this deposit are completely lacking in magnetite, which is widespread in other phlogopite deposits in this region.

### 1.3. Apatite

Apatite deposits are represented by a metasomatic rare earth–phosphorus formation that occurs in Central Aldan. A new apatite ore type is associated with this formation (Bulakh, 1982, 1983), discovered in the Precambrian of the West Aldan block and forming the Seligdar, Oseny List, Niryandzha and Nimgerkan deposits. They occupy a narrow strip extending NE from the river Seligdar, coinciding with the Udokan–Tipton fault in places where it is intersected by NW-striking faults.

*The Seligdar apatite deposit* is the largest and best known. It is situated in the NW part of Central Aldan, 40 km west of Aldan town and contains apatite–dolomite ores. The ore field has an isometric shape in plan view and occurs in a fold structure in Precambrian metamorphic rocks. Regionally, the deposit is located in the intersection zone between NW- and NE-striking faults (Fig. 80). Detailed prospecting began in 1972, the year the deposit was discovered, and the Precambrian crystalline rocks are known to have been complexly folded with the apatite–carbonate ores completely “overprinting” this structure (Fig. 85). The apatite–dolomite ores are low grade and difficult to enrich; they contain 4–6%  $P_2O_5$ . The occurrence in Precambrian metamorphic rocks of apatite–carbonate mineralization, accompanied by the growth of quartz, hematite, chlorite, calcite, gypsum and anhydrite is associated with late-stage, low-temperature processes, reflecting hydrothermal activity under conditions of intense dislocation at the end of an endogenic cycle. Faulting is expressed in the development of brecciated and mylonitized rocks. Thus, the geological setting of the apatite–dolomite ores is defined on the one hand by linear conformity with fold structures in the early Precambrian host rocks, which is reflected in banding in the ores inherited from the host rocks, and on the other hand by the association with fault and shear zones. This indicates a hydrothermal–metasomatic origin for the ores, which formed in regional fault zones at a stage when fold structures were finally being stabilised. The age of mineralization has been estimated at 1500–1400 Ma.

According to several workers (Entin et al., 1984, 1987), apatite–carbonate metasomatic rocks have a paragenetic relationship with basic to ultrabasic alkaline igneous intrusions and on this basis they may be referred to carbonatites. Further evidence for this is the presence in apatite ores of titanoniobates, a higher chlorine content and a heavier carbon isotope composition compared with calciphyres in the host crystalline rocks (Entin et al., 1989). These data could of course also indicate that alkaline basalts were the source of the phosphorus and rare earths. However, Seligdar-type ore mineralization is a consequence not of a metasomatic stage in the magmatic process, but instead results from metasomatic reworking effects being superimposed on metamorphic and igneous rocks in fault zones.

Marbles and calciphyres in the Precambrian metamorphic assemblage acted as a suitable substrate for the formation of the apatite–carbonate ores, and they are also considered to be the source of the ore-generating elements (Bulakh, 1983). A study of

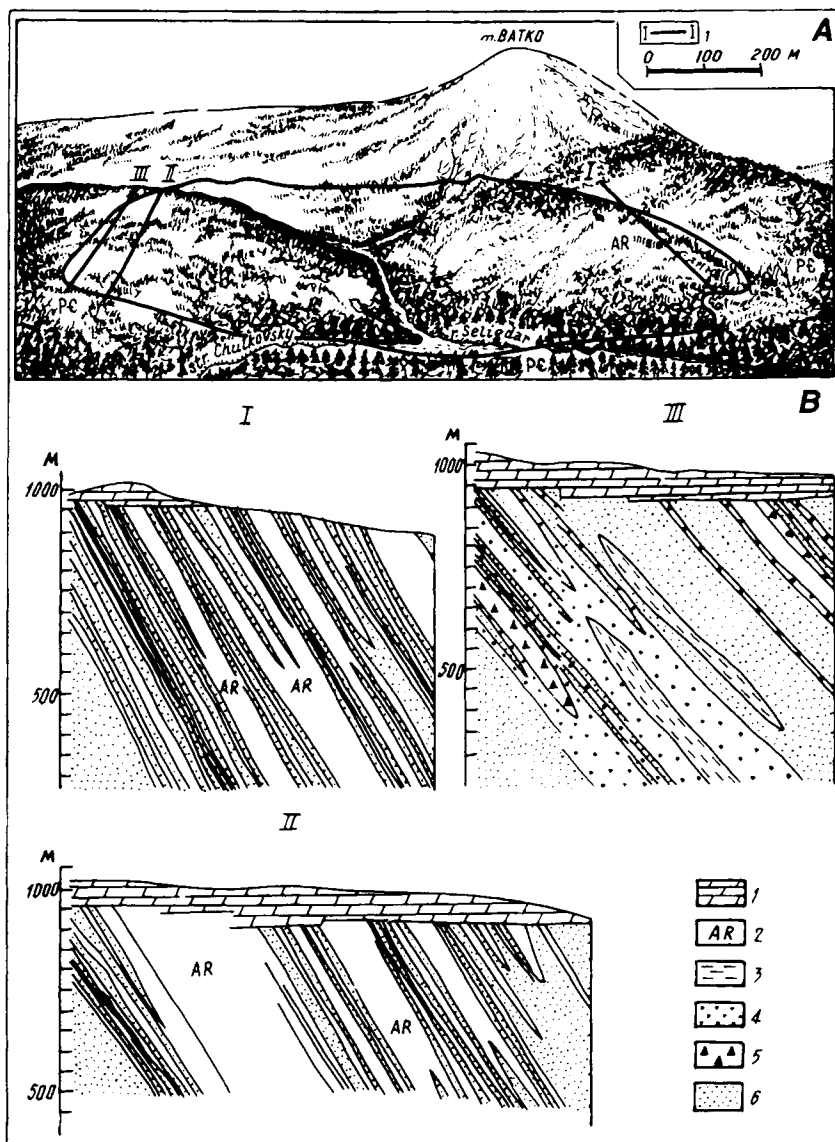


Fig. 85 A.B.

the mineral composition of the rocks in the deposit has shown that besides the apatite-dolomite ores, apatite-forsterite-carbonate ores with minor phlogopite, spinel, magnetite and sulphides, and apatite-pyroxene-calcite ores, being an intermediate stage in the reworking of substrate rocks, are also common and represent the final stage of the metasomatic process. It is worth noting that marbles and calciphyres do not appear to be the main source of phosphorus in the apatite ores that make up the Seligdar deposit. Apatite-pyroxene-calcite ores are closer to metasomatic types found in magnesian

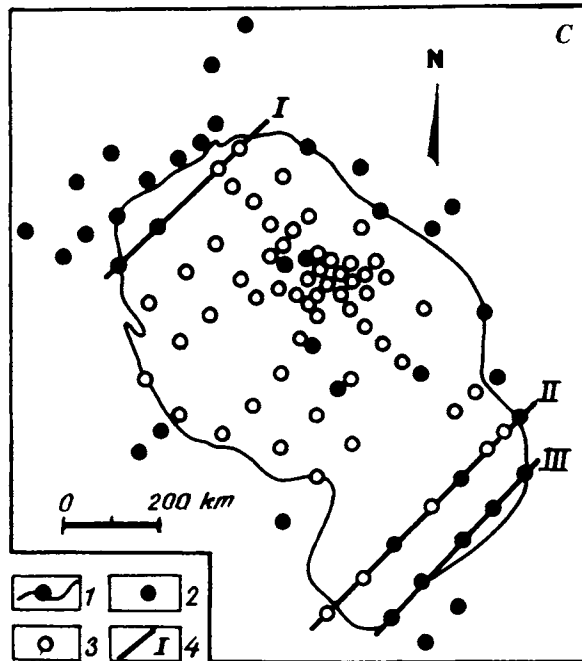


Fig. 85. Panorama, geological sections and plan view of Seligdar apatite deposit (A.G. Bulakh and A.A. Zolotarev, 1983). *A* – panorama of deposit with outlines of ore deposit and section lines I, II, III. *B* – geological sections I, II, III. 1 – dolomite & syenite porphyry lava flows; 2–6 – Archaean basement: 2 – migmatite & gneiss, 3 – ap-carb ore, 4 – ap-dol ore, 5 – ap-forst ore, 6 – schist & gneiss. *C* – plan of ore deposit with exploration drillholes. 1 – outline of deposit, 2 – schist & gneiss, 3 – ap ores, 4 – section lines.

skarns. It has already been pointed out that in several of the Aldan phlogopite deposits (e.g. Kolytkon, Kanku, etc.), apatite is widespread in diopside-phlogopite bodies. The common occurrence of marble and calciphyre in the area around the Seligdar deposit indicates that magnesian skarns, which are also rich in apatite, might be widely developed here.

The distribution of apatite-carbonate ores with sulphates (anhydrite, gypsum, celestine) is evidence for low-temperature processes at the close of hydrothermal activity in fault zones. This is a poorer ore type than apatite-pyroxene-carbonate, apatite-forsterite-carbonate and apatite-dolomite-carbonate types, from which it follows that the culmination and formation of Seligdar-type apatite ores belongs to the apatite-dolomite stage. Forsterite-apatite and pyroxene-apatite ores are either a more suitable substrate for conversion into apatite-dolomite ores, or else they may constitute a separate, independent type of apatite ore which originated at an earlier stage during the formation of rocks in the magnesian skarn type. The sulphate stage apparently led not to the formation of a new ore type, but to the impoverishment of the main type – apatite-dolomite ores, which must be considered to be the major genetic type in this deposit.

#### 1.4. Rock crystal in quartz veins

The Aldan rock crystal formation is represented by vein-type deposits and occurrences in quartzites belonging to the Upper Aldan Formation in the Precambrian Iyengr Group. There are two known areas where veins are located – the upper reaches of the Aldan river where the Greater and Lesser Nemnyrov rivers flow in, and the upper reaches of the Timpton river. The Upper Aldan quartz crystal region is the better known and consists of the Son-Tiit (Kholodnoye, Severnoye, Pustynnoye and other deposits) and the Nimger (Khrustalnoye, Goreloye, Morion and other deposits) groups.

Lithological, structural and tectonic factors have strongly influenced the location of quartz crystal veins. Morphologically, the crystal-rich cavities are represented by simple veins, complex linear vein zones, stockworks, and sometimes pipe-like segregations (Oganesyan, 1983). The occurrence of quartz veins in complexly-folded migmatite gneiss dome structures suggests (Berger, 1962) that they are related to fracture tectonics in various fold zones: gentle flexures, broad open folds and tightly appressed isoclinal folds. Other workers (Mukhin, 1962; Oganesyan, 1983) relate rock crystal formation to fractures which are not directly associated with folding or local faulting. According to them, fracture zones in which rock crystal deposits formed are related to Proterozoic reactivation of high-grade metamorphosed and intensely deformed Archaean rocks. These zones result from the formation of deep faults.

Areas where quartz crystal veins are concentrated have characteristically varied structures, ranging from quartzite members either on anticlinal limbs, or forming basin-and-dome shaped blocks, or in individual quartzite fragments associated with narrow tension gash zones adjacent to faults. Therefore on the one hand the crystal-bearing cavities are spatially related to fracturing of folds, and on the other hand they are controlled by regional fault zones. Usually, fields in which quartz crystal veins are concentrated are partly or wholly bounded by faults. Later faults led to crystal-forming processes in fracture zones initiated during folding, and potentially hosting hydrothermal activity. The most clearly-marked fracture zones occur in quartzites, which are the most brittle rocks, where fracture density reaches 10–20 per metre. In vein zones which are densely fractured areas, there are usually three persistent systems – E-W-striking, horizontal and gently-dipping joints and cross-cutting vertical joints perpendicular to fracture zones. Close to major quartz crystal occurrences such as pockets and veins, there is an increasing density in the veins belonging to these three systems, and new systems appear, such that the final pattern is complex.

Hydrothermal effects in vein zones show up as partial recrystallization of quartzites, which take on a purple hue as a result. Quartz veins within vein zones run parallel to fractures of the major system, or are occasionally arranged *en échelon*. The veins vary in thickness, with a few having rare “bulges” up to 10 m across. Stockworks are usually restricted to such vein sectors, forming a network of variously-oriented veinlets, between which relict quartzites are preserved. Stockworks are usually the most productive parts of vein zones.

The following crystal cavity types have been identified: 1) those located along the contact between quartz veins and quartzites; 2) cavities within veins; 3) cavities located

in areas where quartz veins peter out; 4) those not associated with any vein, so-called tension gashes. The last two types are rare and their importance is low. Nests and hollows are commoner close to intersections between vein zones and amphibolites or pegmatites than farther away. Amphibolites and pegmatites appear to have screened crystal-forming solutions and thus created favourable conditions for quartz crystal growth.

Crystal cavities vary in shape: lenticular, isometric, tubular and irregular. Single-chamber nests occur with thin coatings of vein quartz. The inner surface of nests and hollows is usually covered with fractured quartz crystal bases. Good-quality drusy cavities and crystal druses are rare. Sheared surfaces of fractured crystal bases usually display clear signs of regeneration, indicating that movements which caused crystals to break took place during crystal growth and cavity formation. Crystal-bearing veins contain minor amounts of both substrate minerals (feldspar, scapolite, muscovite) and those that grew during the hydrothermal process (chlorite, hematite, fluorite, calcite, baryte, zeolites). Accessory minerals are represented by zircon, tourmaline, apatite, monazite and garnet. Intense chloritization and argillization are observed in the host rocks around crystal-rich veins.

It has already been noted that the crystal-forming process is related to Proterozoic structural and metamorphic reworking of early Precambrian crystalline rocks of the region. Crystal veins formed in fracture zones associated with early folds, and in faults associated with Proterozoic tectonometamorphic activity which also caused hydrothermal processes to be active in quartzite members. The time of crystal formation thus belongs to the period when Precambrian granulite–gneiss terrains were being stabilized.

Thus, these ore formations belong to a single period of crustal growth which marked the end of the development of this fold terrain. The block structure of Precambrian units, repeated metamorphism, ultrametamorphism and folding, with each event having its own specific features in the different tectonic zones, resulted in the metallogenic signature of the crystalline rocks in these zones being defined by the nature of the geological processes belonging to the period of stabilization. Within this period there was a definite change in ore formations with time, reflecting the tectonic history of the crystalline units. Despite its extent, spanning the interval 2200–1700 Ma ago, in a metallogenic context the entire geological history of the Precambrian evolution of Central Aldan is focused in this period. The reason for this is the change in deformation style in the final fold phase. For high-temperature ore metasomatites (magnesian skarns), a typical feature is their association with both local zones of repeated folding and linear fault zones. Lower-temperature metasomatic and hydrothermal rocks are located exclusively in zones of intense faulting.

## Olyokma Terrain

A.M. LARIN and D.A. MIKHAILOV

The Olyokma granite–greenstone terrain is located in the west of the Aldan Shield. Its southern boundary is marked by the Stanovoy deep fault zone which separates it from the Dzhugdzhur–Stanovoy fold belt. Its western boundary is the Baikal fold belt. The eastern contact of the Olyokma granite–greenstone terrain with the Aldan granulite–gneiss terrain is a complex system of imbricate thrusts along which rocks of the Aldan mega-complex are emplaced above the Olyokma complex. As a result, blocks and lenses of granulites belonging to the Aldan mega-complex occur in and adjacent to the collision zone within the Olyokma terrain. The Olyokma granite–greenstone terrain has three constituent structural complexes: Kurulta and Olyokma (Lower Archaean) and Olondo–Buorsalaa (Upper Archaean). Most of the terrain is occupied by granites showing a variety of ages, amongst which are linear belts and downwarps containing supracrustal rocks belonging to the Olondo–Buorsalaa complex and blocks of retrograde granulites of the Kurulta complex.

The Lower Archaean Kurulta complex is represented by a series of pyroxene-bearing schists and gneisses, interleaved with garnetiferous gneiss, with lenses of ferruginous quartzite and igneous rocks: enderbite, charnockite, garnetiferous granite, also meta-gabbro and meta-ultramafics, altered to schists. The rocks in the complex underwent regional metamorphism and ultrametamorphism at granulite facies conditions. Close to the contacts with the Olyokma complex, blocks of the Kurulta complex have been affected by amphibolite facies retrogressive metamorphism and were repeatedly granitized, making it difficult to discern their mutual relations. The isotopic age of the Kurulta complex is greater than 3400 Ma, using the U–Pb isochron method on zircons.

The Olyokma complex consists mainly of granite–gneiss and biotite–plagioclase gneiss, compositionally equivalent to tonalite. It is cut by granites containing supracrustal relicts – biotite and amphibole plagioclase gneiss, amphibolite and amphibole–plagioclase schist, also rare lenses of quartz gneiss and garnet gneiss. The Olyokma complex underwent high-temperature amphibolite facies metamorphism and granitization. Two such metamorphic episodes are recorded, the second being related to the Late Archaean development of the Olyokma complex, which is the basement to the Late Archaean formations which make up the greenstone belts.

The Late Archaean Olondo–Buorsalaa complex is an analogue of greenstone belts in other Precambrian regions. It forms narrow linear structures elongated in a near N–S direction, superimposed on the Olyokma and Kurulta complexes. Belt structures, which are infilled with rocks of the Olondo, Buorsalaa and Tungurchi groups in varying proportions, reflect a change with time from predominantly volcanogenic

(Olondo Group) deposits through volcanosedimentary (Buorsalaa Group) and finally sedimentary (Tungurcha Group). The Olondo volcanogenic sediments consist of metavolcanics from basic to intermediate and acidic, including komatiites, with thin metasediments at the top of the succession. The age of the Olondo Group is given as  $2960 \pm 70$  Ma by the U–Pb method on zircons from metavolcanics, and a whole-rock Sm–Nd determination yielded  $2966 \pm 16$  Ma (Zhuravlev et al., 1989). The Buorsalaa Group, together with tholeiitic metavolcanics, is represented by garnetiferous amphibolite, including also aluminous schist, quartzite and ferruginous quartzite. The metallogenic signature of this region is mainly defined by ferruginous quartzites. In addition, there are prospects for finding high-alumina raw materials, stratiform tin and tungsten mineralization, also muscovite and rare-metal pegmatites. Ferruginous quartzite deposits, formerly considered to be part of the stratigraphic succession, are associated with Buor–Salaa tholeiitic basalts which fill an extensive linear zone in the Chara–Tokk deep fault. The ferruginous quartzites, which occur amongst basic rocks metamorphosed at granulite facies and repeatedly at amphibolite facies, form a linear iron-ore belt, the northern part of which is represented by the Imalyk group of deposits, and the southern part by the Chara group.

An assemblage of sedimentary rocks of PR<sub>1</sub> age (2.2–2.0 Ga) filling the Udokan intracratonic basin in the western Aldan Shield (Fig. 79) is the youngest formation in the Olyokma granite–greenstone terrain. The internal structure of the Udokan basin is rather complex. According to V.S. Fedorovsky, it was divided by Archaean blocks during sedimentation into two almost equal parts, Kodar and Udokan. Subsequently, the Udokan rocks which make up this structure were subjected to polyphase deformation and zonal metamorphism, then cut by granites belonging to the gigantic Kodar–Kamensky lopolith and the Chiney gabbro–norite layered intrusion. Associated with clastic sediments in the Udokan Group is the huge Udokan cupraceous sandstone deposit. Copper–nickel sulphide and titanium–magnetite mineralization accompanying platinoid mineralization are hosted in basic rocks in the Chiney intrusion. Uneconomic hydrothermal and pegmatitic mineralization types are associated with granitic rocks in the Kodar complex. On the flanks of the Udokan basin at the contact with surrounding Archaean gneisses is the Katuga rare-metal deposit, associated with zones where alkaline metasomatites are developed. Nepheline metasomatites are also associated with zones of regional alkaline metasomatism and their specific composition makes them productive aluminium ore deposits.

## *1. Ore deposits and occurrences*

### *1.1. Iron*

*Ferruginous quartzite deposits in the Chara–Tokk ore region.* The Chara group of deposits in the north of the Chita province is the most intensely studied ferruginous quartzite deposit. Geologically, this group is restricted to the SE part of the Chara microcraton. The largest deposits are found in the Sulumat and Lower Sakukan areas. Metamorphic units hosting the iron ore deposits are the Archaean Chara and

Buorsalaa Groups. Recent studies (Devi et al., 1983; Krivenko, 1981, 1983) have demonstrated that the ferruginous quartzites belong to blastomylonite and cataclastic zones which form N-S regional faults (Fig. 86). The zones vary in width from a few m to 3 km and they are several tens of km long. Previously, these zones were considered

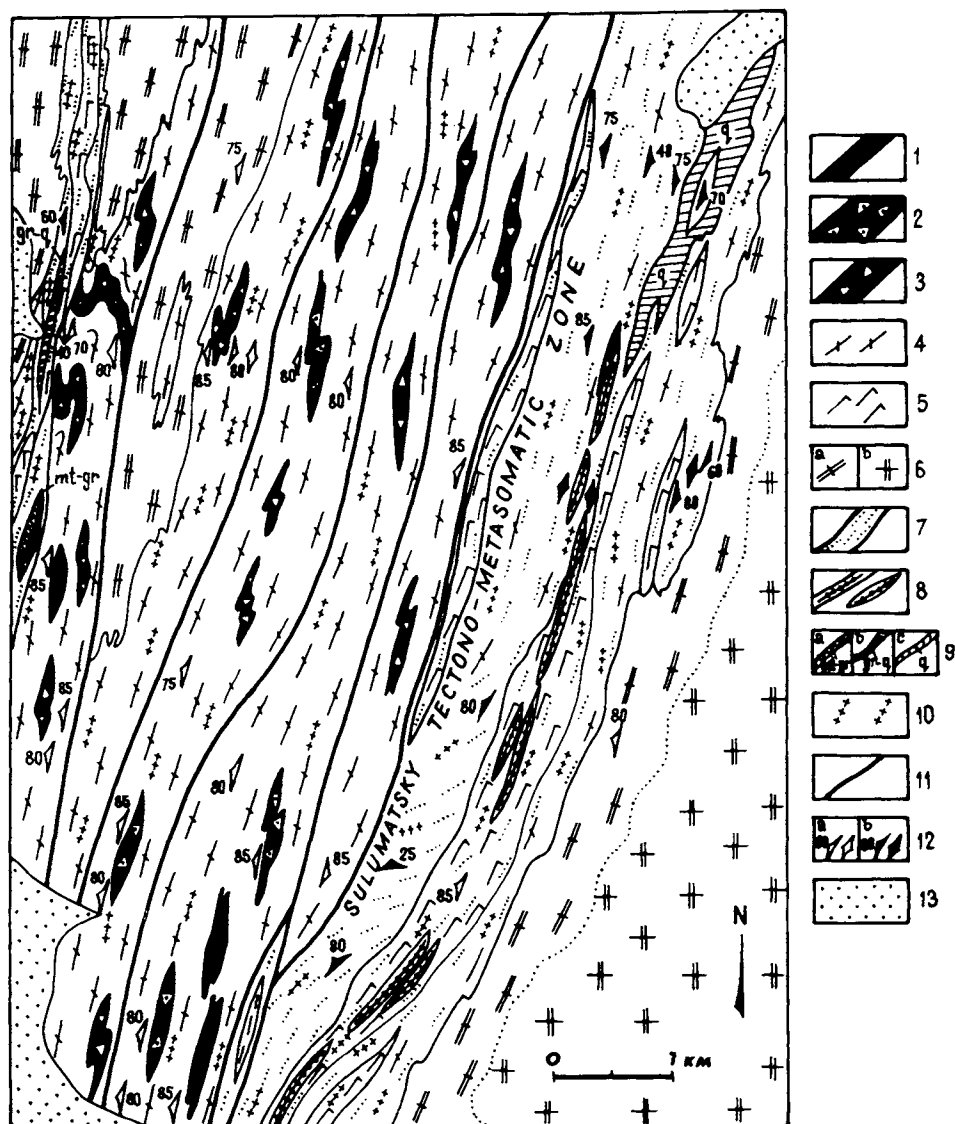


Fig. 86. Geological sketch map of the Chara sector. Compiled by V.A. Krivenko (1977). Chara Schists: 1 - two-px-plag, 2 - cpx-hb-plag, 3 - hb-plag, 4 - Kuandin granite gneiss, 5 - Teprokan metagabbro, 6 - Kuandin granite gneiss (a), massive granite (b), 7 - blastomylonite, 8 - metasomatic Fe quartzite, 9 - metasomatites (a) gt, (b) qz-gt, (c) qz, 10 - granitization, 11 - faults, 12 - attitude, 13 - loose sediment.

to be narrow linear troughs filled with Late Archaean metavolcanics and metasediments. Contacts between these zones and the high-grade metamorphic units – schist, gneiss and enderbite – are gradual; the superimposed schistosity gradually dies out towards the edges of blastomylonite zones.

Ferruginous quartzites within blastomylonite zones form sheet-like bodies of varying dimensions. The largest are over 100 m thick and 3–4 km long; contacts with host rocks are sharp. At the contacts themselves minerals in the blastomylonites are seen to be replaced by quartz and magnetite, resulting in the substrate rocks – mafic schist, amphibolite and various meta-ultramafics – being altered to ferruginous quartzite. Margins of ferruginous quartzite bodies usually contain zones of coarsely-crystalline, frequently massive rocks consisting of quartz, pyroxene, garnet, biotite and amphibole with rare sillimanite and staurolite. Such rocks are considered to be skarn-like metasomatic rocks which appeared during the formation of the ferruginous quartzites. Metasomatic effects are seen in blastomylonitized metamorphic rocks in the form of a eulysite mineral assemblage, which is the initial stage in the formation of ferruginous quartzites. M.N. Devi has noted that some metasomatite varieties are difficult to distinguish externally from corresponding mineralogical varieties of schists in the metamorphic series due to the fact that the banding and mineralogy of the substrate rocks have been inherited. The distinguishing feature is the age relationship with Kuandin granitic rocks, which are younger than the Early Archaean metamorphic rocks. In terms of their age, the ferruginous quartzites in this territory are defined as belonging to regional blastomylonite zones which cut folded Archaean granulite assemblages, and by the fact that the various blastomylonitized rocks display metasomatic replacement features. It is important to note in this context that the ferruginous quartzites themselves show no signs of blastomylonitization or cataclasis.

Ferruginous quartzite bodies contain numerous relicts of gneiss, amphibolite and other strongly sheared metabasic and meta-ultrabasic rocks. Quartz–magnetite material is frequently observed to have penetrated granite–gneiss and granite along breccia zones. Based on these field observations, many workers conclude that the Chara group of deposits is metasomatic in origin. M.N. Devi has subdivided the Chara quartzites into three ore categories based on the total iron to magnetite ratio. The first group has 75 to 100% magnetite, the second 50–75%, and the third < 50%. Ores in the first category account for 53% of the total reserves in the deposit, the second 43%, and the third 3.7%. Reconnaissance has shown that forecast reserves in the Sulumat and Sakukan sections of the Chara deposit are 500–600 million tonnes and 100 m.t. respectively. The content of harmful impurities is low: sulphur 0.01–0.08% and phosphorus < 0.1%. The iron ores contain trace amounts of gold (up to 0.8 g/t) and silver (up to 6.2 g/t). The commonest ferruginous quartzite varieties in the Chara deposit contain 30–45% magnetite, 30–50% quartz and silicate minerals, the main ores being pyroxene and amphiboles. Accessory minerals include apatite, sphene, zircon, pyrite, pyrrhotite, sphalerite, chalcopyrite, tourmaline, rutile, dolomite and calcite, amounting to less than 2%. Studies carried out by the Chita Geological Survey on enrichment of the Chara ores demonstrated that a three-stage process including crushing the ore to 1.0 mm followed by magnetic separation in a low-intensity field (800 Oersted) and subsequent crushing to 0.07 mm size produced an ore concentrate

containing 65.7% iron for a 39.2% yield of 92.9% purity. Sulphur and phosphorus contents were below detectable limits.

### 1.2. Copper

Copper deposits in the Olyokma terrain occur in the Udokan intracratonic basin, located in the west of the Aldan Shield at its boundary with the Baikal–Patom fold belt (Fig. 87). There is no agreement amongst different authors as to the nature of this terrain: it is considered to be a proto platform, an eo platform, a rift, proto orogenic belt, or miogeosynclinal downwarp, aulacogen, or re-entrant angle structure.

### 1.3. Cupraceous sandstone deposits in the Udokan ore region

The stratigraphic setting of the copper mineralization in the Udokan ore region, which was discovered in 1949, and the subdivision of the Udokan Group are discussed in

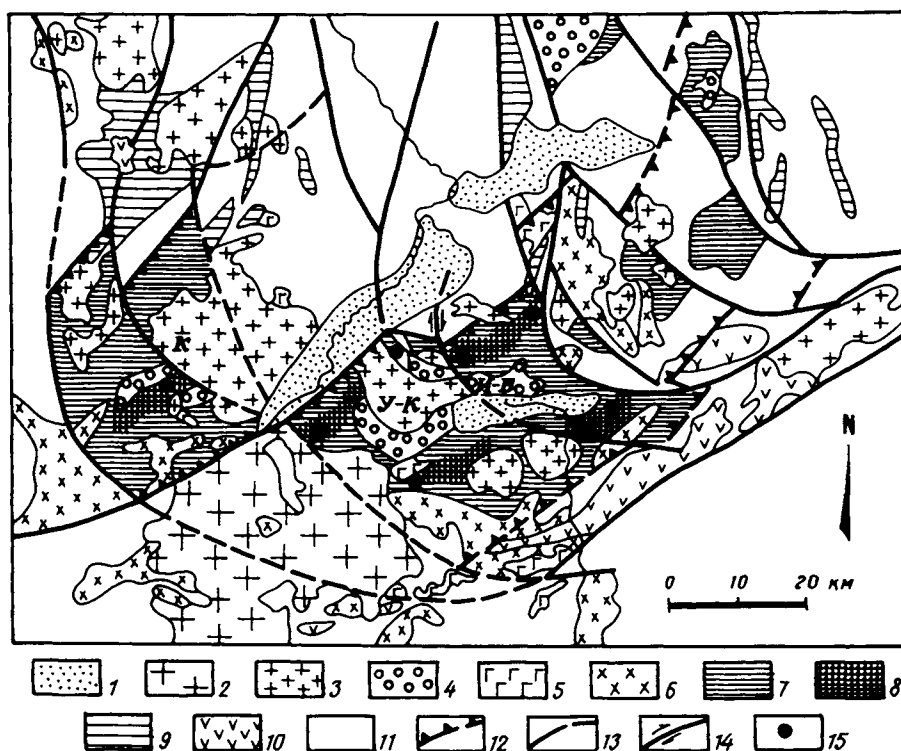


Fig. 87. Geological and structural sketch map of the Kodar–Udokan Zone (O.A. Apolsky, 1982). 1 – Pz. Mz, Cz basins, 2 – Pz granitoids, 3–10 PR<sub>1</sub>, 3 – Kodar granites, 4 – Kamen Gp. 5 – gabbro, gabbro–norite, 6 – Kuandin migmatite–granite, 7–8 – Chiney & Kodar Groups (7 – lagoonal–deltaic, 8 – coastal marine facies), 9 – trough complex, 10 – anorthosite, gabbro–norite, 11 – Archaean gneiss, 12–14 tectonic breaks, 12 – margins of PR<sub>1</sub> rift, 13 – oblique faults, 14 – transcurrent faults, 15 – Chiney Cu sst deposits. Tectonic blocks: K – Kodar, Y–K – Ungur–Katuga, U–B – Ikabya–Burpali.

works by Salop (1975), Bogdanov et al. (1982) and Fedorovsky (1985). The Udokan Group is subdivided into three sub-groups, which are further subdivided into formations; these are, from bottom to top, the Kodar sub-group (Ikabiy and Ayan Fms), the Chiney sub-group (Inyr, Chitkanda, Alexandrov and Butun Fms), and the Kemen sub-group (Sakukan and Namingin Fms), totalling 6–10 km in thickness. Using a microphytolith fossil assemblage, Mikhailova (1985) has determined the age of the Udokan Group as Upper and Lower Proterozoic. Isotopic studies yielded the following results: a) the metamorphic age of the crystalline basement on which the Udokan Group formed is estimated at 3.0–2.6 Ga; b) the depositional age is 1.8–2.0 Ga from U–Pb data provided by Yu.V. Bogdanov et al.; c) metamorphic age: biotite from garnet–biotite schist (K–Ar) 1.94–2.0 Ga, biotite from gneissose granite 1.86–1.9 Ga (K–Ar), muscovite 2.1 Ga (K–Ar), orthite 1.95 Ga (U–Th–Pb), monazite 1.95–2.1 Ga (U–Th–Pb), zircon 2.3 Ga (U–Pb); d) synmetamorphic metasomatites 2.1 Ga (U–Pb), 2.01 Ga (Rb–Sr); synmetamorphic ore mineralization 1.8–2.0 Ga (U–Pb), (Fedorovsky, 1985).

Folding is characterised by a predominance of simple forms, alternation of broad open synclines and box-shaped anticlinal flexures, while minor folds are rare, and typical linear folding is absent. Folds become complicated only in zones of intense granitization and close to intrusions. O.P. Korikovsky has established that high temperature zonal metamorphism of andalusite–sillimanite type affected only the lower parts of the succession, and rocks belonging to the Kemen sub-group were metamorphosed in the low-temperature subfacies of the greenschist facies.

Structural complexes in the Udokan deposit have been studied in detail in terms of lithology, petrochemistry and geochemistry by Bogdanov et al. (1982) and Sochava (1986), who obtained particularly valuable results. Petrochemical analysis has shown the following: 1) a relatively active tectonic regime during Udokanian time; 2) the degree of geochemical differentiation of the rock assemblage increases upwards in the section to reach a maximum in the middle Sakukan sub-group, where metapelites are distinguished on the basis of a higher K<sub>2</sub>O content; 3) the Na<sub>2</sub>O content also increases in the middle of the section; 4) the Fe<sub>2</sub>O<sub>3</sub>/FeO ratio increases from the base of the group to the top. It has thus been demonstrated on the basis of these and other facts that the continental deposits in the middle and upper parts of the succession are metamorphosed redbeds.

Cupraceous sandstone ore deposits and occurrences (Fig. 88) are restricted to certain sections in the stratigraphic succession of the Udokan Group, namely the middle and upper parts. Ore deposit locations are subject to a number of particular patterns. Commonest are ore bodies with a ribbon shape in plan and lenticular cross-section. There are two types of copper-bearing sediment. Firstly, there are cupraceous sandstones forming thick sequences which are impersistent along strike but which have the most important copper concentrations. The second type is represented by siltstones, forming thin horizons that are persistent along strike and contain lower copper concentrations than the first type. The first type is developed in the Lower Chitkanda sub-group (Krasnoye deposit), the Tolokan Group (Burpala, Unkur, Klyukvennoye, Middle Tolokan and Skolkoye deposits) and the Upper Sakukan sub-group (Udokan and Burunin deposits). In the best known Udokan and Krasnoye deposits there is a

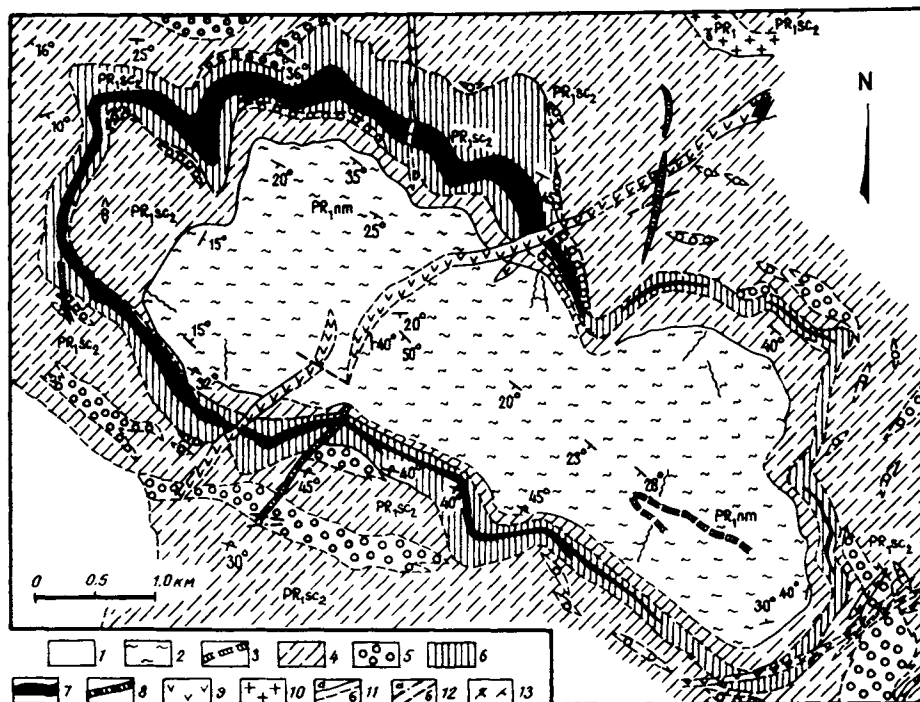


Fig. 88. Lithofacies sketch map of the Udokan deposit (after F.P. Krendelev et al., 1975). 1 – Quaternary. Lithogenetic types of PR<sub>1</sub> sed, 2–5 shallow-water basin: 2 – finely-bedded silty-clayey, 3 – fine, Cu-bearing shallow water basin: 2 – finely-bedded silty-clayey, 3 – fine, Cu-bearing coastal sed. 4 – submarine delta sands, 5 – well-sorted coastal sands with heavy mineral separates: 6–7 subaerial delta deposits, 6 – cross-bedded sands, 7 – Cu-rich sands; 8 – granite-aplite & qz porphyry dykes, 9 – gabbro-diabase dykes, 10 – porphyritic bi granite, 11 – geological boundaries (a) proven, (b) inferred, 12 – tectonic zones (a) proven, (b) inferred, 13 – bedding attitude.

rhythmic alternation of breccioconglomerate, sandstone, silty sandstone, siltstone and shale. Rhythms vary in thickness from 3 m to 15 m, with the copper-bearing sequence and each ore member decreasing upwards in the succession (Bakunin, 1958).

The second copper-bearing sediment type is mainly developed in the Alexandrov and Naminga groups which consist of siltstones, shales and silty sandstones with ripple marks and desiccation cracks. Lithofacies features of the copper-bearing sedimentary suites suggest that they were laid down in shallow coastal lagoons. The strong spatial association between the two cupraceous sediment types is evidence that they both owe their formation to a common source in copper-bearing rocks. Cupraceous facies occur in belts relative to the copper source region. There are three such belts strung out along the present-day southern margin of the Chara microcraton.

Primary copper mineralization is represented by chalcosite, bornite and chalcopyrite, while pyrite, magnetite and titanomagnetite are also common. Rarer minerals include valeriite, molybdenite, sphalerite, marcasite, tennantite, arsenopyrite, galena,

native silver, and bismuth. Ore minerals occur as disseminations in the rock cement, and as pockets and lenticular concentrations and films in sulphide ores. Sulphides often accentuate the cross-lamination and ripple cross-bedding in the sediments. Banded and disseminated-banded rich ores contain quartz-sulphide veinlets associated with cleavage fractures.

Many research workers consider the Kodar-Udokan copper ore mineralization to have a primary sedimentary origin and subsequent copper concentration and the formation of specific ore deposits were associated with later diagenesis and katagenesis. The multistage nature of sedimentation that characterises cupraceous sandstone deposits is not the result of cyclic sedimentation according to Apolsky (1984), but is related to tectonic breaks. Thus for example, the ore mineralization in the Burpali deposit is concentrated directly in a fault zone. Bogdanov and Feoktistov (1982) have noted that the zonal belt distribution of cupraceous sediments relative to erosional source regions, and the presence of stratigraphic and formational control on ore mineralization are the basis for referring the copper mineralization to a primary sedimentary type. Also, the fact that copper mineralization is restricted to the coarsest-grained sandstones with epigenetic carbonate or carbonate-mica-quartz cement, together with structural and textural features in rich ores indicate that late, superimposed processes played a role in ore concentration. Late ore-forming epigenetic stages took the form of intense lateral migration of expelled elysian waters along permeable horizons and favourable structures which resulted from relatively more intense sedimentation in the direction towards the unloading of the artesian basin. Waters with a sodium chloride composition produced an epigenetic concentration of low-grade sedimentary-diagenetic copper mineralization. Traps for copper mineralization were lenses of lagoonal and deltaic sediments located on the slopes of palaeo-elevations.

Epigenetic ore formation had a differentiated origin in Chiney and Kemen time. Epigenetic Chiney ore genesis had already ceased by the onset of Kemen sedimentation. Completion of Kemen ore genesis occurred at the end of this period of sedimentation, and in subsequent episodes of Early Proterozoic tectonic activity. The episodic nature of epigenetic ore formation is confirmed by differences in the composition, rhythmicity, fold styles and degree of metamorphism seen in Chiney and Kemen sediments and the occurrence of local stratigraphic unconformities between these two groups.

The ores which formed in the cupraceous sandstone deposits underwent metamorphism to varying degrees. Externally, these changes are expressed in the disappearance of the red colour of the rocks due to the recrystallization of iron hydroxides, the appearance of pyrrhotite, specular ores, arsenopyrite and cobalt and nickel sulphides. Ores which were most affected by metamorphism contain metamorphic veins and have patchy textures which are characteristic of copper-bearing rocks which have undergone greenschist facies metamorphism.

Copper-bearing rocks experience significant alteration at contacts with cross-cutting gabbro-dyabase dykes and granite intrusions. In the Udokan and Burpala deposits, host rocks are hornfelsed in the contact zones and have been altered to skarns, with sulphides arranged zonally. Bornite-chalcopyrite ores alternate with bornite, chalcopyrite and chalcopyrite-pyrite ores as dyke contacts are approached. Copper from the country rocks is assimilated by the dykes.

Granitic intrusions display more widespread effects on copper-bearing rocks, which were subjected to recrystallization and alteration of sulphide compositions. Contact-metamorphic vein formations are common. Folding and faulting are post-ore in age and were responsible for moving fragments of cupraceous sandstone horizons relative to one another. This was not accompanied by redistribution of ore material near dislocation zones.

The Chiney copper–nickel deposit. This ore deposit is a complex copper–nickel sulphide and titanomagnetite body, genetically related to the Chiney gabbro–norite pluton, which has an area of 100 km<sup>2</sup> and lies 8–20 km from the Udokan cupraceous sandstone deposit. Originally it was known as a titanomagnetite body when M.N. Petrusovich and M.I. Kozin discovered titanomagnetite manifestations in the south of the intrusion in 1931. Lebedev (1962) has studied the petrology and ore mineralization type in the Chiney intrusion. Sviridenko (1963) discovered copper–nickel ores at the base of the lopolith, which were subsequently studied in detail (Sviridenko et al., 1975, 1978).

This pluton has similarities with such ore-bearing layered intrusions as Zlatogorsk, Sudbury, Bushveld and Stillwater, based on its petrological characteristics, geological structure, and metallogenic signature. The intrusion is located at the intersection of a number of long-lived, deep-seated NE- and NW- striking faults. The intrusion is shaped like a typical rhythmically layered lopolith. Its total thickness in vertical section is 2.5–3 km (Fig. 89). Country rocks hosting the Chiney lopolith are Lower Proterozoic clastic terrigenous–carbonate rocks belonging to the cupraceous Udokan Group. Gabbroic rocks and gabbro–norites are cut by Kodar granites, thus defining a Lower Proterozoic age for the intrusion.

The main petrographic features of the Chiney intrusion are expressed as a rhythmic stratification in the sequential crystallization of anorthosite, leucogabbro–norite, gabbro–norite, hypersthene gabbro (ore gabbro), titanomagnetite plagioclasite, and titanomagnetite ore. Gabbroic rocks in the lopolith display a number of petrochemical features indicating that they belong to a shallow-level sub-formation of Precambrian gabbro–norite–anorthosite layered intrusions. The magma in the pluton had a higher alumina content, exceptionally high iron, and higher alkalis. Other elements of interest are increased amounts of Cu, Ni, V, Ag, the first two of which form economic concentrations. The copper–nickel ores are sometimes accompanied by platinoids.

Compositionally and in terms of layering, the Chiney lopolith is divided into three zones: a lower zone of roughly layered leucogabbro–norite up to 650 m thick, a 750 m thick transition zone of norite–gabbro–norite, a finely-layered middle zone of gabbro–norite–anorthosite–titanomagnetite, 1200 m thick, and a 1200 m thick roughly layered norite zone. The basicity of rocks decreases upwards in the rhythms, to the extent that anorthosite with titanomagnetite ore mineralization forms at the tops of rhythms. Individual rhythms formed with the following sequence: anorthosite – gabbro–norite–augite norite – mesocratic norite – melanocratic norite – gabbro–norite – ferro–norite – magnetite plagioclasite – titanomagnetite ore.

Titanomagnetite ore mineralization in gabbroic rocks of the Chiney lopolith is represented by the following morphogenetic types: 1) Accessory (early magmatic) titanomagnetite and ilmenite in gabbro, gabbro–norite and plagioclasite. The ilmenite

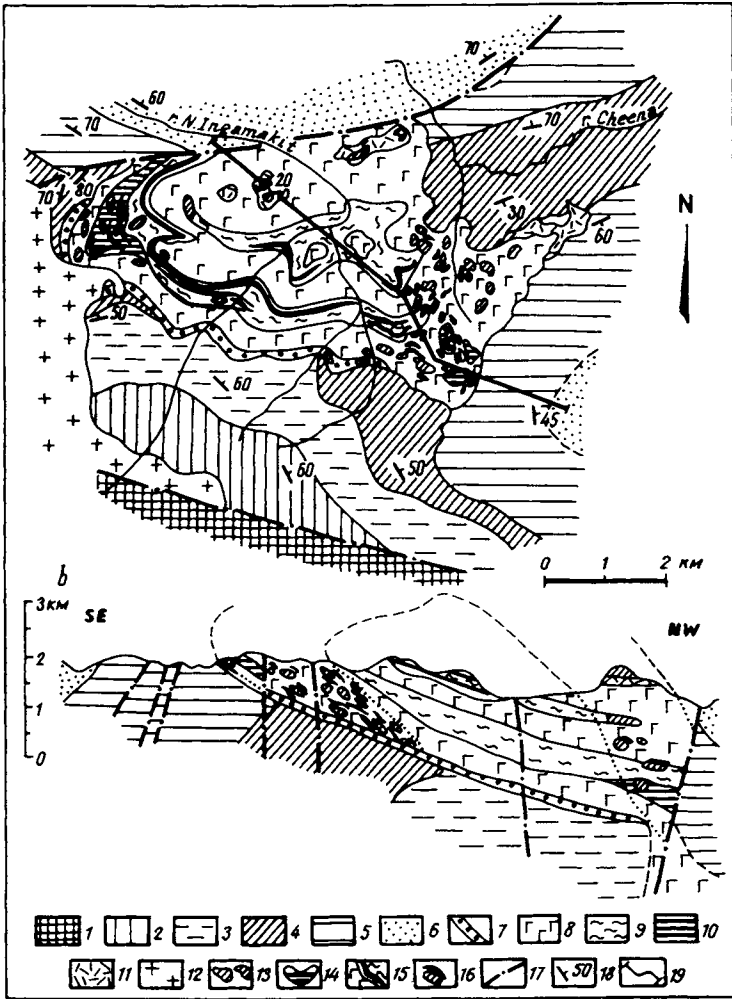


Fig. 89. Geological sketch map (a) and section (b) through the Chiney gabbro-norite pluton (E.G. Kozlov, 1981). 1 - Ar basement, 2-6 PR<sub>1</sub> Udokan Group (2 - Chitkanda, 3 - Alexandrovsky 4 - Butun, 5 - L. Sakukan, 6 - U. Sakukan Fms); 7-11 Chiney intrusive rocks (7 - spotted leucogabbro & anorthosite, basal zone, 8 - massive gabbro-norite, 9 - rhythmically banded gabbro-norite, leucogabbro, anorthosite, 10 - pyroxenite, 11 - qz diorite, monzonite, syenite at inner contact); 12 - Ingamakit granitoids, 13 - Butun xenoliths in Chiney gabbro, 14 - L. Sakukan xenoliths, 15 - sheeted titanomagnetite ores, 16 - vein ores adjacent to xenoliths, 17 - faults, 18 - bedding in Udokan Gp, 19 - section lines.

: magnetite ratio varies from 19 : 81 in ferro-leucogabbro to 43 : 57 in gabbro-norite, and 23 : 77, 33 : 67 in titanomagnetite ores. 2) Early magmatic (cumulate) disseminated ores in gabbro-norite. 3) Late magmatic massive titanomagnetite fusive ores as lenses and laminae at the tops of rhythms. 4) Pegmatitic segregations with ore minerals in pockets. According to Lebedev (1962), the ilmenite to magnetite ratio gradually decreases from the earliest ore accessories to the latest vein-type titanomagnetite,

and reflects the evolution of the ore melt composition during the formation of the pluton.

Chechetkin (1966) and Sviridenko et al. (1975) also recognised several types of mineralization in sulphide ores: 1) Syngenetic stratified liquation ores, occurring as a continuous horizon at gabbro–norite contacts, with disseminated pyrrhotite, chalcopyrite and small amounts of pentlandite. This horizon varies in thickness from a few metres to a few tens of metres. The productive horizon is restricted to the bottom of the lopolith. In addition, there are a further two suspended horizons of disseminated ores 80–100 m above the base. 2) Epigenetic ore cavities, restricted to cataclastic zones, mainly with a NE strike. 3) Disseminated outer contact ores, developed in the Udokan Group host rocks, where sulphide mineralization forms a fine, irregular dissemination. Country rock xenoliths sometimes also contain ore dissemination. 4) Pyrrhotite and chalcopyrite disseminations in titanomagnetite ores. 5) Brecciated bornite–chalcopyrite and chalcopyrite vein-type ores in country rocks. 6) Lead–copper–zinc ores in quartz–calcite veins. 7) Essentially chalcopyrite skarn ores.

Each mineralization type has its own set of specific characteristics. Disseminated ores in contact zones have approximately equal amounts of pyrrhotite and chalcopyrite, but for low-grade ores the ratio is 1 : 15 to 1 : 20, and for rich ores 1 : 25 to 1 : 30. Massive pyrrhotite ore deposits are accompanied by disseminated ores in which chalcopyrite predominates. Massive ores are distinguished by their nickel content ( $\text{Ni} : \text{Cu} = 1 : 8$  to  $1 : 12$ ). Pyrrhotite is absent in skarn ores, while pyrite makes an appearance. Bornite–chalcopyrite and chalcopyrite vein ores occupy a special place, being hosted in tectonic zones within the country rocks. Pyrrhotite is completely absent, while millerite and linneite–polydymite are present. Quartz–calcite veins with sphalerite, galena, chalcopyrite and pyrite crop out in the centre of the massif and are associated with NE-striking fracture zones. Chalcopyrite and pyrite are usually localized close to *zählbands* together with quartz, while sphalerite and galena occur in the centre, together with calcite.

According to Kulikov et al. (1983), the distribution of the various mineralization types in the Chiney intrusion is controlled by internal structural elements, reflecting stages in its emplacement. Negligible amounts of copper sulphide mineralization in the centre of the intrusion and the maximum development of titanomagnetite there indicate a highly magnesian melt which crystallized in a regime where oxygen partial pressure was increasing. The patchy nature of titanomagnetite dissemination in a zone of weakly differentiated rocks is explained by the probably rapid crystallization as compact bodies. But in the zone of sharply differentiated rocks where crystallization was slower, titanomagnetite ores formed rich tabular and *schlieren* deposits. At the margins of the intrusion, country rock assimilation and increasing acidity led to the development of copper–sulphide mineralization. According to Konnikov (1981), the uneven distribution of sulphide mineralization in contact parts of the massif (Fig. 90) is determined by the fact that the body has intruded dolomite and graphitic schist belonging to the Butun Group, from which it was able to assimilate copper during the emplacement of the Chiney pluton.

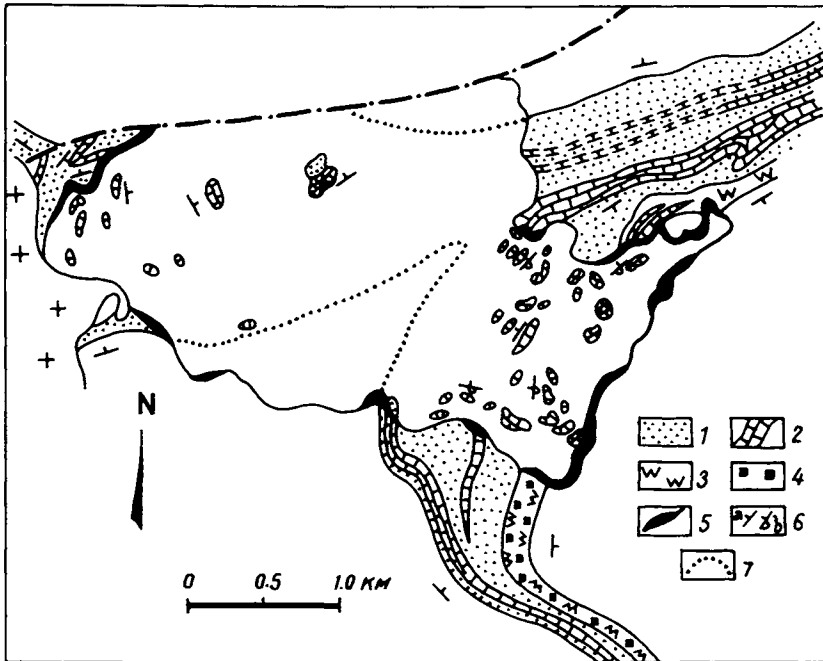


Fig. 90. Rich sulphide ores at contact of Chiney lopolith (E.G. Konnikov, 1981). 1–3 Butun Gp sediments (1 – clastic, 2 – dolomite & dolomitized lst, 3 – graphitic shale); 4 – syngenetic disseminated sulphides in Butun rocks, 5 – sulphide mineralization at intrusive contact, 6 – bedding attitude in Butun seds (a) and xenoliths (b), 7 – inferred location of Butun Gp beneath lopolith.

#### 1.4. Rare metals

The *Katuga rare-metal ore field* is located in the western Aldan Shield in the Kodar–Udokan region, where the Baikal and Stanovoy megablocks are in contact, in a zone affected by the Stanovoy regional fault. The ore field with rare metal mineralization is localized in the southern part of the Early Proterozoic Udokan downwarp at its boundary with Archaean formations in the Chara microcraton, at the southern outer contact with the Kalar rapakivi-type granite intrusions in the Kodar complex (Fig. 91). Country rocks are various schists in the Udokan Group showing amphibolite to greenschist zonal metamorphism, and Archaean granulites in the Chara microcraton, retrogressed at amphibolite facies. Supracrustal rocks hosting the ores form the near-E–W Katuga syncline.

The following summary of the Katuga ore field is based mainly on the work of Arkhangelskaya (1974). Within the ore field, the effects of alkali metasomatic processes are widespread. Metasomatic rocks form two major deposits, Eastern and Western, the latter of which occurs in a fault that complicates the southern limb of the syncline, while the Eastern deposit occurs in the periclinal part of the syncline. Mineral deposits are surrounded by wide aureoles of metasomatically altered country rocks. Metasomatic alteration also affected vein offshoots from the granites in the Kalar intrusion.

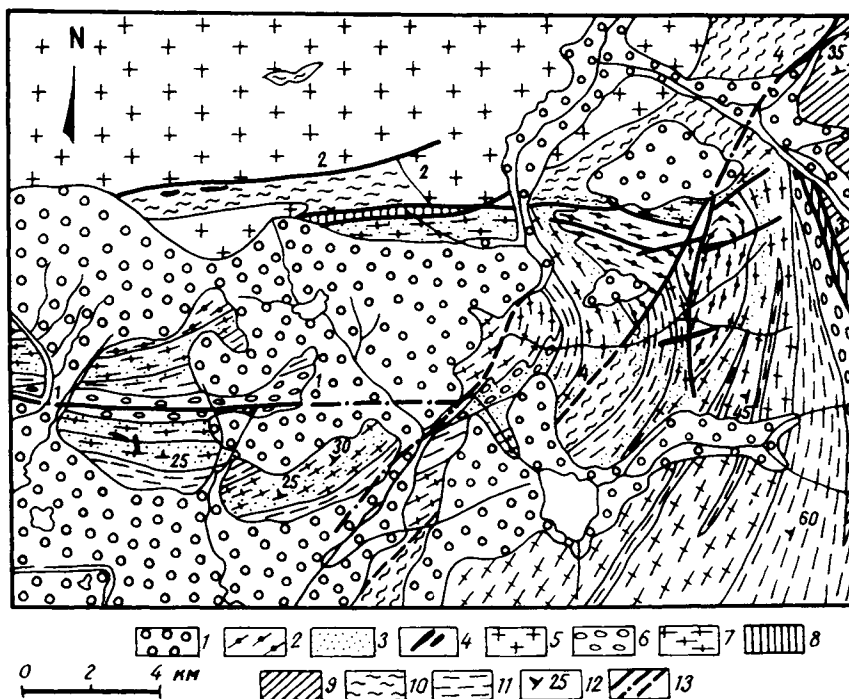


Fig. 91. Sketch map of Katuga field (Arkhangelskaya, 1974). 1 – superficial deposits, 2 – granitic alkali metasomatic rocks, 3 – incompletely metasomatised & hydrothermally reworked gneiss & schist at outer contact of metasomatites, 4 – amph & qz–plag porphyrite, 5 – Kalar granites, 6 – metasomatic quartzite, 7 – granite gneiss & intensely feldspathized gneiss, 8 – retrogressed schist, 9 – mesocratic bi ( $\pm$  gt  $\pm$  silli) schist, 10 – leucocratic Ca-poor bi ( $\pm$  gt) schist & gneiss with cord. musc, st, ky, silli, 11 – mesocratic & melanocratic bi ( $\pm$  amph) schist, in places gt, fibrolite, st; 12 – attitude, 13 – faults (a) visible, (b) buried, (c) inferred. Fields: 1 – Katuga, 2 – Kodar–Katuga, 3 – E–W (Meridian), 4 – Lake (Ozyornoye).

Metasomatic zoning is characteristic of both deposits, but is expressed more evidently in the Eastern deposit. Biotite metasomatites are typical in the upper parts of the deposits, aegerine varieties in the lower parts.

The main groups of ore-bearing quartz feldspar metasomatites are biotite, biotite–amphibole and aegirine–amphibole. Metasomatites usually have a banded structure and a gneissose texture which is partly inherited from the country rocks. Biotite metasomatites consist of quartz (20–25%), acid oligoclase (25–30%), microcline (30–45%), biotite (5–12%). Ore minerals are monazite, zircon, ilmenite, fluorite, malacon (metamict zircon), and rare columbite, columbitized pyrochlore, fergusonite, thorite, and gagarinite. At the contact between biotite metasomatites and schists are zones of mica rock with abundant zircon (malacon), rare earths, fluorite and gagarinite ( $\text{Na-CaY}(\text{F,Cl})_6$ ). Amphibole metasomatites occupy a transitional position between biotite and aegirine–amphibole metasomatites and consist of microcline–perthite (40–45%), albite (10–20%), quartz (30–25%), alkali amphibole (7–15%) and cryolite (1–2 to 5%). Ore minerals are pyrochlore, zircon, neighborite and malacon; gagarinite, fluocerite,

thorite, etc. are sometimes present. The amphibole composition varies from ferro-riebeckite to ferro-arfvedsonite. Aegirine–amphibole metasomatites consist of quartz (10–18%), microcline (30–45%), albite (10–20%), arfvedsonite and aegirine (< 10%). Ore minerals are pyrochlore, zircon and cryolite.

In addition to the metasomatites listed above, independently of the boundaries between individual zones, there are segregations of quartz–feldspar metasomatites with neighborite ( $\text{NaMgF}_3$ ), columbite (or fergusonite), monazite, ilmenite, pyrochlore, zircon, cryolite, thin veins of albitite with zircon, and quartz veins with sphalerite, molybdenite, galena, bornite, pyrite and chalcopyrite. From their chemical composition, the metasomatites correspond to rare-metal alkali granites and granosyenites with the specific ore element assemblage of Ta, Nb, Zr, Be, Sn, Zn, U, Th, Li. Arkhangel'skaya (1974) puts similar alkali metasomatites into the category of rare-metal amagmatic feldspar metasomatites, compositionally and mineralogically close to metasomatic apogranites in the Ulkan intrusion in the east Aldan Shield, the Perzhan granites in the Ukraine, and others. The age of the rare-metal metasomatites in the Katuga ore field is  $2014 \pm 20$  Ma, from the Rb–Sr isochron method, and the initial Sr isotope ratio is very high, at 0.7722 indicating a predominantly crustal nature for the ore genesis. Owing to its ore reserves, the Katuga deposit belongs to the category of major mineral deposits.

### 1.5. Apatite

*The Kalar–Khani region* is one prospective region in the Dzhugdzhur–Stanovoy apatite-bearing province (Belyayev et al., 1981; Gavrilov et al., 1987; Roganov et al., 1986). The region is located in the SW Aldan Shield in the area crossed by the Baikal–Amur Mainline (BAM) railroad. Within its borders are the Ukdus, Kabakhanyr and Yus–Kyuel apatite deposits, associated with Late Archaean pyroxenite intrusions. A typical example from this suite is the Ukdus deposit (Anon., 1983).

*The Ukdus deposit* is situated on the right bank of the river Khani at its confluence with the river Yus–Kyuel, 0.5 km from the BAM rail track. It is associated with an ultrabasic intrusion, controlled by a near-N–S deep fault cutting Buor–Salaa schists and gneisses. The intrusion and surrounding country rocks were affected by intense Early Proterozoic ultrametamorphism during which the country rocks were altered to granite–gneisses, with widespread formation of microcline and quartz–feldspar metasomatites in the fault zone. In plan view, the Ukdus apatite-bearing intrusion is oval- to pear-shaped and elongate in a NW direction, 2 km long by 800 m wide. The intrusion thins out on its SE flank and takes on a dyke-like appearance. It is complex, basically with apatite-bearing meta-pyroxenites showing varying degrees of replacement with biotite, amphibole and feldspar (Fig. 92). Microcline vein bodies up to 75 m wide appear in zones of weaker rock along the contacts of the intrusion. Numerous N–S trending microcline veinlets are observed within the intrusion itself. Apatite mineralization is ubiquitous throughout the rocks of the intrusion. In pyroxenites, the apatite content reaches 20%, forming disseminated and vein-dissemination ore types. A 50–70 m wide zone of brecciated meta-pyroxenite, rich in apatite, can be traced in the middle of the intrusion. The average

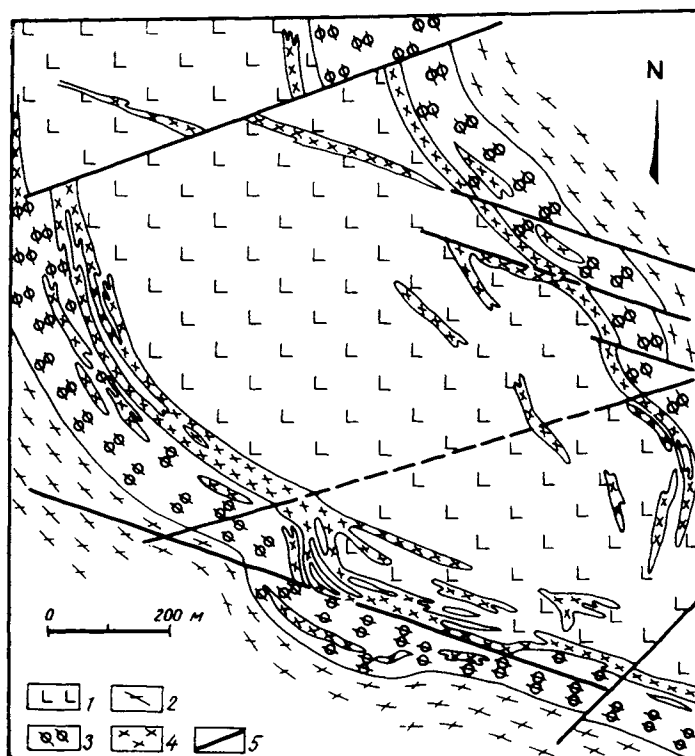


Fig. 92. Geological sketch map of the Ukdus deposit (after M.V. Sukhoverova et al., 1978). 1 – meta-pyroxenite, 2 – bi-amph granite gneiss, 3 – granite gneiss with metapyroxenite relicts (granitization zone), 4 – microcline & qz-feld metasomatites, 5 – faults.

$P_2O_5$  content for the deposit is 4%, and the ore-bearing coefficient is 0.73. Forecast reserves for the deposit, to a depth of 250 m, are estimated at 40 million tonnes  $P_2O_5$ .

This Page Intentionally Left Blank

## Batomga terrain

A.M. LARIN

The Batomga granite-greenstone terrain is situated in the eastern Aldan Shield. The ancient (infracrustal) complex of the terrain consists of the Olenin schists and gneisses and associated basic and ultrabasic intrusions, enderbite, charnockite and trondhjemite, metamorphosed at granulite facies conditions, together with schist, gneiss, amphibolite, quartzite and calciphyre belonging to the younger Batomga Group, metamorphosed at almandine amphibolite facies. These rocks are intensely migmatized in the western part of the terrain, forming broad granite-gneiss fields.

The younger supracrustal complex is similar to greenstone belts and consists of the Chumikan Group in which the dominant rock types are metavolcanics, porphyries, porphyritoids, mica schist, quartzite and calciphyre. The rocks in the supracrustal assemblage have undergone Barrovian zonal metamorphism, from greenschist to low-temperature amphibolite facies. Associated with them are intrusive bodies of metagabbro and biotite granite. In the eastern part of the terrain, the Ulkan volcanoplutonic belt has been superimposed on Archaean structures. The belt is located in the eastern Aldan Shield and is associated with the South Aldan deep fault, an E-W structure separating the Batomga granite-greenstone and Dzhugdzhur-Stanovoy terrains. To the south, the Ulkan belt is bounded by the Dzhugdzhur anorthosite massif, and to the east it is overlain by the Mesozoic Magey volcanics.

Acid volcanics, subalkaline porphyries and minor basic volcanics and trachydolerites, combined with rapakivi and alkali granites into a unified comagmatic volcanoplutonic complex, are the main rocks involved in the Ulkan belt. Sandstones and grits belonging to the Toporikan Fm lie at the base of the clastic terrigenous-volcanogenic succession which makes up the belt. They are overlain by quartz porphyry, syenite porphyry, diabase, amygdaloidal porphyrite, trachyandesite and tuffs with a porphyrite and trachyandesite composition. tuffaceous sandstone, grit and conglomerate belonging to the Elgetey Fm. Lava flows and associated extrusive bodies of komendites and pantellerites are strictly limited in their distribution and occur at the very top of the succession. Clastic terrigenous-volcanogenic rocks in the Ulkan belt attain a total thickness of 4500 m. Folding and faulting are weakly expressed and the rocks are practically unmetamorphosed.

Intrusive formations are represented by granophyric granites (the South Uchuri intrusion), also quartz syenites, subalkaline granites and peralkaline granites (the North Uchuri intrusion). The isotopic age of these granites (U-Pb isochron method on zircons) lies in the interval 1700–1718 Ma (unpubl. data by L.A. Neymark, A.M. Larin, et al.). From their chemical composition, petrology and mineralogy, these

granitic rocks in the Ulkan volcanoplutonic belt are quite close to rocks in the rapakivi granite association. Characteristically they have a pronounced geochemical and metallogenic signature across a wide spectrum of rare metals. In this connection, it should be emphasised that there is an almost total coincidence between the isotopic age of granites in the Ulkan belt and the associated anorthosites in the Dzhugdzhur complex. The Sm-Nd mineral isochron for anorthosites and gabbroic rocks in the Geransky intrusion corresponds to an age of  $1705 \pm 30$  Ma (Sukhanov, 1989). It thus follows that, analogous to the East European craton, these two igneous complexes may be united into a single anorthosite-rapakivi granite formation.

Rare-metal, rare-earth, uranium and thorium mineralization are associated with the subalkaline and peralkaline granites of the North Uchuri intrusion. The igneous rocks in the pluton originated in several phases (Nedashkovsky, 1986): 1) Coarse- to medium-grained, sometimes fine-grained hastingsite syenites. 2) Coarse- to medium-grained, sometimes granophyric rapakivi-type biotite granites and alaskites (the major volume in this phase), commonly containing anorthosite xenoliths. 3) Fine-grained, sometimes porphyritic leucocratic biotite granites, forming stocks and minor sheet-like bodies among main-phase granites. 4) Peralkaline riebeckite, aegirine-riebeckite and astrophyllite-riebeckite granites, forming minor intrusions (the Nygvygan intrusion), stocks and sheets with grorudite and selvsbergite apophyses and with alkali granite pegmatite bodies.

Igneous activity concluded with the intrusion of lamprophyre dykes. Sub-alkali granites are distinguished by having a marked geochemical signature for Sn, W, Mo, Ta and Nb, and peralkaline granites for Be, Ta, Nb, Zr, Hf and Th. Associated with the former are stocks of albitized and greisenized fine-grained granites with contact zones of quartz-topaz-protolithionite greisens with columbite, cassiterite and wolframite mineralization. Also present in the greisens, but less widespread are gelvine, phenacite, molybdenite, pyrite, sphalerite, arsenopyrite and chalcopyrite. Greisen zones occur along E-W faults and are up to 80 m wide and 400 m long. Cassiterite and columbite mineralization are found in albitite zones. Stockwork-type molybdenum occurrences are known in association with third phase biotite granites (Fig. 93). A number of rare-metal deposits and occurrences of different types are known to be associated with the peralkaline granites (Nedashkovsky, 1986), including alkali-granite pegmatites, and various metasomatic and hydrothermally altered rocks. Alkali-granite pegmatites are mainly localized in the outer and inner contact zones of peralkaline granite bodies, as well as in the zone above the intrusive top of these granites, and they are restricted to a 1.0–2.5 km wide E-W band. Pegmatite bodies have a zonal structure, except for contact and schlieren types. Individual bodies are up to 6.0–8.5 m wide and 300 m long. The alkali-granite pegmatites can be divided into three main mineral assemblages, each of which has its own specific rare-metal mineralization. Microcline-astrophyllite-riebeckite-quartz assemblages, which account for the greatest volume of pegmatite bodies, have phenacite mineralization. Columbite, zircon and pyrochlore are associated with albite-aegirine-microcline assemblages, and bertrandite and gentgelvine types are associated with quartz-fluorite-hematite parageneses.

Various metasomatites with rare-metal mineralization are developed along NW and NE faults in rapakivi-type granites in the zone above the intrusive contact of the alkali

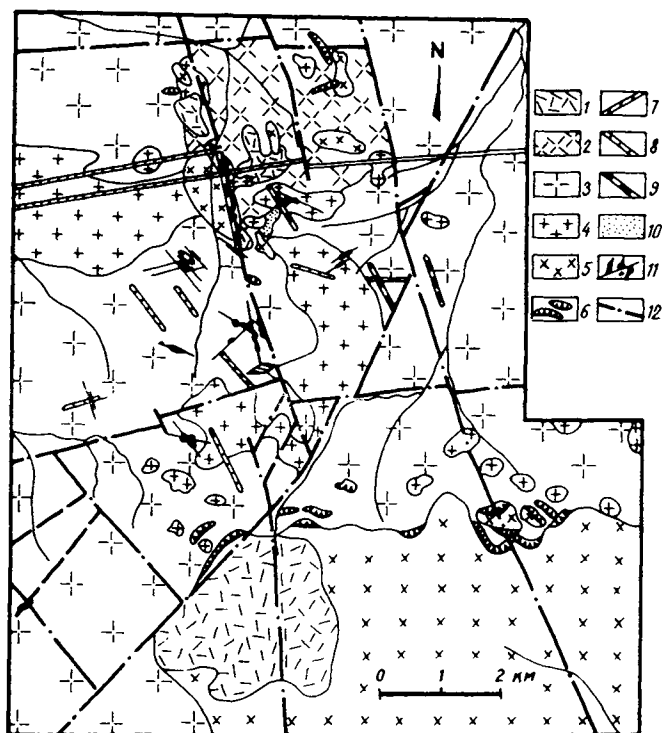


Fig. 93. Geological sketch map showing structure of Ulkan ore field (Nedashkovsky, 1986). 1 – acid volcanic outliers, 2 – rapakivi granosyenite, 3 – rapakivi granite, 4 – fine-grained granite, 5 – peralkaline granite, 6 – alkali granite pegmatite veins, 7 – alkali lamprophyre, 8 – late diabase dykes, 9 – greisen, 10 – qz-molybdenite stockworks, 11 – rare-metal metasomatic & hydrothermal rocks, 12 – late faults.

granite stock. The following compositional types of mineralized metasomatites can be distinguished: 1) Hematite (magnetite)-quartz-feldspar metasomatites with bertrandite, phenacite, beryl and gelvine mineralization (bertrandite predominates). In addition, fluorite, sphalerite, galena, rare pyrite, molybdenite, zircon, bastnesite, columbite, pyrochlore, cyrtolite, thorite, orangite, chalcopyrite, martite and other minerals are present. 2) Hematite (magnetite)-sulphide-quartz metasomatites with gengtgelvine. Also present are sphalerite and galena, less common are pyrite and chalcopyrite. Typical gangue minerals are siderite and rhodonite. 3) Quartz-albite-chlorite metasomatites with euclase. Highly ferric chlorite is the main typomorphic mineral in these rocks. The ore bodies are up to 50 m wide and 440 m long.

Ore-bearing metasomatites and pegmatites are associated with a common zoning and occur in a regular pattern relative to ore-bearing peralkaline granites. Pegmatites are located in the outer and inner contact zone of the intrusion and in the zone above the margin. Hematite-quartz-feldspar metasomatites occur higher than the pegmatites in the zone above the intrusive margin, while hematite-sulphide-quartz and quartz-albite-chlorite metasomatites are farthest from the ore-bearing granites. In exploration

terms, the mineralized metasomatites described above are closest to targets in the fluorite-phenacite-bertrandite formation. An analysis of the spatial distribution of the different types of mineralization and the various granitic rock types suggests that igneous and ore-forming processes in the Ulkan ore field have a polyformational character. We cannot exclude the possibility that Sn, W, Mo and Nb mineralization is associated with hypabyssal granites of the older anorthosite-rapakivi granite formation, while Be, Zr, REE, Th, Nb and Ta mineralization in alkali-granite pegmatites, quartz-feldspar and other metasomatic rocks is associated with the later and deeper alkali-granite formation.

## Dzhugdzhur–Stanovoy terrain

V.A. GORELOV

The Dzhugdzhur–Stanovoy terrain is separated from the Olyokma, Aldan and Batomga terrains by the Stanovoy Fault. To the south and east it is bounded by the Phanerozoic Mongolia–Okhotsk fold belt for a large distance along the Mongolia–Okhotsk tectonic suture, and to the west it is separated by faults from the Baikal–Patom fold belt (Fig. 79). Its Precambrian growth is divided into three structural stages: lower, middle and upper (Rundqvist and Mitrofanov, 1993). The lower structural stage, Archaean in age, consists of a granulite complex which mostly crops out in the northern and southern margins of the terrain, forming extensive zones. Late Archaean metavolcanics and granodiorites of the Stanovoy complex predominate in the central part of the terrain, and constitute the second structural stage. The uppermost third structural stage consists of the Dzheltulak clastic terrigenous assemblage, filling narrow suture zones along the boundaries of block structures in the terrain.

High-grade internal processes in the Dzhugdzhur–Stanovoy terrain are related to the Early Stanovoy cycle of crust-forming events. Tholeiitic and basaltic komatiites formed during this period, together with swarms of parallel dykes. Somewhat later, gabbro–anorthosite and calc-alkali series plutons were emplaced along the northern boundary zone of the granulite belt in the terrain. (Recent geochronological evidence (Sukahnov, 1989) suggests that the gabbro–anorthosites of the biggest Geran massif have an age of  $1705 \pm 30$  Ma. *Editor's note*). The Early Proterozoic cycle concluded with the formation of a large volume of Late Stanovoy granites. Simultaneously, complementary extension zones formed – troughs which were later filled with clastic sediments belonging to the Dzheltulak complex. The tectonic activity of the terrain, which began in the Early Archaean, reached its culmination in the Late Archaean and concluded with cratonization by the end of the Early Proterozoic. Intense tectonomagmatic activity in the Mesozoic manifest itself in the formation of a complexly folded upwarp structure, intruded by numerous granitic bodies, accounting for a large percentage of its area.

Here we do not subdivide the Dzhugdzhur–Stanovoy terrain into type tectonic structures, which may be represented by granulite–gneiss blocks, probably the Pre-Stanovoy tectonothermally reworked belt, rift belts like the Dzheltulak type, and possibly greenstone belts. The metallogenic signature of the terrain in many respects is defined by the polyphase nature of the crust-forming events that produced rock complexes of various ages.

The lower structural stage, during which gabbro–anorthosite plutons formed, controlled the emplacement of ores belonging to the apatite–titanomagnetite formation.

Metavolcanics belonging to the second structural stage, represented by komatiite-tholeiite and andesite-basalt series, are associated with gold-sulphide mineralization. Copper-nickel sulphide mineralization is associated with the appearance of basic to ultrabasic magmatism during the Early Proterozoic cycle. Granitic rocks and associated metasomatites, which mark a prolonged orogenic regime in the Dzhugdzhur-Stanovoy terrain from the end of the Early Proterozoic, have a gold-rare metal signature. The Late Archaean metallogenic epoch in the terrain is marked by the formation of igneous and metamorphic type iron ore, titanium ore and apatite mineralization, and muscovite pegmatites associated with Upper Archaean polygenic-metasomatic granitoids. Ore deposits and occurrences are grouped into the following structural-metallogenic zones: complex apatite-titanium-iron ores in the Dzhugdzhur and Kalar-Olyokma zones, iron ore in the Bomnak zone, and muscovite-rare metals in the Imangra zone. The Early Proterozoic metallogenic epoch manifests itself across the terrain in the formation of gold-rare metal and muscovite mineralization. Identified metallogenic zones are the South Stanovoy gold zone and the Dzheltula gold-copper zone.

## *1. Ore deposits and occurrences*

### *1.1. Iron*

The Bomnak or Upper Zeya zone which extends for over 200 km in an E-W direction is the most typical iron ore zone in the Dzhugdzhur-Stanovoy terrain. It contains the minor Sivakan and Landysh iron ore deposits hosted in gabbro-amphibolites, and numerous ferruginous quartzite occurrences. Forecast reserves for this zone are 800 million tonnes of iron ore (Anon., 1981a). Sivakan is the largest deposit.

*The Sivakan deposit* is located on the right bank of the river Sivakan and the right bank of its tributary, the river Zeya. Precambrian rocks ( $AR_2$ ) that crop out in the region of the deposit are gabbro-amphibolites belonging to the Maya-Dzhanin complex, and Old Stanovoy and Margray granitic complexes ( $AR_2-PR_1$ ) which have migmatized the basic rocks. Precambrian complexes are cut by Mesozoic quartz gabbro-diorites and granodiorites (Fig. 94). All rock complexes in the region have a pronounced NW strike. Dioritic and porphyritic dykes are common. The deposit is hosted in gabbro-amphibolites and consists of 16 ore bodies, concentrated in three sectors. The ore bodies consist of disseminated and disseminated-banded ore types with magnetite-quartz and amphibole-magnetite-quartz composition. No. 1 ore body is the largest, being 500 m long and up to 200 m wide, with a NW strike. Forecast reserves for the deposit are estimated at 120 m.t. of ore with an average iron content of 35%. The deposit is believed to have a metasomatic origin.

### *1.2. Nickel, copper and cobalt*

Several dunite-troctolite-gabbro layered intrusions, including Lukinda, Lucha, Ildeus and others, are found in the southern branches of the Stanovoy mountain range – in

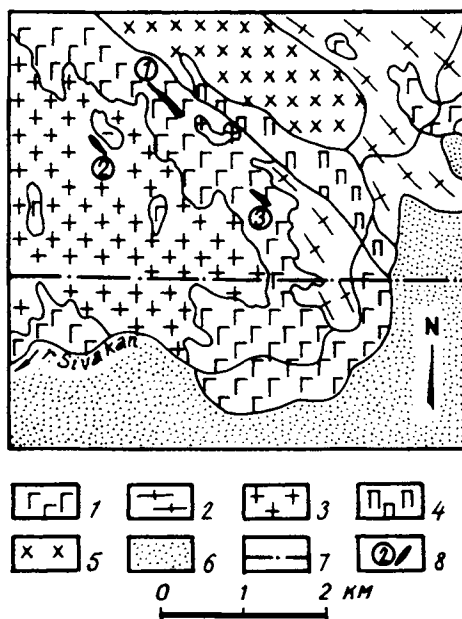


Fig. 94. Geological sketch map of Sivakan deposit area. 1-3 Precambrian complex: 1 - Maya-Dzhanin migmatized gabbro-amphibolite, 2 - Margay gneissose granite & syenite, 3 - granite; 4-5 Mesozoic complex: 4 - qz gabbro-diorite, diorite, 5 - granodiorite; 6 - Quaternary; 7 - faults; 8 - ore sectors 1, 2, 3 in Sivakan deposit.

the upper reaches of the rivers Zeya and Bolshaya Olda, forming part of the peridotite-pyroxenite-norite suite (Malich et al., 1987). The intrusions were emplaced into the Stanovoy and Maya-Dzhanin rock complexes (AR<sub>2</sub>) and are controlled by E-W and NE-striking deep faults (Fig. 96). North of and close to the Lukinda intrusion is a thin strip of Upper Proterozoic rocks, the Tukuringra complex. However, dunite-troctolite intrusions have not been observed among Upper Proterozoic sediments in the Stanovoy range.

The Lukinda and Lucha intrusions are lopoliths in shape, while the Ildeus body is a steeply-dipping sheet. Dunites occur at the base of the suite of intrusions, and amount to around 20% of the total. They contain chromite at the base and gradually grade through diopside and plagioclase varieties to troctolite. The troctolite horizon has troctolite interbanded with plagioclase dunite, then with olivine gabbro. Upper parts of the section consist of gabbro and gabbro-norite with titanomagnetite and are found only in the Lukinda intrusion. All these rocks formed in a single phase. Gabbro-pegmatite dykes, gabbro-norite and gabbro, pyroxenite and anorthosite are derivatives of dunite-troctolite intrusions. Titanium, chromium and copper-nickel sulphide mineralization have been found in these intrusions. Titanium mineralization appears in upper horizons of the Lukinda intrusion, in dykes and at the contacts with gabbro-amphibolite country rocks. Reaction zones at these contacts are thin, up to 2 m, but they typically have high ilmenite and titanomagnetite (up to 36%), in the ratio 1 : 5.

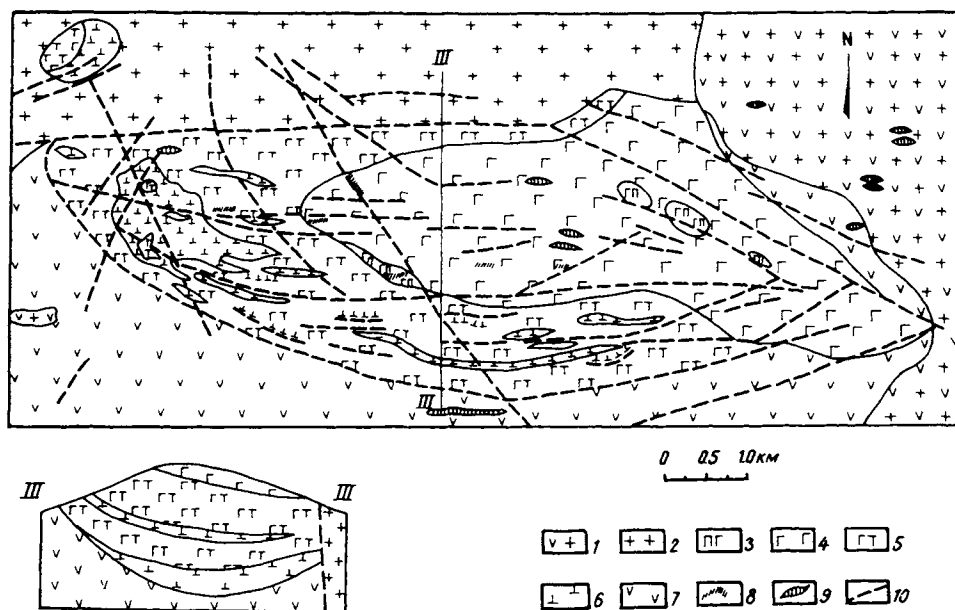


Fig. 96. Schematic geological map and section of the Lukinda intrusion (simplified from S.A. Shcheka, 1969). 1 – AR<sub>2</sub> Old Stanovoy granites. 2 – Mz granites & granosyenites; 3–6 Lukinda intrusion: 3 – pegmatitic gabbro, 4 – olivine gabbro–norite, gabbro, 5 – troctolite, olivine gabbro. 6 – dunite, 7 – leucocratic amphibolite, 8 – gt–musc pegmatite, 9 – felsite dykes, 10 – faults. II–III cross-section.

Chromium mineralization is represented by chrome spinel and is known only in the Lukinda intrusion, where it forms disseminations and plagioclase–chromite veinlets up to 10 cm wide in dunite. The chrome spinel content is 5–15%. Copper–nickel sulphide mineralization is present in all the named intrusions and has been studied most intensely in the Lukinda intrusion. The following account is based on the work of Shcheka (1969).

*The Lukinda intrusion* is emplaced into the Tukuringra deep fault zone. In its northern part, the intrusion is cut by obliquely intersecting feather joints of this fracture. In plan view the intrusion is a lenticular body some 16 km long with a maximum width of 3.5 km. A small body of dunite and olivine gabbro occurs to the NW (Fig. 96). On its southern flank, the massif is in contact with leucocratic granitized amphibolites belonging to the Maya–Dzhanin complex, formed at the expense of gabbro–norite, anorthosite and pyroxenite. Mesozoic alaskitic granites and granosyenites cut the northern part of the intrusion. Selvedges of biotite– and hornblende–oligoclase hornfelses have formed in the contact zone. The major rock types in the intrusion are dunite, troctolite and gabbro–norite. There is a marked increase in the leucocratic nature of the rocks from W to E and from S to N. Copper–nickel mineralization disappears from S to N also. The intrusion is cut by numerous dykes and veins of different ages and compositions. Gabbro–pegmatite dykes, fine-grained gabbro–norite, olivine gabbro and pyroxenite are derivatives of the intrusion. No pattern

has been observed in their orientation or distribution. Felsite, andesite, pegmatite and dacite vein bodies are derived from a granitic magma, and these usually have an E-W strike.

Copper–nickel sulphide mineralization is represented by several types. The earliest is syngenetic dissemination, predominantly in the melanocratic rocks. Disseminated mineralization is evenly distributed, but is not widespread. The nickel and copper contents in syngenetic sulphide dissemination zones is around 0.2%, rarely reaching 0.5%. A very characteristic feature for these ores is the presence of well-formed chromite octahedra. Next in time is cavity–vein mineralization in gabbro pegmatites. Ore-bearing gabbro pegmatites occur as linear zones with the same strike as the long axis of the intrusion. Mineralization is richer in nickel and copper, the contents of which are up to 1.6% and 1.1% respectively. Sulphides corrode rock-forming mineral grains in the pegmatites. The formation of gabbro–norite dykes was accompanied by the formation of metasomatic pyroxenites which everywhere contain low-grade, finely disseminated sulphides. The nickel content in these bodies is 0.1–0.3%, and in rare instances reaches 0.6%. Numerous manifestations of fine, epigenetic sulphide dissemination are found in the leucocratic part of the intrusion, forming extensive linear zones parallel and oblique to the intrusion, with a low (0.2–0.4%) nickel content. The main ore minerals in these types of mineralization are pyrrhotite, pentlandite and chalcopyrite. Mineralized pyroxenites contain in addition magnetite and titanomagnetite. Epigenetic ores contain platinoids and pyrite. Copper–nickel mineralization in the Lukinda intrusion, as in other intrusions in the Stanovoy range, formed in conditions analogous to those in well-known nickel deposits of layered intrusions. Dunite–troctolite intrusions and associated copper–nickel sulphide mineralization in the Stanovoy terrain are considered by Shcheka (1969) to be analogues of Late Proterozoic Pre-Baikal intrusions, including the Iyok-Dovyren and others. Some workers, though, prefer an Early Proterozoic age for these intrusions (Malich et al., 1987).

### 1.3. Molybdenum

The Dzhugdzhur–Stanovoy terrain has recently been acquiring greater importance as a new molybdenum province, the foremost area being the boundary of the terrain with the Aldan Shield, where prospective stockwork molybdenum occurrences have been discovered, genetically related to Mesozoic minor intrusions. As well as the Mesozoic occurrences, others are known from this area which most likely belong to the Proterozoic ore-forming epoch. One of these is the Okhok occurrence, described by Kastykin et al. (in Kuznetsov, 1983), from which the following description is taken.

*The Okhok occurrence* is located in the NW of the Dzhugdzhur–Stanovoy terrain in the Stanovoy deep fault zone, amongst Early Proterozoic faults in Upper Archaean migmatized gneisses and schists. Sutural downwarps have formed along the fault, filled with weakly metamorphosed Early Proterozoic sediments. Concordant with the general E–W strike of the fault are mylonites and retrogressed zones 10s–100s m wide and a few hundred km long, in which graphite, pyrite, iron and silica impregnations are common. Finely disseminated molybdenum occurs alongside the pyrite, and higher

molybdenum concentrations are observed in places where mylonites and N-S faults intersect. The Okhok occurrence is controlled by such a fault, which runs along the Okhok stream and the right tributary of the river Tass-Yurokh. The ore mineral occurrences are represented by a molybdenite-quartz vein and a series of veinlets infilling tension gashes on the hanging wall of the reverse fault controlling the main vein. The vein strikes E-W and dips at 45–50° to the south. It has a width of around 1 m, up to 3.4 m in bulges, and can be traced for 140 m along strike. Quartz has suffered cataclasis and in places where this is most extreme, to the extent of breccia formation, molybdenite concentrations occur, forming films along joint planes and infilling cavities (up to 3–4 cm across) in quartz. Molybdenum is up to a few percent in such places, especially at the outer edges of the vein, while the average content within the vein as a whole is 0.03%.

Close to the vein (up to 100–150 m) there are numerous anastomosing, mainly shallowly-dipping (10–20°) molybdenite-feldspar-quartz veinlets from a few cm to 10–20 cm wide and up to a few tens of m long. Veinlets are spaced a few cm up to a few m apart. Occasionally they are closer together and form sub-parallel series. Molybdenite is medium-grained (1–4 mm), flakey, forming uneven disseminations or rosettes concentrated mainly in zahlband veinlets in the feldspar bands. Pyrite occurs with the molybdenite, magnetite is rarer, and scheelite is found occasionally. Wallrock alteration adjacent to the main vein is weakly expressed, mainly as chlorite, epidote, rarer sericite and silica.

The ore occurrence has a hydrothermal origin, in which several sequential mineral assemblages are identifiable: 1) quartz I + K-feldspar + molybdenite I; 2) quartz II + molybdenite II + pyrite + magnetite; 3) quartz III + molybdenite III + carbonate + hematite. Fluid inclusion studies on quartz indicate that the mineralization temperature was in the interval 250–390°C. Mesozoic magmatism in the region of this mineral occurrence is weakly expressed, mainly as isolated porphyrite dykes. An Early Proterozoic age for the mineralization is most likely. Evidence for this is the fact that the mineralization is restricted to the oldest tectonic zone, with Early Proterozoic granites containing disseminated molybdenite. This does not exclude the possibility that the Mesozoic stage of activity could have been responsible for cataclasis, redistribution and formation of rich ores in the occurrence.

#### 1.4. Gold

Precambrian gold deposits and occurrences in the Dzhugdzhur-Stanovoy terrain can be traced along the southern edge of the Stanovoy block, forming the South Stanovoy gold zone. It has an E-W strike and is controlled by the North Tukuringra and Mongolia-Okhotsk deep faults (Anon., 1981b). Several gold-bearing regions have been delineated within the zone, where native occurrences are found *in situ* (Dambuksa, Sugdzhur, Kupuringra and Chogar regions) alongside Quaternary placer gold deposits. Gold is associated with mineralized retrograde rocks, developed at the expense of Archaean metamorphic units. So far, there are no known deposits with economic significance except for the Zolotaya Gora deposit, now exhausted, but there are a number of practical prospects.

The Zolotaya Gora ("Golden Hill") deposit, discovered in 1917, is located on the Tukuringra ridge in the source region of the Khugdera river, a tributary of the Gilyuy. The area consists of biotite and amphibole gneisses and amphibolites, intruded by numerous Early Stanovoy leucocratic plagioclase granites and Phanerozoic dykes with pyroxenite, hornblendite, syenite and dioritic porphyrite compositions. The gneisses have been retrogressed to varying extents.

The deposit occurs in a shear zone containing intensely retrogressed gneisses and amphibolites, concordant with the host rocks. It has a NW (310–335°) strike, dips to the SW at 20–50°, is up to 200 m wide, and has a strike length in excess of 10 km. The zone has been cut by a number of oblique faults (Fig. 97). It consists of several concordant, sequential veins: quartz–feldspar, quartz, calcite, and zeolite. Gold is mostly associated with the quartz and calcite veins. Quartz veins are found on the footwall of the retrograde zone, forming a suite of six parallel branching veins 0.3–0.6 m thick. The veins consist of quartz showing a variety of grain sizes, and contain xenolithic fragments of country rocks and minerals – mica, amphibole and epidote. The quartz veins are cut by calcite veins. Sulphide mineralization is common in the veins, represented mainly by pyrite and less frequently pyrrotite and occasionally chalcopyrite, galena and molybdenite. Gold in veins is associated with sulphides, and is very unevenly distributed, in separate ore branches. The gold content in veins is typically higher where they are in contact with amphibolite and graphitic gneiss.

Native gold is very fine and as a rule is developed along fractures and in vein cavities, while in host retrogressed rocks it forms flakes around lenticular quartz segregations. An oxidized zone is very intensely developed in the deposit, with gold forming large grains and variously shaped nuggets. The No. 4 quartz vein is the only one in the deposit which is economic, also a calcite vein situated on its footwall. The deposit is hydrothermal in origin and belongs to the gold–quartz–sulphide formation. No association between the ore-bearing quartz and calcite veins and intrusive activity has been established. As far as their age is concerned, they relate to both Early

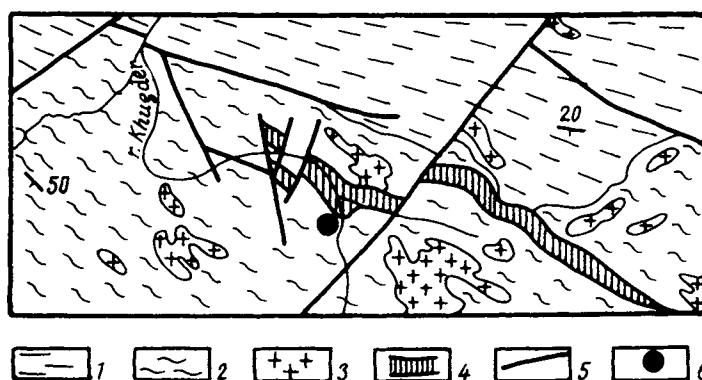


Fig. 97. Geological sketch map of the region around the Zolotaya Gora ("Golden Hill") deposit. 1 - Chimchan gt bi gneiss, 2 - Uryum hb-bi gneiss, 3 - Old Stanovoy granite, 4 - retrogressed rocks, 5 - faults, 6 - Zolotaya Gora ("Golden Hill") ore deposit.

Proterozoic mineralized zones of retrogression, and indirectly to late Jurassic quartz syenite dykes.

### 1.5. Phosphorus, iron and titanium

Over the last decade the Dzhugdzhur–Stanovoy terrain has become a major apatite province in the former Soviet Union, with forecast reserves of  $P_2O_5$  estimated at 640 million tonnes (Roganov et al., 1986). This province occupies most of the area of the terrain as well as the southern marginal zone of the Olyokma terrain and the Precambrian Baladek basement inlier in the Mongolia–Okhotsk geosynclinal system (Belyayev et al., 1981).

Four apatite-bearing geological formations have been identified within the Dzhugdzhur–Stanovoy terrain: marble–gneiss, anorthosite–gabbro, amphibolite–gabbro, and anorthosite (Table 11). The anorthosite is considered to have the greatest prospects for phosphate ores, while the productivity of the others has not been evaluated.

Anorthosite intrusions are exposed over an area greater than 12,000 km<sup>2</sup> and occur in Early Precambrian basement inliers. They possess a number of common features: they occur among granulite-facies metamorphic rocks, with which they have predominantly tectonic contacts, they are accompanied by alkali granites, and in most cases they are intensely retrogressed. The polyphase intrusions have a zonal structure: at the centre is anchi-monominerale anorthosite and at the margins gabbroic rocks are interleaved with anorthosite or less commonly pyroxenite. Two anorthosite varieties can be distinguished on the basis of chemical and mineral composition: labradorite and andesine, which differ in the extent of ore content and the composition of apatite

Table 11

Apatite-bearing geological formations in the Dzhugdzhur–Stanovoy terrain

a) apatite fm b) productivity c) age	Ore formation	Mineral type of deposit	Forecast reserves: $P_2O_5$ content of ore, %	Examples of ore deposits, occurrences
a) marble–gneiss b) unknown c) AR	Phosphorus– rare earth	apatite–REE– carbonate	nil, 5–6%	Chogar, Upper Gar- min, Chagay, etc.
a) anorthosite– gabbro b) low c) AR, PR	Phosphorus–iron– titanium	apatite–ilmenite– titanomagnetite	20/2–4%	Kovaktin, Kruchinin, Alenguy
a) amphibolite– gabbro b) unknown c) AR–PR <sub>1</sub>	Phosphorus–iron– titanium	apatite–ilmenite– titanomagnetite	20–3–4%	Luchin, Utugey, etc.
a) anorthosite b) productive c) AR–PR <sub>1</sub>	Phosphorus–iron– titanium	apatite–ilmenite– titanomagnetite	420/4–8%	Gayum, Bogide, Dzhanin, etc.

occurrence. Overall, the mineral genesis of the anorthosite formation is characterized by complex apatite-ilmenite, apatite-ilmenite-titanomagnetite, rare-earth and zircon occurrences.

Apatite mineralization is seen in all anorthosite intrusions, but economically important accumulations are found only in andesine types (Geran and Segtag), which host a phosphorus-iron-titanium ore formation. This ore formation is represented by early magmatic (Bogide, Maymakan and others) and late magmatic (Dzhanin, Payum and others) genetic types. Four apatite regions have been identified in the Dzhugdzhur-Stanovoy terrain: Geran, Bryantin, Lantar and Chogar (Roganov et al., 1986). The Geran region has normal and poor prospective deposits, mostly complex apatite ores, and the following description is based on material published by Ye.A. Panskikh and V.V. Gavrilov (Anon., 1983; Panskikh, 1986).

*The Geran region* is located in the northern Khabarovsk province, in the Geran anorthosite intrusion, with an area of some 3000 km<sup>2</sup>, which is a fragment of the major Proterozoic Dzhugdzhur pluton. The massif of anorthosites occurs among Early Precambrian rocks, metamorphosed at granulite facies, with which it is in tectonic contact. Country rocks immediately adjacent to the intrusion are subcordant with the configuration of the intrusive boundaries. The intrusion is zoned with anorthosite, gabbro-anorthosite and rare gabbro-norite schlieren at the centre. Gabbroic rocks alternate with anorthosite and occasionally pyroxenite at the edges of the massif, and these rocks have signs of original igneous layering. The massif has been altered by granite and syenite in the western and northern margins where it is in contact with the Proterozoic Ulkan granitoids. Rocks in the southern part of the massif which occur in a regional shear zone, have undergone greenschist facies dynamometamorphism. Two genetic types of complex apatite-ilmenite-titanomagnetite ore have been identified within the Geran intrusion. These are the early magmatic Bogide and Maymakan, and the late magmatic Dzhanin and Gayum deposits, which have been studied to different extents. The Maymakan and Gayum deposits will serve as examples.

*The Maymakan deposit* is found on the northern slopes of the Dzhugdzhur mountain range in the upper reaches of the river Maymakan in the Ayan-Maya region of the Khabarovsk province. It is located in the SE layered margin of the Geran intrusion, bounded to the south by a Cretaceous granitic intrusion. Host rocks form an alternating sequence of pyroxenite, gabbro, gabbro-anorthosite and anorthosite sheets (Fig. 98). Leucocratic rocks increase in amount upwards in the section. All the rocks contain dispersed disseminations of apatite, ilmenite and magnetite. The rocks in the intrusion are cut by granodiorite-porphry and dioritic porphyrite dykes, in places they are schistose and retrogressed, and dislocated along NW-striking faults. From base to top in the deposit, several zones have been identified with disseminated ilmenite-apatite-titanomagnetite mineralization, forming conformable major and minor lenticular and sheet-like deposits from a few m to 200 m thick. The deposits form an ore horizon 700-1400 m wide and some 4 km long, with a NE strike (050-070°). Ores are anorthosite and gabbro-anorthosite, less commonly gabbro and pyroxenite, containing over 12% apatite. Ore deposits are separated by barren rocks of the anorthosite complex. The effects of faulting are widespread throughout the mineral deposit.

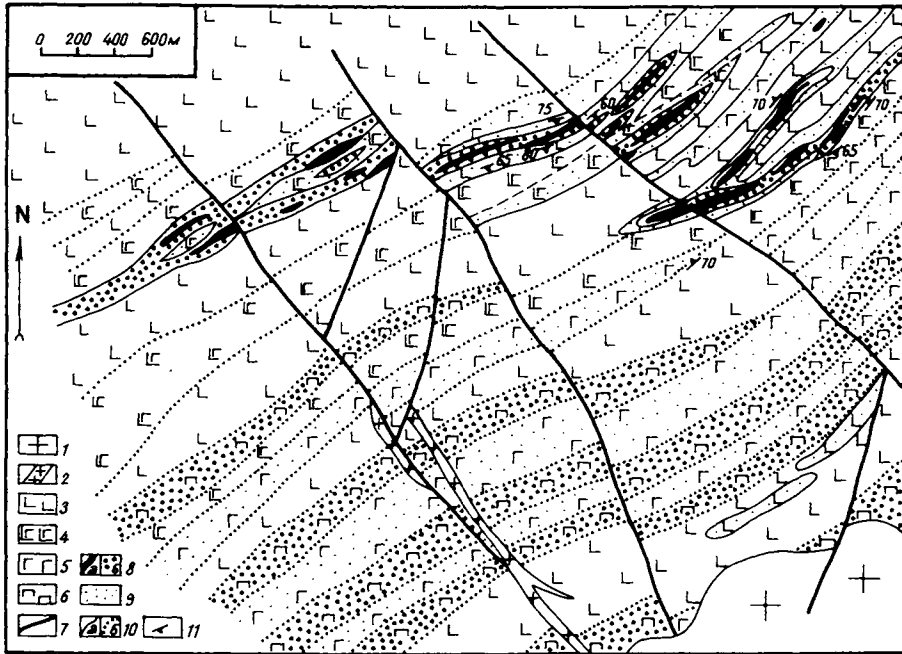


Fig. 98. Geological sketch map of the Maymakan deposit (Smirnov, 1974). 1 - Cretaceous granite, 2 - porphyry veins; 3-6 Geran massif: 3 - anorthosite, 4 - gabbro-anorthosite, 5 - gabbro, 6 - pyroxenite, 7 - faults, 8 - apa-ilm-titanomag ores (a - massive, b - disseminated), 9 - dispersed ore minerals, 10 - geol boundaries (a - various ages, b - facies varieties of rocks), 11 - dip & strike.

The ore deposits have up to five rhythms with a similar structure: massive or patchy ilmenite-apatite-titanomagnetite ore, patchy or patchy-disseminated ore with this same composition and very uneven ore mineral distribution, disseminated ore, anorthosite or gabbro-anorthosite with dispersed apatite disseminations. Mineralization decreases in intensity upwards in the section. Individual rhythms range in thickness from 15 to 60 m, with gradual transitions between the rhythms. In the large bodies, rhythms usually commence with massive or patchy titanomagnetite-apatite-ilmenite ores, containing 25-50% fine-grained apatite. The top and middle parts of ore bodies contain thin (up to 12 m) layers and lenses of ilmenite-apatite ores, with up to 60% apatite, while the apatite content does not exceed 15% in the upper parts of ore bodies. The parameters of the ore bodies and their apatite content are maintained at depth, as confirmed by drilling to depths of 400 m. Forecast reserves for this deposit have been estimated at 110 m.t.  $P_2O_5$ , for a 7.3% grade (Gavrilov et al., 1987). Representative late-magmatic types are the Gayum and Dzhanin deposits, as well as numerous minor occurrences. While the deposits have an overall similarity in ore body morphology (vein, stockwork, complex configuration) and identical apatite-ilmenite-titanomagnetite mineral type, they differ in that the Dzhanin deposit has mostly olivine gabbro, pyroxenite and peridotite, while the Gayum deposit contains anorthosite and has richer ores.

The *Gayum deposit* is located in the axial region of the Dzhugdzhur mountain ridge, 25 km SE of the Maymakan deposit. It occurs in the central anorthositic part of the intrusion, close to its contact with the marginal facies. Country rocks are represented by labradorite with rare lenticular schlieren of gabbro-anorthosite, gabbro, gabbro-norite and norite, 1–40 m thick, which dip gently to the NW at angles of 25–40°. Megacrystic gabbro and gabbro pegmatites are widespread. Within the deposit, the intrusion is cut by several syn-ore faults striking NE and NW. The deposit is represented by three zones – Western, Central and Eastern, separated from one another by 0.5–1.0 km. Each zone contains a group of closely spaced ore bodies (Fig. 99). The Western zone has five major sub-vertical ore veins from 10 m to 70 m wide and 200–950 m long, and four ore pillars measuring from 120 × 300 m to 350 × 400 m. An ore pillar in the Central zone measures 125 × 500 m, and in addition there are two vein-like bodies which join down-dip. The Eastern zone is represented by two ore bodies with maximum thicknesses 57 m and 35 m and strike-length 500 m and 200 m. The ores in this zone lie close to a granitic intrusion and are intensely metamorphosed. The ore bodies lie at a depth of 200 m below the present erosion level.

Four textural varieties of apatite-ilmenite-titanomagnetite ores have been recognised, with anorthosite as their petrogenetic base: massive, ataxitic, patchy and disseminated. Zoning is present in the ore bodies. Massive ilmenite-titanomagnetite ores occur on the footwall, with 10–12% fine-grained apatite, evenly distributed amongst

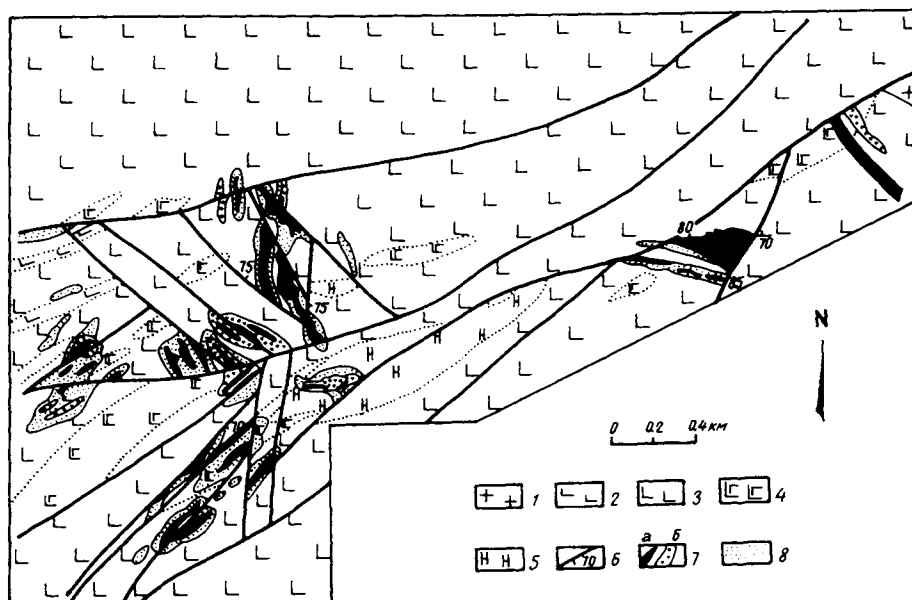


Fig. 99. Geological sketch map of the Gayum deposit (Smirnov, 1974). 1 - Cret. granodiorite; 2-5 anorthosite complex, 2 - labradorite, 3 - andesinite, 4 - gabbro-anorthosite, 5 - norite, gabbro-norite; 6 - faults, dip angle on downthrow side; 7 - apa-ilm-titanomag ores, a - massive, b - patchy & disseminated; 8 - dispersed apatite.

iron–titanium minerals. Both the grain size of apatite crystals and the total amount increase towards the centre of the ore bodies, where there is up to 50% coarse-grained apatite. The apatite content is 15–20% on the hanging wall of the ore bodies. Titanomagnetite and ilmenite in the ores are present in equal amounts. Wallrocks at the contact with the ore bodies contain dispersed apatite disseminations. Forecast reserves for this deposit have been estimated at 100 m.t.  $P_2O_5$  with an 8.4% grade. Average  $P_2O_5$  content in individual ore bodies ranges from 3 to 16%.

## 2. *Conclusions*

Thus, the useful mineral deposits which occur within this terrain belong to both traditional Precambrian ore formations and to those with as yet no analogues. Traditional ore formations, such as ferruginous quartzites, magnesian skarns, rock crystal, poly-metallic in layered basic intrusions, although not differing from types of corresponding ores in other regions, do however from their main characteristics possess a number of features peculiar only to this region. For example, the magnesian skarn formation in Central Aldan from the volume and areal distribution of skarn bodies is the largest in the world, due entirely to its phlogopite content. Magnetite deposits associated with this formation are also almost the only example of such an ore mineralization type. Although ferruginous quartzite deposits are not large in dimension, the magnetite ores of the Chara group are nevertheless similar to ores in the Olenegorsk deposit in the Kola Peninsula, and possess high industrial properties, enabling superconcentrates to be obtained which are suitable for powder metallurgy.

These specific features of the deposits arise due to a combination of lithology, metamorphism and deformation in granulite–gneiss terrains and greenstone belts in the region as a whole. It is possible to select individual ore types and trace the evolution of the ore genesis reflecting the sequence in which geological processes have changed, the main factors being the mobilization, migration and deposition of ore elements. A remarkable feature is the polyphase nature of apatite mineralization in Central Aldan: disseminated mineralization in schists and marbles, occurrences in magnesian skarns and major deposits in metasomatic rocks along deep faults. At Khamar–Daban in the Pre-Baikal region, on the other hand, apatite enrichment in calc-silicates occurred earlier, at the lithogenesis stage, in amounts close to economic, but superimposed processes of dislocation metamorphism and metasomatism did not lead to any significant redistribution and concentration of phosphorus. The Slyudyanka skarns of Khamar–Daban have only minor phlogopite occurrences, while in similar geological settings such as the Precambrian of the Canadian Shield, fairly large apatite deposits were able to form. Exclusive to the Precambrian in this region is its copper content. The formation of the Kodar–Udoka cupraceous sandstones resulted from the favourable combination of a sequence of internal and external processes which not only led to the redeposition of copper, but also its concentration in rocks which had no primary copper enrichment.

In conclusion, it is worth emphasising the following circumstance. In describing the deposits, we noted the complex history of migration and deposition of many ore-

forming elements, expressed as the existence of a series of petrogenic types of the same ore – igneous, metamorphic and metasomatic, formed in different periods. Such complexity in ore mineralization is taken to indicate that the deposits are “polygenic”. However, through the entire extensive period of migration and the multiplicity of geological factors, leading to ore deposition, it is none the less possible to recognise the existence of a definite range of ore genesis through time. The overwhelming majority of deposits belong to metamorphic–metasomatic and hydrothermal–magmatic types, i.e. they have their origin in internal processes. A study of the time of ore mineralization shows that various ore types were formed during the Early Proterozoic epoch (2.2–1.7 Ga), when ancient high-grade metamorphic rocks underwent repeated structural and metamorphic reworking, leading to the redistribution and concentration of ore elements. Within this extended time interval, there was a definite sequence of ore formations, magmatic, metamorphic and metasomatic. This circumstance points to the need for a detailed study of the products of structural, metamorphic and hydrothermal–metasomatic reworking of ancient crystalline rocks, which may have a different geological expression in different terrains.

This Page Intentionally Left Blank

### Section 3:

## Basement inliers around the Siberian craton and adjacent fold belts

V.Ya. KHILTOVA

### *1. General geological features*

Basement inliers around the edge of the ancient Siberian craton previously included the crystalline rocks which crop out along its SW edge (Obruchev, 1949). These are the rocks of the SW Pre-Baikal region, Pre-Sayan region, and the South Yenisey ridge (the Angara-Kan microcraton). These territories are also now quite frequently considered to be similar types of tectonic structure, the mineral deposits of which are grouped together into a single Baikar-Yenisey metallogenic province (Bilibina, 1985). Depending on the volume of information available on the geology and metallogeny of the regions, the whole marginal structure of the craton was subdivided into independent tectonic structures of smaller orders of magnitude, with identified metallogenic zones and belts.

Of all the regions that were previously regarded as marginal basement inliers of the Siberian craton, geochronological and geological evidence confirms that only the Pre-Sayan inlier had a sub-cratonic evolution, beginning in the Early Proterozoic, which establishes beyond doubt that it belongs to ancient cratonic structures. Some workers (Amantov et al., 1988) quote evidence that the stratigraphic cover of Archaean rocks in the South Yenisey inlier consists of Early Riphean platform sediments, indicating that it can also be considered to be part of the craton basement. However, others maintain that the Archaean basement rocks and the Riphean platform sediments are found only in tectonic relationship and the South Yenisey high is a central massif in the Baikaride fold system of the Yenisey ridge. Finally, a third group considers that the Archaean rocks in the south of the Yenisey ridge belong to the basement of the Baikarides (Votakh et al., 1978).

The issue of whether or not the SW Pre-Baikal region (Pre-Olkhon) should be referred to as a structure of the ancient platform basement is particularly controversial. More and more radiometric data are becoming available for this region (material assembled by S.P. Korikovskiy and V.S. Federovskiy) which point to the widespread effects of high-grade crustal processes, including granulite facies metamorphism, during the Early Palaeozoic. Despite the lack of consensus concerning the status of individual segments of the marginal inliers, on the whole they can be treated as a single terrain which evolved during the early Precambrian according to a uniform scheme that was common across the entire region. Differences between individual parts of the region largely result from their later history.

The ore deposits of Western Khamar–Daban are described in the chapter on “Basement inliers”, as well as deposits located in regions traditionally regarded as marginal inliers (Fig. 100). Most researchers regard this region, which borders on the Siberian craton, as being a component of a younger fold belt framework around the ancient Siberian craton. The description of the region’s ore deposits in this section will allow us to present a more complete picture of Precambrian metallogeny in marginal structures.

The oldest rocks in the inliers are Archaean complexes, forming granulite–gneiss terrains: Sharyzhalgay, Biryusa, South Yenisey, Pre-Olkhon and to a large extent Khamar–Daban. At the present time, these terrains are tectonic blocks, traditionally referred to in the literature as “micro-cratons” – Angara–Kan, Baikal, Biryusa and Khamar–Daban. Supracrustal rocks in granulite–gneiss terrains belonging to structures in the Siberian craton basement are Early Archaean (?Katarchaean) in age. However, to regard these regions as independent Early Archaean tectonic structures is hardly justifiable. They all show evidence of extensive crust-forming processes of Late

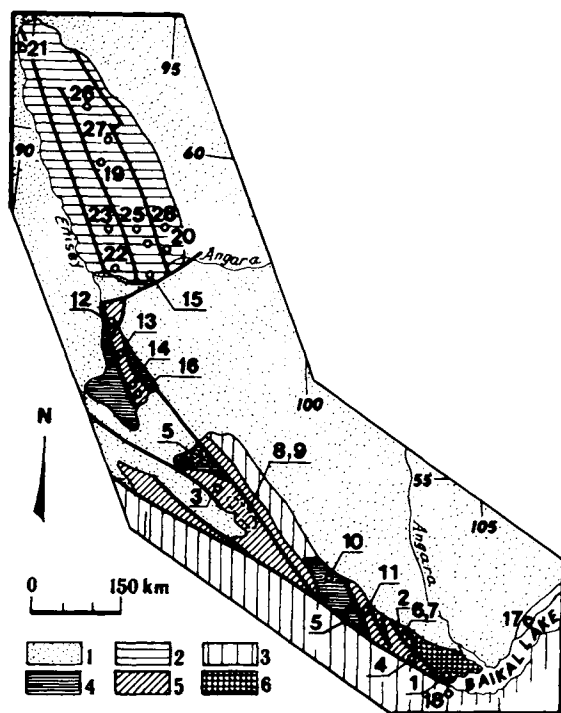


Fig. 100. Distribution of ore deposits and occurrences in Yenisey ridge and Pre-Sayan. 1 – Phanerozoic around Sayan–Yenisey terrain; 2 – PR<sub>2</sub> Trans-Angara; 3 – PR<sub>3</sub> E. Sayan; 4 – PR<sub>1</sub>; 5 – AR<sub>2</sub>; 6 – AR<sub>1</sub>. Deposits: 1 – Baikal Fe, 2 – Sosnovy Bayts Fe, 3 – Maly Tagul Ti-mag, 4 – Kitoy high-Al schist, 5 – rare-metal pegmatite zone, 6 – Kamchadal Talc, 7 – Savvin magnesite, 8 – Biryusa musc pegmatite field, 9 – Neroy-I musc pegmatites, 10 – Belaya Zima Ap, 11 – Bolshaya Tagna Fluor, 12 – Shiver Ti-mag, 13 – Kuzeyev Au, 14 – Bogunayev Au, 15 – Barga musc pegmatites, 16 – Kondakovskoye musc pegmatites, 17 – Sagan Zaba Mn, 18 – Slyudyanka phlog, 19 – Yenashim Fe, 20 – L. Angara Fe, 21 – Porozhinskoye Mn, 22 – Gorevskoye Pb–Zn, 23 – Linear Pb–Zn, 24 – Gerfedskoye Au, 25 – Uderey Sb. Au, 26 – Soviet Au, 27 – Olympiad Au, 28 – Kirgitey magnesite.

Archaean and Early Proterozoic age. Their tectonic structure was formed in the Late Archaean, therefore it is probably more correct to define them using the neutral term granulite–gneiss terrain.

High-grade crustal processes affected all parts of the terrains in the Late Archaean, while Early Proterozoic effects are restricted to the margins of major blocks, i.e. they have an overprinting character. This suggests that the Pre-Sayan inlier and possibly also the Angara–Kan micro-craton, are Late Archaean tectonic structures, in which the basic Archaean structures of upper crustal levels are greenstone belts. In this region, these are the Onot graben in Pre-Sayan, and the Pre-Yenisey (Pre-Divin) belt in the Angara–Kan microcraton. Rocks of the Tepsa complex, which make up synclinal structures, are considered to be the same age as Upper Archaean greenstone belts in the Biryusa microcraton.

Early Proterozoic tectonic structures in marginal inliers include, somewhat provisionally, only the Urik–Iy and Tumanshet grabens in Pre-Sayan, defining them as intracratonic basins. They contain weakly metamorphosed volcanosedimentary rocks, in which clastic terrigenous rocks are an important constituent. High-grade metamorphic complexes (high-T amphibolite facies), the Vesnina and Yenisey groups in the Angara–Kan microcraton, are usually referred to the Early Proterozoic. The nature and type of tectonic structure in which these rocks formed has not been determined, but they were obviously not intracratonic basins. From the end of the Early Proterozoic (1650 Ma), the marginal inliers, like all the ancient cratonic structures, developed in sub-cratonic conditions. Early Precambrian metallogeny is very similar in all the marginal inliers, apart from the Western Khमार–Daban which has its own individual features owing to the peculiar nature of the constituent rocks. Examples here of fold belts adjacent to the marginal inliers are the Yenisey belt (the Trans-Angara part of the Yenisey ridge) and the Baikal–Patom belt (or terrain in this book).

The reason for examining marginal inliers simultaneously with adjacent fold belts is due to the fact that they are not only spatially in contact, but also the mobile belts and marginal inliers were mutually connected during their early Precambrian and later also their Late Proterozoic–Phanerozoic history. Thus, while the Trans-Angara part of the Yenisey ridge evolved independently of the Angara–Kan micro-craton, an identical metallogenic signature is observed over a time span of 1000–800 million years.

The folds belts considered here, especially the Yenisey, are confined to the edge of the Siberian craton. They belong to its folded marginal framework and have both common and distinguishing features. Riphean sediments in each belt were folded and metamorphosed, although the time at which these processes occurred varied. In the Yenisey belt, in pre-Riphean time, a post-Early Proterozoic stabilization event has been clearly established, and here is emphasised by the development of sub-cratonic alkaline igneous complexes (Datsenko, 1984). No such information is available for the Baikal–Patom belt. For the Yenisey belt, geological and geophysical evidence suggest that it evolved on a granulite–gneiss basement. A similar basement for the Baikal–Patom belt can only be supposed for a few zones, such as the Mama, for example. In terms of metallogeny, these two belts have much in common, but there are differences in the time at which the exact same types of useful minerals developed. For example, poly-metallic ore deposits formed at 850 Ma ago (based on lead isotopic studies) in the Yenisey belt, but 750 Ma ago in the Baikal–Patom belt.

This Page Intentionally Left Blank

## The Pre-Sayan inlier

V.YA. KHILTOVA and G.P. PLESKACH

### *1. Geological structure and ore content – general remarks*

Tectonically the Pre-Sayan inlier is a shield made of early Precambrian formations comparable with rocks in the Aldan–Stanovoy shield. To the north, the inlier is overlain by platform sediments, and to the south it is bounded against Precambrian rocks of the younger East Sayan fold belt by the Main Sayan Fault (Fig. 101). Early Precambrian rocks in the Pre-Sayan inlier include Early and Late Archaean and Early Proterozoic. As mentioned previously, there are three components to the early Precambrian tectonic structure of this region – granulite–gneiss terrains, the Sharyzhalgay and Biryusa blocks (micro-cratons); Late Archaean belts, the Onot graben and Tepsa synclinal structures; and finally Early Proterozoic intracratonic basins, the Urik–Iy and Tumanshet grabens.

Basic volcanics play an important role in the composition of the supracrustal rocks that make up the Onot graben, while they are quite insignificant in the Tepsa complex of the Biryusa microcraton. A possible explanation for this could be that only the upper part of the supracrustal assemblage is exposed at the present erosion level in Biryusa, or that the assemblage formed in a special type of structure. The issue remains unresolved. Granulite–gneiss terrains are considered to be Upper Archaean infracomplexes. Early Proterozoic intracratonic basins, located amongst high-grade Early Archaean metamorphic rocks, consist mainly of weakly-metamorphosed volcanosedimentary rocks. Volcanics found in the Urik–Iy graben belong to highly-differentiated series. According to Semeikin (1972), the upper part of the assemblage which makes up the Urik–Iy graben is defined as a molasse, either marine or continental. From its inception, the entire Pre-Sayan region can be considered to have developed in a sub-cratonic regime.

Granulite–gneiss terrains were formed by external and internal crustal processes during the Early Archaean, a feature which is reflected in their metallogeny. Associated with these terrains are such deposits as eulysite-type ferruginous quartzites, e.g. the Baikal deposit, peraluminous schists, e.g. the Kitoy sillimanite deposit, and graphite occurrences. Titanomagnetite deposits around 3 Ga old are common, such as the Malotagul deposit. In addition to Archaean titanomagnetite deposits, the Biryusa granulite–gneiss terrains also typically have younger deposits, such as mica pegmatites, gold, copper, nickel and cobalt occurrences (Khrenov et al., 1988). The Late Archaean greenstone (Onot graben) contains iron ores – the Sosnovy Bayts ferruginous quartzite deposit, magnesite – the Savina deposit, and talc – the Onot group of deposits. There are also tungsten occurrences hosted in carbonates and amphibolites, and cobalt

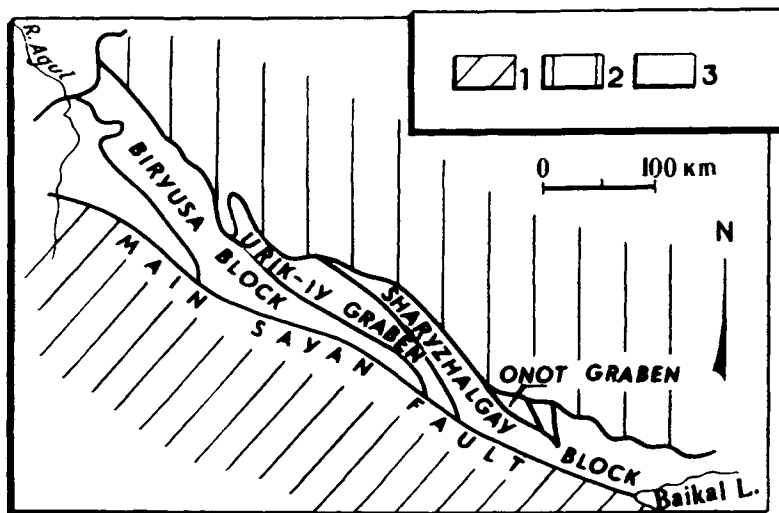


Fig. 101. Sketch map showing tectonic structure of Pre-Sayan basement inlier. 1 - PR + R. Sayan field terrain. 2 - PR-R-Ph platform cover. 3 - A + PR. Pre-Sayan region.

occurrences hosted in diabase dykes. Polymetallic mineralization is associated with the Arban complex of basic rocks. Rare-metal pegmatites and a series of ore shows occur in the Pre-Sayan–Urik–Iy and Tumanshet grabens (mainly the Urik–Iy): Fe (ferruginous quartzites); Ni, Co associated with igneous rocks; Cu, Au, related to hydrothermal processes; Zn, Pb associated with sedimentary rocks and the Early to Middle Proterozoic Gunik complex of granosyenites. Rare-metal mineralization has also been found in the granosyenites. The Pre-Sayan inlier contains ore deposits which originated during the stable stage of development, when the intra-cratonic rift was formed with rare metals, apatite, fluorite and magnetite. These are related to central type alkali-ultrabasic intrusions which occur on the NE edge of the Urik–Iy graben with both Early Archaean Sharzhalgay granulites and the Early Proterozoic intracratonic basin. Irkutsk geologists have determined an age for the alkali-ultrabasic rocks of the Pre-Sayan region within the range 700–550 Ma (Rb–Sr method). Apatite deposits in the alkali-ultrabasic complexes are grouped together under the name “the Pre-Sayan phosphate-bearing region”.

## 2. Ore deposits and occurrences

### 2.1. Iron

The *Baikal iron ore deposit* is located in SE Pre-Sayan in the middle reaches of the river Kitoi and belongs to the Kitoi group of deposits, associated with granulite facies rocks belonging to the Early Archaean Sharzhalgay complex (Fig. 102). Other deposits in the group are Kharabarovsk, Saramtin and Kitoysky Zhidoy, as well as several minor occurrences, including Butukhey, Sharzhalgay, Khondor, etc. (Uchitel et al., 1966).

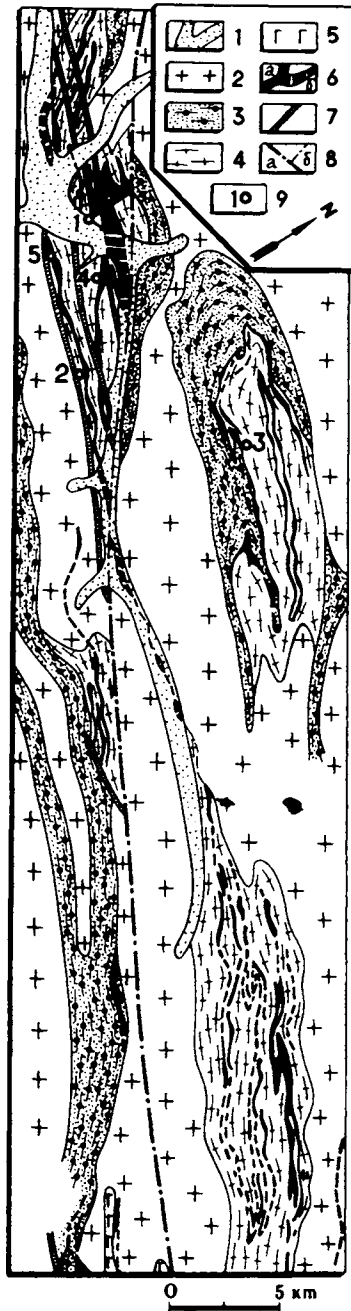


Fig. 102. Geological sketch map of Baikal ferruginous quartzite deposit, compiled by A.A. Shafeyev and Yu.D. Buinov (1981), with material provided by V.M. Speshilov. 1 – Quaternary, 2 – Kitoy gneissose granite, charnockite, enderbite, 3 – quartzite & gneissose granite, 4 – hbl-2-px schist, 5 – gabbro-norite, 6 – ore bodies (a – exposed, b – buried), 7 – diabase dykes, 8 – faults (a – exposed, b – buried) 9 – boreholes.

The Baikal deposit is the largest of its type in the Pre-Sayan region. All the deposits named above constitute the Baikal iron ore zone, stretching in a NW direction for 100 km. The deposit, which was discovered in the early 1960s, has been studied by Uchitel et al. (1966), Shafeyev and Buinov (1981). It is located in a large fold structure, which some claim is an anticline, others a syncline. The ore-bearing unit in which the individual bodies are sited is characterized by a magnetic anomaly of up to 5–7 MOe. Ferruginous quartzite ore bodies occur in either pyroxene and biotite–pyroxene gneisses with thin amphibolite sheets, or in pyroxene–amphibole, biotite and amphibolite sheets, or in pyroxene, amphibole and high-alumina schists. The ore bodies are podiform and sheet-like, and generally concordant with the host rocks (Shafeyev et al., 1981). They are restricted to areas of intense deformation, and vary in length from a few hundred m to 2 km, and from a few m to 10 m thick. Compositionally, the ores are mainly quartz–pyroxene–magnetite, quartz–amphibole–magnetite, and quartz–magnetite, with disseminated and massive textures. They are subdivided into three groups: 1) massive quartz–magnetite with 35–45%  $\text{Fe}_2\text{O}_3$ ; 2) uneven-grained pyroxene–quartz–magnetite with 25–35%  $\text{Fe}_2\text{O}_3$ ; and 3) disseminated pyroxene–feldspar–magnetite with 15–25%  $\text{Fe}_2\text{O}_3$ . Contacts with country rocks are usually gradual and often the ores can be distinguished from the host rock composition by their higher magnetite content. Ore types alternate in a section. From the composition and metamorphic grade of the country rocks, and from the mutual relations of individual rock types, the deposit can be classified as eulysitic type.

*The Sosnovy Bayts deposit* belongs to the Late Archaean Onot group of iron ore deposits in the Pre-Sayan. They have been known since 1887, but they were not studied prior to the 1930s. Then, and later in the 1960s, investigations were carried out in the middle reaches of the river Onot and adjacent territories, leading to the discovery of the Biboy, Southern and New ore deposits and occurrences (Fig. 103). They are all found in graben-type structures, filled with Upper Archaean formations (but previously thought to be Lower Proterozoic). The Sosnovy Bayts deposit (Polyakov, 1936) is located in the centre of the Onot graben and comprises sheet-like deposits among amphibole, chlorite–biotite, garnet–biotite and high-alumina schists. Country rocks display zonal metamorphism from amphibolite to low-temperature epidote–amphibolite facies (sillimanite–kyanite facies series). Useful components in the deposit are magnetite, hematite and martite.

Ore bodies are in beds, traceable for 120 m along strike, with an average thickness of about 1 m (Fig. 104). The ore-bearing member is over 123 m thick, of which 66 m is occupied by ore beds. The deposit contains three mineralogical ore types: 1) cherry-red quartzite and quartz–mica schist in the upper horizons; 2) brownish-grey schistose quartzite in the middle; and 3) even-grained, steel-grey quartzite, the commonest type. The first type is the least common. In these ores, the ore mineral content is around 50%, with magnetite almost completely replaced by hematite. Banding and schistosity are poorly expressed in type 2, although there is a detectable alternation of richer and poorer layers, containing 75–85% and 20–25% ore mineral respectively. Hematite is the main ore mineral and there are frequent relicts showing that it has replaced magnetite. Type 3 ores are massive and usually fine-grained. Banding is either not observed or is wavy and discontinuous. Quartz and the ore minerals are evenly

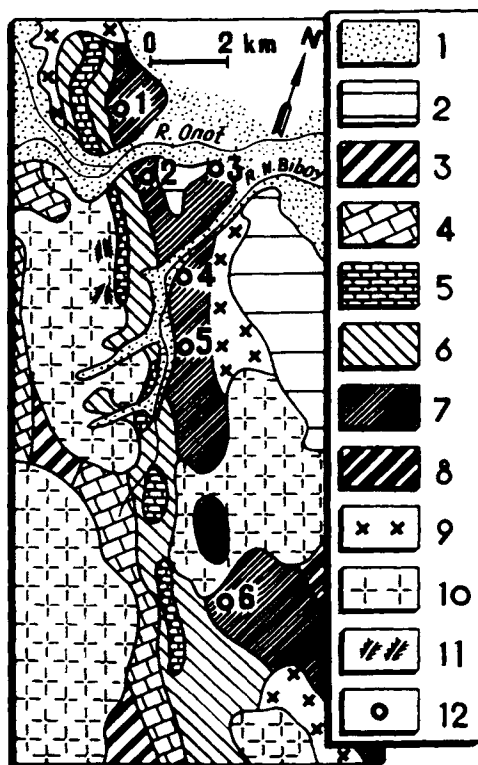


Fig. 103. Geological sketch map showing structure of Onot group of deposits (Polyakov, 1936). 1 – Quaternary, 2 – Cambrian, 3 – L. amphibolite & hbl schist, 4 – L. lst, 5 – U. lst, 6 – U. amphibolite & hbl schist, 7 – Fe-rich schist, 8 – gt amphibolite, 9 – bi gneiss & gneissose granite, 10 – granite, granodiorite, 11 – pegmatite veins, 12 – location of deposits.

distributed. Ore compositions in this deposit are on average 34–36%  $\text{Fe}_2\text{O}_3$ , 3–5%  $\text{FeO}$ , 46–49%  $\text{SiO}_2$ . Massive ores, which form rare podiform deposits upto 5m thick, contain 92%  $\text{Fe}_2\text{O}_3$ , 1%  $\text{FeO}$  and 7%  $\text{SiO}_2$ . Rich martite ores have been bound in a weathered mantle in the continuation of the Sosnovy Bayts deposit beneath the platform cover. Data from two boreholes prove that the ore is less than 2 m thick (Uchitel et al., 1966).

This deposit can be dated only from the age of the host rocks. Recent work done on syntectonic granite–gneiss exposed in the Onot graben (the Onot complex) has yielded an age of  $3250 \pm 50$  Ma (Rundqvist and Mitrofanov, 1993). These granites may have formed at the expense of a rheomorphosed basement, which means that the figure quoted above does not reflect the age of the rocks in the Onot graben. However, thermo-emission data obtained from both Onot graben granites and the country rocks intruded by these granites, suggest that the rocks in the graben formed during the Archaean (Rundqvist and Mitrofanov, 1993).

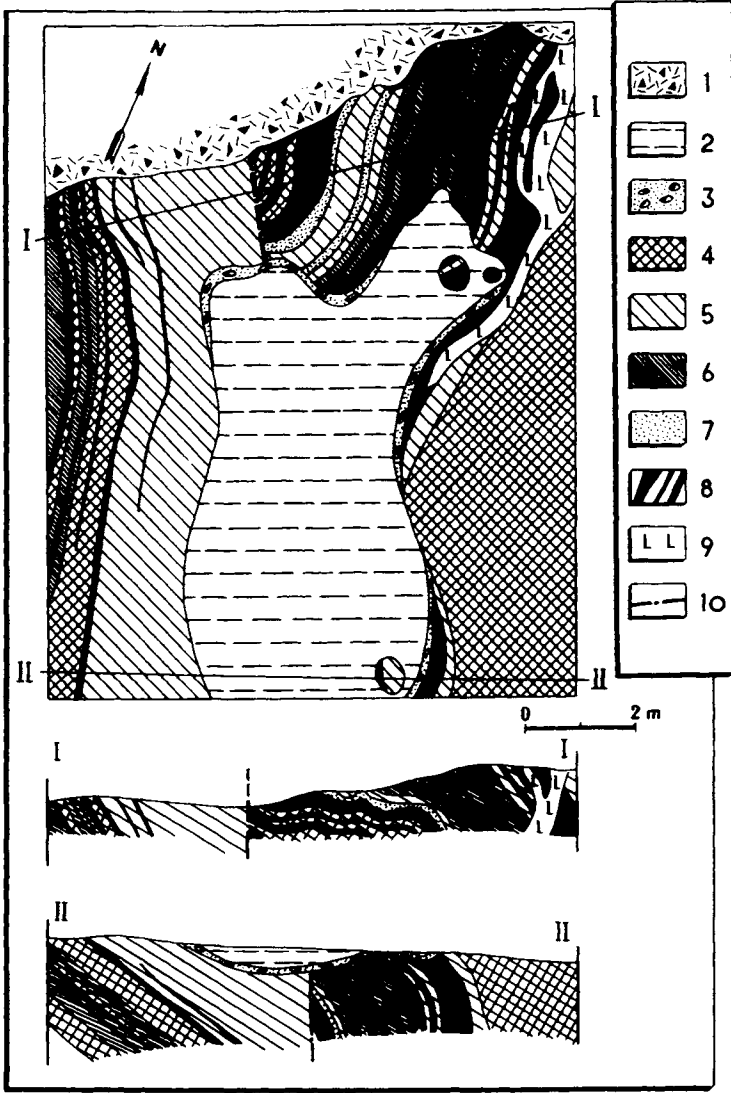


Fig. 104. Sketch map and section showing structure of Sosnovy Bayts productive unit (Polyakov, 1936). 1 – drift, 2 – Cambrian, 3 – basal conglomerate, 4 – amphibolite, 5 – hb schist, 6 – bt-chl schist between ore beds, 7 – bt gneiss, 8 – ores, 9 – diabase, 10 – faults.

At present, there is no agreement on the genesis of the deposits. Mikhailov (1983) emphasises such features found in the Sosnovy Bayts deposit as the presence of massive gabbro–diabase amongst members containing ferruginous quartzites and garnet–mica schists, within which shear zones are found to contain magnetite and quartz that appeared during the emplacement of the gabbro–diabase bodies. This and other evidence has led researchers to conclude that the Sosnovy Bayts deposit, like others in the

group, may be classified as metasomatic. Most workers consider that the deposits belong to jaspilite-type banded iron formations. This is based on such facts as: 1) the close association between ferruginous quartzite and amphibolite, 2) the presence of aluminous rocks (sometimes peraluminous) and carbonate intercalations amongst amphibolites, and these are often finely interleaved with the ferruginous quartzites, 3) fine banding, typical of banded ironstones, and other structural and textural features common in volcanosedimentary rocks.

## 2.2. Titanium

*The Malotagul deposit* was discovered during aerial surveying in 1965, and has been studied by A.S. Baryshev, N.S. Suvorin and O.M. Glazunov, among others. The deposit is located in the Biryusa micraton in the middle reaches of the river Tagul, between the Tagul and Tumanshet rivers. It is associated with metagabbroic rocks, in an ancient granite–gneiss unit within the Archaean Biryusa complex (Fig. 105). The age of the granite–gneiss associated with the metagabbro is  $3260 \pm 50$  Ma, based on a recent Rb–Sr determination obtained by I.A. Romanov and co-workers.

The area in which the metagabbroic rocks occur is structurally inhomogeneous (Mekhanoshin et al., 1980). The internal structure of the various blocks identified here is complicated by faults. Mineralization, amphibolization, and sometimes migmatization occur along NE-striking faults which affect the metagabbros. Primary structures are practically not preserved in the massif, with only occasional examples of primary banding with melanocratic and leucocratic rocks alternating. Primary minerals and textures in gabbroic rocks are equally rare. It is assumed on the basis of relict primary minerals that the original rocks in the intrusion were gabbro, gabbro–norite and their extreme differentiates, pyroxenite and anorthosite. It has also been assumed that the ore bodies occur along the contact between gabbro and granite–gneiss (Fig. 106). Transformations in metagabbro related to regional metamorphism occurred at high temperatures, sufficient to cause eclogitization of these rocks. From their petrochemistry, the metagabbros have high iron and low alkali contents, a relatively high Fe : Ti ratio and higher vanadium, thus the deposit may be considered to be vanadium–iron–titanium. Three main ore types are represented in the deposit: disseminated, massive (rarer), and sideronitic, based on the dominant texture.

Ore bodies usually have a sheet-like or podiform shape, with variable thickness and occasional branching. Lenticular bodies are 50–480 m long and 8–80 m thick. The main minerals are magnetite and ilmenite. Magnetite almost always contains ilmenite and spinel platelets as solid phase dissociation products, while ilmenite has magnetite. Mn-garnet is an associated mineral. Massive and sideronitic ores have sharp contacts with both disseminated ores and with the metagabbroic rocks. Disseminated ores are connected to metagabbros by gradual transitions. The following ores are distinguished, depending on which mineral predominates: titanomagnetite–ilmenite, titanomagnetite–ferro-ilmenite, magnetite–ferro-ilmenite, magnetite–ilmenite, hematite–ilmenite. Massive ores consist of titanomagnetite and ferro-ilmenite aggregates, in which titanomagnetite predominates. Titanomagnetite and ilmenite predominate in the sideronitic ores.

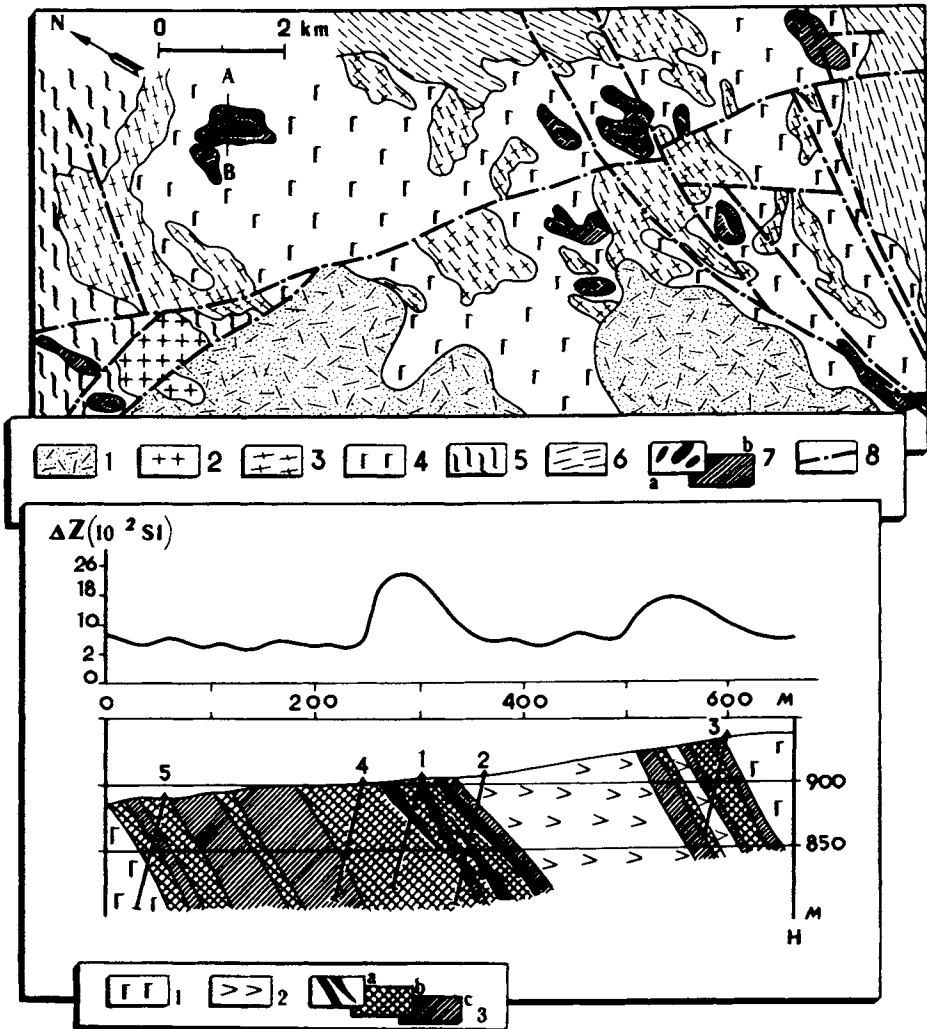


Fig. 105. Geological sketch map and section, *Malotagul* deposit (Shafeyev and Buinov, 1981). 1 – felsite & felsite-porphry (PZ<sub>3</sub>), 2 – granite (D), 3 – gneissose granite (AR<sub>1-2</sub>), 4 – gabbro-anorthosite, 5 – amphibolitized gabbro, 6 – ortho-amphibolite, 7 – Biryusa schist (a) & gneiss (b) (AR<sub>1-2</sub>), 8 – faults. Cross-section: 1 – amphibolitized gabbro, 2 – gabbro-anorthosite, 3 – disseminated ilmenite-magnetite & titanomagnetite ores, with % Fe (a) 30, (b) 10–30, (c) 10–20.

The *Malotagul* intrusion is the largest in the Biryusa microcraton, but there are also smaller bodies. In the Monkres metagabbro intrusion in the eastern Biryusa on the right tributaries of the river Uda there is only low-grade magnetite-ilmenite mineralization. The localization of ores in metagabbroic rocks is related not only to the magmatic process itself, but to a significant extent is also the result of metamorphic processes (Mekhanoshin et al., 1980).

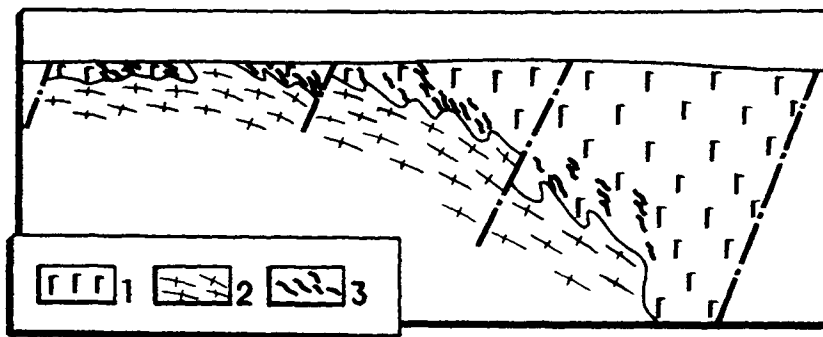


Fig. 106. Schematic model of deep structure of Maly Tagul massif (Mekhanoshin et al., 1980). 1 – metagabbro, 2 – gneiss, 3 – ore bodies.

### 2.3. Aluminium

The *Kitoy (Dabady)* sillimanite schist deposit was discovered by I.M. Shirobokov and other geologists from the Irkutsk Geological Survey. It lies in the SE Pre-Sayan region on the left bank of the river Kitoy and is a constituent of a metamorphic series forming the upper part of Early Archaean rocks. The metamorphic rocks are represented by quartzite, marble, para- and ortho-amphibolites, biotite gneiss and sillimanite gneiss (Fig. 107). The sillimanite schist and marble are thought to form the core of a major synclinal fold. Some workers have proposed that the Kitoy metamorphic assemblage which includes the sillimanite schists and marbles should not be included in the Sharyzhalgay complex, and should be referred to younger (Early Proterozoic) formations. However, Kitoy Group rocks have undergone a complex polymetamorphic history, commencing with a granulite facies event which is typical of the Sharyzhalgay complex, thus it is quite justifiable to relate the Kitoy Group to the Early Archaean.

Sillimanite schists with economic sillimanite contents form a band which has a constant thickness and can be followed along strike for several km (Shirobokov, 1961). It is underlain by amphibole–biotite gneiss. The productive horizon contains cordierite–biotite–sillimanite schist and gneiss, and garnet–andalusite–sillimanite schist, with corundum forming in the schists at their contact with pegmatitic granite veins. The sillimanite content in the 50–150 m thick productive horizon is around 70%. The three schist varieties are: 1) dark grey (from the high biotite content), dense, with 20–25%

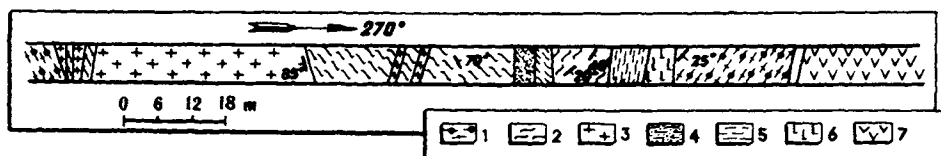


Fig. 107. Kitoy sillimanite schists, River Nukhun-gol (Khiltova, 1971). 1 – bt-amph gneiss, 2 – silli schist, 3 – granite dykes, 4 – bt schist, 5 – bt gneiss, 6 – gabbro, 7 – amphibolite.

$\text{Al}_2\text{O}_3$ ; 2) dense, with wavy-crenulated texture, and well-formed prismatic sillimanite accounting for 20–40% of the rock, with this particular variety making up 50–60% of the total mass of the sillimanite schists; 3) knotted rocks, sometimes coarsely banded, with 40–55%  $\text{Al}_2\text{O}_3$ . In the late 1950s, most researchers considered the sillimanite schists to be primary sediments. Later it was proposed that the schists had formed during acid leaching related to the final stages of regional metamorphism (Khlestov et al., 1965). Subsequent analyses of rock lithology, petrochemistry, geochemistry and metamorphic sequences reconfirmed the primary sedimentary genesis of the sillimanite schists, which began as kaolinitic clays deposited in a shallow-water basin (Khiltova, 1971).

#### 2.4. *Rare Metals*

Rare-metal pegmatites in the Pre-Sayan marginal inlier form an extensive province, over 400 km long. The majority of the rare-metal pegmatites are found in the Urik-Iy graben, which contains Early Proterozoic sediments cut by granites belonging to the Sayan complex. The geology of these pegmatites has been studied by G.Ya. Abramovich, P.S. Shames, among others.

The rare-metal pegmatites contain microcline and are either weakly or intensely albitized. Most occur in western parts of the graben, close to the Belsk-Oka and Main Sayan faults. They are concentrated in four pegmatite fields which may relate to elevations within the graben (Abramovich et al., 1970). A total of 11 pegmatite fields has been identified in the entire Pre-Sayan region (Ryabenko, 1979). Pegmatite veins are broadly controlled by tectonic zones, but against this general background they are localized in minor faults which splay off larger faults, in fractures and in zones with increased jointing. Pegmatite fields are usually associated with ENE- and NE-striking faults, the first of which are often accompanied by increased jointing with characteristic linear magnetic anomalies and associated dykes of various compositions. The pegmatite fields associated with these zones are much wider than other regions (upto 15 m, with average width of 5–7 km). The number of pegmatite veins also increases in the ENE-striking zones. The greatest number of pegmatite veins is restricted to places where ENE zones meet NE-striking faults. Replacement processes in pegmatites, with which their ore content is associated, may have been due to the formation of the ENE-striking fracture zones which acted as channelways for solutions (Fig. 108). Biotite and biotite-muscovite granites in the late phase of the Sayan complex have higher Rb, Tl, U, Th, Li, Be and Y contents, suggesting that the rare-metal pegmatites are genetically related to these very granites.

Pegmatite compositions depend to a large extent on the depth at which the granites were emplaced (Abramovich et al., 1978). Strongly albitized microcline pegmatites with rare-metal mineralization are associated with granites which were emplaced 4.5–5.5 km deep. Less albitized pegmatites are associated with deeper-level granites, and finally barren pegmatites with accessory rare-metal mineralization are spatially restricted to the deepest (7–8 km) granites. These pegmatites are also farthest away from the granitic intrusions (Abramovich et al., 1970). Data provided by I.B. Nedumov, N.A. Solodov and others who have studied the rare-metal pegmatites show that it is possible

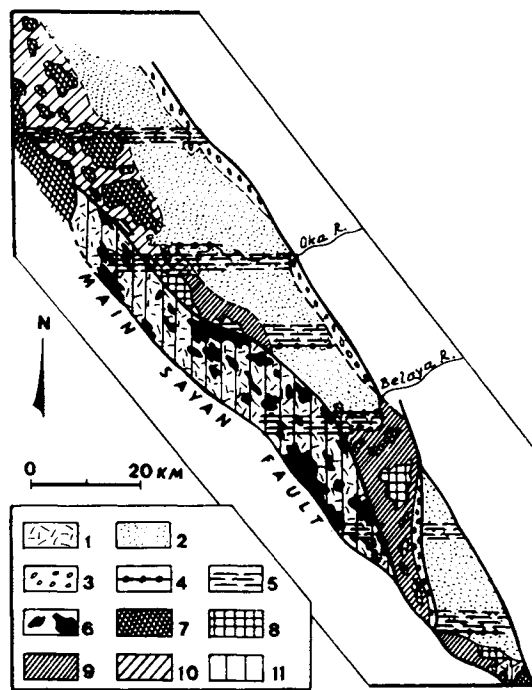


Fig. 108. Distribution of pegmatite fields in Pre-Sayan region (Abramovich et al., 1970). Sediments: 1 – AR, 2 – Pt<sub>1</sub> (undiff.), 3 – PR<sub>2</sub>; 4 – boundary faults, 5 – highly fractured zones. Sayan granitoids PR<sub>1</sub>: 6 – deep-level, 7 – intermediate, 8 – shallow. Pegmatite fields: 9 – albitized microcline, 10 – weakly-albitized microcline, 11 – barren.

to distinguish pegmatites with Ta–Nb–Be, Be–Sn–Li, and complex Be–Sn–Li–Ta–Cs mineralization. Pegmatite veins have complicated forms (Fig. 109) and occur almost exclusively within supracrustal rocks in which amphibolite, amphibolite schist and minor quartzite and mica schist bands predominate. Occasionally they may be found in apical parts of granite intrusions. The most highly differentiated veins contain four or five identifiable zones: 1) aplitic quartz–muscovite, rarer quartz–tourmaline; 2) quartz–microcline–plagioclase; 3) quartz–microcline–spodumene with albite and clevelandite, muscovite, beryl, tourmaline; 4) quartz with a well-expressed core being rare – more often the axial part of a vein has lepidolite, pollucite, rubellite, polychrome tourmaline and other rare-metal minerals in small quantities. Veins with a predominantly quartz–albite–muscovite composition sometimes contain insignificant amounts of cassiterite. Tantaloniobates have been discovered in different zones and mineral assemblages.

A Rb–Sr age determination for the pegmatites yielded a figure of 1700 Ma (Rundqvist and Mitrofanov, 1993). Granites in the Sayan complex have been dated at 1880 Ma by the K–Ar method (Khiltova et al., 1963). Pb–Pb thermo-emission studies have recently been carried out on zircons from the granites. A figure of  $2100 \pm 200$  Ma was obtained for the early granite phase and 1900 Ma for the late phase, thus the Sayan granites are no younger than 1900 Ma.

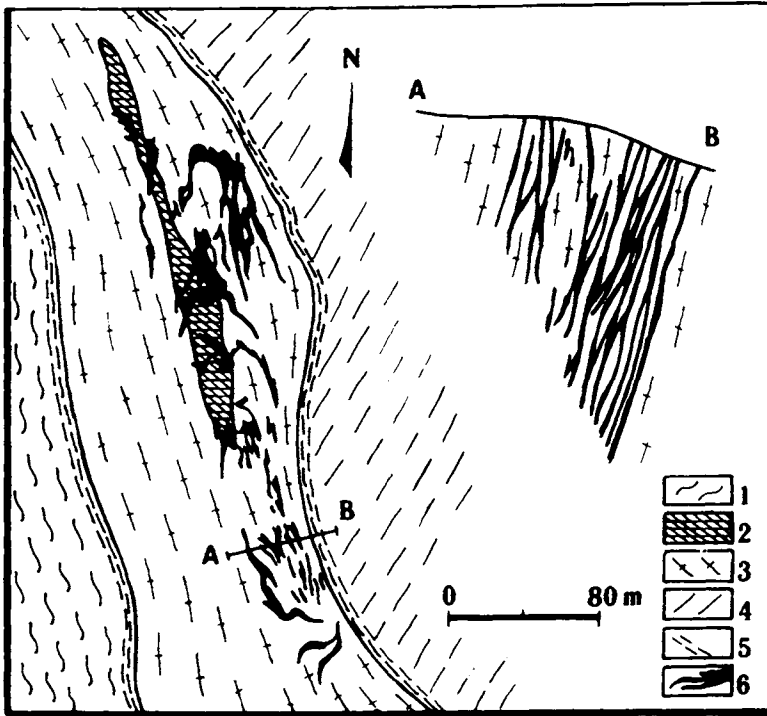


Fig. 109. Geological sketch and section showing structure of spodumene pegmatite deposits (after I.V. Timofeyev, in Smirnov, 1974, vol. 3). 1 - gneiss & mylonite (PR<sub>1</sub>), 2 - massive ortho-amphibolite, 3 - amphibolite & hb schist; 4 - limestone, chlorite-graphite schist, grit (topmost PR<sub>1</sub>), 5 - faults, 6 - spodumene pegmatites.

### 2.5. Talc and magnesite

Talc-magnesite deposits in the Onot graben form a group located in the area between the rivers Onot and Savina. Deposits in this group include Dva Kamnya, Lower Samokhodsk, Kamen, Kamchadal, Vein Suite, and Savina. According to Nadelyayev (1958) and Smolin (1962), the ore field has a total area of 100 km<sup>2</sup> and is associated with a block of rocks (Upper Archaean, from recent studies) that stretches in a NW direction and is separated by faults from a Lower Archaean metamorphic complex to the SW and from Cambrian clastic terrigenous-carbonate (dolomitic) sediments to the NE (Fig. 110).

Rocks in the Upper Archaean block are cut by numerous granite intrusions and younger dolerite dykes. They are divided into the Kamchadal and Sosnovy Bayts groups, the former of which hosts the mineral deposits. There are three horizons - lower (amphibolite), productive (dolomite), and upper (amphibolite). Magnesite and talc deposits occur in the productive carbonate horizon, which due to folding is exposed at the surface as several NW-striking sub-parallel strips. Eastern outcrops of dolomitic rocks contain only small magnesite lenses. The western carbonate strips have

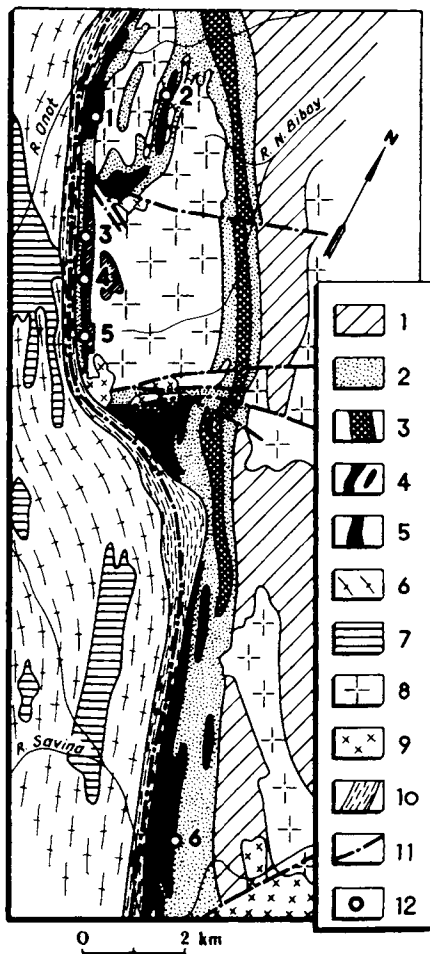


Fig. 110. Deposits in Onot talc field (Nadelyayev, 1958).  $PR_1$  ( $AR_2$ , from recent data): 1 – Sosnovy Bayts Schists & Fe-quartzite, 2 – Upper Kamchadal amphibolite, 3 – Kamchadal productive dolomite, Mg horizon, 4 – Kamchadal productive magnesite, 5 – Lower Kamchadal amphibolite. 6 – Ochkovo granite-gneiss, 7 –  $PR_1$  bt interbanded amphibolite, quartzite, dolomite, 8 –  $PR_1$  bt granite, 9 –  $PR_1$  leucocratic granite, 10 – tectonite zones, 11 – faults, 12 – main talc deposits: 1 – Dva Kamnya, 2 – Lower Samokhodkin, 3 – Kamen, 4 – Kamchadal, 5 – Vein Suite, 6 – Savin.

commercial interest, since they contain large magnesite and talc bodies situated along a SW regional fault. Magnesite deposits are represented by a series of structurally isolated deposits, including sheets restricted to limbs and cores of steeply dipping anticlinal folds. The magnesite is coarsely crystalline, white, light-grey, occasionally pink, brown or dark grey. Textural magnesite types are stellate, radiating or uneven-grained. Impurities present are talc, less commonly chlorite, serpentine, dolomite, quartz, pyrite, iron hydroxides, calcite.

Talc is restricted to magnesite deposits and occurs as disseminations, small veinlets, lenses and large veins both within the magnesites themselves and at the contacts between magnesite and antigorite–chlorite schist, serpentinite and amphibolite. Contacts between talc rock and magnesite are indistinct, indicating that the magnesite has been replaced by talc. Contacts with schist, serpentinite and amphibolite are sharp. Rare magnesite relicts are found within talc veins, also brecciated fragments and serpentinite and schist intercalations. Talc has a fine flakey texture and the colour is greenish-white, light grey, pinkish-white or grey, depending on the impurities. Mineral impurities are chlorite, graphite, hematite, rarer pyrite, magnetite, apatite, dolomite and quartz. Talc-forming processes were most intense in the Kamchadal deposit (Fig. 111), where pure talc rock extends for 500 m with a thickness of around 40 m (Smolin, 1953, 1962). The deposit lies immediately adjacent to a regional fault. Thin silicate intercalations amongst carbonate rocks are characteristic for the productive horizon. In this deposit the talc rocks are basically apomagnesitic, but talc veins are also found within chloritic rocks and contain relicts of the latter. Furthermore, talc

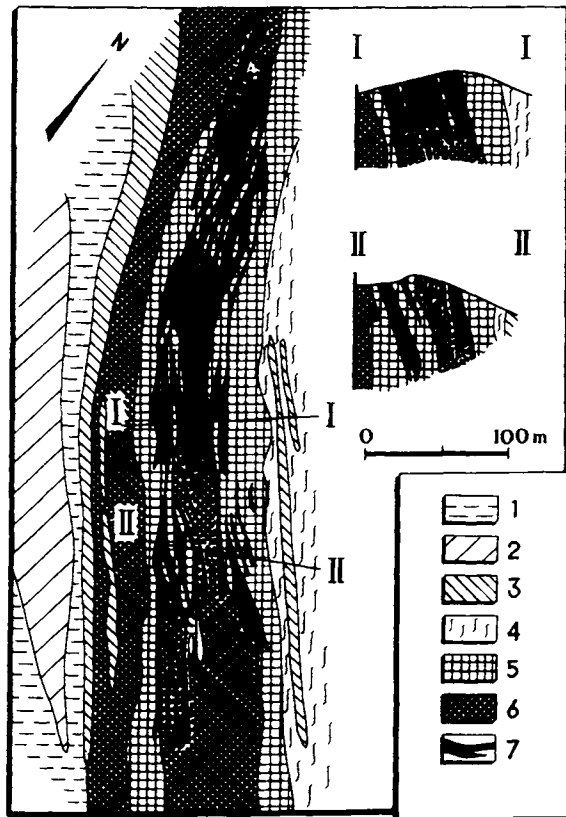


Fig. 111. Geological sketch, Kamchadal deposit (Smolin, 1962). 1 – qzt gneiss, 2 – hbl schist, 3 – epi-chl-hbl schist, 4 – antig-chl schist, 5 – serpentinite, 6 – magnesite, 7 – talc.

ores occur to the west of the main ore body, represented by wide zones of magnesite unevenly replaced by talc, in contact with talc-chlorite apo-amphibolitic rocks. The talc rocks in the Kamchadal deposit have a rather dark greenish colour and are distinguished by their somewhat higher iron content compared to other talc occurrences in the Onot ore field.

Nadelyayev (1958) considered the Onot deposits to be contact-metasomatic, formed under the influence of leucocratic granite intrusions. According to Smolin (1962), deposits in the Onot ore field originated during a retrogressive phase in the metamorphism of the rock assemblage, and the talc ores are contact-reaction formations occupying particular zones in the metasomatic column.

*The Savina magnesite deposit* is one of the world's largest magnesite deposits. It belongs to the Onot-Savina group in the western part of the N-S Onot graben (Poletayev et al., 1975). There is no agreement about the structure of the graben, since it has been completely folded and faulted. Rocks dip at 40° to 80° in the vicinity of the mineral deposit. The deposits in this group are believed to have formed under the influence of the Alagnin-Kholomkhin deep fault, which is thought to have been emplaced during the Late Archaean and judging by the appearance of later magmatism, it was activated twice more.

Kamchadal Group rocks are exposed in the region of the ore deposit, and are here subdivided into a lower essentially carbonate formation and an upper carbonate-clastic terrigenous formation (Fig. 112). Magnesite rocks in the Savina deposit are lithologically related to the carbonate rocks in the lower formation and form a NW-striking, steeply-dipping deposit bounded on the SW by a zone of mylonites and retrogressed rocks along the Lower Biboy fault and on the NE by a system of faults. The total thickness of the magnesites has not been established. Boreholes to 700 and 780 m depth have not reached the base of the magnesite deposit (Poletayev et al., 1975). Most workers currently favour a hypothesis for the origin of the deposit that relates it to metasomatic processes, and the Savina magnesites are regarded as apodolomitic infiltration metasomatites. The source of the magnesian solutions remains an open question at present.

The internal structure of the magnesite deposit is quite complex and is distinguished by a large number of textural varieties, including the following: 1) Fine-grained, blue or bluish-grey, roughly platy, granoblastic. 2) Marble-like, massive or roughly platy, light grey or bluish, medium-grained with a heterogranoblastic texture in the groundmass. 3) Coarsely crystalline, short prisms on the long axis, often with spherical crystal segregations that display a "stellate" texture internally. 4) Brecciated, coarsely crystalline, consisting of 80-85% magnesite and 15-20% talc and chlorite. 5) Fibrous lanceolated varieties, consisting of highly elongate crystals oriented perpendicular to vein walls. Mutual relations between different magnesite ore types indicate that magnesite-forming processes correspond to two phases of magnesite metasomatism.

Magnesite formed during the first phase with fine-grained, marble-like, coarsely crystalline, "stellate" and brecciated textures. Due to the influx of new portions of magnesium-bearing solutions in the second phase, and subsequent recrystallization, fibrous lanceolated textures formed, spatially associated with zones of faulting and intensive jointing. There was a significant time gap between these two phases of

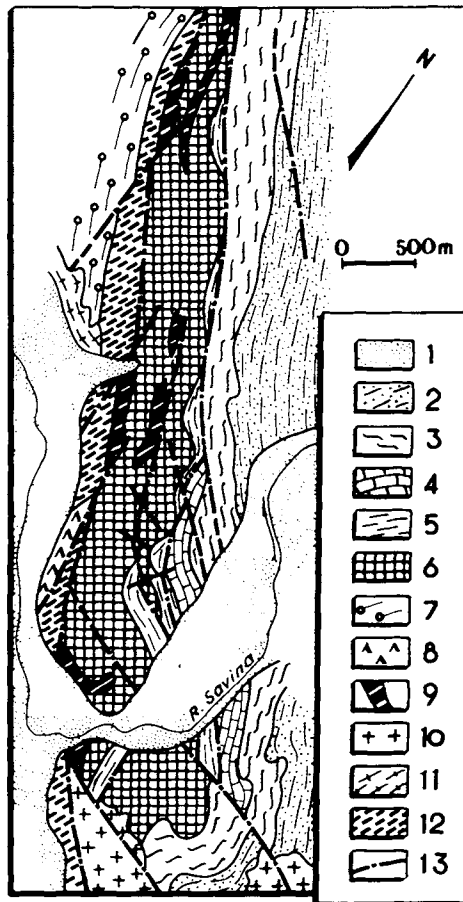


Fig. 112. Geological sketch map, Savin magnesite deposit (Poletayev et al., 1979). 1 – Alluvium. Kamchadal Group (AR<sub>2</sub>): 2 – bt, gt-bt, gt-st, bt-amph schist & gneiss, 3 – carb, chl-serp-carb, talc-chl, bt schists, 4 – dolomite, dolomitic schist, 5 – amphibolite, amph schist, 6 – magnesite. Malo-Iret Group: 7 – migmatized acid-intermediate meta-volcanics. Intrusions: 8 – Nersin diabases, 9 – Arban diabases & ortho-amphibolites, 10 – Sayan granitoids PR<sub>1</sub>, 11 – Onot granite-gneiss AR<sub>2</sub>, 12 – retrogressed rocks & mylonites in Olagnin-Khomolkho shear zone, 13 – faults.

magnesian metasomatism, which are separated by the intrusion of basic dykes, the Arban intrusive complex.

Compositionally, the magnesites of the Savina deposit are an almost monomineralic rock consisting of 75–99% magnesite. They contain from 1% to 25% mineral impurities, represented by talc, chlorite, dolomite, quartz, calcite, pyrite, limonite and rarer amphibole, biotite and brucite. Impurities are unevenly distributed in the mineral deposit, both in terms of composition and amount. Thus, talc and chlorite are more typical for the magnesites in the eastern part of the deposit, where impurities amount to 10–25%. A higher talc and chlorite content is also observed in zones of fractures and tectonic sutures and decreases away from these zones. Relicts of primary dolomites are

found mainly in the south of the deposit. Pyrite is found practically everywhere, although it increases sharply in amount in jointed and tectonic zones. An increase in the pyrite content is also observed in the outer contacts of basic dykes, where an increase in the cobalt content is characteristic, reaching upto 0.57%.

## 2.6. *Muscovite*

Important deposits in the Pre-Sayan inlier are mica pegmatites, which are thought to be related to the Upper Archaean but affected by later events. Pegmatites in the Biryusa inlier are associated with the Tepsa complex which has a predominantly clastic terrigenous composition. There are no more than 10% volcanic rocks in the complex. The pegmatites are referred to as the Gutara-Biryusa pegmatites from the locality where they mostly occur.

*The Gutara-Biryusa mica pegmatites.* Mica pegmatites in the Biryusa inlier are concentrated in a discontinuous strip with a NW strike, concordant with the overall regional structure. The strip extends from the river Iya in the E to the river Tagul in the W for a distance exceeding 100 km. The richest mica-bearing pegmatite veins occur in the area of the rivers Tepsa and Neroy, tributaries of the Bolshaya (Greater) Biryusa river in the middle part of the basement inlier.

Mica pegmatites were first discovered in the 17th century, but it was not until 1925–27 and later in the 1940s that systematic exploration and reconnaissance were carried out to tie down the pegmatite locations. This work proved that the mica pegmatites were more widespread than previously assumed. The deposit is not being exploited at present. The pegmatites occur in Tepsa Group rocks, where schist, quartzite and occasional gneiss predominate. Amphibolite and marble are very subordinate. The commonest schists are two-mica and kyanite-bearing varieties which have a coarsely-crystalline texture adjacent to pegmatite veins. Structural analysis has shown that the pegmatite veins occur in synclines with axes which strike near N–S (Sizykh, 1978).

The Gutara-Biryusa pegmatite strip contains over 10 pegmatite clusters. Veins are highly variable in shape and composition. In many instances they are short and irregular, or are podiform (Figs 113, 114). More rarely they have a sheet-like form. Most are 60–70 m long, though they can reach upto several hundred m, and they are 5–6 m wide. Around 2800 pegmatite veins have been mapped in the region, but only 5–6% have any economic quantities of mica (Dibrov, 1958). They have highly variable internal structure. Some have a uniform, relatively fine-grained texture, others are zoned. Zoned veins show a regular change in texture from aplitic at the contacts to coarsely crystalline, pegmatoid in the centre. Zonation may be uniform, i.e. a similar distribution of zones from the centre to both zählbands, and sometimes it is asymmetric. Economic mica concentrations are associated with coarsely crystalline pegmatites.

## 2.7. *Apatite*

*The Pre-Sayan phosphate region.* Apatite deposits are associated with carbonatites connected to alkali-ultrabasic intrusions. They have been studied by A.A. Frolov, L.K. Pozharitskaya, V.G. Kuznetsov, A.A. Konev and others. Yu.M. Sheinman

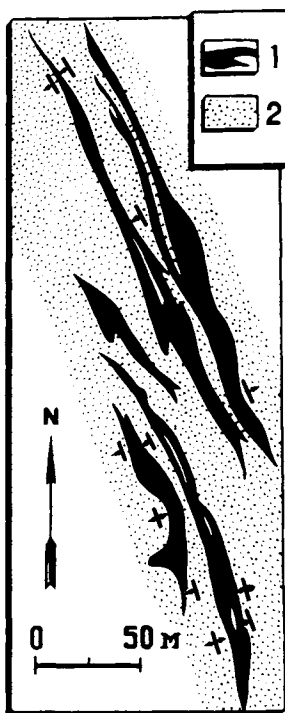


Fig. 113. Pegmatites in Vein Suite deposit (Dibrov, 1958). 1 – mica veins, 2 – Biryusa schist & gneiss.

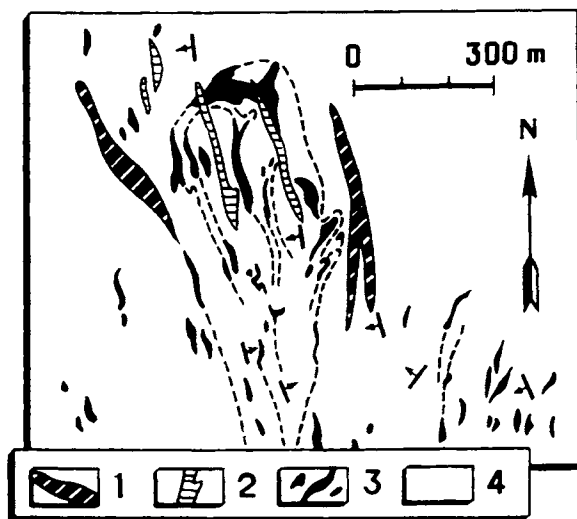


Fig. 114. Pegmatite veins in Neroy-I deposit (Dibrov, 1958). 1 – qz porphyry, 2 – pegmatites, 3 – porphyrite, 4 – Biryusa schist & gneiss.

includes these rocks in an independent igneous province, situated along the southern and western edges of the Siberian craton. The intrusions are typical central-type massifs, emplaced at major NW-striking fault intersections (Frolov, 1968, 1993). The intrusions occur mainly among Early Proterozoic formations and only in one instance in Archaean rocks. Four apatite-bearing carbonatite massifs are known in total. In horizontal section they have an oval or rounded shape with steep to vertical walls. The pipe-like bodies have a zoned ring structure which is usually obscured by linear structures. The ring structure has not been established in at least two of the intrusions. One intrusion will serve as an example of an apatite deposit.

The *Belaya Zima* ("White Winter") deposit is associated with a complex polyphase intrusion of alkali-ultrabasic rocks. The alkali-ultrabasic rocks have an age of  $671 \pm 36$  Ma from Rb-Sr data, and an initial  $^{87}\text{Sr}/^{86}\text{Sr}$  ratio of  $0.70358 \pm 0.00025$  (Chernysheva et al., 1995). According to Frolov (1968) it is a vertical pipe with an oval horizontal section (Fig. 115). Its long axis has a NW strike, typical for the regional faults. The massif consists of pyroxenite and pyroxene-nepheline rocks of the melt-eigite-ijolite-urtite series, nepheline and alkali syenites, picritic porphyrites and breccias, and carbonatite. The internal ring structure is expressed as a change from earlier-

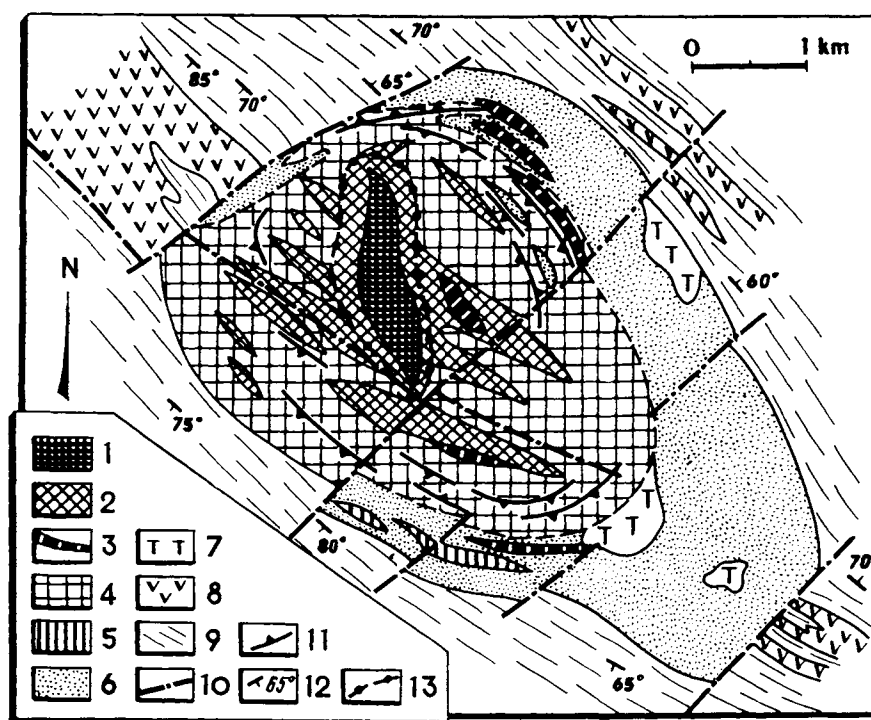


Fig. 115. Structure of carbonatite massif (Frolov, 1968). 1 - ankeritic carbonatite, 2 - amph-ca carbonatite, 3 - fo-di-ca pegmatitic carbonatite, 4 - aug-bt-ca carbonatite, 5 - nepheline & alkali syenites, 6 - ijolite, 7 - melteigite, 8 - gabbro-diabase, 9 - shale & sst. 10 - faults, 11 - shear zones, 12 - banding in carbonatite, 13 - bedding and schistosity.

formed rocks at the periphery to younger in the centre. Originally the entire intrusion would seem to have consisted of pyroxene–nepheline syenite. Pyroxenite was altered to melteigite–ijolite, sometimes urtite, as a result of nephelinization. As a result of carbonitization, these rocks were preserved only as narrow rings around the periphery. Nepheline syenite is present as wide arcuate dykes at the southern edge of the intrusion. Picritic porphyrites and breccias occur as remnants within the carbonatites. The carbonatites have inherited structural elements of central intrusions (stocks, ring dykes) on which linear structures have been superimposed.

Four stages in the carbonatite-forming process have been identified (Table 12). Carbonatites are the main concentrators of apatite, but the different varieties are highly variable in amount (Table 12). Calcitic varieties are richer in apatite than ankeritic. Only in rare instances does the apatite content reach as high as 20–30%. Apatite segregations vary in shape in the different types of carbonatite. In contact zones between silicate rocks and calcitic carbonatites, apatite occurs as lenticular and irregularly-shaped portions, not more than a few metres thick. Here, the apatite is fine-grained, with upto 15%  $P_2O_5$ . Among forsterite–calcite and phlogopite–calcite carbonatites with pegmatitic texture, the apatite concentration is irregular. In this type, apatite is frequently seen together with magnetite, which makes up 5–10% of the rock mass. Several major apatite–magnetite bodies have been discovered by drilling in this rock type. A magnetite–apatite body discovered to the SE of the massif among ijolite–melteigites has the following composition: apatite 5–90%, magnetite 5–50%, perovskite upto 10%. Apatite is relatively uniformly dispersed in fine-grained amphibole–calcite carbonatites with disseminated rare-metal mineralization and in ankeritic carbonatites, and forms clusters of irregularly-shaped and rounded grains. A weathered mantle is developed on the Belaya Zima intrusion: remanent (eluvial) and remanent–infiltration. Generally this mantle occurs along fault zones, where comminution of the rocks facilitated their weathering. The remanent weathered mantle is developed in the central and western parts of the intrusion.

Table 12

Apatite content and structure of carbonatites (after Frolov, 1968)

Carbonatite type and stage of formation	Shapes and dimensions of carbonatite occurrences	Apatite content, in rock, % (range/average)
Augite–biotite–calcite coarse-grained carbonatite; stage I	Oval grains, 0.5–2 mm in size, forming chains along calcite grain boundaries; sometimes irregular aggregates	$\frac{3 - 15}{9}$
Diopside–forsterite–calcite pegmatitic carbonatite; stage II	Fibrous–prismatic crystals, 1–4 mm long, rarely up to 1 cm, fine-grained nest-shaped or veinlet clusters	$\frac{4 - 20}{12}$
Amphibole–calcite fine-grained carbonatite; stage III	Prismatic crystals 0.1–0.5 cm long, forming radial aggregates, also more or less isometric grains (0.1–2 mm) in bands and veinlets, sometimes nests	$\frac{4 - 20}{10}$
Ankeritic carbonatite with fluorite; stage IV	Nests, veinlets and irregular fine-grained intergrowths	$\frac{3 - 12}{8}$

Apatite enrichment of the weathered mantle is directly proportional to the apatite content of the bedrock and its degree of weathering. Among carbonatites, ankeritic types suffered the most weathering. The average  $P_2O_5$  content in the weathered mantle is 10.4% and in carbonatite bedrock, 4.2% (Smirnov, 1980).

The maximum apatite content is found in ochres which represent the top horizon of the weathered mantle. Ochres consist of hydroxides of iron, manganese, hydromicas and clay minerals. They are also enriched in pyrochlore, columbite, magnetite, monzonite and apatite, which are resistant to weathering. The average  $P_2O_5$  content in the ochres is 13.7%. The remanent-infiltration weathered mantle occurs along the SW contact of the massif. Hypergene francolite plays a major role here, and the  $P_2O_5$  content ranges from 10–20% to 36% in this type of weathered mantle. The francolite-bearing zone is tens of metres thick and hundreds of metres long.

## 2.8. Fluorite

*The Bolshaya Tagna deposit* (Frolov, 1968) is associated with an intrusion of alkali-ultrabasic rocks (Rb–Sr age of  $762 \pm 114$  Ma) in Early Proterozoic metamorphic rocks. It was discovered in 1958 and explored in 1968–69. The intrusion is characterised by a relatively small erosion section. It has a zoned ring structure (Fig. 116), with ijolite, alkali and nepheline syenites and carbonatites in sequence. Carbonatites with a pegmatitic texture are missing from the intrusion (which are usually early), while microclinization is very characteristic, resulting in the formation of microcline rock.

Carbonatites form stock-like bodies in the intrusion, with essentially leucocratic calcitic varieties being present. Fluorite-enriched carbonatites are located in the centre of this stock-like body. They are represented by fine-grained varieties, formed during the recrystallization of coarse-grained carbonatites, which probably occurred at 450–150°C (Frolov, 1968). Fluorite is found as veinlets and disseminations. Three ore types are distinguished, based on structural and textural features (Yegorov, 1966): 1) Fine-grained ores in which fluorite crystals are upto 1 mm. Calcite is the main mineral in these ores, 60–75%, with 15–20% fluorite, 5–10% albite, 8% chlorite. Secondary minerals are sulphides, hematite, hydromicas, apatite, celestine, K-feldspar. Fluorite forms lenticles or porphyroblasts. Fluorite porphyroblasts are oriented and distributed in uneven bands, giving the ores a banding. Here the fluorite is white, with a violet tinge. 2) Ores with various grain sizes. Fluorite has light shades of violet, pink and yellow, rarely white. Grains vary in size from a fraction of 1 mm, upto 1 cm. Distribution is regular, and the content is from 5% to 50%. Other minerals are calcite, upto 80%, K-feldspar, upto 45%, albite, hematite, limonite and sulphides. 3) Solid fluorite ores, medium-grained, massive rocks. The fluorite is purple or pink; grains 3–4 mm, sometimes upto 2 cm in size. Ore bodies consist of separate thin veins within other types of ore body, and they have no significance in their own right.

Fluorite-bearing rocks form two large ore zones and a number of minor ore bodies. One of the ore zones is represented by a lens-shaped body, stretched out in a NW direction and dipping at 78–85° to the NE. The body wedges out at depth, from 70 m at the surface to 10 m at depth. A second ore zone is 50–90 m thick and stretches for 800 m along strike, although there are no sharp margins. The average fluorite content is 22%. Some 40–60% of the fluorite in the deposit is observed to occur in two

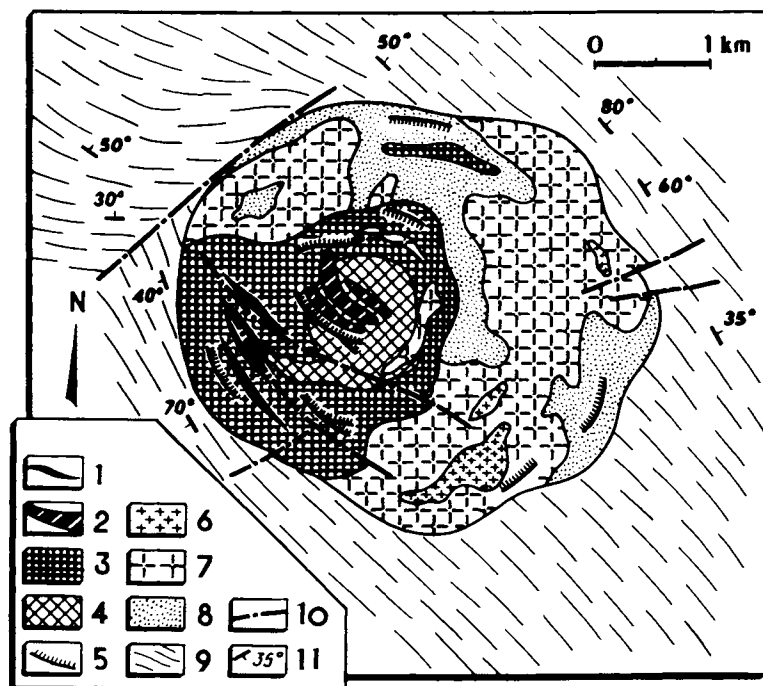


Fig. 116. Structure of Bolshaya Tagna intrusion (Frolov, 1968). 1 – pegmatitic ores, 2 – calcitic carbonatite, with fluorite + hematite, 3 – coarse ca carbonatite, 4 – fine ca carbonatite, 5 – picritic porphyrite–alnite, 6 – nepheline syenite, 7 – K-feldspar syenite, 8 – ijolite & melteigite, 9 – schist, 10 – tectonic zones, 11 – bedding & schistosity.

generations, the earlier of which is purple and deep purple, the later generation being light green to colourless. Purple fluorite has very low uranium and thorium contents, less than in later generations (Vasilkova and Solomkina, 1965). In the earlier fluorite, rare earths total 0.1–0.2%, with 1% Sr, and 0.01% Sr in the later generation, beryllium 0.001% in the earlier generation, 0.0001% in the later. Sulphides found in the deposit (galena, sphalerite, pyrite) formed in the interval between the two fluorite generations. Fluorite, hematite, apatite and other minerals probably formed due to recrystallization of coarse-grained carbonatites into fine-grained, frequently banded varieties in a hydrothermal stage. In places where the ore stage of the hydrothermal process is most complete, upto 25–50% fluorite, 10–25% hematite and 4–5% apatite formed in the carbonatites (Frolov, 1968). Other useful minerals in the deposit apart from fluorite include apatite, however it is much lower in amount than in the Belaya Zima deposit. Zones with higher apatite content are associated with superimposed post-magmatic metasomatic processes. The most widespread ores are apatite–biotite–microcline metasomatic ores, less commonly apatite-bearing alkali syenites and carbonatites. Apatite-bearing rocks form an arcuate zone, conformable with the ring structure of the intrusion. The  $P_2O_5$  content in microcline ores varies from 2.5 to 7%, and in carbonatite ores it is 5% (Yegorov et al., 1980). Rare-earth minerals are present in the deposit, which is thus classified as an apatite–pyrochlore mineral type in the phosphorus–niobium ore formation (Frolov, 1993).

## Angara–Kan inlier

V.Ya. KHILTOVA and G.P. PLESKACH

The Angara–Kan or South Yenisey inlier, situated on the south of the Yenisey ridge, consists of Archaean and Early Proterozoic high-grade metamorphic rocks. Their age has been defined so far on the basis of their metamorphic facies, with granulites assumed to be Archaean and amphibolite facies rocks Early Proterozoic. This approach to determining the age, in use since the time of Kuznetsov (1941), is usually employed even now, since there are still very few radiometric dates for the early Precambrian. Tectonically, the Angara–Kan inlier was often treated as a single structure with no internal subdivisions. It was only in recent years that A.D. Nozhkin separated out the Pre-Divin belt which he described as an Archaean greenstone belt. Relations between the rocks which formed in this belt since the Early Proterozoic (Vesnin or Yenisey Group) have so far not been determined. Iron (in ferruginous quartzites), graphite and aluminous schist occurrences are associated with the granulite–gneisses of the inlier. Archaean basic–ultrabasic intrusions host titanomagnetite deposits: the Shiver and other occurrences. The Kuzeyev and Bogunayev gold ore deposits and muscovite and muscovite with rare-metal pegmatites occupy an important place among the mineral deposits of granulite–gneiss terrains.

### 1. Ore deposits and occurrences

#### 1.1. Titanium

*The Shiver titanomagnetite body.* Titanomagnetite deposits within the Yenisey ridge are associated with an Archaean dunite–pyroxenite–gabbro suite, intrusions of which can be traced along the Pre-Yenisey deep fault zone. Archaean occurrences of this type, typical for the Angara–Kan inlier (Shiver, Zimoveinin, Kimbirka and others) are associated with the Kimbirka complex, the oldest in the inlier. They were studied in the 1970s by T.Ya. Kornev and others. The Shiver titanomagnetite occurrence is located in the east of a layered basic–ultrabasic intrusion in the area between the rivers Kimbirka and Yudinka. The intrusion is elongate in a NW direction, parallel to the general strike of the Kan Group (Fig. 117). It consists of gabbroic rocks and amphibolites, with rarer pyroxenite, anorthosite and diorite. Gabbroic rocks are cut by Taraka granites which have a radiometric age of 1.8–2.0 Ga (Kornev, 1974), and the gabbros themselves belong to the Archaean. They typically have higher Ti contents, although the highest TiO<sub>2</sub> values are concentrated in the lower more strongly layered part.

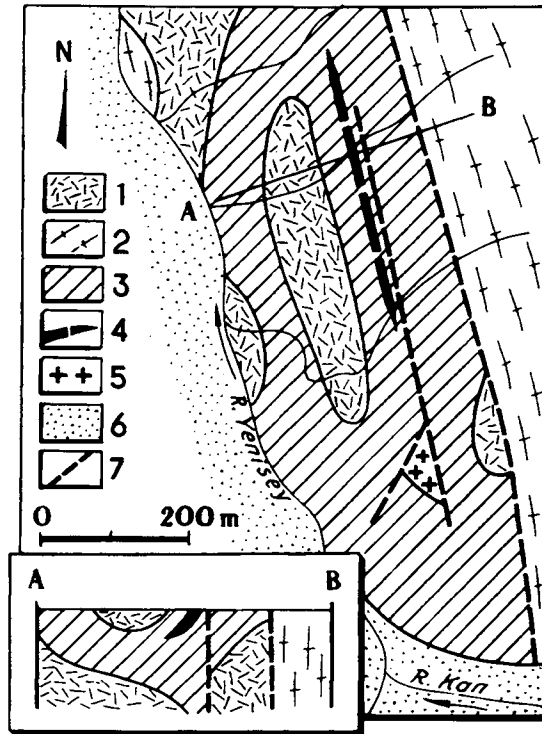


Fig. 117. Geological structure of Shiver occurrence (Kornev, 1974). 1 – qz–chl, qz–bt & act metabasaltic porphyrite, qz albitophyre, rhyolitic porphyry & tuff, 2 – amph & gt–bt schists, quartzite, marble, ortho-amphibolite, 3 – Shiver intrusion (gabbro, pyroxenite, anorthosite), 4 – ore-bearing gabbro, pyroxenite, ortho-amphibolite, 5 – granite & granite gneiss, 6 – Quaternary, 7 – fault zones.

The ore zone stretches for up to 7 km, and has a width of 100–150 m (Kornev, 1961). Strong magnetic anomalies are found along it. Several ore bodies 3 to 20 m thick occur in the ore zone; they are concordant with the gabbro–anorthosites and amphibolized pyroxenites and dip at 50–80° to the SW. In addition to the conformable bodies, there are also those which obliquely intersect the primary banding in the gabbro–anorthosites. These bodies, which occupy various positions, have the same chemical and mineralogical composition and similar textural and structural features. Boundaries between ore bodies and country rocks are usually sharp, rarely gradational. The ore is represented by melanocratic gabbro and pyroxenite enriched in ore minerals and metamorphosed at epidote–amphibolite facies. Titanium in the ores occurs mainly as ilmenite, less commonly as titanomagnetite, rutile and sphene. Magnetite is present in significant quantities with titanium minerals. The ilmenite content in ilmenite–magnetite ores of the Shiver occurrence varies from 8% to 30%. The process of ore genesis was accompanied by amphibolization and enrichment of the rocks in apatite and sulphides, hence impurities in the ores are chlorite, apatite, hematite, chalcocopyrite, pyrrhotite and pyrite. Ore textures are densely disseminated, schlieren and banded.

## 1.2. Gold

The gold deposits in the Yenisey ridge have been studied for many years, but there is no general consensus as to their genesis. Since the work of V.A. Obruchev, the deposits were long considered to be quartz vein type. N.V. Petrovskaya and co-workers as well as L.V. Li and others proposed that the Bogunayevskoye and Kuzeyevskoye deposits in the Angara–Kan microcraton belong to the gold–silver–sulphide formation, which they consider has the following characteristics: the deposits formed during the Late Proterozoic and are mainly hosted in greenschist facies retrogressed zones from granulite facies rocks; the ores generally have higher silver contents, low gold grade, and the sulphur composition in pyrite and galena is close to meteoritic (Li et al., 1986).

*The Bogunayevskoye deposit* (Li et al., 1975) is located in the SE part of the South Yenisey inlier, an anticlinorium complicated by linear and less commonly isometric folds. The deposit was discovered in 1934 by A.S. Khomentovsky. Parallel and oblique faults have a deep-seated origin and are thrusts (Parfyonov, 1963) or steep reverse faults with NE-dipping surfaces. The deposit is situated in the crest of the anticlinorium, on the SW flank of the Pre-Yenisey deep fault. Faults are usually accompanied by retrogression and mylonitization. Rocks hosting the deposit belong to the Kuzeyev Fm (Kan Group), which includes garnet and pyroxene granulites and trondhjemites, with minor biotite–, sillimanite– and cordierite–plagioclase gneisses.

The deposit is situated 10–12 km from the NE contact of the Lower Kan intrusion belonging to a granite batholith formation that has been identified in the Yenisey ridge. A leucocratic granite massif occurs 7.5 km from the deposit, and this is thought to be a satellite from the major Lower Kan intrusion. Adamellite, granodiorite and diorite have been mapped at the margins of the massif. Intrusive rocks play a very minor role within the ore field. They are mainly represented by diabase and diabase porphyry, with minor gabbro. Three age groups of diabase dykes have been identified, all of which are older than and cut by gold-bearing quartz veins. The dykes are sharply reduced in number beyond the confines of the ore field. There is thus a close coincidence between the dykes and the ore field. Pegmatites with small amounts of tourmaline are sometimes found in the ore field. Gabbro–diabase and granite–porphyry dykes have been exposed in underground workings; these dykes, which are less than 2 m wide, cut the quartz veins. They strike NNE and dip steeply ( $> 60^\circ$ ) to the SW.

The Bogunayevo anticline which hosts the deposit plunges steeply NW. The metamorphic rocks have a predominantly NW strike and dip at  $50\text{--}80^\circ$  to the NE. Intense retrogression has taken place in the gneiss unit along a steep, regional NW fault. All economic ore veins are localized on the footwall side of the fault and do not extend beyond its limits. Faults striking E–W, N–S and NE are pre-ore and cross diabase and diabase porphyry dykes. Ore mineralization is represented by numerous quartz veins, which are unevenly distributed throughout the entire ore field, but are concentrated in four distinct areas.

The veins mostly strike NE and NNE, with only a few WNW and NW. Sometimes they have an arcuate shape. They vary in length from a few tens to several hundreds of m, and in individual cases up to 1 km; they are a few cm to 2 m thick. Ore bodies have a fairly simple mineral composition: 70–80% quartz, plus carbonates, sericite and

chlorite. Feldspar, garnet and pyroxene are occasionally found. Ore minerals are pyrite, sphalerite, galena, with secondary chalcopyrite, arsenopyrite, pyrrhotite, native gold, cubanite, marcasite, bravoite, magnetite, stannite, cassiterite and molybdenite. The last three minerals are not found in gold ores in other deposits from this region – this is a distinguishing feature of the Bogunayevo deposit alone. Gold is the only component extracted from the ore, although silver is present in increased concentrations. Typical ore textures are massive, drusy, banded and less commonly brecciated. Gold is associated with sulphides, and to a lesser extent also pyrite, more rarely with galena. Gold distribution in the veins is in pipes and cavities. Wallrock alteration includes quartz, sericite, sulphide and carbonate impregnations.

The issue of the genesis of the deposit is controversial. Quartz–sulphide veins were previously thought to be hydrothermal, but now they are related to either granite magmatism, in particular to the Lower Kan granite intrusion, or they are thought to be products of an intra-telluric ore-forming system (Li, 1982).

*The Kuzeyevskoye deposit* (Li, 1974) is spatially associated with granitic rocks belonging to the Teya complex and occurs at the exo-contact of the Belogorsk granite intrusion. Country rocks to the intrusion are the Early Archaean Kuzeyev and Atamanov assemblages, which were metamorphosed at granulite and amphibolite facies. The granitic massif is surrounded by migmatite aureoles, in which gneissose granites predominate. It is cut by pegmatite veins, sometimes aplite and diabase. Diabase dykes are often associated with faults and mylonite zones.

Large thrust-type faults are developed on the outer contact of the massif, where the ore field is located, with displacement surfaces dipping E and NE at 50–70°. The faults are accompanied by numerous minor fractures, which are frequently represented by mylonite zones, in which quartz veins are usually found. Most veins strike NW, with gentle (35–45°) dips to the NE. They can often be many of hundreds of metres long, but are generally impersistent both along strike and down dip. They vary in thickness from 0.02 m to 0.5 m, rarely up to 2–4 m. Veins are seen to be thicker in areas where fault surfaces bend, and such veins have more intense mineralization.

Gold mineralization is associated with the quartz veins. Their mineral composition is quartz in several generations – white to greyish-white, coarse-grained with pyrite, milky-white with a varied assemblage of sulphides, and bluish-grey to grey, fine-grained, with calcite and siderite. Pyrite and galena are the main ore minerals. Galena contains antimony (in the absence of bismuth), and silver, up to 490 g/t. Grey copper ore is present as a secondary mineral. The gold in this deposit is fine-grained, 0.03 to 0.35 mm, with pellet, dendritic and bent flake shapes. Chemically, the gold is close to electrum (500 grade). The gold is unevenly distributed in the veins, the greatest amount being found where sphalerite clusters occur. Galena in the Kuzeyevskoye deposit has an age of  $900 \pm 150$  Ma (Volobuyev, 1973).

### 1.3. *Muscovite*

Mica-bearing pegmatites in the South Yenisey inlier are known in two deposits, Barga and Kondakovo. Pegmatitic veins occur in amphibolite and granulite facies rocks, but are commoner in the former.

*The Barga deposit* (Althausen, 1937) is located in the NE of the South Yenisey high granite–gneiss terrain. It was discovered last century, but was not surveyed in detail until the 1930s. Archaean crystalline rocks hosting the deposit consist of biotite and hornblende gneisses, with a NW (290–310°) strike in this part of the inlier. The pegmatite veins are often close to sheets and they have the same strike as the host rocks but different dip. Only occasionally, e.g. the Olkhovsky mine, the veins and gneisses both dip to the SW, and usually there is a divergence of 20–30°. Veins vary enormously in shape (Fig. 118). Where they are parallel-walled and close to being sheets, they are continuous along strike for up to 200–400 m and are 1–2 m thick. In rare cases the length is up to 1700 m and the thickness 10–50 m. Vein shapes are defined by the nature of fold structures in the gneisses. Where the gneissose banding is constant, the veins also have sharp margins; but the shape is irregular wherever the gneisses are complexly folded.

Pegmatite veins have an irregular internal structure. Zonation can often be seen, especially in those with high (economic) muscovite contents. Zonation is expressed as a change from fine-grained aplitic rocks in the contact zone, followed by a muscovite zone in coarse-grained pegmatites, then feldspar and finally a quartz zone alternating with aplite at the centre, which contains grey quartz, plagioclase, and rare garnet, biotite and muscovite grains. The feldspar zone consists of pink microcline, nest-shaped quartz clusters, negligible muscovite, black tourmaline, rare-metal minerals,

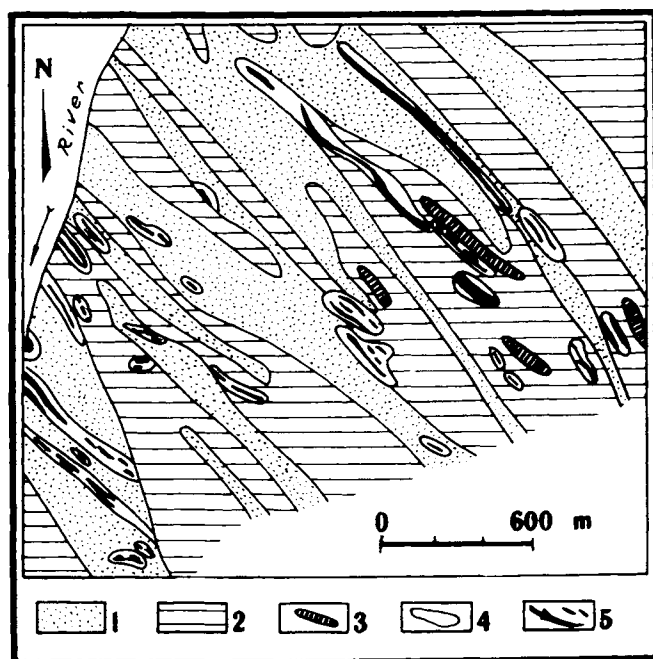


Fig. 118. Sketch showing geological structure of Barga muscovite pegmatite deposit (after M.N. Althausen). 1 – gt gneiss, 2 – px gneiss, 3 – gabbro, 4 – bt gneiss, 5 – pegmatites.

Table 13  
Brief characteristics of mines in Barga deposit, after M.N. Althausen (1933)

Name of mine	No. of veins	Shape of ore body	Strike	Dip	Length, in m	Thickness, in m	Strike length of sector, m	Max. dip length of sector, m
Sluchayny ("Lucky Strike")	2	Elongate, and elongate with two branches at depth	145° 130-150°	40-42°	185-160	1-8, 2-20	105, 55	60, 100
Markovsky	6	Pancakes, sometimes joined	100-120°	58-55°	20-40	0.6-1.5	19-73	23-40
Olkhovsky	2	Branching veins	120-260°	45-90°	230-260	2-15, 4-17	30,20	38,50
Lugovoy	2	Vein with many constrictions	130°	50°	130	1.1	58	43
		Elongate lens	130-140°	40-50°	110	4-6	30	20-25
October	1	Irregular vein with swellings	125°	vertical	200	2-20	41	17

etc. Central parts of veins are represented by quartz segregations. This is not the only type of zoning in the Barga deposit veins, and is typical mainly of those with commercial muscovite, as already noted. The deposit has been exploited in several mines, the geology of which is shown in Table 13.

*The Kondakovo muscovite with rare-metal pegmatite deposit* (Yakzhin, 1937) is located in the south of the Yenisey ridge, on the right bank of the river Kan. The deposit, discovered in 1642, was systematically explored from the early 1930s, in an area of Archaean crystalline rocks which includes gneiss, amphibolite and marble. Diabase and porphyrite form vein rocks. Pegmatite veins themselves are intruded into garnet–mica, garnet–staurolite–mica and epidote–actinolite schists, with mutual transitions between all rock types. Mica schists are the commonest. The pegmatites are assumed to be Upper Archaean to Lower Proterozoic in age.

The pegmatites vary in shape, the main ones being sheet-like, lenses, stocks and nest-like segregations. Pegmatite sheets are the commonest in the region and they often have pinch-and-swell structures and branch where they thin out. The veins vary greatly in thickness, from 1–3 m to 15–20 m in swollen parts. Strike length is from 20 to 350 m, but usually greater than 100 m. Lens-shaped pegmatites, which are rare, are 5–6 m thick and 40 m long. Stock-like and nest-like segregations are rarer still. Mica schists and gneisses, schists and quartzites which host the pegmatites are conformable with them. Pegmatites dip steeply, at 60° to 80°, or 20° in rare cases. Contacts with country rocks are usually sharp. A quartz–mica selvage is often developed at the immediate contact, and contact alteration effects are no wider than 1.5–2.0 m. Selvages mostly contain muscovite, quartz, tourmaline and garnet, with pitch-black tourmaline being particularly abundant. Tourmaline forms clusters in the hanging wall when veins are gently-dipping, and in both zählbands when they are vertical. Minerals vary in proportions, and the greater the variation the coarser the grain size of the pegmatites. A cross-section through a vein has the following composition: unaltered schist in the wall rock, contact-injection gneiss with tourmaline, selvage with coarse mica flakes and tourmaline. In the pegmatite: light aplitic selvage – fine-grained or graphic pegmatite zone – coarse-grained pegmatitic zone – grey or saccharoidal quartz zone – coarse-grained pegmatitic zone – fine-grained or graphic pegmatite zone – light-coloured aplitic selvage. Zoning is clearest and symmetric in vertical and steeply-dipping veins. The quartz to feldspar ratio varies widely in the pegmatites. Where coarse-grained quartz predominates, there is an economic muscovite concentration. Tourmaline, biotite, garnet, apatite and rare-metal minerals occur in all veins, from negligible to quite significant amounts. A total of 30 minerals has been identified in the pegmatites. Sulphides include pyrite, oxides – magnetite (titanomagnetite), silicates – microcline, albite, plagioclase, muscovite, biotite, garnet, tourmaline, sillimanite, kyanite, zircon, chlorite, kaolin, beryl, gilbertite, epidote, orthite, phosphates – apatite, lazulite, graffonite, vivianite.



## Khamar–Daban and Pre-Olkhon inliers (SW Prebaikal)

D.A. MIKHAILOV and V.YA. KHILTOVA

This chapter briefly outlines the known mineral resources in the Pre-Olkhon region and the western part of the Khamar–Daban ridge. Since the publication of one of the earliest works on the tectonics of Eastern Sayan and Khamar–Daban (Obruchev, 1949), and often since then, these regions have been referred to different types of tectonic structure: basement structures of the ancient Siberian craton (Pre-Olkhon) and Precambrian microcratons within younger fold belts (the Khamar–Daban ridge). However, the metallogeny of these regions is usually considered together.

### *1. Pre-Olkhon*

The Pre-Olkhon region is made of mainly high-grade early Precambrian rocks. For a long time all the rocks of the region were treated as belonging to a single Olkhon Group, and it was only relatively recently that new work on the structural geology allowed the metamorphic rocks of the region to be divided into three independent groups: Olkhon, Anga and Sagan–Zaba (Petrova et al., 1984).

The tectonic nature of both the Pre-Olkhon inlier as a whole and its separate parts has so far not been determined. It is also debatable whether or not to include this region as a marginal inlier of the ancient cratonic basement, since, as has already been remarked, folding and metamorphism, including granulite facies events, occurred during the Early Palaeozoic, from radiometric measurements. This ought to imply that the Pre-Olkhon inlier should be grouped with Phanerozoic structures. However, conclusions concerning the extent of intense Lower Palaeozoic processes are so far based only on radiometric data. Their geological interpretation is exceedingly complex, and the possibility cannot be excluded that the Lower Palaeozoic radiometric dates reflect only the time at which the rocks were uplifted from lower crustal P–T conditions to those where the isotopic systems could not be destroyed. This is a perfectly valid proposal, since the Pre-Olkhon inlier is immediately adjacent to a Phanerozoic fold belt, which may have determined the appearance of high temperatures at deep crustal levels which destroyed the isotopic systems. It is quite likely that the tectonic structure of the Pre-Olkhon inlier and its supracrustal rocks originated and formed in the early Precambrian, the more so since structurally and compositionally similar regions adjacent to Pre-Olkhon (the Sharyzhalgay block in Pre-Sayan) have been shown both geologically and radiometrically to have an early Precambrian age. The Pre-Olkhon region has a small area

whose metamorphic rocks contain no known large useful mineral deposits. Manganese deposits and occurrences have been found there (Sagan-Zaba), also graphite and ceramic pegmatites. There are signs that granulated quartz is present.

### 1.1. Manganese

The manganese deposit in the Pre-Olkhon region belongs to the carbonate-manganese formation, which did not produce large mineral deposits in the early Precambrian.

The *Sagan-Zaba deposit* is situated on the western shores of Lake Baikal and is associated with an Archaean (?) assemblage, viz. the carbonate member of the Olkhon Group. According to I.M. Barentsov and V.M. Rakhmanov (in Smirnov, 1974), the main members of the manganese formation are white and grey marbles with manganiferous marble beds and quartzite, gneiss (biotite, amphibole and pyroxene) and amphibolite intercalations. Manganese ores are represented by three beds of manganiferous marbles (Fig. 119), constituents of a 100 m thick bedded or sometimes massive marble member which can be traced in an E-W direction for 700 m. Beds of ore are conformable with the host rocks and dip steeply north at 75–80°. They consist of barren and rich layers from a few cm to 1–2 m thick. The deposit has three ore beds – Northern, Central and Southern. The Northern bed can be followed for 70 m and is 15–18 m thick, with an average manganese content of 6.67%. The Central bed can be traced for 380 m; it is 4–17 m thick and has 6.58% Mn on average. The Southern bed is 325 m long, 10–30 m thick, and contains 3.93% Mn. The manganese content is

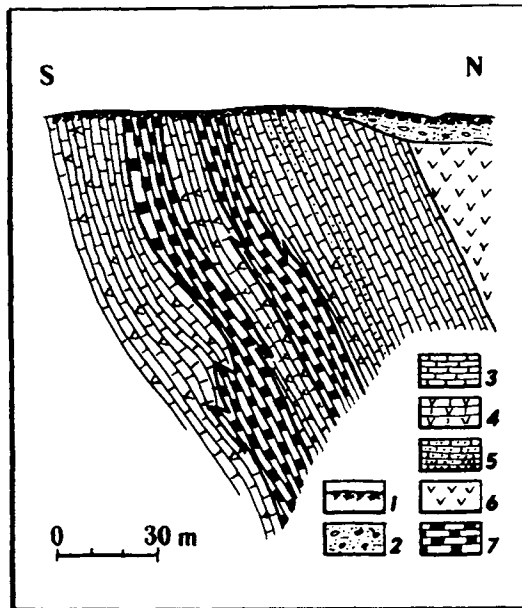


Fig. 119. Geological section, Sagan Zaba deposit (Smirnov, 1974). 1 – soil & Mn ore cap, 2 – alluvium, 3 – grey marble, 4 – marble with porphyrite bands, 5 – white marble, 6 – quartzite, gneiss and amphibolite, 7 – manganiferous marble.

generally uneven in the deposit. It enters into calcite isomorphically, forming a continuous series from manganiferous calcite to manganocalcite. Secondary minerals in the manganese-bearing marbles are quartz, garnet, biotite, muscovite, hornblende and sphene. Intercalations consisting of silicate minerals occur amongst the marbles – garnet, pyroxene, amphibole, in which the Mn content is up to 10%. Manganiferous marbles in the Sagan–Zaba have the following composition (wt.%): Mn 3.93–6.67, Fe 1.47–3.0, P 0.09–0.11, S 0.05–0.13, SiO<sub>2</sub> 7.5–8.1, Al<sub>2</sub>O<sub>3</sub> 0.96–1.57, CaO 39.6–41.7, MgO 2.74–3.5, loss on ignition 32.6–35.37. The ores are subject to surface oxidation in zones 2.3–3.0 m thick in which pyrolusite–psilomelane and psilomelane ores are developed. The Mn content in residual ores in the weathered mantle is 4–44%.

*Manganese occurrences* have been found amongst quartz veins, with the following mineral composition: wad, manganite, psilomelane, graphite, pyrrhotite, etc. Gold is occasionally seen in the pyrrhotite (Kotelnikov 1934). Also, manganese in the marbles and quartzites is associated with tectonite zones, where 16 m thick Mn-rich lenses extend for up to 200 m in a NE direction.

*Graphite occurrences* are found in crystalline limestones, forming disseminated platelets 1–5 mm in size. Graphitization increases close to contacts with ultrabasic minor intrusions. Graphite is also found amongst quartzites, where it can be up to 15% of the total volume of a rock. In the quartzites the graphite is usually in fine flakes. Graphitization is particularly widespread in the black ore zone (the western part of the Pre-Olkhon region).

## 2. *Western Khamar–Daban*

The crystalline rocks of Western Khamar–Daban, divided into the Slyudyanka (Upper Archaean) and Khangarul (Lower Proterozoic) groups, contain a variety of industrial mineral deposits: phlogopite, lazurite, wollastonite, marble for cement and decorative stones, and rare-earth pegmatites. These deposits owe their origin primarily to the widespread distribution of marbles and quartz–diopside rocks and apatite-rich areas. The variety of ore mineralization in this region owes its origin to processes of regional metamorphism, ultrametamorphism and metasomatism. Some researchers consider that repeated deformation (cross-folding) and associated metamorphism, ultrametamorphism and metasomatism, also caused by alkali gabbro intrusions, produced metasomatic formations in carbonate and quartz–diopside rocks.

Contact aureoles in the Asyamovo, Bolshe-Butuy and Malo-Bystrinka gabbro intrusions belonging to the Slyudyanka–Daban basic igneous belt contain wollastonite rocks, developed in carbonate assemblages, and have economic significance. The wollastonite rocks are subdivided into two types. The first is related to polyphase metamorphism and is represented by large bedded bodies in carbonate rocks (in areas where gabbros are located), with the composition wollastonite, quartz, calcite, diopside and apatite. The second type is represented by skarn zones around gabbro intrusions, the composition being wollastonite, albite, K-feldspar, bright green hedenbergite and apatite. Commercial concentrations of wollastonite, used in the manufacture of china, porcelain, glazes, polished facing slabs and other ceramics, occur in both these types.

Later, diopsidic rocks began to be used widely in the production of electro-radioceamics, ceramic pigments, pyro-glass ceramic connectors, glass crystal materials, etc. Therefore productive metamorphic and metasomatic carbonate-silicate rocks and marbles in typical skarns and skarn-like occurrences are viewed as potential targets for discovering not only deposits of phlogopite, lazurite and other hydrothermal-metasomatic rocks, but also for the use of diopside itself. In this regard, the most valuable raw material is low-iron diopside rock. Since quartz-diopside rocks with very low iron oxide, titanium, manganese and alkali metals are widespread in the South Pre-Baikal region, there are considerable prospects for ceramic raw materials.

Quartz-diopside rocks dominate the metamorphic unit which makes up the Slyudyanka Group which contains up to 60% carbonate rocks, divided into calcic and magnesian parts. Quartz-diopside rocks are associated with magnesian marbles which form patches of various dimensions (up to 100 m) involved in complex folding and traceable along strike for tens of kilometres. There are gradations from pure diopside to quartz-diopside rock. They are snow-white rocks with a bluish tinge, mostly massive and with faint patchy textures. Grain size varies from 0.1–1 mm to 3–4 mm. Apatite-rich quartz-diopside rock constitutes a special variety, an example being the Obruch deposit which is exposed close to the Kultuk-Mondy sector. Apatite grains are rounded and are a fraction of 1 mm in size. Chemically, the Obruch apatite is a fluorapatite, and is low in impurities. The apatite is associated with almost all petrographic varieties of crystalline rock in the Obruch assemblage, not only with quartzites, but also with marbles. However, most diopsidic quartzites are apatite-rich. Intercalations and lenses 5–10–20 cm thick often contain up to 85% apatite. Several dozen apatite-rich layers have been discovered in the Obruch assemblage.

Carbonate rocks in zones of polyphase folding and metamorphism are substantially recrystallized and show dedolomitization effects, which has led to the formation of megacrystic almost pure calcite marbles, including one deposit known as Pereval. Here, calcite marble beds are 40–60 m thick, with 3–8% MgO, and are interleaved with forsterite and diopside calciphyres, exploited as raw materials for the cement industry. The greatest interest and metallogenic significance attach to phlogopite and lazurite deposits belonging to the magnesian skarn formation.

### 2.1. *Phlogopite*

*The Slyudyanka phlogopite deposit*, known from the 18th century, has been investigated by many leading scientists: Academician N.I. Koshkarov (1852–1877), Academician D.S. Korzhinsky (1947), and other workers. It was worked in the period from 1928 to 1971. Phlogopite skarn bodies, consisting of diopside, scapolite and calcite are zoned and occur in dolomitic marbles. There are two types: contact-reaction skarn and skarn veins. The first formed during a period of polyphase deformation, metamorphism and ultrametamorphism. Lying at the contact between carbonate and alumino-silicate rocks, the skarns contain narrow phlogopite zones, with crystals no more than 5 cm across. This is the so-called "crust-type" phlogopite concentration. Lazurite-bearing zones are associated with the formation of contact-reaction skarns, which have their greatest expression in the Malo-Bystrinka deposit.

Contact reaction skarns are cut by pegmatite veins and monzonitic bodies, injections of which into these skarns resemble eruptive breccias. Contact-reaction and vein skarns are separated in time by the intrusion of pegmatites and monzonites. Vein skarns form a series of linear veins, being the result of the replacement of granite-pegmatites which cut the metamorphic rocks by diopside-scapolite and diopside-phlogopite zones (Fig. 120). The thickest skarn bodies are represented by the Slyudyanka deposit. Of greatest commercial interest are thick cross-cutting vein bodies with very clearly-expressed symmetrical zoning, where large phlogopite crystals are set in a calcite matrix. Vein bodies of skarn are controlled by joint tectonics, not marble contacts. The overwhelming majority of veins occur in the direction of cross joints which cut pyroxene-amphibole and biotite-cordierite gneisses, which also control the location of the granite-pegmatites hosting the skarns. This type of phlogopite skarn occurrence has been termed the "staircase" type. Regionally, the phlogopite skarns in the Pre-Baikal region are associated with areas where there are local manifestations of polyphase deformation and metamorphism, and within such areas, fracture zones cutting carbonate horizons (Fig. 121). The iron content of phlogopite in vein skarns varies, although it is always higher than in contact-reaction skarns. Therefore the colour of the phlogopite is also variable, so that individual deposits were given names like "Silver", "Amber", "Cherry", "Gypsy girl" during exploitation. Phlogopite has a constant BaO admixture of 0.6 to 2.2%. Crystals are zoned, determined mainly by changes in the B, F, OH, Cr and V contents.

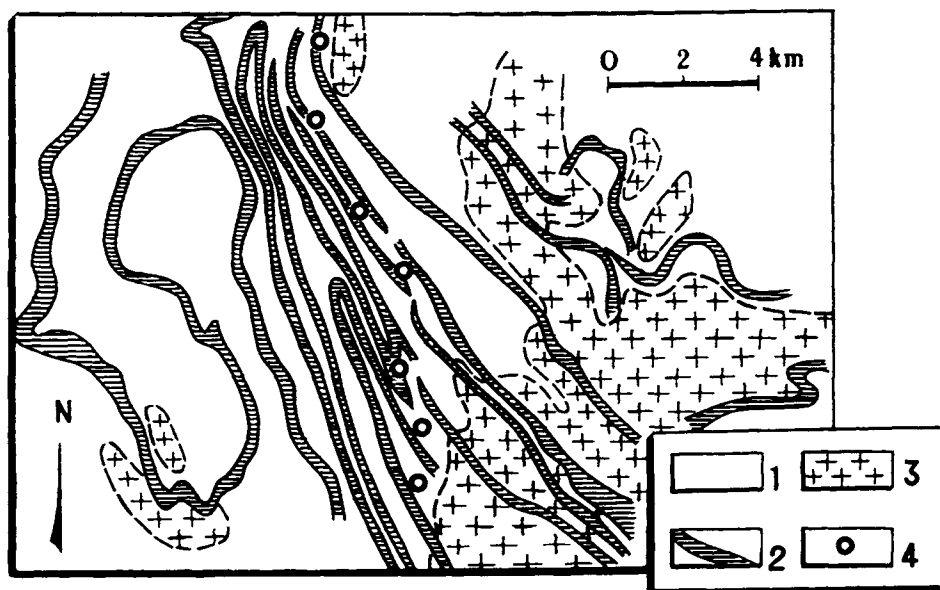


Fig. 120. Location of phlogopite deposits in Sludyanka region (Vasilyev et al., 1969). 1, 2 – stratigraphic markers, 3 – granite & granitized rocks, 4 – phlogopite deposits.

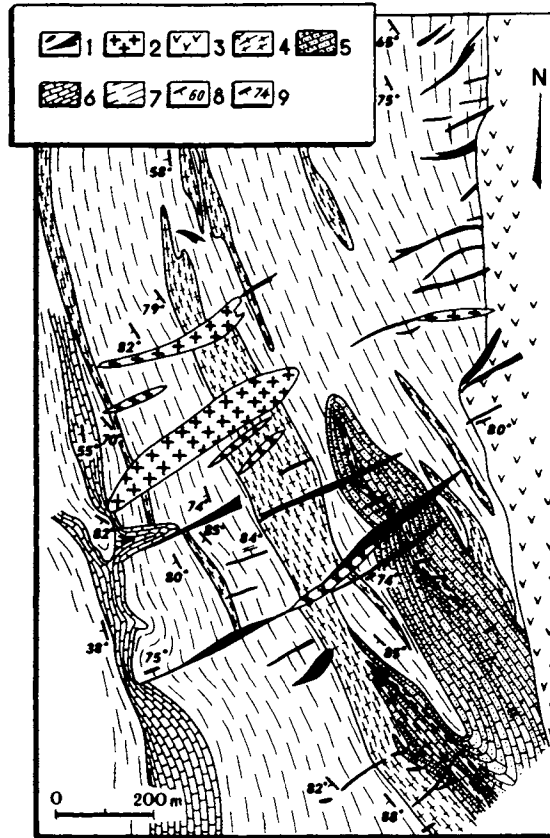


Fig. 121. Location of phlogopite skarns in No. 2 mine, Slyudyanka deposit (after Kuznetsova). 1 - phlog-di-ca veins, 2 - pegmatites, 3 - monzonite, 4 - granitic rocks, 5 - dolomitic marble + calciphyre + amphibolite, 6 - Ca marble, 7 - bt-gt gneiss, bt gneiss, amphibolite, 8 - schistosity, 9 - dip of veins.

## 2.2. Lazurite

The Pre-Baikal region is one of the world's few lazurite provinces. Amongst several known deposits and occurrences in this region is the *Malo-Bystrinka deposit*, discovered in the middle of the last century and located in the upper reaches of the river Malaya Bystrinka, which flows into the river Irkut. The deposit is hosted in a 90 m thick dolomitic marble member and is a series of isolated skarn bodies, replacing granite or sometimes gneiss boudins. The largest lazurite-bearing zones are typical for small boudins, 1–2 m across. Lazurite is a coloured variety of haüyne, which is determined by the presence in the mineral of the  $\text{SiO}_4$  and  $\text{SiO}_3$  radicals requiring oxidized and reduced forms of sulphur. The Pre-Baikal lazurite is intensely coloured, although this is not typical for all lazurite zones, suggesting that the lazurite formed under variable alkaline conditions.

The fact that lazurite occurs precisely in granite boudins (lazurite formation is less in large boudins and inner contacts between marbles and granites) is explained by the metasomatic process having a high alkalinity in such a geological setting. D.S. Kozhinsky (1947) showed that the diopside-lazurite zone appears in magnesian skarns with the highest alkalinity. In small boudins, high alkalinity levels are attained due to the limited quartz content, which impeded the formation of large phlogopite masses, masking the alkalis. Lazurite therefore crystallized immediately after the formation of thin diopside-phlogopite zones. Lazurite areas are also associated with zones of intense shearing and recrystallization in marbles, which formed during dedolomitization.

This brief outline of the mineral deposits inherent to the marginal structures of the Siberian craton, including Pre-Sayan, South Yenisey, Pre-Olkhon and Western Khamar-Daban demonstrates the undoubted similarity in Precambrian mineral deposits for the first two structures, while the second two have different deposits, distinct from those in the first two. The metallogenic scheme in Figure 122 presents a fuller representation of the metallogeny of such a large territory. Comparing the early Precambrian mineral deposits in the first two inliers, it is easy to observe: titanomagnetite deposits associated with ancient differentiated igneous complexes, ferruginous quartzites in Early Archaean, Late Archaean and sometimes Early Proterozoic complexes, micaceous and rare-metal pegmatites of Late Archaean or Early Proterozoic age. Within the South Yenisey and Pre-Sayan inliers, Fe, Cr, Pb-Zn ore deposits and occurrences are associated with tectonic structures of the same type, which consist of a series of structures that formed in sequence over time. For example, Fe deposits: chemogenic-sedimentary eulysite types are hosted in  $Ar_1$  granulite-gneiss supracrustal complexes; volcanogenic-sedimentary jaspilite-type deposits are associated with  $Ar_2$  greenstone belts; and sedimentary deposits are hosted in  $PR_1$  subcratonic rock complexes.

Gold deposits and pegmatites originated during superimposed tectonothermal processes. Similarly, at the end of  $PR_1$ , rare-metal pegmatites were emplaced around the edge of the relatively stable plate belonging to the basement of the Siberian craton, while micaceous pegmatites which had formed at higher P-T conditions are restricted to those parts of the region which were involved in collisional events between the basement platforms of the Siberian craton and the surrounding fold belts. Gold deposits in inliers are restricted to the lowest temperature tectonothermal processes, which formed superimposed zones of retrogression. Ancient crustal blocks – Pre-Olkhon and Khamar-Daban – consist of other rock complexes and consequently are characterised by other useful minerals.

A characteristic feature of the metallogeny of many regions – the repeated appearance over an extensive geological history of exactly the same mineralization – is also reflected in the structures examined here. For example, N.M. Khrenov, G.Ya. Abramovich and others have demonstrated that in the Pre-Sayan region, this feature is most clearly expressed in rare-metal mineralisation, which can be traced here from the Early Proterozoic through to the Mesozoic and against this background it is associated with various ore-magmatic systems. The earliest mineralization occurs in granite pegmatites and is associated with intracratonic basins. Later mineralization is associated with carbonatites, later still with amazonitic sub-alkali granites and, latest of all,

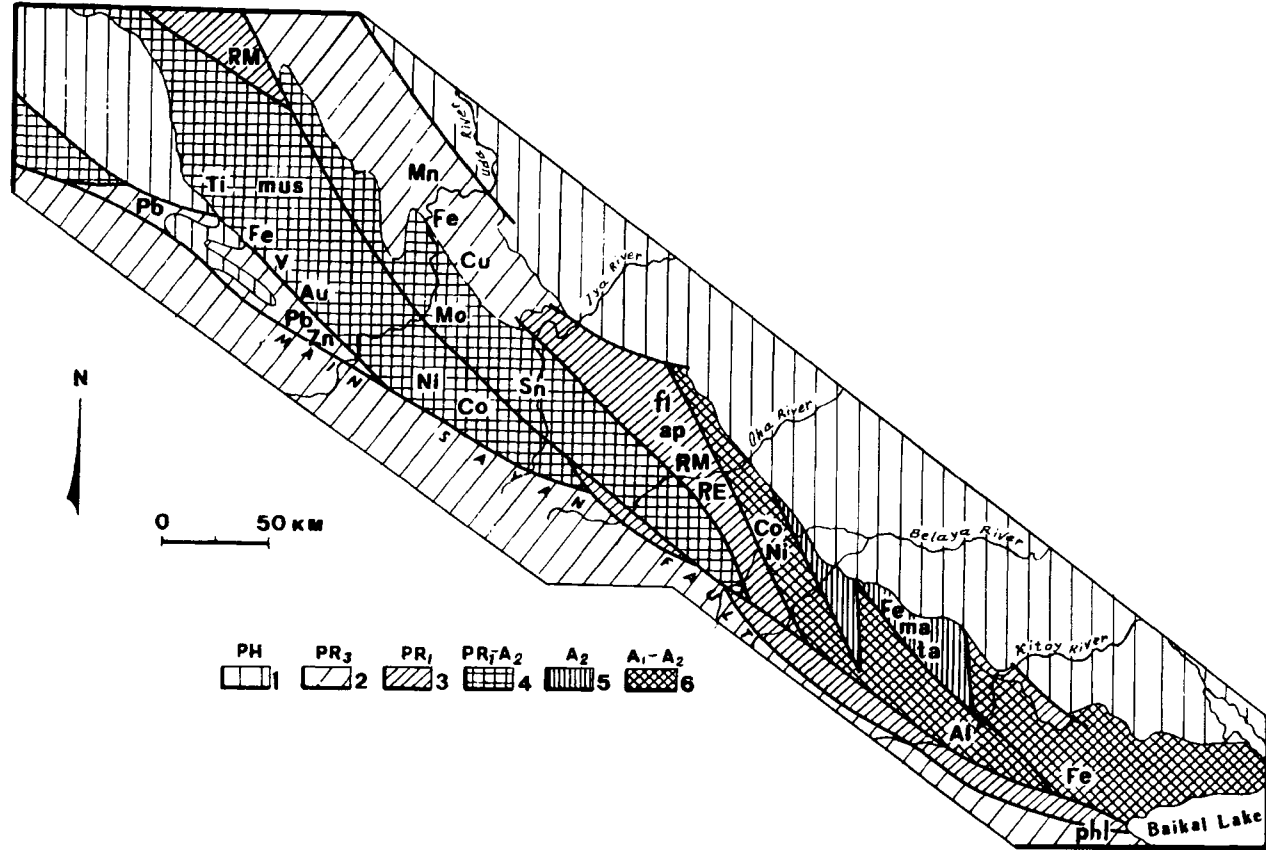


Figure 122. Metallogeny of Pre-Sayan region (data provided by P.M. Khrenov and G.Ya. Abramovich, 1986). 1 – platform cover, 2 – Pt of E. Sayan fold belt & pericratonic basin, 3 – PR<sub>1</sub> of intracratonic basins, 4 – PR<sub>1</sub>-AR<sub>2</sub> of areas of tectono-thermal reworking, 5 – AR<sub>2</sub> of greenstone belts, 6 – AR<sub>1</sub>-AR<sub>2</sub> of granulite-gneiss terrains.

with trachyrhyolites. A common feature in the metallogeny of these regions is a change in the composition of the elements giving rise to concentrations. Thus, elements heavier than Fe are not found in Early Archaean deposits. Judging from the composition of typical Late Archaean deposits, this period was characterized by siderophile–chalcophile geological processes.

This Page Intentionally Left Blank

## Yenisey fold belt

V.Ya. KHILTOVA and G.P. PLESKACH

This belt is situated along the western edge of the ancient Siberian craton and most workers refer it to the Baikalides or more recently to the Ripheides. Its area depends on whether or not the Angara–Kan micro-craton is included. Folded Riphean formations, which define all the belt's features, crop out mainly in the Trans-Angara part of the Yenisey ridge. An important factor in the creation of the belt structure is its situation in the collision zone between the Siberian craton and the West Siberian platform. The belt is characterized by having territories which are highly differentiated on a number of counts: the composition of the sedimentary and volcanosedimentary rocks, their thickness, deformation, the number and composition of volcanic and intrusive rocks.

Depending on these characteristics, the Yenisey belt is divided into three main linear tectonic zones: Eastern (Chernorechenko–Kamenskaya), Central (Teysko–Tatar), and Pre-Yenisey, which in turn are usually further divided into subzones (Fig. 123). Thus, the Pre-Yenisey has the Isakov, Pre-Yenisey and Vorogorsk–Angara sub-zones from west to east. Volcanic formations are restricted to the Central and Pre-Yenisey zones, in which intrusive rocks also play an important role. Recent work in the Isakov zone by V.Ye. Khain, M.I. Volobuyev and Ye.V. Khain (1993), E.G. Konnikov, V.A. Vernikhovsky and others (1994) has produced a complete section of Riphean ophiolites. The ophiolites are tectonically associated with island arc volcanics in this zone (a metarhyolite–andesite–basalt complex). Gabbroic rocks in the ophiolite series have an age of  $1260 \pm 100$  Ma (Rb–Sr method). The ophiolites form thrust sheets, displaced eastwards at the end of the Riphean (600–620 Ma ago) and thrust over Riphean assemblages cut by granites with an age of  $1050 \pm 20$  Ma. In the Pre-Yenisey zone, these are mostly basic rocks, with acid rocks being very minor. In the Central zone there are mostly acid rocks, while the Eastern zone is amagmatic. Nozhkin et al. (1979) have proposed that the elongate zoning in the Yenisey ridge originated during later stages of mobile development, while during the concluding stages at the end of the late Riphean, E–W faults were emplaced and created even greater heterogeneity in the structure of the Yenisey belt.

The Yenisey mobile belt (including the Angara–Kan microcraton) is defined as a single ore belt, the metallogenic features of which are closely related to the composition of the rocks constituting the structural–petrographic zones, and the tectonic structure, in particular deep faults. Brovko et al. (1986) and others have demonstrated that each structural–petrographic zone has its own unique metallogenic features. In the Pre-Yenisey zone, the metallogeny is defined by the widespread distribution of basic rocks, which is particularly the case for the Isakov sub-zone. Characteristic to this sub-zone

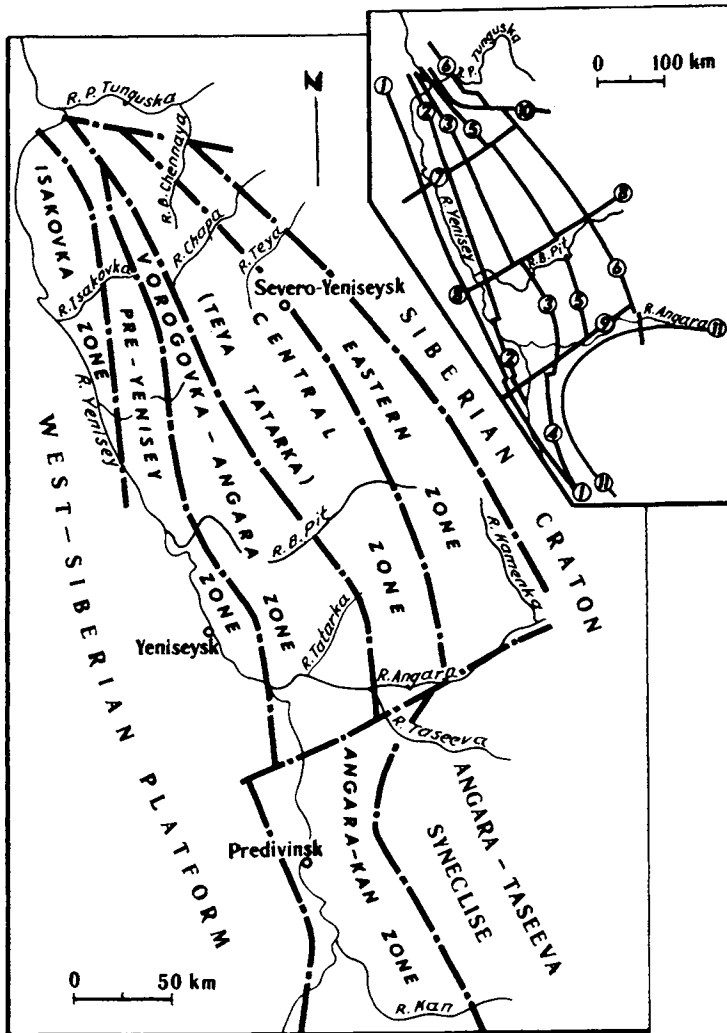


Fig. 123. Structural zones of Yenisey ridge (after Brovko, Kornev and Li, 1986). Inset: faults (Amontov, 1988). 1 - Pre-Yenisey, 2 - Osinovskiy, 3 - Tatar, 4 - Kan-Shilkin, 5 - Motygin, 6 - Belmin, 7 - Yartsevskiy, 8 - Bolshoy Pit, 9 - Lower Angara, 10 - Tungusskiy, 11 - Angara-Kan.

are ferruginous quartzites, chromite mineralization hosted in ultrabasic igneous intrusions, copper-pyrite and pyrite-polymetallic mineralization hosted in basic volcanics, lead-zinc mineralization hosted in carbonate rocks containing volcanics. Many polymetallic ore deposits are found in the Vorogovsk-Angara sub-zone: stratiform pyrite-lead-zinc deposits and occurrences in black shale formations. Iron, manganese and vanadium occurrences are present in this sub-zone.

When considering the Pre-Yenisey zone as a whole, it has to be emphasized that it is mainly characterized by polymetallic, manganese, and chromite mineralization. In the

Central zone, which is dominated by Riphean clastic terrigenous rocks with minor volcanics and widespread granitic intrusions of a batholithic formation, the quartz-ore formation is the most typical. Typomorphic are also metasomatically altered ferruginous quartzites, polymetallic ore mineralization in carbonate and carbonate-volcanic-clastic terrigenous sequences, and baryte-polymetallic. Metallogeny in the Eastern zone is defined by the presence of iron ores (chlorite-hematite-clastic terrigenous formation), magnesite and talc deposits, and phosphorite occurrences.

### 1.1. Iron

Iron is found in all three zones of the Yenisey fold belt. In the Pre-Yenisey zone it is associated with volcanic rocks, forming the ferruginous quartzite type of occurrence. Metasomatically altered ferruginous quartzites are known in the Central zone – the Yenashim deposit. A chlorite-hematite-clastic terrigenous formation is more typical for the Eastern zone – the Lower Angara deposit.

*The Yenashim deposit* was discovered in 1962–64 as magnetite ore deposits and occurrences, treated as a single ore field. The Yenashim ore field extends as a linear strip for some 70 km in a N–S direction in the Central anticlinorium and includes a number of deposits, the largest being the Yenashim which is located in the upper reaches of the river Chirimba, 4.5 km from the town of Yenashiminsky Polkan. According to Komov (1967, 1968) and Kornev (1971), the region is made of metamorphosed volcanogenic-carbonate-clastic terrigenous rocks belonging to the Proterozoic Korda Group. Rocks hosting the ores are quartz-biotite, garnet-biotite, amphibole, mica, and quartz-chlorite-biotite schists. Calcareous and graphitic schists occur sporadically. The rocks are deformed into steep NW-striking folds and are cut by granites belonging to the Chirimba intrusion, which consists of biotite granite, gneissose granite and rarer granodiorite and diorite. Also cropping out in the region around the deposit are rocks consisting of actinolite, epidote, chlorite and magnetite, and defined as metasomatites (Fig. 124). These rocks are found at the contact between granitoids and metamorphic rocks, occurring as bands and lenses, conformable with the contact and dipping at 60–85° to the NE. As a rule, contacts with host rocks are indistinct, and there are transitions across zones with partially altered rocks. It has been assumed that the metasomatites formed in three stages, with the following paragenetic mineral assemblages forming successively: garnet-pyroxene, amphibole-epidote-magnetite, and sulphide-carbonate.

Garnet-pyroxene skarn rocks formed in the earliest pre-ore stage and are preserved only as xenoliths in separate zones, since they in turn were subjected to the effects of later metasomatic processes in the second (ore) stage, as a result of which a new mineral assemblage formed: epidote, amphibole, chlorite, magnetite and others. The ore stage of metasomatism is characterized by a significant influx of iron, magnesium and titanium. In the concluding sulphide phase in the growing mineral assemblage, a new mineral association developed: calcite, pyrite, pyrrhotite and chalcopyrite. A result of the ore stage of metasomatism was the formation of magnetite-rich metasomatites, representing the ore deposit. Ore bodies do not have sharp boundaries and are identified on the basis of chemical sampling as containing more than 26% iron. The ore

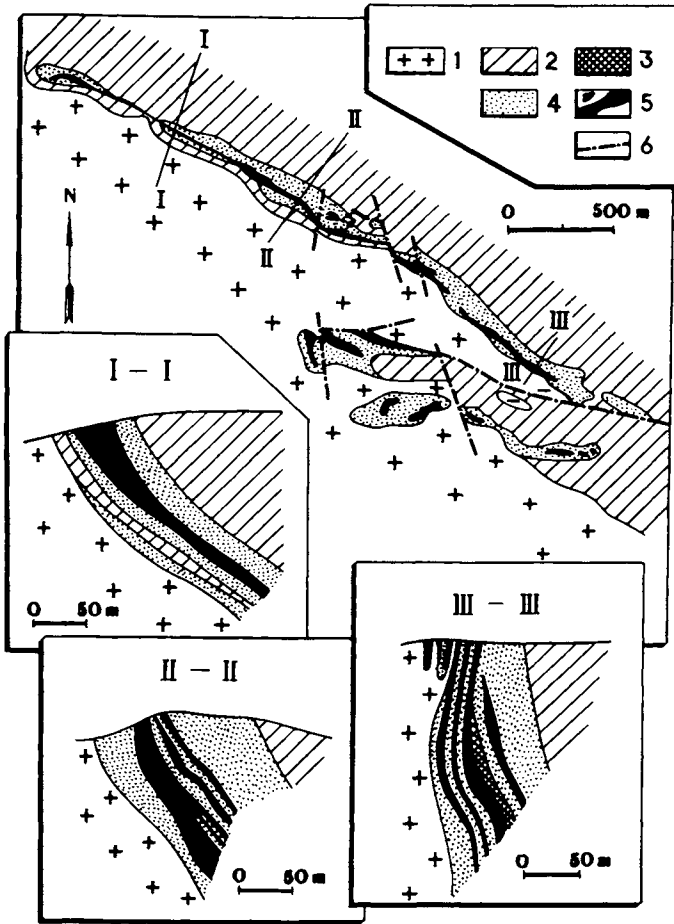


Fig. 124. Geological structure of Yenashimin deposit in section (Kumetz, 1979). 1 - Chirimbin granite, 2 - schist, 3 - quartzite, 4 - hornfels, metasomatites, 5 - magnetite ores, 6 - faults.

bodies are sheet-like and podiform and peter out along strike or sometimes merge with one another. Typically, they have broadly conformable relations with the dip and strike of the metasomatites and their location within the deposit is controlled by NW, sometimes NE faults.

Ten ore bodies have been discovered in the Yenashim deposit, from 200 m to 800 m long and 20 to 70 m thick. Magnetite is the main ore mineral, forming a solid mass, in which the other minerals are seen to form aggregates and veinlets. Pyrrhotite, pyrite, chalcopyrite, melnikovite-pyrite, chalcosite, ilmenite and covellite are present in small quantities in the ores. The following textural varieties are distinguished: 1) massive ores, consisting of magnetite with a small amount of amphibole; 2) disseminated, consisting of amphibole, epidote and dispersed magnetite crystals; 3) banded, represented by alternating magnetite and barren metasomatite bands. Ores in the Yenashim

deposit typically have low sulphur and phosphorus contents. Harmful impurities (arsenic, zinc, copper, lead) are found in minimal quantities. A favourable factor is the presence in the ores of alloying admixtures – nickel, cobalt, manganese, titanium and chrome.

The age of the ore genesis in the deposits of the Yenashim ore field is  $800 \pm 35$  Ma, from vesuvianite separated from skarns in the Uvolzhskoye deposit (Volobuyev et al., 1973); the age of granitic rocks in the Tatar–Ayakhtin complex from radiological data is  $850 \pm 60$  Ma (Volobuyev et al., 1973). Thus, the Yenashim ore deposits and the Chirimba granitic intrusion formed close together in time. Available geological and geochronological data suggest that the magnetite ores in the Yenashim ore field formed due to metasomatic alteration which affected pre-granite primary sedimentary hematite ores during the emplacement of the granite intrusion (Komov, 1969).

*The Lower Angara deposit* is one of the largest in the Angara–Pit iron ore basin, situated in the area between the Angara and Greater Pit river in the Eastern (miogeosynclinal) zone of the Yenisey Trans-Angara region. Information about the presence of hematite ores in this area first appeared in 1933–44. The Lower Angara deposit was discovered in 1946, and in 1947–49 the Udoronga and other deposits were found (Medvedkov, 1981). A large number of occurrences have been found in recent years also. All the ore deposits and occurrences stretch out in a band along the eastern limb of the Central anticlinorium of the Yenisey ridge and are restricted to the western flanks of synclines in the Angara–Pit synclinorium (Fig. 125). The Lower Angara deposit is located on the SW part of the structure. It extends for 20 km, individual beds being 10–15 km, and the beds dip at  $45\text{--}80^\circ$ . On average, the ore zone is 80–100 m thick, occasionally up to 150 m. The ore horizon lies at the base of the Lower Angara Fm in the Upper Riphean Oslyansk Group, which is unconformable on Kirgitey Group sediments. As well as the ore beds, the Lower Angara Fm consists of alternating beds and lenses of argillites, siltstones and sandstones.

Ore bodies are represented by beds of ore-bearing grits, sometimes conglomerates, interbedded with siltstones, sandstones and shales (Fig. 126). The number of ore beds varies both along strike and down dip, and on the flanks they tend to wedge out. Ore beds average 5–8 m thick, the total being up to 50 m. Northwards the ore body is sheared and there is an increase in the total thickness and number of ore beds, but the thickness of individual beds decreases. Contacts between ore bodies and host rocks are sharp, however along strike there is often a gradation into hematized sandstones. The thickest and richest ores lie at the base of the ore horizon.

The main type of ore deposit is ore-bearing grit, varieties being hematitic, sandy-hematitic, and clayey-hematitic grits. Hematite–siderite breccias have been found in the southern part of the deposit. Sandy-hematitic grits containing around 60% of the reserves in the deposit, consist of hematite grit and pebbles, cemented by hematite with significant amounts of quartzose sandstone. About 10% of the reserves are concentrated in hematite grits, distinguished by the lower content of quartzose sandstones in the cement. Clay–chlorite–hematite grits make up around 30% of the hematite ore reserves and consist of hematite pebbles and numerous pebbles of clay–chlorite rocks. Hematite–siderite breccias consist of approximately equal amounts of hematite, chlorite and siderite fragments, cemented by siderite, quartzose sandstone, pyrite and

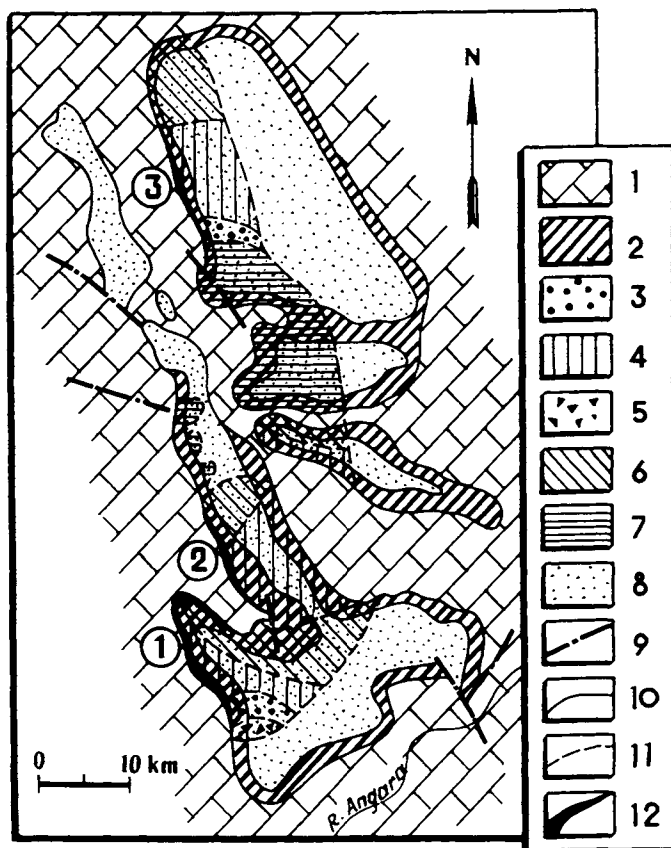


Fig. 125. Geological sketch map of Angara-Pit iron ore basin (Kalugina and Yudin, 1952). 1 –  $PR_3$  limestone, sideritic dolomite, phyllite, siltstone, sst, cgl with hematite lenses, basic lavas beneath ore; 2 – L. Angara clastic-carb ore-bearing formation; 3–7 ore lithofacies: 3 – chl-hema fragmental ores, 4 – chl-hema chemogenic-fragmental ores, 5 – chl-sid-hema breccioconglomerate, 6 – sandy-clayey rocks with thin ores, 7 – clayey rocks in ore-bearing horizon, 8 – dolomite, lst, argillite, phyllite, sst, above ore; 9 – faults, 10 – stratigraphic boundaries, 11 – boundaries of ore lithofacies, 12 – ore deposits (numbers in circles): 1 – Lower Angara, 2 – Udorongo, 3 – Ishimbin.

dispersed magnetite and hematite. Ore-forming minerals are hydrohematite, hematite, goethite, occasionally siderite and very rarely magnesite and pyrite. Non-ore minerals include quartz, lepto-chlorite and other chlorites, clay minerals and sericite. The average iron content in the ores is about 40%, with very low contents of harmful and alloying impurities.

### 1.2. Manganese

Manganese deposits are most characteristic for the Pre-Yenisey zone of the belt. Manganese is found in various ore formations: oxidised and carbonate stratiform and

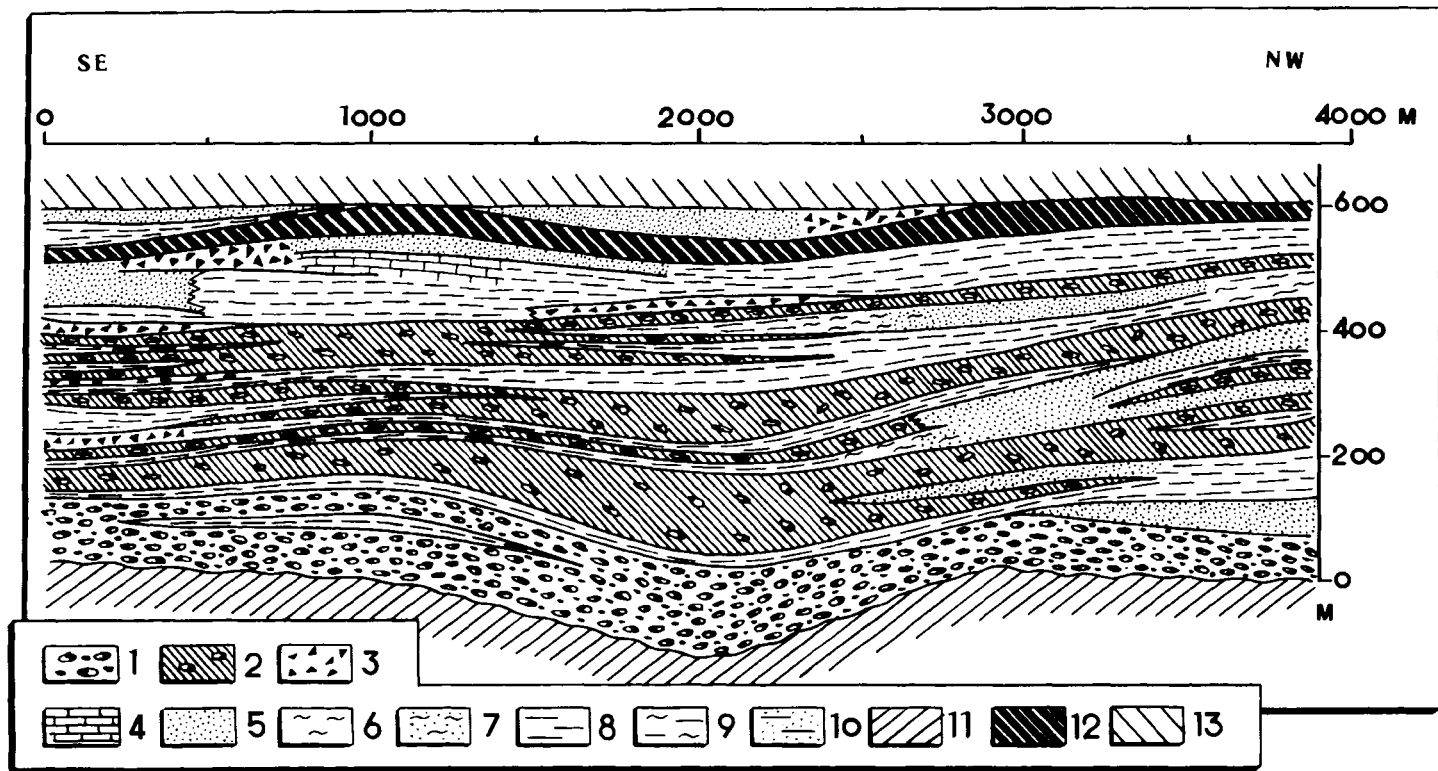


Fig. 126. Longitudinal schematic section of ore-bearing horizon in Lower Angara deposit (after Yudin, 1963). 1 - fragmental ores, 2 - chemogenic fragmental ores, 3 - chl-sid hema breccioconglomerate, 4 - chl argillite, 5 - sst, 6 - siltstone, 7 - sandy siltstone, 8 - argillite, 9 - silty argillite, 10 - sandy argillite, 11 - Kirgitey argillite, 12 - chemogenic ore, 13 - Lower Angara argillite.

oxidised manganese-hypergene (Porozhinskoye deposit) and manganese-carbonate stratiform (Tayozhnoye deposit).

The *Porozhinskoye deposit* was discovered in 1975. It is located in the north of the Yenisey ridge and in the Vorogov depression, which consists of Upper Riphean and Vendian molasse-flyschoidal sediments, overlain by Lower Cambrian platform deposits (Musatov et al., 1980). Manganese ore mineralization is associated with a carbonate-silica member in the Vendian Podyom Fm (Fig. 127). There are four units in the manganiferous formation, from bottom to top these are dolomite, manganese ore, tuffaceous-silica and clastic terrigenous (Mkrtychyan et al., 1982). The sub-ore dolomitic unit consists of grey and light-pink dolomites with a massive or sometimes banded texture with lenses of oncolitic dolomite and thin dolomitic breccio-conglomerate beds. The dolomites are barren, although at the top of the member there are pockets and veinlets of manganese oxides, probably of infiltration origin. The dolomitic unit is 350–400 m thick. The ore-bearing tuffaceous unit lies conformably on

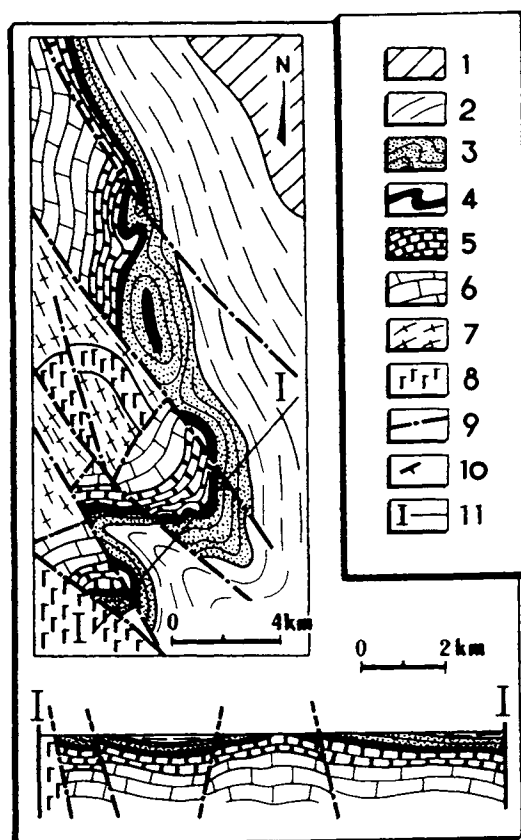


Fig. 127. Sketch map of Porozhin deposit (Mkrtychyan et al., 1982). Vendian: 1 – Nemchan sst. red grit, 2–5 Podyom Fm, 2 – grey sst & shale, 3 – siliceous tuff, 4 – Mn-ore member, 5 – dolomite; 6 – Sukhorechka lst, limey sst; PR<sub>3</sub> complex: 7 – schist, 8 – ultramafics, 9 – faults, 10 – dip & strike, 11 – section line.

dolomites and consists of siliceous tuffites at the base, overlain by manganiferous tuffites and tuffs, giving way to siliceous tuffites. The main part of the ore unit consists of manganiferous tuffites – dark grey to black rhythmically layered rocks, consisting of impersistent sandstone and siltstone beds, and siliceous intercalations, interlayered with manganese ore beds. The colour of these rocks is defined not only by the presence of manganese mineralization, but also the large amount of dispersed organic matter (Golovko et al., 1982). The productive unit is 12 to 85 m thick. A tufogenic-siliceous member, 80–120 m thick, consisting of tufosilicites conformably overlies the manganese ore unit.

The geological structure of the succession containing the ore unit is fairly constant over the area of the deposit, although the ore deposit itself differs in its varied mineral composition, ore texture and structure, and ores of different genetic types are encountered. Ores in the Porozhinskoye deposit fall into two types, based on mineral composition and conditions of formation, primary (oxide and carbonate) and secondary (oxidized-infiltration and residual-infiltration). Primary ores form beds and lenses in manganiferous tuffites and occur mainly at the base of the unit. Beds vary in thickness from 0.9–1.5 m to 8 m. Bedded deposits are typical mainly for the NW part of the deposit, and wedge out towards the SE. At the base of the unit there are thin comminuted zones with manganese mineralization (Golovko et al., 1982).

Carbonate ores crop out mainly in the east of the deposit. Beds containing manganese carbonate are thin in most of the deposit, becoming thicker towards the east and merging together to form a single zone of carbonate ores. Manganese carbonate in tuffites occurs as lenticular, rounded, ellipsoidal, slightly flattened concretions, 0.5 to 2–3 mm in size. The manganese content in the carbonate ores does not exceed 5–15%. Rhodochrosite is the main ore mineral, manganosiderite being less common. Admixtures include siderite, pyrite, apatite, occasionally vernadite and ranseyite.

Oxide ores are predominantly developed in the NW of the deposit. Ore beds are concretions, clusters and irregularly-shaped ore fragments, embedded in a brownish-black silica-clay matrix. Manganite is the main ore mineral, accounting for 70–80% of the ore. Pyrolusite, psilomelane, vernadite; goethite, kaolinite, quartz are present in minor amounts. Small concretions found in the ore beds also have a manganitic composition. A colloidal structure is the most typical for manganese oxide ores, which is characteristic for cryptocrystalline manganite masses. However, there are also ores with a sedimentary structure, lenticular-bedded manganiferous tuffites with thin intercalations of ore material. In addition, partial crystallization of the gel-like masses has led to the formation of manganitic ores with radial, snowstorm and fibrous textures, while dehydration of the gel-like substance and subsequent infilling of resulting fractures have produced an ore with cockscomb texture. Primary oxide ores were affected by diagenetic processes with redistribution of the ore material and partial replacement by tufas, leading to the formation of ores with a brecciated-laminated (?) texture.

At the contact between dolomites and siliceous tufas at the base of the ore-bearing unit, there are brecciated ores with montmorillonite-rhodochrosite mineralization, which formed due to the action of post-magmatic solutions (Golovko et al., 1982). Here, the maximum thickness for such altered rocks is 5–6 m. Sometimes they are

present at the top of the ore-bearing unit, and occasionally this type of rhodochrosite ore is associated with magnetite ore beds. Rhodochrosite mineralization in this type of ore is later, since rhodochrosite veinlets cut the manganitic ores. The manganese content in brecciated ores is variable, and reaches 16–20%.

During the Cretaceous–Palaeogene, primary manganese ores were in the near-surface zone and partially subjected to weathering, as a result of which oxidized infiltration–residual ores formed, richer in comparison to primary ores. This type of ore is more developed in the NW part of the deposit, where ore bodies of this type are up to 8–10 m thick. Since bedded manganitic ores and rocks in the brecciated and infiltration zones were also subjected to hypergene processes, two types of oxidised ores formed respectively – pyrolusite and ranseyite–vernadite which differ not only in their mineral content, but also texturally and structurally.

Pyrolusite ores are the most widespread, forming clusters, concretions and irregularly-shaped ore fragments, embedded in a spongy quartz–clay matrix. Oxidized ores often inherit structural and textural features from manganitic ores, and relict primary manganite is found in them, partially replaced by pyrolusite. In addition, vernadite, goethite and ranseyite are present in insignificant amounts. The manganese content in pyrolusite ores is not usually more than 50%, although it can be up to 80%. Ranseyite–vernadite ores are sharply different from pyrolusite ores and are light porous rocks with a brownish-black colour and relicts of leached dolomite. Vernadite and ranseyite are the main ore minerals, with pyrolusite and goethite admixtures. The manganese content in this type of ore is up to 40%.

### 1.3. Lead and Zinc

Investigations over a 50–60 year period in the Yenisey ridge have established the presence of a belt of polymetallic mineral deposits that stretches in a N-S direction for over 400 km. These deposits are mainly associated with the Upper Proterozoic Tungusik Group of volcanosedimentary rocks. According to Okhapkin and Brovkov (1976), many of the ore deposits and occurrences in the polymetallic belt (over 300) have a number of features in common. These are: a relatively small number of mineral types of ore, and a simple mineral composition; the predominant role of carbonates amongst host rocks, and significant distance from intrusions. Researchers distinguish the following formations amongst the host rocks: 1) galena–sphalerite–carbonate mineral type (e.g. the Gorevskoye lead–zinc carbonate deposit); 2) galena–sphalerite black shale (the Linear deposit, pyrites–lead–zinc black shale); 3) pyrite–polymetallic, associated with silicate rocks of volcanic origin (the Khariuzikhin occurrence).

*The Gorevskoye deposit* belongs to the lead–zinc group, associated with carbonate rocks. It was discovered in 1956 by Yu.N. Glazyrin, and has been studied by many workers, including M.N. Sherman, V.N. Vydrin, G.N. Brovkov, I.A. Okhapkin, T.Ya. Kornev, V.G. Ponomaryov, E.G. Distanov (Okhapkin et al., 1976; Ponomaryov, 1974; Sherman, 1968). The deposit is situated in the southern Trans-Angara region. The area around it, and the belt as a whole, is characterized by N-S and E-W faults. The deposit is hosted in the top part of the Upper Proterozoic Tungusik Group, which consists of shallow water sediments belonging to a clastic terrigenous–dolomite–carbonate

formation, around 1 Ga old (Brovkov et al., 1986). Carbonate rocks greatly dominate the succession. They contain up to 2–4% carbonaceous matter. Rocks hosting the ores are limestones interbedded with thin intercalations of graphitic carbonate–iron–silica (0.1–1–2%), carbonate–clay, and siliceous shales. The dolomite content in limestones sometimes reaches 11%, and clastic material is usually present. There are many diabase dykes in the SE of the ore body, less than 10 m wide and a few hundred m long. Their age is estimated variously from Proterozoic to Mesozoic; however, they cut all Proterozoic rocks, but are not present amongst Phanerozoic formations.

There are three main ore bodies in the deposit: Main, West and North-West, and several minor bodies (Fig. 128). The bodies are a few m up to 90 m thick. The ore bodies are podiform in shape and form a horseshoe outcrop, with a NW strike and SE dip. Sometimes a group of podiform (or other shape) bodies is disconnected and separated by only weakly mineralized rocks.

The North-West deposit has the greatest development of sphalerite, whereas the Main and West bodies are characterized by having the maximum extent and a mainly galena composition with a Pb : Zn ratio of 5 : 1. The ore bodies are hosted in quartz–siderite rocks with lenticular microquartzite zones. They are concordant with their host rocks and display the same degree of deformation. Galena, pyrrhotite and sphalerite are the main ore minerals. Sulphides make up 16–20%, siderite–ankerite 32–42%, quartz 32–38%. Ore mineral assemblages in the deposit are pyrrhotite, galena–

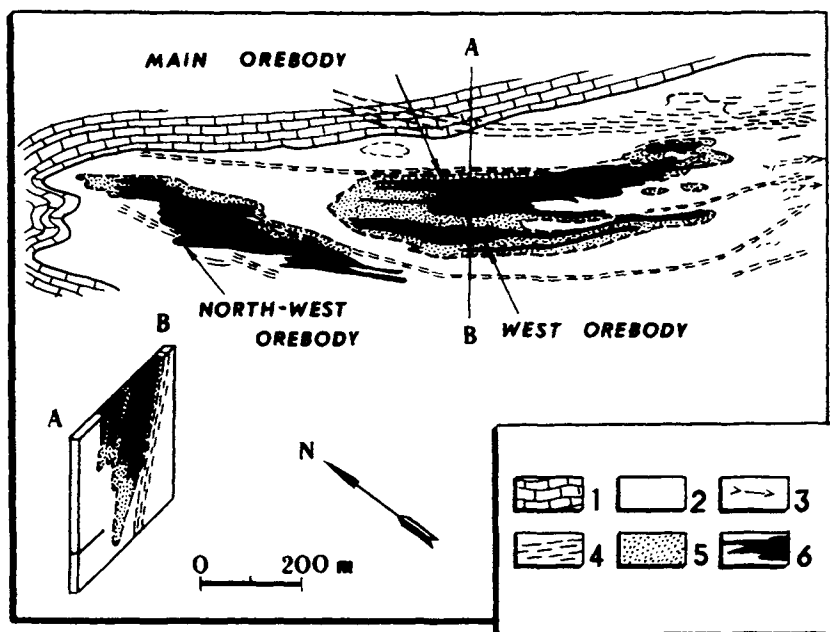


Fig. 128. Surface plan and geological cross-section of Gorevskoye deposit (Ivankin, 1973). 1 - lst, 2 - silicified lst, ore host, 3 - dolerite dykes, 4 - crush zones & shear zones, 5 - hydrothermally altered rock, 6 - ore bodies.

pyrrhotite-sphalerite, and galena. Pyrrhotite and siderite are widespread in the ores of the deposit. Secondary minerals include pyrite, marcasite, magnetite, burnonite, boulangerite, jaspilite, arsenopyrite, ilmenite, chalcopyrite and gudmundite. The geochemical signature of the ores is a higher than host rock content of Ag, Cd, As, Sb, Mn, Ce, Tl, Hg.

Three ore types are distinguished on the basis of the major components: lead-zinc, with  $Pb/Zn < 1$ ; lead,  $Pb/Zn$  up to 6-8; and pyrrhotite. The last type follows the root zones of ore bodies and in the lowest horizons, pyrrhotite ores form independent deposits. Essentially sphaleritic mineralization is concentrated on the hanging wall of the ore zone, and galena on the footwall. The average  $Pb : Zn$  ratio is 4 : 1. Lead ores account for 74% of the reserves in the deposit. Also present are silver, cadmium, thallium, tellurium and mercury. Sphalerite is iron-rich (Fe up to 9.80%) and manganese (MnO = 0.55%). Ore textures are brecciated vein-disseminations, less commonly banded or massive. Heavy sulphur isotopes are typical for the major ore-forming minerals ( $\delta^{34}S$  from + 12 to 24%); pyrite has lighter sulphur, with  $\delta^{34}S$  from 2 to 15%. Mineralization has been dated at  $870 \pm 100$  Ma from the lead isotope composition (Volobuyev et al., 1973).

Various hypotheses exist regarding the genesis of the deposit. Several workers regard it as hydrothermal-metasomatic. Others consider it to be hydrothermal-sedimentary in origin, based on the fact that the Gorevskoye deposit has a strictly lithostratigraphic setting and no direct associations with intrusive formations in the region have been found, there are no adjacent ore metasomatites, and the ores have a simple composition (Brovko et al., 1986).

*The Linear deposit* was discovered in 1959 by L.G. Savanovich and investigated by A.Ye. Miroshnikov, A.A. Okhapkin, G.N. Brovko, E.G. Distanov, T.Ya. Kornev, and many others. It is located in the Teva-Tatar zone (Brovko, Li et al., 1986). The region in which the deposit occurs is dominated by an E-W-striking fault which has the same trend as the fold structures here. The region consists of Upper Riphean rocks belonging to the Shuntar Group, low-grade metamorphics. Intrusive rocks are represented by a few rare diabase dykes. The rock succession hosting the ores is divided into two parts. At the base are weakly mineralized phyllitic siltstone, calcareous mica schist, graphite-mica schist, graphite-mica calcareous schist, and micaceous limestones with thin syn-sedimentary carbonate breccias. The upper part of the succession which actually hosts the mineral deposit consists of phyllitic-graphitic siltstone, quartz-mica schist, quartz-carbonate-mica schist, and sericite quartzite. Volcanogenic rocks have been found in various parts of the section, according to data provided by N.A. Okhapkin (in Ruchkin, 1984).

Mineralization gravitates towards a carbonaceous quartz-sericite schist member in which sericite, hydromica, quartz and carbonaceous matter are the main constituents, with secondary pyrite, siderite, chlorite, chloritoid, phlogopite and paragonite. Typically, the schists are highly dislocated. All these rocks form an anticlinal fold, limestones in the core of which are steeply dipping (Fig. 129).

The ore bodies are complex lenticular deposits, forming a single arcuate ore zone. Bodies strike at  $290-300^\circ$  and dip to NE at  $40-60^\circ$ ; they are a few m to 30 m thick and can be traced for several hundred metres along strike. Within the ore bodies there is an

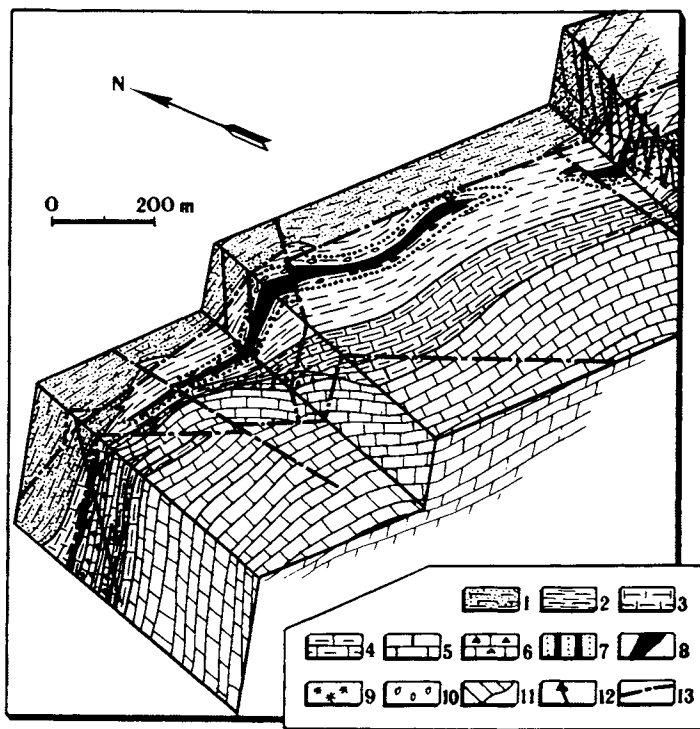


Fig. 129. Block diagram of Linear deposit (Miroshnikov et al., 1977). 1-3 qz-seric schists: 1 - silty, 2 - carbonaceous, 3 - carbonaceous-limey. 4 - clayey lst. 5 - cryptogenic & chemogenic lst. 6 - bedded & brecciated lst, 7 - qz-pyrite sand, 8 - sulphide ores. 9 - brown ironstone, 10 - bleached rocks near ores. 11 - weathered mantle, 12 - boreholes, 13 - faults.

alternation between laminae of solid pyrite ores and mineralized carbonaceous quartz-sericite schist. Quantitatively, the ratio between these types is not constant, but pyrite laminae are always in the majority. Ores have a banded texture. Sphalerite and galena in the ore mass form disseminated and vein-disseminated aggregates. Ore minerals are pyrite in two generations (I and II), sphalerite (I, II), galena. Secondary minerals are pyrrhotite, chalcopyrite, arsenopyrite, ilmenite, and burnonite. Pyrite II accounts for 50-60%; the sphalerite II and galena contents in places drop to 30-40%, with sphalerite being 5.5% on average, and galena 1.2%. Ore mineral assemblages are early sphalerite-pyrite and later galena-sphalerite-pyrite. The richest lead-zinc mineralization is associated with areas of intense phlogopite growth. The deposit formed at relatively high temperature (greenschist facies) as a result of which the sphalerite present is iron-rich. From XRF work, the deposit is known to contain cobalt, nickel, tungsten, tin, antimony and bismuth. The sphalerite and galena are characterised by having heavy sulphur isotopes.

A weak zonation is observed in the lead and zinc distribution. Lead occurs in relatively higher amounts in the upper parts of the ore bodies. The ore zone has a zoned

primary aureole. Parts above the ore are enriched in barium and lead, and beneath the ore – zinc and manganese. As the ore zone tapers out in the geochemical area, there is an increase in the lead to zinc ratio. The tops of ore bodies have been subjected to oxidation, with the formation of iron hard pans. Wall-rock alteration in the deposit is weakly expressed and has been completely ignored by some workers (Ponomaryov, 1974). This type of alteration includes silicification, sideritization and ankeritization. Host rocks have an Upper Riphean age, while the mineralization in the deposit is two-stage, at 900 Ma and 650 Ma.

As well as the deposits considered above, the Yenisey ridge is host to polymetallic occurrences associated with volcanogenic–clastic terrigenous assemblages. Ruchkin (1984) has proposed that the ore-hosting formations in this region – black shale and carbonate which host the lead–zinc deposits – form a single lateral series of formations which also encompasses the volcanogenic–sedimentary sequences. Volcanics in these sequences are represented by a basalt–andesite–liparite magmatic series. Uniting the host formations into a single lateral series (Fig. 130) presupposes a paragenetic relationship between the ore deposits.

#### 1.4. Gold

Most gold mineralization (occurrences and ore deposits) in the Yenisey belt is located in the Central zone, which has widespread granite intrusions, with which the gold is often associated. Gold has been found in various ore formations: gold–quartz (Gerfedskoye, Soviet), gold–antimonite–quartz (Uderey), and gold–sulphide (Olympiad).

##### 1.4.1. The Gerfedskoye gold ore field

The Gerfedskoye deposit was discovered in 1890 and was first described in 1910 by A.K. Meister as the “Main Vein”. According to Li et al. (1976), this deposit forms the main

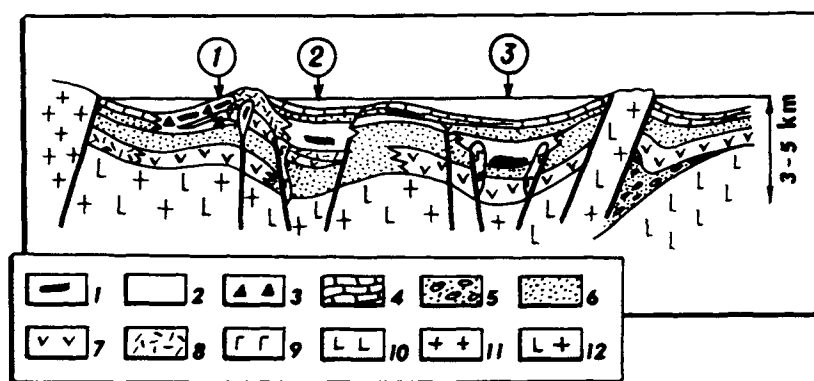


Fig. 130. Idealised sketch of palaeotectonic environments hosting stratiform polymetallic ore deposits (Ruchkin, 1984). 1 - ore deposits. 2 - basins. 3-9 host rocks. 3 - volcanic, 4 - carbonate, 5 - cgl & sed breccia, 6 - clastic, 7 - basic volcs, 8 - acid volcs, 9 - basic intrusions: 10-12 types of weathered mantle 10 - oceanic, 11 - continental, 12 - transitional. Deposits (numbers in circles): 1 - Linear, 2 - Gorevskoye, 3 - Khariuzikhin

part of the Gerfedskoye ore field which runs in a near N-S direction and is located in the eastern axial part of the southern termination of the Central anticlinorium. Cropping out in the anticlinal core are granitoids belonging to the Tatar massif, and rocks of the Lower Proterozoic Penchenga Group. It is assumed that the deposits in this ore field are spatially and genetically related to the granitic intrusion. The spatial association has been established by gravity surveys (Fig. 131; Li et al., 1975). The deposit is situated on the outer contact of the intrusion, 5–6 km away from its eastern edge, and is hosted in sediments at the top of the Penchenga Group at its boundary with the Korda Group (Li et al., 1975). The upper part of the Penchenga Group consists of carbonatized quartz–chlorite schist and limestone lenses, greenish quartz–chlorite schist interbedded with black phyllite. Near the contact, the Korda Group consists of carbonaceous–clay shale, and sandstone with tuffite and porphyrite lenses. Structurally, the ore field is defined as a monocline with a gentle (20–25°) easterly dip, though occasionally this is up to 45°, and up to 70° where small-scale folds are developed. Minor fold axes usually strike almost E–W, while the regional strike of the host rocks is more nearly N–S, as are the faults. Mineralized areas are restricted to carbonatized and silicified rocks, containing lenticular and bedded deposits of quartz–carbonate, carbonate–quartz and muscovite–carbonate metasomatites. Deposits are

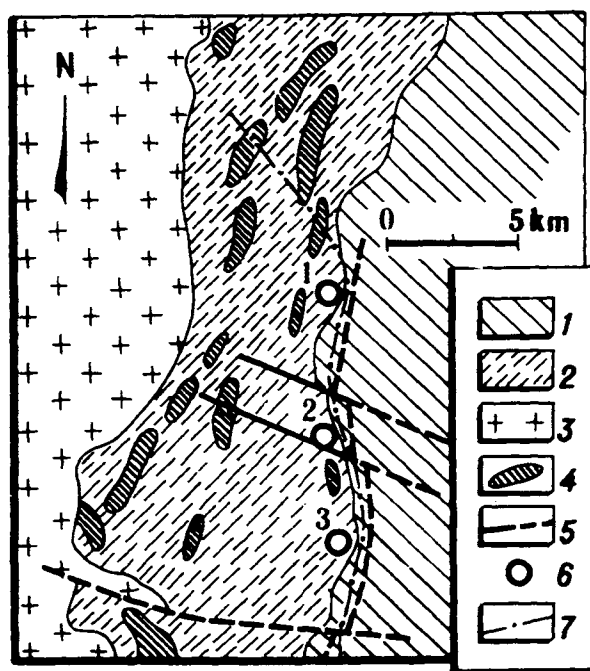


Fig. 131. Geological sketch map of Gerfedskoye ore field (Li and Shokhina, 1976). 1 – Korda Gp (PR<sub>3</sub>), 2 – Penchenga Gp (PR<sub>1</sub>), 3 – granitoids, 4 – diabase, gabbro–diabase, 5 – faults, 6 – Au deposits: Nikolayevskoye (1), Upper Uderey (2), Gerfedskoye (3); 7 – granite outlines, inferred from gravity data.

from a few cm to 20 m thick and can be followed for a distance of 150–210 m. Footwall contacts with host rocks are usually straight and linear, while hanging wall contacts often have bulges.

Metasomatite bodies are sub-concordant with host rock structures and are localized along the boundary between the Penchenga and Korda groups. They are cut by steeply-dipping quartz veins and veinlets. Places where veins are highly concentrated form stockwork bodies, which themselves are ore deposits. Veins and veinlets are composed of grey-white, milky-white and sometimes bluish quartz with tiny amounts of carbonate. Ore mineralization includes pyrite, pyrrhotite, arsenopyrite and magnetite. Secondary minerals are chalcopyrite, galena, gold, ilmenite, sometimes bismuthite, native bismuth and silver. Gold forms either visible segregations in places where pyrrhotite, pyrite and chalcopyrite have accumulated, situated among coarsely crystalline quartz, or it occurs as microscopic segregations in arsenopyrite, pyrrhotite and pyrite associated with quartz in cross-cutting veins. Here the gold fills fractures in sulphides and occurs along grain boundaries. The commonest ore types in the Gerfedskoye deposit are arsenopyrite–pyrite and pyrite–sphalerite–galena. According to Li and Shokhina (1976), the deposit originated due to rock replacement and infilling of fracture spaces under the influence of hydrothermal ore processes induced by granitic emplacement. M.I. Volobuyev has provided data showing that the Tatar granitic intrusion is  $850 \pm 60$  Ma old. The N–S zone which includes the Gerfedskoye ore field also contains the Nikolayevo and Upper Uderey deposits, which have different ore types from the Gerfedskoye. For example, pyrrhotite–pyrite ores are more widespread in the Nikolayevo deposit. The Gerfedskoye deposit belongs to the gold–quartz formation, which is typical of many ore deposits and occurrences in the Yenisey ridge, in particular the Soviet deposit.

*The Soviet deposit* (Smirnov, 1974; Li and Shokhina, 1978) has been investigated by N.V. Petrovskaya, V.A. Bogdanovich, P.V. Ivankin, L.V. Li and O.I. Shokhina, among others. It is a 10 km long, 1 km wide strip running in a NW direction. The deposit is located in a tectonic block at the junction between the Central and Eastern zones. Host rocks are dark grey to black and greenish-grey phyllitic schists and silty-clayey shales. Drill cores prove that with depth these schists gradually merge into greenish-grey and green quartz–chlorite–sericite and quartz–sericite schists. No intrusive rocks have been found directly within the area of the deposit. They are seen only 2.0–2.5 km to the NNE and 5 km to the ENE, represented by diabase and gabbro–diabase which are cut by small mica lamprophyre and syenite–porphyry dykes. A poorly-exposed granite intrusion has been found here. The structure of the ore field is defined by the internal structure of the schist unit and the faults which affect it. Typically it contains zones which display greater schistosity which predate the ore and have a complex history of development. The schist unit itself is deformed into arcuate, curvilinear or sometimes isoclinal folds which have a more or less constant NW strike and axial surfaces dipping SW at angles greater than  $60^\circ$ . Fold axes plunge SE at  $15\text{--}20^\circ$ . The main mass of quartz veins and veinlets in the ore field is affected by a penetrative cleavage. The deposit has seven productive quartz vein zones which differ in thickness but have constant dip and strike: steep ( $70\text{--}80^\circ$ ) SW or NE dip and NW ( $305\text{--}310^\circ$ ) strike. Zones are 200–1000 m long and a few m to 300 m wide.

Vein zones consist of a large number of short quartz veins and veinlets extending in the strike direction of the zones. The veins often contain numerous wallrock inclusions, completely unaffected by any alteration. Sericitization and chloritization of inclusions is seen only rarely. Rocks hosting the veins have been more or less sericitized and chloritized. Tourmaline, apatite, rutile after ilmenite, and carbonate veinlets are frequently observed. Ores in this deposit belong to the low-sulphide type, with sulphides amounting to about 1% usually, occasionally 3–5%. Quartz is the main vein mineral, in four generations: 1) the commonest is milky-white, coarsely crystalline, everywhere showing signs of deformation; 2) semi-transparent saccharoidal and finely prismatic; 3) transparent, fine cockscomb habit; and 4) clear as water, acicular. Ore minerals are pyrite (which accounts for 80% of the total mass of sulphides) and arsenopyrite. Secondary minerals are pyrrhotite, sphalerite, galena, chalcopyrite, marcasite, rare bismuthite, native silver, feibergite, maucherite, violarite, and calaverite. Ore types in the deposit are: homogenous quartz, quartz with host rock relicts, quartz–arsenopyrite, quartz–sulphide with an admixture of polymetallic sulphide group (the most productive type). Mineral assemblages show a zonation within the quartz vein zones. At the centre is an economic essentially arsenopyrite assemblage. In the peripheral zone at the edges of economic ore bodies, the pyrite assemblage is dominant, giving way to quartz veinlets along strike, which contain disseminated, fine-grained pyrite and an admixture of carbonates. The polymetallic sulphide assemblage occurs unevenly at the centre and on the flanks. Gold often forms microscopic segregations in the quartz, but the greater part is in sulphides. The gold grade is 918 to 983.5, being 940 on average in upper horizons and 954 in lower horizons.

Various points of view exist regarding the genesis of the mineralization. N.V. Petrovskaya is of the opinion that it has a hydrothermal origin, relatively high-temperature, fairly deep level, and formed in several phases. L.V. Li and O.I. Shokhina maintain that as well as veins with a hydrothermal origin, there are those which arose due to the regrouping of quartz–silt material in the wall rocks during further recrystallization while hydrothermal processes were taking place. Such veins are poor in gold.

*The Uderey gold–antimony deposit* was discovered in 1966 and has been investigated by A.T. Stebleva, L.V. Li, E.G. Distanov, O.I. Shokhina and others. It is situated in a central strip of flat-lying folds in a N–S syncline on the eastern limb of the Tatar anticlinorium – the Teya–Tatar zone. The deposit lies in Proterozoic metamorphosed clastic terrigenous and carbonate rocks belonging to the Uderey, Gorbylok and Korda formations (Fig. 132).

In the region around the deposit, the Korda Fm consists of quartzose sandstone, tuffite and porphyrite. The Gorbylok Fm consists of dark-green phyllite (quartz–sericite–chlorite composition) with thin siltstone intercalations and limestone lenses. The Uderey Fm consists of dark grey, grey–black, grey and greenish-grey phyllitic clay and silty–clayey schists. Over the area of the deposit the rocks are deformed into broad, open synclines and anticlines with a NE strike. Ore-controlling structures are thrusts and reverse faults parallel to the strike of the NE folds. These faults are often accompanied by intense zones of shearing, crushing and schistosity (Fig. 133). Quartz veins strike NE (10–50°) and dip at 35–60° to the NW. Very few have a NNE strike. Morphologically, the veins are comparatively simple, with a straight, linear strike.

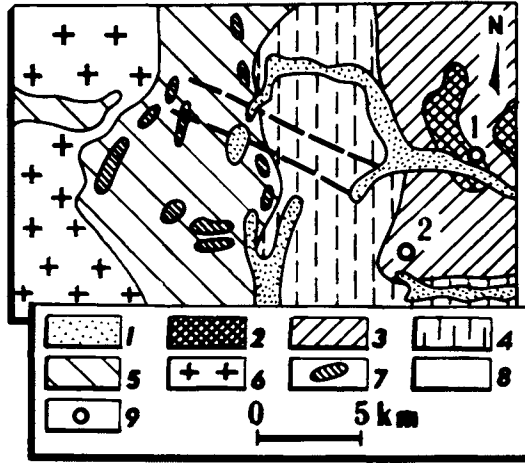


Fig. 132. Geological sketch of structure of Vasilyevo and Uderey deposits (Li et al., 1971). 1 – Tertiary & Quaternary, 2-4 PR<sub>2</sub>: 2 – Uderey Gp. 3 – Gorbilok Gp. 4 – Korda Gp. 5 – Penchenga (PR<sub>1</sub>), 6 – granite, trondhjemite, granodiorite, syenite, 7 – gabbro-diorite, diorite, amphibolite, 8 – faults, 9 – ore deposits: 1 – Uderey, Sb. 2 – Vasilyev, Au.

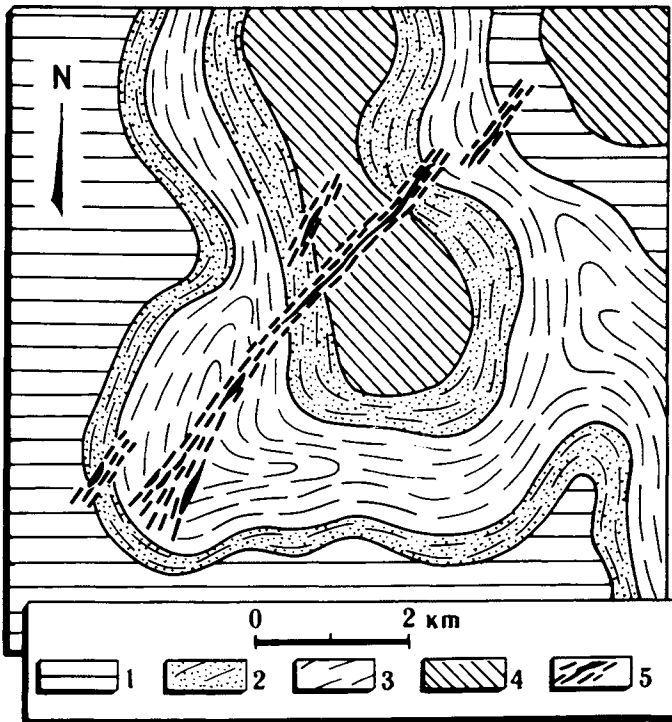


Fig. 133. Geological sketch map showing structure of Uderey deposit (Li et al., 1971). 1 – Korda phyllite, 2 – Gorbilok siltstone, 3 – Gorbilok phyllite, 4 – Uderey phyllite, 5 – ore bodies & shear zones.

Sometimes they are conformable with the bedding in the host rocks and folded together with them, and sometimes they cut the bedding. Podiform, vein-like and columnar bodies are distinguished. Due to changes in thickness and strike, they have wavy outlines. Ore bodies regularly consist of several sub-parallel veins and impregnated schists which host the veins.

The Uderey ore field contains three sub-parallel ore zones: North, Burakhtin and Main (Stebleva, 1971). Gold in the ores is associated with both quartz veins containing pyrite and arsenopyrite, and with antimony-bearing veins. The main minerals in the gold ore veins are quartz and small amounts of carbonate and albite. Ore minerals include pyrite, arsenopyrite, specular ores and sphalerite. Sulphides amount to no more than 5% in total, thus the Uderey deposit was previously classified as a sulphide-poor formation by N.V. Petrovskaya et al. Gold occurs disseminated and in small cavities, usually in quartz. Native gold grains are in clusters or extended into thin wispy outlines and threads. It is unevenly distributed and is found as traces, or up to a few tens of g/t. The greatest concentration has been found in the Central part (Stebleva, 1971). Antimony mineralization is located to the NE of the gold-bearing structure. Quartz-gold veins give way to quartz-antimonite veins in that direction. Wallrock alteration effects include pyritization, arsenopyrite growth, silicification, sericitization and carbonatization. Veins with antimony mineralization contain in addition to quartz and antimonite as major minerals, bertierite, pyrite, siderite, rare sphalerite, chalcopryrite, arsenopyrite, etc. The antimony content is highly variable, from traces to 89%. As main ore minerals, gold and antimony are clearly individualized spatially but they do have a number of similarities, such as their geological setting and ore morphology.

According to L.V. Li, gold and antimony mineralization formed during different stages in a single process, suggesting that the deposit can be treated as a plutonic-hydrothermal type. E.G. Distanov et al. (1971) classify it as a telethermal type, in which gold-quartz and quartz-antimonite mineralizations of different ages occur together. The age of the first quartz-gold mineralization has been estimated at 850–900 Ma, and about 660 Ma for the later quartz-antimonite.

Recently, several deposits and occurrences in the gold-antimony-quartz formation, in particular the Vedugin occurrence, have been referred to the auriferous metasomatite-beresite formation (Sazonov et al., 1995). The metasomatites are present in Riphean chlorite-sericite schists, with the following composition: biotite, chlorite, chloritoid, sericite, plagioclase, graphitic material. The metasomatic column presumably had four zones: 1) chloritized schists with calcite, dolomite and pyrite; 2) sulphide-impregnated schists with carbonate-ankerite and carbonate-enriched crenulated schists (with siderite); 3) sericitic quartzites (with up to 60% sericite); 4) quartzites containing rutile, pyrite, pyrrhotite and arsenopyrite in addition to quartz.

Three of these zones (2, 3, 4) are auriferous metasomatites. Polymetallic ore mineralization is developed in them, consisting of pyrite, pyrrhotite and arsenopyrite, with additionally microscopic aggregates of berthierite, antimonite, marcasite, pentlandite, chalcopryrite, sphalerite, galena, cubanite, cobaltine, ulmannite, breithauptite, gudmundite, tennantite, sartorite, jamesonite, tetrahedrite, boulangerite, falkmanite, burnonite, sakharovaite, joseite-B, hessite, argentite, aurostibite, electrum, native antimony, bismuth and three generations of gold (Sazonov et al., 1995).

Gold I – yellow, assay 917–975%. Gold flakes 0.02–0.05 mm in size occur as isometric drop-shaped inclusions in pyrite, pyrrhotite, chalcopyrite and arsenopyrite,

Gold II – pale yellow, assay 885–949%. Contains admixture of up to 1.5% silver and up to 6–7% mercury. Forms irregularly shaped segregations in intergranular spaces between quartz and ankerite. Gold flakes are 0.1–0.2 mm in size.

Gold III – pale reddish-orange, assay up to 975%. Contains admixture of up to 1% copper, up to 4.5% antimony. Gold flakes form films, rims and platelets replacing antimony minerals. Size 0.0015–0.07 mm.

Gold II and III (with mercury and antimony) are typomorphic minerals for the metasomatite–beresite formation. K–Ar studies show that the age of the metasomatite–beresite formation is 682–715 Ma. This value is slightly less than the age of quartz vein type gold deposits, determined by the same method (692–795–850 Ma, Sazonov et al., 1995).

*The Olympiad deposit* is located in the middle tectonic zone of the Trans-Angara Yenisey ridge, in the upper reaches of the river Yenashimo. It belongs to the gold–sulphide formation. Originally, in the early 1950s, it was defined as an uneconomic antimony deposit. In the mid-1970s, L.V. Li and colleagues defined it as a gold deposit, since they managed to determine that the distribution of antimony mineralization did not coincide with the distribution area of gold. The deposit (Li, 1976) is located in a sag in the roof zone of a granite intrusion and occurs in a zone affected by the Tatar deep fault, in the area where it has a knee-bend flexure. It is hosted in a Riphean meta-sedimentary assemblage (Korda Fm in the Upper Proterozoic Sukhoy Pit Group) and is located in the part where the intrusion is more than 1 km deep, from gravity measurements. Rocks hosting the deposit are quartz–mica schist, quartz–carbonate–mica schist with limestone bands, and carbonaceous quartz–muscovite schist. Where they have been affected by the intrusion, the schists are hornfelsed (biotite, amphibole, muscovite) and the limestones have been altered to skarns. The deposit is situated in a fault-bounded block in which the constituent rocks show complex, high-strain fold effects and widespread small-scale faulting. Faults include conformable and sub-conformable interlaminar shear zones, strike-slip faults along the contact between different lithological horizons and transverse, steeply-dipping faults and strike-slip faults.

Disseminated sulphide ore mineralization is associated with various metasomatite compositions, which are most intensely expressed at the boundaries between different lithological horizons. Quartz–carbonate–mica schists and limestones are particularly strongly altered. Mineralization is localized in the contact zone between quartz–carbonate and quartz–muscovite–graphite schists (Fig. 134). Quartz–muscovite–graphite schists are assumed to have acted as a screen during the influx of ore-bearing solutions. Ore bodies with disseminated gold–sulphide ores are sheet-like, extending along the axes of gently E-dipping antiforms and recumbent folds. L.V. Li considers that interlaminar slip zones played a particularly important role in the localization of the mineralization. Mineralization is concentrated on both sides of these slip zones, but is commoner on the footwall. Transverse faults are also thought to have been important in the ore emplacement. Along interlaminar zones there is frequently a highly-altered weathering mantle, inheriting a primary ore concentration. The ore mineralization has a complex composition. Pyrrhotite and arsenopyrite are the main ore-forming minerals,

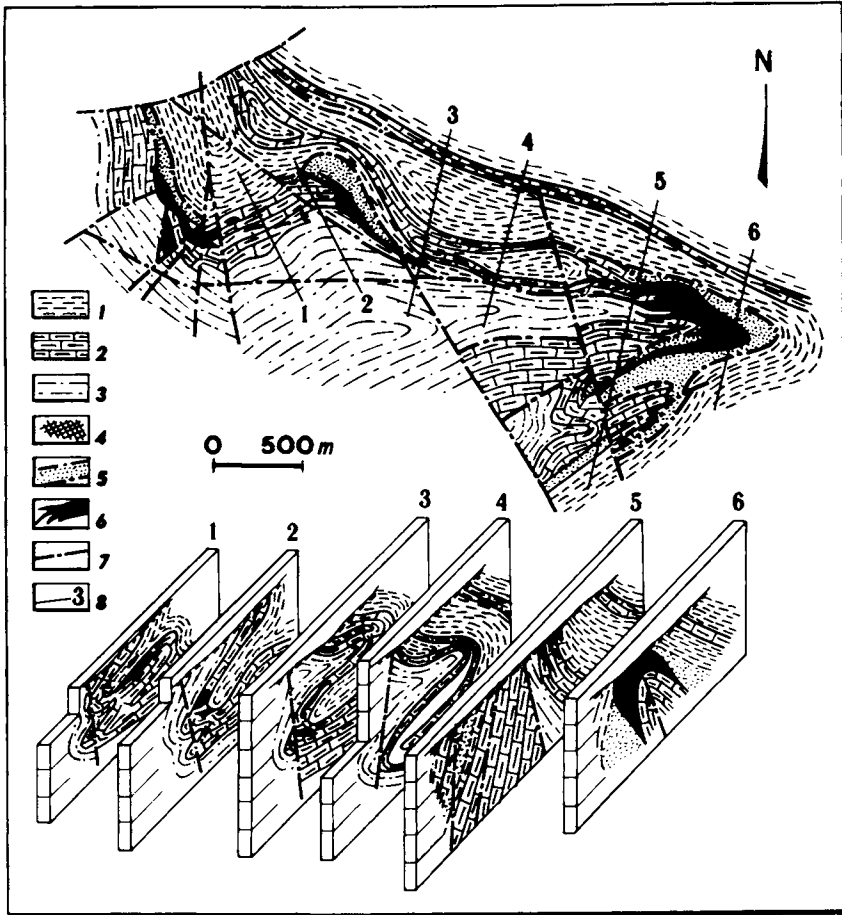


Fig. 134. Plan and diagrammatic block sections of Olympiad deposit (after Kruglov and Li, 1986). 1-3 schists: 1 - graphite-qz-musc, 2 - qz-carb-mica, 3 - qz-mica; 4 - gt-hbl-px-microcline skarnoids. 5 - products of weathered mantle, 6 - ore bodies, 7 - faults, 8 - sections.

represented by three generations. Less common are pyrite, antimonite, berthierite and gold; and there are rare occurrences of galena, sphalerite, chalcopyrite, grey copper ore (tetrahedrite-tennantite), jamesonite, bismuthite, marcasite, magnetite, titanomagnetite, ilmenite and scheelite. Detailed microscopic studies have revealed the presence of individual inclusions of pentlandite, molybdenite, gudmundite, native antimony, burtonite, native silver, violarite, aurstibite, ulmannite and alabanite. The sulphur isotopic composition in sulphides is characteristically variable, from 1.1 to + 17.4%. Gold forms small, dispersed aggregates 0.003 to 0.1 mm across. It is associated with pyrrhotite, arsenopyrite, pyrite and micro-granoblastic quartz (up to 25% gold intergrown with quartz and rock, up to 75% with sulphides and up to 3% free gold). Most often, the gold is associated with arsenopyrite, with which it is intimately intergrown or

infilling minute fractures in grains. Neutron activation analysis has shown that gold is present in all arsenopyrite crystals, but is unevenly distributed even in crystals taken from the same sample (Genkin et al., 1994). The edges of arsenopyrite are usually enriched in gold, where its content sometimes reaches 2000 g/t. The gold content in pyrrhotite and pyrite is about half that in arsenopyrite. Different bodies in the deposit have different gold contents (Genkin et al., 1994). The average is between 2.5 and 7–8 g/t, with a maximum from 10 to 84 g/t. In the weathered mantle developed around the ore bodies, the gold content is approximately twice as much. According to L.V. Li and L.N. Grinenko who have worked on the Olympiad deposit, it belongs to the plutonic–hydrothermal type, which owes its origin to hydrothermal–metasomatic processes which developed during the emplacement of the granitic intrusion.

### *1.5. Talc and magnesite*

*The Kirgitey deposit.* The Yenisey ridge hosts one of the largest talc and magnesite deposits in the former USSR – the Kirgitey. It belongs to the Uderoy ore field (Smolin, 1961), located in the area between the rivers Greater and Lesser Kirgitey, on the SW limb of the Angara–Pit synclinorium, in the Eastern zone of the Trans-Angara region (Fig. 135). The deposit was opened in 1948. The region around the Kirgitey deposit consists of weakly metamorphosed rocks belonging to an Upper Proterozoic clastic terrigenous–carbonate sequence (Fig. 136), represented by sandstone, siltstone and argillaceous shale (Pogoryny Fm); limestone and shale (Kartochka Fm); dolomite (Aladyino Fm); argillaceous shale, limestone and quartzite (Potoskuy Fm). Talc occurrences gravitate towards the contact between Aladyino dolomites and Potoskuy argillaceous shales. They are controlled by major faults with a N–S strike and associated minor splay faults (Smolin, 1962). The total length of the N–S–trending ore field which includes the Kirgitey deposit is around 2 km.

A characteristic feature of the Kirgitey deposit is the presence of various talc ore types, which differ in origin, geological setting, and economic importance. In addition to hypogene ores, represented by primary crystalline talc rocks, there are also hypergene ores – residual powdery talc weathered crusts and redeposited powdery talc which is presumed to be of Tertiary age (Ignatova, 1962). According to M.D. Ignatova, primary crystalline talc has a hydrothermal–metasomatic origin and is represented by two genetic varieties – apo-carbonate which formed at the expense of Aladyino dolomite, and apo-silicate which formed due to metasomatic replacement of Potoskuy quartzite. The source of the hydrothermal solutions remains an open question at the moment. Hypogene ores are represented by dense, finely-crystalline talc rock (steatite) and foliated talc schists with a greasy feel. Talc rocks are white, bluish, grey and yellowish. Impurities include small amounts of rutile, magnesite, and carbonaceous–clayey material. Powdery talc rocks are fine-grained, snow-white, floury talc mass, naturally enriched due to the removal of impurities by weathering. Ores of this type are distinguished by their high purity, and they are especially valuable.

Six ore bodies have been recognised in the deposit, running in a N–S direction (Fig. 137). A southern group of ore bodies constitutes a single vein-type deposit, 550 m long, with a steep dip, and consisting of a main vein around 20 m thick and minor talc

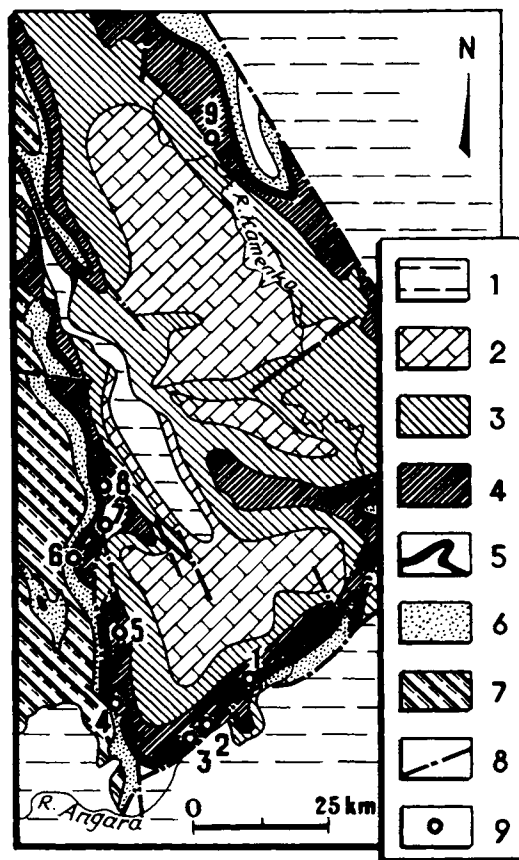


Fig. 135. Talc and magnesite deposits, Uderey ore field (Kirichenko et al., 1965). 1 - PZ, 2 - 1st, etc., Dashkin & L. Angara Fms, Osloyan Gp, 3 - shale, etc., Dadyktin & Shuntar Fms, Tungussik Gp, 4 - 1st etc., Potoskuy Gp, 5 - Aladyin Fm, Sukhoy Pit Gp, Kartochnka Fm, 6 - shale, etc., Pogoryny Fm, 7 - phyllite & sst, Uderey Fm, 8 - faults, 9 - talc & magnesite deposits: 1 - Bykovskoye-I, 2 - Bykovskoye-II, 3 - Meshkovskoye, 4 - S. Kirigitey, 5 - Kirigitey, 6 - Talskoye, 7 - Rybinskoye, 8 - Udorong, 9 - Kardakan.

veins which splay off it, alternating with dolomite interbeds. The deposit is divided into three ore bodies, I, II and III, by two constrictions. The mineral deposits in the bodies are represented by dense apo-carbonate talc rocks. The ore texture in the extreme southern part (ore body I) is almost massive, shearing increases northwards, and in the third ore body the foliated varieties are close to talc schists. Contacts between talc rocks and dolomite wall rocks are sharp, although the dolomite at the contact is highly impregnated with talc. The ore bodies in the northern part of the deposit also represent a single deposit with a steep easterly dip, extending for over 800 m and divided by a constriction into two bodies, V and VI. In its upper part the northern deposit consists of powdery talc rock, a weathered crust 50-100 m thick, giving way at depth to dense primary talc rock. In body V at depth, many dolomite interbeds and inclusions also

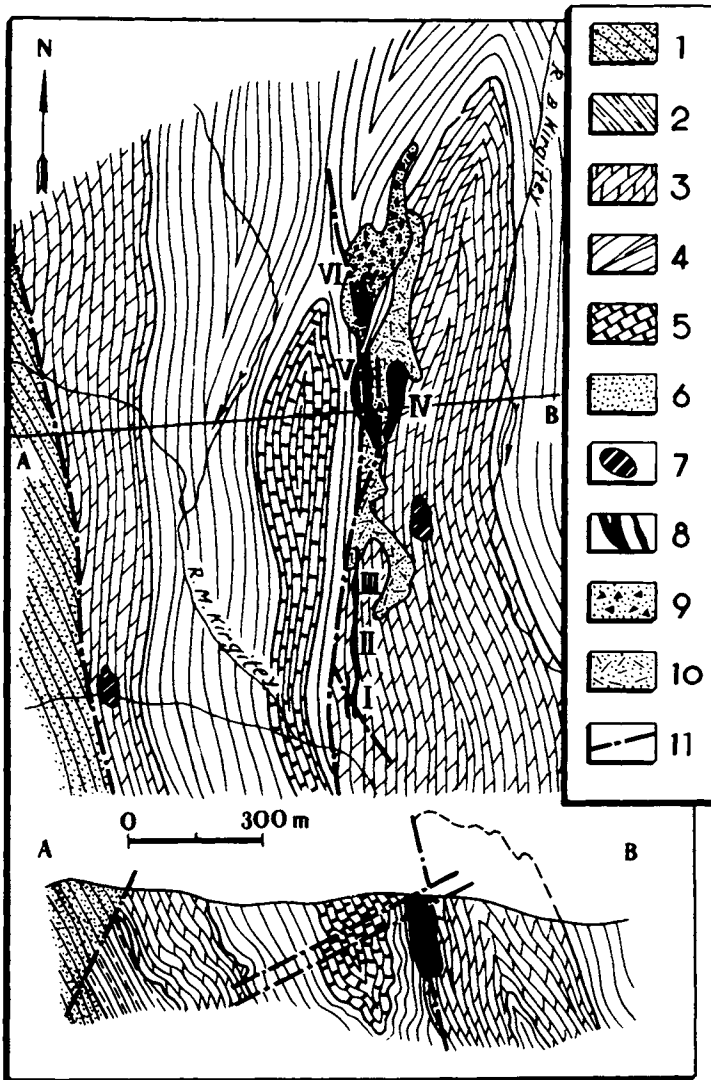


Fig. 136. Sketch showing geological structure of Kirgitey talc deposit (Smolin, 1961). 1-7 PR<sub>2</sub> sediments: 1 - Pogoryny shale, 2 - mottled lst & shale, 3 - Aladyin dolomite, 4 - Potoskuy mottled shale, 5 - Potoskuy black algal lst, 6 - Potoskuy quartzite, 7 - magnesite pods in Aladyin dolomite, 8 - talc ore bodies (I-VI), 9 - marshallitic eluvium from quartzite, 10 - unconsol. Tert. bauxitic seds, 11 - faults.

appear, constituting from 30 to 60% of the ore body's thickness. The structure of body VI is complicated by large inclusions of marshalite and quartzite which break it into a main pod some 30 m thick, and a series of smaller pods. Genetically, the talc rocks in body V are similar to the ores in the southern part of the deposit, i.e. they are apodolomitic, while in No. VI they are represented by apo-silicate varieties. Ore body No. IV consists of powdery redeposited ores in a gently-dipping bedded deposit within

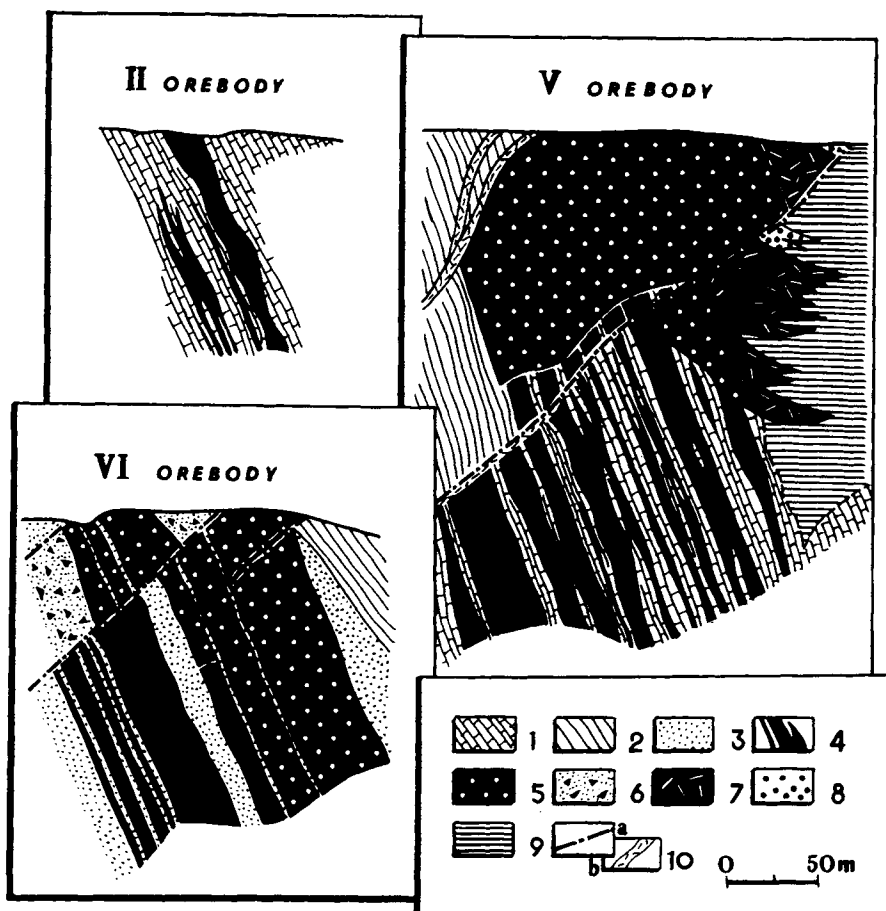


Fig. 137. Geological cross-sections, Kirgitey talc deposit (Smolin, 1961). 1 - dolomite, 2 - shale, 3 - quartzite, 4 - dense talc ore, 5 - powdery talc, 6 - marshallitic eluvium from quartzite, 7 - redeposited powdery talc, 8 - sand (weathered quartzite), 9 - clays in karstic depressions, 10a - faults, 10b - shear zones.

an assemblage of unconsolidated sediments in the east of a karst depression which runs in a N-S direction. The ore deposit extends for about 300 m and has an average width of 50 m; the thickness is not constant, and varies from a fraction of 1 m to 30 m.

### 1.6. Rare metals

Tungsten, tin and molybdenum occurrences are known in the Yenisey ridge. Tungsten as scheelite is found in metasomatic quartzite (Olenegorsk deposit), and skarn (Ilyin deposit) which are located in the outer contact of a granitic intrusion. Molybdenum occurs in quartz veins, skarns, gneisens and pegmatites. Quartz-muscovite greisens and pegmatites containing fluorite, topaz and wolframite are known in the contact zones of

batholithic granites (Amantov et al., 1988). Tin occurrences have been discovered at granite intrusion contacts, in a cassiterite–greisen formation (Levo-Landakh occurrence), a cassiterite–skarn formation (Tyradin), and a wolframite–cassiterite–quartz formation (Goltsovoye).

2. Conclusions

The Precambrian mineral deposits and occurrences of the Yenisey belt described in this chapter on the whole reflect the metallogenic features of the region. The metallogenic scheme (Fig. 138), which is a summary representation of the signatures of the tectonic

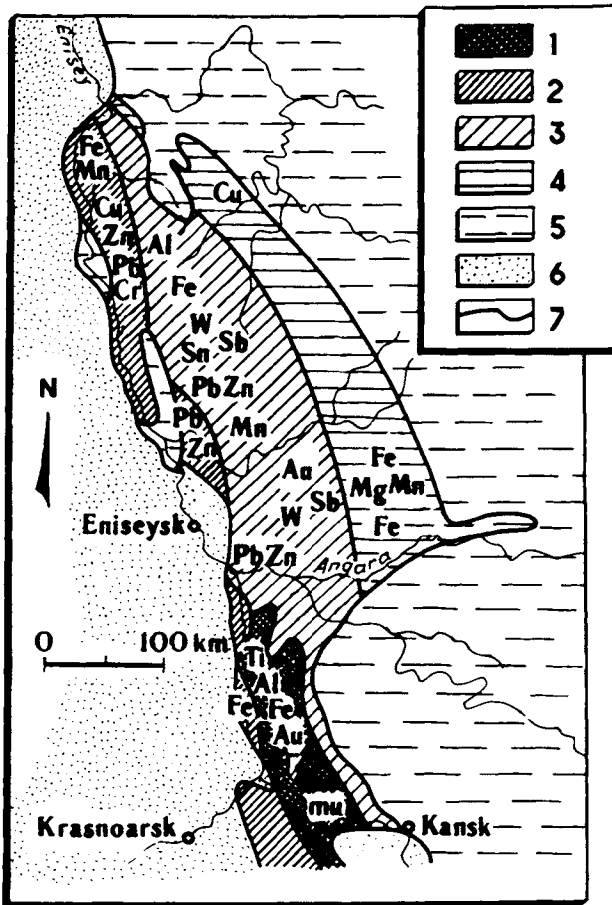


Fig. 138. Metallogeny of Yenisey ridge (Amantov et al., 1988). 1 - AR<sub>1</sub> (Kan zone), 2 - PR<sub>1</sub>-PR<sub>2</sub> (Pre-Yenisey zone), 3 - PR<sub>1</sub>-PR<sub>2</sub> (Central zone), 4 - PR<sub>2</sub> (Chernorechka-Kamenka zone), 5-6 platform cover, 7 - geological boundaries.

zones, reflects significant metallogenic differences between them, due to the different dynamics of evolution and consequently different compositions of their constituent complexes. The metallogeny of the Western (Pre-Yenisey) zone is due to the dominant presence of Riphean ( $R_{2-3}$ ) island arc and ophiolite complexes. Differences between the mineral deposits in the Central zone are due to the fact that Riphean supracrustal and igneous complexes of varied compositions formed there, as well as rock complexes that formed under Early Proterozoic and possibly Late Archaean processes. The metallogeny of the Eastern zone was influenced by its pre-platform setting during the Riphean. A characteristic feature of the Yenisey belt is the variety of formations hosting particular useful components (Table 14), as a result of the deposits having originated in various palaeotectonic environments. This fact relates mainly to iron, gold and polymetals. Many of the deposits formed close to one another in time. Thus, gold ores display a spatial and genetic relationship with 960–850 Ma old granitic rocks, which are characterised by higher basicity and are represented by granodiorite, diorite, trondhjemite–adamellite (Datsenko, 1984). Polymetallic ore deposits – lead–zinc formation in carbonate rocks, massive sulphide–lead–zinc formation and polymetallic in essentially silicate rocks probably formed simultaneously (Ruchkin, 1984). In this region there is a marked association between useful minerals and particular geological processes. Thus, iron, manganese, vanadium, lead and zinc ore formations are associated with sedimentary processes. Titanomagnetite and chrome are associated with basic and ultrabasic intrusive magmatism. Polymetals occur in paragenetic relationship with basaltic volcanism. During the time at which Late Riphean granitic rocks were

Table 14

Ore formations in deposits of the Yenisey ridge, using material by G.N. Brovkov, L.V. Li, et al. (1986)

Metal	Ore formation	Ore deposit
Iron	Titano-magnetite	Shiver
	Siderite	Gorevskoye
	Ferruginous quartzite	Predivinskoye
	Metasomatically altered ferruginous quartzite	Yenashim
	Chlorite–hematite clastic terrigenous	Lower Angara
Manganese	Hypergene manganese oxide	Porozhinskoye
	Manganese–carbonate stratiform	Tayozhnoye
Lead–zinc–copper	Pb–Zn in carbonates	Gorevskoye
	Pyritic Pb–Zn in black shales	Linear
	Polymetallic in silicate host (carbonate–volcanic–clastic hosted subformation)	Khariuzikhin
Gold	Gold–quartz	Gerfedskoye, Soviet
	Au–Ag–quartz–sulphide	Bogunayev, Kuzeyev
	Au–Sb–quartz	Uderey
Tin	Cassiterite pegmatite	Yenashim
Tungsten	Scheelite skarn	Ilyin
Mica	Pegmatite	Kondakovo, Barga

being emplaced, gold deposits and occurrences were forming, as well as tin and tungsten. The relationship between deposits and particular geological processes resulted in the spatial distribution of deposits in the belt, such that a link has been established between deposits not only in any particular tectonic zone, but also between tectonomorphological structures. Thus, gold, tin, tungsten and antimony deposits are hosted in anticlinoria, and iron, manganese, lead and others in synclinoria (Brovkov et al., 1986).

## Baikal–Patom fold belt

A.M. LARIN, Ye.Yu. RYTSK and Yu.M. SOKOLOV

### *1. Geological structure and metallogeny*

The Baikal–Patom fold terrain is one of the most interesting and at the same time the most complex terrain in the development of the Precambrian in the former USSR, which explains the controversy surrounding the interpretation of the tectonic structure of this region. Despite the fact that there are several well-known mineral deposits in a relatively small area, such as the Kholodninskoye lead–zinc, Molodyozhnoye chrysotile–asbestos, gold targets in the Bodaibo region, the Mama mica-bearing region, potash and alumina ores in the Synnyr complex, granulated quartz deposits and others, their association with different types of tectonic structures, the nature of these structures themselves and their time frames, are still highly controversial issues (Amontov et al., 1988; Salop, 1964; Fedorovsky, 1985). The present authors adhere to the broad outlines of the tectonic structure and the boundaries of the Baikal–Patom fold belt as set out in the companion volume “Precambrian Geology of the USSR” (Rundqvist and Mitrofanov, 1993) with some amendments, based on new geological and geochronological evidence for this region. In general terms, we regard the Baikal–Patom region as an example of a fold terrain with a prolonged history of polycyclic development, the main role being played by tectonic structures dating from the Riphean stage, reworked by tectonomagmatic crustal processes in the Phanerozoic. The following major tectonic structures are distinguished: Early Proterozoic Baikal fold belt (protogeosynclinal) with blocks of reworked Archaean–Early Proterozoic (?) basement, the Riphean Baikal–Patom fold belt, including miogeosynclinal and eugeosynclinal zones, the Olokit riftogene depression, and the Bodaibo intracratonic basin (Fig. 139).

*The Baikal fold belt* consists of three structural–lithological zones: Chuya–Tonod miogeosyncline, Baikal–Muya eugeosyncline, and the Akitkan volcanoplutonic belt. Reworked basement blocks are distinguished as independent structural elements – Chuya, Nechersky and Muya. Basement blocks consist of granulite facies metamorphic complexes, intensely granitized and retrogressed at amphibolite facies conditions. In some places, evidence has been found for a further episode of superimposed high-temperature retrogression, associated with kyanite–sillimanite Barrovian-type metamorphism. This is particularly well-expressed in the Patom Highlands. Constituents of these polyphase metamorphic complexes are mainly various gneisses and migmatites, forming granite–gneiss dome structures. Ortho-amphibolite and marble play a minor role. Early Proterozoic syn-collisional granites belonging to the Chuya–Kodar complex

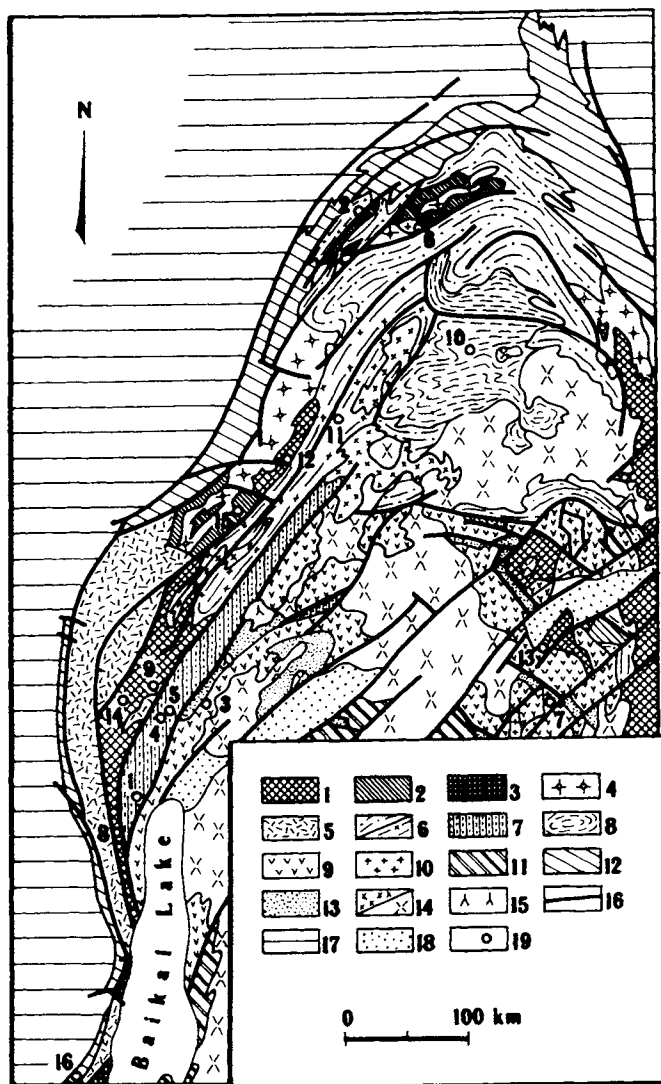


Fig. 139. Structural sketch map of Baikol-Patom fold terrain, 1: 5,000,000 scale. 1-4 Early PR Baikol fold belt: 1 - reworked AR-PR<sub>1</sub> basement blocks, 2 - Chuya-Tonod miogeosyncline, 3 - Baikol-Muya eugeosyncline, 4 - Chuya granitoids 5 - Akitkan PR<sub>1</sub> anorogenic volcanoplutonic belt; 6-10 Late Riphean Baikol-Patom fold belt: 6 - Mama-Patom miogeosyncline. 6a - Patom sub-zone, 6b - Mama sub-zone; 7 - Olokkit rift, 8 - Bodaibo intracratonic basin, 9 - Baikol-Vitim eugeosyncline, 10 - granitoids; 11 - Riphean faulted cover of Barguzin-Vitim central massif; 12 - Mid-Late Riphean Pre-Baikol pericratonic basin; 13 - Vendian-Cambrian basins; 14 - PZ granitoids a - synmetamorphic, b - postmetamorphic; 15 - PZ alkali rocks; 16 - faults; 17 - Siberian platform cover; 18 - CZ rifts; 19 - main ore deposits: 1 - Tyva Fe, 2 - Vitim Fe, 3 - Chaya Cu-Ni, 4 - Dovyren Cu-Ni, 5 - Kholodninskoye pyrite-polymetallic, 6 - Tuyukan Sn, 7 - Mokhovoye Sn, 8 - Davan rare metals, 9 - Abchada rare metals, 10 - Lena Au, 11 - Mama musc pegs, 12 - Chuya ceramic pegs, 13 - Molodyozhnoye chrysotile-asbestos, 14 - gem cordierite, 15 - lazulite, 16 - Pre-Baikol Pb-Zn.

are widely distributed in the basement blocks, forming major batholithic bodies. Ore targets, currently with economic significant, are practically unknown within the basement blocks. Minor occurrences of ceramic and rare-metal pegmatites, rare-metal and tin ore occurrences, and gem-quality cordierite mineralization are associated with processes involving Proterozoic and Phanerozoic reworking of older granulite complexes.

The Baikal fold belt itself consists of the Chuya–Tonod and Baikal–Muya structural–formational zones. The Baikal–Muya eugeosynclinal zone was first identified by Salop (1964). Some workers (Dobretsov, 1982; Fedorovsky, 1985) consider it to be a greenstone belt. Recently obtained geological and geochronological data enable two structural–lithological complexes of different ages to be separated out within the traditional boundaries of the Baikal–Muya zone. An Early Proterozoic complex includes the Sarma and Muya groups in the area between the rivers Pravaya (Right) Mama–Yana–Gorbylak, and the Parama Group in the Samokut trough. A Riphean complex includes the Nyurundukan Group in the North Pre-Baikal region and the Muya Group in the Central Vitim mountains. Early Proterozoic geosynclinal formations are distinguished by their relatively large volumes of metaterigenous and volcanomict rocks. Basic, intermediate and acidic metavolcanics rarely account for more than 50% of the succession. Rocks in the Baikal–Muya Zone are intensely deformed and have undergone regional zonal metamorphism, from greenschist to amphibolite facies. Trondhjemites and migmatites are common in places, and high-temperature retrogression has also been observed. Sokolov and Kovaleva (1983) have determined the age of the zone as early Precambrian. Metarhyodacite porphyrites in the Sarma Group yield an isotopic age of  $1835 \pm 8$  Ma, and a synmetamorphic trondhjemite in the Kocherik complex is  $1900 \pm 30$  Ma old, a U–Pb zircon age (Bibikova et al., 1987). Ore deposits in the Baikal–Muya zone, directly associated with Early Proterozoic structural–lithological complexes, are virtually absent. Gold occurrences in the zone are related to Phanerozoic tectonomagmatic processes.

The Chuya–Tonod miogeosynclinal zone was also first defined by Salop (1964). Rock complexes in the zone are combined into the Kevakta Group (Tonod upwarp), Chuya Group (Chuya upwarp), Khodokan Group (north of the Necher upwarp). These subdivisions are dominated by quartz–feldspar metasandstone, metasilstone, quartz–mica schist, including graphitic varieties. Successions typically display flyschoidal or crudely rhythmic structure. Metamorphic effects are uneven: in the Tonod upwarp the rocks show greenschist facies effects, whereas those in the Chuya upwarp were metamorphosed under greenschist to amphibolite facies conditions. The geological age of the rocks in the Chuya–Tonod Zone is defined on the basis that they are cut by the Early Proterozoic Chuya–Kodar granites. There are practically no ore deposits of Early Proterozoic age within this zone.

The Akitkan volcanoplutonic belt is located at the NW edge of the Baikal–Patom fold terrain, and runs along the southern edge of the Siberian craton. According to S.I. Turchenko and Yu.M. Sokolov (in Rundqvist and Mitrofanov, 1993), it is a proto-orogenic zone, formed at the end of the Early Proterozoic, an event which completed the proto-geosynclinal development of the Baikal fold belt. Other authors regard it as an early activation structure (Bukharov, 1987), or as a non-geosynclinal volcanoplu-

tonic belt in a tectonically active regime (Khrenov, 1981). The Akitkan belt has an arcuate shape, with a NNE strike in the south, gradually swinging round to the NE. Its total length is around 1000 km, and it is up to 60 km across. At its base the belt consists of Akitkan Group clastic terrigenous–volcanogenic formations which Bukharov (1987) divides into two. The lower of the two is the Domugda Fm which is dominated by volcanic rocks: trachytic, trachyandesitic, trachylyparitic, sometimes felsitic porphyries, granosyenite porphyry and tuffs with the same composition. Volcanics are interbedded with coarse clastic terrigenous sediments and redbeds. In the upper part of the Akitkan Group are the Chaya and Khibelen Fms, both dominated by variegated continental clastic terrigenous sediments, in which there are quartz porphyry tuffs, tuffaceous rocks, quartz porphyry and amygdaloidal porphyrite.

Associated with the Akitkan Group are subvolcanic and hypabyssal intrusions – granites belonging to the Irel and Primorye complexes, forming both minor dykes and stock-like bodies often with a ring structure, and fairly large massifs. Compositions range from diorite, granodiorite, quartz monzonite to granosyenite, granite and alaskite. Petrochemically, many of the granitic varieties approximate to rapakivi. Rocks in the Akitkan belt are practically unmetamorphosed and dynamothermal metamorphic effects are seen only along major tectonic sutures, where there are blastomylonite zones and alkaline metasomatic and retrograde alteration. The age of the Akitkan volcano-plutonic belt is bracketed by the unconformity between the Akitkan Group and the underlying Lower Proterozoic Sarma schists, and the overlying Riphean Baikal Group carbonate–clastic terrigenous sediments. The isotopic age of granitic rocks in the Irel complex, which cut Khibelen volcanics, is  $1860 \pm 30$  Ma, a U–Pb zircon age (Neymark et al., 1987). By the same method, volcanic rocks in the Domugda and Chaya Fms in the Akitkan Group lie in the interval 1860–1820 Ma (Neymark et al., 1991).

Varied mineralization is associated with the plutonic and volcanic complexes in the Akitkan belt, but basically none of it has any economic importance at present. Sn, W, Bi, Mo, Be, Ta, Nb, REE occurrences are found in association with the granitic rocks, in quartz–feldspar metasomatic veins, quartz veins and greisens. Polymetals, fluorite, W, Sn and Au occurrences are found in extrusive and vent facies.

The Baikal–Patom fold belt, of Riphean age, contains the Baikal–Vitim eu-geosynclinal and the Mama–Patom miogeosynclinal zones, the Olokita rift, and the Bodaibo intracratonic basin. Structural–lithological complexes in the Baikal–Vitim zone include the Nyurundukan Group in Northern Pre-Baikal, and the Muya Group in the Central Vitim Highlands. Klitin et al. (1975), Dobretsov (1982), and a number of other workers have demonstrated the presence of an ophiolite association in this structural zone, including alpine-type ultrabasics, metagabbroic rocks, tholeiitic metabasalts, keratophyres, and a parallel dyke swarm. The rock complexes are dominated by tholeiitic–basaltic and rhyodacitic metavolcanics, metasandstone and meta-greywacke, including siliceous and carbonaceous schist horizons and marbles. Olistostrome formations are characteristic (Dobretsov, 1982; Khain et al., 1988), the olistoliths of which are seen to host meta-ultrabasic rocks. Barrovian-type zonal metamorphism, from low-temperature greenschist to amphibolite facies, has affected the rocks in the Baikal–Patom zone. Complex polyphase folding is typical. The isotopic age of basic rocks in the Nyurundukan Group is  $1050 \pm 120$  Ma (Sm–Nd isochron

method, carried out by L.A. Neymark, A.A. Nemchin et al.), while the Chaya pyroxenite–gabbro–norite differentiated pluton yields an age of  $650 \pm 35$  Ma (Amelin et al., 1990).

Among the ore deposits found in the Baikal–Vitim Zone, an important place is held by the Molodyozhnoye chrysotile–asbestos deposit, and nephrite deposits, which are related to retrogressive effects on ultrabasics in the Parama complex. Small copper–nickel sulphide ore deposits (Chaya) are hosted in ultrabasic to basic differentiated plutons, as well as titanomagnetite mineralization (Slyudinskoye and others).

The Mama–Patom miogeosynclinal zone occupies an extensive area in the North Baikal and Patom Highlands. It consists of a single, thick complex, part of the Patom Group and the Mama assemblage. The succession displays a characteristic rhythmic structure, from flyschoidal members to major rhythms, corresponding to sub-groups. Erosion products from an ancient weathered mantle occur at the base of the rhythms, alternating with monomict and oligomict clastic rocks, with carbonate members at the top. Polyphase folding is intimately related to the evolution of regional metamorphic processes, which progressed from uniform greenschist facies to kyanite–sillimanite type zonal metamorphism. Granite–gneiss domes and thrusts are common, at various erosion levels. The Mama synclinorium occupies a rather special place in the structure of the miogeosynclinal zone. Typically, it has a relatively truncated section and significant development of highly aluminous products from the erosion of an ancient weathered mantle, indicating that it formed under stable conditions of a palaeo-upwarp or basement high. In terms of the metamorphic zonation of the Mama–Patom zone, the Mama downwarp stands out because of the widespread development of products of ultrametamorphism, granite–gneiss domes and pegmatites. Neymark (1990) obtained Hercynian ages of  $350 \pm 10$  Ma for granites and  $320 \pm 10$  Ma for pegmatites, by the U–Pb method on zircon. In addition to the well-known economic muscovite pegmatite deposits in the Mama mica-bearing province, the Mama–Patom zone also hosts iron ore targets in the Vitim ore region, associated with an iron-rich horizon in the Medvezhevo Fm.

The Olokit rift is a 20–25 km wide linear structure stretching for over 250 km from the northern shores of Lake Baikal to the lower reaches of the river Mama. It is bounded to the NW by the Levomin and Abchada faults and to the SE by the Chaya–Nyrundukan deep fault. In the tectonic structure of the Baikal–Patom folded terrain, it is a long-lived system of narrow trough structures, superimposed on a folded basement of the Karelides. The most extensive is the Olokit–Mama foredeep, genetically related to the Bodaibo intracratonic basin. In the SE part of the belt a series of downwarps – Nyrundukan, Tyya–Kholodnin, Orkolikan–Dzhalokan – is separated by blocks of remobilized basement. Broadly speaking, the structure of a section through the Olokit zone resembles the rhythmic succession in the Mama–Patom zone, and differs in containing contrasting differentiated volcanic sequences, hundreds of m to 2 km thick. Rocks in the stratified complex and the intrusive suites were metamorphosed under kyanite–sillimanite type zonal metamorphic conditions, and are retrogressed in deep fault zones. The deformation history of rocks in the Olokita zone includes several episodes of folding accompanied by metamorphism, and superimposed thrusts and reverse faults.

There are conflicting views regarding the age of the Olokit Group. Some workers (Rundqvist and Mitrofanov, 1993; Fedorovsky, 1985) consider that it belongs to the Early Proterozoic, others that it is Riphean (Anon., 1986; Distanov et al., 1985). From a geochronological study carried out on rocks in the Olokit zone, an Early Proterozoic age has been established for metaporphyrries in the Ilovir Fm, forming the visible base of the Olokit Group –  $1863 \pm 5$  Ma, and granitic rocks in the Abchada massif which are comagmatic with these –  $1866 \pm 5$  Ma (Neymark et al., 1990). Metaporphyrries in the Synnyr Fm at the top of the Olokit Group have been dated by the U–Pb method on zircons at  $700 \pm 20$  Ma (Neymark et al., 1990). The Dovyren layered intrusion which cuts the middle of the Olokit Group has been dated by an array of different methods (Sm–Nd, Rb–Sr, Pb–Pb) also at  $700 \pm 20$  Ma (Neymark et al., 1989). In estimating the age of the Olokit Group, it is important to take into account Pb-model ages obtained on galena and pyrite from the Kholodnin deposit, situated in the middle of the succession:  $740\text{--}760 \pm 10$  Ma (Neymark et al., 1990). Thus, most of the Olokit Group would appear to have an Upper Riphean age. It should be pointed out that during the Upper Riphean there was magmatic activation of Early Proterozoic structures, expressed in the emplacement of hypabyssal and sub-volcanic intrusions of the Bambukoy and Zhanok tin-bearing granitic complexes in the region of the Muya microcraton, and the Yuzov complex in the Tonod basement high.

The Olokit belt is one of the largest productive structures in the Baikal–Patom fold terrain. Associated with volcanogenic–carbonate–black shale sediments are massive sulphide–polymetallic ores in the Kholodnin deposit, and a number of prospective occurrences. Small-scale baryte–polymetallic targets are hosted in carbonate rocks, including the Yoko–Rybachy deposit among others. Silica–iron greenschists in the Nyurundukan depression host the Tyya Mn–Fe quartzite deposit, and similar occurrences are found in the same assemblage in the river Abchada basin. Layered intrusions in the Dovyren complex host copper–nickel sulphide mineralization, and a similar composition is found in association with meta-ultrabasic rocks in the Avkita occurrence.

The Bodaibo intracratonic basin is situated in the NE of the Baikal–Patom fold terrain, and is made up of a rock assemblage belonging to the Bodaibo Group. The Bodaibo Group is divided into two sub-groups, with different compositions. The lower of these is the Kropotkin sub-group, which is characterised by metasediments and metasilstones with phyllitic and graphitic intercalations. The upper Bodaibo sub-group proper differs in that it contains polymict and greywacke-type metasediments and shales with thin carbonate intercalations at the top of the succession. The internal structure of the intra-cratonic basin is characterised by two second-order downwarps (Bodaibo and Marakan–Tunguska), separated by the Kropotkin high. Sedimentary assemblages in the basin are deformed into a system of E–W syn-metamorphic folds, complicated by thrust structures. Metamorphic conditions throughout most of the basin do not exceed the chlorite–sericite sub-facies of the regional greenschist metamorphic facies. On moving towards the basement highs surrounding the basin, there is a sharp increase in metamorphic grade, accompanying polyphase superimposed folding and granite–gneiss dome formation.

Igneous rocks are represented by insignificant Hercynian granitoids and a lamprophyre and granite–porphyry dyke swarm. The age of the structural–litho-

logical complex in the Bodaibo basin is considered by most workers to be Late Riphean, as confirmed by a 610 Ma zircon age on the Konstantinovo granite plug (Neymark et al., 1990). The Bodaibo intra-cratonic basin hosts the Lena gold ore cluster. *In-situ* gold deposits of the “Sukhoy Log” disseminated-vein type have an extensive polyphase history of formation, controlled by zones of moderately graphite- and sulphide-rich schists, combined with structural, metamorphic and metasomatic factors.

## 2. Ore deposits and occurrences

### 2.1. Iron

Iron deposits in the Baikal–Patom fold terrain have a very limited distribution and are almost entirely restricted to rocks in the Teptorgo Group within the Olokit and Mama–Patom structures. This rock complex has a two-fold structure, with highly mature erosion products of an ancient weathered mantle at the base (Purpol, Chukcha and other formations), overlain by a clastic succession altered to a variety of different schists, with tholeiitic–metabasaltic lava flows and meta-diorite sills (Medvezhevka, Tyya and other formations). Iron-rich schists gravitate towards the lower part of the succession, while productive banded ironstones and iron-ore metasomatites occur nearer the top. According to Golovenko (1976) and other workers, the iron-ore assemblage in the Teptorgo Group is related to the sub-platform stage in the evolution of the Baikal fold terrain. The Tyya deposit and the Vitim ore field will be used as examples of type iron-ore targets.

*The Tyya deposit.* The discovery and investigation of the Tyya iron ore zone are associated with the names of V.V. Dombrovsky and A.S. Kulchitsky and geologists and geophysicists working with the North Baikal exploration team – P.P. Sofronov, A.G. Krapivin, V.P. Meshcherov, I.T. Alsaydayev, A.A. Darizhapov and P.Ch. Shobogorov. Various issues relating to the geology of this ore region have been examined in publications and reports written by V.U. Bolonev, V.G. Kushev, V.Ye. Rudenko, Yu.G. Popov, V.D. Belogur, and others. The Tyya iron ore zone is a narrow (1–3 km) band of outcrops of the productive horizon in Tyya greenschists, which can be traced for about 50 km in a NE direction. A series of ore districts has been found in this band (Sevelikon, Senogda, Gorbylak, Tyya–Kavynakh), which are distinguished on the basis of their very high content of productive banded ironstone beds. Formation analysis indicates that the ore-hosting sediments together with the banded ironstones belong to a silica–iron greenstone formation, lying in the linear structure of the Nyurundukan graben–syncline on the SE edge of the Olokit continental margin palaeorift downwarp (Fig. 140). Only the SE limb of the structure can be traced for a considerable distance, and the overturned NW limb can be mapped only intermittently, being tectonically overlain by a thick nappe of blastomylonitized gneisses belonging to the Early Proterozoic Ungdar assemblage. The greenschist formation is distinguished by its regionally distributed, disseminated magnetite which gives rise to an aeromagnetic anomaly of varying magnitude in the Olokit zone.

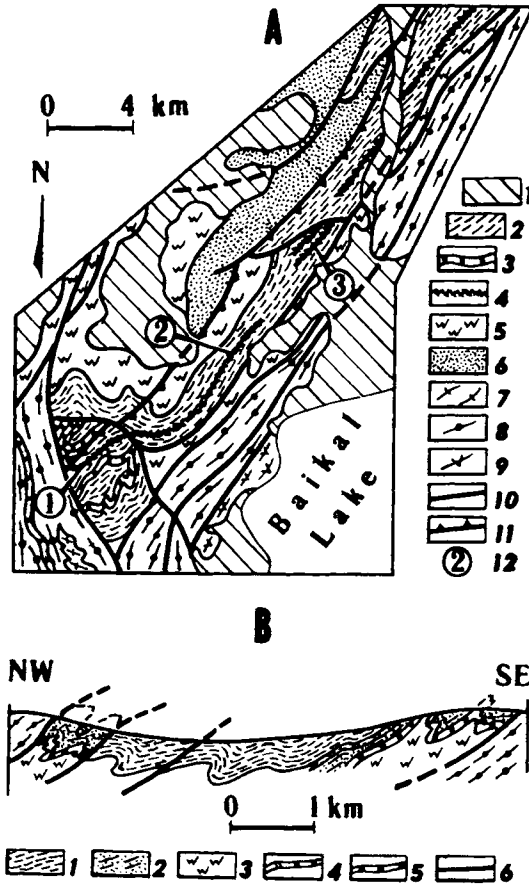


Fig. 140. Sketch showing geological structure (A) and section (B) of SW Nyurundukan graben, Tyra iron-ore deposit. 1 - Quaternary, 2 - Fe-rich greenschist, 3 - lst, 4 - Fe-quartzite, 5 - high-Al schist, 6 - quartzite, 7 - gneissose granite, 8 - blastomylonite, 9 - amphibolite, 10 - faults, 11 - thrusts, 12 - ore sectors (1 - Sevelikon, 2 - Gorbylok, 3 - Senogda). Section: 1 - upper greenschist, 2 - graphitic schist, 3 - lower greenschist, 4 - dolomite, 5 - lst, 6 - faults.

The greenschist formation hosting the ores is divided into three members. The lowest consists of green amphibole, biotite-amphibole, biotite-quartz-amphibole and quartz-epidote-amphibole  $\pm$  garnet schists, with a visible thickness in excess of 50 m. The middle member - the productive horizon - is a monotonous unit of finely-banded greenschists ( $Qtz \pm Ab + Ep \pm Chl \pm Czo \pm Mag \pm Act \pm Ser \pm Carb$ ), including carbonate marker horizons at the base and top, represented by grey limestone and dolomite, as well as quartzites, including ferruginous varieties. The total thickness probably does not exceed 0.8-1.0 km. The topmost member crops out only in the area where the core of the structure is preserved, in the river Sevelikon basin, and consists of grey and black carbonaceous schists ( $C_{org} + Qtz + Carb$ ,  $C_{org} + Carb + Ms + Qtz$ ,  $Carb + Bt + Ms + Qtz$ ) with rare quartzite and limestone intercalations. The

thickness is up to 250 m. The greenschist formation which hosts the ore consists in the main of fine-grained metasandstone, iron-carbonate metasandstone, metasilstone and tuffaceous metasandstone with or without carbonate. Essentially amphibole schists are most likely derived from tuffs originally. Only the amphibole schists and amphibolites in the lowest member probably formed from basic volcanics, as confirmed by reconstructions based on AKF diagrams and geochemical data.

By analysing the metamorphic mineral assemblages in these rocks, it has proved possible to establish elements of metamorphic zoning, subordinate to the structure of the Nyurundukan graben. Along its axis in the Tyya and Gorbylak valley the biotite zone in the greenschist facies can be mapped, surrounded by the garnet zone (almandine-chlorite-chloritoid sub-facies). The metamorphic zone boundary is established from a change in the paragenesis  $Act + Chl + Ep + Ab + Qtz + Carb \pm Ser \pm Mag$  to a higher temperature one that includes hornblende. The highest metamorphic grade, corresponding to the top of the garnet zone and (or) staurolite facies, is found in the Sevelikon district ( $Grt + Hbl$  and  $Qtz + Bt$  and  $Czo + Chl + Mag \pm Mu$ ). A very characteristic feature for the entire zone is the Fe-rich chlorite, and in the Sevelikon district it is easy to locate precisely the replacement of biotite by later chlorite, an effect related to retrogression adjacent to a fault. Retrogressed rocks are controlled by a thrust suture on the NW flank of the Nyurundukan graben, and it is often difficult to distinguish this from prograde metamorphosed greenschists. Mapping has shown that the location of the ferruginous quartzites does not depend on metamorphic zoning or folding.

Two ore varieties can be identified on the basis of textural and structural features – banded, with up to 90% Mgt and disseminated, with 20–60% Mgt, and compositionally – magnetite, magnetite-hematite and hematite ores. Morphologically, the ores are typical beds and packets, with fine internal banding due to the alternation of ore-rich and barren laminae. In relatively high-temperature metamorphic zones, this banding is metamorphic in nature. Magnetite occurs disseminated throughout the rock mass, either concentrated in  $Qtz + Czo + Pl$  laminae in the metasandstones or  $Chl + Bt + Ep + Qtz$  in greenschists. In ore laminae associated with lenticles of coarse-grained recrystallized quartz and single grains of  $Carb_{Fe}$ , magnetite is clearly more coarsely crystalline, suggesting that the ore material recrystallized during both prograde and retrograde metamorphic episodes. Partially associated with these processes is the replacement of hematite by magnetite, and also the appearance of unique Mn-rich metasomatites ( $Grt + Carb_{Fe} + Bt + Ms + Chl + Qtz$ ). The number of ferruginous quartzite beds is highly irregular within the space of the ore zone and amounts to 1–3 up to 6–10 within a thickness of 10–25 m to 6.0–7.3 m on average. In the Senogda district the total thickness of ferruginous quartzite beds reaches 22–37.5 m. The iron content in the ores is not constant, but varies from 17–20% to 45–52%. A characteristic geochemical feature of the ores is the higher manganese concentration from 0.1 to 8.3%, and up to 19% in “skarnoids”. Other elements are V (0.003–0.05%), Ti (up to 0.5%), P (0.02–0.57%); Co, Zn and in places Pb, Ni, Cu and Cr are higher.

The Abchada iron ore zone in the NW part of the Olokit–Mama depression has a similar composition and structure – the Tuluokit, Abchada, Nyurik and other districts

– but differs in the much higher contrast in the ore-hosting Tyya succession, with the presence of acid and basic metavolcanic rocks, the higher manganese content in the ores, variable lithofacies and as a result relatively low parameters for the ore bodies.

The evidence presented above suggests syndimentary, stratiform banded ironstone horizons for the Tyya deposit and occurrences in the Olokit zone as a whole, with the main control being exercised by litho-formational factors. The association with basaltic volcanism against this background is paragenetic. A Riphean age for the host assemblage, the lack of similarity between the Olokit complex and ore-bearing siliceous schist and schistose amphibolite formations contradicts the point of view that the Tyya deposit belongs to the jaspilite formation. The negligible volume of volcanics in the ore hosting successions, the higher manganese content in the ores, the composition and structure of the sub-platform ore-hosting complex, in the author's opinion indicate that the targets under discussion in the Olokit zone should be classified in the silica-hematite group of ore deposits. This group is distinguished on the basis of the variety of formational types of ore targets, from pure hematite sedimentary deposits in the Angara–Pit sub-platform basin in a clastic terrigenous formation of redeposited products of a chemical weathered mantle, to hematite–magnetite banded ironstones in metamorphosed volcano-sedimentary formations in geosynclinal assemblages.

## 2.2. *Nickel, copper, cobalt*

Copper–nickel sulphide ore deposits in the Baikal–Patom fold terrain are found in only two types of structure: the Baikal–Vitim eugeosynclinal zone of the Baikal fold belt, and the Late Riphean Olokit riftogene basin. There are no economic copper–nickel deposits.

*The Chaya deposit* occurs in the ore-bearing massif of the same name (Fig. 141), on the western limb of the Baikal–Muya basic–ultrabasic belt, within the fold structure of the Baikal–Vitim proto-ophiolite zone. The age and formational association of the Chaya massif have not been determined. A number of workers consider it to be a component of the Baikal–Muya basic–ultrabasic belt. However, some hold the opinion that it has a younger, Riphean, age. Some others refer it to the Dovyren peridotite–pyroxenite–norite complex (Rundqvist, 1986), gabbro–pyroxenite–dunite (Lesnov, 1972), or gabbro–norite formation (Truneva et al., 1979). Moreover, Truneva et al. (1979) consider it to have a polyphase genesis, with the ultrabasic component belonging to an earlier complex, affected by gabbroization from a basic magma. The Chaya intrusion is located on the NW limb of the Kichera–Mama anticlinorium in the zone where this structure meets the Olokit synclinorium, and it cuts the Nyurundukan metamorphic complex (Lesnov, 1972). The intrusive body has a lenticular shape and extends in a NE direction, conformable with the fold structures. Contacts with country rocks are injection-type, in places with eruptive breccias. In the inner contact zones, hybrid diorite and quartz diorite have formed, while hornfelses and skarnoids occur in the country rocks. Faults divide the intrusion into two unequal parts. Ore mineralization is concentrated exclusively in the lower part of the intrusion, which is a steeply-dipping, sheet-like body with subvertical contacts (Fig. 141). Primary banding is extremely weakly expressed. Thus, the internal structure has the following particular

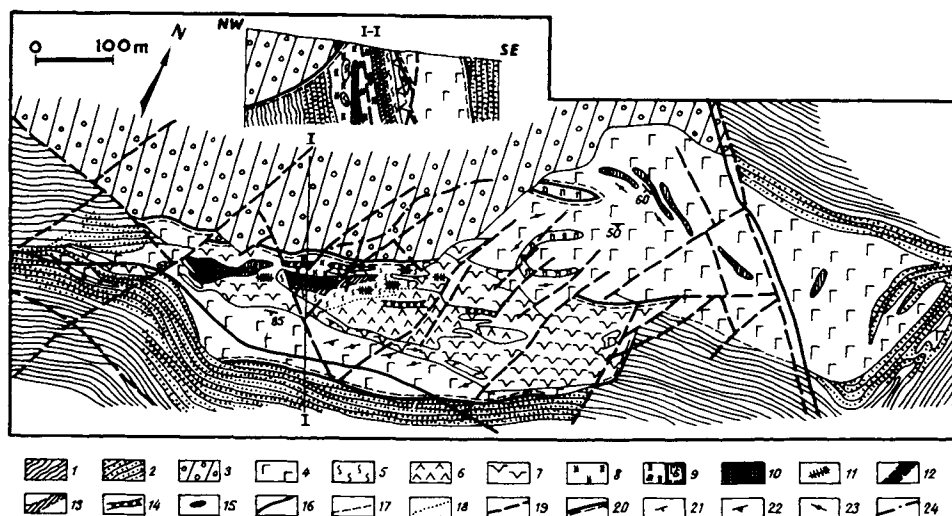


Fig. 141. Geological sketch map of the Chaya basic-ultrabasic intrusion (Cheshenko and Baburin, 1970). 1 – Riphean schist, 2 – as 1, hornfelsed, 3 – L. Cambrian cgl & sst. PR igneous complex: 4 – gabbro, 5 – serpentinite, 6 – dunite, 7 – peridotite, 8 – pyroxenite, 9a – plagi-peridotite, 9b – as 9a, with poor ores, 10 – as 9, with densely disseminated sideronite Ni-sulphide mineralization, 11 – dykes. Ores in brecciated serpentinite: 12 – rich, 13 – poor. Projections of buried ore bodies to the surface: 14 – disseminated ores, 15 – massive sulphide ores. Rock contacts: 16 – proven, 17 – inferred, 18 – transitional. 19 – faults, 20 – contact faults. Attitude: 21 – rock contacts, 22 – igneous banding, 23 – strike of banding; 24 – NW contact, inferred from magnetic survey.

zonation (Cheshenko et al., 1970): at the centre of the body – dunite and serpentinite, surrounded by a band with pyroxenite-peridotite composition; the margins consist of gabbroic rocks. On this basis, Lesnov (1972) considers the pluton to be a polyphase intrusion.

Sulphide mineralization is present to some extent in all the rocks of the intrusion, but ore concentrations exist only in the ultrabasic rocks. The two main ore varieties are disseminated and vein-type. Disseminated mineralization occurs in plagioclase peridotite layers and can be followed along strike and down dip for several hundred metres and through several metres of thickness. The dominant type is fine xenomorphic dissemination of sulphides, up to 0.2–1.0 mm in size, rarely up to 5 mm. The average Ni content in disseminated ores is 0.4–0.8%, up to 1.15%; Co 0.018–0.028%; Cu 0.17–0.25%. Vein ores are widely developed in the brecciated, mineralized serpentinite zone, and also close to the lower contacts of the intrusion. From textural and morphological features, the types identified are brecciated, massive and disseminated-vein. In the first, Ni on average is 1.5–2.5%, in the second from 4.5–6.0% to 7.4–9.5%; Co 0.19–0.23%; Cu 1.1–2.7%; in the third, Ni 2.5–3.1%, Co 0.022–0.025%, Cu 0.31–0.59%.

The deposit contains two relatively large ore bodies, hosted in ultrabasic rocks (Lesnov, 1972; Truneva, 1979). Ore body No. 3 is in the SW part of the intrusion and is a sheet-like ore zone with steep contacts, hosted in second-phase peridotites, broadly concordant with the overall structure, and occupying a “hanging” position. Rich ores

often concentrate at its base. It wedges out at depth or breaks up into a number of thin lenses. The ore body is up to 80–100 m thick and extends for around 1000 m. Disseminated ores predominate; intimately associated brecciated and massive ores form a sub-vertical body of rich ores with a complex configuration and zonal structure, where massive ores make up the central part. Ore body No. 2 is along strike from No. 3 body, and can be followed for 500 m with a thickness of about 40 m. It is associated with a zone of brecciated serpentinite, gabbro–pegmatite and pyroxenite, and consists of disseminated and vein-disseminated ores. Brecciated and massive ores are less common. Pyrrhotite is the main ore mineral, amounting to over 50% of the total ore mineral content. Pentlandite and chalcopyrite are present in smaller quantities. Depending on the type of ore, magnetite, pyrite, titanomagnetite, chromite, ilmenite, sphalerite, violarite, marcasite, melnikovite and makkinawite are found in varying proportions. Regarding its genesis, most workers treat the Chaya deposit as a magmatic type, with syngenetic and epigenetic ores.

*The Dovyren ore field.* The Yoko–Dovyren ore-bearing massif belongs to the Dovyren layered intrusive complex in the peridotite–pyroxenite–norite formation. It is located in the Olokit riftogene depression and cuts volcanosedimentary assemblages of the Avkit and Ondok formations which are overlain by Lower Cambrian Avgol Fm sediments. It has a lenticular shape with dimensions  $28.5 \times 4.0$  km and is conformable with the fold structures in the host rocks. As with the host rocks, the intrusion was “turned on its head” during folding and now has a secondary steep attitude (Gurulev, 1965). Rock types in the intrusion include peridotite, olivinite, troctolite, pyroxenite, mesocratic, leucocratic and melanocratic olivine gabbro, gabbro–norite and gabbro–diorite. The intrusion is accompanied by ultrabasic and basic dyke-like bodies running parallel to the intrusion’s NW contact. The intrusion has an asymmetric structure due to the layering, in which the ultrabasic rocks lie at the base, the footwall. The frequent interlayering of rocks with closely similar composition at different horizons in the intrusion and gradual transitions between rocks within individual horizons led Shishkin (1964) to suggest that differentiation processes are incomplete. Some workers consider that the massif is a multiple intrusion, identifying up to four intrusive phases.

The ore field has several deposits (Ozernoye (Lake), Tsentralnoye (Central), Rybachye (Fisherman), and others), and two main ore types: disseminated and vein-type. Disseminated sulphide ore mineralization is found in all rock types in the intrusion, although its maximum expression is characteristic for plagioclase peridotite and contact gabbro where several ore zones are found. One of these forms a contact deposit at the NW extremity of the intrusion. Another is associated with the lower dyke-like plagioclase peridotite body, forming a hanging-wall deposit in close proximity to the footwall of this body. The deposits are estimated to be a few m thick and to extend for several hundred m along strike and downdip. Ore mineralization in these bodies is represented by fine-grained, unevenly distributed, and dense sulphide dissemination. Additionally, in contact gabbros, there are coarse (up to 20 mm), irregularly-shaped grains.

The main ore minerals in the disseminated ores are pyrrhotite, magnetite, pentlandite, chalcopyrite; secondary valeriite, chromite, titanomagnetite, ilmenite; rare sphalerite and cubanite. Silicates are highly altered as a rule, with serpentinite, chlorite, hornblende and pelitic material developed at their expense. Late sulphides sometimes

form due to replacement of silicate minerals. The Ni content in disseminated ores reaches 1.2%, Co 0.22%, Cu 0.23%, Ni/Co = 11, Ni/Cu = 1.3. As a rule, disseminated ores are accompanied to some extent by vein mineralization, especially in tectonically reworked zones, where secondary replacement processes are expressed most intensely in the rocks. Shishkin (1964) has identified the following mineralization types among the vein ores: 1) mineralized pegmatitic gabbro, 2) vein-like bodies with a brecciated structure, 3) mineralized zones of crushed rock, 4) mineralization along joints in the intrusive rocks, 5) quartz-carbonate veinlets with sulphide mineralization. Only the first two types have any economic significance.

Mineralized pegmatite dykes are found in the outer NW contact of the massif, and among the dyke-like bodies. They are a few m wide and can be followed along strike for hundreds of m. Sulphide mineralization is developed along joints and forms large disseminated grains, clusters and veinlets, sometimes with a texture resembling brecciation. Mineralization is very unevenly distributed. The main ore minerals are pyrrhotite, chalcopyrite, pentlandite; secondary ilmenite, magnetite; rare sphalerite and galena. Primary silicate minerals in the dykes are extensively replaced by chlorite, actinolite, zoisite, clinozoisite, epidote, etc. The Ni content in ore bodies within the pegmatitic gabbros is up to 1.8%, Cu 0.2%, Co 0.05%. Vein-like sulphide ore bodies are exposed in the inner contact zone of the intrusion. Lenticular ore bodies consist of brecciated ore. Primary silicate mineral fragments are almost completely replaced by chlorite, serpentine and other minerals. In certain areas the brecciated ores grade into massive sulphide ores. Based on mineralogy, there are two types of ore body, pentlandite-chalcopyrite-pyrrhotite and pyrite-pyrrhotite. The first type also contains magnetite, pyrite, sphalerite, ilmenite, titanomagnetite, rare valeriite and cubanite. And in ores of the second type – magnetite, chalcopyrite, occasionally pentlandite and valeriite. In these ores Ni is up to 2.9%, Co 0.05%, Cu 0.5%. The Ni/Co and Ni/Cu ratios in vein-type ore bodies are 18 and 3.6 respectively.

From the mineralogy and chemical composition, the copper-nickel sulphide ores in the Dovyren ore field are closest to the ores of the Pechenga region (Shishkin, 1964). Genetically the sulphide ores in the Dovyren field belong to the magmatic type and their formation is inextricably linked to that of the massif. Depending on their conditions of formation, Denisova (1961) and Shishkin (1964) identify syngenetic (disseminated) ores which crystallized directly from the melt, and epigenetic (veins), which have a metasomatic origin. The emplacement of the nickeliferous Upper Proterozoic layered intrusions of the Dovyren complex appears to have been due to Upper Riphean rifting processes. The isotopic age (Sm-Nd isochron) of the Yoko-Dovyren massif is  $700 \pm 35$  Ma, according to data provided by L.A. Neymark, Yu.V. Amelin et al.

### 2.3. Lead and Zinc

*The Kholodninskoye massive sulphide-polymetallic deposit* is one of the biggest and best studied ore targets in the Baikal fold terrain. It was discovered in 1968 by V.N. Kostenko during geophysical exploration for nickel. Exploration results by V.P. Bushuyev, R.S. Tarasova and V.A. Mogilev and long-term investigations by G.V. Ruchkin, V.D. Konkin, T.P. Kuznetsova, E.G. Distanov, N.L. Dobretsov, Yu.M. Sokolov and

others demonstrated that the Kholodninskoye deposit is comparable in scale with such unique Precambrian ore targets as Sullivan (British Columbia) in Canada, Mount Isa (Queensland), Macarthur (Northern Territories) and Broken Hill (New South Wales) in Australia.

The deposit is hosted in a black shale sequence of a volcanogenic–carbonate–black shale (graphitic–clastic terrigenous–flyschoidal) formation at the edge of the Tyaa–Kholodninskoye palaeorift depression in the Olokit continental margin zone. The age of the host formation and the Olokit productive complex as a whole is Upper Riphean and is “bracketed” in the interval 1050–700 Ma. This estimate is based on the results of isotopic dating of Nyurundukan metabasalts underlying the productive complex (the lower boundary), and Sm–Nd dating of Dovyren gabbroic rocks which cut the ore-hosting sediments and U–Pb zircon dating of acid volcanics at the very top of the productive horizon (Neymark et al., 1990) (the upper boundary).

The main feature of the Kholodninskoye deposit is the high metamorphic grade of the sulphide ores and the host rocks. An early kyanite–sillimanite type zonal regional metamorphic and superimposed local greenschist facies retrogression have been established. Biotite–muscovite gneiss, staurolite and greenschist facies, including garnet and biotite zones, replace one another in sequence, from SE to NW. Mineral parageneses in the metamorphic rocks taken together with PT data indicate that metamorphic zoning occurred under PT conditions of 550–650°C and up to 7 kbar. Products of a retrogressive metamorphic event are widespread, represented by Fe–Mg–Ca and quartz–muscovite metasomatites of an acid leaching facies. Metamorphic zoning is complicated by retrogression in shear zones, including various blastomylonites and phyllonites. The age of regional metamorphism in the vicinity of the Kholodninskoye deposit has been determined by the Rb–Sr method on small samples of the host metapelites. Estimates obtained agree with Sm–Nd results on garnetiferous ortho-amphibolite dykes which cut sheeted ore bodies in the deposit, and a Sm–Nd estimate for the metamorphic age of garnetiferous amphibolites in the Nyurundukan assemblage, in the range 600–550 Ma. Geochronological results suggest a large time gap between the sedimentation and metamorphism of the host assemblage.

The formation hosting the Kholodninskoye ore deposit is usually divided into a lower productive unit with a metatuff–carbonate–black shale composition, and an upper unit of quartzite and black shale with polymetallic ore mineral occurrences. The productive part of the ore-bearing formation is represented by carbonate-rich graphitic shales, riddled with pyrite–pyrrhotite veinlets, porphyroblastic rocks with a variable mineral composition where graphitic quartzose sandstones and amphibolites play a minor role. Black graphitic shales containing around 3%  $C_{org}$  on average, are fine-grained primary sedimentary rocks in the pelite–siltstone series, with relict bedding and are distinguished by variations in the composition of the carbonate–silica–clay cement, recrystallized into a fine-grained aggregate of metamorphic minerals. Attempts at reconstructing the primary composition of the black shales indicate two broad groups. The first includes primary clay–tuffaceous sediments, formed under the influence of distal volcanism, and primary hydromica clays associated with physical weathering of basic rocks. The second group forms black shales after primary kaolin-rich highly mature erosion products of an ancient residual weathered mantle on a continental

landmass and hydromica clays resulting from intense chemical weathering of basic rocks. Banded pyrite-polymetallic ores are associated exclusively with the first group of black shales, which is an indirect indication that ore genesis is related to distal volcanism. Porphyroblastic rocks include metamorphic-metasomatic and metamorphosed primary sedimentary rocks which are distinguished on the basis of the regular position in the succession of rhythms of different orders, relict sedimentary structures, and geochemical features. Some of the amphibolites were formed from gabbroic sheet intrusions and dykes. They have a massive structure and relict primary igneous textures.

The deposit includes three *en échelon* ore zones coinciding with different stratigraphic levels in the host rock succession (Fig. 142). The First zone is the most intensely studied and consists of alternating bedded ore bodies and host graphitic shales with intercalations and lenses of metamorphic-metasomatic rocks and ortho-amphibolites. Some workers consider that the structure of the First zone results from the complex, multiple folding of a single ore bed (Tarasova et al., 1981; Distanov et al.,

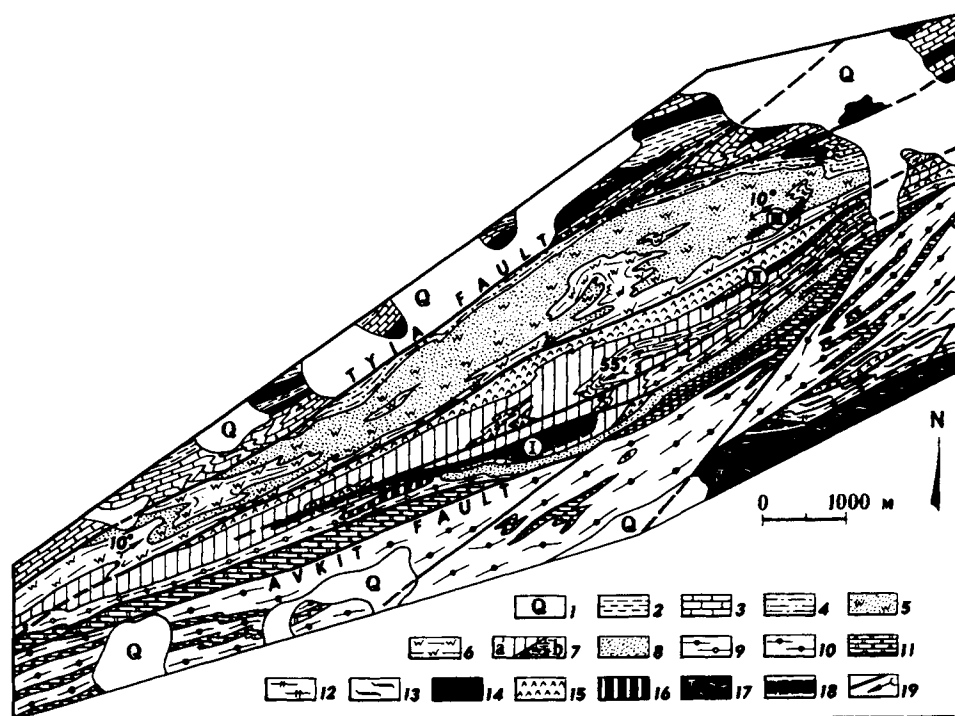


Fig. 142. Sketch showing geological structure of Kholodninskoye deposit. 1 - Quaternary. 2-3 - rocks above ore, 2 - phyllite, 3 - marble; 4-6 upper ore-quartz schist: 4 - metasiltstone, 5 - quartzite, 6 - graphitic-gt-qz schist, 6 - grit; 7-9 lower graphitic productive unit: 7a - schist, 7b - marble. 8 - quartzite; 9 - knotted schist, transitional member; 10-14 units beneath ore: 10 - Avkita schists, 11 - dolomitic marble, 12 - high-Al schist, 13 - retrogressed greenschist; 14 - metagabbro & metadiabase; 15 - orthoamphibolite; 16 - meta-ultrabasic, 17 - melanocratic orthogneiss; 18 ore zones (I, II, III) faults and dip of fold bends.

1982; Dobretsov et al., 1987), others view it as reflecting primary palaeotectonic facies conditions that controlled the localization of stratiform ores (Konkin et al., 1987). According to our evidence, the bedded ore bodies are demonstrably involved in complex folding together with their host rocks, although there are no high amplitude folds, such as the Kholodninskaya and Rudnaya ("Ore") synclines within the area of the deposit. One of those which has actually been mapped out is a steeply-plunging knee-shaped structure ( $F_2$ ) on the NE flank of the First ore zone. Thanks to the generally monoclinial attitude of the host rocks and ores, the Lower, Main and Upper bedded ore bodies in the First zone can be confidently traced for over 5 km towards the SW flank of the deposit. The Second and Third ore zones situated stratigraphically higher have a distinctly lesser extent and a relatively simpler structure. Local ore-hosting horizons occupy a very precise position in the established cyclical structure of the host succession, in the transition zone between transgressive and regressive rhythms.

In terms of morphology and banding in the host rocks, there are two morpho-structural types of ore body – bedded, which define the economic value of the deposit, and cross-cutting vein and vein-dissemination types. Bedded ores are characterised by later and vertical (across the thickness) zoning with an increase in the polymetallic constituent upwards in the section and away from essentially pyrite lenticular bulges (Moseikin et al., 1982; Zubkov et al., 1990). Compositionally, the bedded ores are essentially zinc-rich ( $Pb/Zn = 1/2-1/4$  and over) and low in impurity elements (As, Cd, Sb, Ge). Cross-cutting ores are controlled by faults synchronous with the folding, and are intimately associated with the quartz-muscovite metasomatic facies of acid leaching and occur as complexly-branching zones superimposed on both host rocks and on bedded ores. They account for only a few percent of the total reserves in the deposit.

Among the genetic types, it is possible to divide the ores into metamorphosed and those that originated during metamorphic processes. The first type includes bedded ores, consisting of the main productive sulphide association with varying textural and structural characteristics. Usually they are fine-grained disseminated-banded, densely disseminated, finely and coarsely banded, with alternating massive and disseminated ores, frequently with sub-concordant veinlets and fine-grained aggregates of galena and sphalerite. Densely-disseminated and bedding-disseminated pyrite ores in graphitic quartzites contain relict primary sulphide ores with a colloidal texture, including aggregates of framboidal pyrite. An unbroken sequence of metamorphic changes can be observed in primary ores, from those recrystallized *in situ* to coarse-grained aggregates of massive and granoblastic pyrite. According to several workers (Ruchkin et al., 1973), the formation of "spherulitic" ores, represented by fine-grained pyrite-galena aggregates with or without coarse-grained galena with rounded quartz or sometimes quartz-carbonate "nodules" is associated with the prograde metamorphic maximum. Also of metamorphic origin are those cross-cutting vein and vein-dissemination ores with variable mineral composition – galena-pyrrhotite, galena-sphalerite-pyrrhotite, galena. Most workers (Ruchkin et al., 1975; Dobretsov et al., 1987; Distanov et al., 1982) have shown that the formation of these ores is related to a retrogressive regional metamorphic episode.

The issue of the genesis of the Kholodninskoye deposit still remains a fiercely debated subject. Two models are well-founded, pre-metamorphic and metamorphic. According to the pre-metamorphic model (Ruchkin et al., 1975; Distanov et al., 1977, 1982; Konkin et al., 1987), economic deposits formed during hydrothermal-sedimentary ore genesis, synchronous with the host graphite-silica-carbonate-clay sediments in the ore-controlling environment of a palaeo-depression. Metamorphism, accompanied by metasomatism and folding, led to metamorphic recrystallization in place of the primary ores, complicated morphology of the bedded ore deposits with ore material being forced locally into fold cores, and the formation of cross-cutting, regenerated, uneconomic vein-disseminated mineralization. In the metamorphic model (Sokolov et al., 1981; Dobretsov et al., 1987; Bushmin, 1990), the deciding factor in the formation of economic ores are regional metamorphic processes accompanying retrogressive metasomatism and deformation with a leading role in ore-controlling isoclinal folding and fault zones synchronous with folding. In this scenario, it is considered that around 70% of the ores in this deposit have a metamorphic-metasomatic origin, concentrated in fold cores as "ore pillars" due to redeposition of primary ores during plastic flow and acid leaching (Dobretsov et al., 1987).

Adherents of both models put forward very similar arguments, since in either case they proceed from the recognition that there were both synsedimentary and metamorphic stages in the formation of the deposit. The main difference is in the geological evaluation of the significance of each stage in the formation of economic ore bodies. The debate exposes the inadequacy of the geological arguments for resolving the key issue in this problem: was either of these the factor that determined the formation of large-scale ore deposits, or is the uniqueness of the reserves in the deposit due precisely to a two-stage history of formation?

In order to evaluate the proposed genetic models, the Institute of Precambrian Geology and Geochronology undertook a detailed study of the lead isotopic composition in the different ore types. For initially low-grade redeposited ores, the lead isotopic composition should have a variable radiogenic Pb component, accumulated in the host rocks from the time of deposition to metamorphism and taken up by sulphides during their metamorphic recrystallization. In this case, we should expect meaningful variations in the lead isotopic composition in sulphides. From the results of earlier work carried out on the lead isotopic composition in sulphides from the Kholodninskoye deposit (Tugarinov et al., 1976; Mirkina et al., 1977; Karpenko et al., 1981; Anon., 1988b), it was impossible to evaluate the constancy of Pb isotopic characteristics either because the sampling was unrepresentative or because the isotope analysis was insufficiently precise. A total of 24 samples was selected for Pb-isotopic analysis, which were characteristic of the Lower, Main and Upper bedded massive sulphide-polymetallic ores in deposits in the First and Second ore zones, as well as a complete suite of their metamorphic equivalents.

In any examination of Pb isotopic data for sulphides in actual ore targets, the existence and magnitude of variations in isotopic ratios is especially significant, since major stratiform deposits typically do not show a deviation exceeding 0.1–0.2% (Doe and Stacey, 1974). Compared with previously published results, our data form highly compact ellipses in the conventional coordinate system (Fig. 143) and, being statisti-

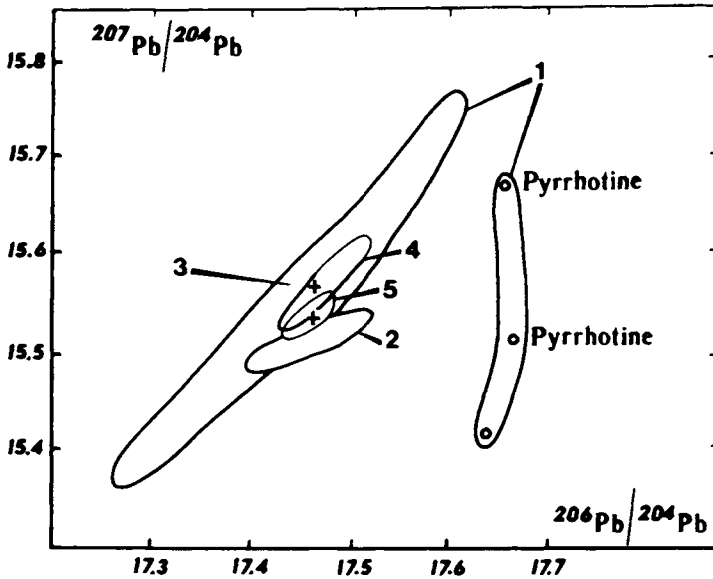


Fig. 143. Comparison of isotopic Pb composition in sulphides from Kholodninskoye deposit. 1 – Mirkina et al., 1977, 2 – Tugarinov et al., 1976, 3 – Karpenko et al., 1981, 4 – Precambrian Institute, MI-1320 instrument, 5 – as 4, MAT-261 instrument.

cally representative, they indicate a lack of natural variations in the lead isotope ratios in different types of ore. The maximum  $Pb^{207}/Pb^{206}$  “scatter”, distorted to the least degree by instrument mass fractionation, is less than 0.1% (Fig. 144). This result demonstrates that the Kholodninskoye deposit is identical in terms of this parameter to the majority of large stratiform deposits in the world with an exhalative-sedimentary (sedex) origin. On the graph showing model curves for the evolution of the lead isotopic composition, constructed for major or stratiform deposits of different ages, our data coincide precisely with the growth curve for the “orogen” model of plumbotectonics (Zartman and Doe, 1981) for both uranium and thorogenic Pb isotopes (Fig. 145a). Computed values for the model age and “ $\mu$ ” and “ $\kappa$ ” parameters according to the Stacey and Kramers model (1975), the growth curve for which practically coincides with that for the plumbotectonic “orogen” model, corresponds to an average value of  $740 \pm 10$  Ma for  $\mu$  ( $U^{238}/Pb^{204}$ ) = 9.64 and “ $\kappa$ ” ( $Th^{232}/U^{238}$ ) = 3.79, while the last two values are very close to the “ $\mu$ ” and “ $\kappa$ ” values (9.74 and 3.78 respectively) taken in the model. The agreement between calculated and model parameters, and the fact that for all major stratiform sulphide deposits when there is such an agreement, the model age of ore lead satisfactorily corresponds with the age of the host rocks (Stacey and Kramers, 1975), suggests that the figure obtained for the model age of ore lead is close to the age of the host rocks. This conclusion is also confirmed by the distribution of our Pb isotopic data on the growth curve relative to the results for other major stratiform sulphide deposits of the world (Fig. 145b). As can be seen from the diagram, the point for the isotopic composition of ore lead in the

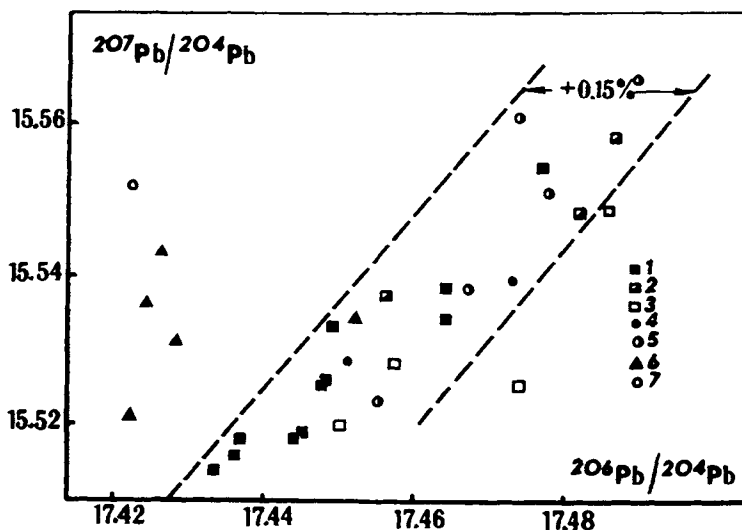


Fig. 144. Pb-isotopic characteristics of sulphides in Kholodninskoye massive sulphide-polymetallic deposit, compared with Olokite baryte-polymetallic deposits and occurrences. Kholodninskoye 1-5: 1 - galena, bedded ores, First zone, 2 - Second zone, 3 - galena from regenerated vein ores, 4 - galena from "spherulitic" metamorphic ores, 5 - pyrite from various ore types; 6 - galena, Yoko-Rybachye barite-polymetallic deposit, 7 - galena, Ondoko barite-polymetallic occurrence.

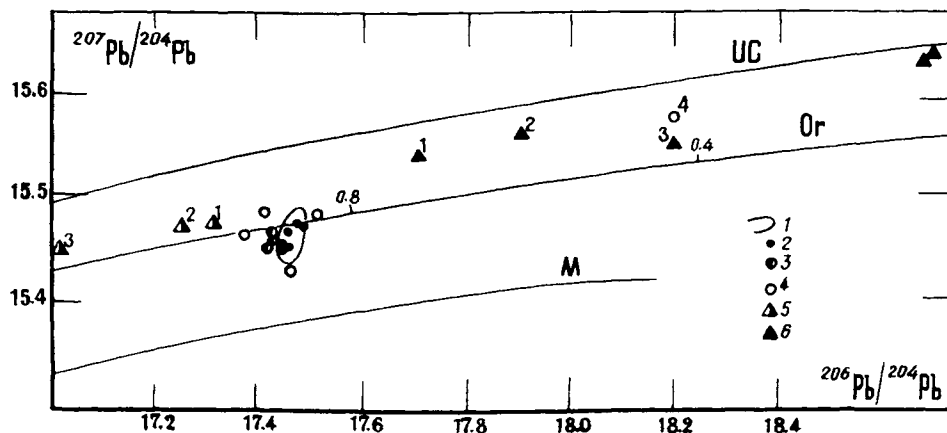


Fig. 145a. Pb-isotopic characteristics of sulphides in Kholodninskoye deposit compared with Olokite and Yenisey ridge Pb-Zn deposits. 1 - Kholodninskoye deposit, 2 - Ovgol pyrite - polymetallic occurrence, 3 - Yoko-Rybachye baryte-polymetallic deposit, 4 - baryte-polymetallic occurrences, 5 - Yenisey ridge deposits (1 - Maryanikhin, 2 - Merkurievo, 3 - Gorevskoye), 6 - Olokite vein occurrences (1 - disseminated galena in Ovgol granite dyke, 2 - Malygin, 3 - Mramornoye, 4 - Upper Chuya, 5 - Kudushkit). UC - upper crust, Or - orogen, M - mantle (plumbotectonic model growth curves Doe, Zartman, 1979).

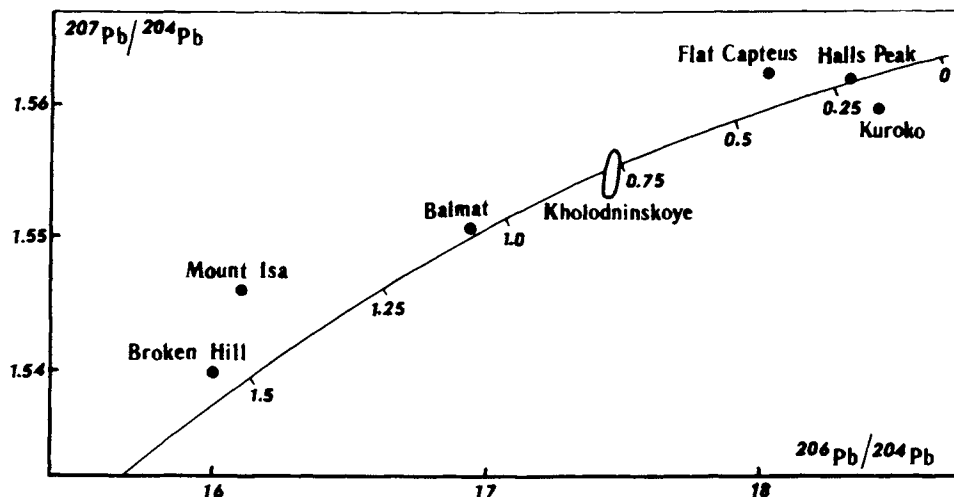


Fig. 145b. Lead isotopic growth curve for major stratiform deposits in the world, and position on it of Kholodninskoye deposit.

Kholodninskoye deposit lies between those for Balmat (USA) with an age of 1060 Ma, and Captain's Flat (Australia), which has an age of 420 Ma.

Lead isotopic data for the Kholodninskoye deposit cannot be satisfactorily reconciled with the hypothesis that the mineralization has a superimposed origin, since in such a case there would have to be ideal homogenization of the lead isotopic composition in different ore types. The "transparent" preservation of homogeneous isotopic characteristics in the whole range of products of metamorphic recrystallization from primary bedded ores to "spheritic" and regenerated vein-disseminations, suggests that the lead was mainly concentrated syngenetically. Proof of this conclusion is also to be found in results from investigating the lead isotopic composition in massive sulphides from different ore types, including framboidal pyrites in primary ores. It can be seen that the lead isotopic compositions of pyrite and galena from the deposit are quite identical. Thus, our results provide evidence that the bedded economic pyrite-polymetallic ores formed during a syngenic stage in exhalative-sedimentary ore genesis.

#### 2.4. Tin

Tin mineralization in the Baikai-Patom fold terrain has an extremely limited distribution and does not form any economically valuable targets. All presently known mineral deposits and occurrences are located in either basement inliers of the Chuya-Vitim zone or in the Akitkan volcanoplutonic belt. Greatest interest attaches to the tin ore targets in the Chuya-Vitim zone. On the one hand, these are varied quartz-feldspar metasomatites and pegmatites with tin-rare metal mineralization, hosted in the Davan-Abchada shear zone (described below), and on the other hand, pure tin ore or tin-sulphide deposits and

occurrences hosted in sub-volcanic granitic complexes. At present, ore targets in the Tuyukan ore region have the greatest interest among the deposits of the second type.

*The Tuyukan tin-ore region* was discovered fairly recently during geological surveying by the "Irkutsk-Geology" Company, in the Tonod basement high of the Chuya-Vitim zone. Ore targets are localized mainly in the external and internal contact zones of the huge Chuya-Kodar granite batholith, occasionally in the middle of it, in association with tectonic slabs of the Purpol Fm (Teptorga Group). Host rocks are Early Proterozoic metamorphic complexes of the Kevakta Group (Mikhailovo and Albaza Fms) and the Chuya-Kodar granites of the same age which cut them. Individual mineralization points have also been noted among Purpol and Medvezhye Fm sediments, overlying Chuya-Kodar granites. According to A.I. Ivanova et al. (Lugov, 1986), the tin-ore objects of the region are associated with minor sub-volcanic granite-porphphy intrusions of the Late Riphean Yazovo complex. Evidence for a link between mineralization and Yazovo complex granites is the fact that the granites are closely associated with the same deep fault, the granite-porphphyries have a tin geochemical signature, and they contain accessory cassiterite.

The occurrences described here are closest to deposits in the cassiterite-silicate ore formation. Mineral types of ore include sericite-quartz-cassiterite-sulphide, sericite-quartz-cassiterite, quartz-tourmaline-cassiterite, occasionally albite-quartz-cassiterite and quartz-microcline-cassiterite. Ore bodies of different compositions have a predominantly similar morphology and are represented by linear zones of veins, crush zones, occasionally metasomatic deposits. The best-studied occurrence is the Nakhodka, located in the middle of the NE ore-controlling fault zone. The main ore body with sericite-quartz-cassiterite-sulphide mineralization has a linear stockwork shape and is hosted in Mikhailovo Fm silicified graphitic schists. The rocks are deformed into tightly appressed folds and are cut by Chuya-Kodar granites. Associated with cassiterite in the ore bodies are arsenopyrite, galena, sphalerite, chalcopyrite, pyrrhotite, acantite, etc. Tin is unevenly distributed and varies from a few tenths to several percent. It is important to note the presence of silver in the ores, which can occasionally be up to 500 g/t. Maximum thicknesses and ore contents (ore columns) occur in the complex intersection zone between a NE fault and NNE strike-slip faults (Lugov, 1986). Also associated with this same Late Riphean period is the formation of the Zhanoksy volcanoplutonic granite complex in the surroundings of the Muya microcraton, with associated tin mineralization in feldspar metasomatites (Mokhovoye, Korotkoye, Skalistoye and other occurrences).

### 2.5. Rare metals

Rare metal occurrences are quite widespread in the Akitkan volcanoplutonic belt and the Chuya-Vitim zone of anticlinal highs in the Baikal fold belt, although there are no economic deposits. Numerous minor occurrences are known in the Akitkan volcano-plutonic belt - Sn, W, Bi, Mo, Be, Ta, Nb, REE in quartz veins, greisens, quartz-feldspar metasomatites associated with granitic rocks of the Irel, Primorye and Chuya-Kodar complexes. Polymetallic, fluorite and gold occurrences are associated with sub-volcanic bodies developed amongst acid volcanics of the Akitkan Group. The

most interesting rare-metal mineralization is known in the Davan–Abchada shear zone, distinguished by having a prolonged polycyclic evolution.

*Rare-metal occurrences in the Davan–Abchada shear zone.* This zone belongs with the marginal suture system of the Siberian craton. In the Baikal–Patom fold terrain, it follows the boundary of Archaean basement inliers (the Chuya–Vitim zone), partly overlain by the Akitkan volcanoplutonic belt, and supracrustal assemblages in the Baikal–Vitim, Mama and Olokit structures. There are two structural–metallogenic zones in the Davan–Abchada shear zone – the Davan and Abchada.

The Davan structural–metallogenic zone is controlled by the Davan shear belt, which runs along the axis of the Baikal and Akitkan ridges within the Western and North-Western Pre-Baikal regions (Fig. 146). This zone extends for over 200 km and has 5 km wide outcrops in the S and 50 km in the N. It was first identified in 1964 by M.P. Lobanov, V.M. Shemyakin, and A.N. Artemyev (Lobanov, 1966). Geotectonically, the Davan zone is genetically related to a long-lived, deep-seated fault first emplaced in the Early Proterozoic. In this connection, the kinematics of differential movements in its domain of influence encompass rocks of the lower structural stage (Sarma and Chuya groups), and rocks of the upper structural stage, represented by sedimentary–volcanic and intrusive complexes of the Akitkan volcano–plutonic complex. Within the Davan structural–metallogenic zone are faults belonging to a variety of genetic types, inhomogeneous dynamothermal metamorphism and metasomatism, which control metamorphic ore genesis in the zone, as confirmed by the corresponding iso-facies ore parageneses between vein formations and thermodynamic conditions of formation of metamorphic zoning (Table 15). The table shows that the veins form a metallogenic zoning that is subordinate in general features to the metamorphic zoning.

- 1) For the amphibolite facies belonging to the andalusite–sillimanite facies series in terms of PT parameters, high-temperature quartz–feldspar melt derivatives are typical: granite, aplite, quartz–feldspar and rare-earth pegmatites.
- 2) Metasomatic effects are most pronounced within the epidote–amphibolite facies zone, forming thick (up to 10–15 m) zoned deposits: a) quartz–microcline (amazonite), b) quartz–microcline (amazonite)–albite, c) quartz–albite, d) essentially quartz. Rare-metal and rare-earth mineralization are associated with the metasomatic zones.
- 3) Gold–sulphide mineralization is associated with sericite–quartz metasomatites in greenschist facies zones.

The geochemical spectrum of each metamorphic zone differs in its individual character. In the epidote–amphibolite facies zone, the most typical ore elements are rare metals (Mo, Sn, Be, Nb), rare earths (Y, Yb), rare alkalis (Li, Rb, Cs), and mineralizing elements (F). Amounts of these elements are lower in shear zones and anatectic zones, and in the transition to the amphibolite facies zone. Genetically, the rare metal–rare earth metasomatites belong to the rheometamorphic class of formations. A geochronological study of ore-hosting metasomatites in the Davan zone, carried out by L.A. Neymark and colleagues in the isotope laboratory of the Institute of Precambrian Geology and Geochronology using material provided by A.M. Larin and N.N. Predtechensky, identified two main pulses of ore formation at 1750–1850 Ma and 320 Ma (U–Pb isochron method on zircon). The first pulse is close in time to igneous processes in the Akitkan volcanoplutonic belt, the second corresponds to Hercynian events, so pervasive in the Baikal fold belt.

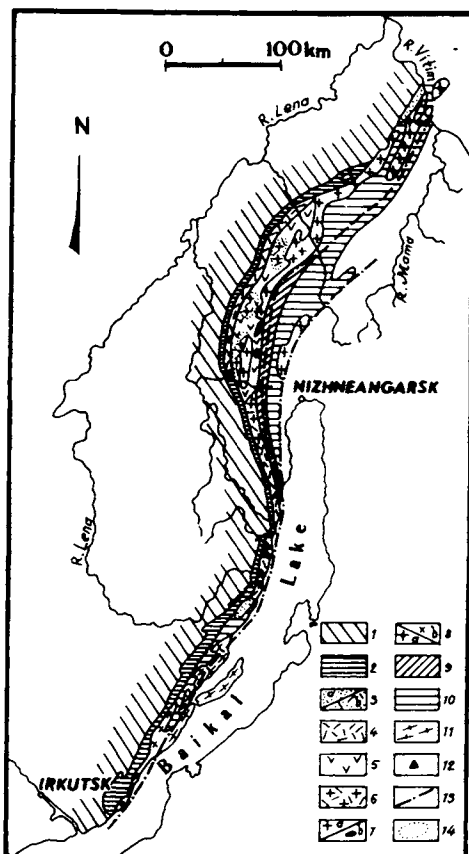


Fig. 146. Sketch of Davan shear zone in Pre-Baikal structures. 1 - L. PZ clastic & carbonate seds, 2 - U. PR Baikal Gp clastic-carb seds, 3-9 L. PR Akitkan volcanoplutonic belt: 3a - Teptorga Gp seds, 3b - Chaya Fm (Akitkan Gp), volcanosedimentary; 4-5 - Khibilen Fm (Akitkan Gp) acid lavas & tuffs; 6 - Irel sub-volcanic intrusions (porphyritic granite, granodiorite), 7a - Irel hypabyssal intrusions (granodiorite, granite, granosyenite), 7b - Kutim minor intrusions & dykes (diorite, granodiorite, gabbro), 8a - Chuya-Vitim granites, 8b - Primorsky granites, 9 metamorphic & metasomatic rocks in Davan shear zone; 10 - L. PR (?) metaseds, 11 - AR metamorphics, Baikal microcraton, 12 - relicts of central-type volcano (A.A. Bukharov), 13 - main fault lines, 14 - contours of subvolcanic rocks, genetically close to effusives.

The Abchada rare-metal zone is located in the northwards continuation of the Davan zone and is a rare-metal pegmatite field. Pegmatites with rare-metal mineralization, corresponding to the spodumene-free microcline-albite sub-group in N.A. Solodov's classification, were discovered after World War II during geological surveying by V.A. Dvorkin-Samarsky. They were subsequently studied by Manuylova et al. (1964), Makrygina (1981), Sizykh (1985) and Sokolov (1975, 1982). Swarms of pegmatite veins are localized in a narrow band 8-10 km wide, extending for around 100 km in a NE direction along the Abchada fault.

The pegmatites are located in greenschist-facies retrogressed shear zones. Host rocks, represented by biotite, cordierite-sillimanite-phlogopite, cordierite-anthophyl-

Table 15

Characteristics of ore genesis in the Davan structural-metallogenic zone (after Lobanov, 1970, interpreted by Yu.M. Sokolov)

	Diagenesis stage (non-metamorphic rocks)	Greenschist facies	Epidote-amphibolite facies	Amphibolite facies
Host rocks	Pelites: graphite-clay shale, siltstone, sandstone. Calc & calc-silicate rocks: limestone, dolomite, clay carb, carbonate-talc	Sericite-chlorite, sericite-carbonate schists. Carbonate-chlorite, epidote-quartz-chlorite schists, cataclasites, mylonites	Biotite, biotite-amphibole blastomylonites, porphyroids, blastoporphyritic and augen orthogneiss, biotite and two-mica microschists	Two-mica, biotite-amphibole, sillimanite, garnet-two mica gneisses, schists, quartzites, amphibolites, gneissose granites
Vein facies	Quartz, quartz-calcite veins with phlogopite, baryte, sphalerite, galena, pyrite and chalcopyrite; chalcedony, aragonite, calcite	Hydrothermal-metasomatic deposits, vein zones: with chlorite, sericite, epidote, albite, baryte, pyrite, chalcopyrite, galena, sphalerite, grey copper ores, antimonite, arsenopyrite	Metasomatic zones, deposits, quartz, quartz-feldspar veins with sub-alkali amphibole, muscovite, biotite, fluorite, cassiterite, molybdenite, mangerite, pyrrhotite, fergusonite, orthite and rare metals	Granites, aplites, amazonite pegmatites with rare metals, metasomatic zones with rare metals, granulated quartz
Ore mineral paragenesis of host rocks	Galena, cleopane, pyrite (impurities: chalcopyrite, grey copper ores)	Galena, sphalerite, pyrite, chalcopyrite (impurities: grey copper ores, pyrrhotite and arsenopyrite)	Rare-metal mineralization (impurities: molybdenite, cassiterite, pyrrhotite, arsenopyrite, magnetite)	Rare-metal mineralization, pyrrhotite, magnetite
Morphology of ore	Disseminations; large pockets, podiform deposits, cross-cutting laminar veinlets	Disseminations, stockworks, conformable veins	Disseminations, pockets, rare veinlets	Disseminations, vein-disseminated accumulations
Au content of veins in zones	Trace	3-6 g/t	≤ 0.012 g/t	

lite-mica and aegirine gneisses, gneissose granite, amphibolite and marble were metamorphosed in the andalusite-sillimanite facies series of the sillimanite-biotite-orthoclase and sillimanite-garnet-cordierite-orthoclase sub-facies of cummingtonite amphibolites. Post-metamorphic potash metasomatic effects are common in the country rocks. Within the Abchada pegmatite zone there is later ore zoning which correlates well with metamorphic zoning. Rare-metal microcline (amazonite)-albite pegmatites crop out directly in a fault zone, associated with the andalusite-cordierite assemblage, while to the NW, where sillimanite-cordierite assemblages are developed in the host rocks, it is mainly biotite-rare earth pegmatites with orthite and xenotime which occur. The pegmatite veins are 100-500 m long, and range in width from 2-3 m to 15 m, with sharp margins, slab-like and lenticular shapes. In terms of composition and texture, they are classified into weakly differentiated (graphic, with a predominantly primary granitic matrix), wholly differentiated, muscovite-microcline, and replacement, muscovite-quartz-albite. Vein structures are zoned and cellular-zoned. Textural varieties include graphic, block and various quartz-albite replacement textures and a complex quartz-muscovite texture.

Pegmatites in the Abchada zone differ from rare-metal pegmatites in other provinces in their type of rare-metal mineralization. Thus, they do not contain lithium minerals (spodumene, lepidolite, etc.) nor polychromatic tourmaline, boron minerals are very rare, while at the same time they contain minerals typical of the rare-metal pegmatite formation: beryl, cassiterite, phenacite, danalite, samarskite-euxenite, gadolinite, fluorite, and ilmenorutile. Sizykh (1985) has noted the presence of clusters of polychromatic aquamarine and heliodor crystals in the pegmatites, associated with an albite-oligoclase replacement assemblage, forming economic concentrations of gem-quality material. This assemblage is associated with epidote-amphibolite facies retrogressed zones in which granulated quartz also forms.

Genetically, these pegmatites are related to high-temperature, post-metamorphic migmatization processes, so that for example the formation temperature of plagioclase migmatites is 530°C using the biotite-amphibole geothermometer, and 500°C for microcline migmatites. The pegmatite bodies are not genetically or spatially connected to granites, their distribution being totally controlled by retrograde shear zones, while their internal structural elements are determined by their position in the metasomatic column. The geochemical REE spectrum is identical for migmatites and pegmatites. All these factors together suggest that the deposits belong to the ortho-metamorphic class of the metamorphic genetic type. Geochemical data on the composition of minerals in the pegmatites show that they are shallow-depth formations (andalusite-sillimanite facies series).

## 2.6. Gold

Gold ore deposits in the Baikal fold terrain are usually grouped into two main formational types – gold-black shale (“Sukhoi Log”) and gold-sulphide-quartz veins. Economic targets of the first type are known only in the Lena gold ore complex, where they are intimately associated with quartz vein and placer deposits. Economic quartz-vein gold ore targets occur over a much wider area and are found in a number of gold

ore complexes, where they are accompanied by polymetallic and rare-earth mineralization (South Muya, Oktokit–Chipchikon and Pravaya Mama complexes).

The Lena gold ore complex since 1884 has been one of the country's largest producers of placer gold, and more recently *in-situ* gold as well. Deposits in the gold ore complex are located in the relatively small area of the Bodaibo intracratonic basin, consisting of an Upper Riphean carbonate–clastic terrigenous rock assemblage (Fig. 147). Two sub-groups are distinguished in this assemblage, corresponding to depositional rhythms. The lower Kropotkin rhythm is made up of monomict and oligomict quartzites and quartz–sericite schists which give way to black graphitic sericite–quartz schist, metasiltstone and metasandstone. The upper Bodaibo rhythm consists of variable grain-sized polymict and greywacke-type metasandstones, including thin intercalations of carbonaceous phyllitic schists, metasiltstone, metagrit and limestone which are overlain by an assemblage of interbedded metasandstone, phyllitic schist and dolomite. Gold mineralization shows no clear stratigraphic control, tending towards members with fewer carbonaceous schists and metasiltstones, both in the Bodaibo and the underlying Kadalikan assemblage which has a similar composition. There have been recent reports that tuffs and tephra have been found among the

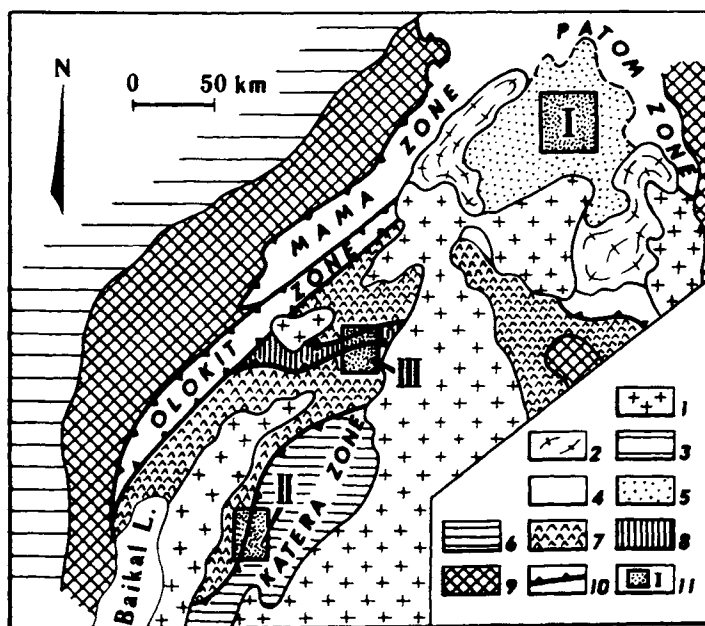


Fig. 147. Geological setting of gold ore complexes in Baikal fold terrain. PZ granitoids (1–2): 1 – Barguzin, Telmama, Konkudero–Mamakan granite plutons, 2 – Mama–Oron gneissose granites. 3 – Siberian platform cover; Riphean clastic–carbonate assemblages (4–6): 4 – structural zones in external belt of Baikal terrain, 5 – Bodaibo epicratonic basin, 6 – internal belt of Baikal terrain; Riphean eugeosynclinal complex (7–8): 7 – Baikal – Vitim belt, 8 – Orkolikan–Dzhalokan trough; 9 – AR–L. PR complexes in basement highs; 10 – zone boundaries; 11 – gold complexes (I – Lena, II – Oktokit–Chipchikon, III – Pravaya Mama).

metasediments (Buryak, 1987), suggesting that there was contemporaneous basaltic volcanism. In a structural sense, the mineralization is associated with the Bodaibo and Marakan–Tunguska internal basins separated in the structure of the epicratonic basin by the Kropotkin basement high. As Rundqvist and Rundqvist (1990) have shown, the Bodaibo epicratonic basin on the whole is genetically related to the Olokit palaeorift zone, more precisely the Olokit–Mama palaeorift trough. The buried continental palaeorift can be traced beneath the axis of the basin as a zone of linear geochemical and geophysical anomalies with a higher density of fractures, and this controls the most productive gold ore fields. Gold–black shale mineralization within the internal basins is subordinate to a system of intraformational thrusts, linked to ridge-like anticlinal folds. These ore-controlling structures may be identified with linear-type lateral dislocation zones (Yanovsky, 1990).

The sedimentary assemblage in the epicratonic basin was metamorphosed under chlorite–sericite subfacies conditions of the greenschist facies, with which the dominant E–W first-order folds are associated (Fedorovsky, 1985). The basin is bordered to the E and W by high-grade zonal metamorphism of kyanite–sillimanite type with second- and third-order folds and granite–gneiss domes. Against these broad features, a flexure in the first-order fold axial surfaces, caused by subsequent deformation, can be clearly mapped out (Flaass, 1971). Thus, in the syn-metamorphic field of regional strain, the Bodaibo epicratonic basin is “overprinted” by a relatively simple single deformation episode.

Igneous rocks in the Lena gold-ore complex are represented by granitoids and minor amounts of basic rocks. Of the three igneous rock groups identified, the earliest are syn-metamorphic gneissose granites of the Mama–Oron complex, forming dome structures in the cores of thermal anticlines. Geological estimates of the age of the Mama–Oron granites and the synchronous metamorphic aureole range from Early Proterozoic (Korikovskiy and Federovskiy, 1980) to Upper Riphean (Salop, 1967; Kazakovich et al., 1971), and using K–Ar results, upper Palaeozoic (Velikoslavinskii et al., 1961). The Mama–Oron granites of the Bolshe-Patom dome, which cut a significant part of the Bodaibo Group succession, have been dated at  $354 \pm 12$  Ma by the U–Pb method on zircon (Neymark et al., 1990). From a K–Ar date on biotite and muscovite, it is possible to fix the ending of thermal events in the interval 280–310 Ma. Different zircon morphologies from muscovite pegmatites in the Kolotovka mine determine an isochron corresponding to an age of  $322 \pm 5$  Ma, and the K–Ar age of muscovite is  $330 \pm 10$  Ma. This result points to a Hercynian age for the metamorphic aureole and superimposed strain in the Patom Highlands, which had previously been thought to be Precambrian.

The second group is represented by large plutons in the Telmama and Konkudero–Mamakan post-metamorphic granite complexes which occur on the S and SE edges of an intracratonic basin. An exception is the Dzhegdakar intrusion, located in the centre of the gold-ore complex. The intrusions are surrounded by high-temperature hornfels contact aureoles, which overprint zonal metamorphic rocks, and have an age of 320 Ma (U–Pb, on zircons; V.A. Khalilov, 1990, pers. comm.). The third group comprises dykes in the Kodali–Butuin and Aglan–Ayan complexes. The first of these complexes is represented by lamprophyres, dioritic porphyrites, and microdiorites (Kazakevich et al.,

1971). According to Kondratenko (1977), basic dykes are mainly concentrated in an extensive N-S belt, practically cutting at right angles the major structural elements of the Bodaibo basin.

The geological age of the Kodali-Butuin dykes has been determined as Upper Palaeozoic, whereby the dykes are not only post-granite, but also cross-cut the quartz-gold veins (Sher, 1959). Lamprophyres have been dated by the Sm-Nd method at  $313 \pm 59$  Ma,  $\epsilon_{Nd}(T) = -10.3$  (Neymark et al., 1990). The Aglan-Ayan swarm consists of plagioclase granite-porphry, granite-porphry, and quartz porphyry. They form a series of dykes and minor stocks, also concentrated in a N-S belt, similar in situation to the Kodali-Butuin dykes. Direct field observations have confirmed that lamprophyres are cut by granite-porphry dykes, with xenoliths of the former (Kondratenko, 1977). From the results of a U-Pb study of zircon and sphene from plagioclase granite-porphries in the Konstantinovo stock, the age of the complex is  $290 \pm 20$  Ma with relatively older inherited zircon (from 530 to 650 Ma according to the  $^{207}\text{Pb}/^{206}\text{Pb}$  ratio).

The main economic value of the Lena gold-ore complex are "Sukhoi Log" type targets with vein-disseminated sulphide mineralization in the form of almost bed-like mineralized zones associated with graphite-rich silty pelite members. Such zones are tens of m thick and tens of km long, with low gold contents of 3-6 g/t. Within the framework of the metamorphic-hydrothermal genetic model proposed by Buryak (1975, 1982, 1987), the mineralized zones contain several identifiable sulphide generations. The earliest - sedimentary-diagenetic - is represented exclusively by massive sulphide and contains practically no gold. Early metamorphic pyrite-pyrrhotite vein-type with rare sphalerite, chalcopyrite and arsenopyrite segregations is subordinate to the structural direction of a cleavage and secondary schistosity in host silty pelites, and characteristically has a higher gold content. The main gold-bearing association compares with metamorphic-hydrothermal formations and consists of pyrite with an arsenopyrite admixture, which are accompanied by higher silver and arsenic concentrations, and as a rule is found in quartz veinlets and veins in mineralized zones. Productive gold-bearing zones are accompanied by low-temperature sericite-carbon dioxide listvenite-berezite type metasomatic wall rock alteration overprinting regional metamorphic-metasomatic changes, similar to deep-seated propylites. In the post-magmatic concept, gold-sulphide mineralization is considered to be superimposed on quartz veinlets in graphitic schists and syngenetic with post-magmatic quartz veins with a sulphide assemblage of grey copper ores, galena, occasionally arsenopyrite and chalcopyrite. A recently proposed model combining a hydrothermal and plutonic origin for the formation of economic gold content in carbonaceous clastic terrigenous assemblages (Narseyev et al., 1989; Yanovsky, 1990) envisages a paragenetic connection between gold and granitic magmatism with local primary concentrations of gold in favourable lithostratigraphic horizons, with subsequent redistribution into long-lived ore-localizing zones in so-called lateral dislocations. Published geological and geochronological data indicate two major stages in the formation of the Lena gold-ore complex - Baikalian and Hercynian, the latter of which, with the appearance of varied granitoid magmatism, determined the economic gold content of the ore targets in the complex.

The Oktokit–Chipchikon ore complex is associated with the Namama regional fault system in the tectonic collision zone between the Svetlin block of melanocratic rocks in the Baikal–Vitim eugeosynclinal belt and the Katera basin with its carbonate–clastic terrigenous assemblage (Fig. 147). Gold-ore targets in the complex include gold–quartz veins in the Chipchikon deposit and gold–polymetallic ores in carbonate rocks and metasomatites in the Oktokit deposit. The Chipchikon deposit is hosted in plagioclase–amphibole schist, amphibolite and plagioclase migmatite in the Upper Riphean Nyurundukan Fm with large almost sheet-like pyroxenite–gabbro–norite intrusions. Ore-controlling structures are NNE-trending strike-slip faults and anticlinal crests. Gold–sulphide–quartz veins are hosted in extension joints splaying off faults, and together with sub-parallel swarms of fine-grained trondhjemitic dykes of the Kachoy complex they form two levels, the lower of which is situated beneath the screen of a gabbroic allochthon. Gold–sulphide–quartz veins are accompanied by weakly-expressed listvenitization with disseminated sulphides.

The Oktokit deposit is represented by a series of productive mineralized zones of listvenite–berezite metasomatites, associated with thrust–nappe tectonic sutures between a Riphean metamorphic complex of melanocratic rocks and a Lower Cambrian carbonate assemblage, and with intraformational thrust structures. Despite the different geological and structural settings, the deposits in the Oktokit–Chipchikon gold-ore complex show the same stages in the hydrothermal ore process. The earliest gold–sulphide–quartz associations (pyrite–chalcopyrite and pyrite–arsenopyrite) alternate with gold–polymetallic and gold–chalcopyrite–grey copper ore associations with economic gold, silver, lead, zinc, copper and antimony concentrations, although these are extremely unevenly distributed. There is local development of a gold–sulphotelluride–tetrahedrite–bismuth ore association. A characteristic feature is the intense development of oxygen compounds of the main metals in the hypergene zone. Free gold is finely-dispersed in most sulphides in all the ore associations and has a relatively low purity. The hypergene zone has much more, high purity redeposited gold. Gold grade ranges from a few tenths of one percent to 28 g/t, reaching up to 65–138 g/t in places. Thus, the deposits in the Oktokit–Chipchikon gold-ore complex constitute a typical example of hydrothermal formations, coinciding with regional fault zones. Table 16 compares the essential features in the sequence of geological events in the Lena and Oktokit–Chipchikon gold-ore complexes, using the latest geochronological data obtained by the Institute of Precambrian Geology and Geochronology.

A detailed lead isotopic study of sulphides in ore targets and feldspars from associated igneous rocks was undertaken in order to elucidate the genesis of the gold target in the Baikal fold terrain. Our results are shown in Figure 148, from which it can be seen that sulphides from comparable Lena and Oktokit–Chipchikon ore complexes differ markedly in all Pb-isotopic ratios, indicating that the rocks and ores originated from different depths. Attention is drawn to the fact that the isotopic composition of lead from all the morphogenetic types of gold–sulphide mineralization of “Sukhoy Log” type is identical, as is that of *in-situ* and placer gold in the Lena ore complex, which may indicate that the economic gold content of the ore complex as a whole has a single genesis. A quite different situation pertains to the Oktokit–Chipchikon ore complex. Isotope compositional points for individual deposits and independent

Table 16

Comparison of main geological events in the history of formation of the Lena and Olokit–Chipchikon gold-ore complexes

Age	Main geological events and geochronological data			
	Lena gold-ore complex	Au	Olokit–Chipchikon gold-ore complex	Au
Cz	Arch uplift, rifting	placers	Arch uplift, rifting	placers
Mz	?		?	
	Metasomatites, including wall rock, dyke swarms, 290 and 313 Ma (U–Pb and Sm–Nd)	quartz–vein	Chivyrkuy granite pluton 298 Ma (U–Pb)	
Pz <sub>2</sub>	Post-orogenic granite plutons and mica pegmatites, 320 Ma (U–Pb)			
	Zonal metamorphism and migmatite granites, 350 Ma (U–Pb)	vein disseminated	Metasomatites, including wall rock and ore-bearing, dyke swarm	quartz-vein and mineralized zones
Pz <sub>1</sub>			Barguzin granite batholith, 380 Ma (U–Pb), tonalite plutons, 470 Ma (U–Pb). Low-temperature metamorphism	
V–Cm			Volcanism; deposition of Baramyi Group	
PR <sub>3</sub>	Greenschist facies metamorphism Deposition of Patom Group	higher conc. primary conc.	Metamorphism, granitoids Sedimentation and volcanism, Katera and Nyurundukan Groups	
PR <sub>1</sub>	Continental crust older than 2.0 Ga (basement)	source	Continental crust older than 2.0 Ga (basement)	source

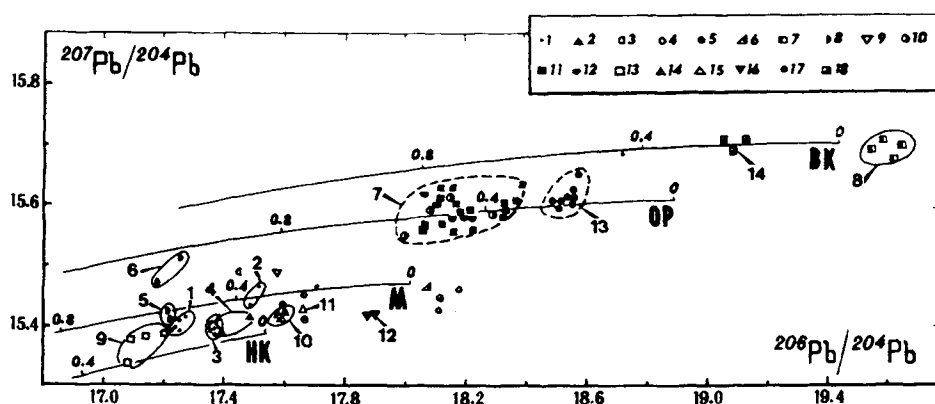


Fig. 148. Lead isotopic characteristics for sulphides and feldspars in ores and rocks of gold-ore complexes in the Baikal fold terrain. Pb isotopic growth curves constructed according to the Zartman and Doe (1981) "plumbotectonics-2" model (UC - upper crust, LC - lower crust, OR - orogen, M - mantle). Sulphides (1-12). Oktokit-Chipchikon ore complex (1-5): 1 - galena, Oktokit ore field & Ogemi sector, 2 - pyrrhotite & chalcopyrite, Chipchikon deposit, 3 - chalcopyrite, Pravaya Berimya occurrence, 4 - pyrite & chalcopyrite, Myodin ore zone, Oktokit field, 5 - pyrite-pyrrhotite veins, Arbun Mo occurrence; Katera basin (6-7): 6 - disseminated pyrite, Pyandon schists, 7 - pyrite, bedded ores, graphitic schists; Pravaya Mama ore complex (8-9): 8 - galena from ore sectors, 9 - disseminated galena; Lena ore complex (10-12): 10 - gold, 11 - pyrite, 12 - auriferous pyrite. Feldspars (13-18). Katera-Barguzin region (13-15): 13 - granite, 14 - monzodiorite, 15 - trondhjemite; Bodaibo region (16-18): 16 - lamprophyre, 17 - gneissose granite, 18 - mica pegmatite. Numbers on figure: ore zones & gold ore complexes (1-8) & intrusive complexes (9-14): 1 - Sukhoy stream, 2 - Barytes stream, 3 - Ogemi sector, 4 - Chipchikon deposit, 5 - Ukuchikta sector, 6 - Vysotny sector, 7 - Lena ore complex, 8 - Katera basin; 9 - Barguzin, 10 - Kachoy stocks, 11 - Kachoy dykes, 12 - Kodali-Butuin dykes, 13 - Mama-Oron complex & Konstantinvo stock, Aglan-Ayan complex; 14 - Mama mica pegmatites.

mineralized zones form small and as a rule non-overlapping compact fields relative to the homogenized isotope composition (see Fig. 148), which most likely is due to different mineral-forming episodes and (or) wall rock effects. The spread of experimental points at the start of the mantle curve results from superimposed processes in the hypergene zone causing a restructuring of the Pb-isotopic system in sulphides with low lead concentrations.

Looking at the overall lead isotopic data for sulphides and feldspars, there is reasonably good coverage of their isotopic compositional fields, which may point to a genetic link between granite- and ore-forming processes. Experimental Pb isotopic compositional points for granites and sulphides in the investigated ore complexes form a trend on the Pb-Pb diagram (Fig. 148) from Barguzin granites with the most primitive Pb isotopic composition to Mama mica-rich pegmatites, between which are points for sulphides and feldspars from Mama-Oron granites and dykes. The established trend may indicate a similarity in the age of the processes that produced the economic gold content of the Lena and Oktokit-Chipchikon ore complexes during the Hercynian stage and a closeness in the ages of the ore material sources. If we accept the suggested Hercynian age for the ore-forming processes (productive stages in any case), then using the constraints imposed by the trend obtained, the age of the crustal lead

sources can be estimated at 2.0–2.1 Ga. Overall then, the observed distribution of lead isotope ratios, using Zartman's (1984) terminology, is typical of "rejuvenated cratons" – segments of sufficiently old continental crust, subsequently reworked (including the effects of ore forming processes) during a much later period of geological time. This conclusion is confirmed by studies of the Sm–Nd isotopic system, using whole-rock granite samples from the investigated gold-ore complexes. From the TDM data obtained, the model age of the Mama–Oron granites and the lamprophyre dykes in the Bodaibo downwarp are identical with the Barguzin granitoids in the region of the Oktokit–Chipchikon gold-ore complex and corresponds to a crustal source age of around 2.0–2.1 Ga. Taking the Pb–Pb data into account, a consequence of this is the need to acknowledge that the material sources have the same age for granitoids and gold-ore formations in comparable ore complexes, which was the lower and upper continental crust. As distinct from the Lena complex, a significant part of the granitoids in the region of the Oktokit–Chipchikon gold-ore complex are the products of reworking of relatively young melanocratic crust, with a Riphean age (TDM = 0.72–0.95 Ga). Monzodiorites and trondhjemites in the Kachoy complex within the gold-ore complex itself are characterised by intermediate model age values TDM = 1.5–1.6 Ga, which may be due to mixing of Upper Riphean and Early Proterozoic crust during the formation of these granites. From this characteristic, the dykes in the Oktokit–Chipchikon ore complex are strikingly different from similar rocks in the Lena ore complex.

In concluding this overview of the gold ore targets in the Baikal fold terrain, we emphasise that our isotope geochemical results provide fairly reliable answers to two key questions concerning the geology of the gold ore deposits. The main source of the ore material was Early Proterozoic continental crust; the age of the main ore-generating processes corresponds to the Palaeozoic stage in the polycyclic evolution of the region. Thus, it is possible to consider that the potential extent of the period involving "removal" of the useful component from a rock sequence with its background distribution and concentration to an economic level may have amounted to no less than 1.5 billion years. Obviously, during such a vast time interval, extremely varied processes must have played their part in concentrating the gold, with the major role belonging to metamorphism and granitic magmatism, i.e. the main rock-forming processes. Depending on the geodynamic setting, the sequence of actual geological events could have been significantly different. For example, in the relatively stable conditions existing in an epicratonic basin, primary gold accumulation began in the Upper Riphean and was associated with sedimentary processes in which organic matter played a part. Early greenschist metamorphism led to the first local concentrations of gold in favourable lithostratigraphic and structural horizons. Powerful Hercynian continental collisional processes with high geothermal gradient zonal metamorphism and various forms of granitic magmatism created favourable conditions for subsequent gold concentration from both host sediments and from a primary source. Dykes and associated gold content probably fix the concluding, and more local, stage of ore genesis. Thus, metamorphic and plutonic genetic models for the formation of "Sukhoy Log" type gold ore deposits are not alternatives, but instead reflect one aspect of a single and extensive ore forming process. In this connection, "Sukhoy Log" type gold deposits in sedimentary assemblages are the clearest representatives of polygenetic and poly-

chronic ore targets. In active continental margin conditions, restored in the Katera-Barguzin region, there is no intermediate stage of primary gold accumulation in sedimentary successions, and economic gold content is related to post-magmatic hydrothermal activity. We may surmise that this condition is one reason for the lower productivity of the Oktokit-Chipchikon ore complex as a whole.

### 2.7. *Muscovite*

The Baikal-Patom fold terrain contains the largest muscovite province in the former Soviet Union, where hundreds of muscovite pegmatites are concentrated.

*The Baikal-Patom muscovite province* is situated in the North-West Pre-Baikal region, the North Baikal and Patom Highlands within the Mama structural-formational zone of the Baikal fold belt. The productive area of the muscovite province is up to 45 km wide and extends for about 400 km. From geophysical data, a prism of metamorphic rocks which host the muscovite pegmatites can be traced down to depths of 2-4 km. The prism is gently inclined at 2-5° to the NE (045°), such that due to erosion it is possible to observe the top of the prism towards the NE flank of the province, in the source region of the rivers Bolshoy (Greater) Patom-Anangra-Mara, while on the SW flank, the deep zones of the Baikal fold belt are exposed, represented by migmatite and granite-gneiss fields, containing non-reworked micro-blocks of Mama Group metamorphic rocks. In addition, the Zhuya structural-pegmatitic zone (Bushev, 1979) occurs to the NE in the watershed of the rivers Vitim and Zhuya, while there are small muscovite pegmatite fields in the SW of practically no economic importance (Levaya (Left) Minya river basin, middle reaches of the river Chaya, and watershed between the rivers Tukulakh-Nalimda-Magdana).

Tens of thousands of pegmatite bodies are concentrated in the Baikal-Patom province, of which only a tiny number have economic muscovite contents. These veins are concentrated in pegmatite fields and veins, historically referred to as deposits (Fig. 149; Tarasov et al., 1975). The best known are, from NE to SW: Anangra, Mara, Bolshe-Severnoye, Vitim, Takhtygan, Kalotovka, Slyudyansk, Kamnizhskoye, Lugovskoye, Sogdiondonskoye, and a group of numerous deposits in the Chuya structural-pegmatitic zone. However, it should be borne in mind that these fields also contain pegmatitic granite veins which are essentially separate deposits. Such veins are common in the Chuya zone, for example vein No. 15 (Golets Oboronny), from which around 20 tonnes of muscovite were extracted when it was operational, and veins in the Mochikit, Davgokit and other sectors. The muscovite pegmatite deposits occur in the outcrop area of the Mama Group, concerning the age of which, and that of the pegmatites, there exist different viewpoints, which were considered above.

The following values were obtained for the isotopic age of the pegmatites: K-Ar 300-400 Ma, Rb-Sr (isochron) 400 Ma, Rb-Sr (model) 450 Ma, Pb (model) 320 Ma, U-Pb (isochron, zircons) 300 Ma, Pb-Pb (on zircons) 300, 800, 1300, 1700, 1900 Ma. Such a wide range of values for isotopic ages, from Hercynian to Svecofennian, combines numerous tectonomagmatic events in the geological evolution of southern Siberia (the Baikal mountain region), of Caledonian and Hercynian age, during which enormous masses of granitic intrusions were emplaced (Angara-Vitim batholith,

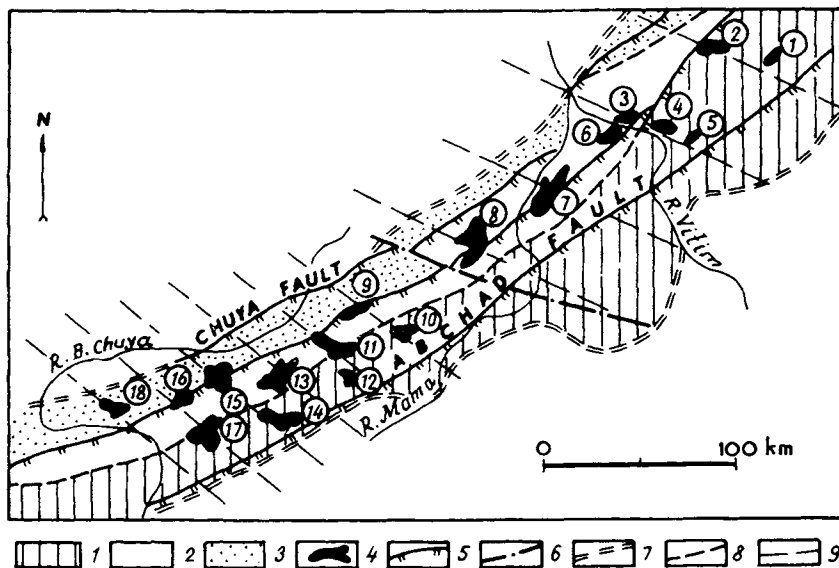


Fig. 149. North Baikal muscovite deposits (after V.P. Vasileva, 1975). Zones: 1 – voluminous injections, 2 – normal injections, 3 – solitary veins, 4 – muscovite deposits, 5 – thrust-nappes & strike-slip faults, 6 – deep fault, 7 – boundaries of pegmatite distribution, 8 – boundaries of abundant pegmatites, 9 – empirical shear stress lines. Numbers in circles (1–18): pegmatite vein clusters.

plutons in the Central Vitim Mountains, Konkudero granites and others, cutting fossiliferous Cambrian rocks). This question was considered by M.M. Odintsov as long ago as 1972, but even up to the present there are still attempts made to suggest that the regional metamorphism was a Palaeozoic event. Summarising all the geological and geochronological evidence, the author concludes that the Baikal–Patom pegmatite province formed at 1.9 Ga ago, during a global event in the system of metallogenic pulses of Precambrian crust-forming internal processes (Kosygin and Kulish, 1984)\*, which corresponds in time to a low-gradient kyanite–sillimanite facies series metamorphic event. It has been established from its PT conditions that this metallogenic pulse was the most productive for the formation of pegmatites in the muscovite and rare metal–muscovite formations.

The geotectonic setting of the pegmatite province is determined by the fact that it occupies the southern segment of the East Siberian pegmatite ring belt. It is perfectly likely that horizontal compression had a significant role to play in the dynamics of formation of structural–metallogenic zones and pegmatite fields concentrated between the cratons of the Siberian plate and the Baikal–Muya greenstone belt, as has been

\* (However, recent data obtained by L.A. Neymark and others in the isotope laboratory at the Precambrian Institute in St Petersburg, using samples collected by Yu.M. Sokolov, S.P. Korikovskiy and A.I. Sezko, suggest a Hercynian age for both Mama–Oron synkinematic granites ( $350 \pm 15$  Ma) and their associated muscovite pegmatites ( $320 \pm 10$  Ma), using the U–Pb isochron method on zircons. – Editor's note).

established for pegmatite fields in the Indostan Shield (Moralev et al., 1976). Using satellite images, several investigators (Fomin et al., 1987) undertook an attempt at reconstructing the palaeostructure controlling the distribution of pegmatite metallogenic zones in the Baikal–Vitim pegmatite province. For example, their results show that the dimensions of a proposed Baikal–Patom palaeo-arch are 300 km SE–NW and 650 km SW–NE. The Mama–Chuya palaeo-graben, the outlines of which coincide with the Chuya–Vitim muscovite pegmatite zone, occupies the centre of this palaeo-arch. On the limbs of the palaeo-arch are the Zhuya (muscovite zone), North Baikal (rare metal–muscovite zone), Minyo–Kutim (muscovite zone) and Yangudin–Param palaeo-grabens. Thus, the first-order ore-controlling structure to which the majority of economic muscovite veins belong, is an ancient arch structure. Second-order structures are palaeo-grabens, controlling rare-metal pegmatite zones, and third-order ore-controlling structures are deep-seated faults, represented by fragments of joint zones filled by pegmatite veins. The attitude of the pegmatite fields in the Mama zone is defined by its internal structural features and episodes of folding, metamorphism and metasomatism.

The Mama synclinorium has a NE strike and an asymmetrical structure: the NW limb dips relatively gently, while the SE limb is steep. The NW limb consists of amphibolite facies metamorphic rocks and on the SE limb the same rocks are at lower grade, with well-expressed Barrovian-type zones. In cross-section from NW to SE, the synclinorium is divided into three structural–formational zones: NW (isoclinal folds), central (late-inversion domes and arches), and SE (isoclinal folds and kyanite–sillimanite metamorphic zoning). Thus, the deep zones of the Chaya–Chuya block are exposed on the SW flank, characterised by sillimanite–biotite–garnet–orthoclase sub-facies metamorphism, intense migmatization and correspondingly few muscovite-bearing pegmatite veins. Farther to the NE is the Chuya–Mama productive block, with biotite–staurolite–muscovite–kyanite sub-facies rocks and weakly-expressed migmatization. And, finally, the Angara–Patom block is exposed on the extreme NE flank, representing the province’s upper structural stage where there are no migmatites, and pegmatites occur as granite and aplite veins. The block structure determines the formation of unequal, concentrated clusters of pegmatitic material, which is beautifully illustrated on the pegmatite distribution map for the central part of the Mama crystalline belt, compiled by V.N. Chesnokov.

Detailed structural research by A.S. Flaass has demonstrated that there are several gold generations of different ages in the Mama productive sector –  $F_1$ ,  $F_2$ ,  $F_3$  and  $F_4$ . Most of the pegmatites (group II) are concentrated in  $F_3$  positive structures. In the general evolution of folding in the pegmatite province, it is expedient to distinguish pre-inversion, inversion and late post-inversion stages which are characterised by different structural and metamorphic parageneses that determined pegmatite formation at each stage. During the pre-inversion stage, pegmatites formed according to the scheme: Na-metasomatism (porphyroblast growth) → porphyroblast homogenisation → replacement of porphyroblasts by quartz (diablastic growth) → collector recrystallisation → weak K-metasomatism → group I pegmatites. Lower pressure and volume expansion during the inversion stage allowed anatectic (possibly paligenic) granites to form, which were subjected to patchy recrystallization – group II pegmatites

during the transition from prograde to retrograde metamorphic episodes at the end of the stage. Finally, metasomatic alteration of the quartz-feldspar matrix (feldspar hydrolysis, muscovitization, growth of metasome minerals) occurred during late and post-inversion stages. This scheme was further elaborated by Butvin (1988), based on detailed work over many years, and he developed the following classification: I. Pegmatitic granites and group I pegmatites. Essentially plagioclase granitoids: a) metamorphic-metasomatic, b) anatectic. Pegmatites: a) plagioclase-muscovite-quartz composition, b) plagioclase-quartz-muscovite. II. Pegmatitic granites and group II pegmatites. Palingenic pegmatitic granites and pegmatites: a) non-replaced plagioclase-microcline composition b) replaced plagioclase-microcline composition, c) replaced plagioclase composition. Metasomatic pegmatites: a) in replaced granite and pegmatite bodies: essentially plagioclase and essentially plagioclase-microcline compositions, b) plagioclase-microcline composition in non-replaced granite and pegmatite bodies, c) zones of recrystallization and metasomatism in group I granites and pegmatites. According to this classification, V.V. Butvin devised a taxonomy for the pegmatite fields in the North Baikal structural-pegmatite zone and established a particular zonation of the pegmatite fields, illustrated in Figure 150.

Stratigraphy has been an important factor in the distribution of muscovite pegmatites. Some time ago, Zavaliskin and Lvova (1954) were able, owing to the flyschoidal structure of the Mama Group, to identify in the succession productive horizons characterised by finely interlaminated kyanite and less aluminous beds, which reflect definite lithofacies. Later research in the Mama Group (Anon., 1983) showed that the overall succession represents two formational series – a clastic terrigenous-flyschoidal series in the lower sub-group, and a sandy-clayey-carbonate series in the upper sub-group. Pegmatites have the greatest concentration in the lower and upper aluminous schist formations. The association between rich muscovite pegmatite veins and peraluminous (kyanite-rich) rocks exists in reality, reflecting the individual development of pegmatites in the Mama Group.

Korzhinsky (1937) established that genetic links exist between the evolution of regional metamorphism and pegmatite formation stages (prograde and retrograde). This pattern was confirmed for the first time in the practice of metallogenic analysis during evaluations of the potential for muscovite sources in the whole Baikal-Patom province by Sokolov (1970) and Velikoslavinsky et al. (1960). Table 17 synthesises all the latest data and illustrates patterns of phylogenetic and ontogenetic links in the pegmatite-forming cycle during the evolution of regional metamorphism of the Mama Group. It follows from the information in Table 17 that the pegmatite-forming cycle was determined by the parameters of the monometamorphic cycle of the Mama Group under kyanite-sillimanite facies series conditions. Regional studies carried out in recent years by B.V. Petrov, V.A. Makrygina, S.P. Korikovskiy, V.S. Fedorovskiy, V.V. Butvin and other researchers in the Baikal Highlands confirm this point of view. At the same time, a number of workers who have studied areas of high-grade metamorphic zones in the group came to the conclusion that metamorphic evolution involved two events (M. Ye. Salye, V.N. Podkovyrov), thereby reviving A.N. Neyelov's views.

The overall muscovite content in a regional sense owes its origin exclusively to the Chuya-Mama block, where all the economic deposits are concentrated. It is separated

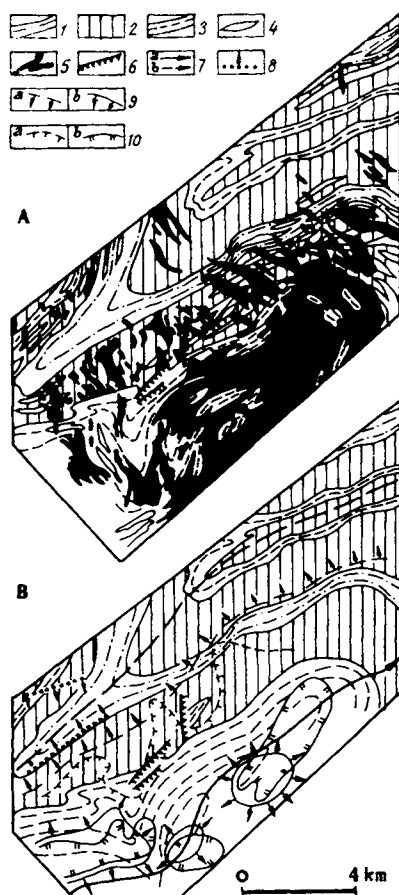


Fig. 150. Geological map (A) and sketch of zoning (B) for Bolsheversky pegmatite field (Butvin, 1988). 1 – ky-gt-musc-bt gneiss, 2 – grey gneiss, quartzite, marble, 3 – ky gneiss, 4 – group I granites & pegmatites, 5 – group II granites & pegmatites, 6 – faults, 7 – structural axes: a – Bolsheversky antiform, b – Gremuchin synform; zone elements: 8 – metamorphic-metasomatic stage, zones 1/2 transition, 9 – magmatic stage, a – zones 2/3 transition, b – zones 1/2 transition, 10 – post-magmatic stage, a – muscovite for electronics, b – coarse pegmatitic muscovite.

from the uneconomic Chuya–Chaya block by the sillimanite isograd surface and from the Angara–Patom block by a large jump in the appearance of huge masses of vein granites and aplites. Economic muscovite mineralization formed in stages, in accordance with retrograde metamorphic processes. In group I pegmatites (plagioclase–quartz–biotite), muscovite (so-called joint muscovite) replaces biotite and (or) is associated with quartz (pine-needle, wedge-shaped muscovite). In group II pegmatites, muscovite is present as a quartz–muscovite replacement assemblage, formed during feldspar hydrolysis (first-generation muscovite according to V.D. Nikitin) or metasomatic–pegmatitic muscovite, associated with giant feldspar and quartz blocks (second-generation muscovite according to V.D. Nikitin). Muscovitization of pegmatite veins

Table 17

Genetic association between mineral assemblages of a metamorphic cycle and zonal metamorphism of the Mama Group and isofacies vein formations (after Yu.M. Sokolov)

Subfacies	Main metamorphic mineral assemblages		Degree of migmatization & granitization	Degree of crystallinity; intensity of retrograde metamorphism	Vein formation: main mineral assemblages in vein rocks	Potential evaluation of formation		
	quartz-feldspar pelites	calcic and basic				degree of recrystallization of pegmatites and intensity of retrograde metamorphism	Productivity of useful mineral resource	
<b>CHLORITE ISOGRAD</b>								
chlorite-sericite (pre-biotite)	sericite + chlorite + quartz (± opaque miner, albite <sub>0 5</sub> , calcite)	epidote + chlorite + quartz + actinolite (± albite <sub>1 9</sub> , opaque miner, calcite)		Finely banded phyllites, schists, meta-sandstones, effusives; graphite-rich matrix	Quartz, quartz-albite, carbonate veins, concretions (Qtz, Ser, Chl, Ep, Ab, Ms, Tur, Sd). Sulphides: pyrite, chalcopyrite, galena, sphalerite, grey copper ores, pyrrhotite, pentlandite, arsenopyrite, cubanite		Quartz-vein formation, initial qz-vein crystal, gold-ore mineralization of Lena province: gold-quartz & gold-sulphide formations	
<b>BIOTITE ISOGRAD</b>								
biotite-chlorite (biotite)	biotite + sericite + chlorite + quartz (± albite <sub>5 11</sub> , opaque miner, calcite); chloritoid + sericite + chlorite + quartz (± albite, opaque miner)	epidote + chlorite + quartz + actinolite (± albite <sub>1 9</sub> , opaque miner, calcite)			Sulphides in veinlets, elongate pods, disseminations			
<b>GARNET ISOGRAD</b>								
(pyrope = 5.7%, spessartine = 6.55% in metapelites)								
almandine-chlorite-chloritoid	chloritoid + kyanite + garnet; garnet + biotite + albite <sub>5 11</sub>	amphibole + epidote + albite <sub>3 7</sub> + quartz (± biotite, ores,					Mainly porphyroblastic; ground-mass noticeably	Quartz veins, quartz veins with kyanite and actinolite

+ quartz ± muscovite; garnet + kyanite + staurolite + biotite + quartz + plagioclase

carbonate); amphibole + actinolite + plagioclase

recrystallized; gradual decrease in graphitic matter

**PLAGIOCLASE (18% ANORTHITE) ISOGRAD**  
(pyrope = 10.5%, spessartine = 2.75% in metapelites)

staurolite-chloritoid

garnet + kyanite + staurolite + Pl<sub>28-35</sub> + quartz (± Ms)

amphibole + epidote + Pl<sub>20-12</sub> + quartz (garnet, biotite)

Quartz-feldspar, pegmatite-like veins with green muscovite

Initial pegmatite formation

**ISOGRAD MARKING APPEARANCE OF PEGMATITES, ANATECTITES & ALKALI METASOMATISM**

kyanite-biotite-muscovite (staurolite-biotite-kyanite-Ms)

Bt + Pl + Qtz; Grt + Bt + Pl + Qtz; Grt + St + Bt + Pl + Qtz; Grt + Ky + Bt + Pl + Qtz; Grt + Ky + St + Pl + Qtz; Grt + Ky + St + Pl + Bt + Qtz; ± Ms; Pl<sub>19 48</sub>

Grt + Bt + Pl + Sep + Qtz + calcite; Grt + Amph + Pl + Qtz; Di + Amph + Pl + Qtz ± Ms

Small amount of migmatization, rare granite-gneiss (migmatitic) domes

Total recrystallization of matrix; coarsely banded schists & gneisses dominate; strong graphitization

Strong retrograde metamorphism (muscovitization). Complete recrystallization series in pegmatites. Mainly in Chuya-Mama block of groups I and II pegs; in Angara-Patom block, group II

Orthometamorphic formations; muscovite, graphite, talc. Muscovite-rich zones in pegmatitic veins, with economic concentrations of high-quality muscovite

**SILLIMANITE ISOGRAD**  
(pyrope = 14.5%, spessartine = 1.7% in metapelites)

sillimanite-biotite-garnet-orthoclase

Sil + Bt + Pl + Mc + Qtz; Sil + Grt + Bt + Pl + Qtz; Sil + Ky + Bt + Pl + Qtz ± Ms

Pl + Amph; Qtz + Pl + Amph; Qtz + Pl + Ky + Amph; Qtz + Pl + En + Grt + Amph

High degree of migmatization, metamorphic rocks preserved as unstable relicts ("scyaliths")

Quartz-feldspar pegmatites, initial muscovite-rich pegmatite formation

Low degree of retrograde metamorphism (muscovitization) of metamorphic rocks (Chuya-Chaya block). Mainly group I pegmatites

Ceramic and low muscovite pegmatite formation. Muscovite bearing zones rare, low-grade muscovite, closely associated with magnetite, hence uneconomic

took place in a single event corresponding to the amphibolite facies retrograde metamorphic stage. Morphological features of pegmatite veins in the different structural-facies zones, their dimensions, structural settings and the distribution of muscovite zones within them are illustrated in the summary table (Table 17), compiled by V.N. Chesnokov and O.N. Fillipov, and require no elaboration.

### 2.8. *Ceramic pegmatites*

*The Chuya ceramic pegmatite zone* is situated within the Chuya–Vitim zone of anticlinal upwarps in the Baikal fold belt, located mainly in the Chuya ancient basement inlier. Field evidence suggests that the pegmatites fall into two age groups.

1) The oldest pegmatites in the Baikal fold belt are those of the quartz–feldspar (ceramic) pegmatite formation, located within the Chuya–Vitim granulite–gneiss zone, occupying a band stretching from the right bank of the river Vitim (Yazovago river basin) to the watershed between the rivers Malaya (Lesser) Chuya and Chaya. These pegmatites are associated with porphyroblastic biotite, biotite–microcline–plagioclase and muscovite–plagioclase granites and gneissose granites. They are contemporaneous with the folding of the Chuya assemblage (synkinematic) non-replaced migmatitic pegmatites, emplaced during ultrametamorphism when metamorphic differentiation was taking place with weakly-developed anatexis (biotite pegmatites according to V.A. Makrygina, 1981). In this context, metasomatic processes are restricted in them, and only occasionally is it possible to find rare deformed and ribbon-like muscovite crystals 2–3 cm across.

2) The next group of pegmatites in age belong to the quartz–feldspar formation and are also found in the granulite–gneiss zone (left bank of the river Chuya in the area between its two tributaries, the rivers Tyksha and Pravaya (Right) Bramya). These pegmatites are very different from the previous ones: a) they form both single veins and swarms of large pegmatitic bodies in the Mama Group; b) they have a typical vein shape with sharp contacts and contain mainly hypidiomorphic textural varieties of rocks, evidence that they formed from a melt; c) collective recrystallization in initial metasomatic manifestations is widely developed in the pegmatites; and finally d) recrystallization is always found in them, genetically related to the kinematics of the tectonometamorphic cycle of Mama Group time, evidence for an early Precambrian age. Genetic relations of pegmatites are determined by regional metamorphism of the Chuya Group at amphibolite facies PT conditions, kyanite–sillimanite type. The isotopic age of pegmatites in these groups has been determined only by the K–Ar method on micas, and varies from 1.92 to 2.16 Ga and evidently reflects only an upper age limit for these rocks.

### 2.9. *Chrysotile–asbestos*

At present there is only one chrysotile–asbestos deposit known in the Baikal–Patom fold terrain, the Molodyozhnoye, which is distinctive in terms of the reserves and high quality of the resource.

*The Molodyozhnoye chrysotile–asbestos deposit* occurs in northern Buryatiya within the Baikal–Vitim eugeosynclinal zone of the Baikal fold belt. Asbestos-bearing ultra-

basic rocks were discovered in this region in 1957 by A.A. Malyshev during survey work to produce 1: 200,000 scale geological maps. The Molodyozhnoye deposit was discovered in 1958–59 during investigations of these occurrences by the Buryat Geological Survey.

The deposit belongs to the cross-fibre chrysotile–asbestos formational type in dunite–harzburgite rocks (Rundqvist, 1986) of the Bazhenov sub-type, distinguished by the extremely high fibrous asbestos content, and uniquely rich in textile varieties. Ore-bearing alpine-type ultramafics in the Param intrusive complex form part of the Baikal–Vitim structural–formational complex, which several authors consider to be an Early Proterozoic greenstone belt (Dobrzhinetskaya, 1985) or a proto-ophiolitic belt (Dobretsov, 1982). Intrusions in the Param complex are controlled by the NW-striking Kilyan tectonic zone which can be followed for over 150 km, forming the Anye–Kilyan ultramafic belt (Zamanshchikov et al., 1966). There are no age constraints for the ultramafics in the Param complex. Bashta (1974) considers that the intrusions originated in the Lower Proterozoic and they were finally emplaced as igneous bodies during the interval from the Lower to Upper Proterozoic or Lower Palaeozoic. Dobrzhinetskaya (1985) considers the Param ultramafics to be Early Proterozoic protrusions, emplaced in the final shearing stage of the Baikal–Vitim greenstone belt. A close similarity has been noted between these ultramafics and those in Phanerozoic ophiolite terrains, and with oceanic varieties.

The asbestos-bearing Molodyozhny massif is located in the centre of the mafic–ultramafic belt in the collision zone between supracrustal rocks in an Early Proterozoic downwarp and Archaean gneisses of the Muya microcraton. It extends for over 5 km in a NW direction, with a maximum width of 0.55 km and is a sheeted intrusion, perfectly concordant with the trend of linear folds affecting Lower Proterozoic Kilyan assemblage volcanosedimentary rocks. The massif consists mainly of harzburgite and dunite. As a result of hydrothermal alteration, primary rocks have been converted to serpentinites of various compositions: lizardite, chrysotile–lizardite, chrysotile–antigorite–lizardite, brucite–chrysotile–lizardite, antigorite, etc. In addition, carbonitization and listvenitization are widespread. The asbestos deposit has an elliptical shape, and is restricted to the thickest, central part of the intrusion. Its maximum thickness is 489 m and it can be followed for 768 m, along a NW strike, conformable with the general orientation of the intrusion. The structural setting of the deposit is controlled by NW-striking zones at the margins of the intrusion. It has a concentric zoned structure (Fig. 151), resulting from the regular alternation of zones with different asbestos types from the centre to the edges of the mineral deposit (Bashta, 1970; Tatarinov and Artemov, 1967). The richest and highest quality ores occur in a zone of simple splay veins, distinguished by the high content of long-fibre, high-quality asbestos, and in a “large net” zone containing the highest concentration of rocks with asbestos fibres. Zoning in the deposit is also enhanced by differences in the mineral composition of the ores. Chrysotile and fine-grained serpentine typify serpentinite at the core, zones of simple splay veins, and large and fine networks. Serpentinites in zones of network and oriented cross-fractures, as well as fine networks at the edge of the deposit are represented mainly by lizardite. Intensely sheared serpentinites most often consist of antigorite (Zamanshchikov et al., 1966).

The formation of the deposit involved two distinct phases (Bashta, 1970; Tatarinov and Artemov, 1967). The first was a phase of autometamorphic serpentinization of the intrusive rocks, the extent of serpentinization increasing from the edge to the centre of the intrusion. The second, essentially productive, phase due to subsequent metamorphic processes, created the chrysotile–asbestos mineral deposit. Superimposed metamorphic effects are seen more intensely at the intrusion margins. According to Bashta (1970) the concentric zoning results from two processes coinciding – uniform tectonic flattening and late serpentinization. The first process caused fracturing to occur more intensely at the edges of the massif, and the formation of the asbestos deposit is related to late serpentinization. The source of the solutions which were responsible for the late serpentinization and associated asbestos formation is completely unknown. Some authors (Tatarinov and Artemov, 1967) connect them with a buried granitic intrusion. The presence of granite is established by the presence of the Kachoy granite–porphyry dyke complex, hosted in the immediate outer contact zone of the Molodyozhnoye massif. Others (Bashta, 1970) do not rule out a connection between late serpentinization and fluids with a metamorphic origin.

#### 2.10. *Decorative stones*

*The Param nephrite deposit* is associated with the Param ultrabasic igneous intrusion, in the Baikal–Vitim eugeosynclinal zone of the Baikal fold belt. The Param intrusion is a rootless lenticular body 22 km long with a maximum width of 4 km. According to Dobrzhinetskaya (1985), it is a typical example of mantle peridotite, harzburgite subtype, emplaced into a volcanosedimentary complex by a protrusive route under the control of strike-slip deformation in the final shearing stage of the Baikal–Vitim eugeosynclinal zone. The massif has a zoned structure (Gurulev et al., 1973), the centre being made of serpentinized harzburgites, in which lenticular and sheeted, sometimes branching, dunite bodies are seen, usually very weakly serpentinized. The extent of serpentinization increases towards the contacts, and serpentinized dunites and harzburgites give way to patchy serpentinites.

The Param nephrite deposit is restricted to the western contact between the intrusion and a sheeted amphibolite body, a constituent of the Lower Proterozoic host volcanosedimentary assemblage. Epidote and tremolite metasomatic rocks crop out at the contact between the serpentinite mass and the amphibolites. Nephrite mineralization is hosted in tremolitic rocks occurring between epidiosites, developed at the expense of amphibolites and serpentinites (Fig. 152). Metasomatic zoning is seen in the contact zone. A 20 cm wide zone of epidotized rocks is developed near the immediate contact with amphibolites, which themselves are intensely sheared and chloritized. Closer towards the serpentinites, a 50 cm wide zone of tremolitic rocks can be followed, and these in turn grade into a 1.5 m wide nephrite body. The nephrite in the Param deposit is a dense, massive, crypto-crystalline rock. Polished slabs vary in colour from deep-green to grass-green, in places moss-green due to chlorite impurities. The nephrite consists of an aggregate of fine, short tremolite fibres, creating a disoriented texture. According to Gurulev and Shagzhiyeva (1973), this is a contact-metasomatic deposit, evidence being metasomatic zoning in rocks at the contact. An important factor in the

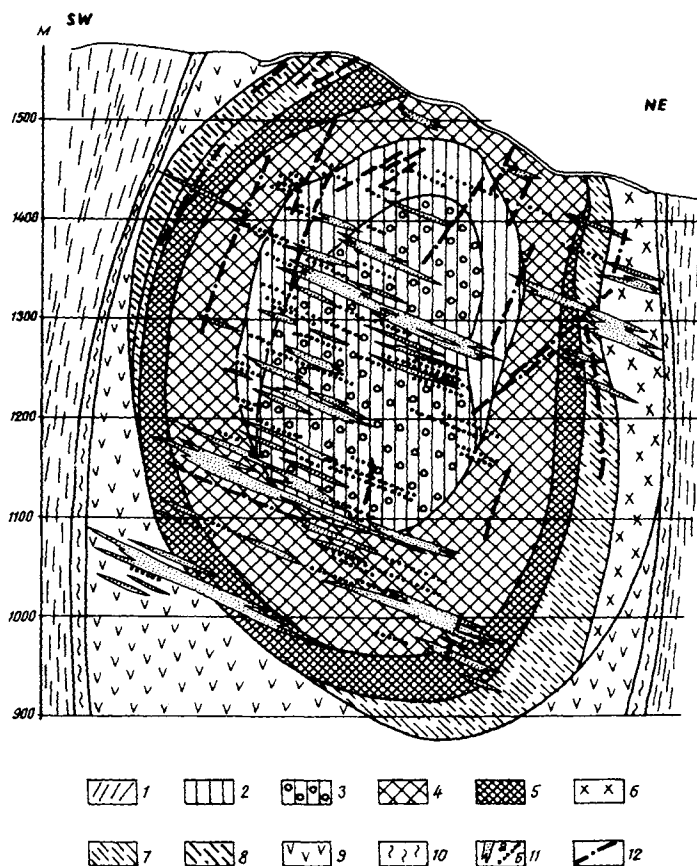


Fig. 151. Geological section of Molodyozhnoye chrysotile-asbestos deposit (simplified from Bashta, 1970). 1 – Kilyan schists ( $R_3$ ), 2, 3 – serpentized harzburgite. 4 – serpentinite with large asbestos nets, 5 – with fine asbestos nets, 6 – marginal serpentinite with oriented asbestos veins, 8 – asbestos cross-cuts, 9 – roughly foliated serpentinite, 10 – intensely foliated serpentinite, 11 – apodunite serpentinite, a – large bodies, b – small bodies, 12 – faults & shear zones.

lithological control of nephrite mineralization is the presence of basic rocks, amphibolites, amongst the original rocks, for it is precisely the amphibolites which predetermined the development of metasomatic zoning, thereby creating favourable conditions for nephrite formation.

Occurrences of decorative cordierite are located within the Chuya–Vitim zone of anticlinal basement highs of the Baikal fold belt. They were discovered by Sizykh (1985) in the basin of the rivers Ukuchikta, Kutima and Abchada. The occurrences, in shear zones, are associated with quartz–cordierite–muscovite metasomatites which most probably formed during a retrograde metamorphic event, in an acid leaching stage, evidence being the paragenetic association of quartz with cordierite. A productive strip of cordierite-rich rocks 4–6 km broad can be traced for some considerable distance and shear zones within it are sometimes as much as 900 m wide. Dimensions of

quartz–cordierite segregations in which pale lilac and pale green transparent cordierite occurs as a semi-precious raw material, vary from 5 to 50 cm across, 10–15 cm on average. Semi-precious cordierite deposits are typically ortho-metamorphic and appear to be related to the second regional metamorphic event in the Chuya–Vitim granulite–gneiss zone. An extreme figure for the isotopic age of zircon from these rocks is 2.26 Ga (Pb–Pb method).

*Decorative lazulite occurrences*, including economic accumulations, were discovered by Lobach-Zhuchenko (1953) in the watershed between the left tributaries of the Bolshaya (Greater) Chuya and the rivers Baragda and Sosnovka, within the Chuya–Vitim zone of anticlinorial upwarps. Lazulite mineralization is restricted to a magnetite–kyanite–chloritoid schist horizon, consisting of interleaved muscovite–kyanite, kyanite–chloritoid, magnetite–chloritoid and chloritoid schists. Lazulite occurs as an accessory mineral together with garnet, tourmaline and apatite, distributed evenly throughout kyanite-rich rocks, high in alumina and iron. Lazulite occurrences and minor economic accumulations are found in quartz–lazulite veins up to 50–60 cm wide in chloritoid schists. Lazulite in the veins has an indigo-blue colour, forming crystalline aggregates up to 10–15 cm in diameter. Other minerals in the veins include albite, sericite, apatite, garnet, amphibole, clinopyroxene and aegirine. Lazulite in metamorphic rocks is usually associated with peraluminous schists with a particular geochemical signature and forms during prograde regional metamorphism, hence it is an ortho-metamorphic mineral. Occurrences are known in Armenia, Kazakhstan, Polar Urals, Pre-Baikal region and North Carolina, USA.

### 3. Conclusions

As has already been pointed out, the history of the geological development of the Baikal–Patom fold terrain is exceptionally complicated and is characterised by polycyclic evolution over a huge time interval from Archaean to Cenozoic. The oldest Archaean stage is quite indistinct. At present, outcrops of the ancient basement are found only in Archaean crustal blocks in the Chuya–Vitim zone of the Early Proterozoic Baikal fold belt. Archaean crustal relicts in basement blocks are represented by a complex of schists, quartzites and gneisses, metamorphosed under granulite facies conditions, compositionally similar to Archaean complexes in adjacent terrains. Associated with the Archaean stage are a few uneconomic mineral deposits. These are metamorphic graphite and manganese occurrences, hosted in Olkhon Group carbonate rocks, also ceramic pegmatites in the Chuya zone (this does not rule out the possibility that they may have formed in connection with an Early Proterozoic crust-forming event).

The two main crust-forming events in the Proterozoic of the region were Early Proterozoic (Svecofennian) and Late Riphean (Baikalian). During the first, the Baikalian protogeosynclinal fold belt formed, with its various structural–formational zones which have very different metallogenic signatures. In the Baikal–Vitim eu-geosynclinal zone which is dominated by proto-ophiolitic complexes and some island arc complexes, practically all known mineralization is associated with alpine-type ul-

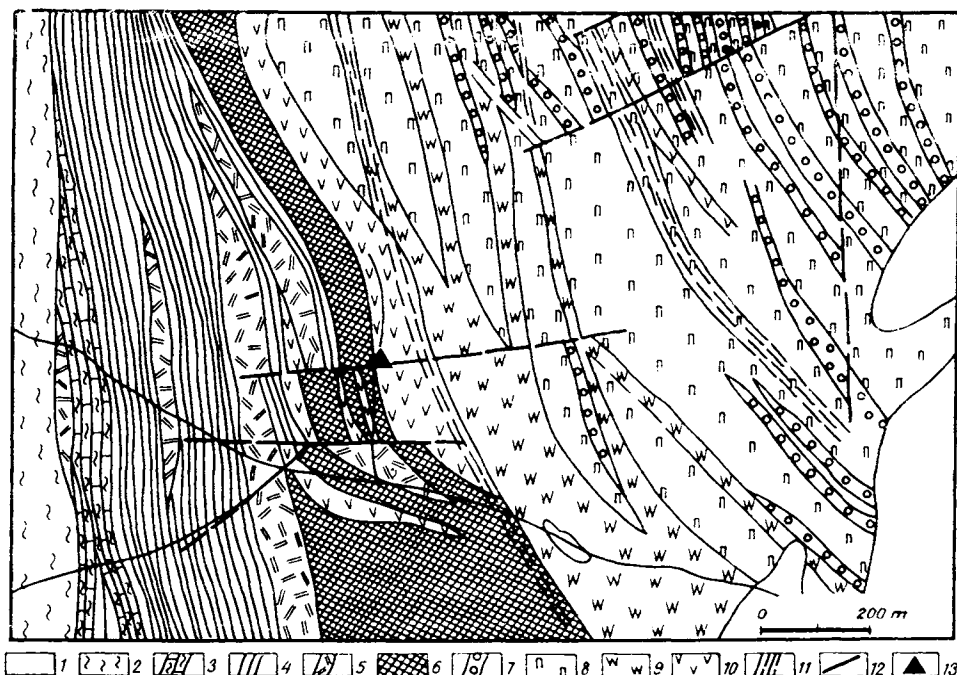


Fig. 152. Geological sketch showing structure of Param nephrite deposit. 1 – alluvium, 2–6 Ra Kilyan volcanosed. unit; 2 – chl schist, 3 – carb-chl schist, 4 – graphite seri schist, 5 – metalavas, 6 – ortho-amphib; 7–10 Param ultramafics, 7 – dunite, 8 – peridotite, 9 – patchy serpentinite, 10 – intensely sheared serpentinite; 11 – shear zones; 12 – fault lines; 13 – Param nephrite deposit.

tramafrics in the Baikal–Muya ultramafic belt. Most interest attaches to the Molodyozhnoye chrysotile–asbestos deposit. All other ore targets have no economic importance at present. The Akitkan continental margin volcanoplutonic belt concludes the development of the Early Proterozoic proto-geosyncline. Numerous rare-metal, tin, tungsten, fluorite, polymetals and gold occurrences belonging to various genetic types are associated with granitic intrusions and volcanics in this zone, but there are no economic ore targets.

The most productive stage in the history of the region was the Upper Riphean. During this stage, the Olokit riftogene depression originated with its black shale complex and the associated huge Kholodninskoye massive sulphide–polymetallic deposit. Copper–nickel sulphide mineralization is associated with the Dovyren layered intrusion. Consolidated structures in the Early Proterozoic fold terrain, especially blocks which were consolidated early, were affected by igneous processes, resulting in the formation of sub-volcanic and volcanoplutonic granitic complexes, with associated tin mineralization – the Mokhovoye deposit and the Tuyukan ore region. In its NE continuation, the Olokit riftogene depression merges with the Bodaibo intracratonic basin, which also has an Upper Riphean age. A black shale succession in the Bodaibo basin hosts the large-scale gold mineralization of the Lena gold-bearing region.

The next important metallogenic epoch in this territory was the Hercynian. Emplacement of large volumes of rare-metal granites, the Konkudero–Makan complex, took place during Hercynian tectonomagmatic events, as well as the Synnyr complex of central-type alkali intrusions with their huge reserves of potash and alumina raw materials. During this period in the Mama Zone there was intense folding and kyanite–sillimanite type regional metamorphism, emplacement of the Mama–Oron gneissose granite complex, and formation of muscovite pegmatites on a gigantic scale. Regional metamorphism and granite-forming processes were responsible for a new pulse of gold mineralization in the Lena gold-bearing region. Rare-metal quartz–amazonite metasomatites and pegmatites formed during this period in the Davan–Abchada shear zone.

**Section 4:**

Platform cover of the Siberian Craton

This Page Intentionally Left Blank

## Tectonic evolution and metallogeny

A.K. ZAPOLNOV

The Precambrian part of the platform cover of the Siberian craton is considered in this work to be in the Upper Proterozoic – Riphean and Vendian (Yudomian). Riphean sediments form the lower or palaeo-cratonic cover assemblage. Vendian (at least Upper Vendian) sediments then form the upper, platform assemblage.

In many ways, the palaeocratonic assemblage of the Siberian craton differs substantially from the corresponding assemblage of the Russian craton. The Riphean cover on the Siberian plate, especially the north, has many products of repeated volcanism. A significant number of Riphean dykes, grouped into regularly-oriented swarms, have been mapped in the Aldan Shield, and particularly within the Anabar massif. Highly explosive basic magmas have left their imprint on the significant content of redeposited volcanoclastic material in terrigenous clastic successions. Another specific feature is the set of tectonic structures, composed of various Riphean subdivisions. This feature is underlined by the fact that, unlike the Russian craton, the Siberian is almost totally covered by Middle and Upper Riphean sediments, except for some marginal areas in the E and SW. Against this background, Riphean sediments form negative and positive structural forms, which grade smoothly into one another, and with definite similarities to structural forms of the platform cover (synclises and antclises). Specific formational and structural features of the palaeocratonic assemblage of the Siberian craton also determine its metallogenic signature. The Riphean is richer in metal ores here than in the Russian craton, especially on the W, SW and E margins (Table 18).

Across the Siberian craton as a whole, the complete cycle of arcogenesis occurred, as for the Russian craton, although less vigorously in Siberia. This may be explained by much less activity in the Early Proterozoic of the epi-Archaean craton compared with the East European craton and a correspondingly greater degree of consolidation by the beginning of the Riphean. Nevertheless, during the palaeocratonic (Riphean) period, it is possible to see the same three main phases in the evolution of the craton as are seen on the Russian craton, although somewhat provisionally. However, the relative importance of each of these phases is essentially different here, and so the set of tectonic structures is correspondingly different also.

The initial stage of arcogenesis encompasses the first half of the Early Riphean. During this time, an arch-type geostructure with clearly-expressed asymmetry formed on the site of the stabilized craton. Highest amplitudes on this upwarp were displaced towards the NE half of the arch and were compensated by the initiation and formation

Table 18

## Mineral deposits in the cover of the Siberian craton

Useful component	Ore formation	Age	Tectonic setting	Ore deposits, occurrences
Iron	Limonite-hematite in quartz sandstones	R <sub>1</sub> , Gonam Fm	Uchur basin	Numerous minor occurrences
Iron	Limonite-hematite in quartz sandstones	R <sub>2</sub> , Talyn Fm, Totta Fm	Maya basin	Numerous minor occurrences
Iron	Siderite-limonite and chamosite-hematite in sandy-clayey seds	R <sub>3</sub> , Lakhanda Group	Maya basin	Numerous minor occurrences
Iron	Hematite, clastic terrigenous	R <sub>3</sub> , Oslyan Group	Pre-Yenisey pericratonic basin*	Lower Angara, Ishimbinskoye, Udorong and many occurrences
Iron-titanium-vanadium	Titano-magnetite in ultrabasic rocks		Aldan Shield	Minor occurrences in Kondera, Inagli & other intrusions
Manganese	Weathered mantle (pyrolusite-psilomelane)	Carbonates of Sukhoy Pit (R <sub>2</sub> ) & Tungusik (R <sub>3</sub> ) groups	Pre-Yenisey pericratonic basin*	Gremyachinskoye, Nizhneye (Lower), & other occurrences
Manganese-iron	Hausmanite-hematite in sandstones and conglomerates	R <sub>2</sub> , Tagul Fm (Karagas Group)	Pre-Sayan pericratonic basin	Arshan occurrence
Manganese	Weathered mantle (psilomelane)	R <sub>2</sub> , Tagul Fm (Karagas Group)	Pre-Sayan pericratonic basin	Nikolayevskoye, Shangulezh
Manganese	Manganiferous clastic terrigenous	R <sub>2</sub> , Unguokhtakh Formation	Udzha intracratonic basin	Tomtor occurrence
Lead-zinc	Galena-sphalerite in sandstones	R <sub>1</sub> , Mukun Group	Kotuy Fomichev graben	Kotuykan occurrence
Lead	Galena in quartzose sandstones	R <sub>2</sub> , Golousten Formation	Pre-Baikal pericratonic basin	Minor occurrences
Lead-zinc	Stratiform fluorite-sphalerite-galena in dolomites	Golousten (R <sub>2</sub> ) and Uluntuy (R <sub>3</sub> ) formations	Pre-Baikal pericratonic basin	Tabor, Khibelen, Lugovoye & others
Lead-zinc	Stratiform galena-sphalerite in dolomites	V <sub>1</sub> , Sardana Formation	Yudoma-Maya basin	Sardana, Uruy, Perevalnoye and many occurrences

Lead-zinc	Galena-sphalerite in dolomites	V, Staraya Rechka Fm	West Anabar monocline	Numerous minor occurrences
Lead-zinc-copper	Pyrite-chalcopyrite-sphalerite-galena in clastic terrigenous-carbonate sediments	V, Sukharikha Formation	Turukhan basin	Numerous minor occurrences
Copper	Cupraceous sandstones	V, Izluchinskaya Formation	Turukhan basin	Numerous minor occurrences
Copper	Cupraceous sandstones	V, Taseyevo Group	Pre-Yenisey basin	Numerous minor occurrences
Copper	Cupraceous sandstones	V, Ushakov Formation	Pre-Baikal basin	Numerous minor occurrences
Copper	Cupraceous sandstones	V, Oselok Group	Pre-Sayan basin	Numerous minor occurrences
Magnesite, talc	Talc-magnesite	Aladyino (R <sub>2</sub> ) & Potoskuy (R <sub>3</sub> ) shale & dolomite	Pre-Yenisey pericratonic basin*	Kirgitey
Phlogopite	Magnetite-phlogopite in alkali ultrabasic rocks	V <sub>1</sub>	Aldan Shield	Minor occurrences in Kondera, Chada & other intrusions
Phosphorite	Phosphatic clastic terrigenous	R <sub>2</sub> , Uluntuy Formation	Pre-Baikal pericratonic basin	Minor occurrences
Phosphorite	Phosphatic clastic terrigenous	R <sub>3</sub> , Ipsit and Techn Fms (Karagas Group)	Pre-Sayan pericratonic basin	Minor occurrences
Bauxite	Weathered mantle on dolomite	After Tsipanda Group (R <sub>2</sub> ) dolomites	Yudoma-Maya pericratonic basin	Gornostil & other occurrences
Bauxite	Weathered mantle on dolomite	After Golousten Group (R <sub>2</sub> ) dolomites	Pre-Baikal pericratonic basin	Minor occurrences

\*Many authors consider the Pre-Yenisey to be an external (pre-cratonic) zone of the Yenisey miogeosyncline. In this book, mineral deposits in the Pre-Yenisey peri-craton are described in the section on the Baikal Yenisey marginal inlier.

of a chain of linear pericratonic depressions along its northern and eastern margins. An additional structural complexity in the north was a radial system of major fractures, along which deep basins (grabens) developed – Kyutungda, Udzha, Kotuy–Fomichev. The deposition of continental redbeds was strictly localized in these structures, the only exception being the initiation at this time of the extensive Uchur basin on the southern margin of the craton, and filled with littoral-facies clastic terrigenous sediments (the Gonam Fm). Sediments in the Uchur basin are amagmatic. Lavas (mainly alkali–basic) and silica–alkali pyroclastics play a negligible role overall in the pericratonic basins and grabens in the north of the craton.

Prospects of finding economic concentrations of metals in sediments of this stage are extremely slim. The presence of finely disseminated ore minerals in the carbonate cement of sandstones in the Kotuy–Fomichev graben and the general appearance of minerals such as pyrite, galena, sphalerite and cinnabar in the heavy fraction of rocks is hardly grounds for hoping to discover economic deposits owing to the absence of a limestone–dolomite unit in the succession – a lithological factor in the location of stratiform deposits of this type. Many iron ore deposits of sedimentary origin are known in the Uchur basin.

The next stage, the aulacogenic stage proper, is very clearly expressed in the Russian craton, less so in the Siberian. The less distinctive block structure of the crystalline basement did not facilitate the formation of an interconnected network of aulacogens. At present only the Urinsky and Irkineyevsky aulacogens can be identified with any certainty in the Siberian craton, and the complex Kempendyay and Ygyattin graben system and associated Suntar horst. Thick carbonate–clastic terrigenous and volcanoterrigenous, mainly green-coloured, and carbonaceous assemblages accumulated here in an actively developing trough during the Middle Riphean. At the end of the aulacogenic stage (in pre-Valyukhtin time), 30–100 m thick basic sills were intruded. Valyukhtin Group sediments (end Middle Riphean), transgressing far beyond the edges of the Urinsky trough, marked the transition to the next, concluding, stage in the formation of the palaeocratonic assemblage.

Over most of the Siberian craton, the transition to this concluding stage occurred much earlier, from the second half of the Early Riphean. Overall, this stage is characterized by a gradual collapse of the whole cratonic mega-arch. This took place unevenly, as on the Russian craton, since it is possible to identify two or three sub-stages in the process. During the first (second half of the Early Riphean), there was only some “overlapping” of sedimentary assemblages beyond the edges of radial basins and a simultaneous change from continental redbeds to grey clastic terrigenous–carbonate sediments, and from alkali–basic to basic in the composition of volcanics.

During the second sub-stage (from the Middle Riphean), there was further settling of the craton. Sedimentation extends sharply beyond the edges of the Early Riphean basins, with the formation of a discontinuous sedimentary cover of clastic terrigenous–carbonate and carbonate composition. However, in many cases the maximum thicknesses coincide spatially with previous basins.

Also from the Middle Riphean, second generation pericratonic basins became established along the S, W and NE margins of the craton, a phenomenon unknown on the Russian craton. The main concentrations of useful minerals in this stage are

associated with precisely these second generation pericratonic basins. A number of stratiform Pb–Zn and Pb ore deposits and occurrences are hosted in Middle Riphean sediments in the Pre-Baikal basin. Sedimentary occurrences of Mn and Fe–Mn (Pre-Sayan and Pre-Yenisey basins), phosphorites (Pre-Baikal, Pre-Sayan basins), as well as weathered mantle deposits (manganese, bauxite) are known in pericratonic Middle and Upper Riphean sediments. Various non-metallic mineral occurrences are also found in these sediments. For example, hydrothermal–metasomatic magnesite and talc deposits are restricted to deep fault zones in the Pre-Yenisey basin. They are hosted in dolomites at the top of the Middle Riphean (Aladyin Fm) and base of the Upper Riphean (Potoskuy Fm).

Carbonate and clastic terrigenous-carbonate basinal sediments of this stage are relatively less metalliferous. Known occurrences are also spatially restricted here to earlier depressions or to their rims. For example, geographically associated with the Yudoma–Maya basin are massive and oolitic sedimentary limonite–hematite and chamosite–siderite ores (deposits in the Aimchan and Lakhanda Groups in the Maya basin, and in the Totta Group on the Omnya basement high), also bauxites and zinc occurrences. Manganese occurrences are found in the region of the Udzha basin.

The development of this sedimentary stage concludes with the formation at end Riphean–early Vendian (?) of sedimentary groups containing evident molassic deposits. These sediments mainly crop out around the craton edges, especially in pericratonic basin regions, where orogenic-type compensatory basins formed in the concluding stage of their development. As a rule, the succession in these basins is two-fold. The lower part, not always present, consists of variegated clastic terrigenous or terrigenous-carbonate sediments (Kandyk Fm of the Uy Group, Oslyanka Group and correlates). Continental redbeds dominate the upper part of the succession (Taseyeva Group, Ushakovka Fm and correlates).

Iron mineralization is associated with the variegated part of the succession in the Pre-Yenisey basin, where economic hematite ore deposits and occurrences are hosted at the base of the Oslyanka Group. Copper mineralization occurs amongst redbeds. The copper concentration increases in lateral transition zones from redbeds to variegated formations (the Taseyeva Group in the Pre-Yenisey basin, Izluchina Fm in the Turukhan basin, upper horizons of the Uy Group in the Yudoma–Maya basin, the Ushakovka Fm in the Pre-Baikal basin, Oselok Group in the Pre-Sayan basin, and others).

Activation of basins which originated in the Early Riphean also occurred in this time interval, with the appearance of basic–ultrabasic magmatism in the Udzha basin region (the Tomtor and Bogdo intrusions), the Pre-Verkhoyan basin (established geophysically), and the Yudoma–Maya basin. Iron–titanium mineralization, apatite ores and phlogopite pegmatites are associated with intrusions in the last case. Iceland spar occurrences are associated with hydrothermal calcite veins in the Anabar massif, probably also at the same time. Thus, the productivity of Riphean sediments shows an overall increase in the transition from one stage to the next, and is particularly clear in the transition to the latest palaeocratonic period, more especially its final stage, when alkali–ultrabasic magmatism appeared.

Beginning from the late Vendian (possibly the start of the Vendian in SE regions), a new platform period in the development of the Siberian craton was established. The

main propelling force for this development were oscillatory epeirogenic movements, regulating repeated alternations of transgressions and regressions. Most important in Vendian mineral genesis were polymetallic ores, with a predominantly zinc signature. Economic stratiform Pb–Zn deposits are known in the region of the Yudoma–Maya Riphean basin (the Sardana ore belt). Numerous small galena and sphalerite occurrences are also known in the north of the craton, in the Staraya Rechka Fm on the western slopes of the Anabar massif and in Manykay dolomites (?L. Cambrian) on the eastern slopes. Sphalerite and galena in the Turukhan basin region (Sukharikha Fm) are associated with copper minerals – chalcopyrite, bornite and chalcocite. Finally, in sediments transitional between U. Vendian and L. Cambrian (Manykay Fm, Variegated Fm) there are the oldest phosphate horizons in the platform sedimentary cover.

## *1. Mineral deposits and occurrences*

### *1.1. Manganese*

*Manganese deposits of the Lower Uda ore region.* The Lower Uda group of numerous small manganese deposits and occurrences is hosted in Riphean sediments of the Pre-Sayan pericratonic basin on the SW margin of the Siberian craton. Here the Riphean succession consists of continental redbeds and carbonate sediments belonging to the Karagassky Group (R<sub>2</sub>–R<sub>3</sub>) and grey clastic terrigenous sediments of the Oselok Group (R<sub>3</sub>–Kudash?). Formations in the Karagassky Group are, from the base upwards, Shangulezh, Tegul, Ipsit and Techin. Higher manganese concentrations are restricted exclusively to the base of the Tagul (Inzan) Fm. Host rocks are shallow marine arkosic sandstones and siltstones, giving way at the base of the formation to coarser clastic varieties. There is a very gentle overall dip to the SW. Most mineral occurrences are concentrated on the SW limb of the extensive and very gentle Uvat dome-like basement high, where the ore-bearing member can be traced for 30 km.

In addition to oxidized (secondary) ores, this region is also known for its accumulations of weakly metamorphosed primary oxide ores, which may have formed in the Precambrian (Late Riphean). Primary manganese oxide ores have been found in the Arshan occurrence (Demchenko et al., 1967; Suslov et al., 1967). Here, a lenticular ore body measuring 0.9 m thick by 130 m long has been mapped in sandstone and small pebbly conglomerate horizons. Ore texture is coarsely- or finely-banded. The ores are often shot through with thin baryte, calcite and other veinlets. Ore minerals fill the spaces between angular dolomite and quartz fragments in clastic rocks, as aggregates of small isometric grains, or else they form conformable veinlet-type ore laminae as aggregates of elongate crystals. The main ore mineral is hausmanite, and braunite is secondary; other manganese minerals being rhodochrosite (several generations), manganocalcite and friedelite. Calcite, baryte and antigorite are the main gangue minerals. The manganese content in the ores is up to 45%.

Primary manganese oxide deposition took place in shallow marine conditions, which frequently alternated with draining of the area. Confirmation that coastal marine sediments and initial ore material were syngenetic lies in the almost total lack of

any signs that the clastic material has been replaced by a cementing ore aggregate. The action of hydrothermal solutions had an effect on the subsequent transformation of primary manganese concentrations in addition to diagenetic and initial metamorphic processes. Particular evidence for this are veinlet structures, the paragenetic association of hausmanite and antigorite, and the presence of friedelite. This last fact suggests a possible link between hydrothermal activity (with chlorine influx) and the intrusion of diabase sills and dykes – the Nersin complex – into the Karagassky Group.

Primary iron and phosphorus concentrations are also hosted in the Karagassky coastal marine sediments. Hematite ores are somewhat separate from manganese. Either they are interbedded with manganese ores, as in the Arshan occurrence, or else they replace them upwards in the succession. Phosphorite-rich horizons belong at the very top of the Karagassky Group, in the Ipsit Fm and the base of the Techin Fm.

The oxidized (secondary) ore deposits and occurrences which predominate in the region are also hosted in Tagul Fm sediments (Nikolayevskoye, Shangulezh, Kettskoye and others). The ore deposits belong to the residual and residual–infiltration types. Manganese and ferro-manganese ores are restricted to a chemical weathered mantle on sandy–dolomitic sediments. The weathered mantle is up to 170 m thick, with a 20–30 m thick productive member at the base. Mineral types are psilomelane, psilomelane–pyrolusite and psilomelane–vernadite ores. The manganese grade of these ores is up to 45–50%.

Ore horizons are bedded. Economic grade ore clusters are unevenly spaced, irregularly shaped and restricted to local joint zones in the host sediments. Mineralization can be followed downdip to depths of 400–500 m. Most rocks are disintegrated arkosic sandstones with a dolomite cement and with clastic dolomite interbeds, showing weak primary manganese mineralization. Ore structures are varied, especially in the manganese cap, and include massive, concretionary, conchoidal–botryoidal, earthy, sooty, and others. Common textures are cemented, collomorphic, granular, columnar–acicular, etc. Main ore minerals are psilomelane (cryptomelane), pyrolusite, vernadite, hollandite; secondary – manganite and various iron hydroxides. The age of ore formation has not been determined, but the weathered mantle seems to have originated in the Cenozoic.

## 1.2. Lead and Zinc

*The Pre-Baikal pericratonic basin.* This basin runs along the NW shore of Lake Baikal as a narrow strip (maximum width 25–30 km) as far as the river Chara, separated by transverse highs into a chain of local basins. From S to N these are Buguldey, Iliktin and Ulkan. The total length of the basin is around 1700 km. The succession in the Pre-Baikal pericratonic basin includes the Middle Riphean Goloustnaya and Uluntuy Formations and Upper Riphean Kachergat Fm. These are succeeded above an erosion surface by the Vendian Ushakov Fm conglomerates and greywackes. The lower part of the Goloustnaya Fm consists of quartz sandstones with thin siltstone and dolomite intercalations. The top of the Goloustnaya Fm and the Uluntuy Fm are clastic terrigenous–carbonate formations: organic and chemical limestone and dolomite, interbedded with siltstone and clayey shales. Sandstone, siltstone and shale are then found

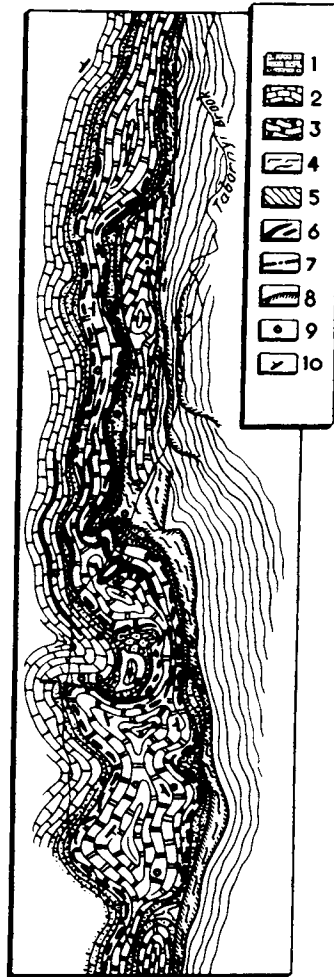


Fig. 153. Tabor deposit (Tychinsky et al., 1977). 1 – Uluntuy siltstone, dolomite; 2–5 Golousten Gp. 2– banded lst, 3 – dolomite, 4 – talc rock. 5 – variegated siltstone etc.; 6 – ore bodies; 7 – zone of mylonites, boudinage, crushing; 8 – thrusts; 9 – boreholes; 10 – bedding.

in the overlying Kachergat Fm. Riphean sediments in the Buguldey and Ilikin basins are up to 3 km thick, of which the clastic terrigenous–carbonate formation is about a third. Disseminated and vein-disseminated galena and galena–sphalerite ores are found throughout the peri-cratonic basin (Ruchkin, 1984; Malich et al., 1987).

In addition to polymetallic ores, Goloustnaya and Uluntuy sediments also host bauxite and phosphorite occurrences. At the base of the Goloustnaya Fm there are two horizons of redeposited chemical weathered mantle on a dolomite surface. Bauxite bodies in karstic palaeo-relief depressions are up to 0.5 m thick. In the area of the Anga high (between the Buguldey and Ilikin depressions), the Uluntuy Fm has several thin

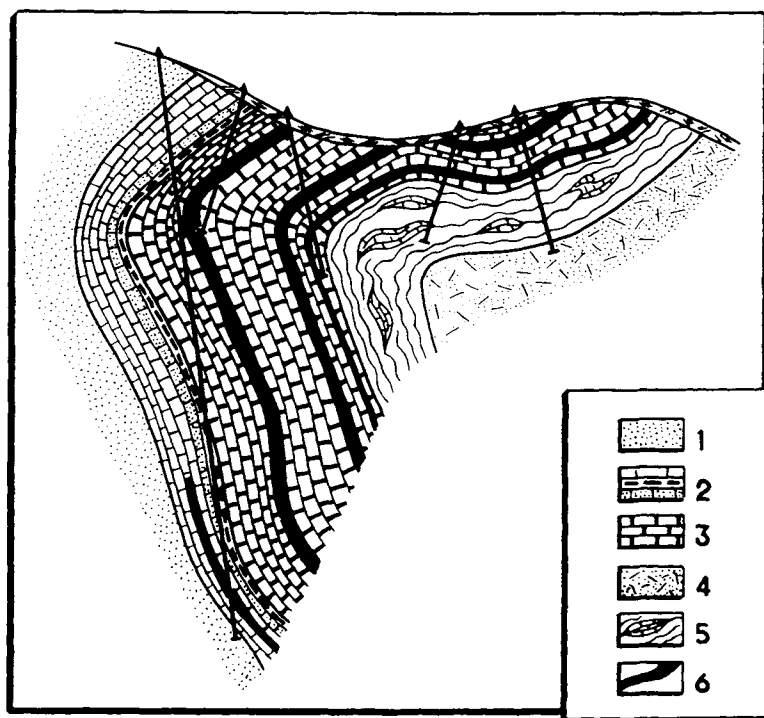


Fig. 154. Geological section of Tabor deposit (Ruchkin, 1984). 1 – Kachergat siltstones; 2 – Uluntuy carbonates; 3–5 Golousten Gp, 3 – 1st, dolomite, 4 – siltstone, 5 – talc-carb rock; 6 – ore bodies.

monophosphate horizons up to 1.5–2 m thick, containing 35–40%  $P_2O_5$  and carbonate-silica, clayey and sandy phosphorites with up to 33%  $P_2O_5$ .

The lower quartzose sandstone part of the Goloustnaya Fm hosts galena mineralization, but not at economic grade. The ores are disseminated and cavity-disseminated, the main ore minerals being galena and pyrite, with chalcopyrite and tetrahedrite as secondary minerals. The horizon hosting the ore is no more than 5–10 m thick. Greatest interest in the Pre-Baikal pericratonic basin attaches to economic reserves of galena-sphalerite and fluorite-sphalerite ore types. These deposits are hosted in a clastic terrigenous-carbonate member forming the upper part of the Goloustnaya Fm and the Uluntuy Fm. They belong to the lead-zinc ore formation in carbonate rocks. E.I. Kutuyev (in Rundqvist, 1986) classifies them as Barvin type – lead-zinc often with baryte and fluorite in a bedded karstic carbonate formation. A type deposit for this classification is the Tabornoye deposit, described in detail by Ruchkin (1984).

*The Tabor deposit* is located in the Ilikin depression. The main ore bodies are hosted in the upper carbonate member of the Goloustnaya Fm (Figs. 153, 154), in dolomitized limestone horizons. One ore body is hosted in talc-rich carbonates and pure talc rocks. The deposit occurs in a steep monocline, closer to the surface of a complex elongate box-fold with an amplitude of 200–250 m. Faults are generally

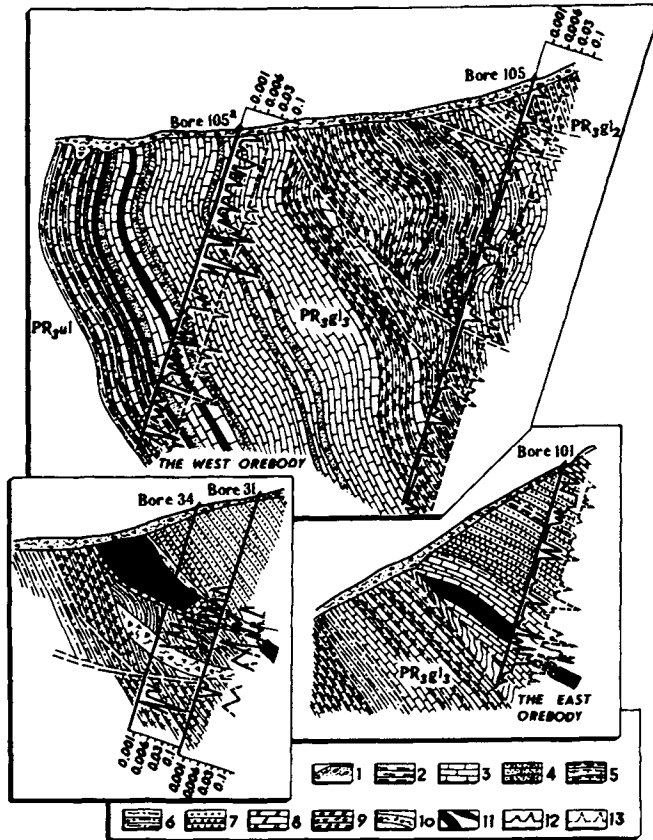


Fig. 155. Geological sections along exploration traverses, Khibelen deposit (Tychinsky et al., 1977). 1 – Quaternary, 2 – shale, 3 – lst, 4 – oolitic lst, 5 – talc rock, 6 – siltstone, 7 – argillite, 8 – dolomite, 9 – sands & grits, 10 – crush zones, 11 – ore bodies (a – E, b – W), 12–13 point–furrow sampling of Pb (12) and Zn (13) contents (spectral analysis).

conformable with the layering of the rocks. Shear zones along which talc-rich rocks are developed may have an ore-controlling role.

Ore bodies are tabular and as a rule conformable with host dolomitized limestones. They can be followed for several hundred m along strike. Contacts are indistinct, and the ores are vein-disseminations. However, massive ores are found in shear zones, giving way sharply to banded ores at the contact, due to alternating sphalerite, fluorite and silicified limestone bands. Ore textures are granular and metacolloidal. Metasomatic alteration structures and textures are also widespread. Subsequent dynamo-metamorphism related to late folds has caused bending of ore mineral crystals and the development of gneissose textures. Sphalerite and galena are the main ore minerals. pyrite and arsenopyrite are secondary, while chalcopyrite, grey copper ores, boulangerite, bismuthite, cassiterite, etc. are rare. Gangue minerals are fluorite, quartz, dolomite, calcite, ankerite and others. Cadmium is present in the ores as an impurity.



Fig. 156. Geological sketch of central part of Yudoma–Maya basin (simplified from Ruchkin et al., 1977). 1 – Riphean, 2 – Vendian (Yudomian), 3 – Camb., 4 – undiff. Palaeoz., 5 – Jurassic, 6 – basic ig rocks, 7 – faults, 8 – outline of Bas–Dukat palaeo-upwarp, 9 – Pb–Zn occurrences, 10 Sardana ore region. Anticlines: Yu – Yurkanda, K – Kurunga, Ch – Chagda. Synclines: S – Sardana, B – Byttakh. Faults: G – Guvindin, Che – Chelat.

Wall rock alterations in the host are expressed as ankeritization, dolomitization, fluoritization, silicification and calcitization. Homogenization studies of fluid inclusions in fluorite crystals indicate high ore-forming temperatures, in the range 150–350°C. It is assumed that primary lead and zinc concentrations which formed during sedimentation and subsequent katagenesis became involved in the hydrothermal–metasomatic process. The Khibelen, Lugovoye and other deposits belong to this type, as well as the Tabor (Fig. 155).

A different type of ore deposit and occurrence (e.g. Novo–Anay) is characterised by the absence of wall rock alteration, banded structure, and often metacolloidal and oncolitic textures. These features, together with low ore-forming temperatures (70–140°C), and great continuity of host beds (up to 10 km), suggest that this type of

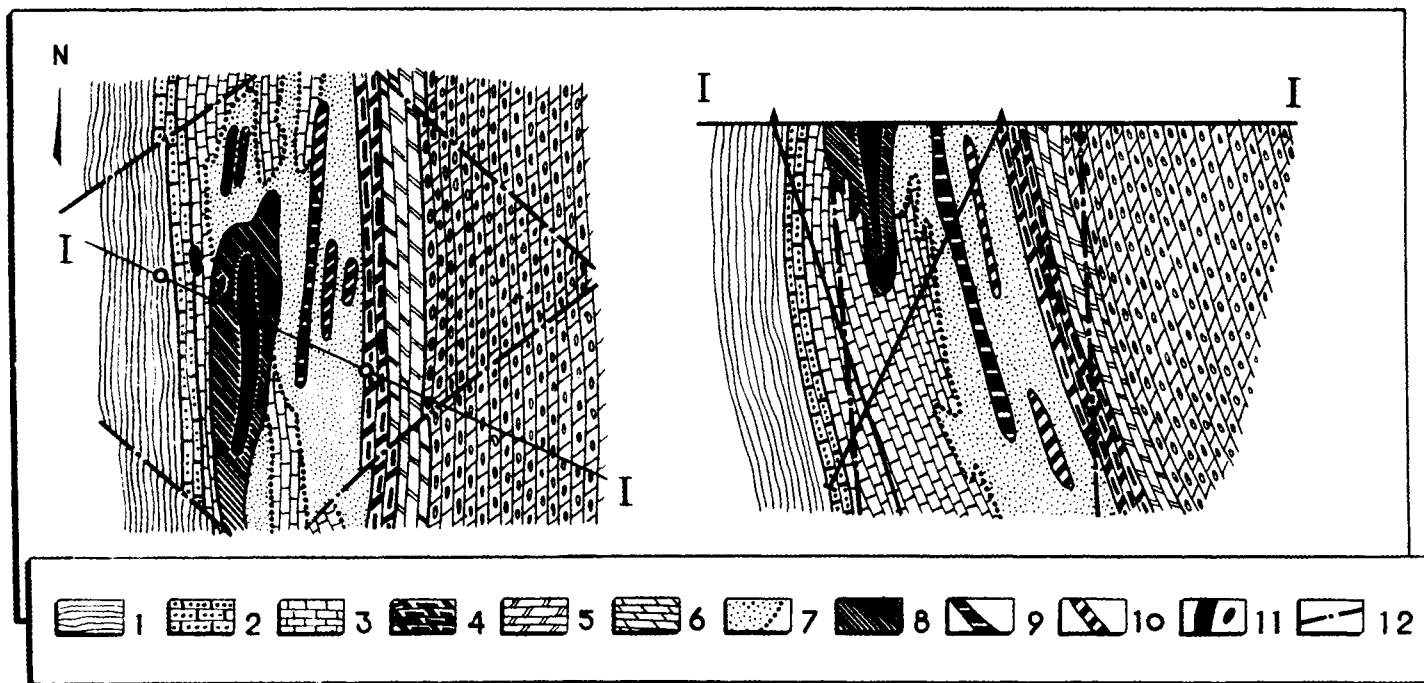


Fig. 157. Geological map and section, Sardana deposit (Ruchkin et al., 1977). L. Camb.: 1 - Inikan shale, 2 - Ist; Vendian (Yudomian): 3-5 Sardana G: 3 - Ist, 4 - bituminous dolomite & Ist, 5 - fine-grained dolomite, 6 - Yukanda Ist; 7 - metasomatic dolomite. Ore zones: 8 - upper level, 9 - middle level, 10 - lower level; 11 - ore bodies; 12 - faults.

deposit had already been completely formed at the stage of katagenesis. The isotopic composition of ore lead is highly anomalous (J-type) and close to that in Mississippi Valley-type lead-zinc deposits, for which an epigenetic origin has been clearly established. However, a number of workers consider the Pre-Baikal basin lead-zinc ores to be syngenetic, but underwent subsequent alteration during diagenesis, katagenesis and regional metamorphism.

*Lead-zinc deposits of the Sardana ore region.* The lead-zinc deposits of Sardana, Uruy, Perevalnoye, and numerous minor occurrences making up the Sardana ore region are hosted in Yudomian carbonate successions overlying Riphean sediments in the Yudoma-Maya pericratonic basin on the SE of the Siberian craton. The biggest deposit in the region is the Sardana, discovered in 1971. The following description of the ore region is based on Ruchkin et al. (1977). The contemporary structural plan of the region was created as the result of numerous tectonic reworking events. Thickness distribution points to synsedimentary fold formation. However, the growth of linear folds with clearly expressed asymmetry on the limbs and a regional system of N-S thrust-nappes belong to the Cretaceous and are synchronous with the development of the Mesozoic Verkhoyan fold system.

The largest fault zones in this ore region are the Guvinda in the west and the Chelat in the east (Fig. 156). Folds mapped in the region include the Yurkanda, narrow crestal Kurunga and Chagda anticlines, separated by the Sardana and Byttakh synclines. Western synclinal limbs dip at 20–40°, eastern limbs are steep to overturned. The Sardana syncline is complicated by additional minor folds, and synclinal cores are filled with Yudomian (Vendian) and Cambrian sediments. Synclines narrow southwards or are pinched out completely in response to the growth immediately to the SW of the extensive Sardana palaeo-uplift. Yudomian deposits in this region are divided into the Yukanda (lower) and Sardana (upper) formations, separated by stratigraphic unconformities. The Sardana Fm consists of carbonate rocks (the Yudomian type section, according to Semikhatov and Serebryakov, 1983). There are three members, from the base upwards: fine- and coarse-grained dolomite; dark bituminous dolomite and limestone (marker horizon); fine-grained bedded limestone and dolomite. The formation is 120–130 m thick. Lower Cambrian variegated glauconitic limestone lies above an obvious unconformity (with erosion).

Lead-zinc mineralization is hosted in all three members of the Sardana Fm, although the main economic grades are concentrated in the top member, where ore bodies occur at three levels. Host horizons are from a few to 20–30 m thick. Relative to bedding, the ore bodies occupy a conformable or gently cross-cutting position (Fig. 157). All the main ore bodies are hosted in steep eastern synclinal limbs. The actual position of any one specific ore body is determined by low-displacement faults: brecciation zones within beds, with which ores are directly associated, and local NE-striking faults bounding the ore bodies. Host rocks are saccharoidal dolomites with well-formed grains, which form lenticular bodies a few tens of m thick and from a few tens of m to 1 km long. Dolomite bodies hosting the ores are surrounded by a limestone halo 0.5–5 m wide, with intense vein-type dolomitization. The metasomatic nature of host dolomites is confirmed by the presence of relict limestone inclusions with diffuse outlines.

Ore bodies at various stratigraphic levels in the upper member have different shapes: pillar-like (with average thickness-to-length ratio 1 : 10) in the top level, tabular (1 : 30) in the middle level, and ribbon-like (from 1 : 200 to 1 : 100) in the bottom level. As a general rule, the ore bodies have sharp boundaries. They also wedge out sharply, accompanied in places by nests and pockets of monomineralic galena, up to half a metre across.

Economic ore grades relate to essentially sphalerite, sphalerite–galena and galena–sphalerite types. Secondary minerals are pyrite, marcasite, arsenopyrite, smithsonite, cerussite and anglesite, while dolomite and calcite are the main gangue minerals. The lead to zinc ratio for different deposits ranges from 1 : 2 to 1 : 10. The ores also contain germanium and silver. The ore deposits formed in three stages: pyrite–sphalerite, galena–sphalerite, and dolomite–calcite. Mineral assemblages in the pyrite–sphalerite stage (dolomite–pyrite–marcasite, dolomite–sphalerite, pyrite–marcasite–arsenopyrite) have negligible distribution. The dolomite–sphalerite assemblage may form pillar-like monomineralic ore deposits in the top ore horizon. Sphalerite segregations typically display a fine-grained texture. Metasomatic structures are common.

The mineral assemblage in the galena–sphalerite stage forms the main mass of economic ore deposits which are hosted in all three levels where mineralization is developed, and they have different shapes at each level. Ores are vein-disseminated, and also occur as separate lenses and nests as far as the earliest fine-grained sphalerite ores are concerned. Cocarde and crustification textures are also common. Sphalerite is represented by allotriomorphic aggregates, with pyrite disseminations. Galena aggregates are concentrated in sub-parallel laminae amongst “zebra dolomites” (zones of internal brecciation), and also amongst earlier fine-grained sphalerite. In addition to the major ore minerals, the assemblage also contains antimony and arsenic sulphosalts, pyrite, plus dolomite and calcite. Finally, the mineral assemblage in the dolomite–calcite stage is also widespread, accompanying ore bodies, but not forming independent economic ore segregations. As well as calcite and dolomite, the assemblage also contains antraxolite, sphalerite and galena. There are also solitary quartz veinlets, as well as quartz crystals in cavities where late dolomite veins have been leached.

Overall, the lead–zinc mineralization in the Sardana ore region has features of both syngenetic and epigenetic origin. Mineralization is clearly associated with a particular stratigraphic horizon, which maintains a constant lithological composition and thickness. An important role in the location of economic deposits is undoubtedly syndimentary structures, both folding and faulting, including a deep-seated zone that evolved over a long period and controlled facies changes (types of succession) immediately NW of the ore region. Finally, syn-sedimentary textures such as brecciation are seen in the ore bodies. At the same time, the metasomatic nature of the ores is confirmed by facts such as the presence of metasomatic dolomite relicts in the ores, replacement textures of dolomite by early sphalerite, rapid lateral wedging-out of ore bodies, and tectonic control by a network of low-displacement faults. Studies based on isotope thermometry and fluid inclusion homogenization temperatures in sphalerite, dolomite and calcite indicate high temperatures of ore formation in the pyrite–sphalerite stage (200–220°C) and galena–sphalerite stage (260–360°C). During the galena–sphalerite stage there was almost total recrystallization of early pyrite and

sphalerite ores, accompanied by their frequent redeposition with the formation of vein-type ores. The frequent redeposition of lead–zinc ores occurred later, in the third stage, initiating late dispersed dissemination.

Isotopic studies of ore lead, relating to crypto-anomalous J-type lead, do not provide a definitive answer to the question of the age of the ore mineralization. The presence of mid-Palaeozoic gabbro–diabase dykes in the Uruy deposit defines the upper age boundary for the ore formation. Ore deposits in the Sardana region belong to the lead–zinc ore formation in carbonate rocks. E.I. Kutyrev (in Rundqvist, 1986) defines them as an independent Sardana type of lead–zinc deposit in a karstic–carbonate riftogene formation.

This Page Intentionally Left Blank

## **Part III**

### **Patterns of minerals deposit evolution in precambrian structures**

This Page Intentionally Left Blank

## Evolutionary patterns of mineral deposits in precambrian terrains

A. M. LARIN, S. I. TURCHENKO and D.V. RUNDQVIST

The type examples of the varied mineral deposits in Precambrian terrains examined in the present work broadly define the features of the ore content in Precambrian tectonic structures on two ancient cratons. The sequence in which tectonic structures and rock complexes replace one another in time often continues in such a fashion that later structures inherit features of earlier-formed structures. Therefore, the ore content in the identified structures reflects not only the actual situation in each tectonic structure in Precambrian terrains, but also the entire sequence of geological processes – from the time at which the structure had finally formed as a type structure up to the last events affecting it, i.e. its evolutionary (“retrospective” according to Kosygin (1988)) character. An important problem in metallogenic research relates to the time at which Precambrian deposits formed. Attempts at solving this have a long history in Russia, and results are considered in works by Bilibina et al. (1984), Sokolov and Kratz (1984), Rundqvist and Sokolov (1986), among others. When analysing the problem of the time of formation of mineral deposits in crustal structures, we inevitably have to address the issue that many deposits formed in a partially discrete manner. Precambrian deposits very often have a much more complex nature, possessing features of polygenetic–polychronous mineral deposits. These features are due, as a rule, to the complex polycyclic history of the geological evolution of most Precambrian terrains, during which there was frequent reworking, remobilization and removal of ore material often from different sources. Primary disseminated concentrations and stratiform deposits were transformed into metamorphic and metamorphosed deposits as a result of regional and contact metamorphic effects or retrogression. Against this background, rich ores could have formed, as well as the impoverishment or even destruction of primary ores. In some cases when similar processes have acted over a long period, they may adopt features of newly-formed hydrothermal–metasomatic deposits of different types. Such deposits would then have been forming for tens or hundreds of millions of years. This is particularly true for ferruginous quartzite deposits, some types of pegmatite deposit, iron, phlogopite and apatite deposits in magnesian skarn formations, gold ore, massive sulphide and other deposits. Rundqvist and Sokolov (1986) have observed in this connection that even for deposits whose history of formation has stretched out over hundreds of millions of years, the actual ore-forming processes themselves are short-lived and correspond to separate pulses, with reworking pulses being mainly associated with metamorphic and igneous peaks in subsequent cycles. It is these particular features in Precambrian ore genesis which complicate the metallogenic

periodicity in the Precambrian – the identification of metallogenic epochs and pulses. In this work, the term “metallogenic epoch” follows the definition by Yu.A. Bilibin, V.I. Smirnov, G.A. Tvarchrelidze and others as meaning a relatively long time interval of development, during which the complete spectrum of useful minerals forms by internal and surface processes. The term “metallogenic pulse” proposed by Sokolov and Kratz (1984), means a relatively brief time interval, characterised by a peak of mineral deposit development.

An analysis carried out on the distribution of more than 300 Precambrian mineral deposits in the former Soviet Union in different tectonic structures and of different ages has brought to light several common features in the ore content of tectonic structures and patterns of formation of Precambrian deposits with time. The time boundaries for tectonic epochs referred to in the Preface have metallogenic significance for Precambrian terrains in the former Soviet Union and allow the following metallogenic epochs to be defined:

- (1) Saamian–Aldanian, 3.4–3.0 Ga.
- (2) Rebolian, 3.0–2.6 Ga.
- (3) Seletskian, 2.5–2.35 Ga.
- (4) Svecofennian–Udokanian, 2.2–1.8 Ga.
- (5) Gothian, 1.75–1.3 Ga.
- (6) Dalslandian, 1.2–0.9 Ga.
- (7) Baikalian, 0.8–0.6 Ga.

### 1. *Archaean metallogenic epochs*

*The Katarchaean epoch* (> 3.4Ga) is fairly well represented in the ancient cratons of the southern continents, but so far has not been subjected to metallogenic evaluation in Precambrian terrains in this country due to a lack of reliable information about mineral deposits in such extremely old tectonic structures.

*The Saamian (Aldanian) metallogenic epoch* on the whole is poor in useful mineral deposits. Minor deposits and occurrences of elements in the iron group, graphite and high-alumina raw materials in two types of structure – granulite–gneiss terrains and early generations of greenstone belts – are the main types (Fig. 158, 159).

Granulite–gneiss terrains within the boundaries of the former USSR occur as separate blocks in the shield areas of the East European craton and occupy extensive areas in the shields of the Siberian craton. Examples of this type of structure in the East European craton include the Central Kola block and the Korva–Kolvitsa zone in the Baltic Shield, and similar formations in the Ukrainian Shield are present in the Podolsk, West Azov and, in part, the Volyn blocks. Distinct from this, the shields in the Siberian craton consist mainly of this type of structure. Here, granulite–gneiss terrains make up almost the entire Aldan Shield, the Chara block in the Olyokma terrain and blocks in the Anabar Shield.

Granulite–gneiss terrains typically contain eulysite-type iron ore mineralization, represented by two-pyroxene magnetite schists and magnetite quartzite, forming lenses and laminae in mafic granulites. Mineralization of a similar nature is common in Early

Archaean complexes that make up the Zvelev Group in the Sutam, Kholodninsk and Larbin iron ore regions in the south of the West Aldan block; a constituent of the Daldya and Upper Anabar groups in the Anabar Shield; and also within the Tipton Group in the East Aldan block. Two-pyroxene–magnetite schist lenses and bodies and associated ferruginous quartzites are known at the base of the Kola gneisses (Shonguy–Volshpakh zone, Simbozero and Pinkeljavr deposits) on the Kola Peninsula; with the Volyn–Podolian and Pre-Azov blocks in the Ukrainian Shield; and in the granulite–gneiss blocks of the Pre-Sayan region (Baikal deposit).

Small-scale titanomagnetite deposits are associated with basic intrusions, altered to eclogitic rocks as a result of metamorphism, in the Angara–Kan and Biryusa microcratons in the Siberian craton. Minor chromite and Cu–Ni sulphide occurrences hosted in ultrabasic bodies are found in the Aldan and Anabar Shields. Besides uneconomic Cu–Ni sulphide mineralization in peridotite–pyroxenite–gabbro minor intrusions in relict granulite–gneiss complexes in Late Archaean granite–greenstone terrains in the Voronezh crystalline massif, the East European platform also has small deposits of these ores (the Lovnozero ore region).

Graphite, sillimanite, garnet, corundum and kyanite deposits are quite common in schists, plagioclase gneisses and quartzites in granulite–gneiss terrains. In the Aldan Shield they are mostly hosted in the Iyengra Group (the Nadezhda graphite deposit) and the Tipton Group (Dzhelinda corundum and kyanite deposit); the Archaean Khapchan Group in the Anabar Shield; and the Kitoy Group in the Sharyzhalgay microcraton in Pre-Sayan. Graphite deposits (Makharinetsk) in the kinzigite formation in the Ukrainian Shield are hosted in granulite–gneiss blocks – the Volyn–Podolian and Pre-Azov.

Granite–greenstone terrains began to form in the Siberian craton during the second half of this epoch. In the subsequent Rebolian epoch, this type of tectonic structure had already become the dominant one for both cratons. In tectonic terms, granite–greenstone terrains are subdivided into tonalite–gneiss and granite–gneiss areas, and greenstone belts. Tonalite–gneiss and granite–gneiss areas form the basement to greenstone belts and are considered to be grey gneiss complexes, forming the oldest crustal segments with an age of 3.5–3.0 Ga, and cut by granitoids of various ages (including the oldest). Petrochemically, the grey gneisses correspond to tonalite, trondhjemite, granodiorite and quartz diorite. In the Archaean cratons of the former Soviet Union, such structures are composed of tonalite and oligoclase granite (Karelia and the Kola Peninsula), also gneissose granite and granitic rocks of the Dnieper complex in the Ukrainian Shield. Similar formations have been found in the Olyokma granite–greenstone terrain within the Vitim–Aldan Shield (Drugova et al., 1985). An inherent feature of tonalite– and granite–gneiss areas is repeated granite formation, which is characterised by a change from calc-alkaline to normal granites, then highly-alkaline granites. In terms of their metallogeny, the grey gneiss complexes themselves are probably “barren”, at least there is no known mineralization in them at present.

Greenstone belts can be divided into two groups on the basis of the age and composition of their constituent formations. The first group, “old”, are 3.5–3.0 Ga old with mafic–ultramafic komatiitic–basaltic and bimodal basaltic–rhyolitic associations. Some of the greenstone belts in the Dnieper and Olyokma granite–greenstone terrains

in the Pre-Sayan region probably belong to this group. "Young" belts form the second group, with an age of 3.0–2.7 Ga and contain komatiitic and andesitic–basaltic volcanics accompanied by subsequently differentiated series (basalt–andesite–dacite–rhyolite) and clastic terrigenous assemblages. Examples are the Karelian granite–greenstone terrain (Parandovo–Tikshozero, Sumozero–Kenozero, Vedlozero–Segozero, etc.), Tersk–Allarechka and Kolmozero–Voronye on the Kola peninsula, and individual belts in the Dnieper and Kursk granite–greenstone terrains.

Typical deposits in Archaean greenstone belts are iron ore, gold ore, volcanogenic massive sulphide, copper–nickel, also rare metal–pegmatite, molybdenum–porphyry and talc–magnesite mineralization. In addition, there are differences in the ore content of greenstone belts of different ages and regions. An analysis of the distribution of different mineralization types with time for Precambrian terrains (Meyer, 1984) shows that iron and gold ore mineralization are developed in greenstone belts of any age, whereas nickel sulphide and massive sulphide deposits are mainly characteristic of young belts. It is probable that, depending on the location of greenstone belts of different age in Archaean cratons and their depth of occurrence, their ore contents will be different. However, despite differences in the metallogeny of greenstone belts, it should be noted that in all Archaean cratons, greenstone belts always have economic mineralization of one type or another. Thus, there is no doubt about the prospects of greenstone belts, and this raises the question of the intensification of reconnaissance and exploration efforts in Archaean greenstone terrains in the East European and Siberian cratons, for which mineral deposits and minor occurrences, typical for greenstone belts, are known.

The earliest generation of greenstone belts in the Olyokma block has an age of 3.23 Ga (Sm–Nd method), according to the latest unpublished data by A.A. Nemchin and V.L. Dook. The Onot greenstone belt in the Pre-Sayan region has a similar age, at 3.25 Ga approximately. Associated with these ancient greenstone belts are the earliest minor jaspilite-type banded iron formations in the Siberian craton. A typical example is the Sosnovy Bayts deposit in the Onot belt of Pre-Sayan. Iron ores in this deposit are clearly associated with metavolcanics of mainly basic composition. Here also within the Onot belt are major talc–magnesite ore deposits, which have a long and complex history of formation. In the greenstone belts of the Olyokma granite–greenstone terrain, the most prospective iron ore reserves occur in areas where younger greenstone belts crop out. It is important, though, to point out that the Early Archaean epoch has still not been studied well enough compared with subsequent epochs, as far as geology, geochronology and metallogeny are concerned.

*The Rebolian (Late Archaean) metallogenic epoch* signifies a qualitatively new stage in crustal evolution, sharply different from the previous stage both in the nature of tectonic structures and the particular features and scale at which ore-generating processes operated. This epoch differs in the widespread development of greenstone belts, while at the same time polycyclic structures begin to make their mark in the form of tectonothermally reworked belts. At the end of this period, intracratonic basins emerged as the first sub-cratonic structures in stabilized basement blocks. A much broader spectrum of useful mineral deposits is associated with the Rebolian epoch, both in genetic and formational types, as well as the range of ore components. Major

economic deposits appear in both cratons for the first time. Besides the extremely large iron ore deposits in the form of ferruginous quartzites, copper–nickel sulphide and massive sulphide deposits begin to make an appearance. Moreover, essentially new types of deposit appear, such as rare-metal pegmatites, Cu–Mo, gold and others (Figs 158, 159).

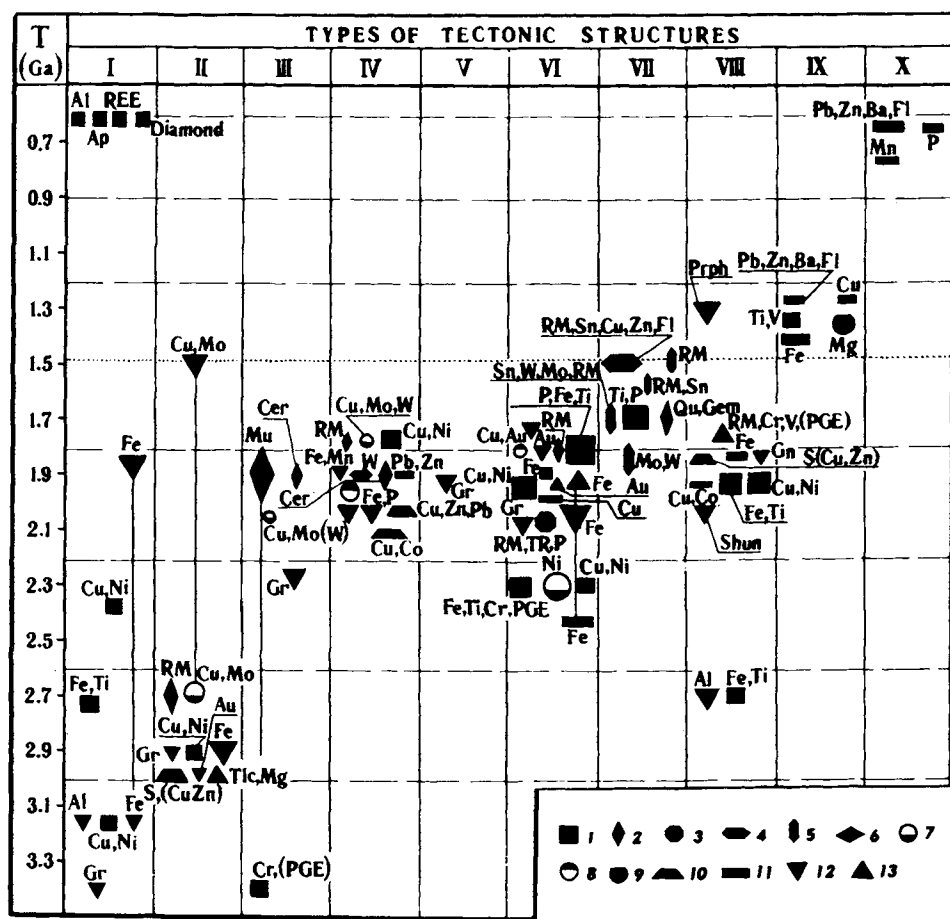


Fig. 158. Precambrian mineralization of East European craton by structure and metallogenic epoch. I – granulite–gneiss terrains, II – granite–greenstone terrains, III – reworking zones, IV – fold belts, V – intracratonic fold belts, VI – rift belts, VII – anorogenic volcanoplutonic belts, VIII – intracratonic basins, IX – pericratonic depressions, X – platform cover. Genetic mineralization types: 1 – magmatic, 2 – pegmatitic, 3 – carbonatitic, 4 – skarn, 5 – greisen, apo-granitic, 6 – alkali metasomatites in deep fault zones, 7–9 hydrothermal (7 – plutonic, 8 – volcanic, 9 – non-magmatic); 10 – massive sulphide, 11 – stratiform in seds, 12 – metamorphosed, 13 – metamorphic. Industrial minerals: Mus – muscovite, Cer – ceramics, Gr – graphite, Talc, Mag – magnesite, Fl – fluorite. Phl – phlogopite, Q – piezo-quartz, Prph – pyrophyllite, Asb – asbestos, Neph – nephrite, Sh – shungite. Size of symbol proportional to scale of mineralization.

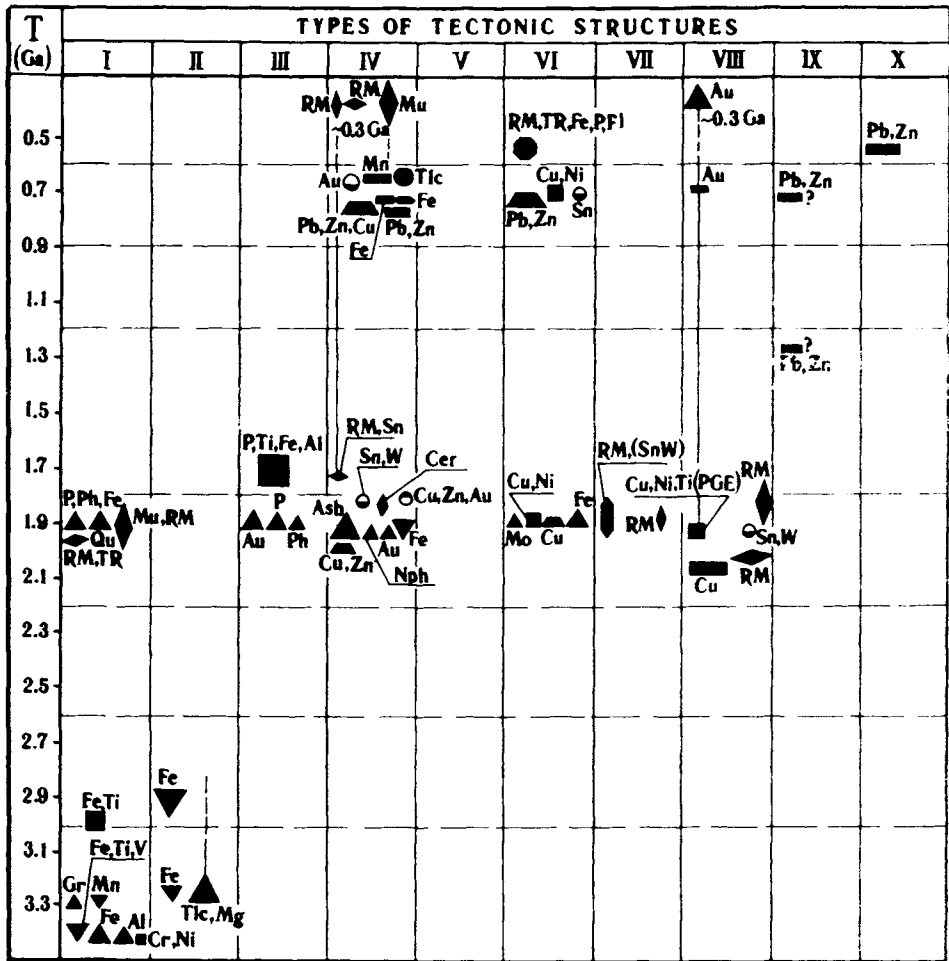


Fig. 159. Precambrian mineralization of Siberian craton. See Fig. 158 for symbols and legend.

The Late Archaean metallogenic epoch had its fullest and most intense expression in the East European craton. Ferruginous quartzite deposits in the Kostomuksha ore region formed in 3.0–2.9 Ga old greenstone belts in the Karelian granite–greenstone terrain of the Baltic Shield. Iron ores in this area are very clearly associated with a thick acid metavolcanic unit. Similar types of deposit are found in the Hautavaara and Mangin structures in Karelia, but for these ones, iron–silica–schist type mineralization is more typical. Major iron ore deposits of this type (Kostomuksha, Gimola, Bolshozero) have been discovered in the Gimola–Kostomuksha greenstone belt, while small deposits and minor occurrences are also known in the Vedlozero–Segozero and other belts. The main iron ore reserves of Karelia, amounting to hundreds of million tons of iron, are associated with this type of mineralization.

The metamorphic (hydrothermal–metasomatic) type of iron ore mineralization has a limited distribution and is represented by isolated bodies of rich hematite–magnetite ores or thin veins of pure magnetite amongst iron-rich ferruginous quartzite host rocks. The emplacement of such ore bodies is usually controlled by zones where faults of various orientations intersect. This mineralization type is known in the iron ore deposits of Karelia, the Kola Peninsula and the greenstone belts in the Kursk granite–greenstone terrain.

Massive sulphide type mineralization in noticeable amounts in greenstone belts in the basement to the East European craton is known in the Karelian granite–greenstone terrain, where it is represented by three types of deposits and occurrences: mainly massive sulphide (Hautavaara, Nyalmozero, Vediozero, Parandovo; sometimes with copper pyrites (Yalonvaara), and pyrite–polymetallic (Vozhmin) mineralization. A common feature of massive sulphide mineralization in greenstone belts is its stratiform nature and constant association with volcanosedimentary formations. Sheet-like conformable massive sulphide ore bodies belong essentially to volcanogenic (predominantly dacite–andesite and dacite–rhyolite series) and sedimentary (siliceous and black shale) associations. In many deposits the ores are metamorphosed at epidote–amphibolite and amphibolite facies and have suffered reworking accompanied by superimposed copper–nickel mineralization, and preserve textural signs of volcanogenic–chemogenic origin (banded, concretionary, globular, framboidal).

Copper–nickel sulphide deposits do not as a rule attain economic grades. The majority are hosted in meta-ultramafic sheet-like bodies in the dunite–pyroxenite–gabbro and harzburgite–olivinite formations, associated with komatiitic–tholeiitic volcanic complexes, which also contain minor Cu–Ni occurrences. The ores are usually metamorphosed and the richest mineralization belongs to the rheometamorphic type. Copper–nickel mineralization can be divided into two genetic types, depending on composition and conditions of formation: syngenetic liquation and superimposed hydrothermal–metasomatic.

Syngenetic liquation mineralization is represented by dispersed pentlandite–pyrrhotite disseminations in peridotitic komatites and sill-like ultramafic bodies. Occurrences of this type are known in the Karelian granite–greenstone terrain, where a number have been found in the Sumozero–Kenozero greenstone belt (Vozhmin, Lebyazhye). The most significant Cu–Ni deposits (Ailarechka, Vostok) and isolated occurrences are hosted in the Tersk–Ailarechka greenstone belt on the Kola Peninsula. It is important to note that although many workers consider the Ailarechka to be a liquation–magmatic deposit, it does bear signs of a metamorphic (hydrothermal–metasomatic) origin (Turchenko, 1978). A similarly complex genesis for Cu–Ni mineralization has been established in basic–ultrabasic intrusions in the Pre-Dnieper granite–greenstone terrain in the Ukrainian Shield (the Pravdin deposit).

Hydrothermal–metasomatic Cu–Ni mineralization is epigenetic in nature and mineralogically extremely varied. This is due to repeated metamorphism, leading to regeneration of primary–magmatic disseminated ores, or mobilization of ore-generating elements from ultramafic source material. Moreover, it is important to point out that mineralization in all cases is localized within ultramafic bodies which have been subjected to metamorphic–metasomatic and tectonic reworking. This type is repre-

sented by heazlewoodite (Vozhmin and Svetlozero intrusions in the Sumozero–Kenozero belt, Karelia), and polydymite–millerite mineralization (Kosinovo sector of the Kursk granite–greenstone terrain). Talc and listvenite formation in ultramafics is accompanied by pentlandite–pyrrhotite and maucherite–bravoite–pentlandite mineralization, typical for greenstone belts in the Pre-Dnieper granite–greenstone terrain, the Zolotyie Porogi and Svetlozero sectors of the Sumozero–Kenozero belt, and for the Hautavaara deposit in the Karelian granite–greenstone terrain.

Rare-metal mineralization in greenstone belts in granite–greenstone terrains on the East European craton is rarely observed. The only one of this type are rare-metal pegmatites and their host metasomatically altered gabbro–anorthosites in the Kolmozero–Voronya belt, Kola terrain. Pegmatites are associated with differentiated tourmaline–muscovite potassic granite intrusions of Late Archaean age. Although this type of mineralization has been known about for a long time, it has significance in terms of forecasting reserves in relation to the interpretation of the Kolmozero–Voronya zone as a greenstone belt, and for other structures of similar type. The same importance attaches to previously-known and newly-discovered Cu–Mo deposits (Pellapakhk in the Kola terrain), hosted in hypabyssal intrusions of the gabbro–trondhjemite association. The ores contain Ag and Au accompanying the ore constituents. These can be categorised as small- and medium-scale deposits. Minor targets also exist in the Karelia terrain, close in type to Cu–Mo deposits and with a similar age, but associated with meso-abyssal and abyssal potassic granite intrusions (Päävara, Kichany, etc.).

At the end of the Late Archaean in the Baltic Shield, the Keivy intracratonic basin was initiated, the formation of which signified the beginnings of craton stabilization and a transition to conditions typical of a sub-cratonic regime. A typical feature of this structure is the presence of thick highly aluminous kyanite schist units in the succession, which formed during the metamorphism of kaolinitic and hydromicaceous clays, and essentially siliceous metasedimentary rocks. The huge kyanite reserves in these deposits have a metamorphic origin (prograde and retrograde types). Small- and medium-scale titanomagnetite deposits with high vanadium contents formed at the margins of the Keivy structure, related to gabbro–labradorite intrusions (Tsagin, Magazin–Myusyur, Acha), while Early Proterozoic alkali granites which cut the Keivy rocks, carry rare-metal mineralization.

During the Late Archaean epoch, the Siberian craton, like the East European, is characterized by the widespread development of greenstone belts, although as was previously mentioned, these structures had already begun to form as early as the Early Archaean on the Siberian craton. In the Late Archaean then, the gigantic structure of the Dzhugdzhur–Stanovoy belt was initiated, as a zone of tectonothermal reworking. However, in its metallogenic aspect the Late Archaean epoch in the Siberian craton is more weakly expressed and differs in having a much poorer spectrum of useful minerals (Fig. 159).

In greenstone belts of the second age generation ( $\sim 2.96$  Ga), the main type of mineral deposit determining the economic significance of this type of structure are ferruginous quartzite deposits. In these ones, as distinct from the earlier generation ( $\sim 3.25$  Ga), large-scale economic deposits formed, mainly hosted in basic metavolcanics. The biggest targets in the Chara–Tokk ore region occur in the Olyokma granite–

greenstone terrain. Intense iron deposition in the ferruginous quartzite formation took place twice: at the start, during active basic volcanism, and at the end, when sedimentary rocks began to dominate. Two iron ore quartzite horizons formed as a result, which crop out in the Chara–Tokk, Tasmiyeli, Nelyukan and Khanin iron ore region. In addition, supracrustal assemblages in greenstone belts host minor occurrences of scheelite and polymetallic mineralization, while ultramafics host chromium, nickel and asbestos occurrences. Mineral deposits that usually typify granite–greenstone terrains, such as rare-metal pegmatites, Cu–Mo and porphyry–Mo, Cu–Ni sulphide, pyrites, and other types, are missing from the Siberian craton.

## 2. Proterozoic metallogenic epochs

Considerable crustal reworking took place in the Early Proterozoic, much more significant than that at the beginning of the Late Archaean. There was a sharp change in the type of tectonic movement; the entire structural plan was reassembled; changes to the internal regimes took place; and qualitatively new types of tectonic structures appeared – mainly linear rift belts, fold belts and volcanoplutonic belts. Structures initiated in the preceding epoch continued to evolve, such as intracratonic basins and belts of tectonothermal reworking. From the middle Early Proterozoic, apparently, plate tectonic mechanisms began to operate, approximately the same as now. It was from this particular period that fold belts began to form, a typical example being the Svecokarelian belt in the Baltic Shield, in which it is already possible to distinguish proto-ophiolite complexes, continental shelf and slope successions, island arc associations, and continental margin volcanic belts. Much commoner in this period were intracratonic basin type structures, reflecting a sub-cratonic regime in the most stabilized blocks. Specific structural types such as independent intracontinental volcanoplutonic belts appear from the end of the Early Proterozoic. In the Late Proterozoic, aulacogens, pericratonic basins and intracratonic fold belts also began to form. At the same time, Proterozoic structures in many cases developed as inherited Archaean structures, dating from the start of the Late Archaean. These are tectonothermally reworked belts, which in many instances (e.g. the Belomorian belt in Karelia, the Pre-Stanovoy and Dzugdzhur–Stanovoy and others) formed in a polycyclic manner and extended over an extremely long period, from the Late Archaean to the end of the Early Proterozoic, sometimes even into the Late Proterozoic.

The metallogenic style also changed sharply, beginning from the Early Proterozoic. In addition to deposits inherited from earlier epochs (banded iron formations, Cu–Ni sulphide, rare-metal pegmatites, etc.), substantially new ones also appeared: copper–nickel–pyrite, pyrite–polymetallic, lead–zinc, hydrothermal–metasomatic rare metal, rare metal–polymetallic skarns, various uranium deposits, deposits hosted in foiditic complexes, and other types (Figs 156, 157). Two metallogenic epochs are recognisable in the Early Proterozoic: the Seletskian, 2.5–2.35 Ga, and the Svecofennian (Udokanian), 2.1–1.8 Ga.

*The Seletskian metallogenic epoch* is quite clearly marked in the East European craton, and either practically does not appear or has not been recognised in the

Siberian craton. Associated with this epoch is the formation of the Earth's first typical rift systems in the continental crust. In terms of its metallogeny, the epoch does not have a rich variety of useful minerals, the main ones being elements in the siderophile-chalcophile group (Fe, Cr, Ni, Cu, Ti, V, PGE). Economic Fe-Ti-V and Cu-Ni sulphide deposits with platinoids (the Olanga group of intrusions, 2.45–2.35 Ga old in North Karelia, and the Moncha deposit on the Kola Peninsula) are hosted in basic-ultrabasic layered igneous intrusions associated with the Sumian-Sariolian rift-type belts in the Baltic Shield. In SE Karelia there is the Burakov intrusion of the same age and similar formational affinity, with Cr and Fe-Ti-V ores with platinoids, also secondary nickel silicate ores in serpentinized ultrabasic rocks. Reserves of these silicate ores with easily-extractable nickel are huge. This new type of nickel ore seems to have formed in relation to autometasomatic processes. Gold-sulphide type vein occurrences (Maya) are hosted in basic volcanics in the North Karelian rift.

Initiation of the Krivoy Rog rift system in the Ukrainian Shield, with its long, polycyclic history of development, belongs to this epoch, with the Krivoy Rog ferruginous quartzite deposits. This is an extensive linear structure, over 200 km long in a N-S direction. Within its borders, the succession comprises mainly quartz-sericite and silica-iron schists, quartzite and ferruginous quartzite and rare metavolcanics, amounting to around 6 km thick. These sediments host chlorite-magnetite, quartz-magnetite-hematite and solid magnetite ores of metamorphic origin. This does not exclude the fact that primary iron accumulation in metasedimentary assemblages in this structure had already started in this epoch and reached its culmination in the later Svecofennian epoch. A rift origin is also suggested for linear structures in the Voronezh crystalline massif containing Kursk Group sediments which host the major iron ore deposits of the Kursk Magnetic Anomaly.

*The Svecofennian (Udokanian) metallogenic epoch*, which appeared from the second half of the Early Proterozoic, is the main ore-bearing epoch for both the East European and Siberian cratons. The most genetically varied deposits formed then, similar in the range of ore formations to the Phanerozoic, but yet preserving an entire complex of deposits specific only to the Precambrian. Uniquely large-scale deposits formed during this particular epoch (Fig. 160). The Svecofennian epoch has an important role in determining the metallogenic signature of major structures in the craton basement, and is the major and most productive ore-generating epoch in the Precambrian of both cratons. The most important deposits of this epoch are ferruginous quartzites, Cu-Ni sulphides, cupraceous sandstones, iron ore and phlogopite in magnesian skarns, muscovite pegmatites, rare-metal pegmatites, rare-metal alkali metasomatites, and others. In the East European craton, the most important ore targets – ferruginous quartzites and sulphide deposits – are associated with rift-type structures, which partly inherit rift belts from the previous Seletskian epoch in their tectonic evolution. Rift-type belts as ore-hosting structures are most easily identified in the Baltic Shield. They are represented by the Pechenga-Imandra-Varzuga belt, which cuts the Kola metallogenic province in a SW direction, the Kuola-Vygozero belt, emplaced along the collision zone between the Karelian granite-greenstone terrain and the Belomorian tectonothermally reworked belt. The Krivoy Rog-Kremenchug belt in the Ukrainian Shield may be a similar type of structure.

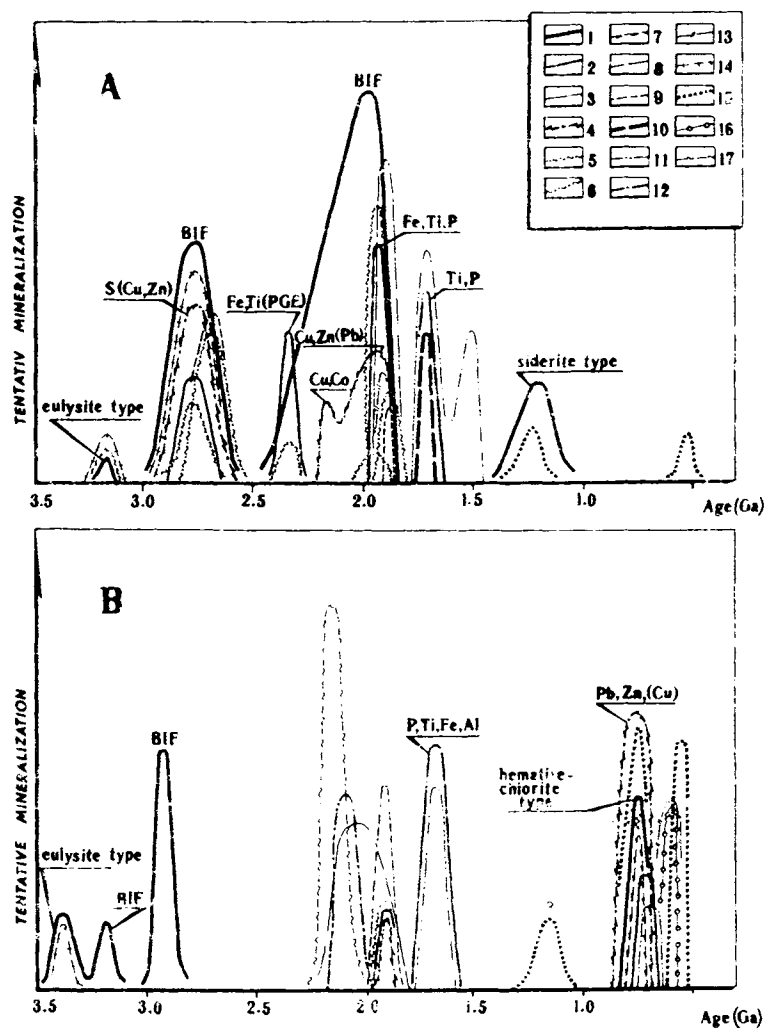


Fig. 160. Evolution of Precambrian ore formation in (A) East European and (B) Siberian cratons. Deposit types: 1 - Fe ore; 2 - Ti-Fe in basic-ultrabasic complexes; 3 - Fe, phlog. ap deposit magnesian skarns, metamorphic complexes; 4 - massive sulphide; 5 - Cu-Ni sulphides; 6 - Cu-Mo porphyry; 7 - vein gold; 8-9 - pegmatites: 8 - muscovite, 9 - rare-metal; 10 - quartz crystal; 11 - hydrothermal-rare metal deposits hosted in granites; 12 - rare metal deposits hosted in alkali metasomatites in deep fault zones; 13 - carbonatites hosting rare metals, rare earths, Fe, apatite and other deposits; 14 - high-Al; 15 - Pb-Zn stratiform in carbonates; 16 - sedi. Mn; 17 - Cu ss.

During the Svecofennian epoch, major Pechenga-type economic sulphide deposits were again associated with rift-type structures. The Pechenga-Imandra-Varzuga belt encompasses an area in the Kola terrain where Svecofennian crustal processes were operating, and includes the outcrop area of Pechenga and Varzuga supracrustal groups and the Archaean basement complex, which were subjected to Early Proterozoic

igneous and metamorphic processes. The first stage in the creation of the belt was the emplacement of a system of deep faults and the intrusion of layered igneous complexes: gabbro–norite–peridotite in the Moncha, Panskiye and Fedorovskiye tundras, gabbro–labradorite in the Moncha–Chuna–Volchiye tundras, belonging to the Seletskian epoch and having an age of 2.45–2.35 Ga. A subsequent stage was the accumulation of picritic–andesitic–basaltic and clastic terrigenous–trachybasaltic assemblages, evidence that the belt was evolving in an extensional regime. Intrusion of lenticular gabbro–wehrlite bodies occurred at 1.98–1.90 Ga, contemporaneous with the formation of the volcanogenic–clastic terrigenous assemblages in the Pechenga zone, hosting the Cu–Ni sulphide ores. Pechenga ores are represented by two genetic types: 1) primary magmatic disseminated and schlieren ores, 2) epimagmatic metamorphic and hydrothermal vein-disseminated and vein-type ores, formed during Dalslandian regeneration (Rundqvist and Mitrofanov, 1993). Native copper occurrences have been found in the Varzuga zone of this rift belt, in the outcrop area of trachybasalt–trachyandesite series meta-volcanics in the Umba Group. Copper–nickel sulphide mineralization also exists in other types of tectonic structures, particularly intracratonic basins: however, it does not have the same importance as in rift belts. A suitable example is to be found in minor Cu–Ni–Co deposits in the Voronezh crystalline massif, hosted in the Mamonov suite of dunite–peridotite–gabbro–norite layered intrusions. Specific Cu–Ni sulphide mineralization, apparently similar to “fahlband” type, is found amongst ferruginous quartzites and schists of the Krivoy Rog rift belt. Co, Pb and Bi are also associated with the Cu–Ni mineralization.

The next and most important type of deposit in the Svecofennian epoch are the ferruginous quartzites. The Early Proterozoic is the second in time and the most important epoch of iron accumulation in ferruginous quartzites in the East European craton. Deposits of this type are also associated with rift belts situated in the south of East European craton within the Ukrainian Shield and the Voronezh crystalline massif. As distinct from the essentially volcanogenic Cu–Ni signature for mineralization in belts in the Baltic Shield, the rift-type structures in southern parts of the craton consist mainly of clastic continental sedimentary assemblages. The major Krivoy Rog deposits have a chemogenic–sedimentary origin and are intimately associated with iron–chert–carbonate and iron–chert–silicate formations. The mineralization has a complex, polygenetic nature. It has already been remarked upon that this does not exclude the fact that primary chemogenic–sedimentary ores had already started forming during the preceding Seletskian epoch. During Svecofennian regional metamorphism, the ores were transformed and partially redeposited, although the highest-grade ores were formed post-metamorphism in zones subjected to alkali metasomatism, where they are commonly associated with economic uranium mineralization. Small sedimentary–volcanic type ferruginous quartzite deposits (Mariupol and Pobug types) formed during this period in the fold belt of the Pre-Azov metallogenic province in the Ukrainian Shield. Small uneconomic deposits of the iron–chert clastogenic formation originated in intracratonic basins in the Voronezh crystalline massif.

The most varied mineralization (Fe, Ti, P, REE, F, rare metals, etc.) is associated with foiditic igneous complexes in the Svecofennian stage of rifting. In fact, they appear

in such large volumes for the first time in the evolution of the crust. Foiditic complexes are completely atypical for rift structures in the preceding Seletskian epoch.

The largest P–Fe–Ti deposit is the Gremyakha–Vyrmes, hosted in an alkali gabbro intrusion, located in the Pechenga–Varzuga rift belt in the Baltic Shield. Intrusions of ultrabasic rocks with carbonatites, nepheline syenites and mariupolites crop out in the Pre-Azov block in the Ukrainian Shield. Apatite and rare metal–rare earth mineralization with fluorite is hosted in carbonatites and various alkali metasomatites (the Chernigovo and October (Mazurov) deposits). In the Pre-Azov terrain in the Ukrainian Shield and the Kola terrain in the Baltic Shield, rare metal–rare earth occurrences are found in pegmatites, alkali metasomatites and hydrothermal rocks.

Economic graphite deposits, the Petrov group in the Ukrainian Shield are hosted in peraluminous, carbonate and quartzitic successions. A similar type of graphite deposit is known also in fold belts (Troitskoye) and in small intracratonic basins of the Ukrainian Shield. Distinct from this, the intracratonic basins of the Baltic Shield, which are characterised by a much lower grade of regional metamorphism, contain major shungite deposits. Of the other types of mineralization associated with these structures, the most typical are auriferous conglomerates, copper–epidote, cupraceous sandstones, copper–zinc–pyrites, and others.

Intracratonic basins in the eastern Baltic Shield are mainly located within the Karelian granite–greenstone terrain and are represented by structures of the Jatulian assemblage. Partially isometric in plan view, the basins in which these assemblages are developed are associated with extensive linear structures in which the same formations crop out, but are thicker. Similar structures can be considered to be proto-aulacogens, forming a type of structure transitional to rift belts. The Jatulian assemblage consists of volcanosedimentary rocks, formed in the time interval 2100–1850 Ma ago. Jatulian sediments are located in narrow troughs and superimposed synsedimentary depressions adjoining the Kuola–Vygozero rift belt.

Copper pyrites occurrences in the Segozero–Yangozero basin are hosted in andesite–basalt and trachybasaltic volcanogenic assemblages. A similar type of mineralization in gabbro–diabase of the Lehti structure (Shuyezero and Ushakov mineral occurrences) are distinguished by their higher Ag and Au contents. Besides typical copper pyrites occurrences, the Onega and Yangozero basins also host cupraceous sandstones (Voronov Bor, Maimajärvi), Cu–Co shales (Kuzoranda) and shungite deposits (Zazhogin).

An extremely interesting type of ore mineralization, currently with no obvious analogues anywhere else, has been discovered in one of the intracratonic basins in the Baltic Shield, but its economic prospects have not yet been evaluated. This is U–Cr–V–PGE–Au mineralization in “alkali–amphibole propylites” and mica rocks which crop out in a carbonate–black shale assemblage. The mineralization has no obvious connection to magmatism and is controlled by a deep-seated regional fault zone. From a number of specific features, this type resembles the Zholtyye Vody “Yellow waters” (Zholtaya Rechka, “Yellow Brook”) uranium deposit in the Ukrainian Shield.

Deposits belonging to the Fe–Ti ore formation are known from areas surrounding the intracratonic basins, in association with faintly layered gabbro–diabase intrusive

sheets. The largest such deposit, at Pudozhgora, is hosted in the flank of the Onega structure in the southern Baltic Shield.

One of the most important types of ore-bearing structure in the Svecofennian epoch are belts of tectono-thermal reworking, which host the uniquely large-scale rare metal-muscovite pegmatites of the Yona and Chupa-Loukhi regions in the Belomorian polymetamorphic belt (Salye et al., 1976). The formation of these deposits coincides with the concluding stage of the Svecofennian kyanite-sillimanite facies series of a Barrovian-type metamorphic event. Muscovite pegmatite fields are strictly related to Loukhi peraluminous gneiss horizons. Only ceramic pegmatites are found beyond these.

Intense tectonothermal reworking in the Ukrainian Shield is evident in junction zones between different structural types (Golovanov, Orekhovo-Pavlograd), where Archaean complexes were metamorphosed in deep fault zones, basic-ultrabasic and granitic intrusions were emplaced, and metasomatic alteration occurred. Such zones are characterised by iron ore, chromite (the Kapitanov deposit), molybdenum and copper-molybdenum mineralization (Lipovenkov, Lyubar, Ostropol occurrences), also graphite deposits and occurrences in a khondalite formation (Zavalyev).

Fold belts constitute an extremely important type of ore-bearing structure in any analysis of the metallogeny of the Svecofennian epoch in the evolution of the East European craton. One example in the Baltic Shield is the Ladoga belt, a constituent of the Svecokarelian fold terrain, which is situated mainly in Finnish and Swedish territory. In the Ukrainian Shield there is the fold belt.

In a metallogenic sense, the Svecokarelian terrain was formerly identified as the Svecofennian sulphide ore province (Turchenko, 1978), due to its clear copper pyrites, massive sulphide-polymetallic, copper-nickel and rare metal-sulphide ore specialization. Supracrustal and igneous rocks in the Ladoga belt are associated with the development of tectonic and internal crust-forming processes of the Svecokareliides and form the SE continuation of the ore-bearing structures of the Main Ore Belt in Finland (Kahma, 1973). During the Svecofennian, this belt was an extensive, internally differentiated mobile terrain, initiated on Upper Archaean sialic crust, it is characterised by repeated folding, early basic and later granitic magmatism, restricted to the inner zones, where the Sortavala Group volcanogenic-carbonate assemblages crop out. The external parts of the belt consist of Ladoga Group clastic formations. Andalusite-sillimanite facies series metamorphic zoning is present, increasing from greenschist facies near the zone adjacent to the Karelian granite-greenstone terrain, to granulite facies and ultrametamorphic zones in the SW. Mineralization types in the Ladoga belt include pyrite-pyrrhotite, copper pyrites and pyrite-polymetallic occurrences, also graphite and scheelite, mostly in inner parts of the belt, and hosted mainly in the Sortavala volcanosedimentary group. There is also a regular association between mineralization and metamorphic zoning (Turchenko, 1978). All the pyrite-polymetallic and copper pyrites occurrences are located close to isograds in the ultrametamorphic zones and within staurolite-almandine sub-facies zones. Only pyrrhotite mineralization is preserved in ultrametamorphic zones, but ceramic pegmatites are common. Sulphide mineralization in the staurolite-almandine zone is represented by sphalerite-galena, sphalerite and chalcopyrite-pyrrhotite and scheelite, hosted in marbles and amphibio-

lites, altered to skarns, or associated with silicification and muscovitization zones. Gabbro intrusions are typical for the inner parts of the belt, hosting titanomagnetite mineralization (the Velimäki occurrence).

The sequence of ore genesis development within the entire Svecokarelian fold terrain has the following characteristic features. The earliest mineralization formed within the Main Sulphide Belt, located in a "pre-subduction" rift zone. The Cu-Zn-Co-Ni pyrite deposit at Outokumpu, with an age of around 2.0 Ga is hosted in a proto-ophiolitic complex and appears to have formed under "oceanic" conditions. The same zone hosts younger (~2.0-1.9 Ga) Cu-Zn-Co pyrite (Pyhäsalmi) and Cu-Ni sulphide (Kotalahti) deposits. Similar in age are cupraceous sandstone type deposits (Hamaslahti) and pyrite-polymetallic (Vihanti), which formed in continental slope conditions (miogeosynclinal zone). Cu-pyrite, Cu-Zn-pyrite, Pb-Zn, Fe-Mn and P-Fe deposits in the Bergslagen and Skjellefte ore regions, which formed in an island arc setting, are around 1.9 Ga old. The youngest Cu-Au, Cu-Mo, Mo-W and Pb-Zn and other vein deposits and rare-metal pegmatites, hosted in late- and post-orogenic granites, conclude the Svecofennian metallogenic epoch at 1.85-1.80 Ga ago.

The Litsa-Araguba plutonic belt formed simultaneously with the concluding stages of the Svecofennian orogeny in the consolidated part of the Baltic Shield immediately adjacent to the fold belt. It consists mainly of hypabyssal granitic rocks in the granodiorite-granite series with an age of 1.84-1.78 Ga. These granitoids host Mo-W deposits, and combine features of Mo-W greisen and Mo-porphyry ore formations.

Mention has already been made of the fact that the Seletskian metallogenic epoch did not appear in the Siberian craton. Early Proterozoic ore-forming processes were most intense here and in the East European craton in the 2.2-1.85 Ga interval in the Svecofennian (Udokanian) epoch. In the Siberian craton, this period was characterised by the development of extremely varied tectonic regimes. In the Aldan granulite-gneiss terrain and in the Anabar Shield, tectonomagmatic and tectonometamorphic processes affected older crystalline complexes over a very wide area. A polycyclic belt of tectonothermal reworking continued to evolve in the Dzhugdzhur-Stanovoy terrain, with powerful granite-forming processes, and the emplacement of minor Dzheltulak-type rifts. At the same time, independent volcanoplutonic belts were initiated in the eastern Aldan Shield, while intracratonic basins formed in the west. Fold belts and intracratonic basins formed around the W and SW margins of the Siberian craton, with tectonothermal reworking being common in Archaean basement inliers in these structures. Compared with the East European craton, fold belts and rift-type belts are very weakly developed in the Siberian craton, which is an important difference. The specific nature of the tectonic evolution of the Siberian craton during the Early Proterozoic also determined the metallogenic signature of the Svecofennian (Udokanian) epoch.

The large-scale occurrence of tectonometamorphic and tectonomagmatic changes which affected the Aldan granulite-gneiss terrain during the Proterozoic led to the formation of highly specific metamorphic-metasomatic deposits of iron, phlogopite and apatite in the magnesian skarn formation (Emeldzhak-Tayozhnaya group of deposits), belonging to the orthometamorphic class of deposits. In the West Aldan block the same processes were responsible for the formation of metasomatic Seligdar-

type apatite–rare earth metasomatic deposits in forsterite–carbonate and pyroxene–carbonate metasomatites. Metamorphic reworking of Archaean structures in Central Aldan during Proterozoic crustal activity produced rock crystal deposits, controlled by the development of joint systems, mainly in quartzitic horizons. Similar phlogopite, apatite and lazurite deposits in magnesian skarns formed in early Precambrian complexes of Khamar–Daban and the SW Pre-Baikal region. The development of alkali metasomatism, related to Early Proterozoic granitization, of ultrabasic rocks in the Olyokma granite–greenstone terrain led to the formation of the Ukdu's apatite deposit in a metaperidotite intrusion. A characteristic feature of all the above-mentioned types of deposit is the long time they took to form and the polyphase nature of the ore-forming processes.

The polycyclic development of regional metamorphism, ultrametamorphism and retrogression in the Dzhugdzhur–Stanovoy tectonothermally reworked belt led to the formation of specific iron and gold deposits within its borders during the Svecofennian epoch (the Kholodnikan ore region). Magnetite–quartz and amphibole–magnetite–quartz ores in the Sivakan deposit have an obvious metasomatic origin and are hosted in zones of intense migmatization of Late Archaean mafic rocks. Gold-ore vein deposits in the South, North and East Stanovoy gold-ore zones belong to gold–quartz and gold–sulphide–quartz formations. The gold-ore zones are controlled by deep-seated regional faults. Ore mineralization is associated with greenschist retrograde metamorphism, developed at the expense of Archaean metamorphic complexes.

However, the most productive type of ore-bearing structure in the basement of the Siberian craton in the Svecofennian (Udokanian) epoch were intracratonic basins that formed in the interval  $\sim 2.2$ – $2.1$  Ga ago. A typical example is the Udokan basin with its unique cupraceous sandstone deposits. The huge Katugan rare-metal deposit, hosted in alkali metasomatites, is located on the flanks of this structure, in a regional deep fault zone. Mineralization at  $\sim 2.1$  Ga old shows no connection with igneous activity. Large rapakivi-type granite intrusions belonging to the Kodar complex were emplaced during the late stages of development of this structure (1.9–1.85 Ga), with their associated Sn, W, Mo and U greisen and quartz-vein mineralization types, also the Chiney layered gabbro–norite lopolith intrusion with Cu–Ni and titanomagnetite mineralization with platinoids. Minor rare-metal pegmatite deposits are also related to this late stage of basin development, and these are hosted in the country rocks at the flanks of the structure.

In the Pre-Sayan region, in the SW of the craton, major rare-metal pegmatite deposits formed in this epoch. Pegmatite fields here are also hosted in intracratonic basin structures (the Urik–Iy graben). Similar rare-metal and muscovite–rare metal pegmatite deposits formed in the Angara–Kan basement inlier in the Yenisey ridge. Within the Dzhugdzhur–Stanovoy terrain, gold–sulphide and chalcopyrite mineralization are hosted in the Lower Proterozoic Dzheltulak graphite schists in small rift-type structures in the Dzheitulak zone.

Fold belts play a special role in the metallogeny of the Svecofennian (Udokanian) epoch. A type example is the Baikal fold belt, which to a large degree is covered by younger Riphean structures. Only fragments of the fold belt are exposed at the present surface: a microgeosynclinal complex (Sarma Group, Kutim, Chuya, Mikhailovsky

and Albazin Formations) and the Akitkan anorogenic volcanoplutonic belt. Isotope geochemistry studies by L.A. Neymark and Yu.V. Amelin confirm the view that Early Proterozoic structures are present in the basement to the Baikhalides. There are no economically important mineral deposits in structures belonging to the Early Proterozoic Baikal fold belt. Various types of rare metal, polymetallic, fluorite and gold ore mineralization are common in the Akitkan volcanoplutonic belt, which concluded the development of the Baikal fold belt as a whole at 1.8–1.9 Ga ago. Rare-metal mineralization is mainly hosted in hypabyssal and meso-abyssal sub-alkaline potassic granitoid intrusions belonging to the Irel, Primorsk and other complexes, as well as in alkali metasomatites adjacent to fault zones, while polymetallic and gold ores are hosted in Akitkan acid volcanics. However, there are no economic targets within the proto-orogenic volcanoplutonic belt.

*The Gothian metallogenic epoch* is clearly marked only in the territory of the East European craton. Anorogenic volcanoplutonic belts of the Gothian epoch (1.75–1.35 Ga) were initiated along the western edge of the craton after Svecofennian orogenic processes had been concluded and the fold structures had been consolidated at 1.85–1.80 Ga ago. In the Sveconorwegian zone (Sweden and Norway) in the extreme SW of the Baltic Shield, the Gothian fold belt formed in this period, and was subsequently reworked during the Dalslandian orogeny.

Anorthosite–rapakivi granite is the typomorphic igneous association in the volcanoplutonic belts of this epoch. It is important to emphasise that plutons belonging to this association were not emplaced simultaneously in different belts, or even within a single belt. The oldest representatives of the association (1.75 Ga) are known in the Ukrainian Shield. In the Baltic Shield there are two age generations within the Ladoga–Dalekarlian belt: the Vyborg and other intrusions (1.67–1.65 Ga), Salmi and Ulyaleg intrusions (1.55 Ga). Supracrustal formations in such structures are represented by Hoglandian assemblages and the Pugachev and Ovruch Groups. In addition to the coarse clastic sediments, mainly continental redbeds, there are also trachyandesite, trachybasalt and liparite lava flows and tuffs of the same age, as is also the case for the associated intrusions in the anorthosite–rapakivi granite formation. The concluding stage in the evolution of volcanoplutonic belts is characterised by Jotnian basic magmatism (~1.35 Ga). As well as the intrusion of dolerite–monzonite dykes and sills, continental trachybasalts were also erupted. Volcanic rocks usually alternate with coarsely clastic continental redbeds (the Salmi Fm in the Pasha graben). Intrusions belonging to the anorthosite–rapakivi granite association and superimposed Hoglandian and Jotnian basins are controlled by a system of orthogonal faults. For instance, the Ladoga–Dalekarlian belt coincides with an E–W fault zone along the southern edge of the Baltic Shield. The 200 km wide belt extends for around 1600–1800 km. North–south fault zones in the Ukrainian Shield control the emplacement of the Korosten and Korsun–Novomirgorod anorthosite–rapakivi granite massifs.

Intrusions of this association host a variety of ore deposits (Fig. 158). In the Ukrainian Shield, Ti–P mineralization occurs in the Korosten and Korsun–Novomirgorod massifs. The same intrusions contain a strip of hybrid rocks, hosting the Konstantinovo field of cavity pegmatites with piezo-quartz, morion, topaz and gem-quality beryl. Be, Sn, W, Mo, F and rare earth mineralization are known to be asso-

ciated with rapakivi granites in the Suschan–Perzhan zone, hosted in various alkali metasomatics, greisens, propylites, etc. The ores have an identical age to the host granites, 1.75 Ga. Economic mineralization is also known in the Ladoga–Dalekarlian belt. Iron–tin–beryllium–polymetallic skarn deposits in the Pitkäranta ore region are hosted in the Salmi rapakivi granite intrusion. The age of mineralization is 1.55 Ga. Volcanoplutonic belts in the East European craton therefore formed over a 400 million year period. A bimodal anorthosite–rapakivi granite magmatic phase and associated complex mineralization occupied the 200 million year interval from 1750 to 1550 Ma.

Similar structures in the Siberian craton (described above) formed slightly earlier, at around 1.85 Ga, practically simultaneously with the final stage in the growth of Svecofennian fold belts. The largest-scale deposits are hosted in the Ulkan volcano-plutonic belt (Khrenov, 1981). Greisen-type Sn–W mineralization is hosted in sub-alkaline rapakivi-like granites in this belt, while peralkaline granites host rare metal (Be, Zr, Nb, Ta, REE, Th) deposits in alkali-granite pegmatites, fenites and feldspathic metasomatites. P–Ti–Fe ores are hosted in Dzhugdzhur anorthosites, associated with the Ulkan granites of the same age (~1.70 Ga). In terms of phosphorus reserves, this is the largest apatite province in the former Soviet Union. A similar asynchronicity in the development of identical tectonic structures in the East European and Siberian cratons is especially well-expressed in the formation of anorogenic volcanoplutonic belts. An even more pronounced difference between the two cratons in terms of their metallogeny appeared in the Late Proterozoic after the volcanoplutonic belts had ceased forming.

*The Dalslandian metallogenic epoch* in both cratons is characterised by a relatively stable tectonic regime, when mostly sub-cratonic type tectonic structures originated, and only in the extreme SW Baltic Shield, outside Russia, did the Sveco-Norwegian orogenic belt form. In broad terms, this epoch is marked in both cratons by very low metallogenic productivity. Associated with this epoch in the East European craton are sedimentary siderite deposits in carbonate rocks in the Bashkirian pericratonic basin (the Bakal and Zigazin–Komarov group of deposits). In the same basin and at about the same time, the major Satka magnesite deposit and minor polymetallic, baryte and fluorite deposits formed (Fig. 156). No significant concentrations of useful minerals are associated with this epoch in the Siberian craton.

*The Baikalian metallogenic epoch* is characterised by sharply different tectonic activity and metallogenic productivity in the East European and Siberian cratons. As far as the East European craton is concerned, this epoch is practically barren in terms of metallogeny. The most typical structures are platform assemblages. The present platform cover began to accumulate only from the top of the Vendian. Stratiform fluorite–baryte–zinc mineralization, similar to Mississippi Valley-type, is known in these assemblages around the margins of the Ukrainian Shield. Just as characteristic for this epoch were aulacogens, forming a dense network of structures in the basement of the Russian platform. The ore content of these formations is not clear. The Timan–Kanin intracratonic fold belt formed at the same time on the NE edge of the East European craton, directly associated with the Ripheides of the Urals. Uneconomic Cu–Ni mineralization is known in this belt, hosted in gabbro–diabases, and tin mineralization, hosted in granitoids. Ore-generating processes during the Late Riphean were incomparably more intense in the Siberian craton, in relation to general activity along

the W and SW margins, accompanied by the establishment of geosynclines, riftogene depressions and intracratonic basins (Fig. 159).

Copper pyrites, massive sulphide–polymetallic, lead–zinc–pyrite deposits in black shales and volcanogenic complexes, and Pb–Zn stratiform deposits in carbonate rocks formed in the eugeosynclinal zone of the Baikalides in the Trans-Angara region, forming a single lateral series of deposits. The age of ore genesis is about 850 Ma. Gold-ore targets belonging to four formational types originated in the central anticlinorium of the Trans-Angara fold belt in this period. Greatest significance attaches to the gold–quartz type, associated with Late Riphean granite batholiths (850 Ma). Iron and manganese ore deposits and minor bauxite and phosphate occurrences were formed in the miogeosynclinal zone. Here also the major Kirgitey hydrothermal talc and magnesite deposit formed in a deep fault zone, hosted in a carbonate–schist assemblage.

A whole series of tectonic structures formed in the Baikal fold belt during the Late Riphean epoch, differing in metallogenic signature. These are the Baikal–Vitim protoophiolite belt, the Olokit riftogene depression, the Bodaibo intracratonic basin, the Pre-Baikal pericratonic basin, and others. Asbestos, nephrite and gold deposits formed within the Baikal–Vitim protoophiolitic belt (~0.65 Ga), related to retrogressive metamorphism of dunite–harzburgite ultrabasic formations and basic volcanic complexes. The Molodyozhnoye chrysotile–asbestos is worth a special mention in terms of the scale and quality of the mineral resource. The Tyya ferruginous quartzite is associated with a phase of andesite volcanism which concluded the development of this belt. The final formation of the deposit is related to late processes of superimposed folding and metamorphism. Low-grade Cu–Zn–pyrite mineralization is mainly hosted in volcanic complexes in the zone.

The major Kholodnin Pb–Zn–pyrite deposit is hosted in a black shale sequence in the Olokit riftogene depression. The age of the mineralization is about 750 Ma. Subsequent folding and regional metamorphism (up to amphibolite facies) during the Vendian created ore pillars rich in Pb–Zn ores. The same belt also contains the 700 Ma old Dovyren peridotite–pyroxenite–norite layered intrusion with low-grade Cu–Ni mineralization. Late Riphean rifting activated rigid early Precambrian basement inliers in the Baikal fold terrain, and the intrusion into them of subvolcanic and hypabyssal granitoids and the formation of tin ore deposits and minor occurrences belonging to the cassiterite–silicate formation (the Mokhovoye, Nakhodka and other deposits). Fluorite–lead–zinc stratiform deposits (Tabor, Khibelen, etc.), similar to Mississippi Valley-type deposits, formed in carbonates in the Pre-Baikal pericratonic basin at this time.

Basins which had initially formed around the edges of the Siberian craton were affected by a certain amount of activity at the Upper Riphean–Vendian boundary, with the appearance of alkali-ultramafic magmatism. Major apatite, rare metal, iron and fluorite deposits are hosted in carbonatites of this suite in the Pre-Sayan region. Carbonatites of the same type and age in South Yakutia host rare earth–rare metal and apatite–phlogopite mineralization, while aulacogens of this time (Udzha) in the north of the Siberian craton host vein occurrences of galena, fluorite, baryte and sphalerite, localized in eruptive–sedimentary parts of the succession, as well as apatite–titanomagnetite ores in alkali–ultrabasic complexes and rare earth–rare metal mineralization in carbonatites.

Yudomian (Vendian) sediments, which form the platform cover assemblages of the Siberian craton, contain pyrite–chalcopyrite–chalcocite–bornite mineralization in places, hosted for example in cross-bedded sandstones of the Ushakov Fm in the middle reaches of the river Angara. But the most characteristic is stratiform lead–zinc mineralization, represented by the Sardana deposit in the Yudoma–Maya pericratonic basin. Densely disseminated and finely dispersed lead–zinc ores in this deposit form sheets and pods amongst dolomites and limestones in the thick Yudomian (Vendian) succession.

### *2.1. Phanerozoic metallogenic epochs*

Particular features of Phanerozoic metallogeny in Precambrian terrains are in many ways predetermined by the nature of their previous geological history. The most characteristic internal ore formations in the Phanerozoic of Precambrian cratons, frequently forming extremely large and unique deposits of phosphorus, rare metals, potash and alumina raw materials, iron, phlogopite, diamonds, etc., hosted in foidite complexes. These complexes may have formed mainly under conditions of rigid, long-stabilized regions with a thick cratonised continental crust, which had experienced tectonic activity in the Phanerozoic. The material that formed these deposits had a deep source – a mainly mantle origin.

Phanerozoic mineral deposits in Precambrian terrains remain somewhat apart in having a more complex genesis. Their formation in post-Precambrian time was directly caused by the character of the Precambrian history of ore-hosting crustal blocks. They are usually polychronic deposits, which took hundreds of millions of years to form, across more than one metallogenic epoch. As a rule, the source of the ore material has a crustal or mixed origin and underwent a long and complex development during the cyclical evolution of the Earth's crust. The most typical examples of such targets are the gold ore and muscovite deposits of the Baikal fold terrain, which until recently had been thought to be Precambrian in their entirety.

Isotope geochemistry on the gold deposits of the Baikal fold terrain by L.A. Neymark, using material supplied by I.K. Rundqvist and others, has shown that they have an Early Proterozoic crustal source, a long and complex subsequent history, with the formation of stratiform gold concentrations in the Late Riphean, and final formation of large deposits of vein gold during Hercynian tectogenesis. Also associated with this Hercynian period was the formation of unique muscovite pegmatite deposits, hosted in peraluminous Precambrian complexes in the Mamskaya zone of the Baikal fold terrain. The long polycyclic evolution of the Davan–Abchada shear zone in the same region led to the emplacement in it of rare-metal mineralization, related to at least two metallogenic pulses: Early Proterozoic and Hercynian.

### *3. Conclusions*

The above analysis of distribution patterns of different mineralization types for each Precambrian metallogenic epoch in different tectonic structures has allowed us to

explain some of the commonest features in the evolution of ore formation in the Precambrian and to compare ore genesis in the East European and Siberian cratons (Fig. 160).

(1) The possibility of identifying the various types of ore-bearing tectonic structures outlined in the Preface has been confirmed. The whole range of structures is presented in summary form (Table 16). It has already been remarked that each type of structure developed in a definite time interval, measured in hundreds of millions of years. These ore-bearing structures may appear repeatedly in different regions, permitting age generations to be identified. Examples would be the two generations of greenstone belts (Early and Late Archaean) in the Olyokma granite–greenstone terrain; Seletskian and Svecofennian rift belts in the Baltic Shield and younger Late Riphean rifts in the Baikal fold terrain; intracratonic basins which first appeared in the Late Archaean (Keivy), reached their maximum in the Early Proterozoic (Udokan, Onega, etc.) and completed their evolution in the Late Riphean (Bodaibo). Table 16 presents the sequence of ore-bearing tectonic structures, reflecting the typical way in which they appeared in time during the evolution of Precambrian terrains.

(2) Moving from older to younger epochs, crustal structure becomes progressively more complex but in a spasmodic way, owing to changes in geodynamic environments with time. The appearance of new and more complex tectonic structures and their greater variety with time is reflected in the metallogenic evolution of Precambrian terrains. The Katarchaean and most of the Early Archaean epochs are characterised by weak crustal differentiation and the almost universal development of granulite–gneiss type structures with an essentially siderophile weakly-expressed metallogenic signature and a predominance of elements belonging to the iron group in deposits with metamorphic origin. Continued evolution of the Precambrian lithosphere led to the formation in the Siberian craton at the end of the Early Archaean of the first greenstone belts with parallel development of tectonic structures belonging to an earlier stage. Early Archaean greenstone belts have an indistinct iron signature.

The Late Archaean (Rebolian) was an epoch which saw the rapid formation of structures in granite–greenstone terrains and belts of tectonothermal reworking, as well as powerful granite formation with the first appearance of huge masses of potassic granites in the evolution of the crust. Intense iron accumulation took place in this epoch, as ferruginous quartzites, and a whole series of qualitatively new types of deposit formed, such as massive sulphide, Cu–Mo porphyry, rare-metal, pegmatites, etc. Thus, against a dominant background of a siderophile ore signature in this epoch, features of both chalcophile and lithophile signatures had already begun to appear.

The Early Proterozoic was a period when tectonic processes in the Precambrian lithosphere were at their most active, accompanied by pronounced changes in the types of tectonic movements, reworking of the structural plan, changes in internal crustal regimes, and emergence of a geochemically inhomogeneous mantle. Qualitatively new types of tectonic structures originated in this period, such as rift belts, fold terrains, volcanoplutonic belts, and others. The main structures to form in the Early Proterozoic, during the Seletskian epoch, were rifts with a predominantly siderophile assemblage of ore elements (Fe, Ti, Cr, Pt, Cu, Ni). A variety of structures formed in the subsequent Svecofennian epoch, with an exceptionally broad spectrum of mineral

deposits. In fact, the Svecofennian was the most productive epoch in terms of metallogeny. Besides deposits of ore elements in the siderophile group, chalcophile and lithophile group elements also obtain a wide distribution. For the first time in the history of the crust, deposits appear in foiditic igneous complexes, indicating a highly mature continental crust at this time. Unique Fe, Cu, Ni, rare-metal, muscovite and other deposits belong to this epoch.

The Gothian epoch was one in which ancient cratons became relatively stable, and specific structures formed – anorogenic volcanoplutonic belts with rare metal and rare metal–polymetallic signatures. The Dalslandian epoch is distinguished by an even more stable tectonic regime, and the formation of minor Fe, Pb, Zn and Ba sedimentary deposits in sub-cratonic structures.

Tectonic activity increased sharply at the craton margins during the Baikalian epoch, when rift-type depressions, fold belts and intracratonic basins became established. The process was felt most intensely in the Siberian craton and led to the formation of major Au, polymetallic, Fe, Mn and rare-metal deposits. This epoch determined the foundations of most Caledonian and Hercynian fold belts in the former Soviet Union. Additionally, the ancient East European and Siberian cratons had become completely stabilized by this time, allowing platform cover assemblages and aulacogens to form, with specific ore contents.

It is possible to construct an evolutionary series for the evolution of mineralization in the various metallogenic epochs for each of the two cratons. For the East European craton: AR<sub>1</sub>: (Fe, Gt, Cr, Cu, Ni, Al) → AR<sub>2</sub>: Fe, S, Al, RM, Cu, Mo, Gt, Talc, (Ti, Ni) → PR<sub>1</sub><sup>1</sup>: Cu, Ni, Fe, Ti, Gt, Pt, (Au) → PR<sub>1</sub><sup>2</sup>: [Fe, Musc], Cu, Ni, P, Ti, Zn, RM, REE, Gt, (Mo, W, Au, Ag) → R<sub>1</sub>: RM, Sn, Ti, P, Q, Fl, (Cu, Zn, Pb) → R<sub>2</sub>: Mag, Fe, Pb, Zn, (Ti, V, Cu, Ba) → R<sub>3</sub>-V: (Fe, Mn, Pb, P, Ba, Phlg). For the Siberian craton: AR<sub>1</sub>: Fe, Ti, Al, Gt, (Cr, Ni) → AR<sub>2</sub>: Fe → PR<sub>1</sub><sup>1</sup>? → PR<sub>1</sub><sup>2</sup>: [Cu], RM, Fe, Phlg, P, Q, Au, (Ti, Ni, Zn) → R<sub>1</sub>: Fe, Ti, Al, RM → R<sub>2</sub>? → R<sub>3</sub>-V: [Pb, Zn, Talc, Asb], Cu, RM, REE, Mn, Au, Fe, P, (Sn, Ni).

(Note: boxed symbols = unique mineral deposits, underlined = major, in brackets = minor deposits and occurrences. Abbreviations: Gt – garnet, RM – rare metals, Musc – muscovite, Mag – magnesite, Q – piezoquartz, Fl – fluorite, Phlg – phlogopite, Asb – asbestos).

(3) Despite the fact that there are common features in the metallogenic development of the East European and Siberian cratons, some differences are discernible, due in large measure to their particular geological history, in particular the lack of synchronicity in the evolution of similar tectonic structures and associated mineral deposits. Currently available data suggest that the geological evolution of the Siberian craton began slightly earlier than the East European craton. For example, eulysite-type iron deposits in granulite–gneiss terrains of the Siberian craton had already begun to form in the Katarchaeon, but only in the Early Archaean in the East European craton. Granulite–gneiss terrains in the Siberian craton are generally characterised by corundum, kyanite, sillimanite, phlogopite, apatite, rock crystal and lazurite deposits and occurrences which are missing from similar types of structures in the East European craton.

The first greenstone belts with ferruginous quartzite deposits became established in the Siberian craton almost 300 million years earlier, i.e. at the end of the Early

Archaean epoch. The Late Archaean metallogenic epoch most intensely and completely manifest itself in the East European craton and is much reduced in the Siberian craton (deposits in the Fe and P group).

Clear differences emerged between the development of the two cratons during the Early Proterozoic (Fig. 158). The East European craton was much more mobile then, and major deep-seated structures were initiated – rift belts with widespread mantle magmatism, Svecofennian-type fold belts, marked differentiation into eugeosynclinal and miogeosynclinal zones and characterised by clearly-expressed metallogenic zoning. Similarly, specific features in internal processes were also responsible for the metallogenic signature of the East European craton during this epoch, primarily as an assemblage of siderophile–chalcophile group elements (Fe, Ti, Cu, Ni, Pt, Zn, P, and others).

Tectonic processes were less intense in the Siberian craton during the Early Proterozoic. The Seletskian metallogenic epoch is practically not represented here. The Svecofennian epoch on the other hand is quite distinct, and appeared almost simultaneously in the East European craton, albeit in a distinctive form. Rifting processes did not produce mature rift belts with widespread basaltic magmatism. Continental crustal growth processes around the craton margins are smaller-scale in comparison to the East European craton. Intracratonic crustal processes predominated, appearing as intense tectonothermal and tectonomagmatic reworking of Archaean structures, also the formation of Udokan-type intracratonic basins. The specific crustal nature of Early Proterozoic internal processes in the Siberian craton produced deposits of essentially lithophile–chalcophile group ore elements (copper, rare metals), and industrial minerals.

Anorogenic volcanoplutonic belts of the same time, with rare-metal mineralization, took place over a 100–150 Ma time interval in both cratons. Whereas they were initiated in the East European craton after the very end of the Svecofennian orogeny, in the Siberian craton these belts formed somewhat earlier, practically parallel with the conclusion of orogenic processes in Svecofennian fold belts. In the Siberian craton, the Baikalian epoch was extremely intense compared to the East European craton, with fold belts, rifts and intracratonic basins forming around the craton margins, and a variety of ore deposits, such as Fe, Au, Cu, Zn, Pb and rare metals.

(4) Each metallogenic epoch is an ordered spectrum of metallogenic pulses – brief time intervals, characterised by the maximum development of useful mineral deposits. As a rule, metallogenic pulses are much shorter than the time intervals separating them. An example is the sequence of metallogenic pulses of the Svecofennian epoch in the Svecokarelian fold terrain: Cu, Co, Ni (2.0 Ga) → Cu, Zn, Ni, (Co, Pb) (1.9–2.0 Ga) → Fe, Mn, P, Pb, Zn (1.9 Ga) → Cu, Au, Mo, W (1.85 Ga) → Pb, Zn (1.85–1.80 Ga). An equally illuminating example is the distribution of metallogenic pulses in the Gothian volcanoplutonic belts of the East European platform. As in the previous version, the evolution of mineralization follows a strictly-defined path, although in this case the same anorthosite–rapakivi granite association stands out as an ore-bearing complex: Be, Ti, P, REE, Nb, Ta, Zr, (Sn, W, Mo) (1.75 Ga) → Be, Sn, (Pb, Zn, Cu) (1.65 Ga) → Sn, Be, Cu, Zn, Pb (1.55 Ga). A characteristic feature of these series, despite substantial differences, is the gradual reduction in the role of siderophile

elements and an increase in lithophile–chalcophile and later essentially chalcophile elements from initial members of the series to end members.

(5) In the course of crustal evolution from ancient to younger structures, the types of ore mineralization also changed in a regular fashion. The oldest high-grade metamorphic complexes are host to mainly metamorphic deposits, both in the prograde and retrograde classes. These deposits play a less important role on the whole as we move towards younger structures. Orthometamorphic deposits are more typical for tectonic structures displaying polycyclic development, such as belts of tectonothermal reworking, granulite–gneiss terrains subjected to pervasive tectonometamorphic and tectonomagmatic processes, long-lived suture zones, etc. This class of mineral deposit mainly characterises Late Archaean–Early Proterozoic structures, but sometimes also appears in younger structures. Many of them have a polychronous and polygenetic nature.

Typical sedimentary, volcanosedimentary, magmatic, pegmatitic and hydrothermal deposits appear beginning from the Late Archaean, usually more or less transformed during subsequent metamorphic and metasomatic processes. Carbonatite deposits make their appearance from the middle of the Early Proterozoic. As tectonic structures “become younger” there is a regular increase in the variety of genetic types of deposit and the total range of useful minerals. It is important to note that, against this background, some mineral deposits have a “transparent” distribution nature in time. For example, Cu–Ni sulphide and Fe–Ti deposits, hosted in basic–ultrabasic complexes, can be traced from the Early Archaean to the Late Riphean and Phanerozoic, reaching a culmination in the Svecofennian epoch. At the same time, a whole range of deposits exists, typical exclusively of the Precambrian or even a particular metallogenic epoch. Examples are ferruginous quartzites, P–Fe–Ti deposits in anorthosites, metaliferous conglomerates, alkali metasomatites with rare-metal mineralisation in deep fault zones, etc.

For some types of deposit, there is a regular evolution in the transition from old structures to younger. Eulysitic-type ferruginous quartzites in high-grade Early Archaean metamorphic complexes change to ferruginous quartzites in greenstone belts, where they are associated with volcanic complexes of various compositions, forming major ore deposits. By the Early Proterozoic they become ferruginous quartzites in “continental” rifts, hosting uniquely large-scale deposits and ferruginous quartzites in fold terrains (both in mio- and eu-geosynclinal zones). In the Riphean they become bedded hematite–chlorite ores in miogeosynclinal assemblages. Rare-metal pegmatites in Late Archaean granite–greenstone terrains give way in the Svecofennian epoch to muscovite, rare metal–muscovite, rare metal, rare earth and ceramic pegmatites, formed in various tectonic environments. Cavity pegmatites with piezoquartz, topaz and beryl formed in the Gothian epoch. Massive sulphide deposits also changed in a regular pattern with time. In Late Archaean greenstone belts, massive sulphide deposits are replaced in the Svecofennian epoch by Cu–Zn deposits, often with Co and Ni in fold belts. In the Middle–Late Riphean they give way to pyrite–polymetallic and lead–zinc deposits in eugeosynclinal zones of fold belts. Pb–Zn–pyrite deposits had already formed in the Late Riphean in rift belts, with the parallel development in pericratonic basins of Pb–Zn deposits in carbonate rocks.

Later still, at the Vendian–Palaeozoic boundary, only Pb–Zn deposits formed in carbonates in platform cover assemblages.

(6) One specific feature that relates to some Precambrian mineral deposits is their weak “differentiation”. For example, in the author’s opinion, features of Mo–W greisen and Mo–porphyry formations combine together in the Jaurijoki Mo–W deposit in the Baltic Shield. The Seligdar apatite–rare earth deposit combines features of a carbonatite deposit and magnesian skarn formations. Tin–rare metal–polymetallic skarn deposits in the Pitkäranta ore region display features of different ore formations. It is important to mention in this regard that these examples relate to simple, non-polygenetic and polychronous deposits, where the multiple formations are caused for other reasons.

In conclusion, it should be pointed out that the major ore-forming epochs affecting the East European and Siberian cratons generally correlate well with the main crust-forming events found in the Precambrian of other ancient cratons. However, attention has to be paid to certain differences. In particular, the oldest metallogenic epochs – Katarchaeon and Early Archaean – are well represented in the ancient cratons of the Southern Hemisphere, but are practically not seen in the East European and Siberian cratons. The Gothian and Dalslandian epochs are also weakly expressed. Anorogenic volcano-plutonic belts with mainly rare metal mineralization formed almost exclusively in the Gothian, and only in the East European craton. In other ancient cratons at the same time, besides volcanoplutonic belts there are many instances of rift belts and aulacogens with polymetallic Pb–Zn mineralization, intracratonic fold belts with rare-metal mineralization, intracratonic basins with polychronous U–Ni mineralization, and belts of tectonothermal reworking. A sub-cratonic regime dominated in both cratons during the Dalslandian epoch, except for the Sveco-Norwegian zone of tectonothermal reworking at the edge of the Baltic Shield. In other cratons at the same time, anorogenic volcanoplutonic belts, intracratonic fold belts and belts of tectonothermal reworking with rare-metal and tin mineralization continued to evolve. The relative stability during epochs of internal crustal processes has great practical significance, since the most important economic mineral deposit types display a definite distribution pattern on a geological time scale.

This Page Intentionally Left Blank

## A Classification of Precambrian mineral deposit types

D.V. RUNDQUIST, V.A. GORELOV, S.I. TURCHENKO  
and A.M. LARIN

A type classification of Precambrian mineral deposits presents special complexities due to the widespread distribution of metamorphic deposits in ancient crustal structures, for many of which the primary genetic nature of the ores has either not been established or is ambiguous. Very many deposits formed in two or three stages, as noted above, separated in time – primary ore genesis and subsequent alteration and the appearance of new mineral parageneses. The sum total of this means that in many cases determining the time of ore formation and the genetic type of a deposit are also very complicated. A systematic approach to treating data for Precambrian mineral deposits often involves the simplest version – subdividing them on the basis of the raw material. Such an approach to distinguishing formational types of ores, reflecting the variety of ore formations similar in composition and structure, originating in different geological environments is generally accepted in “special” metallogeny. The mineral deposits and occurrences in the East European and Siberian cratons described in this work are grouped into 60 major ore formations for 30 useful minerals (Table 19). However, there are sharp differences in the significance of these ore formations in the country’s mineral raw material resources. The main role in iron ore deposits belongs to Precambrian ferruginous quartzite formations. This type appears in all the shield areas, from Early Archaean to Late Proterozoic and is mainly concentrated in Late Archaean–Early Proterozoic structures.

Precambrian titanium deposits have large resources; these are mostly complex, containing iron, vanadium, phosphorus, occasionally small quantities of copper, nickel and cobalt. Most of these deposits are genetically linked to gabbro–anorthosites and occur widely in the Baltic, Ukrainian and Aldan shields and marginal inliers around the Siberian craton. The Kolar–Dzhugdzhur zone with gabbro–anorthosites, located in the junction zone between the Aldan and Stanovoy terrains, is unique in terms of resources and will obviously be important in the future.

Manganese and chromium are less typical of Precambrian structures in these cratons, compared to foreign examples, where Mn and Cr reserves in Precambrian ore deposits amount to 89% and 98% of the total respectively (Bykhover, 1984). The recent discovery of the Porozhin deposit in Vendian–Riphean sediments in the Yenisey ridge, belonging to the manganiferous carbonate formation, widens the prospects of Late Precambrian structures for manganese raw materials.

Table 19

## Precambrian Deposits in the East European and Siberian Cratons

Formational type of deposit		Examples of deposits (tectonic block, terrain, belt)	Mineral deposit characteristics		
Ore formation	Host formation		Mineral type	Genetic type	Ore-forming epoch
<b>METALLIFEROUS DEPOSITS</b>					
1. Iron					
Eulysitic iron ore	Fe-silica in granulite gneiss & two-px schist	Pinkeljavr (Kola terrain), Baikal (Pre-Sayan), Olympiad (Aldan) Central Anabar occurrences	Magnetite, hematite-magnetite	Metamorphic	AR <sub>1</sub> PR
Ferruginous quartzite	Fe-silica in amphibolite gneiss	Olenegorsk (Kola terrain), Chara etc. in Chara-Tokk group (Olyokma terrain)	Hematite-magnetite	Metamorphic (volcano-sed.)	AR <sub>2</sub>
	Fe-silica in amphibolite gneiss	Mariupol (Pre-Azov block)	Hematite-magnetite	Metamorphic (volcano-sed.)	PR <sub>1</sub>
	Fe-silica in schist & gneiss	Kostomuksha (Karelia)	Hematite magnetite	Metamorphic (volcano-sed.)	AR <sub>2</sub>
	Fe-silica in amphibolitic schist	Chertomlyk etc., Krivoy Rog basin (Pre-Dnieper block); Sosnovy Bayts, Onot group (Pre-Sayan); Tyva (Baikal-Patom terrain)	Hematite-magnetite	Metamorphic (volcano-sed.)	AR <sub>2</sub> PR <sub>1</sub>
	Fe-silica in shale, conglomerate & sst	Ingulets etc., Krivoy Rog basin (Pre-Dnieper block); Kursk Magnetic Anomaly (KMA)-Yakovlevo, Lebedin (Voronezh Massif), Vitim ore field (Baikal-Patom terrain)	Hematite magnetite	Metamorphic (clastic sed.)	PR <sub>1</sub>
Silica-hematite iron ore	Siltstone-sandstone-shale	Lower Angara etc. Angara-Pit basin (Yenisey ridge)	Hematite-leptochlorite	Sedimentary (metamorphosed)	R <sub>2</sub>
Limonite-hematite iron ore	Quartzose sandstone	Uchur ore zone (platform cover of Siberian craton) Maya ore zone (platform cover of Siberian craton)	Limonite-hematite	Sedimentary	R <sub>1</sub> R <sub>2-3</sub>
Sideritic iron ore	Limestone-dolomite	Bakal (East European craton)	Siderite	Sedimentary	R <sub>1</sub>
Magnesian skarn iron ore	Two-pyroxene schist, calciphyre	Tayezhnoye (Aldan terrain)	Apatite-phlogopite-magnetite	Metamorphic (metasomatic)	PR <sub>1</sub>

2. Titanium					
Fe-Ti	Gabbro-anorthosite	Tsagin (Kola Peninsula)	Ilmenite-titanomagnetite	Meta-igneous	AR <sub>2</sub>
		Volodar-Volyn (Volyn block)	Ilmenite-titanomagnetite	Meta-igneous	PR <sub>2</sub>
	Clinopyroxenite-wehrlite	Central (Kola terrain)	Ilmenite-titanomagnetite	Meta-igneous	AR <sub>2</sub>
	Gabbro-diabase	Pudozhgora (Karelia terrain)	Ilmenite-titanomagnetite	Meta-igneous	PR <sub>1</sub>
	Gabbro-gabbro norite	Malo-Tagul (Pre-Sayan)	Ilmenite-titanomagnetite	Meta-igneous	AR <sub>2</sub>
P-Fe-Ti	Dunite-pyroxenite-gabbro	Shivero (Yenisey ridge)	Ilmenite-titanomagnetite	Meta-igneous	AR <sub>2</sub>
	Gabbro-anorthosite	Gayum, Maymakan (Dzhugdzhur-Stanovoy terrain)	Apatite-ilmenite-titanomagnetite	Meta-igneous	AR <sub>2</sub>
		Stremigorod (Volyn block)	Apatite-ilmenite-titanomagnetite	Meta-igneous	PR <sub>1</sub>
		Occurrences in Anabar Shield (Magan block)	Apatite-ilmenite-titanomagnetite	Meta-igneous	AR
	Alkali gabbro	Gremyakha-Vyrmes (Kola terrain)	Apatite-ilmenite-titanomagnetite	Meta-igneous	PR <sub>1</sub>
Cu-Fe-Ti	Gabbro-norite	Chiney (Olyokma terrain)	Chalcopyrite-titanomagnetite	Meta-igneous	PR <sub>1</sub>
3. Manganese					
Manganiferous silica-carbonate	Silica-carbonate	Porozhin (Yenisey ridge)	Manganosiderite-rhodochrosite	Sedimentary	
Manganif. qz-glauc.sand-clay	Sandy-shaly	Nikolayev (Pre-Sayan basin, platform cover of Siberian craton)		Sedimentary	
Mn-carbonate	Dolomite limestone	Sagan-Zaba (W. Pre-Baikal)	Manganocalcite	Sedimentary	AR
4. Chromium					
Chromite	Dunite-peridotite	Kapitanov (Golovanev suture zone)	Sulphide-chromite	Magmatic	AR <sub>1</sub>
5. Aluminium					
High-Al schist	High-Al schist	Shuururta, Keyvy group (Kola terrain)	Sillimanite-kyanite	Metamorphic	
		Kitoy (Pre-Sayan)	Sillimanite	Metamorphic	
High-Al weathered mantle	Dolomite	Gornostil (Maya basin, platform cover of Siberian craton)	Bauxite	Laterite	
6. Nickel					
Cu-Ni sulphide	Gabbro-wehrlite	Kaula, Pechenga group (Kola terrain)	Chalcopyrite-pentlandite-pyrrhotite	Magmatic	PR <sub>1</sub>

Table 19 (Continued)

Formational type of deposit		Examples of deposits (tectonic block, terrain, belt)	Mineral deposit characteristics		
Ore formation	Host formation		Mineral type	Genetic type	Ore-forming epoch
	Olivinite-harzburgite	Allarechka (Kola terrain)	Chalcopyrite-pentlandite -pyrrhotite	Magmatic	PR <sub>1</sub>
	Olivinite-wehrlite	Lebyazhe (Karelia terrain)	Chalcopyrite-pentlandite -pyrrhotite	Magmatic	PR <sub>1</sub>
	Peridotite-pyroxenite-norite	Monchegorsk group (Kola terrain) Chaya (Baikal-Patom terrain)	Chalcopyrite-pentlandite -pyrrhotite	Magmatic	PR <sub>1</sub> , R <sub>1</sub>
	Websterite gabbro norite	Lovnozero (Kola terrain)	Chalcopyrite-pentlandite -pyrrhotite	Magmatic	PR <sub>1</sub>
	Dunite peridotite gabbro norite	Nizhnemamon (Voronezh crystalline massif)	Chalcopyrite-pentlandite -pyrrhotite	Magmatic	PR <sub>1</sub>
	Dunite troctolite gabbro	Lukinda (Dzhugdzhur Stanovoy terrain)	Chalcopyrite pentlandite -pyrrhotite	Magmatic	PR <sub>1</sub>
		7. Copper			
Cupraceous sandstones	Siltstone-sandstone	Udokan (Olyokma terrain)	Chalcosite bornite chalcopyrite	Metasedimentary	PR <sub>1</sub>
		Occurrences in Pre-Yenisey, Pre-Sayan, Pre-Baikal basins (platform cover of Siberian craton)	Chalcosite bornite chalcopyrite	Metasedimentary	
Co-Cu in shales	Dolomite-shale diabase	Kuzoranda (Karelia terrain)	Chalcopyrite pyrite with cobalt	Volcano-sedimentary	PR <sub>1</sub>
Cu ore in basalts	Basalt	Occurrences in Volyn basin, platform cover on East European craton	Native copper	Volcanogenic-hydrothermal	
		8. Lead, zinc			
Stratiform Pb-Zn	Carbonate	Gorevsk (Yenisey ridge)	Galena-sphalerite	Volcanogenic-sedimentary	R <sub>2</sub>
	Carbonate	Sardana (Yudoma-Maya basin, platform cover on Siberian craton)	Galena-sphalerite	Volcanogenic-sedimentary	
Pb-Zn pyrites	Carbonaceous shales	Linear (Yenisey ridge); Kholodninskoye (Baikal-Patom terrain)	Galena-sphalerite-pyrite	Volcanogenic-sedimentary	

Fluorite-Pb- Zn	Graphitic-shale-carbonate	Tabor etc. (Pre-Baikal basin, platform cover on Siberian craton)	Fluorite-galena-sphalerite	Volcanogenic-sedimentary	R <sub>2,3</sub>
Pb-Zn veins	Unidentified	Bazarnaya Guba (Kola terrain)	Sphalerite-galena	Hydrothermal	PR <sub>2?</sub>
Mo in greisens	Graphitic, granite-porphyry	9. Molybdenum Yaurijoki (Kola terrain)	Fluorite-molybdenite	Greisen	PR <sub>1</sub>
Mo in granites	Granite	Päävara (Karelia terrain), Lyubar (Podolsk block), Okhok (Dzhugdzhur-Stanovoy terrain)	Molybdenite	Hydrothermal	PR <sub>1</sub>
Mo-porphyry	Gabbro-plagiogranite	Lobash (Karelia terrain)	Molybdenite	Hydrothermal	AR <sub>2</sub>
Cu-Mo-porphyry	Leucogranite, alaskite	Pellapakhk (Kola terrain)	Chalcopyrite-molybdenite	Hydrothermal	AR <sub>2</sub>
W in skarns	Granite	10. Tin, tungsten Latvasyrä (Ladoga belt)	Scheelite	Skarn	PR <sub>1</sub>
Fe-Zn-Sn in skarns	Anorthosite-rapakivi granite	Pitkäranta, Kittilä (Ladoga belt)	Chalcopyrite-magnetite-sphalerite-cassiterite	Skarn	R <sub>1</sub>
Cassiterite silicate	Granite	Tuyukan tin-ore region (Baikal Patom terrain)	Cassiterite sulphide	Hydrothermal	R <sub>3</sub>
		11. Rare metals and rare earths (Ta, Nb, Cs, etc.)			
Rare metal pegmatite	Granite (granitic pegmatites)	Voronya Kolmozero zone (Kola terrain)	Tantalite pollucite	Pegmatite	AR <sub>2</sub>
	Granite (granitic pegmatites)	Pegmatite field in Urík-Iy graben	Tantalite	Pegmatite	PR <sub>1</sub>
Rare metal rare earth pegmatite	Granite-migmatite? (granitic pegmatites)	Occurrences in Abchad zone (Baikal-Patom terrain)		Pegmatite	PR <sub>1</sub>
Rare metal-rare earth fenite	Granite-granosyenite, syenite	October (Pre-Azov block)	Zircon pyrochlore	Hydrothermal metasomatic	PR <sub>1</sub>
Rare metal-rare earth feldspath.	Granite-alkali granite	Suschan-Perzhan zone (Volyn block)	Zircon pyrochlore	Hydrothermal metasomatic	PR <sub>1</sub>
Rare metal-REE feld-greisen	Unidentified	Katuga ore field (Olyokma terrain)	Zircon-pyrochlore	Hydrothermal-metasomatic	PR <sub>1</sub>
	Alkali-granite	Ulkan ore field (Batomga terrain)	Columbite-cassiterite-wolframite	Hydrothermal metasomatic	PR <sub>1</sub>

Table 19 (Continued)

Formational type of deposit		Examples of deposits (tectonic block, terrain, belt)	Mineral deposit characteristics		
Ore formation	Host formation		Mineral type	Genetic type	Ore-forming epoch
Rare metal-REE carbonatite	Granite Alkali-ultrabasic-carbonatite	Occurrences in Davan zone (Baikal-Patom terrain) Chernigov (Pre-Azov block)	Cassiterite-gelvine-columbite-fergusonite Zircon-pyrochlore	Hydrothermal-metasomatic Carbonatite	PR <sub>1</sub> PR <sub>1</sub>
Au-sulphide-quartz	Unidentified	12. Gold Voitskoye (Karelia terrain), Zolotaya Gora ("Gold Hills") (Dzhugdzhur-Stanovoy terrain)	Gold-chalcopyrite	Hydrothermal	PR <sub>1</sub>
Au-black shale	Black shale	Sukhoy Log (Baikal-Patom terrain)	Gold-pyrite	Hydrothermal	R?
Au-quartz	Granite	Gerfedskoye (Yenisey ridge)	Gold-pyrite	Hydrothermal	R <sub>3</sub>
Au-Ag-quartz-sulphide	Granite	Bogunayevo (Yenisey ridge)	Gold-pyrite	Hydrothermal	R <sub>3</sub>
Au-Sb-quartz	Granite	Uderey (Yenisey ridge)	Gold-antimonite	Hydrothermal	R <sub>3</sub>
Fe-U	Ferruginous-silica in hornblende schists	13. Uranium Zheltaya Rechka ("Yellow River") (Pre-Dnieper block)	Mg-sulphide-nasturanium	Metasomatic	PR <sub>1</sub>
INDUSTRIAL MINERALS					
Ceramic and musc. pegmatite	Migmatitic granite assoc. with high-Al gneiss	1. Muscovite Rikolatva, White Sea province (Belomorian belt); Vitim, Mama-Chuya province (Baikal-Patom terrain) Occurrences in Khapchan block, Anabar Shield Tepsa, Gutara-Biryusa belt (Pre-Sayan region) Barga (Yenisey ridge)	Muscovite-quartz-feldspar	Metamorphic-metasomatic	PR <sub>1</sub>  PR <sub>2</sub> ? AR?
Rare metal-muscovite	Migmatitic granite assoc. with high-Al gneiss	Kodakovskoye (Yenisey ridge)	Muscovite	Metamorphic-metasomatic	AR-PR <sub>1</sub>

Phlogopite– Mg skarn	Two-pyroxene schist, calciphyre	Emeldzhak (Aldan terrain); Slyudyanka (West Khamar– Daban)	2. Phlogopite Apatite–magnetite– phlogopite	Metamorphic– metasomatic	PR <sub>1</sub>
REE–P	Carbonatite (?), dolomite (?)	Seligdar (Aldan terrain)	3. Apatite Apatite–dolomite	Carbonatitic (?) metasomatic	PR <sub>1</sub> (?)
Phosphorus P–Fe–Ti (see under “Titanium”) P–Fe–REE	Pyroxenite (?) Carbonatite, alkali ultrabasic	Ukdus (Olyokma terrain) Belaya Zima (“White Winter”) (Pre-Sayan)	Apatite Apatite–magnetite– pyrochlore	Magmatic Carbonatite	AR <sub>2</sub> PR <sub>1</sub>
Talc–magnesite	Dunite–peridotite  Dolomite	Pravdin (Pre-Dnieper block)  Onot, Savvina (Pre-Sayan)  Kirgitey	4. Talc and magnesite Talc–magnesite  Talc–magnesite  Talc–magnesite	Hydrothermal– metasomatic  Hydrothermal– metasomatic  Hydrothermal– metasomatic	AR <sub>2</sub>  AR <sub>2</sub>  R
Chrysotile– asbestos	Dunite–harzburgite	Molodyozhnoye (Baikal–Patom terrain)	5. Chrysotile–asbestos Chrysotile–asbestos	Hydrothermal– metasomatic	PR <sub>1</sub>
Graphitic kinzigite Graphitic gneiss	Kinzigite and khonda- litic carbonaceous Amphibolite–gneiss	Burtyn (Volyn block)  Skalistoye (Kola terrain) Ihala ore field (Ladoga belt), Zavalyevskoye (Volyn block), Petrov group (Kirovograd block), Troitskoye (Pre-Azov block)	6. Graphite Graphite  Graphite	Metamorphic  Metamorphic	AR <sub>2</sub>  AR <sub>2</sub>
Ceramic pegmatites	Migmatitic granite	Kuruvaara etc. (Belomorian, Lyupikko– Ladoga belt); Chuya zone of ceramic pegmatites (Baikal–Patom terrain)	7. Ceramic raw materials Quartz–feldspar	Metamorphic– metasomatic	AR <sub>2</sub> – PR <sub>1</sub>
Pyrites	Keratophyre–spilite	Hautavaara (Karelia terrain)	8. Pyrites Pyrrhotite–pyrite	Stratiform volcano-sedim.	AR <sub>2</sub> – PR <sub>1</sub>

Table 19 (Continued)

Formational type of deposit		Examples of deposits (tectonic block, terrain, belt)	Mineral deposit characteristics		
Ore formation	Host formation		Mineral type	Genetic type	Ore-forming epoch
		9. Quartz			
Quartz-crystal in pegmatites	Anorthosite-rapakivi granite	Volyn pegmatite field (Volyn block)	Topaz-quartz	Pegmatite	PR <sub>1</sub>
Quartz-crystal in quartzites	Quartzite, quartzitic gneiss	Kholodnoye etc. Upper Aldan quartz crystal region (Aldan terrain)	Quartz	Hydrothermal	PR <sub>1</sub>
		10. Shungite			
Shungite	Schist	Zazhogin (Karelia terrain)	Shungite	Metasedimentary	PR <sub>1</sub>
		11. Pyrophyllite			
Quartz-pyrophyllite	Quartz porphyry, sandstone	Zbrankov (Volyn block)	Quartz pyrophyllite	Metamorphic hydrothermal	PR <sub>2</sub>
		12. Fluorite			
Fluorite in carbonates	Carbonate, alkali ultrabasic	Bolshaya Tagna	Fluorite	Carbonate	PR <sub>1</sub> ?
Fluorite in sandstones	Sandstone	Bakhtyn in Podolsk Pre Dnestr region (platform cover on East European craton)	Fluorite	Sedimentary hydrothermal	

Peraluminous kyanite and sillimanite types of raw material are known in all Precambrian regions of the country and constitute targets at various scales, the largest of which is the Keivy kyanite ore basin on the Kola Peninsula.

The most famous Precambrian copper–nickel sulphide ores appear in the Kola terrain of the Baltic Shield. Smaller-scale deposits are known in Karelia, the Voronezh crystalline massif and the Pre-Baikal region, and insignificant ones in other Precambrian regions. Economic-scale deposits in komatiites, which are known in the Precambrian abroad (Kambalda type in Australia, for example) have not been discovered in the former Soviet Union, although indications of copper–nickel mineralization (with heazlewoodite,  $\text{Ni}_3\text{S}_2$ ) have recently been found in serpentinized komatiites in Northern Karelia.

The largest Precambrian copper ore deposits belong to the cupraceous sandstone formation. As well as the known Udokan deposit in the West Aldan Shield, similar deposits have been forecast in other structures in this shield area (Uguy, Dzheltulak), and possibly also in Vendian–Riphean sediments in the Sayan, Baikal and Yenisey basins, formed at the margins of the platform cover of the Siberian craton.

During the last decade, unique massive sulphide and stratiform lead–zinc deposits have been found in Precambrian structures elsewhere: MacArthur River in Australia, Pine Point in Canada, Hamsberg in South Africa, etc. The Kholodnin, Gorevskoye, Sardana, Tabor and other deposits, formed in Riphean fold belts and marginal basins around the Siberian craton, belong to this genetic type. The importance of these types of deposits in the overall balance of lead–zinc ores for the country has increased sharply in recent years, such that the lead–zinc prospects of Precambrian structures in Siberia are far from exhausted. In the East European craton, polymetallic stratiform mineralization in carbonate rocks has been discovered in the Bashkirian basement high, although generally here and in other regions of the craton this type of ore mineralization is less typical. Precambrian shields in the former Soviet Union also characteristically contain rare metal deposits – tantalum, niobium, cesium, REE, genetically related to pegmatites, carbonate alkali and feldspar metasomatites; gold deposits of various types are hosted mainly in the fold structures surrounding the Siberian craton. As distinct from shield areas in Africa, South America and Canada, molybdenum, tin and tungsten deposits are not typical in the former Soviet Union and are found only as minor deposits (Pitkäranta, etc.) and occurrences.

Industrial minerals of Precambrian age largely satisfy the economy in muscovite, ceramic raw materials, graphite, talc, magnesite, phlogopite and piezo-quartz. A new resource – shungite – forms deposits with huge resources in the Onega intracratonic basin in Karelia. Graphitic sediments are common in all the country's Precambrian shields, hosting deposits at various scales of mostly fine platy graphite of the type being extracted from the Zavalyev deposit in the Ukrainian Shield. The deposits contain significant graphite reserves. Economic deposits of phlogopite, talc, magnesite, asbestos, piezo-quartz and fluorite predominate in Precambrian structures of the Siberian craton, but are less typical for the East European craton.

Comparing data on the breadth and the scale of distribution of the various types of mineral deposits in the Precambrian regions of the former Soviet Union and their connection to geological formations (Tables 20, 21), a number of conclusions emerge.

Table 20

## Main genetic types of Precambrian ore deposits in the former USSR

I. Deposits hosted in igneous complexes		
1) in basic and ultrabasic complexes:	2) in intermediate and acid rocks:	3) in alkali-ultrabasic, -basic and alkali rocks:
a) in intrusions (igneous proper, hydrothermal) Cr, Fe-Ti, Cu-Fe-Ti, P-Fe-Ti, Cu-Ni sulphide, anthophyllite-chrysotile-asbestos, talc-magnesite	a) in intrusions (post-magmatic hydrothermal, metamorphic-metasomatic, skarn, greisen) Mo, Cu-Mo, W-Mo, W, Sn, RM-REE, Au, Sb porphyry	a) in intrusions (igneous proper, carbonatites, metasomatic, hydrothermal) R-Fe-RM, CaF <sub>2</sub> -RM, RM-REE, P-Fe-Ti
b) in volcanics (volcano-exhalative, post- magmatic, hydrothermal) Cu-Ni sulphides, Cu, Pb-Zn-pyrites, S-pyrites - volcano-sedimentary	b) not usually hosted in volcanics	b) not usually hosted in volcanics
II. Deposits not usually hosted in weathered mantles (see IV 2a for bauxite weathered mantles and high-Al corundum metamorphic ores)		
III. Deposits hosted in sedimentary assemblages		
1) in clastic terrigenous	2) in carbonates	3) not usually hosted in sulphate halogen rocks
Fe - silica-hematite	Fe - siderite	(some metamorphic B, F, Cl, P-bearing rocks and
Mn - quartz-glaucophane	Mn - carbonate	ores are considered to be altered analogues of sul-
Cu - in sandstones	Pb-Zn - carbonate	phate-halogen rocks - see IV 2b)
quartz crystal	talc-magnesite-carbonate	
1-2 hosted in clastic terrigenous-carbonate-graphitic rocks		
Cu, Pb-Zn, Au, Au-Sb		
IV. Deposits hosted in metamorphic complexes		
1. Metamorphosed, para-metamorphic	2. Metamorphic proper, a) rheo-metamorphic	b) ortho-metamorphic: ceramic, mica, rare-metal,
Fe - quartzites, high-Al deposits, and others	Rich ores; black shale, pyrite, ferruginous quartzite; graphite, kyanite, corundum, apatite and other deposits	quartz crystal pegmatites; Fe-B-apatite skarnoids, phlogopite-rich, metamorphic-metasomatic ores in outer metamorphic zones and ultrametamorphism: Au - quartz, Au - sulphides, and others

Table 21

Examples of genetic types of Precambrian deposits in the East European and Siberian cratons

Ore formation	Host geological formation	Examples of mineral deposits
I. Deposits genetically associated with igneous complexes		
1a. Hosted in basic & ultrabasic igneous intrusive complexes		
Chromite	Dunite-peridotite	Kapitanov (Ukraine)
Iron-titanium	Dunite-pyroxenite-gabbro	Shivero (Yenisey ridge)
	Clinopyroxene-wehrlite	Central (Kola Peninsula)
	Gabbro-gabbro norite	Malotagul (Pre-Sayan)
	Gabbro-labradorite	Tsagin (Kola Peninsula)
	Gabbro-anorthosite	Volodarsk-Volyn (Ukraine)
	Gabbro-diabase	Pudozhgora (Karelia)
Copper-iron-titanium	Gabbro-diorite	Chiney (Aldan)
Phosphorus-iron-titanium	Gabbro-anorthosite	Stremigorod (Ukraine), Gayum,
		Maymakan (Dzhugdzhur-Stanovoy)
Copper-nickel sulphide	Olivinite-harzburgite	Allarechka (Kola Peninsula)
	Olivinite-wehrlite	Lebyazhi (Karelia)
	Dunite-peridotite-gabbro-norite	Nizhnemamon (Voronezh crystalline massif)
	Dunite-troctolite-gabbro	Lukinda (Dzhugdzhur-Stanovoy)
	Peridotite-pyroxenite-norite	Monchegorsk group of deposits (Kola Peninsula)
	Gabbro-wehrlite	Pechenga group (Kola Peninsula)
Apatite	Websterite-gabbro-norite	Lovnozero (Kola Peninsula)
	Pyroxenite (?)	Ukdu (Aldan)
Chrysotile-asbestos	Dunite-harzburgite	Molodyozhnoye (Pre-Baikal)
Talc-magnesite	Dunite-peridotite	Pravdin (Ukraine)
1b. Hosted in basic & ultrabasic volcanics		
Copper-nickel sulphide	Komatiite	Zolotyye Porogi (Karelia)
Pyrites	Keratophyre-spilite	Hautavaara (Karelia)
2. Hosted in acid & intermediate igneous intrusive complexes		
Molybdenum	Gabbro-plagiogranite	Lobash (Karelia)
	Granite	Päävara (Karelia), Okhok (DST)
	Granite-porphry	Jaurijoki (Kola Peninsula)
Cu-Mo porphyry	Leucogranite, alkaskite	Pellapakhk (Kola Peninsula)
W-Mo	Granite	Lyubar (Ukraine)
Tungsten	Anorthosite-rapakivi granite	Latvasyrä (Lake Ladoga)
Fe-Zn-Sn	Anorthosite-rapakivi granite	Pitkäranta, Kitilä (Lake Ladoga)
Cassiterite-silicate	Granite	Tuyukan tin ore region (Pre-Baikal)
Rare metal	Granite	Voronya-Kolmozero zone (Kola Peninsula), Urik-Iy belt (Sayan)
		Davan zone occurrences (Baikal)
Rare metal-rare earth	Granite	Abchada zone occurrences (Baikal)
	Granite-migmatite	Gerfedskeye (Yenisey ridge)
Gold-quartz	Granite	Bogunayevo (Yenisey ridge)
Au-Ag-quartz-sulphide	Granite	Uderey (Yenisey ridge)
Gold-antimony-quartz	Granite	Volyn pegmatite field (Ukraine)
Quartz crystal	Anorthosite-rapakivi granite	
3. Hosted in alkali-ultrabasic, basic & alkali intrusive complexes		
P-Fe-rare metal	Alkali-UB & carbonatite	Belaya Zima (Pre-Sayan)
Fluorite-rare metal	Alkali-UB & carbonatite	Bolshaya Tagna (Pre-Sayan)

Table 21 (Continued)

Ore formation	Host geological formation	Examples of mineral deposits
Rare metal P-Fe-Ti	Alkali-UB & carbonatite Alkal gabbro	Arbarastakh (Aldan) Gremyakha-Vyrmes (Kola Pen.), Yeletozero (Karelia)
Rare metal-rare earth	Alkali-UB & carbonatite Grano-syenite, syenite  Alkali-granite	Chernigov (Ukraine) October, Suschan-Perzhan zone (Ukraine) Katuga ore field (Pre-Baikal), Ulkan ore field (Aldan)
II. Deposits genetically associated with weathered mantles		
Bauxite weathered mantle after dolomite	Dolomite	Gornostil (sedimentary cover on Siberian craton)
III. Deposits genetically associated with sedimentary rocks		
1. Hosted in clastic terrigenous rocks		
Silica-hematite iron ore	Siltstone-sandstone-shale	Angara-Pit basin (Yenisey ridge)
Limonite-hematite iron ore	Quartzose sandstone	Uchuri and Maya ore zones (sedimen- tary cover, Siberian craton)
Mn-rich quartz-glaucinite sandy-clayey	Sandstone-shale	Nikolayevskoye (sedimentary cover Siberian craton, Pre-Sayan)
Cu ore in sandstones	Siltstone-sandstone	Udokan (Aldan)
Quartz crystal	Quartzitic	Upper Aldan quartz crystal region
2. Hosted in carbonate rocks		
Sideritic iron ore	Limestone-dolomite	Bakal (Urals)
Mn-rich carbonate	Silica-carbonate	Porozhin (Yenisey ridge)
Lead-zinc	Carbonate	Gorevsk (Yenisey ridge), Sardana (platform cover, Siberia)
Talc-magnesite	Dolomite	Onot, Savin (Pre-Sayan)
3. Hosted in graphitic clastic terrigenous-carbonate rocks		
Cobalt-copper ore	Dolomite-shale	Kuzoranda (Karelia)
Lead-zinc pyrites	Graphitic-silica-carbonate Black shale	Kholodnin (Pre-Baikal) Linear (Yenisey ridge)
Fluorite-lead-zinc	Graphitic-clayey-carbonate	Tabor (Pre-Baikal)
Gold-sulphide-quartz	Black shale	Sukhoy Log (Pre-Baikal)
Shungite	Graphitic shale	Zazhogin (Karelia)
IV. Deposits genetically associated with metamorphic rocks		
1. Metamorphosed (parametamorphic): the overwhelming majority of types I-III deposits are altered		
2. Metamorphic proper		
2a. Rheometamorphic		
Eulysitic iron ore	Ferruginous-siliceous	Olympiad (Aldan), Baikal (Sayan)
Ferruginous quartzite	Ferruginous-siliceous	Olenegorsk (Kola Peninsula), Kosto- muksha (Karelia), Krivoy Rog basin (Ukraine), Kursk Magnetic Anomaly (Voronezh massif), Chara-Tokk region (Aldan), Vitim ore field (Pre-Baikal)
Aluminous in schists	High-Al schists	Keyvy basin (Kola Peninsula)
	Gneiss-carbonate	Kitoy (Pre-Sayan)
Graphitic gneiss	Amphibolite-gneiss	Skalistoye (Kola Peninsula), Ihala (Lake Ladoga), Zavalyevsk (Ukraine), Nadezhdinskoye (Aldan)

Table 21 (Continued)

Ore formation	Host geological formation	Examples of mineral deposits
Rare metal-phosphorus	Carbonate-dolomite (possibly carbonatite)	Seligdar (Aldan)
2b. Orthometamorphic Ceramic pegmatites		Kuruvaara etc. (Belomorian belt), Pirtima (Ladoga), Chuya ceramic pegmatite zone (Pre-Baikal)
Ceramic & muscovite pegmatites	Migmatite-granite associated with aluminous gneisses	Rikolatva etc. (Belomorian belt), Vitim etc., Mama-Chuya province (Pre-Baikal), Tepsa etc., Gutar-Biryusa belt (Pre-Sayan), Anabar Shield occurrences
Rare metal-muscovite	Migmatite-granite associated with aluminous gneisses Migmatite-granite associated with bt-amph gneisses	Kondakovo (Yenisey ridge)  Bargin (Yenisey ridge)
Rare metal pegmatites	Granite	Voronya-Kolmozero zone (Kola)
Phlogopite-magnesian skarns	Dolomite, pyroxene- amphibole schist	Emeldzhak (Aldan), Slyudyanka (West Khamar-Daban)
Apatite-magnesian skarns	Dolomite, pyroxene- amphibole schist	Emeldzhak (Aldan), Slyudyanka (West Khamar-Daban)
Iron ore-magnesian skarns	Dolomite, pyroxene- amphibole schist	Tayezhnoye (Aldan)

(1) Amongst Precambrian endogenic deposits in the former USSR as in other Precambrian regions around the world, magmatic deposits are represented most fully, hosted in basic and ultrabasic intrusions (Cr, REE, Fe, Ti, Cu, Ni, Co), and metamorphic-metasomatic or hydrothermal-metasomatic, which originated during subsequent alteration (chrysotile-asbestos, talc).

Deposits hosted in basic volcanics are much less important here than in other regions like Canada, Western Australia and India. All that has been discovered in this country to date are large pyrite deposits (Hautavaara, Parandovo, Karelia), solitary polymetallic-pyrite (Kholodninskoye in the Pre-Baikal region), and only signs of copper-nickel occurrences associated with komatiites (Zolotyie Porogi in Karelia).

(2) The "spectrum" of deposits hosted in acid igneous intrusions is much narrower than in Phanerozoic terrains. Only the full range of pegmatitic deposits appears - ceramic, mica, rare-metal and quartz-crystal types. High-temperature metasomatites are also characteristic - feldspathoids, albitites and skarns with rare-metal mineralization (Sn, W, Mo, Ta, Nb, etc. in the Sutschan-Perzhan zone in the Ukraine, the Katuga ore field in Aldan, the Davan zone in the Pre-Baikal region, and others).

A characteristic feature of deposits associated with granitic magmatism is their close genetic and spatial connection with zones of ultrametamorphism and migmatization. Against this background, it is difficult to refer each individual deposit to one particular concrete genetic type. It has already been mentioned above that Precambrian deposits

typically have signs that metasomatites of different affinities are combined together – feldspathites and albitites, albitites in silicification, skarn and greisen zones, etc. Attention is also drawn to “intermediate” genetic types of mineralization between copper–molybdenum–porphyry and copper–massive sulphide, tin–quartz vein greisens and apo-granites (feldspatholitic) and others.

Acid volcanics in Precambrian structures in this country typically remain poor in ores. Extensive zones of hydrothermal alteration are known in which the affected rocks display signs of rare-metal, fluorite, molybdenum, gold, and polymetallic mineralization, increased radioactive contamination, but not a single deposit of practical significance is known. Elsewhere in the world, acid volcanics in orogenic and post-orogenic development stages host major magnetite–apatite ores, such as the Kiruna type (Sweden), also gold and rare metals (Brazil).

(3) Deposits hosted in alkali, alkali–ultrabasic and basic intrusive complexes are very characteristic of Precambrian terrains in the former Soviet Union. However, most of them developed in Precambrian structures much later in time, in the Palaeozoic (Devonian–Carboniferous mainly) and Mesozoic (Triassic and Jurassic) and are related to rifting processes inherited from earlier periods (Khibiny and Lovozero on the Kola Peninsula, Synnyrskoye in the Lake Baikal region, etc.). Separate alkali intrusive complexes with rare metal–rare earth mineralization, apatite, phlogopite and sometimes platinoids appear in the Proterozoic (Gremyakh–Vyrmes in the Kola Peninsula, Yeletzero in Karelia, October in the Ukraine, etc.). This group is represented fairly completely compared with other Precambrian provinces in the world. However, they are less ore-rich in comparison to Phanerozoic alkali complexes.

(4) Sedimentary deposits in Precambrian structures are most complete where they are associated with a group of carbonate and graphitic formations. Riphean polymetallic stratiform deposits (Gorevskoye, Sardana, etc.) in structures surrounding the Siberian craton are the most typical among carbonate formations. Magnesite and siderite deposits are also being exploited (Satka and Bakal in Bashkiria). Clastic terrigenous and carbonate–black shale formations host numerous fields of gold–sulphide, gold–antimony and gold–quartz metamorphic and polymetallic stratiform (“black shale”) types. Deposits hosted in black shale formations usually originate with the widespread participation of subsequent metamorphic and hydrothermal–metasomatic processes, which as we have seen in the example from the Lake Baikal region, the Yenisey ridge and elsewhere, were active in the Palaeozoic or even the Mesozoic. Individual large deposits are also hosted in variegated clastic successions and continental redbeds, in particular the cupraceous sandstone deposits of Udokan (Aldan). Typically non-metamorphic sulphate, halide and boron-rich formations and associated mineral deposits are completely absent from Precambrian sedimentary assemblages.

(5) Deposits in weathered mantles of Precambrian age can be distinguished only provisionally since they can all be classified as metamorphic with justification, because of later high-grade metamorphism, for example the Keivy type of peraluminous schist (Kola Peninsula) or the corundum deposits in Aldan, which are the metamorphosed products of ancient weathered mantles.

(6) The most characteristic feature of Precambrian deposits is the wide distribution of ores belonging to the metamorphic class (para-, ortho-, and rheo-metamorphic).

Practically all Precambrian deposits are metamorphosed. However, the importance of metamorphic processes during the formation of ore bodies in different deposits is highly variable.

Metamorphism in Precambrian deposits, as noted earlier, shows up not only in altered ore structures and textures, ore body morphology, location in shear zones and fold hinges, etc., but in highly altered mineral parageneses. In sum total this produced original skarnoid complexes, metasomatic quartzites, amphibolites, skeletal andalusite-cordierite metasomatites, hisovarite metasomatites with a kyanite-sillimanite composition, and other types. Ores in such deposits are as a rule banded and show signs of intense plastic flow, boudinage and mylonitization. Undoubtedly, the most typical feature of Precambrian deposits is the widespread development of strictly metamorphic deposits, formed during metamorphic differentiation. Some of them – rheometamorphic – originated in previously existing zones, parts of horizons containing higher concentrations of useful components. Examples are graphite, kyanite and apatite (Seligdar type) and apatite-rare earth deposits, rich ore deposits of ferruginous quartzites, pyrite deposits, etc. Others – orthometamorphic – are more intimately related to ultrametamorphic processes and metamorphic-metasomatic formations which were developing simultaneously at higher crustal levels. These deposits were created entirely during metamorphism. In addition to mica, rare-metal and other pegmatites, magnesian skarn deposits with magnetite, apatite, phlogopite and precious stones are usually classified with this type. Also referable to this group might be some purely metasomatic and quartz vein redeposited material in outer metamorphic zones. A particular example would be the Zholtyye Vody type uranium deposit in the Ukraine, certain gold-quartz, gold-carbonate-quartz and gold-sulphide deposits of the Yenisey ridge, the Baikal-Patom region, etc. This subdivision of deposits on the basis of types of raw material, ore formations and formation types (based on relations with geological formations) allows us finally to point out some general features in the metallogeny of the European and Siberian cratons (Table 22).

Table 22

Typical mineral resources of the cratons

Useful minerals	East European craton	Siberian craton
Typical of both cratons	Ferruginous quartzites, Fe-Ti ( $\pm$ V, Cu) hosted in anorthosite and gabbro; ceramic, muscovite, rare-metal pegmatites, rare-metal metasomatites, Sn-W-rare metal skarn-greisen, quartz vein	
More typical of one craton	Cu-Ni, pyrites (Cu-pyrites), U and U-apatite albititic, shungitic, graphitic	Fe-phlogopite-apatite skarn, poly-metallic pyrites, stratiform carbonate and black shale; Au-black shale, Au-Sb, apatite stratiform, talc and magnesite in carbonates, asbestos in ultramafics, Cu-sandstones, optic and piezo-quartz
Atypical	Au-conglomerates, Au-quartz and Au-sulphide in greenstone belts, U-Mo, U-Ni, U-Au-Cu, Cu-Mo-porphyry, Mn carbonate, siliceous, gonditic PGM in layered intrusions	

What are the metallogenic signatures of the East European and Siberian cratons related to? Is it due to differences in the extent to which they have been investigated, or is it a result of differences in geological evolution and geological structure?

The second of these assumptions is well-justified. The present authors have previously noted many specific features which distinguish the two cratons: various quantitative relations between major tectonic structures – granulite–gneiss, granite–greenstone, rift–intra-cratonic; differences in the degree of structural inhomogeneity, in particular, those in the East European craton; asynchronous development with a certain delay in the consolidation of structures in the Siberian craton, etc.

It is especially important for understanding differences in metallogeny between the two cratons to note the much greater distribution of Archaean and Early Proterozoic carbonate successions in supracrustal complexes in Siberia. This also seems to have determined the predominant growth here of phlogopite, talc, magnesite, asbestos and Seligdar-type apatite deposits. However, differences in metallogenic signatures between the East European and Siberian cratons may also have been determined by much deeper factors. We refer back to the “ranging” of the world’s Precambrian shields based on geopotential anomaly, conducted by I.I. Abramovich and I.K. Klushin. These authors concluded from the predominant crustal thicknesses and average P-wave speeds that the shields of the East European craton – the Baltic and Ukrainian – are closer to the Greenland shield and are substantially different from the shields of the Siberian craton – the Aldan and Anabar, which are closer in terms of their deep structure to the Brazilian and Australian shields.

## References

1. Abramovich, G.A., Gundobin, G.M., Ryabenko, V.Ye. and Shames, P.I., 1970. Structural and magmatic controls on the emplacement of rare-metal pegmatite fields in E. Sayan. *Razvedka i okhrana nedr*, no. 3, p. 10–15.
2. Ainberg, L.F., 1933. The Pre-Azov Alkali Intrusion. 184 p.
3. Althausen, M.N., 1937. The Barga deposit. In: *Micas of the USSR*, Moscow, p. 281–309.
4. Amantov, V.A., Kuznetsov, V.A., Matrosov, P. S. (eds), 1988. *Geological Structure of the USSR and Distribution Patterns of Useful Minerals*, vol. 7, Altay–Sayan and Trans-Baikal–Upper Amur regions, pt. 2, Trans-Baikal–Upper Amur region, Leningrad, Nedra, 239 p.
5. Amelin, Yu.V., Belyayev, A., Larin, A. et al., 1991. The Salmi batholith and the Pitkäranta ore field in Soviet Karelia. *Geological Survey of Finland, Guide No. 33*, 57 p.
6. Amelin, Yu.V., Neymark, L.A., Larin, A.M. et al., 1990. Age of ores in the Pitkäranta ore region, North Ladoga, and association with the Salmi rapakivi granite intrusion. In: *Isotopic dating of ore formations*, Abstracts, Kiev, p. 155–157.
7. Andreyev, G.A. (ed.), 1987. Structural and mineralogical constraints on metamorphic ore mineralization—massive sulphide deposits as a case study, Novosibirsk, 166 p.
8. Anon., 1971. The Lena gold ore region, Moscow, Nedra, 163 p.
9. Anon., 1973. Stratiform Copper Deposits of the USSR, Leningrad, Nedra, 312 p.
10. Anon., 1977. Techniques for exploring and evaluating semi-precious stone deposits (jewelry, facing stones and polished stones). No. 17, Garnet. Moscow, USSR Ministry for Geology, 74 p.
11. Anon., 1981a. Metallogenic Map of the BAM Region, 1:1,500,000 scale. Explanatory Memoir, Leningrad, VSEGEI, 140 p.
12. Anon., 1981b. Metallogeny of the Precambrian, Irkutsk, 380 p.
13. Anon., 1983a. Phosphorite and Apatite Deposits of Siberia and the Far East, Novosibirsk, 187 p.
14. Anon., 1983b. Petrochemistry of Precambrian Sedimentary and Volcano-sedimentary Assemblages, Leningrad, Nauka, 256 p.
15. Anon., 1985. *Geological Structure of the USSR and Distribution Patterns of Useful Minerals*, vol. 1, Russian Craton, Leningrad, Nedra, 356 p.
16. Anon., 1988a. *Distribution Patterns of Useful Minerals*, vol. 15, Metallogeny of Siberia, Moscow, Nauka, 269 p.
17. Anon., 1988b. Lead isotopes and ore genesis. *Trudy VSEGEI, new series*, vol. 342, Leningrad, 243 p.
18. Apolsky, O.P., 1982. Tectonic nature of the Kodar–Udokan structural–formational zone. *Doklady Akad. Nauk SSSR*, vol. 256, no. 4, p. 931–934.
19. Apolsky, O.P., 1984. Geotectonic setting of Early Proterozoic cupraceous sandstones, Eastern Siberia. *Doklady Akad. Nauk SSSR*, vol. 277, no. 2, p. 438–442.
20. Arkhangelskaya, V.V., 1974. Rare-metal alkali complexes in the southern margins of the Siberian craton. Moscow, Nedra, 128p.
21. Bakun, N.N. 1958. Conditions of formation and secondary alteration of sedimentary rocks in the Udokan cupraceous sandstone deposit, Chita province. *Izvestiya vuzov. Geol. i razvedka*, no. 11, p. 41–48.
22. Bashta, K.G., 1970. The Molodyozhnoye chrysotile–asbestos deposit. Ore content and structures of deposits in the Buryat ASSR. Ulan-Ude, p. 117–131.
23. Bashta, K.G., 1974. Geology and asbestos content of alpine-type ultrabasics in the region of the Molodyozhnoye chrysotile–asbestos deposit. In: *Asbestos in the USSR*, vol. 1, p. 122–134.
24. Batashov, V.G., Onopriyenko, M.Ye., Kudlayev, A.R. and Tarkhanov, A.V., 1984. The Zholtaya Rechka uranium deposit. Abstracts, 27th Int. Geol. Congress, vol. 9, pt 1, p. 330–332, Moscow, Nauka.
25. Belevtsev, Ya.N. (ed.), 1974. *Metallogeny of the Ukraine and Moldavia*, Kiev, Naukova Dumka, 511 p.

26. Belevtsev, Ya.N., 1981. Development of a theory of ore formation and Precambrian metallogeny in the Ukrainian Academy of Sciences. In: *Ore Formation and Metallogeny*, Kiev, Naukova Dumka, p. 5–36.
27. Belevtsev, Ya.N. (ed.), 1982. Ore deposits of the Ukraine. In: *Excursion Guide C-1*, 4th MAGRM Symp., Tbilisi, Sept. 1982, Tbilisi, Metsniereba, 54 p.
28. Belevtsev, Ya.N., 1985. Conditions of the origin of metamorphic iron–chert formations in the Precambrian of the East European platform. In: *Proc. Conf. Precambrian Metallogeny*, Tabor, May, 1985. Prague, p. 113–116 (in English).
29. Belevtsev, Ya.N. 1986. Geological setting of metamorphosed Precambrian iron ore deposits of the East European craton. In: *Deep Crustal Conditions in Ore Formation*, Moscow, Nauka, p. 114–125.
30. Belevtsev, Ya.N., 1987. Evolution of iron accumulation in the Precambrian crust. *Geol. Zhurnal*, vol. 47, no. 3, p. 3–11.
31. Belevtsev, Ya.N. (ed.), 1988. Ferruginous quartzites in the Precambrian of European USSR: Stratigraphy, Tectonics and Formation Types, 3 volumes, Kiev, Naukova Dumka.
32. Belevtsev, Ya.N., Babkov, Yu.B., Verigin, M.I. et al., 1974. The Krivoy Rog–Kremenchug metallogenic zone. In: *Metallogeny of the Ukraine and Moldavia*, Kiev, Naukova Dumka, p. 412–425.
33. Belevtsev, Ya.N., Batashov, B.G., and Koval, V.V., 1984. Uranium deposits at Zholtyye Vody and the Krivoy Rog iron ore deposit. In: *27th Int. Geol. Congress, Field excursion 108*, Kiev, Naukova Dumka, 32 p.
34. Belevtsev, Ya.N. and Galetsky, L.S., 1984. Metallogeny of the Ukrainian Shield. In: *Geology and Mineral Resources of Ancient Cratons (Indo-Soviet Symposium)* Moscow, Nauka, p. 60–64.
35. Belevtsev, Ya.N., and Yepatko, Yu.M. (eds), 1986. *Metamorphic Ore Formation in the Precambrian. Distribution Patterns and Exploration Criteria for Metamorphic Deposits*, Kiev, Naukova Dumka, 188 p.
36. Belevtsev, Ya.N., Yepatko, Yu.M., Verigin, M.I. et al., 1981. *Iron Ore Deposits in the Ukraine and their Evaluation Forecasts*, Kiev, Naukova Dumka, 230 p.
37. Belkov, I.V., 1963. *The Keivy Kyanite Schists*. Moscow and Leningrad, Acad. Sciences publishers, 321 p.
38. Belkov, I.V. (ed.), 1985. *Magmatic Formations in the NE Baltic Shield*, Leningrad, Nauka, 175 p.
39. Belyayev, A.M. and Lvov, B.K., 1981. Mineralogy and geochemical signature of the Salmi rapakivi granite intrusion. *Vestnik Leningrad State Univ.*, no. 6, p. 15–24.
40. Belyayev, Ye.V., Panskikh, Ye.A., Faizulin, R.M. et al., 1981. Mineral genesis and prospect evaluation of the Dzhugdzhur–Stanovoy apatite province. *Geology and Geophysics*, no. 12, p. 55–63.
41. Bepalko, N.A., 1975. Metasomatites in the Suts chan–Perzhan zone. In: *Criteria for Forecasting Mineral Deposits in the Ukrainian Shield and Surrounding Regions*, Kiev, Naukova Dumka, p. 225–230.
42. Bibikova, Ye.V., Belov, A.Ye., Gracheva, G.V. and Rozen, O.M., 1985. An upper age limit for the granulites of the Anabar Shield. *Izvestiya Akad. Nauk SSSR. Ser. geol.*, no. 8, p. 19–24.
43. Bibikova, Ye.V., Korikovskiy, S. P., Kirnozova, T.I. et al., 1987. Geochronological age determination of rocks in the Baikal–Vitim greenstone belt. In: *Isotopic Dating of Metamorphic and Metasomatic Processes*, Moscow, Nauka, p. 154–164.
44. Bilibina, T.V. (ed.), 1980. *Metallogeny of the Eastern Baltic Shield*, Leningrad, Nedra, 247 p.
45. Bilibina, T.V. and Shaposhnikov, G.N. (eds), 1976. *Geological Formations and Metallogeny of the Aldan Shield*, Leningrad, Nedra, 337 p. (Trudy VSEGEI, new series, vol. 276).
46. Bilibina, T.V., 1985. Global problems in metallogeny and Precambrian tectonics. *Soviet. geol.*, no. 6, p. 19–34.
47. Bilibina, T.V., Kazansky, V.I. and Laverov, N.P., 1984. Main Precambrian ore-bearing structural types. In: *Early Precambrian Metallogeny of the USSR*, Leningrad, Nauka, p. 14–32.
48. Bilibina, T.V., Laverov, N.P., Parfenov, L.M. et al., 1984. Metallogenic provinces in shield areas and their continental tectonic setting. In: *Problems of Precambrian Metallogeny*, Leningrad, Nauka, p. 30–41.
49. Biske, N.S., Bolshakova, V.Z. and Atyutsky, V.I. 1977. Graphite–rich rocks around Ihala. In: *Mineral Raw Materials of Karelia*, Petrozavodsk, p. 47–56.

50. Bogachev, A.I. and Gorelov, V.A., 1968. Structure and ore minerals of the Allarechka Cu-Ni sulphide deposit. In: *Geology of Ore Deposits*, no. 2, p. 74-78.
51. Bogdanov, Yu.V. and Feoktistov, V.P., 1982. A genetic model. *Doklady Akad. Nauk SSSR*, vol. 263, no. 4, p. 949-952.
52. Bogdanov, Yu.V., Kochin, G.G., Kut'yev, E.I. et al., 1966. Copper-rich sediments in the Olyokma-Vitim Highlands, Leningrad, Nedra, 388 p.
53. Brovko, G.N., Li, L.V., Kornev, T.Ya., Okhapkin, N.A. et al., 1986. *Geology and Metallogeny of the Yenisey Ore Belt*, Trudy SNIIGGIMS, Krasnoyarsk, 290 p.
54. Brovko, G.N., Li, L.V., Ponomarev, V.G. et al., 1988. Metallogeny of the Yenisey ridge. In: *Mineral Distribution Patterns*, vol. 15, *Metallogeny of Siberia*, Moscow, Nauka, p. 140-148.
55. Bukharov, A.A., 1987. Proto-activation zones of ancient cratons, Novosibirsk, Nauka, 202 p.
56. Bulakh, A.G. 1982. Genetic types of apatite-rich rocks in the Seligdar deposit. In: *Geology, Exploration and Reconnaissance of Industrial Mineral Deposits*, Leningrad, Leningrad State Univ. Press, no. 6, p. 101-108.
57. Bulakh, A.G. and Zolotarev, A.A. 1983. Geological nature of the Seligdar field of apatite-rich carbonate rocks, Aldan shield. *Soviet. geol.*, no. 6, p. 96-101.
58. Buldygerov, V.V. and Gerasimov, N.S., 1983. The Olokit basin and its metallogeny. In: *Precambrian Basins and Metallogeny, Baikal-Amur Region*, Novosibirsk, Inst. Geol. and Geophys., Siberian Branch, Ac. Sc. USSR, p. 26-27.
59. Bulgatov, A.N. 1983. *Tectonics of the Baikhalides*, Novosibirsk, 192 p.
60. Buryak, V.A., 1975. A Metamorphic-Hydrothermal Type of Economic Gold Mineralization, Nauka, 45 p.
61. Buryak, V.A., 1982. *Metamorphism and Ore Formation*, Moscow, Nedra, 255p.
62. Buryak, V.A., 1987. The formation of gold mineralization in graphitic rocks. *Izvestiya Akad. Nauk SSSR, Geol. series*, no. 12, p. 94-105.
63. Bushev, A.G., 1979. Mica pegmatite veins in the Zhunin deposit, Baikal-Patom Highlands. In: *Criteria for Exploring and Evaluating Mica Pegmatites*, Moscow, VIMS, p. 5-8.
64. Bushmin, S.A., 1990. Connection of ore formation with mineral facies of metasomatic rocks and fluid acidity-alkalinity. An example of the Kholodninskoye deposit, N. Baikal region, E. Siberia. 8th IAGOD, Ottawa, p. A39 (in English).
65. Butvin, V.V., 1987. The pegmatitic granites of the Mama-Oron complex. *Soviet. geol.*, no. 6, p. 89-94.
66. Butvin, V.V., 1988. Pegmatite fields in the N. Baikal muscovite province, PhD thesis abstract, Irkutsk, 17 p.
67. Bykhover, N.A., 1984. *World Distribution of Mineral Resources by Ore-Forming Epochs*, Moscow; Nedra, 576 p.
68. Chechenko, Yu.A. and Baburin, L.M., 1970. Structure of the Chaya intrusion, N. Pre-Baikal. *Izvestiya Akad. Nauk SSSR, Geol. series*, no. 2, p. 151-155.
69. Chechetkin, V.S., 1966. Cu-Ni mineralization in the Chiney gabbro-norite layered intrusion. *Geol. and Mineral Res. of Trans-Baikalia, Chita*, p. 54-56.
70. Chernov, V.M., Inina, K.A., Gorkovets, V.Ya. and Rayevskaya, M.B., 1970. *Volcanogenic Iron-Chert Formations of Karelia*, Petrozavodsk, 285 p.
71. Chernysheva, E.A., Sandimirova, G.P., Bankovskaya, E.B., Kuznetsova, S.V., 1995. Rb-Sr age and Sr isotopic composition in dyke rocks of Pre-Sayan carbonatite complexes. *Doklady Akad. Nauk SSSR*, vol. 345, no. 3, p. 388-393.
72. Chernyshov, N.M., 1971. *Cu-Ni Sulphide Deposits in the SE Voronezh Crystalline Massif*, Voronezh, Voronezh Univ. Press, 312 p.
73. Chernyshov, N.M., 1972. Structural-facies types and Ni content of basic-ultrabasic intrusions in the Mamonov complex, Voronezh massif. In: *Precambrian Geology and Metallogeny of the Voronezh Crystalline Massif*, Voronezh, Voronezh Univ. Press, p. 13-17.
74. Chernyshov, N.M., 1976. Precambrian igneous rocks and their metallogeny in the Voronezh massif. In: *Precambrian Geology and Metallogeny of the Voronezh Crystalline Massif*, Voronezh, Voronezh Univ. Press, p. 55-57.
75. Chernyshov, N.M., 1986a. A new type of Ni sulphide mineralization in the Voronezh massif. *Geol. of Ore Deposits*, no. 3, p. 34-45.

76. Chernyshov, N.M., 1986b. Types of Ni-rich intrusions and Cu-Ni mineralization in the Voronezh massif, *Soviet. Geol.*, no. 12, p. 42-54.
77. Chernyshov, N.M., Bocharov, V.L. and Frolov, S.M., 1981. Ultramafics of the Voronezh massif, Voronezh, Voronezh Univ. Press, 252 p.
78. Chernyshov, N.M., Molotkov, S.P., Kostyukov, V.I. et al., 1978. Petrology and geochemistry of Ni-rich differentiated magma chamber intrusions in the Voronezh massif. In: *Petrological Constraints on the Formation of Cu-Ni Sulphide Deposits and Forecast Criteria*, Petrozavodsk, p. 27-29.
79. Chuyko, D.G. and Lomayev, V.G., 1963. Geology and genesis of the Gorevskoye deposit. In: *New Data on the Geology of the Krasnoyarsk District*, Krasnoyarsk, p. 295-303.
80. Dagalaisky, V.B., 1984. Iron ore formations. In: *Foundations of Metallogeny in Precambrian Metamorphic Belts*, Leningrad, Nauka, p. 144-158.
81. Danilevskaya, G.A., 1987. Mineralogical and tectonic mapping of diopsidic rocks, a new type of mineral resource in the phlogopite deposits of Aldan. In: *Mineralogy and the National Economy*, Leningrad, Nauka, p. 168-169.
82. Datsenko, V.M., 1984. Granitic Magmatism at the SW Margins of the Siberian Craton, Novosibirsk, Nauka, 120 p.
83. Demchenko, V.M., Kuznetsov, V.G. and Chernyshov, G.B., 1967. Manganese prospects in the Pre-Sayan marginal depression. In: *Manganese Deposits of the USSR*, Moscow, Nauka, p. 373-376.
84. Denisova, M.V., 1961. Cu-Ni sulphide mineralization in a basic-ultrabasic intrusion in the Baikal fold terrain. In: *Geology and Mineralogy of Ore Deposits of the USSR*, new series, vol. 60, Leningrad, p. 37-45.
85. Devi, M.N. and Rutshtein, I.G., 1983. Structural geological setting of ferruginous quartzites in the Kodar-Udokan zone in relation to problems of Precambrian troughs. In: *Precambrian Troughs in the Baikal-Amur Region and their Metallogeny*, Novosibirsk, Nauka, p. 50-51.
86. Dibrov, V.Ye., 1958. Geological Structure of the Gutaro-Biryusa Mica Region, Voronezh, Voronezh Univ. Press, 126 p.
87. Distanov, E.G. and Ponomarev, V.G., 1980. Geology and genesis of the Gorevskoye Pb-Zn deposit. *Geology and Geophysics*, no. 12, p. 27-37.
88. Distanov, E.G., 1977. The Massive Sulphide-Polymetallic Deposits of Siberia, Novosibirsk, Nauka, 351 p.
89. Distanov, E.G., Kovalev, K.R., Shobogorov, P.Ch. et al., 1977. Formation of metamorphosed hydrothermal-sedimentary massive sulphide-polymetallic ores in the Kholodninskoye deposit. In: *Genesis of Stratiform Pb-Zn Deposits of Siberia*, Novosibirsk, Nauka, p. 5-43.
90. Distanov, E.G., Kovalev, K.R., Tarasova, R.S. et al., 1982. The Kholodninskoye Massive Sulphide-Polymetallic Deposit in the Precambrian of the Pre-Baikal Region, Novosibirsk, Nauka, 206 p.
91. Distanov, E.G., Ponomarev, V.G. and Kovalev, K.R., 1985. Geological evolution and metallogeny of the Olokit trough, Baikal Highlands. In: *Precambrian Trough Structures in the Baikal-Amur Region and their Metallogeny*, Novosibirsk, Nauka, p. 53-67.
92. Distanov, E.G., Ponomarev, V.G. and Stebleva, A.T., 1971. Geology and Ore Deposits of Central Siberia, Krasnoyarsk, p. 81-83 (*Trudy SNIIGGIMS*, vol. 114).
93. Dobretsov N.L., Gabov, N.F., Volkova, N.I. and Kartovchenko, V.G., 1981. Metamorphism and ore content of sedimentary assemblages around the Kholodninskoye deposit, N. Pre-Baikal region. In: *Petrology and Mineralogy of Metamorphic Formations in Siberia*, Novosibirsk, p. 56-69.
94. Dobretsov, N.L., 1982. Ophiolites and the problem of the Baikal-Muya ophiolite belt. In: *Magmatism and Metamorphism along the Baikal-Amur Railroad (BAM) Zone, and their Role in the Formation of Useful Mineral Deposits*, Novosibirsk, Nauka, p. 11-18.
95. Dobretsov, N.L., Melyakhovetsky, A.A., Ashepkov, I.V. et al., 1987. Structural and Mineralogical Controls on Metamorphic Ore Mineralization, Novosibirsk, Nauka, 166 p.
96. Dobrzhinetskaya, L.F., 1985. Petrochemistry and geochemistry of basic-ultrabasic volcanic and plutonic rocks in the Early Proterozoic Baikal-Vitim greenstone belt. *Geokhimiya*, no. 7, p. 930-945.
97. Dodin, L.L., 1979. The Geology and Mineralogy of Southern Siberia, Moscow, Nedra, 236 p.
98. Doe, B.R. and Stacey, S.S., 1984. The application of lead isotopes to the problem of ore genesis and ore prospect evaluation: a review. *Econ. Geol.*, vol. 69, p. 757-776 (in English).

99. Doe, B.R. and Zartman, R.E., 1979. Plumbotectonics I, the Phanerozoic. In: *Geochemistry of Hydrothermal Ore Deposits*, 2nd edn. New York, Wiley Interscience, p. 22–70 (in English).
100. Dorgan, M.N., Kachan, V.G., Kiseleva, V.S. et al., 1964. Metallogeny of structural regions in the Ukraine, Kiev, Naukova Dumka, p. 120–125.
101. Drannik, A.S. and Bogatskaya, I.V., 1967. New data on the composition, structure and stratigraphic position of the Precambrian Ovruch volcano-sedimentary group. *Problems of Precambrian Sedimentary Geology*, no. 2, Moscow, Nedra.
102. Drugova, G.M., Bushmin, S.A. and Kharitonov, A.L., 1985. Early Precambrian crust-forming processes in the W. Aldan Shield. In: *The Early Precambrian of the Aldan Massif and Adjacent Regions*, Leningrad, Nauka, p. 35–52.
103. Dubrovsky, M.I., 1969. Petrography, mineralogy and geochemistry of the Yuvoaivi granitoid complex. In: *Mineralogy of the Kola Peninsula*, Leningrad, Nauka, p. 26–81.
104. Dubyna, I.V., 1939. Graphite Deposits in the Ukrainian SSR, Kharkov, GONTI NKTP Press, 208 p.
105. Entin, A.R., Belousov, V.M. and Galkin, G.F., 1977. New information on the geology of the Seligdar apatite deposit. In: *Apatites of the Aldan Shield*, Yakutsk, p. 5–16.
106. Entin, A.R., Sobotovich, E.V. and Olkhovik, Yu.A., 1984. Conditions of formation of the Seligdar apatite deposit (Central Aldan). *Soviet. geol.*, no. 8, p. 17–27.
107. Entin, A.R., Tyan, O.A. Makhotko, V.F. and Kravchenko, Ye.M., 1989. Titanio-niobates in Seligdar-type ores. *Soviet. Geol.*, no. 2, p. 83–90.
108. Entin, A.R., Zaytsev, A.I., Nenashev, N.I. and Olshtynsky, S.P., 1987. Genesis of Seligdar-type apatite-carbonate rocks, Aldan. *Doklady Akad. Nauk SSSR*, vol. 237, no. 5, p. 1228.
109. Etingof, M.M., Solovitsky, V.N., Yesipchuk, K.Ye. et al., 1986. Amendments to the correlation of the Precambrian stratigraphic scheme for the Ukrainian Shield. *Geol. zhurnal*, vol. 46, no. 3, p. 3–6.
110. Fedorovsky, V.S., 1985. Lower Proterozoic of the Baikal Mountains – Geology and formation of the continental crust in the Early Precambrian, Moscow, Nauka, 200 p. (*Proc. Geol. Inst. USSR Acad. Sc.*, vol. 400).
111. Fedotova, M.G., 1978. Characteristics of Pb–Zn veins on the southern shores of the Kola Peninsula. In: *Geology and Mineral Resources of the Kola Peninsula*, Apatity, p. 130–136.
112. Fedotova, M.G., Ingurman, V.A. and Menshikov, Yu.P., 1971. Mineralogy of polymetallic ores on the Murmansk coast. In: *Mineralogy of the Kola Peninsula*, Leningrad, Nauka, no. 8, p. 153–167.
113. Fersman, A.Ye., 1941. *Useful Minerals of the Kola Peninsula*, Moscow–Leningrad, USSR Acad. Sc. Publ., 345 p.
114. Flaass, A.S., 1971. Structural evolution of the Mama–Bodaibo Group. *Geotectonics*, no. 6, p. 58–64.
115. Fomin, Yu.M., Yuutev, A.G. and Zorin, B.I., 1987. Discovery of ancient and recent mica ore-controlling structures using satellite images. *Izvestiya Akad. Nauk SSSR, Geol. series*, no. 9, p. 91–99.
116. Frolov, A.A., 1968. Geological structure and apatite content of an intrusion of alkali ultrabasic rocks and carbonatites in E. Sayan, In: *Apatites*. Moscow, p. 198–210.
117. Frolov, A.A., 1993. Carbonatite ring complexes – their metallogeny and criteria for predicting their ore content. *Otechestvennaya Geologiya*, no. 5, p. 21–28.
118. Galetsky, L.S., 1970. A new type of apo-granite. *Geol. Zhurnal*, vol. 30, no. 6, p. 61–71.
119. Galetsky, L.S., 1974. The Volyn metallogenic province. The Sutschan–Perzhan sub-zone. In: *Metallogeny of the Ukraine and Moldavia*, Kiev, Naukova Dumka, p. 374–378.
120. Galetsky, L.S., and Ryabenko, V.A., 1974. The Podolsk metallogenic province. In: *Metallogeny of the Ukraine and Moldavia*, Kiev, Naukova Dumka, p. 386–396.
121. Galetsky, L.S., Gorlitsky, B.A., Kipnis, L.A., et al., ed. Storchak, P.N., 1984. *Geology and Metallogeny of the Precambrian of the Ukrainian Shield*, explanatory memoir to a set of maps at 1:1,000,000 scale. Kiev, Ministry of Geology, Ukrainian SSR.
122. Galetsky, L.S., Kolosovskaya, V.A., Ilkevich, G.I. et al., 1987. Correlation of structures, geological and ore formations between the Ukrainian Shield and the Belorussian and Voronezh crystalline massifs. *Geol. zhurnal*, vol. 47, no. 4, p. 52–59.
123. Galetsky, L.S., Polskoy, F.R. and Taranyuk, M.F., 1986. Carbonaceous formations in the Ukrainian Shield and their ore content. *Geol. zhurnal*, no.1. p. 21–26.

124. Galetsky, L.S., Zaritsky, A.I. and Chernitsyn, V.B., 1987. The evolution of ore-forming systems in the Ukrainian Shield. In: Conditions of Ore Deposit Formation, Proc. 6th MAGRM Symposium, Nauka, vol. 1, p. 102–107.
125. Gavrillov, V.V., Panskikh, Ye.A. and Vorobyov, S.I., 1987. Apatite prospects in the Dzhugdzhur–Stanovoy structural–metallogenic zone. *Razvedka i okhrana nedr*, no. 3.
126. Genkin, A.D., Lapatin, B.A., Savelyev, R.A., Safonov, Yu.G., Sergeev, N.B., Kerzin, A.L., Tsepina, A.I., Amshtuts, Kh., Afanasyeva, Z.B., Vagner, F., Ivanova, G.F. 1994. Gold ore in the Olympiad deposit, Yenisey Ridge, Siberia. *Geology of Ore Deposits*, vol. 36, no. 2, p. 111–137.
127. Gerasimov, Ye.K., Matukhin, R.G. and Sukhoverkhova, M.V., 1978. An apatite-rich formation in a Proterozoic weathered mantle in the Aldan Shield. *Soviet. geol.*, no.4, p.112–119.
128. Gladky, V.N., Galetsky, L.S., Kalyayev, G.I. et al., 1971. Tectonics and metallogeny of the Ukrainian Shield. In: *Regional Tectonics of the Ukraine and Distribution Patterns of Useful Minerals, Abstracts. First Republican Meeting on Tectonics*, Kiev, Naukova Dumka, p. 34–36.
129. Glagolev, A.A., Devi, M.N. and Myznikov, I.K., 1986. Alkali metasomatites in ferruginous quartzite deposits of the Chara Group. *Izvestiya Akad. Nauk SSSR. Geol. ser.*, no. 3, p. 62–75.
130. Glagoleva, A.A. Kravchenko, V.M. and Boronikhin, V.A., 1978. High-grade hypogene iron ores in the Chara–Tökk region, W. Aldan Shield. *Doklady Akad. Nauk SSSR*, vol. 238, no. 5.
131. Glazovsky, A.A., Gorbunov, G.I. and Sysoyev, F.A., 1974. Cu–Ni sulphide magmatic ore deposits. *Ore Deposits of the USSR*, vol. 2. Moscow, Nedra, p. 29–33.
132. Glevassky, Ye.B. and Krivdik, S.G., 1977. Ultrabasic and alkaline rocks in a Precambrian carbonatite complex in the Pre-Azov region. *Geol. zhurnal*, vol. 37, no. 6, p. 95–109.
133. Glevassky, Ye.B. and Krivdik, S.G., 1978. Precambrian carbonatites in the Pre-Azov region, *Geol. zhurnal*, no. 2, p. 83–98.
134. Glevassky, Ye.B. and Krivdik, S.G., 1981a. A Precambrian Carbonatite in the Pre-Azov Region, Kiev, Naukova Dumka, 226 p.
135. Glevassky, Ye.B. and Krivdik, S.G., 1981b. Metallogeny of the Chernigov carbonatite intrusion. In: *Ore Formation and Metallogeny*, Kiev, Naukova Dumka, p. 72–76.
136. Golivkin, N.I. (ed.), 1982. *Precambrian Iron ore Formations in the Kursk Magnetic Anomaly (KMA) and their Evaluation*, Moscow, Nedra. 227 p. (Geol. Production Enterprise Co. of Central Regions).
137. Golovenok, V.K., 1957. Stratigraphy of the NE margin of the Patom Highlands. *Vestnik Leningrad Univ., Geol.–Geog. series*, vol. 4, no. 24, p. 54–64.
138. Golovenok, V.K., 1976. *Lithology, geochemistry and sedimentary environment of the Teptorgo Group in the Baikal Mountains*, Moscow, Nedra, 120 p.
139. Golovko, V.A. and Nasedkina, V.Kh., 1982. Composition and genesis of manganese ores in the Porozhinskoye deposit. In: *Geology and Geochemistry of Manganese*, Moscow, Nauka, p. 104–109.
140. Golovko, V.A., Mstislavsky, M.M., Nasedkina, V.Kh. et al., 1982. Manganese content of the Precambrian in the Yenisey ridge. In: *Geology and Geochemistry of Manganese*, Moscow, Nauka, p. 94–104.
141. Gorbunov, G.I., 1968. *Geology and Genesis of the Pechenga Cu–Ni Sulphide Deposits*, Moscow, Nedra, 353 p.
142. Gorbunov, G.I., (ed.), 1981. *Mineral Deposits of the Kola Peninsula*, Leningrad, Nauka, 272 p.
143. Gorbunov, G.I. and Papunen, H. (eds), 1985. *Cu–Ni Deposits of the Baltic Shield*, Leningrad, Nauka, 329 p.
144. Gorbunov, G.I., Zaytsev, Yu.S. and Chernyshov, N.M., 1969. Main features of the stratigraphy and magmatism of the Voronezh crystalline massif. *Soviet. geol.*, no. 10, p. 8–25.
145. Gorkovets, V.Ya. and Rayevskaya, M.B., 1986. *Iron Ores of Karelia, Petrozavodsk*, 55 p. (Abstract Preprint).
146. Gorkovets, V.Ya., Rayevskaya, M.B., Belonsov, Ye.F. and Inina, K.A., 1981. *Geology and Metallogeny of the Region around the Kostomuksha Deposit, Petrozavodsk*, 143 p.
147. Gorlov, N.V., 1975. Structural basis for forecasting mineral deposits in pegmatites of the NW White Sea region. In: *Muscovite Pegmatites of the USSR*, Leningrad, Nauka, p. 159–162.
148. Goryainov, P.M., 1976. *Geology and Genesis of Iron–Chert Formations in the Kola Peninsula*, Leningrad, Nauka, 146 p.

149. Grechishnikov, N.P. (ed.), 1983. Structures of ore fields and deposits of ferruginous quartzites and high-grade iron ores in the Ukrainian Shield and Voronezh massif, Kiev, 66 p. (Preprint, IMGF Publ., Ukrainian Acad. Sciences).
150. Grishin, M.P., Lotyshev, V.I. and Surkov, V.S., 1982. Structure of the basement of the Siberian craton and its influence on the formation of Riphean basins. In: *Geophysical Methods in Regional Geology*, Novosibirsk, Nauka, p. 102–110 (Trudy Inst. Geol. and Geophys., Siberian Branch, USSR Ac. Sciences, vol. 543).
151. Grivakov, A.G., 1971. Mineralogy of the Slobodovskoye garnet deposit, Vinnitsa province. In: *Geology and Composition of Ore Deposits in the Ukraine*, vol. 4, Scientific Proc. Inst. Mineral Resources, Moscow, p. 119–124.
152. Grokhovskaya, T.L., Distler, V.V., Zakharov, A.A. et al., 1989. Platinum group metals in the Lukulaisvaara layered intrusion, N. Karelia. *Doklady Akad. Nauk SSSR*, vol. 306, no. 3, p. 430–434.
153. Gurulev, S.A. and Shagzhiyev, K.Sh., 1973. Geology and conditions of formation of the Param nephrite deposit, E. Siberia. In: *Industrial Minerals in Ultramafic Bodies*, Moscow, Nauka, p. 234–247.
154. Gurulev, S.A., 1965. Geology and Conditions of Formation of the Yoko-Dovyren gabbro-peridotite intrusion, Moscow, Nedra, 122 p.
155. Haapala, I. and Ramo, O.T., 1990. Petrogenesis of the Proterozoic rapakivi granites of Finland. In: Stein, H.J. and Hannah (eds), *Ore-bearing granite systems: petrogenesis and mineralizing processes*. Geol. Soc. Am. Spec. Paper, vol. 246, p. 275–286 (in English).
156. Haapala, I., 1983. Metallogeny of Precambrian granitoids of Finland. In: *Metallogeny of Precambrian Granitoids*, Moscow, Nauka, p. 25–71.
157. Ignatova, M.D., 1962. The Kirgitey talc deposit. In: *Useful Minerals in the Krasnoyarsk Region*, Moscow, Acad. Sc. USSR Publ.
158. Ilvitsky, M.M. and Shrubovich, F.V., 1969. Cu–Ni sulphide mineralization in the Pravdin ultrabasic intrusion, Central Pre-Dnieper region. In: *Geology and Ores of Southern Ukraine*, vol. 2, Dnepropetrovsk, p. 42–60.
159. Ivanov, A.I., Rozhok, S.N., Strazova, T.M. and Yakovlev, V.P., 1981. A new iron-ore region in Eastern Siberia. In: *Precambrian Metallogeny*, Irkutsk, p. 247–248.
160. Ivantsiv, O.E., 1972. Geology and Genesis of Graphite Deposits in the Ukraine, Kiev, Naukova Dumka, 134 p. (in Ukrainian).
161. Ivashchenko, V.I., 1987. Sn–Sb Skarn Mineralization in the Southern Baltic Shield, Leningrad. Nauka, 240 p.
162. Kahma, A., 1973. The main metallogenic features of Finland. *Bull. Geol. Surv. Finland*, no. 265, p. 1–36 (in English).
163. Kalyayev, G.I., 1967. Metamorphic analogues of geosynclinal sedimentary formations in the Ukrainian Shield. In: *Problems in Precambrian Sedimentary Geology*, Moscow, Nedra, p. 227–237.
164. Kanevsky, A.Ya., 1981. The use of Ni, Co, Cr and Ti concentration coefficients in elucidating the metallogenic signature of ultramafic intrusions in the Central Bug region, Ukrainian Shield. *Geol. zhurnal*, no. 6, p. 117–121.
165. Karpenko, S., Delovan, M.H. and Doe, B.R., 1981. Lead isotope analyses of galenas from selected ore deposits of the USSR. *Econ. Geol.*, vol. 76, p. 716–742 (in English).
166. Kavetsky, M.L., Mkrtchyan, A.K., Storozhenko, A.N. and Ustalov, V.V., 1980. The Porozhinskoye manganese deposit. *Razvedka i okhrana nedr*, no. 3, p. 13–17.
167. Kayryak, A.I., Negrutza, V.Z. and Gumenny, Yu.K., 1975. Gold in the Kareliides. In: *Precambrian Metallogeny. Abstracts, First All-Union Meeting on Precambrian Metallogeny*, Leningrad, p. 74–76.
168. Kazakevich, Yu.P., Sher, S.D. and Zhdanova, T.P., 1971. The Lena Gold Ore Region, vol. 1, Moscow, Nedra, p. 88–133.
169. Kazansky, V.I. and Laverov, N.P., 1977. Uranium deposits. In: *Ore Deposits of the USSR*, vol. 2., (ed. Smirnov, V.I.), Pitman, London (in English).
170. Kazansky, V.I., 1972. *Ore-Bearing Tectonic Structures in Activated Terrains*, Moscow, Nedra, 240 p.
171. Kazansky, V.I., 1988. *Evolution of Precambrian Ore-Bearing Structures*, Moscow, Nedra, 285 p.
172. Khain, V.Ye. and Bozhko, N.A., 1988. *Historical Geotectonics. The Precambrian*, Moscow, Nedra, 382 p.

173. Khazov, R.A., 1973. Geological features of tin mineralization in N. Ladoga, Leningrad, 87 p. (Proc. Geol. Inst. Karelian Branch, USSR Acad. Sc., vol. 15).
174. Khazov, R.A., 1982. Metallogeny of the Ladoga-Bothnian Geoblock, Baltic Shield, Leningrad, 192 p.
175. Khiltova, V.Ya. and Krylov, I.N., 1963. The age of Precambrian formations in the Oka river basin, E. Sayan. In: Absolute Age of Precambrian Rocks of the USSR, Leningrad, Nauka, p. 136-142.
176. Khiltova, V.Ya., 1971. High-Al rocks in the Kitoy Group, E. Sayan: their lithology and conditions of formation. In: Precambrian Lithology, Leningrad, Nauka, p. 96-108.
177. Khlestov, V.V. and Ushakova, Ye.N., 1965. Metamorphism of the Kitoy Group, E. Sayan. In: Genetic and Experimental Mineralogy, Novosibirsk (Proc. Inst. Geol. and Geophys., vol. 36).
178. Khrenov, P.M., 1981. Non-Geosynclinal Volcano-Plutonic Belts in the Continental Massif of Eastern Siberia, Moscow, Nedra, 223 p.
179. Khrenov, P.M., Abramovich, G. Ya., Lobanov, M.P., Popov, Yu.P., 1988. Metallogeny of marginal structures around the Siberian craton. In: Distribution Patterns of Useful Minerals, vol. 15, Metallogeny of Siberia, Moscow, Nauka, p. 100-113.
180. Klitin, K.A., Dolminina, Ye.A. and Rile, G.V., 1975. Structure and age of an ophiolite complex in the Baikal-Vitim elevation. Bull. Moscow Naturalists, Geol. section, vol. 50, no. 1, p. 82-94.
181. Komarov, A.N. and Ilupin, I.P., 1978. New fission-track evidence for the age of kimberlites in Yakutia. Geochemistry, no. 7, p. 1004-1014.
182. Komov, I.L., 1967. New data on magnetite mineralization in the central Yenisey ridge. Soviet. geologiya, no. 9, p. 110-113.
183. Komov, I.L., 1968. Distribution patterns of iron ore deposits in the central Yenisey ridge. In: Geology of Ore Deposits, no. 4, p. 83-86.
184. Komov, I.L., 1969. Geological structure, composition and conditions of formation of the Yenashim magnetite deposit, Yenisey ridge. Geol. i razvedka, no. 3, p. 91-96.
185. Kondratenko, A.K., 1977. Igneous complexes in the central Lena province and their metallogenic signature, Moscow, Nedra, 141 p.
186. Konkina, V.D., Ruchkin, G.V., Ryt'sk, Ye.Yu. et al., 1987. A multidisciplinary approach to forecasting and exploring massive sulphide-polymetallic deposits in Precambrian carbonaceous-clastic assemblages. In: Multidisciplinary Methods in Forecasting and Exploration, vol. 21, Moscow, Nedra, 68 p.
187. Konnikov, Z.G., 1981. The role of the environment in the emplacement of magmatic-hosted mineralization in the Chiny pluton, E. Siberia. In: Geology of Precambrian Mineral Deposits, Leningrad, Nauka, p. 135-147.
188. Korikovskiy, S.P. and Fedorovskiy, V.S., 1980. The Early Precambrian of the Patom Highlands, Moscow, Nauka, 300 p.
189. Korikovskiy, S.P. and Fedorovskiy, V.S., 1983. Correlation of Lower Proterozoic stratified complexes and internal processes in the Olyokma-Vitim mountains and the Patom Highlands. In: Precambrian Stratigraphy of Central Siberia, Leningrad, Nauka, p. 37-50.
190. Korikovskiy, S.P., 1967. Metamorphism, Granitization and Post-Magmatic Processes in the Precambrian of the Udokan-Stanovoy Zone, Moscow, Nauka, 298 p.
191. Korikovskiy, S.P., Sumin, L.V., Arakelyants, M.M. et al., 1985. Age of Precambrian granitoids in central N. Pre-Baikal region, Olokit Zone, using Pb-Pb evaporation and K-Ar techniques. Doklady Akad. Nauk SSSR, vol. 280, no. 3, p. 688-693.
192. Kornev, T.Ya., 1961. Titanium in basic rocks of the Kimbir complex, S. Yenisey ridge. In: Geology and Useful Minerals in the Krasnoyarsk District, Krasnoyarsk, p. 155-160.
193. Kornev, T.Ya., 1971. A new type of volcano-sedimentary iron ore in the Yenisey ridge and its association with massive sulphide mineralization. In: Ore Content and Geology of Central Siberia, Trudy SNIIGGIMS, vol. 114, Krasnoyarsk, p. 83-88.
194. Kornev, T.Ya., 1974. Magmatic-hosted ore deposits in the Yenisey ridge. In: Ore Content and Metallogeny of Structures in the Yenisey Ridge, Krasnoyarsk, p. 3-8.
195. Korzhinsky, D.S., 1937. Petrological analysis of phlogopite and muscovite deposits in E. Siberia. In: Micas of the USSR, Moscow-Leningrad, p. 93-114.
196. Kosygin, Yu.A. and Kulish, Ye.A. (eds), 1984. Main Types of Ore Formations, Moscow, Nauka, 316 p.

197. Kosygin, Yu. A., 1988. *Tectonics*, Moscow. Nedra, 461 p.
198. Kotelnikov, L.G., 1984. In-situ gold deposits on Olkhon island and the genesis of brown iron and manganese ores in the Olkhon district. *Izvestiya Akad. Nauk SSSR, Math. and Natural Sciences Section*, no. 2, p. 209–215.
199. Kozlovsky, Ye.A. (ed.), 1989. *Geological Structure of the USSR and Distribution Patterns of Useful Minerals*, vol. 10, pt. 2, *Distribution Patterns of Mineral Deposits*, Leningrad, Nedra, 611 p.
200. Kozubova, L.A., Mirkina, S.L., Rublev, A.G. and Chukhonin, A.P., 1980. Radiogenic age and composition of the Chivyrkuy pluton, Baikal Highlands. *Doklady Akad. Nauk SSSR*, vol. 251, no. 4.
201. Kratz, K.O. (ed.), 1979. *Main Problems of the Structure of the Russian Platform*, Leningrad, Nauka, 120 p.
202. Kratz, K.O. (ed.), 1983. *The Earth's Crust and Metallogeny of the SE Baltic Shield*, Leningrad, 304 p.
203. Kratz, K.O. (ed.), 1984. *Foundations of Metallogeny of Precambrian Metamorphic Belts*, Leningrad, Nauka, 340 p.
204. Krestin, Ye.M., 1988. The Kursk granite–greenstone terrain. In: *Greenstone Belts in the Basement of the East European Craton, Part 1*, Leningrad, Nauka, p. 15–18.
205. Krivenko, V.A., 1981. The role of tectonic and metallogenic processes in the formation of iron ore deposits in the Kodar range. In: *Metallogeny of the Precambrian. Abstracts, 2nd All-Union Meeting, Irkutsk*, p. 310–312.
206. Krivenko, V.A., 1983. Geology of the Itchilyak "trough", NE Udokan range. In: *Precambrian Troughs in the Baikal–Amur Region and their Metallogeny*, Novosibirsk, p. 68–69.
207. Krogh, T.E. and Gulson, B.L., 1973. Old lead components in the young Bergeell massif, SE Swiss Alps. *Contrib. Mineral. Petrol.*, vol. 40, no. 3, p. 239–252 (in English).
208. Krylov, I.N., Gorokhov, I.M., Kutuyavin, E.P. et al., 1980. Dating of polyphase metamorphic rocks in the Sharyzhalgay Group. In: *Geochronology of Eastern Siberia and the Far East*, Moscow, p. 80–94.
209. Kudryavtsev, V.A., 1982. Tectonic setting and faults in the Chara–Tokk iron ore region. In: *Faults and Endogenic Mineralization of the Baikal–Amur Region*, Moscow, p. 88–101.
210. Kudryavtsev, V.A., 1987. Formational and economic types of Archaean ferruginous quartzites in the Aldan–Stanovoy region. *Soviet. geol.*, no. 4, p. 30–38.
211. Kudryavtsev, V.A., Krylov, V.V., Vollosovich, N.N. et al., 1985. Lower Archaean magnetite quartzites in the Aldan–Stanovoy region—an iron ore source. *Soviet. geol.*, no. 9, p. 51–62.
212. Kulakovskiy, A.L. and Pertsov, A.N., 1987. Allochthonous carbonatites in the Precambrian of Central Aldan. *Izvestiya Akad. Nauk SSSR, Geol. series*, no. 1, p. 52–68.
213. Kulakovskiy, A.L., 1985. Platinoids in rocks and ores of the Tayozhnoye magnetite skarn deposit, Central Aldan. *Doklady Akad. Nauk SSSR*, vol. 381, no. 1, p. 129–133.
214. Kulikov, A.I., Krynkov, V.K., Melnikov, K.M. and Belova, A.B., 1983. The Chiney gabbro intrusion and its ores. *Izvestiya VUZ, Geol. series*, no. 3, p. 19–26.
215. Kushev, V.G., and Sinitsyn, A.V., 1984. The Role of ore–metamorphic processes in the formation of metallogenic assemblages in Precambrian greenstone basins and mobile belts. In: *Regional Metamorphism and Metamorphic Ore Formation*, Kiev, Naukova Dumka, p. 277–286.
216. Kushev, V.G., Bolonev, V.U., Zamoshchikov, M.Ye. et al., 1981. The Tyra iron ore region. N. Pre-Baikal. In: *Geology of Precambrian Mineral Deposits*, Leningrad, Nauka, p. 51–70.
217. Kuzmenko, V.I., 1946. The Petrovo–Gnutovo parsite deposit, Ukrainian SSR. *Soviet. geol.*, no. 12, p. 49–61.
218. Kuznetsov, V.A. (ed.), 1983. *Geology of Ore Deposits in the Baikal–Amur Railroad (BAM) zone*, Novosibirsk, Nauka, 192 p.
219. Kuznetsov, V.A. (ed.), 1985. *Precambrian Troughs in the Baikal–Amur Region and their Metallogeny*, Novosibirsk, 200 p.
220. Kuznetsov, V.G. and Khrenov, P.M. (eds), 1982. *Geological map of the Irkutsk province and adjacent territories, 1:500,000 scale*.
221. Kuznetsov, V.G., 1979. Main distribution patterns of apatites in intrusions of the E. Sayan province of ultrabasic rocks and carbonatites. In: *Major Features of the Geology of E. Sayan*, p. 108–114.
222. Larin, A.M., 1980. Zoned mineralization in the Pitkäranta ore region. *Bull. Moscow Naturalists, Geol. section*, vol. 55, no. 3, p. 73–82.

223. Larin, A.M., 1989. Precambrian rare-metal deposits. In: *Geology of Ore Deposits*, no. 4, p. 12-22.
224. Larin, A.M., Amelin, Yu.V., Neymark, L.A., 1991. Age and genesis of complex skarn ores in the Pitkäranta ore region. *Geology of Ore Deposits*, vol. 33, no. 6, p. 15-33.
225. Larin, A.M., Neymark, L.A., Baskakov, A.V. et al., 1990. Isotope geochronological evidence for the lack of a link between Mo mineralization and granitic magmatism in the Lobash deposit, E. Karelia. In: *Isotopic Dating of Endogenic Ore Formations, Abstracts*, Kiev, p. 118-120.
226. Larin, A.M., Neymark, L.A., Gorokhovskiy, B.M. and Ovchinnikova, G.V., 1990. Relationship between complex skarn mineralization in the Pitkäranta region and rapakivi granites of the Salmi massif from Pb-isotopic data. *Izvestiya Akad. Nauk SSSR, Geol. series*, no. 5, p. 47-57.
227. Larin, A.M., Nikitina, V.D. and Kozlov, V.S., 1981. Tin in limestone skarns in the Pitkäranta ore region, S. Karelia. In: *Genetic Models of Endogenic Ore Formations, Abstracts*, vol. 3, Novosibirsk, p. 57-60.
228. Lazarenko, Ye.K., Pavlishin, V.I., Latysh, V.T. et al., 1973. *Mineralogy and Genesis of Cavity Pegmatites in Volynya, Lvov*, Lvov Univ. Press, 360 p.
229. Lazarev, Yu.I., 1971. *Structural and Metamorphic Petrology of Ferruginous Quartzites in the Kostomuksha Deposit, Leningrad*, Nauka, 192 p.
230. Lazko, Ye.M., Kirilyuk, V.P., Sivoronov, A.A. and Yatsenko, G.M., 1975. *Lower Precambrian of the W. Ukrainian Shield, Lvov, Vishcha Shkola Publ.*, 236 p.
231. Lebedev, A.P., 1962. The Chiney gabbro-anorthosite pluton. *Trudy Inst. Geol. Ore Deposits (IGEM), USSR Ac. Sc.*, vol. 80, Moscow, 100 p.
232. Leonenko, I.N., Golivkin, N.I., Zaytsev, Yu.S. et al., 1976a. Structure and formational sub-division of the Precambrian in the Voronezh crystalline massif. In: *Geology, Petrology and Metallogeny of Crystalline Rocks in the East European Craton. Vol. 1, Geology and Deep Mapping of the Buried Basement*, Moscow, Nedra, p. 83-91.
233. Leonenko, I.N., Raskatov, G.I., Pavlovskiy, V.I. et al., 1976b. Methodology and main results of deep geological and geophysical analysis of the Precambrian of the Voronezh crystalline massif. In: *Geology, Petrology and Metallogeny of Crystalline Rocks in the East European Craton. Vol. 1, Geology and Deep Mapping of the Buried Basement*, Moscow, Nedra, p. 179-189.
234. Lesnov, F.P., 1972. *Geology and Petrology of the Chaya Ni-rich Gabbro-Peridotite-Dunite Pluton, North Pre-Baikal region, Novosibirsk*, Nauka, 228 p.
235. Li, L.V., 1974. Gold mineralization in the S. Yenisey ridge. In: *Mineral Deposits of Central Siberia*, no. 4, Krasnoyarsk.
236. Li, L.V., 1982. Relationship between endogenic mineralization and tectono-magmatic processes in the Angara-Kan micro-craton. *Doklady Akad. Nauk SSSR*, vol. 263, no. 3, p. 676-679.
237. Li, L.V., Mikheyev, V.G., Dorofeyev, A.P. and Bychkov, A.I., 1971. Geological and structural controls on the hosting and ratio of Au and Sb mineralization in the S. Yenisey region, Yenisey ridge. In: *Ore Content and Geology of Central Siberia*, Krasnoyarsk, p. 60-66.
238. Li, L.V. and Shokhina, O.I., 1975. Gold distribution in granitic rocks and indications of gold in intrusions in the Yenisey ridge. In: *Geology of Mineral Resources in the Lower Pre-Angara Region, Krasnoyarsk*, p. 113-119.
239. Li, L.V. and Shokhina, O.I., 1976. Genetic features of gold ore deposits in the Gerfedskoye ore field in the Yenisey ridge. In: *Metallogeny of the Krasnoyarsk District, Krasnoyarsk. (Trudy SNIIG-GIMS, vol. 241)*.
240. Lichak, I.L., 1959. *Pyrophyllite schist deposits of Volynya*. In: *Geology of the USSR*, vol. 5, Moscow.
241. Lichak, I.L., 1972. The Ovruch volcanoclastic assemblage. In: *Stratigraphy of the Ukrainian SSR, vol. 1, Precambrian*, Kiev, Naukova Dumka (in Ukrainian).
242. Litvinovskiy, B.A. and Zankilevich, A.N., 1976. *Palaeozoic Granitic Magmatism in Western Pre-Baikalia, Novosibirsk*, Nauka, 139.
243. Lobach-Zhuchenko, S.B., 1957. Retrograde metamorphism of the Mama quartzite-gneiss group. *Proc. Lab. Precambrian Geol. (LAGED)*, vol. 7, p. 247-267.
244. Lobach-Zhuchenko, S.B., 1963. A lazulite discovery in the Baikal Highlands. *Trans. All-Union Min. Soc. (VMO)*, series 2, part 92, p. 714-715.

245. Lobach-Zhuchenko, S.B. (ed.), 1988. Greenstone Belts in the Basement of the East European Craton, Leningrad, Nauka, 212 p.
246. Lobanov, M.P., 1966. The Davan shear zone (NW Pre-Baikal) and its relationship with dynamo-metamorphism, metasomatism and ore mineralization. In: *Geology and Mineral Resources of the Baikal-Patom Highlands*, Irkutsk, p. 168-184.
247. Lugov, S.F. (ed.), 1986. *Geology of Tin Ore Deposits of the USSR*, vol. 2, pt 2, Moscow, Nedra, 200 p.
248. Lutz, B.G., 1964. Granulite Facies Petrology of the Anabar Massif, Moscow, 124 p.
249. Lutz, B.G., 1984. Mantled gneiss domes in the Anabar massif and Aldan Shield. *Bull. Moscow Naturalists, Geol. section*, vol. 85, no. 2, p. 27-35.
250. Makarova, G.V., 1971. Tungsten occurrences around NW Ladoga, Karelia. In: *Mineralogy and Geochemistry of Tungsten Deposits*, Leningrad Univ. Press, p. 205-207.
251. Makrygina, V.A., 1981. *Geochemistry of Medium- and Low-Pressure Regional Metamorphism and Ultrametamorphism*, Novosibirsk, Nauka, 198 p.
252. Malich, N.S., Masaytis, V.L., Surkov, V.S. (eds), 1987. *Geological Structure of the USSR and Distribution Patterns of Useful Minerals*, vol. 4, Siberian Craton, Leningrad, Nedra, 356 p.
253. Manches, G., Minster, J.F. and Allègre, C.J., 1978. Comparative U-Th-Pb and Rb-Sr study of the St Severin amphoterite: consequences for early Solar System chronology. *Earth and Planet. Sci. Letters*, vol. 39, no. 1, p. 14-24 (in English).
254. Manuylova, M.M., Vaskovsky, D.P. and Gurulev, S.A., 1964. *Precambrian Geology of the North Pre-Baikal Region*, Moscow-Leningrad, Nauka, 226 p.
255. Marakushev, A.A., 1958. Petrology of the Tayozhnoye iron ore deposit in the Archaean of the Aldan Shield. *Trudy Far Eastern Branch, USSR Acad. Sc., Geol. series, Magadan*, vol. 5, p. 1-121.
256. Mashchak, M.S., 1973. Petrochemistry of diabase and dolerite dykes, S. Anabar Shield. In: *Geology and Geochemistry of Basic Rocks in the East Siberian Craton*, Moscow, p. 78-86.
257. Medvedkov, V.I., 1981. The Lower Angara deposit. In: *Iron Ore Deposits of Siberia*, Novosibirsk, Nauka (Siberian Branch), p. 134-135.
258. Mekhanoshin, A.S., Glazunov, O.M. and Burmanina, G.V., 1980. *Geochemistry and Ore Content of Metagabbros, Eastern Sayan*, Novosibirsk, Nauka, 102 p.
259. Metalidi, S.V. and Nechayev, S.V., 1983. *The Sutschan-Perzhan Zone: Geology, Mineralogy and Ores*, Kiev, Naukova Dumka, 136 p.
260. Metalidi, V.S., Bukovich, I.P., Vysotsky, V.L. et al., 1986. A new complex molybdenum deposit in the Ukrainian Shield. *Geol. zhurnal*, no. 5, p. 102-105.
261. Meyer, C., 1984. Ore-forming processes in geological history. In: *Genesis of Ore Deposits* (Skinner, B.M., ed.), vol. 1, p. 13-71 (in English).
262. Mikhailov, D.A. and Klimov, L.V., 1959. Geology of iron ore deposits. In: *Precambrian Geology of the Aldan Mining Region*. Proc. Lab. Precambrian Geology (LAGED), vol. 8, p. 266-318.
263. Mikhailov, D.A., 1973. *Precambrian Ore-rich Mg-Ca Metasomatites*, Leningrad, Nauka, 144 p.
264. Mikhailov, D.A., 1978. Origin of Precambrian ore-rich magnesian skarns. *Izvestiya Akad. Nauk SSSR, Geol. series*, no. 12, p. 145-151.
265. Mikhailov, D.A., 1983. *Metasomatic Origin of Precambrian Ferruginous Quartzites*, Leningrad, Nauka, 168 p.
266. Mikhailov, D.A., 1986. Constraints on Precambrian Ore-rich Metasomatites, Leningrad, Nauka, 112p.
267. Mikhailova, N.S., 1985. Proterozoic microphytofossils in the western Aldan Shield and the internal zone of the Patom Highlands. *Bull. Moscow Naturalists, Geol. section*, vol. 60, no. 4, p. 95-104.
268. Mirkina, S.L., Zhidkov, A.Ya., Chukhonin, A.P. et al., 1977. Multidisciplinary isotope geochronological study of rocks and ores in the Kholodninskoye deposit. *Geochemistry*, no. 6, p. 854-862.
269. Mironyuk, Ye.P. and Petrov, A.F., 1976. The role of faults in the location of prospective ferruginous quartzite deposits in the western Aldan Shield. In: *Fault Tectonics of the Yakutsk ASSR*, Yakutsk, p. 126-135.
270. Miroshnikov, A.Ye., Brovko, G.N., Golyshev, S.I. and Okhapkin, N.A., 1977. Carbonaceous matter in Riphean sulphide-rich black shales in the Linear Pb-Zn deposit, Yenisey ridge. *Lithology and Mineral Resources*, no. 3, 141-148.

271. Mkrtychyan, A.K., Savinyak, Yu.V., Ustalov, V.V. and Tsykin, R.A., 1982. Manganese formations in the Yenisey ridge. In: *Geology and Geochemistry of Manganese*, Moscow, Nauka, p. 89–94.
272. Moralev, V.M. (ed.), 1986. *Structure of the Earth's Crust in the Anabar Shield*, Moscow, Nauka.
273. Moralev, V.M. and Shmakin, B.M., 1976. Tectonic and physico-chemical conditions of formation of Precambrian pegmatite fields in India. *Geotectonics*, no. 1, p. 130–133.
274. Moralev, V.M., 1978. Typical features of the metallogeny and tectonic nature of Precambrian greenstone belts. In: *Problems of Precambrian Metallogeny*, Leningrad, Nauka, p. 205–211.
275. Moseikin, V.V., Konkin, V.D. and Kuznetsova, T.P., 1982. Geochemical zoning of ore bodies in the Kholodninskoye massive sulphide–polymetallic deposit. *Geology of Ore Deposits*, no. 6, p. 74–84.
276. Mukhin, V.A., 1962. Zones of increased tectonic activity in the western Aldan Shield and association with quartz crystal veins. *Trudy VNIIP*, vol. 7, p. 77–87.
277. Musatov, D.I., Ustalov, V.V., Kachevsky, L.K. et al., 1980. Precambrian manganese mineralization in the Yenisey ridge. In: *New Data on Manganese Deposits in the USSR*, Moscow, Nauka, p. 200–205.
278. Musatov, D.P., Levitova, F.N. and Chernyshov, N.M., 1981. Deep structure of the Anabar Shield. In: *General and Regional Geology and Geological Mapping*, Moscow, p. 1–17 (Review of VIEMS, no. 6).
279. Nadelyayev, K.M., 1958. The Onot talc and magnesite deposit. In: *Light metal Resources of Eastern Siberia*, Moscow, Acad. Sc. USSR Publ., p. 265–272.
280. Narseyev, V.A., Kurbanov, N.K., Konstantinov, M.M. et al., 1989. *Gold Exploration and Forecasts*, Moscow, TSNIGRI, 237 p.
281. Nechayev, S.V., 1978. Geological and geochemical nature of ore mineralization in the sedimentary cover of the western part of the East European craton, Kiev, Naukova Dumka, 192 p.
282. Nechayev, S.V., Yegorova, L.N. and Sharkin, O.P., 1987. Polytypy and rhenium-rich molybdenite in the Ukrainian Shield, their practical application and scientific significance. *Geol. zhurnal*, no. 1, p. 78–88.
283. Nedashkovsky, P.G., 1986. *Rare-Metal Alkali-Granite Pegmatites and Fenites*, Moscow, Nauka, 89 p.
284. Neymark, L.A., 1988. Ore Pb isotopes and the origin of deposits. In: *Isotope Geochemistry of Ore-Forming Processes*, Moscow, Nauka, p. 99–116.
285. Neymark, L.A., Amelin, Yu.V., Larin, A.M., 1994. Pb–Nd–Sr isotopic and geochemical constraints on the origin of the 1.54–1.56 Ga Salmi rapakivi granite–anorthosite batholith (Karelia, Russia). *Mineralogy and Petrology*, vol. 50, p. 173–193 (in English).
286. Neymark, L.A., Larin, A.M., Yakovleva, S.Z. et al., 1991. New data on the age of the Akitkan group in the Baikal–Patom fold belt, from results of U–Pb dating of zircons. *Doklady Akad. Nauk SSSR*, vol. 320, no. 1, p. 182–186.
287. Neymark, L.A., Mirkina, S.L., Rublev, A.G. et al., 1987. Age of the Irel granitic complex. Pre-Baikal region, from isotopic evidence. *Izvestiya Akad. Nauk SSSR. Geol. series*, no. 5, p. 18–25.
288. Neymark, L.A., Ovchinnikova, G.V., Gorokhovskiy, B.M. et al., 1990a. Age and origin of gold ore deposits in the Baikal Highlands. In: *Isotopic Dating of Endogenic Ore Formations, Abstracts*, Kiev, p. 230–232.
289. Neymark, L.A., Rytsk, Ye.Yu., Levchenkov, O.A. et al., 1990b. An Early Proterozoic–Upper Archaean age for the Olokit complex (N. Pre-Baikalia) using U–Pb geochronology. In: *Precambrian Geology and Geochronology of the Siberian Craton and Margins*, Nauka, p. 206–222.
290. Neymark, L.A., Sokolov, Yu.M., Drubetskoy, Ye.R. et al., 1990c. Age of regional metamorphism and muscovite pegmatite formation in the Mamo–Bodaibo depression, Baikal Mountains. In: *Isotopic Dating of Endogenic Ore Formations, Abstracts*, Kiev, p. 130–131.
291. Nikolayev, A.F., Faizullin, L.D. and Ismagilov, I.Sh., 1985. Main graphite-bearing provinces and regions of the USSR, Moscow, 30 p. (*Geol. methods for industrial mineral exploration, VIEMS Review*).
292. Nosikov, V.V., 1960. Kyanite deposits in the Kola–Karelia region as a new raw material base for the refractory industry. In: *Geology and Mineral Resources of the NW Russian Federation*, vol. 2, p. 47–67.
293. Nozhkin, A.D. and Boldyrev, M.V., 1979. Riphean volcanism, tectonic zoning and metallogeny of the Yenisey ridge. *Geology and Geophysics*, no. 10, p. 47–61.

294. Nozhkin, A.D., 1985. Early Precambrian trough complexes in the SW Siberian craton and their metallogeny. In: *Precambrian Trough Structures of the Baikál-Amur Region and their Metallogeny*, Novosibirsk, Nauka, p. 34–46.
295. Odintsov, M.M., 1972. Structural–metallogenic regional mapping of eastern Siberia. *Geology and Geophysics*, no. 6, p. 15–26.
296. Oganessian, L.V., 1983. Structural constraints on Precambrian rock crystal mineralization in the southern Aldan Shield. *Express Information. VIEMS*, no. 1, p. 11–20.
297. Okhapkin, N.A., Miroshnikov, A.Ye., Brovko, G.N. and Kornev, T.Ya., 1976. Characteristics of ore targets in the Yenisey polymetallic belt. In: *Polymetallic Mineralization of the Yenisey ridge*, Krasnoyarsk, p. 38–52.
298. Orlov, V.P., Golivkin, N.I., Dimitriyev, V.P. et al., 1984. Metallogenic Regions and an Evaluation of Forecasts for Iron Ore Reserves in the Kursk Magnetic Anomaly, Kiev, 56 p. (Preprint, IGF, Ukrainian Acad. Sc.).
299. Osadchiy, V.K. and Stadnik, V.A., 1977. Genesis of carbonatite complex rocks, Chernigov zone, western Pre-Azov region. In: *Mineralogical Criteria for Rare and Non-Ferrous Metal Exploration in the Ukrainian Shield. Abstracts, Republican Symp., Dneprorudnoye, May 1977*. Kiev, Naukova Dumka, p. 112.
300. Osokin, A.S., 1987. Distribution and Composition of Apatite–Titanomagnetite–Ilmenite Ores in the Gremyakhá–Vyrmes Intrusion, Apatity, 90 p.
301. Ovchinnikova, G.V., Larin, A.M., Neymark, L.A., Gorokhovskiy, B.M., Sergeeva, N.A., 1995. Pb-isotopic constraints on the origin of the Lobash Mo-porphry deposit, E. Karelia, Russia. *Precambrian of Europe: Stratigraphy, Structure, Evolution and Mineralization. Abstracts, 9th Meeting of MAEGS, Russian Acad. Sciences, St Petersburg*, p. 83–84.
302. Panskikh, Ye.A. and Sukhanov, M.K., 1982. Geological structure, petrology and ore content of anorthosite massifs of the Far East, USSR. In: *Petrology and Ore Content of Natural Rock Associations*, Moscow, Nauka, p. 138–157.
303. Panskikh, Ye.A., 1986. Genetic types of ilmenite ores in the Far East and their conditions of formation. In: *Pacific Geology*, Novosibirsk, Nauka, no. 2, p. 83–87.
304. Parfenov, L.M., 1963. Tectonics of Siberia, vol. 2, Novosibirsk, Siberian Branch, USSR Acad. Sc. Publ.
305. Parfenov, V.D. and Yudin, N.I., 1976. Apatite in the Precambrian of Central Aldan. *Doklady Akad. Nauk SSSR*, vol. 229, no. 5, p. 1192–1194.
306. Parfenov, V.D. and Yudin, N.I., 1982. Metamorphic Apatite in Ancient Assemblages of Central Aldan, Moscow, Nauka.
307. Parfenov, V.D., Chekhovskiy, M.M. and Yudin, N.I., 1987. Types and prospects of metamorphic apatite mineralization in Central Aldan. *Soviet. geol.*, no. 8, p. 66–80.
308. Pavlov, V.A. and Cherdakov, V.I., 1985. Iron ore distribution patterns in the Dyosovo deposit, S. Yakutia. *Geology of Ore Deposits*, no. 1, p. 40–47.
309. Pavlov, V.A., Cherdakov, V.I. and Komarov, P.V., 1986. Factors controlling ore mineralization, and criteria for forecasting and evaluating the Aldan iron ore region. *Soviet Geol.*, no. 12, p. 54–65.
310. Pearce, J.A., Harris, N.B.W. and Tindle, A.G., 1984. Trace element discrimination diagrams for the tectonic interpretation of granitic rocks. *J. Petrology*, vol. 25, no. 4, p. 956–983 (in English).
311. Pekki, A.A. and Razorenova, V.I., 1977. Ceramic pegmatites of Karelia. In: *Mineral Resources of Karelia*, Petrozavodsk, p. 15–26.
312. Perevozchikova, V.A. (ed.), 1974. Tectonics of the Eastern Baltic Shield, Leningrad, Nedra, 288 p.
313. Pertsev, N.N. and Kulakovskiy, A.L., 1988. An Iron-Rich Assemblage in Central Aldan. Moscow, Nauka, 237 p.
314. Petrov, R.P., Karpenko, V.S. and Mershchersky, Yu.A., 1969. *Uranium Deposits in Precambrian Iron Ore Formations*, Moscow, Atomizdat, 72 p.
315. Petrova, Z.I. and Levitsky, V.I., 1984. Petrology and Geochemistry of Granulite Complexes in the Pre-Baikal Region, Novosibirsk, Nauka, 200 p.
316. Petrovskaya, N.V., Safronov, Yu.G. and Sher, S.D., 1976. Formations of gold ore deposits. In: *Ore Formations of Endogenic Deposits*, Moscow, Nauka, vol. 2, p. 3–110.
317. Peyve, A.V. et al., 1977. Ophiolites: the current situation and research problems. *Geotectonics*, no. 6, p. 4–12.

318. Plaksenko, N.A. and Shchegolev, I.N., 1977. Major features of metallogeny of supracrustal assemblages in the Precambrian of the Kursk Magnetic Anomaly. In: *Geology of the Kursk Magnetic Anomaly*, Voronezh, Voronezh Univ. Press, no. 1, p. 3–11.
319. Plaksenko, N.A., 1966. Major Patterns of Sedimentary Iron Ore Deposition in the Precambrian of the Kursk Magnetic Anomaly, Voronezh, Voronezh Univ. Press, 264 p.
320. Plaksenko, N.A., Chernyshov, N.M., Shchegolev, I.N. et al., 1976. Precambrian ore formations in the Voronezh crystalline massif. In: *Precambrian Geology and Metallogeny of the Voronezh Crystalline Massif*, Voronezh, Voronezh Univ. Press, p. 50–54.
321. Pochtarenko, V.I. and Bachay, L.V., 1974. Molybdenum in the Lyubarskoye and other sectors of the western Ukrainian Shield. In: *Criteria for Forecasting Mineral Deposits in the Ukrainian Shield and Surroundings*, Kiev, Naukova Dumka, p. 334–336.
322. Poletayev, I.A., Shames, P.I. and Shcherbakov, A.F., 1975. Geological structure of the Savina magnetite deposit. In: *Geology and Mineral Resources of Eastern Sayan*, Mem. Irkutsk Geol. Surv.
323. Poletayev, I.A., Shames, P.I. and Shcherbakov, A.F., 1979. Geological Structure of the Savina magnetite deposit. In: *Main Geological Features of Eastern Sayan*, Irkutsk, p. 114–125.
324. Polkanov, A.A., Yeliseyev, N.A., Yeliseyev, E.N., Kavardin, G.I. et al., 1967. The Gremyakha–Vyrmes Intrusion, Kola Peninsula. Moscow–Leningrad, Nauka, 236 p.
325. Poltorykhin, P.I., 1986. Metalliferous deposits in the Precambrian, SW part of the East European craton. *Soviet. geol.*, no. 12, p. 64–69.
326. Polyakov, M.V., 1936. *Geology of the Northern group of deposits in the Onot Iron Ore Region*, Irkutsk, 106 p.
327. Ponomarev, V.G., 1974. Stratiform massive–polymetallic deposits in Proterozoic sediments of the Yenisey ridge. *Geol. and Geophysics*, no. 11, p. 59–66.
328. Popov, V.Ye., 1975. A new type of deposit in tectonomagmatic terrains: southern Karelia and other regions. In: *Distribution Patterns of Useful Minerals*, vol. 11, Moscow, Nauka, p. 235–243.
329. Popov, V.M., 1962. Genesis of Stratiform Deposits of Non-Ferrous Metals. *Izvestiya Kirgiz Acad. Sc.*, no. 2.
330. Popov, V.Ye. (ed.), 1985. Analysis of ore content in prospective areas of the Baltic Shield. *Trudy VSEGEI*, new series, vol. 235, 288 p.
331. Popov, V.Ye. and Rundqvist, D.V. (eds), 1984. Metallogenic Map of the Kola–Karelia Region, 1:1,000,000 scale. Leningrad, VSEGEI.
332. Proskurin, G.P., 1984. Apatite–ilmenite mineral zoning in gabbros of the Korosten pluton. In: *Vertical Zoning in Magmatic Ore Deposits*, Moscow, Nauka, p. 44–67.
333. Proskurina, V.P., 1974. Structures controlling pegmatite emplacement in the NE Yenisey region. In: *Muscovite pegmatites of the USSR*. Leningrad, Nauka, p. 159–162.
334. Pukharev, A.I., 1959. Geology and hosting of south Yakutian iron ore deposits. *Geol. Ore Deposits*, no. 1, p. 70–76.
335. Rabkin, M.I., 1959. Geology and Petrology of the Anabar crystalline shield. *Trudy NIIGA*, vol 87, 164 p.
336. Reshetnyak, V.V. and Yefimenko, N.G., 1984. Iron–chert formations in the Krivoy Rog iron ore basin. *Geol. zhurnal*, no. 5, p. 18–25.
337. Reznitsky, L.Z., Vasilyev, Ye.P., Vishchnyakov, V.N. et al., 1989. Quartz–diopside rocks in southern Pre-Baikalia. *Izvestiya VUZ, Geol. and Expl.*, no. 3, p. 54–63.
338. Robonen, V.I. and Rybakov, S.I., 1983. Massive sulphide deposits of Karelia. In: *Pyrites Deposits of the USSR*, Moscow, Nauka, p. 162–178.
339. Robonen, V.I., Rybakov, S.I., Ruchkin, G.V. et al., 1978. Massive sulphide Deposits of Karelia. Leningrad, Nauka, 192 p.
340. Roganov, G.V. and Seleznev, N.N., 1986. Agricultural Resources of the Baikal–Amur Railroad (BAM) Region. In: *Pacific Geology*. Novosibirsk, Nauka, no. 2, p. 88–96.
341. Romanov, I.A. and Gerasimov, N.S., 1987. Rb–Sr dating of Precambrian acid rocks of the Malo-Tagul deposit, eastern Sayan. In: *Geology, Tectonics, Petrology and Ore Deposits in the Precambrian of the Siberian Craton and Surroundings*. Abstracts. Irkutsk, p. 226–227.
342. Romanovich, I.F., 1973. Deposits in European Russia and Trans-Caucasia. Dnepropetrovsk–Zaporozhets region. In: *Talc Deposits of the USSR*, vol. 2. Moscow, Nedra, p. 27–28.

343. Rozen, O.M. and Dimroth, E., 1982. Ancient meta-greywackes in the basement of the continental crust: investigation of primary mineral composition – examples from Canada and the USSR. In: *Sedimentary Geology of High-Grade Precambrian Metamorphic Complexes*, Moscow, Nauka, p. 155–179.
344. Rozen, O.M., 1981. Enderbitic rocks of Anabar and the grey gneiss problem. In: *Ancient Granitoids of the USSR–Grey Gneiss Complexes*, Leningrad, Nauka, p. 125–135.
345. Rub, M.G., Pavlov, V.A., Gladkov, N.G. and Yashukhin, O.N., 1982. Tin- and Tungsten-rich Granitoids in the USSR, Moscow, Nauka, 261 p.
346. Ruchkin, G.V., 1984. *Precambrian Stratiform Polymetallic Deposits*, Moscow, Nedra, 238 p.
347. Ruchkin, G.V., Bogovin, V.D., Donets, A.K. et al., 1977. Pb–Zn mineralization in Vendian carbonate assemblages in the SE Yakutia–Sardana ore region. *Geol. Ore Deposits*, no. 4.
348. Ruchkin, G.V., Bushuyev, V.P., Varlamov, V.A. et al., 1975. The Kholodninskoye deposit – a representative Precambrian massive sulphide–polymetallic deposit. *Geol. Ore Deposits*, no. 5, p. 3–17.
349. Ruchkin, G.V., Konkin, V.D. and Kuznetsova, T.P., 1973. Metamorphism of massive sulphide–polymetallic ores in the Kholodninskoye deposit, north Pre-Baikal region. *Geol. Ore Deposits*, no. 6, p. 67–78.
350. Rudenko, S.A., 1962. Genesis and textural features of mariupolites. *Trans. Leningrad Mining Inst.*, vol. 23, no. 2, p. 3–35.
351. Rudenko, V.Ye. and Rudenko, Yu.L., 1979. *Reconstruction of Precambrian Metamorphic and Metasomatic Rocks*, Novosibirsk, Nauka, 172 p.
352. Rundqvist, D.V. (ed.), 1981. *Ore Content and Geological Formations in Crustal Structures*, Leningrad, Nauka, 423 p.
353. Rundqvist, D.V. (ed.), 1986. *Evaluation Criteria in Forecasting Useful Mineral Deposits of Regions*, Leningrad, 751 p.
354. Rundqvist, D.V. and Mitrofanov, F.P. (eds), 1993. *Precambrian Geology of the USSR*. Amsterdam, Elsevier, 528 p. (in English).
355. Rundqvist, D.V. and Sokolov, Yu.M., 1986. Major metallogenic epochs in the Precambrian of the European part of the USSR. In: *Int. Conf. on Metallogeny of the Precambrian (IGCP Proj. 91)*, Czech Geol. Survey (UUG), Prague, p. 93–109 (in English).
356. Rundqvist, D.V. and Turchenko, S.I., 1989. Precambrian tectonic structures of the Siberian craton and their ore content. In: *Precambrian Geology and Geochronology of the Siberian Craton and Surrounding Fold Belts*, Leningrad, Nedra.
357. Rundqvist, D.V., 1990. Geological evolution and metallogeny of the Baikallides. In: *Fundamental Problems in Ore Formation and Metallogeny*, Leningrad, Nauka, p. 44–65.
358. Rusakov, N.F. and Kravchenko, G.L., 1986. Structure of the Chernigov carbonatite intrusion. *Geol. zhurnal.*, no. 4, p. 112–118.
359. Rusakov, N.F., Lapchuk, A.J. and Sinitza, A.N., 1980. Discovery of new carbonatites in W. Pre-Azov. *Geol. zhurnal*, no. 2, p. 151–153.
360. Ryabenko, V.A. and Moskina, O.D., 1978. A graphitic clastic terrigenous assemblage in the Ukrainian Shield and associated graphite deposits. *Geol. zhurnal*, no. 2, p. 22–111.
361. Ryabenko, V.A., 1976. Basic distribution patterns of mineral deposits in Ukrainian Shield structural belts. In: *Tectonics and Stratigraphy*, Kiev, Naukova Dumka, no. 10, p. 30–35.
362. Rybakov, S.I. and Kulikov, V.S., 1985. Nature and dynamics of evolution of Archaean greenstone belts in the Baltic Shield. In: *Precambrian Trough Structures of the Baikal–Amur Region and their Metallogeny*, Novosibirsk, Nauka, p. 164–170.
363. Rybakov, S.I., Kulikov V.S., Chekulayev, V.P. et al., 1987. Ore prospects in Archaean greenstone belts in the basement to the East European craton. In: *Geology and Ore Prospects of Ancient Cratonic Basements*, Leningrad, Nauka.
364. Salop, L.I., 1964. *Geology of the Baikal Mountains*. vol. 1. Stratigraphy, Moscow, Nedra, 515 p.
365. Salop, L.I., 1967. *Geology of the Baikal Mountains*. vol. 2. Magmatism, Tectonics and Geological Evolution, Moscow, Nedra, 669 p.
366. Salop, L.I., 1973. *General Stratigraphic Scale of the Precambrian*, Leningrad, 309 p.
367. Salye, M.Ye. and Glebovitsky, V.A., 1976. *Metallogenic Signature of Pegmatites*, Leningrad, 188 p.

368. Salye, M.Ye., 1975. Metallogenic pegmatite formations in the eastern Baltic Shield. In: *Muscovite Pegmatites of the USSR*, Leningrad, Nauka, p. 15–36.
369. Sazonov, E.A., Zvyagina, A.E., Romanovsky, A.E., Shvedov, G.I., Leontiyev, S.I., 1995. Apo-schist Au-bearing metasomatites of beresite formation (Yenisey Ridge). *Geology and Geophysics*, no. 4, p. 53–61.
370. Semenenko, N.P. (ed.), 1975. *Constraints on Forecasting Mineral Deposits in the Ukrainian Shield and Adjacent Areas*, Kiev, Naukova Dumka, 560 p.
371. Semenenko, N.P., Ladyeva, V.D., Bordunov, I.N. et al., 1978. *Ferruginous Quartzite Formations of the Ukrainian Shield*, vol. 1, 327 p., vol. 2, 367 p.
372. Semeykin, N.I., 1972. Lithofacies characteristics of Proterozoic clastic sediments in the south Iya-Urik graben. In: *Geology and Gold Content of Riphean and Vendian Conglomerates in the southern Margins of the Irkutsk Amphitheatre*, Irkutsk, p. 26–45.
373. Shafeyev, A.A. and Buinov, Yu.D., 1981. Magnetite quartzites in eastern Sayan. In: *Iron Ore Deposits of Siberia*, Novosibirsk, p. 76–77.
374. Shakhov, G.P., 1983. Intrusive calciphyres in the river Sutam basin. *Doklady Akad. Nauk SSSR*, vol. 272, no. 4, p. 941–946.
375. Sharov, V.N., Shmotov, A.P. and Konvalov, I.V., 1978. *Metasomatic Zoning and Associated Mineralization*, Novosibirsk, 102 p.
376. Shchegolev, I.N., 1981. Precambrian iron formations in the Kursk Magnetic Anomaly and the Ukrainian Shield. *Geol. zhurnal*, no. 5, p. 62–69.
377. Shchegolev, I.N., 1985. *Precambrian Iron Ore Deposits and their Investigation*, Moscow, Nedra, 197 p.
378. Shcheka, S.A., 1969. *Petrology and Ores in Ni-Rich Dunite-Troctolite Intrusions in the Stanovoy Range*, Moscow, Nauka, 133 p.
379. Shcherbak, N.P., Artemenko, G.V., Bartnitsky, Ye.N. et al.; ed. Sobotovich, E.V., 1989. *Geochronological Scale for the Precambrian of the Ukrainian Shield*. Kiev, Naukova Dumka, 144 p.
380. Shcherbakov, A.F. and Poletayev, I.A., 1977. Magnesite ores in the Savin deposit. *Lithology and Mineral Resources*, no. 6, p. 85–98.
381. Sher, S.D., 1959. Basic igneous veins in the Bodaibo river basin and their association with quartz veins. In: *Handbook on the Geology of Ferrous, Non-Ferrous and Rare Metals*, Moscow, vol. 4, p. 104–114.
382. Shergina, Yu.P., Larin, A.M., Chukhonin, A.P. et al., 1982. Age of the Salmi rapakivi granite intrusion and associated mineralization. *Izvestiya Akad. Nauk SSSR, Geol. series*, no. 12, p. 64–76.
383. Shergina, Yu.P., Murina, G.A. and Kozubova, L.A., 1980. Rb-Sr age of Barguzin granites. *Trudy VSEGEI, new series*, vol. 307, p. 108–115.
384. Sherman, M.L., 1968. The Gorevskoye Pb-Zn deposit. In: *Geological Research in the Krasnoyarsk District and Tuva*, Kyzyl, p. 32–38.
385. Shirobokov, I.M., 1961. The Kitoy sillimanite schist deposit. In: *Geology and Mineral Resources of the Irkutsk Province*, Irkutsk, vol. 1.
386. Shishkin, N.N., 1964. Cu-Ni sulphide mineralization in the Yoko-Dovyren basic-ultrabasic intrusion. *Geol. of Ore Deposits*, no. 1, p. 93–98.
387. Shmakin, B.M. (ed.), 1978. *Mineralogy of the Pre-Baikal Region*. Irkutsk, 222 p.
388. Shmakin, B.M., 1976. *Muscovite and Rare Metal-Muscovite Pegmatites*. Novosibirsk, Nauka, 367 p.
389. Shpunt, P.R. and Sochneva, E.G., 1981. Early Riphean carbonatites in the Anabar massif. *Doklady Akad. Nauk SSSR*, vol. 289, no. 4, p. 946–951.
390. Sinitsyn, A.V., Kushev, V.G. and Markov, Ye.I., 1986. Tectonic regions of the Ukrainian Shield. *Vestnik Leningrad Univ., Geol. and Geog.*, vol. 1, no. 6, p. 5–11.
391. Sizykh, A.I., 1978. Structure of the Biryusa belt and stages in its formation. In: *Crustal Dynamics of Eastern Siberia*, Novosibirsk, Nauka, p. 102–112.
392. Sizykh, A.I., 1985. *Petrology of Metamorphic Belts in the North Pre-Baikal Region*. Novosibirsk, Nauka, 120 p.
393. Sizykh, V.I. (ed.), 1978. *Tectonics and Metallogeny of Eastern Siberia*. Irkutsk, Irkutsk Univ. Press, 190 p.

394. Smirnov, A.D., Altukhov, Ye.I. and Buldakov, I.V., 1967. Ripheids of Southern Siberia and Structural Setting of Pegmatites, Moscow, Nauka.
395. Smirnov, F.L., 1980. Geology of Apatite Deposits of Siberia, Novosibirsk, Nauka.
396. Smirnov, V.I. (ed.), 1974. Ore Deposits of the USSR, 3 vols, London, Oliver & Boyd (in English).
397. Smirnov, V.I. (ed.), 1981. A Course in Ore Deposits, Moscow, Nedra, 348 p.
398. Smirnov, V.I., 1982. Geology of Mineral Resources, Moscow, Nedra, 669 p.
399. Smolin, P.P., 1961. The Kirgitey low-Fe talc deposit, Krasnoyarsk district. In: Talc – a Mineral and a Resource, Moscow, Acad. Sc. Publ. (Trudy IGEM, no. 63).
400. Smolin, P.P., 1962. Distribution patterns of economic talc deposits in the USSR and constraints on valuable Fe-free talc. In: Distribution Patterns of Mineral Resources, Moscow, Acad. Sc. Publ., p. 493–548.
401. Smolin, P.P., Shevelev, A.I., Urasina, L.P. et al., 1984. Genetic Types, Distribution Patterns and Forecasts of Brucite and Magnesite Deposits, Moscow Nauka, 318 p.
402. Sochava, A.V., 1986. Upper Archaean and Proterozoic Petrochemistry of the Western Aldan-Vitim Shield, Leningrad, Nauka, 144 p.
403. Sokolov, V.A. (ed.), 1975. Shungites of Karelia and their Utilization, Petrozavodsk, 240 p.
404. Sokolov, V.A. (ed.), 1981. Shungitic Rocks in Karelia, Petrozavodsk, 175 p.
405. Sokolov, V.A. (ed.), 1982. Geology of Shungitic Proterozoic Volcano-Sedimentary Formations in Karelia, Petrozavodsk, 208 p.
406. Sokolov, V.A. (ed.), 1987. Geology of Karelia, Leningrad, Nauka, 231 p.
407. Sokolov, Yu.M., 1965. Preliminary sketch of geological and geochronological regional distribution of pegmatites in the Baikal-Patom pegmatite belt. In: Absolute Age of Precambrian Rocks of the USSR, Leningrad, Nauka, p. 167–174.
408. Sokolov, Yu.M., 1970. Metamorphic Muscovite Pegmatites, Leningrad, Nauka, 189 p.
409. Sokolov, Yu.M., 1982. Cycles of mineral formation in the tectono-metamorphic evolution of the Baikal fold terrain. In: Magmatism and Metamorphism in the Baikal-Amur Railroad (BAM) Region and their Role in the Formation of Useful Mineral Deposits, Novosibirsk, Nauka, p. 29–35.
410. Sokolov, Yu.M. (ed.), 1988. Multidisciplinary exploration criteria for mica pegmatites in the White Sea region. Leningrad, Nauka, 152 p.
411. Sokolov, Yu.M. et al., 1966. Garnet as a criterion for delimiting pegmatite fields. In: Precambrian Geology and Geochronology, Moscow-Leningrad, Nauka, p. 312–322 (Proc. Lab. Precambrian Geol. (LAGED), vol. 19)
412. Sokolov, Yu.M. and Kovaleva, S.Yu., 1983. Tectono-metamorphic cycles in the Baikal Mountains and their metallogenic signature. In: Metamorphism of the Precambrian in the Region of the Baikal-Amur Railroad, Leningrad, Nauka, p. 199–226.
413. Sokolov, Yu.M. and Kratz, K.O., 1984. Metallogenic pulses of internal crustal activity in the Precambrian. In: Early Precambrian Metallogeny of the USSR, Leningrad, Nauka, p. 4–14.
414. Sokolov, Yu.M., Glebovitsky, V.A. and Turchenko, S.I., 1975. Genetic classification of metamorphic-type useful mineral deposits. Sov. geol., no. 2, p. 52–66.
415. Sokolov, Yu.M., Sumin, L.V., Timofeyev, B.V. et al., 1985. Geological age of metamorphic and ore formations of the Baikal-Patom fold terrain. Geol. Ore Deposits, no. 1, p. 48–57.
416. Sokolov, Yu.M., Turchenko, S.I. and Bushmin, S.A., 1981. Geology and genesis of the Kholodninskoye deposit. In: Geology of Precambrian Useful Mineral Deposits, Leningrad, Nauka, p. 167–233.
417. Stacey, V.S. and Kramers, V.D., 1975. Approximation of terrestrial lead isotope evolution by a two-stage model. Earth and Planet. Sci. Letters, vol. 13, no. 2 (in English).
418. Stanton, R.L. and Russell, R.D., 1959. Anomalous leads and the emplacement of lead sulfide ores. Econ. Geol., vol. 54, no. 4 (in English).
419. Stebleva, A.T., 1971. The Uderey antimony deposit. In: Ore Deposits and Geology of Central Siberia, Krasnoyarsk, p. 81–83 (Trudy Krasnoyarsk SNIIGGIMS, vol. 114).
420. Sukhanov, M.K. and Rachkov, V.S., 1984. Apatite-rich gabbro-norites of the Anabar Shield. Izvestiya Akad. Nauk SSSR, Geol. series, no. 12, p. 115–118.
421. Sukhanov, M.K. and Zhuravlev, D.Z., 1989. Sm-Nd dating of Precambrian anorthosites of Dzhugdzhur. Doklady Akad. Nauk SSSR, vol. 304, no. 4, p. 964–968.

422. Suslov, A.T. and Andrushchenko, P.F., 1967. New data on the mineral composition and structure of ores in manganese deposits in the Pre-Sayan manganese region. In: *Manganese Deposits of the USSR*, Moscow, Nauka, p. 377–406.
423. Sviridenko, V.T. and Kudryavtsev, B.Ye., 1975. Petrochemistry and ore content of the Chiney lopolith. *Geol. and Geophysics*, no. 10, p. 35–47.
424. Sviridenko, V.T. and Terentyev, V.M., 1978. Magmatic evolution and plutono-magmatic formations of the Kodar–Udokan region in relation to their metal ore content. *Trudy VSEGEI, new series*, vol. 302, p. 21–34.
425. Tankilevich, I.M. and Kulikovskiy, V.K., 1977. Pyrophyllite formation in Upper Proterozoic Ovruch Group rocks. In: *Geology, Hydrogeology, Geochemistry and Geophysics of the Ukraine and the RSFSR (Russian Federation)*, Kiev. *Vishcha Shkola*, vol. 13, p. 40–42.
426. Tankilevich, I.M., 1976. New information on the genesis of pyrophyllite in rocks of the Ovruch Group, Upper Proterozoic. *Geol. zhurnal*, no. 3, Kiev, Naukova Dumka, p. 88–96.
427. Tankilevich, I.M., 1977. Pyrophyllites in the NW Ukrainian Shield, PhD Thesis Abstract, Kiev.
428. Tarasenko, V.S. and Panskikh, Ye.A., 1982. A new genetic type of apatite–ilmenite ores in gabbro-anorthosite intrusions of the Korosten pluton, Ukrainian Shield. *Acad. Sc. USSR Publ., Geol. Series*, no. 11, p. 100–110.
429. Tarasov, Ye.V., Galkin, G.A. and Dorokhin, V.K., 1975. Pegmatite distribution patterns in the N. Baikal muscovite province. In: *Muscovite Pegmatites of the USSR*, Leningrad, Nauka, p. 191–197.
430. Tarasova, R.S., Mogilev, V.A. and Dobretsov, N.L., 1981. Structural features and structural and metamorphic evolution of the Kholodninskoye massive sulphide–polymetallic deposit. *Geology and Geophysics*, no. 4, p. 34–46.
431. Tarkhanov, A.V. and Poluarshinov, G.P., 1989. Spatio-chronological position of Precambrian uranium deposits. In: *Metallogenesis of Uranium Deposits*, Vienna, JAEA, p. 201–210 (in English).
432. Tarkhanov, A.V., Kudlayev, A.R., Petrin, A.V. and Kozyrkov, V.D., (in press). The first economic V–Sc deposit.
433. Tatarinov, P.M. (ed.), 1969. *A Course in Industrial Mineral Deposits*, Moscow, Nedra, 472 p.
434. Tatarinov, P.M. and Artemov, V.R. (eds), 1967. *Chrysotile–Asbestos Deposits of the USSR*, 512 p.
435. Tayersky, V.M. and Tayerskaya, Z.K., 1961. New data on the stratigraphy of the Mama crystalline belt. In: *Geology and Mineral Resources of the Irkutsk District*, Irkutsk, vol. 1, p. 7–39.
436. Terentyev, V.M., Komaristy, A.K., Rudnik, V.A. et al., 1973. An Early Proterozoic age for meta-somatic rocks in the Baikal structural suture zone. In: *Absolute Age of Ore Deposits and Younger Magmatic Processes*, Abstracts, 28th Int. Geol. Congress, Moscow, Nauka, p. 79–81.
437. Tishkin, A.I., Tarkhanov, A.V. and Streltsov, A.A., 1990. *Uranium Deposits in Ancient Shields*, Moscow, Nedra, 144 p.
438. Tretyakov, G.A., Mikhailov, Yu.Ya. and Kalugin, I.A., 1981. Fault tectonics and structural control of iron ore mineralization in the Charo–Tokk region of Yakutia. *Geology and Geophysics*, no. 7, p. 37–42.
439. Truneva, M.F., Gurulev, O.A., Zhmodin, S.M. and Ogurtsov, A.M., 1979. Genesis of Cu–Ni sulphide ores in the Chaya deposit. In: *Contact Effects and Mineralization in Gabbro–Peridotite Intrusions*, Moscow, Nauka, p. 97–107.
440. Tsarovskiy, I.D., 1954. Structural types of alkaline rocks in the Ukrainian SSR. *Izvestiya Akad. Nauk SSSR, Geol. series*, no. 4, p. 101–112.
441. Tsarovskiy, I.D., 1964. Nepheline syenites in Central Pre-Dnieper and Pre-Azov regions. *Proc. Lab. Precambrian Geol. (LAGED)*, vol. 19, p. 272–276.
442. Tsarovskiy, I.D. and Kravchenko, G.L., 1962. Structure of the south Kalchik syenite intrusion, eastern Pre-Azov region. *Doklady Akad. Nauk SSSR*, no. 2.
443. Tugarinov, A.I., Varlamov, V.A., Karpenko, S.F. et al., 1976. Lead isotopic composition of galena in the Kholodninskoye deposit and host rocks. *Geochemistry*, no. 2, p. 202–210.
444. Turchenko, S.I., 1978. *Metallogeny of Metamorphic Sulphide Deposits of the Baltic Shield*, 120 p.
445. Turchenko, S.I., 1992. Precambrian metallogeny related to tectonics in the eastern part of the Baltic Shield, *Precambrian Research*, vol. 58, p. 121–141 (in English).

446. Tychinsky, A.A., Sinchuk, Yu. A., Shipilov, L.D. and Pokrovsky, I.G., 1977. Source of ore material and genesis of stratiform Pb-Zn mineralization – the Pre-Baikal polymetallic ore belt. In: *Genesis of Stratiform Pb-Zn Deposits of Siberia*, Novosibirsk, Nauka, p. 111–119.
447. Uchitel, M.S. and Korobeynikov, V.V., 1966. The east Sayan iron ore province, Irkutsk district, Irkutsk (Proc. Irkutsk Polytech. Inst., vol. 30), p. 109–116.
448. Vaasjoki, M.O., 1981. The lead isotopic composition of some Finnish galenas. *Geol. Surv. Finland, Bull.* 316, 25 p. (in English).
449. Valeyev, R.N., 1978. *Aulacogens in the East European Craton*, Moscow, Nedra, 153 p.
450. Velikoslavinsky, D.A., Kazakov, A.N. and Gerling, E.K., 1961. Age of geological formations in the north Baikal Highlands, *Proc. Lab. Precambrian Geol. (LAGED)*, no. 12, p. 281–290.
451. Velikoslavinsky, D.A. and Sokolov, Yu.M., 1960. The relationship between the genesis and mineralization of pegmatites in the Mama region and regional metamorphism, *Zap. VMO*, vol. 12, part 89, p. 208–213.
452. Verger, V.I., 1962. Structural controls on the emplacement of quartz crystal veins in the southern Aldan shield. *Trudy VNIIP*, vol. 7, p. 61–77.
453. Vilor, N.V., Fefelov, N.N., Solodyankina, V.N. and Brandt, S.B., 1982. Isotopic composition of ore lead in some Sayan-Baikal deposits. *Geology and Geophysics*, no. 3, p. 65–70.
454. Vinogradov, A.N. and Vinogradova, G.V., 1987. The ore-magmatic system of the Yuvoaivi granite-porphphy complex, *Apatity*, 92 p.
455. Vishnevsky, A.N., 1978. *Metamorphic Complexes of the Anabar Shield*, *Trudy NIIGA*, vol. 184, Leningrad, Nedra, 213 p.
456. Volobuyev, M.I., Stupnikova, N.I. and Zykov, S.I., The Yenisey ridge. *Geochronology of the USSR*, vol. 1, Leningrad, Nedra, p. 189–202.
457. Volobuyev, M.I. and Zykov, S.I., 1963. Age and geochemical features of lead occurrences in the Yenisey ridge. *Geology and Geophysics*, no. 12, p. 22–31.
458. Votakh, O.A., 1968. *Precambrian Tectonics of the Western Edge of the Siberian Craton*, Moscow, Nauka, 136 p.
459. Votakh, O.A., Zhabin, V.V. and Kozlov, G.V., 1978. The Yenisey ridge. In: *Precambrian of the Continents. Fold Belts and Young Platforms of Eastern Europe and Asia*, Novosibirsk, Nauka, p. 38–56.
460. Yakovlev, Yu.A., Yakovleva, A.K., Balabonin, N.A. and Orsoyev, D.A., 1979. *Cu-Ni Ores in a Granulite Complex*, Leningrad, 208 p.
461. Yakzhin, A.N., 1937. The Kondakovskoye deposit. In: *Micas of the USSR*, Moscow.
462. Yanovsky, V.M., 1990. *Ore-Controlling Structures in Clastic Miogeosynclines*, Moscow, Nedra, 244 p.
463. Yegin, V.I. and Kichagin, L.N., 1973. Characteristics of and prospects for apatite mineralization in Central Aldan. *Novosti geologii, Yakutsk*, vol. 3, no. 3, p. 87–90.
464. Yegorov, I.I., Ovchinnikov, I.P. and Nikiforov, K.A., 1966. A new type of fluorite ore. *Razvedka: okhrana nedr*, no. 9.
465. Yeliseyev, N.A., Gorbunov, G.I., Yeliseyev, E.N. et al., 1961. *Ultrabasic and Basic Intrusions of Pechenga*, Moscow-Leningrad, USSR Acad. Sc. Publ., 357 p.
466. Yeliseyev, N.A. and Kushev, V.G., 1964. Intrusions of alkali-earth syenites, their internal structure and chemistry, Pre-Azov region. *Proc. Lab. Precambrian Geol., (LAGED) USSR Acad. Sc.*, vol. 19, p. 255–271.
467. Yeliseyev, N.A., Nikolsky, A.P. and Kushev, V.G., 1961. *Metasomatites in the Krivoy Rog ore belt*. *Proc. Lab. Precambrian Geol., (LAGED) USSR Acad. Sc.*, vol. 13, 204 p.
468. Yeliseyev, N.A., Yeliseyev, E.N., Kozlov, Ye.K. et al., 1956. *Geology and Ore Deposits of the Monchegorsk Pluton*, Moscow, Leningrad, Acad. Sc. Publ., 328 p.
469. Yemelyanov, A.A., Kastykina, V.M. and Kastykin, Yu.P., 1985. New data on the geological structure and metallogeny of the Dzheltulak trough. In: *Precambrian Troughs in the Baikal-Amur Region and their Metallogeny*, Novosibirsk, Nauka, p. 151–157.
470. Yeskin, A.S., 1969. Ancient metamorphic complexes in the western Pre-Baikal region. In: *Geology of the Pre-Baikal Region*, Irkutsk, p. 114–149.
471. Yeskin, A.S., Ez, V.V., Grabkin, A.V. et al., 1979. *Correlation of Internal Processes in Precambrian Metamorphic Complexes, Pre-Baikal Region*, Novosibirsk, Nauka, 118 p.

472. Yeskin, A.S., Obulov, S.P. and Feldman, M.S., 1975. Stages of Precambrian Magmatism, Leningrad, Nauka, p. 70-71.
473. Yeskin, A.S., Odintsov, M.M., and Belichenko, V.G., 1969. The oldest metamorphic complexes in the Pre-Baikal region. *Geol. and Geophys.*, no. 7, p. 21-25.
474. Yudin, B.A., 1987. Fe-Ti Oxide and Fe Ores in Igneous Rocks of Karelia and the Kola Peninsula, Petrozavodsk, 209 p.
475. Zamanshchikov, M.Ye. and Bashta, K.G., 1966. The Molodyozhnoye chrysotile-asbestos deposit, Buryat ASSR. *Razvedka i okhrana neдр*, no. 5, p. 5-9.
476. Zartman, R.E., 1984. Pb, Sr and Nd isotopic characteristics of ore deposits and their dependence on geological setting. In: *Metallogeny and Ore Deposits, 27th Int. Geol. Congress, Section 12, Moscow, Nauka, vol. 12, p. 44-56.*
477. Zartman, R.E. and Doe, B.P., 1981. Plumbotectonics. The model. *Tectonophysics*, vol. 75, no. 1-2, p. 135-162 (in English).
478. Zavalishin, M.A. and Lvova, N.A. 1954. Stratigraphy and geological structure of the NE Mama region. *Trudy Giproniislyuda (Proc. Mica Research Inst.)*, vol. 13, p. 4-72.
479. Zaytsev, Yu.S., Ageykin, A.S., Golyshkina, R.I. et al., 1970. New data on the Precambrian geology of the SE Voronezh crystalline massif. In: *Precambrian Petrography of the Russian Craton. Proc. First Regional Meeting on the Petrography of European USSR, Kiev, Naukova Dumka, p. 59-73.*
480. Zhdanova, V.V. and Dayn, A.A., 1975. Gold mineralization in the Precambrian of the Kola Peninsula. In: *Metallogeny of the Precambrian. Abstracts, First All-Union Meeting on Precambrian Metallogeny, Leningrad, p. 76-77.*
481. Zlobenko, I.F., Dusyatsky, V.A. and Fomin, A.B., 1977. Cu-Ni sulphide occurrences in the west Ukrainian Shield. *Razvedka i okhrana neдр*, no. 2, p. 8-11.
482. Zubkov, V.V., Konkin, V.D. and Solovyov, Ye.B., 1990. Zoning in massive sulphide-polymetallic ore mineralization and carbonaceous clastic terrigenous-flyschoidal assemblages. *Obzor VIEMS, Moscow, p. 44.*
483. Zubkov, Yu.D., 1986. Morphology and prospects of the Legliyer magnetite skarn deposit, southern Yakutia. *Geology and Geophysics*, no. 8, p. 118-123.

## Index of Deposits

- Aivar, 17  
 Akkim, 38  
 Aleksandrov, **130**  
 Alenguy, 238  
 Allarechka, **12**, 37, 389, 412, 419  
 Anangra, 349  
 Angara-Pit iron ore basin, 293, 326, 410, 420  
 Annama, 38  
 Annin, 170  
 Arbarastakh, 420  
 Arshan, 366, 371  
 Azov graphite region, **144**
- Baikal, 410, 420  
 Bakal group, 174, 410  
 Bakhtyn, 177  
 Balakhovskoye, 141  
 Barginskoye, 420  
 Bazardaya Guba, 42, 413  
 Begim-Chokrak, **136**  
 Belgorod type ore, **164**  
 Belozimin, 415, 419  
 Beregov type ore, **161**  
 Bergaul, 71  
 Besedin type ore, **161**  
 Bezmyannaya, **27**  
 Biboy, 252  
 Bogide, 238-239  
 Bogunayevoye, 271, 273-274, 315, 414, 419  
 Bolotnoye, **199**  
 Bolshaya Gleyevatka, 118  
 Bolshe-Severnoye, 349  
 Bolshetagnin, 416, 419  
 Bolshezero, 53  
 Bolshoy Rov, **27**  
 Bomnak iron ore zone, 232  
 Bryantnin apatite-bearing region, 239  
 Burpala, 216, 218  
 Burtyn, 117, 141, 145, 415  
 Burunin, 216  
 Butukhey, **250**
- Central, **12**, 23, **24**, 302  
 Chagay, 238  
 Chalka, 71  
 Chara, **213**, 214, 410  
 Chara group, 197, 214, 424  
 Chara-Tokk ore region, 197, 212, 391, 410, 420  
 Chaya, 321, 326, 412  
 Chebolak, 74
- Chepovich intrusion, 112, 127  
 Chernigov, 117, 130, **135**, 395, 413, 420  
 Chernigov-Tokmachan, 136  
 Chertomyk, 113, 117, **121**, 410  
 Chervurta, **27**  
 Chiney, **215**, 219-220, 411, 419  
 Chogar, 238  
 Chogar apatite region, 238-239  
 Chogar gold region, 238  
 Chupa, **12**, 81, 396  
 Chuya ceramic pegmatite zone, 336, 349, 356, 414-415
- Davan-Abchad rare metal zone, **336**, 419  
 Dolgaya Guba, **42**  
 Dovyren ore field, 401  
 Dva Kamnya, **260**  
 Dyos, 197-198  
 Dzhanin, 238-240  
 Dzhelindin, 385  
 Dzhugdzhur structural-metallogenic zone, 232
- Elgorash, 40  
 Elkon group, 202  
 Elmeldzhak, **201**, 202, **203-204**, 205, 415, 421  
 Emeldzhak group, 202, 397
- Faimoguba, 74  
 Fyodorov group, 195, 202
- Gayum, 238-240, **241**, 411  
 Geranskiy apatite region, 239  
 Gerfedskoye, **302-303**, 304, 315, 413, 419  
 Gologorskoe, 174  
 Goluboye, 202  
 Goreloye, 209  
 Gorevsk (Pb-Zn), 298, 300, 315, 412, 417, 420  
 Gorishneplavninskoye, 118  
 Gornostil, 367, 420  
 Gremyakha-Vyrmes, **12**, 24, **25**, 395, 411, 420  
 Gutara-Biryusa Pegmatites, 265  
 Gutaro-Biryusa belt, 420
- Hautavaara, **12**, 72, 389, 415, 419  
 Heinäjoki, 88  
 Heposelkä, **90**, 92, 94  
 Hetolambi, 83  
 Himola, 53  
 Hirvi-Navolok, 62

- Hopunvaara, **90**, 92  
 Huhtervu, 102  
 Hukkala, 70
- Ihala, **12**, 103, 415, 420  
 Ildeus, 232–233  
 Ilyin, **313**, 315  
 Inagli, 366  
 Ingulets, 118, 410  
 Ishimbin, 366
- Jakkima, 88  
 Jalonvara, **12**  
 Jaurijoki, **12**, 43, 413, 419  
 Jokiranta, 88
- Kabakhanyr, 224  
 Kalchik, 130  
 Kamchadal, **260**, **262**, 263  
 Kamenskoye, **150**, 117  
 Kammikivi, **31**  
 Kamnizhskoye, 349  
 Kanku, 208  
 Kapitanov, 112, 117, **123**, 396, 411, 419  
 Karachunovo–Lozovat zone, 113, 117, **128**  
 Karagay, 174  
 Katuga, 212, 398, 413, 420  
 Katuga rare metal ore field, 222, **223**  
 Kaula, **31**, 33, **34**, 411  
 Kettskoye, 371  
 Keyvy basin, 27, 420  
 Khanin ore region, 391  
 Kharabarov, 250  
 Khariuzikhin, 298, 315  
 Khibelen, 366, **374**, 401  
 Kholodnikan ore region, 202, 398  
 Kholodninskoye, 317, 329, **331**, **334**, **336**, **361**,  
 401, 412, 417, 420  
 Kholodnoye, 209, 415  
 Khondorsk, 250  
 Khrustalnoye, 209  
 Khuduchin, 202  
 Kichany, 70, 390  
 Kimbir, 271  
 Kirgitey, 310, 367, 401, 415  
 Kirovogorsk, 17  
 Kitelä, **90**, 92–93, 96, **98**, 99, 419  
 Kitoy, 249, **250**, **257**, 411, 420  
 Kitovsky Zhidoy, 250  
 Klyukvennoye, 216  
 Kolosjoki, 32  
 Koltykon, 208  
 Komarich anomalies, **161**  
 Kommunar, 88
- Komsomolskoye (Fe), 200  
 Kondakovo, 274, 277, 315, 420  
 Konstantinovo pegmatite field, 145, 323, 399  
 Korosten, 130  
 Korpanga, 53  
 Kostomuksha, **12**, 53, 55, 388, 410, 420  
 Kotselvaara, **31**  
 Kotuykan, 366  
 Kovaktin, 238  
 Koykari, 57  
 Krasnoye, 216  
 Krivokhizhintsevo, 176  
 Krivoy Rog district (graphite), **144**  
 Krivoy Rog–Kremenchug iron ore basin, 113,  
 117, **118–120**, 392, 410, 420  
 Kruchinin, 238  
 Kuksungur, 122  
 Kuranakh group, 202  
 Kurkenpakh, 17  
 Kursk iron ore province, **160**, 410, 420  
 Kuruvaara, 83, 415, 420  
 Kuzeyevskoye, 273–274, 315  
 Kuzoranda, 62, 395, 412, 420  
 Kyrpurta, **27**
- Landysh, 232  
 Lantar apatite ore region, 239  
 Larbin, 202  
 Latvasyrjä, **12**, 88, 413, 419  
 “Layer-330” **36**  
 Lebedin, 158, 410  
 Lebyazhi, **12**, 59, 412, 419  
 Legliyer, **199**  
 Legliyer group, 197–198  
 Lena gold region, **342**, 343–344, 348, **361**, 362  
 Levo–Lendakh, **314**  
 Lipovenkovo, 117, 123, 130, 396  
 Lobash, **12**, 67, **68–69**  
 Lovnozero, **12**, 412, 419  
 Lower Angara, 315, 366, 410  
 Lucha, 232–233  
 Luchin, 238  
 Lugovoye, 366, 375  
 Lugovskoye, 349  
 Lukinda, 232–235, **234**, 412, 419  
 Luonjoki, 40  
 Lyubar, 112, 117, **131–132**, 396, 413, 419  
 Lyuppiko (ceramics), 100  
 Lyuppiko (Sn), **90**, 92, 99
- Magazin–Musyur, 20  
 Magnetitovoye, **199**  
 Magnetitovy Log, 23  
 Maimjärvi, 62, 395

- Makharinetsk, 112, 385  
 Maleyevo, 130  
 Malinovaya Varaka, 81  
 Malobratulov, 130  
 Malotagul, 249, 255, **256**, 411, 419  
 Malo-Bystrinskoye, **284**  
 Mamskaya zone, 402  
 Manyuk, **27**  
 Mariupol, 113, 117, **122**, 394, 410  
 Maya, 392, 420  
 Maya ore zone, 410  
 Maymakan, 239, **240**, 419  
 Mezherich, 126  
 Mensunvara, 88  
 Middle Tolokan, 216  
 Mikhailov (Fe), 156, 158, 161, **163-164**  
 Mirona, **31**  
 Moiseyevo, 130  
 Mokhovoye, 337, **361**, 401  
 Molodyozhnoye, 317, 321, 356-357, **359**, 401, 415, 419  
 Monchegorsk, **12**, 35, **36**, 412, 419  
 Morion, 209  
 Moroshkovoye lake, **36**  
 Murovan-Kurilovets, 176  
  
 Nadezhdinskoye, 385, 420  
 Nagoryansk, 112, 151  
 Nakhodka, 337, 401  
 Neblogorsk, 79  
 Nelyukan ore region, 391  
 Neroy-1, 265  
 New Ore Field, **90**, 92  
 Nigozero, 74  
 Nikolaevskoye, 304, 366, 371, 411, 420  
 Nimger group, 209  
 Nittis-Kumuzhya-Travyanaya (NKT), 35, **36**  
 Nizhnemamon, 158, 161, 165, **166**, 167  
 Nizhneye, 366  
 North Souker, **31**  
 Novobakal, 174  
 Novomirgorod area, 126  
 Novopoltava, 136  
 Nusa-1, **27**  
 Nusa-3, **27**  
 Nyalmozero, 71, 389  
 Nyud-II, 36  
  
 October, 395, 413, 420  
 Okhok, 235, 236  
 Oktokita, 345, **347**  
 Oktober, 117, 130, **133**  
 Old Ore Field, **90**, 92, 94  
 Olenegorsk (Fe), **12**, 16, 17, 242, **313**, 410, 420  
 Olenegorsk (W), 313  
 Olimpiad, **302**, 308, 310, 410, 420  
 Olkhovsk, 275  
 Olympic, 202  
 Onki, **31**  
 Onot, 247, 249, 252, **253**, **260**, 263, 410, 415, 420  
 Ostropol, 112, 117, 396  
 Otradnoye, 83  
 Oyumrak group, 202  
  
 Päävara, 70, 390, 413, 419  
 Pahtajärvi, 32  
 Param, 358  
 Paromovka, 125-126  
 Parandovo, **12**, 71, 389  
 Payum, 239  
 Pecheguba, 17  
 Pechenga ore field, **12**, 30, **31**, 419  
 Pellapahk, 46, 390, 413, 419  
 Perevalnoye, 366, 377  
 Pervomaysk, 118, 130  
 Pervozvanov, 130  
 Perzhan, 130  
 Petrov (graphite), 117, 141, 415  
 Petrov group, **144**, 395  
 Petrovo-Gnutovo, 117, **134**  
 Pinkeljavr, 385, 410  
 Pinyazevichi, 126  
 Pionerka, 200  
 Pirtima, 83, 420  
 Pitkäranta, **12**, 89, **90**, **95**, 100, **101**, 413, 417, 419  
 Podkolodnovo, 158, 161, 165, **166**  
 Porozhin, **296**, 297, 315, 411, 420  
 Pravdin I (Ni), 117, **128-129**, 389  
 Pravdin II (talc), 113, 117, **150**  
 Predivin, 315, 415  
 Professor Bauman, 17  
 Promezhutochnoye, 30, **31**  
 Prostorov, 136  
 Pudozhgora, **12**, 57, 396, 411, 419  
 Pustynnoye, 209  
  
 Raisa, **42**  
 Raisoavi, **31**  
 Raivämäki, 102  
 Rikolatva, 79, 414, 420  
 Ristiniemi, **90**, 92  
 Rudnichnoye, 174  
 Runnijoki, 38  
 Ryzhany, 125-126  
  
 Sachkinsko-Vishnyakovskoye, **145**  
 Sagan-Zaba, 279, **280**, 281, 411

- Samuil, **42**  
 Saramtin, **250**  
 Sardana, 366, **376**, 377, 412, 417, 420  
 Sardana ore region, **375**, 377  
 Satka group, 174, 400  
 Savina, 249, 263, **264**  
 Seligdar, 197, 206, **207–208**, 397, 415, 420  
 Semiletka, **31**  
 Severnoye (quartz), 209  
 Shangulezh, 366, 371  
 Sharyzhalgay, **250**  
 Shikhan, 174  
 Shiversk, 315, 411, 419  
 Shumigorodok, 83  
 Shunga, 74  
 Shuururta, **12**, 28, **29**, 411  
 Shuya, 71  
 Sivakan, 232, **233**, 398  
 Sivaglin group, 197–198  
 Skalistoye (graphite), 50, 337, 415, 420  
 Skelevat–Magnetitovoye, 118  
 Skolkoye, 216  
 Slobodov, 112, 117, **149**  
 Slyudyanka, 242, 281–283  
 Slyudyansk, 349  
 Sofia, 42  
 Son-tiit group, 209  
 Sopcha, 35, **36**  
 Sortavala ore region, **88**  
 Sosnovy Bayts, 249, 252, **253–254**, 260, 386, 410  
 Souker, **31**  
 South Kakhozero, 17  
 South Stanovoy metallogenic zone, 232, 236  
 Sputnik, **31**  
 Starokrymskoye, **145**  
 Stepnoye, 174  
 Stoylen, 158  
 Stremigorod, 117, 126–127, 411, 419  
 Styrtta, 126  
 Subtugur, 202  
 Sueynlagash, 40  
 Sukhoy Log, 323, 341, 344–345, **347**, 348, 413, 420  
 Sursk, 130  
 Sushchan–Perzhan zone, 117, **137**, **139**, 413, 420  
 Svetlozero, **59**  
 Tabor, 366, **372–373**, 401, 412, 417, 420  
 Takhtygan, 344  
 Tarskoye, 174  
 Tasmiyeli ore region, 391  
 Taurta, **27**  
 Tayezhnoye (Fe), 198, **199**, 200–201, 397, 410, 421  
 Tedino, 81  
 Tepsa, 420  
 Ternovka, 126  
 Terrasa, **36**  
 Tervijärvi, 102  
 Tinskoye, **199**  
 Tomtor, 366  
 Troitskoye, 117, 141, **144**, 395, 415  
 Tsagin, **12**, 20, **21**, 410, 419  
 Tukan, 174  
 Tussagan, 174  
 Tuyukan tin ore region, 337, **361**, 413, 419  
 Tyapsh–Manyuk, 27  
 Tyradin, **314**  
 Tyyskoye, 401, 410  
 Uchur ore zone (Fe), 202, 410, 420  
 Uderey, **302**, 304–305, 307, 310, 315, 414, 419  
 Udokan, 212, 216, **217**, 218, 412, 417, 420  
 Udorong, 293, 366  
 Ukdsu, 224, **225**, 398, 415, 419  
 Uksa, **90**, 91  
 Ulkan, **229**, 413, 420  
 Unkur, 216  
 Upper Aldan region, 416, 420  
 Upper Garmin, 238  
 Urik–Iy belt, 419  
 Uruy, 366, 377, 379  
 Utomitelnoye, **199**  
 Utugey, 238  
 Vedlozero, 71, 389  
 Verbin, 130  
 Verkhovtsevo, 113  
 Veselyansk, **150**  
 Virov, 130  
 Vitim (Mu), 349, 413, 420  
 Vitim ore field (Fe), 410, 420  
 Voitskoye, 70, 413  
 Volchegorskoe, 174  
 Volodarsk–Volyn, 112, 410, 419  
 Volotov, 158  
 Volyn pegmatite field, 117, 145, **146–147**, 416, 419  
 Volyn region (graphite), **145**  
 Vorgelurta, **27**  
 Vostok, 389  
 Voyevodchino, 177  
 Vozhminskoyoe, 58

- Yagelurta, **27**  
Yaginda, **202**  
Yakovlev-type ore, **164**, 410  
Yalonvaara, 67, 389  
Yelan, 158, 161, 166, **168–169**  
Yeletozero, 420  
Yenashmin (Fe), 315  
Yona, **12**, 396  
Yugok, 130  
Yuktin, 202  
Yunges, 40  
Yus-Kyuel, 224
- Zapolyarnoye, **31**  
Zarechnoye, **199**
- Zavalyevskoye, 112, 117, 141, **143–144**, 396,  
415, 420  
Zazhogin, **12**, 74, 395, 416, 420  
Zbrankov, 112, 117, **151**, 416  
Zhdanov (Ni), **31**  
Zheleznaya Varaka, 17  
Zheltorechka, 117, **138–141**, 395, 414  
Zhyoltyye Vody, 395  
Zigazin-Komarov group, 174, 400  
Zimoveynin, 271  
Zolotaya Gora, 236, **237**, 414  
Zolotyye Porogi, 58, **59**, 419
- “15 Years of October”, 17

This Page Intentionally Left Blank

## Subject Index

- Abchada zone, 419  
 Aivar, 17  
 Akkim, 38  
 Aleksandrov, 130  
 Alenguy, 238  
 Allarechka, 12, 37, 389, 412, 419  
 Anangra, 349  
 Angara-Pit basin, 410, 420  
 Angara-Pit iron ore basin, 293  
 Angara-Pit, 326  
 Annama, 38  
 Annin, 170  
 Arbarastakh, 420  
 Arshan, 366, 371  
 Asbestos-bearing Molodyozhny massif, 357  
 Azov graphite region, 144
- Baikal, 410, 420  
 Bakal group, 174  
 Bakal, 410  
 Bakhtyn, 177  
 Balakhovskoye, 141  
 Bargin, 421  
 Bazarnaya Bay occurrence, 42  
 Bazarnaya Guba, 413  
 Begim-Chokrak, 136  
 Belaya Zima ("White Winter"), 415  
 Belaya Zima, 419  
 Belgorod type ores, 164  
 Berdichev graphite region, 141  
 Beregov type ores, 161  
 Bergaul, 71  
 Besedin type ores, 161  
 Bezymyannaya, 27  
 Biboy, 252  
 Bogide, 238-239  
 Bogunayev, 271, 315  
 Bogunayevo, 274, 414, 419  
 Bogunayevskoye deposit, 273  
 Bogunayevskoye, 273  
 Bolotnoye, 199  
 Bolshaya Gleyevatka, 118  
 Bolshaya Tagna, 416, 419  
 Bolshe-Severnoye, 349  
 Bolshezero, 53  
 Bolshoy Rov, 27  
 Bomnak or Upper Zeya zone, 232  
 Bryantin, 239  
 Bulpala, 216, 218
- Burtyn graphite deposit, 145  
 Burtyn, 117, 141, 415  
 Burunin, 216  
 Butukhey, 250
- Central deposit, 23  
 Central zone, 302  
 Central, 12  
 Chagay, 238  
 Chalka, 71  
 Chara deposit, 214  
 Chara group of deposits, 214  
 Chara group, 242  
 Chara sector, 213  
 Chara, 410  
 Chara-Tokk ore region, 212  
 Chara-Tokk region, 420  
 Chara-Tokk, 391  
 Charo groups, 197  
 Charo-Tokk group, 197, 410  
 Chaya deposit, 326  
 Chaya, 321, 412  
 Chebolak, 74  
 Chepovich intrusion, 127  
 Chepovich intrusions, 112  
 Chernigov apatite-carbonatite and rare metal-rare earth deposit, 135  
 Chernigov, 117, 130, 414, 420  
 Chernigov-Tokmachan, 136  
 Chernigovo, 395  
 Chertomlyk, 113, 117, 410  
 Chertomlyk ferruginous quartzite deposit, 121  
 Chervurta, 27  
 Chiney copper-nickel deposit, 219  
 Chiney Cu sst deposits, 215  
 Chiney, 220, 411, 419  
 Chogar, 238-239  
 Chupa, 12, 81  
 Chupa Loukhi, 396  
 Chuya ceramic pegmatite zone, 356, 421  
 Chuya structural-pegmatitic zone, 349  
 Chuya zone of ceramic pegmatites, 415  
 Chuya-Vitim zone, 336  
 Crystal region, 416
- Davan zone, 419  
 Davan-Abchada shear zone, 336  
 Dolgaya Bay, 42

- Dovyren peridotite–pyroxenite–norite layered intrusion with low-grade Cu–Ni mineralization, 401
- Dva Kamnya, 260
- Dyos, 197–198
- Dzhanin, 238–240
- Dzhelinda corundum and kyanite deposit, 385
- Dzhugdzhur, 232
- East Vozhminkoye, 59
- Elgorash, 40
- Elkon, 202
- Emeldzhak deposit, 202, 204–205
- Emeldzhak phlogopite deposit, 203
- Emeldzhak, 201–202, 415, 421
- Emeldzhak–Tayozhnaya group, 397
- Faimoguba, 74
- Fyodorov Group, 195
- Fyodorov, 202
- Gayum deposit, 241
- Gayum, 238–240, 411
- Geran, 239
- Gerfedskeye deposit, 302, 304
- Gerfedskeye gold ore, 302
- Gerfedskeye ore field, 303–304
- Gerfedskeye, 315, 414, 419
- Gologorskoye, 174
- Goluboye, 202
- Gora, 414
- Gorevskoye, 315, 417
- Goreloye, 209
- Gorevsk, 412, 420
- Gorevskoye deposit, 298, 300
- Gorishneplavinskoye, 118
- Gornostil, 367, 411, 420
- Gremyakh–Vyrmes deposit, 23
- Gremyakh–Vyrmes, 12, 25, 395, 411, 420
- Gutar–Biryusa belt, 421
- Gutara–Biryusa mica pegmatites, 265
- Hautavaara deposit, 72–73
- Hautavaara, 12, 389, 415, 419
- Heinäjoki, 88
- Heposelkä, 90, 93–94
- Hetolambi, 83
- Himola, 53
- Hirvi–Navolok, 62
- Hopunvaara, 90, 92
- Huhtervu, 102
- Hukkala, 70
- Ihala graphite region, 103
- Ihala ore field, 415
- Ihala, 12, 420
- Ildeus, 232–233
- Ilyin, 313, 315
- Inagli, 366
- Ingulets, 118, 410
- Ishimbinskoye, 366
- Jakkima, 88
- Jalonvaara, 12
- Jaurijoki deposit, 43
- Jaurijoki, 12, 419
- Jokiranta, 88
- Kabakhanyr, 224
- Kalchik, 130
- Kalotovka, 349
- Kamchadal deposit, 262
- Kamchadal, 260, 263
- Kamenskoye deposit, 150
- Kamenskoye, 117
- Kammizhskoye, 349
- Kanku, 208
- Kapitanov deposit, 396
- Kapitanov, 112, 117, 123, 411, 419
- Karachunov–Lozovat zone, 117
- Karachunovo–Lozovat, 113
- Karachunovo–Lozovat sulphide mineralization zone, 128
- Karagai, 174
- Katuga field, 223
- Katuga ore field, 413, 420
- Katuga rare-metal deposit, 212
- Katuga rare-metal ore field, 222
- Katugan rare-metal deposit, 398
- Kaula deposit, 33–34
- Kaula, 31, 411
- Keivy ore-bearing zone, 27
- Kettskoye, 371
- Keyvy basin, 420
- Khanin iron ore region, 391
- Kharabarovsk, 250
- Khariuzikhin occurrence, 298
- Khariuzikhin, 315
- Khibelen deposit, 374
- Khibelen, 366, 401
- Kholodnikan ore region, 398
- Kholodnikan, 202
- Kholodnin Pb–Zn–pyrite deposit, 401
- Kholodnin, 417, 420
- Kholodninskoye deposit, 331, 334, 336

- Kholodninskoye massive sulphide-polymetallic deposit, 329, 361  
 Kholodninskoye, 317, 412  
 Kholodnoye, 209, 416  
 Khondor, 250  
 Khrustalnoye, 209  
 Khuduchin, 202  
 Kichany, 70, 390  
 Kimbirka, 271  
 Kirgitey deposit, 310  
 Kirgitey hydrothermal talc, 401  
 Kirgitey, 367, 415  
 Kirovogorsk, 17  
 Kitilä, 419  
 Kitoy (Dabady) sillimanite schist deposit, 257  
 Kitoy group of deposits, 250  
 Kitoy sillimanite deposit, 249  
 Kitoy, 411, 420  
 Kitovsky Zhidoy, 250  
 Kittelä deposit, 98-99  
 Kittelä, 90, 92-93  
 Kittilä deposit, 96  
 Klyukvennoye, 216  
 Koikari titanomagnetite deposits, 57  
 Kolosjoki occurrences, 32  
 Koltykon, 208  
 Komarich-type, 161  
 Kommunar, 88  
 Komsomolsk, 17  
 Komsomolskoye, 200  
 Kondakovo muscovite with rare-metal pegmatite deposit, 277  
 Kondakovo, 274, 315, 421  
 Konstantinovo field of cavity pegmatites, 399  
 Konstantinovo granite plug, 323  
 Konstantinovo pegmatite field, 145  
 Korosten, 130  
 Korpanga, 53  
 Kostomuksha deposit, 55  
 Kostomuksha ore region, 53, 388  
 Kostomuksha, 12, 53, 410, 420  
 Kotselvaara-Kammikivi, 31  
 Kotuykan occurrence, 366  
 Kovaktin, 238  
 Krasnoye deposits, 216  
 Krivokhizhintsovo, 176  
 Krivoy Rog basin, 410, 420  
 Krivoy Rog graphite region, 144  
 Krivoy Rog-Kremenchug basin, 117  
 Krivoy Rog-Kremenchug belt, 392  
 Krivoy Rog-Kremenchug iron ore basin, 113  
 Krivoy Rog-Kremenchug zone, 116  
 Krivoy Rog-Kremenchug, 118  
 Kruchinin, 238  
 Kuksungur, 122  
 Kuranakh, 202  
 Kurkenpakkk, 17  
 Kursk iron ore province, 160  
 Kursk Magnetic Anomaly (KMA), 410  
 Kursk Magnetic Anomaly, 420  
 Kuru-Vaara deposit, 83  
 Kuruvaara, 415, 421  
 Kuru-Vaara, 83  
 Kuzeyev, 315  
 Kuzeyevskoye deposit, 274  
 Kuzeyevskoye, 273  
 Kuzoranda occurrence, 62  
 Kuzoranda, 395, 412, 420  
 Kyrpurta, 27  
 Lake Moroshkovo, 36  
 Lake Svetloye, 59  
 Landysh, 232  
 Lantar, 239  
 Larbin regions, 202  
 Latvasyrä, 413, 419  
 Latvasyrjä, 12, 88  
 Layer 330, 36  
 Lebedin, 158, 410  
 Lebyazhe, 412  
 Lebyazhi deposit, 59  
 Lebyazhi, 12, 59, 419  
 Leglier group, 197-198  
 Leglier, 199  
 Lena gold ore complex, 342-344  
 Lena gold-bearing region, 361-362  
 Lena ore complex, 348  
 Levo-Landakh occurrence, 314  
 Lipovenkov, 396  
 Lipovenkovo, 117, 123, 130  
 Lobash deposit, 67  
 Lobash molybdenum deposit, 68-69  
 Lobash, 12  
 Lovnozero, 12, 412, 419  
 Lower Angara, 315, 366, 410  
 Lucha, 232  
 Luchin, 238  
 Lugovoye, 366, 375  
 Lugovskoye, 349  
 Lukinda and Lucha intrusions, 233  
 Lukinda intrusion, 234  
 Lukinda, 232, 412, 419  
 Luonjoki, 40  
 Lupikko, 92  
 Lyubar molybdenum occurrence, 132

- Lyubar, 112, 117, 131, 396, 413, 419  
 Lyupikko deposit, 99–100  
 Lyupikko, 90
- Magazin–Musyur, 20  
 Magnesite deposit, 401  
 Magnetitovoye, 199  
 Magnetitovy Log, 23  
 Maimjärvi, 395  
 Maimjärvi occurrence, 62  
 Makharinetsk, 112, 385  
 Maleyevo, 130  
 Malinovaya Varaka, 81  
 Malobratulov, 130  
 Malo-Bystrinka deposit, 284  
 Malotagul deposit, 249, 255–256  
 Malo-Tagul, 411  
 Malotagul, 419  
 Mamskaya zone, 402  
 Manyuk, 27  
 Mara, 349  
 Mariupol ore deposit, 122  
 Mariupol, 113, 117, 394, 410  
 Maya ore zone, 410  
 Maya ore zones, 420  
 Maya, 392  
 Maymakan deposit, 239–240  
 Maymakan, 239, 419  
 Mensunvaara, 88  
 Mezherich, 126  
 Middle Tolokan, 216  
 Mikhailov iron ore deposit, 163  
 Mikhailov, 158, 161, 164  
 Mirona, 31  
 Mokhovoye deposit, 361  
 Mokhovoye, 337, 401  
 Molodyozhnoye chrysotile–asbestos deposit, 321, 356, 359  
 Molodyozhnoye chrysotile–asbestos, 401  
 Molodyozhnoye, 317, 415, 419  
 Monchegorsk group of deposits, 419  
 Monchegorsk group, 412  
 Monchegorsk pluton, 36  
 Monchegorsk, 12  
 Moiseyevo, 130  
 Morion, 209  
 Murovan–Kurilovets, 176
- Nadezhda graphite deposit, 385  
 Nadezhdinskoye, 420  
 Nagoryansk, 112  
 Nagoryansk pyrophyllite deposits, 151  
 Nakhodka, 337, 401
- Neblogorsk, 79  
 Nelyukan, 391  
 Neroy I deposit, 266  
 New Ore Field, 90, 92  
 Nigozero deposit, 74  
 Nikolayev, 411  
 Nikolayevo, 304  
 Nikolayevskoye, 366, 371, 420  
 Nimger groups, 209  
 Nittis–Kumuzhyc–Travyanaya (NKT), 35  
 Nizhne-Mamon deposit, 166  
 Nizhne-Mamon ore deposit, 167  
 Nizhne-Mamon, 158, 161, 165  
 Nizhneye, 366  
 NKT, 36  
 North Souker, 31  
 Novobakal, 174  
 Novomirgorod areas, 126  
 Novopoltava, 136  
 Nussa 1, 27  
 Nussa 3, 27  
 Nyalmozero, 71, 389  
 Nyud-II, 36
- October intrusion, 133  
 October, 117, 130, 395, 413, 420  
 Okhok occurrence, 235–236  
 Okhok, 413  
 Oktokit deposit, 345  
 Oktokit ore field, 347  
 Old Ore Field, 90, 93–94  
 Olenegorsk deposit, 242  
 Olenegorsk, 12, 16–17, 313, 410, 420  
 Olkhovsky mine, 275  
 Olympiad deposit, 308  
 Olympiad, 302, 310, 410, 420  
 Olympic, 202  
 Onki, 31  
 Onot deposits, 263  
 Onot graben, 247, 260  
 Onot group of deposits, 249, 253  
 Onot group, 252, 410  
 Onot, 415, 420  
 Ore deposits in the Monchegorsk pluton, 35  
 Ostropol, 112, 117, 396  
 Otradnoye, 83  
 Oyumrak, 202
- Päävaara, 70  
 Päävara, 390, 413, 419  
 Pahtajärvi, 32  
 Param nephrite deposit, 358  
 Parandovo, 12, 71, 389

- Paromovka, 125–126  
 Payum, 239  
 Pecheguba, 17  
 Pechenga group, 419  
 Pechenga ore field, 30–31  
 Pechenga, 12  
 Pellapahk deposit, 46  
 Pellapakhk, 390, 413, 419  
 Perevalnoye, 366, 377  
 Pervomaysk, 118, 130  
 Pervozvanov, 130  
 Perzhan, 130  
 Petrov group, 144, 395, 415  
 Petrov, 117, 141  
 Petrovo–Gnutovo, 117  
 Petrovo–Gnutovo rare-earth occurrence, 134  
 Pinkeljavr deposits, 385  
 Pinkeljavr, 410  
 Pinyazevichi, 126  
 Pionerka, 200  
 Pirtima, 83, 421  
 Pitkäranta, 12, 413, 417, 419  
 Pitkäranta deposits, 100  
 Pitkäranta ore region, 89–90, 95, 101  
 Podkolodnovo deposit, 166  
 Podkolodnovo deposits, 165  
 Podkolodnovo, 158, 161, 170  
 Porozhin deposit, 296  
 Porozhin, 411, 420  
 Porozhinskoye deposit, 296  
 Porozhinskoye, 315  
 Pravdin deposit, 128, 150, 389  
 Pravdin ultrabasic intrusion, 129  
 Pravdin, 113, 415  
 Pravdin-1, 117  
 Pravdin-2, 117  
 Predivinskoye, 315  
 Professor Bauman, 17  
 Promeshutochnoye, 30–31  
 Prostorov, 136  
 Pudozhgora deposit, 57  
 Pudozhgora, 12, 57, 396, 411, 419  
 Pustynnoye, 209  
  
 Raisa, 42  
 Raisoavi, 31  
 Raivamäki, 102  
 Rare-metal occurrences in the Davan–Abchada shear zone, 338  
 Rikolatva deposit, 79  
 Rikolatva, 414, 421  
 Ristiniemi, 90, 92  
 Rudnichnoye, 174  
  
 Runnijoki, 38  
 Ryzhany, 125–126  
  
 Sachkinsko–Vishnyakovskoye deposit, 145  
 Sagan–Zaba deposit, 280  
 Sagan–Zaba, 279, 281, 411  
 Samuil, 42  
 Saramtin, 250  
 Sardana deposit, 376  
 Sardana ore region, 375, 377  
 Sardana, 366, 377, 412, 417, 420  
 Satka group, 174  
 Satka magnesite deposit, 400  
 Savin magnesite deposit, 264  
 Savina deposit, 249  
 Savina magnesite deposit, 263  
 Seligdar apatite deposit, 197, 206, 208  
 Seligdar, 397, 415, 421  
 Semiletka, 31  
 Severnoye, 209  
 Shangulezh, 366, 371  
 Sharyzhalgay, 250  
 Shikhan, 174  
 Shiver, 315  
 Shivero, 411, 419  
 Shumigorodok, 83  
 Shunga, 74  
 Shuururta (Kyanite), 12  
 Shuururta deposit, 28–29  
 Shuururta, 411  
 Shuya, 71  
 Sivaglin, 197–198  
 Sivakan deposit, 232–233, 398  
 Sivakan, 232  
 Skalistoye graphite deposit, 50  
 Skalistoye, 337, 415, 420  
 Skelevat–Magnetitovoye, 118  
 Skolzkoye, 216  
 Slobodov garnet deposit, 149  
 Slobodov, 112, 117  
 Slyudyanka phlogopite deposit, 282  
 Slyudyanka, 242, 281  
 Slyudyansk, 349  
 Sofia, 42  
 Sogdiondonskoye, 349  
 Son–Tiit, 209  
 Sopcha vein deposits, 35  
 Sopcha, 36  
 Sortavala ore region, 88  
 Sosnovy Bayts deposit, 252, 386  
 Sosnovy Bayts, 249, 254, 260, 410  
 Souker, 31  
 South Kakhzero, 17

- South Stanovoy gold zone. 232, 236  
 Sputnik. 31  
 Starokrymskoye deposit. 145  
 Stepnoye. 174  
 Stoylen. 158  
 Stremigorod ores. 127  
 Stremigorod. 117, 411, 419  
 Stremigorod type. 126  
 Styrtta areas. 126  
 Subtugur. 202  
 Sueynlagash. 40  
 Sukhoy Log. 323, 341, 344-345, 348, 414, 420  
 Sukhoy stream. 347  
 Sursk. 130  
 Suschan-Perzhan zone. 413, 420  
 Sustchan-Perzhan zone. 117, 137, 139  
  
 Tabor. 366, 401, 413, 417, 420  
 Tabor deposit. 372-373  
 Takhtygan. 349  
 Tarskoye. 174  
 Tasmiyeli. 391  
 Tavurta. 27  
 Tayezhnoye. 410, 421  
 Tayozhnoye deposit. 198, 200-201  
 Tayozhnoye. 199  
 Tedino muscovite pegmatite deposit. 81  
 Tedino. 81  
 Tepsa. 421  
 Ternovka. 126  
 Terrasa. 36  
 Tervijärvi. 102  
 The Geran region. 239  
 Tinskoye. 199  
 Tomtor occurrence. 366  
 Troitskoye. 117, 141, 144, 395, 415  
 Tsagin deposit. 20  
 Tsagin intrusion. 21  
 Tsagin. 12, 20, 411, 419  
 Tsentralnoye (Central) deposit. 24  
 Tukan. 174  
 Tussagan. 174  
 Tuyukan ore region. 361  
 Tuyukan tin ore region. 419  
 Tuyukan tin-ore region. 337, 413  
 Tyapsh-Manyuk. 27  
 Tyradin. 314  
 Tyya. 401, 410  
  
 Uchur groups. 202  
 Uchur ore zone. 410  
 Uchuri. 420  
  
 Uderey deposit. 307  
 Uderey deposits. 304  
 Uderey gold-antimony deposit. 305  
 Uderey ore field. 307  
 Uderey. 302, 310, 315, 414, 419  
 Udokan cupraceous sandstone deposit. 212  
 Udokan deposit. 216-217, 417  
 Udokan. 216, 218, 412, 420  
 Udorong. 366  
 Udoronga. 293  
 Ukodus apatite deposit. 398  
 Ukodus deposit. 224-225  
 Ukodus. 224, 415, 419  
 Uksa. 90, 92  
 Ulkan ore field. 229, 413, 420  
 Unkur. 216  
 Upper Aldan quartz crystal region. 420  
 Upper Aldan quartz. 416  
 Upper Garmin. 238  
 Urik-Iy belt. 419  
 Uruy deposit. 379  
 Uruy. 366, 377  
 Utomitelnoye. 199  
 Utugey. 238  
  
 Vedlozero. 71, 389  
 Verbin. 130  
 Verkhovtsevo. 113  
 Veselyansk deposit. 150  
 Virov. 130  
 Vitim ore field. 410, 420  
 Vitim. 349, 414, 421  
 Voitskoye occurrence. 70-71  
 Voitskoye. 70, 414  
 Volchegorskoye. 174  
 Volodar Volyn. 112, 411  
 Volodarsk-Volyn. 419  
 Volotov. 158  
 Volyn graphite region. 145  
 Volyn pegmatite field. 117, 145-146, 416, 419  
 Vorgelurta. 27  
 Vostok. 389  
 Voyevodchino. 177  
 Vozhmenskoye. 58  
  
 Yagelurta. 27  
 Yaginda deposit. 202  
 Yaginda. 202  
 Yakovlev type ores. 164  
 Yakovlevo. 410  
 Yalonvaara. 67, 389  
 Yaurijoki. 413  
 Yelan deposit. 168

- Yelan, 158, 161, 166, 168  
Yeletozero, 420  
Yenashim, 315  
Yona, 12, 396  
YUGOK, 130  
Yuktin, 202  
Yunges, 40  
Yus-Kyuel apatite deposits, 224
- Zapolyarnoye, 31  
Zarechnoye, 199  
Zavalyev, 417  
Zavalevskoye graphite deposit, 143  
Zavalyev, 396  
Zavalyevsk, 420  
Zavalyevskoye, 112, 117, 141, 415  
Zazhogin deposit, 74  
Zazhogin, 74, 395, 416, 420  
Zazhogino (shungite), 12
- Zbrankov, 112, 117, 416  
Zbrankovsk, 151  
Zhdanov, 31  
Zheleznaya Varaka, 17  
Zheltaya Rechka, 414  
Zheltorechka deposit, 140  
Zheltorechka, 117  
Zheltorechka uranium deposit, 138  
Zholtaya Rechka, 395  
Zholtyye Vody, 395  
Zigazin Komarov group of deposits, 400  
Zigazin Komarov group, 174  
Zimoveinin, 271  
Zolotaya Gora deposit, 236  
Zolotaya Gora, 237  
Zolotaya, 414  
Zolotyie Porogi, 58-59, 419
- 15 Years of October, 17

This Page Intentionally Left Blank